

Site C Clean Energy Project

**Site C Reservoir Fish Food Organisms Monitoring
Program (Mon-6)**

**Peace River Fish Food Organisms Monitoring Program
(Mon-7)**

Construction Year 4 (2018)

**Ecoscape Environmental Consultants Ltd.
#102 – 450 Neave Court
Kelowna, BC V1V 2M2**

April 2019



Site C Clean Energy Project

Site C Reservoir and Peace River Fish Food Organisms Monitoring



Prepared For:
British Columbia Hydro and Power Authority

Prepared By:
Ecoscape Environmental Consultants Ltd.

April 2019

Site C Clean Energy Project Reservoir Fish Food Organisms Monitoring

Prepared For:
British Columbia Hydro and Power Authority

Prepared By:
Ecoscape Environmental Consultants Ltd.
#102 – 450 Neave Court
Kelowna, BC
V1V 2M2

Authors:
Jason Schleppe, M.Sc., R.P.Bio
Heather Larratt, H.B.Sc., R.P.Bio.
Rachel Plewes, M.Sc.

Modellers:
Joe Thorley, PhD., R.P.Bio
Rachel Plewes, M.Sc.



April, 2019

Ecoscape File No. 17-2056



ACRONYMS AND ABBREVIATIONS

AFDW	ash free dry weight
AICc	Akaike information criterion corrected for small sample sizes
ANCOVA	Analysis of covariance
BC Hydro	British Columbia Hydro and Power Authority
CFU	colony forming unit
chl-a	Chlorophyll-a
CLs	Confidence Limits
Didymo	<i>Didymosphenia geminata</i>
EAC	Environmental Assessment Certificate
EPT	Ephemeroptera (mayflies), Plecoptera (stoneflies), Trichoptera (caddisflies)
FAHMFPP	Fisheries and Aquatic Habitat Monitoring and Follow-up Program
FNU	Formazin Nephelometric Unit
km	kilometer
L	litre
m	metre
masl	metres above sea level
max	maximum value
min	minimum value
n	sample size
NMDS	Non-metric multidimensional scaling
NTU	nephelometric turbidity units
PAR	Photosynthetically active radiation
PERMANOVA	permutational multivariate analysis of variance
RVI	relative variable importance
RTK	real-time kinematic
SD	standard deviation
TSS	total suspended solids



DEFINITIONS

The following terms are defined as they are used in this report.

Term	Definition
Accrual rate	A function of cell settlement, actual growth and losses (grazing, sloughing)
Algae bloom	A super-abundant growth of algae
Anaerobic/anoxic	Devoid of oxygen
Autotrophic	An organism capable of synthesizing its own food from inorganic substances, using light or chemical energy
Benthic	Organisms that dwell in or are associated with the sediments
Benthic production	The production within the benthos originating from both periphyton and benthic invertebrates
Catastrophic flow	Flow events that have population level consequences of >50% mortality
Cyanobacteria	Bacteria-like algae having cyanochrome as the main photosynthetic pigment
Diatoms	Algae that have hard, silica-based "shells" frustules
Diel	Denoting or involving a period of 24 hours
Epilithic algae	Algae that grow on hard inert substrates, such as gravel, cobbles, boulders
Eutrophic	Nutrient-rich, biologically productive water body
Flow	The instantaneous volume of water flowing at any given time (e.g. 1200 m ³ /s)
Freshet	The flood of a river from melted snow in the spring
Functional Feeding group	(FFG) Benthic invertebrates can be classified by mechanism by which they forage, referred to as functional feeding or foraging groups
Heteroscedasticity	Literally "differing variance", where variability is unequal across the range of a second variable that predicts it, from errors or sub-population differences.
Heterotrophic	An organism that cannot synthesize its food and is dependent on complex organic substances for nutrition.
Laminar	Non-turbulent flow of water in parallel layers near a boundary
Light attenuation	Reduction of sunlight strength during transmission through water
Limitation, nutrient	A nutrient can limit or control the growth of organisms e.g. P or N limitation
Linear Regression Model	Linear regression attempts to model the relationship between two variables by fitting a linear equation to observed data
Macroinvertebrate	An invertebrate that is large enough to be seen without a microscope
Mainstem	The primary downstream segment of a river, as contrasted to its tributaries
Mesotrophic	A body of water with moderate nutrient concentrations
Microflora	The sum of algae, bacteria, fungi, <i>Actinomyces</i> , etc., in water or biofilms
Morphology, river	The study of channel pattern and geometry at several points along a river
Oligotrophic	A body of water with low nutrient concentrations
PAR	Photosynthetically Active Radiation -sunlight spectra used by plants
Peak biomass	The highest density, biovolume or chlorophyll-a attained in a set time on a substrate
Periphyton	Microflora that are attached to aquatic plants or solid substrates
Phytoplankton	Algae that float, drift or swim in water columns of reservoirs and lakes
Ramping of flows	A progressive change of discharge into a stream or river channel
Riffle	A stretch of choppy water in a river caused by a shoal or sandbar
Riparian	The interface between land and a stream or lake
Salmonid	Pertaining to the family <i>Salmonidae</i> , including the salmon, trouts, chars, and whitefishes.
Substrates	Substrate (sediment) is the material (boulder cobble sand silt clay) on the bottom of a stream or lake.
Taxa Taxon	A taxonomic group(s) of any rank, such as a species, family, or class.
Thalweg	A line connecting the lowest points of a river, usually has the fastest flows
Zooplankton	Minute animals that graze algae, bacteria and detritus in water bodies



Suggested Citation:

Schleppe, J., H. Larratt, and R. Plewes, 2019. Site C Clean Energy Project: Reservoir Fish Food Organisms Monitoring 2018 Annual Report. Prepared for BC Hydro. Prepared by Ecoscape Environmental Consultants. 71 pg + appendices.

Key Word Tags:

Mon-6: fish food organisms | periphyton production | Benthic invertebrates | Dinosaur Reservoir | Williston Reservoir | Peace River sites PR1 PR2 PR3 | Halfway River | Moberly River | areal biomass | photic zone | trophic condition |

Mon-7: Q1. areal biomass | fish food organisms | primary productivity | benthic invertebrates Peace River sites PD1 PD2 PD3 PD4 PD5 | reach-wide biomass |

Mon-17: hydrologic regime | catchability estimates | fish habitat | periphyton production | Benthic invertebrate | flow fluctuation effects |

© 2019 BC Hydro.

No part of this publication may be reproduced, stored in a retrieval system, or transmitted, in any form or by any means, electronic, mechanical, photocopying, recording, or otherwise, without prior permission from BC Hydro, Burnaby, BC.



ACKNOWLEDGEMENTS

This project would not have been realized without the assistance and contributions from the following individuals:

- Michael McArthur, Senior Environmental Coordinator, Site C Clean Energy Project (project management and coordination)
- Nich Burnett, M.Sc., R.P.Bio., Senior Environmental Coordinator, Site C Clean Energy Project (data / logistics / coordination)
- Brent Mossop, Environmental Specialist, BC Hydro (project management and coordination)
- Joe Thorley, Computational Biologist, Poisson Consulting (data analysis and model development)
- Jordan Akers, H.ABSc., Ecoscape Environmental Consultants Ltd., Data Analysis Technician
- Sue Salter, Cordillera Consulting (benthic invertebrate taxonomy)
- Scott Finlayson, Coridillera Consulting Ltd. (benthic invertebrate taxonomy)
- Kyle Hawes, B.Sc., R.P.Bio, Ecoscape (field data collection)
- Mary Ann Olson-Russello, M.Sc., R.P.Bio., Ecoscape (field / logistics)
- Robert Wagner, B.Sc., Ecoscape (field data collection)
- Tina Deenik, B.Sc., Ecoscape (field data collection)
- Golder Field Crews and Dustin Ford, B.Sc., R.P.Bio. (Fish Stomach Collection)



EXECUTIVE SUMMARY

BC Hydro developed the Site C Fisheries and Aquatic Habitat Monitoring and Follow-up Program (FAHMFP) in accordance with Provincial Environmental Assessment Certificate Condition No. 7 and Federal Decision Statement Condition Nos. 8.4.3 and 8.4.4 for BC Hydro's Site C Clean Energy Project. The Site C Reservoir Fish Food Organisms (Mon-6) and Peace River Fish Food Organisms (Mon-7) Monitoring Programs represent two components of the FAHMFP that monitor the factors affecting periphyton and benthic invertebrates that contribute to food for fish. This study builds on monitoring completed since 2010 using replicate methods and sample sites. Sampling in 2018 marked the second year of monitoring since the Project construction began in 2015, and the fifth year of baseline information prior to river diversion in fall 2020 and reservoir filling in fall 2023. This report covers the Mon-6 and Mon-7 results to date, using comparison of 2010-2012 data with 2017-2018 data.

The transformation of the Site C reach of the Peace River to an approximately 50 m deep reservoir will create a new aquatic environment that is expected to support a community of equal or greater productivity than the existing riverine ecosystem. The Project will result in a loss of 29.6 km² of lotic habitat in the mainstem and the lower reaches of tributaries, and a gain of 9.4 km² of littoral habitat and 83.6 km² of pelagic habitat, resulting in a net gain of 63.4 km² of aquatic habitat. These expected changes could alter fish food communities within and downstream of the future Site C Reservoir.

Sampling for Mon-6 and Mon-7 focused on identifying how physical processes in the Peace River and Williston and Dinosaur reservoirs affect benthic productivity and subsequent availability of fish forage items. In 2017 and 2018, samples were collected in upstream Dinosaur and Williston Reservoirs (control) and at twelve riverine sites, including two new sites in Alberta (PD4 and PD5). All sites were either within the future Site C Reservoir (PR/MD/HD sites) or downstream of it (PD sites). Sites above and below tributaries (Halfway and Moberly rivers) within the future Site C Reservoir were also sampled (Figures 2-1 and 2-2).

Both Williston and Dinosaur reservoir phytoplankton samples showed very low productivities that were numerically dominated by pico-cyanobacteria with brief pulses of diatoms, flagellates, and green algae. The depths of the reservoir photic zones were turbidity-driven, dynamic, and varied seasonally from 3.6 to 12 m in Williston Reservoir and from 1.5 to 10 m in Dinosaur Reservoir. Both reservoir pelagic areas were classified as intermediate between oligotrophic and ultra-oligotrophic using standard nutrient and productivity metrics. The 2017 and 2018 data showed that heavy freshets, intense summer storms, and wildfire ash can increase reservoir nutrient supplies.

Total zooplankton biomass fluctuated with phytoplankton densities seasonally and interannually. Samples from both reservoirs had similar, low-density communities dominated by copepods. Pelagic zooplankton samples from Williston Reservoir had greater productivity than Dinosaur Reservoir pelagic samples. Within Dinosaur Reservoir, littoral samples had double the pelagic zooplankton abundance and biomass in the 2017 and 2018 growing seasons.

The Dinosaur Reservoir littoral area contributed more to standing crop per unit area than the larger but less productive pelagic area. Within Dinosaur Reservoir, littoral periphyton productivity data were variable but generally increased with submergence time and with water temperature. Upstream reservoir communities were different and less productive than those in riverine areas. Dinosaur Reservoir periphyton biomass estimates were all less than half of the downstream riverine reach estimates.



Reservoir invertebrate communities were also distinct (more dipterans, gastropods but fewer Ephemeroptera, Plecoptera, Trichoptera taxa), with lower overall diversity, abundance, and biomass than downstream riverine areas. Within the reservoir littoral zone, invertebrate biomass and abundance increased with depth to peak at 3 m. Stomach contents from Arctic Grayling, Mountain Whitefish and Rainbow Trout from all years indicate that Dipterans provided the most forage in Williston and Dinosaur reservoirs.

The main producers of chlorophyll-a in the Peace River were algae. Periphyton community structures varied seasonally and annually, where fall was always more productive than spring. In riverine areas, key factors that influenced periphyton abundance, biovolume, and chlorophyll-a were substrate submergence and available light, as influenced by turbidity and water depth. These factors were influenced by timing and magnitude of managed flows and by tributary inputs.

Riverine benthic invertebrate community structure was mostly influenced by substrate submergence, as well as annual, seasonal, and site variability. In response to life cycle and seasonal flows, cold summer freshet flows allowed more oligochaetes and chironomid biomass, while stable warmer fall flows permitted greater benthic invertebrate biomass, with proportionately more EPT abundance.

When Site C Reach PR sites are considered, PR1 and PR2 located immediately downstream of Dinosaur Reservoir had the most available light to the substrates and low turbidity that together allowed the greatest in situ productivity. Added to this, PR1 and PR2 experienced greater settlement of reservoir taxa and Didymo proliferation. It is reasonable to expect a similar habitat to develop below Site C Reservoir.

Benthic productivity in Site C Reach PR sites had moderate invertebrate biomass compared to downstream PD1-PD3 sites. Chironomids and oligochaetes were the most abundant invertebrates in Site C reach summer rock basket samples, while high annual variation in the percent abundance of EPT, hydrozoans, chironomids and oligochaetes occurred in fall samples.

The Peace River downstream of the Project is a bar/pool system where turbidity typically exceeds 5 to 10 NTU. A shallow photic zone occurred under the existing turbidity regime that contracted further during freshet and summer storms, particularly at sites affected by tributaries. Numerical modelling of light data confirmed that turbidity strongly restricted light penetration to the riverbed. Available light at submerged substrates controlled periphyton production.

The Downstream reach sites (PD1-PD3) had high light and velocity regimes, and showed summer invertebrate communities dominated by chironomids and oligochaetes. Annual variability in percent Ephemeroptera, Plecoptera, Trichoptera (EPT) was observed in the fall sampling sessions at PD1-PD3, where Fall 2012 and 2018 had higher EPT abundances compared to Fall 2011 and 2017 when higher percent abundances of chironomids and oligochaetes occurred. Further investigation with the Random Forest statistical model showed PD1 and PD3 had higher invertebrate biomass and higher EPT+Dipterans biomass compared to the PR and other PD sites. The furthest downstream sites PD4 was warmer, more turbid and had lower benthic productivity than the upstream Peace River sites.

Of the benthic invertebrates found in the Peace River, EPT and Dipterans were important forage for fish, consisting of at least 75% of the taxa sampled from the stomachs of Arctic Grayling, Mountain Whitefish, and Rainbow Trout. Oligochaetes were abundant in rock basket samples but were rarely utilized. Invertebrates that often enter the drift (e.g., Ephemeropteran Baetidae and Corixidae) were preferred by Rainbow Trout and Arctic



Grayling, while Chironomids and Glossosomatidae are less likely to drift and were utilized by the bottom feeding Mountain Whitefish. The fish stomach contents demonstrated different feeding styles.

To address the questions of Mon-17 (and Mon-6 / Mon-7 total productivity estimates), a reach-wide productivity model was developed in 2018. It considers the timing and magnitude of flow fluctuations and key physical habitat parameters that influence periphyton and invertebrate growth to provide reach-wide estimates of fish food biomass. Please refer to the Mon-17 Technical Memo for this work (Schleppe et al. 2019).



TABLE OF CONTENTS

1.0	INTRODUCTION.....	13
1.1	Mon-6 Management Questions	15
1.2	Mon-7 Management Questions	15
1.3	Mon-17 Management Questions	15
2.0	METHODS	17
2.1	Study Area and Sampling Locations.....	17
2.2	Site-level Water Elevation	22
2.3	Productivity Sampling Program Overview.....	22
2.3.1	Artificial Sampling Design, Deployment, and Retrieval.....	23
2.3.2	Mon-6 and Mon-7 Sampling Program Summary	26
2.3.3	Physical Habitat Parameters.....	27
2.3.4	Periphyton and Invertebrate Post Processing	28
2.4	Statistical Procedures.....	29
2.4.1	River and Reservoir Water Elevations.....	29
2.4.2	River and Reservoir Water Levels.....	30
2.4.1	Light Availability	30
2.4.1	Periphyton and Invertebrate Community Responses	31
2.4.2	Periphyton and Invertebrate Productivity Responses	32
2.4.3	Fish Stomach Contents.....	37
2.4.4	Zooplankton and Phytoplankton.....	37
2.5	Assumptions.....	37
3.0	RESULTS	39
3.1	River and Reservoir Water Elevations	39
3.2	Reservoir Physical Habitat Parameters	39
3.3	Reservoir Primary Productivity	41
3.4	Reservoir Zooplankton	42
3.5	Reservoir Periphyton	43
3.6	Reservoir Invertebrates	43
3.7	Periphyton and Invertebrate Community Structure	44
3.7.1	Periphyton.....	44
3.7.2	Invertebrates.....	45
3.8	River Physical Habitat Parameters	51
3.8.1	Depth	51
3.8.2	Light.....	51
3.8.3	Turbidity.....	53
3.8.4	Temperature	54
3.9	Riverine Periphyton and Invertebrate Productivity	54
3.9.1	Periphyton River Productivity	55
3.9.2	Rock Basket River Samples.....	58
3.10	Riverine Zooplankton.....	61
3.11	Fish Stomachs.....	61
4.0	DISCUSSION	63
4.1	Reservoir (Mon-6)	63
4.1.1	Physical Parameters	63
4.1.2	Reservoir Phytoplankton	64
4.1.3	Reservoir Zooplankton	65
4.1.4	Reservoir Periphyton	65



4.1.5	Reservoir Invertebrates.....	66
4.2	River (Mon-7)	66
4.2.1	Physical Habitat Parameters.....	66
4.2.1	River Phytoplankton.....	66
4.2.2	River Periphyton	67
4.2.3	Invertebrates.....	69
5.0	REFERENCES.....	72



FIGURES

Figure 1-1:	Conceptual model of fish food organism responses to habitat change associated with construction of Site C.....	14
Figure 2-1:	Map of the Peace River study area and sampling locations.	20
Figure 2-2:	Map of the Peace River tributaries and sampling locations.	21
Figure 2-2:	The typical deployment (left) of the sampling apparatus (right) used.....	25
Figure 3-1:	The relationship between the diffuse percentage of light transmission depth, under varying turbidity conditions. Dotted lines represented 95% Confidence Limits (CLs).....	53
Figure 3-2:	Average daily turbidity (FNU) at each downstream site in the Peace River over the duration of deployment in 2018.	54
Figure 3-3:	Relative abundance of Diptera, Ephemeroptera, Plecoptera, and Trichoptera in Arctic Grayling (GR), Mountain Whitefish (MW), and Rainbow Trout (RB).	62



TABLES

Table 2-1:	Mon-6 monitoring stations, sample types, UTM coordinates, and site description.	18
Table 2-2:	Mon-7 Monitoring Stations, Sample Types, UTM Coordinates and Site Description.....	19
Table 2-3:	Naming Convention of Sampling Depths and Corresponding Depth Strata	23
Table 2-4:	Summary of lost samplers and delayed sampler retrieval during summer 2018 deployment.	24
Table 2-5:	Artificial Sampler Deployment and Recovery Rates in 2018.....	26
Table 2-6:	River Elevation Stations Graphed on the Peace River	29
Table 2-7:	Explanatory Variables for for both Periphyton and Benthic Invertebrates,	32
Table 2-9:	Responses for Periphyton, bolded variables were used in mixed effects and random forest models.	36
Table 2-10:	Responses for Benthic Invertebrates, bolded variables were used in mixed effects and random forest models.	37
Table 3-1:	Reservoir / Lake Classification by Trophic Status.....	41
Table 3-2:	Summary of invertebrate taxa richness, percent EPT (abundance and biomass) for Site C reach invertebrate rock basket samplers 2010-2012 and 2017-2018....	47
Table 3-3:	Summary of invertebrate taxa richness, percent EPT (abundance and biomass) for Downstream reach invertebrate rock basket samplers 2010-2012 and 2017-2018.....	49
Table 4-1:	Riverine Periphyton Comparison.....	68



APPENDICES

APPENDIX A	DETAILED SITE MAPS	81
APPENDIX B	DETAILED SAMPLING METHODS	93
APPENDIX C	RESERVOIR STATION ELEVATION PLOTS	96
APPENDIX D	RIVER STATION ELEVATION PLOTS	98
APPENDIX E	SITE DEPTH PLOTS.....	105
APPENDIX F	SITE LIGHT PLOTS	110
APPENDIX G	RESERVOIR AND RIVERINE PAR PROFILES	115
APPENDIX H	RESERVOIR MULTIMETER TEMPERATURE / TURBIDITY PROFILES 126	
APPENDIX I	FORT ST. JOHN WEATHER RESULTS	131
APPENDIX J	LIGHT MODEL RESULTS.....	132
APPENDIX K	TEMPERATURE PLOTS.....	146
APPENDIX L	PHYTOPLANKTON SUMMARY STATS	151
APPENDIX M	PERIPHYTON RESPONSE SUMMARY STATS	152
APPENDIX N	PERIPHYTON BROAD GROUP SUMMARY STAS	163
APPENDIX O	PERIPHYTON ECOLOGICAL-GUILD SUMMARY STATS.....	172
APPENDIX P	PERIPHYTON SHALLOW WATER STRIP PRODUCTIVITY RESULTS AND CORRELATIONS.....	176
APPENDIX Q	RESERVOIR ZOOPLANKTON SUMMARY	177
APPENDIX R	INVERTEBRATE RESPONSE SUMMARY STATS.....	179
APPENDIX S	PERIPHYTON COMMUNITY ANALYSIS USING NMDS	198
APPENDIX T	INVERTEBRATE COMMUNITY ANALYSIS FROM ROCK BASKETS USING NMDS	200
APPENDIX U	INVERTEBRATE COMMUNITY ANALYSIS IN ECKMAN DREDGE USING NMDS INVERTEBRATE RESULTS.....	202
APPENDIX V	EKMAN SAMPLES INVERTEBRATE DOMINANT TAXA BY FAMILY 204	
APPENDIX W	RESERVOIR PERIPHYTON MODEL RESULTS	210
APPENDIX X	RESERVOIR INVERTEBRATE ROCK BASKET PRODUCTIVITY MODEL RESULTS.....	216
APPENDIX Y	PERIPHYTON 2010-2011 AND 2017-2018 RIVERINE SITES DREDGE RESULTS.....	222
APPENDIX Z	RIVER PERIPHYTON FULL TRANSECT MODEL RESULTS.....	225
APPENDIX AA	RIVER PERIPHYTON FULLY SUBMERGED SITES MODEL RESULTS 232	
APPENDIX BB	RIVER PERIPHYTON RANDOM FOREST RESULTS	238
APPENDIX CC	INVERTEBRATE 2010-2011 AND 2017-2018 RIVERINE SITES DREDGE RESULTS	242
APPENDIX DD	RIVER MODEL INVERTEBRATE RESULTS FOR MOSTLY SUBMERGED ROCK BASKETS.....	245
APPENDIX EE	RIVER MODEL RESULTS FOR ALL ROCK BASKETS	252
APPENDIX FF	RIVER BENTHIC INVERTEBRATES RANDOM FOREST RESULTS 258	
APPENDIX GG	FISH STOMACH NMDS ANALYSIS AND PERCENT ABUNDANCE 262	
APPENDIX HH	INVERTEBRATE TAXONOMIC METHODS.....	268



1.0 INTRODUCTION

BC Hydro developed the Site C Fisheries and Aquatic Habitat Monitoring and Follow-up Program (FAHMFP) in accordance with Provincial Environmental Assessment Certificate Condition No. 7 and Federal Decision Statement Condition Nos. 8.4.3 and 8.4.4 for BC Hydro's Site C Clean Energy Project. The Site C Reservoir Fish Food Organisms (Mon-6) and Peace River Fish Food Organisms (Mon-7) Monitoring Programs represent two components of the FAHMFP that monitor the factors affecting periphyton and benthic invertebrates, which contribute food for fish. This study builds on monitoring completed since 2010 using compatible methods and sample sites. Sampling in 2018 marked the second year of monitoring since the Project construction began in 2015, and the fifth year of baseline data prior to river diversion in fall 2020 and reservoir filling in fall 2023. This report covers the Mon-6 and Mon-7 results to date, using comparison of 2010-2012 with 2017-2018 data.

The transformation of the Site C reach of the Peace River into an approximately 50 m deep reservoir will create a new aquatic environment that is expected to support a community of equal or greater productivity than the existing riverine ecosystem (BC Hydro EIS 2013). These expectations are based on prior research in the upstream Williston and Dinosaur Reservoirs. The Site C Clean Energy Project (the Project) will result in a loss of 29.6 km² of lotic habitat in the mainstem and the lower reaches of tributaries, a gain of 9.4 km² of littoral habitat, and a gain of 83.6 km² of pelagic habitat, for a net gain of 63.4 km² of aquatic habitat.

In addition to the altered hydraulic conditions, the major physical changes to the aquatic ecosystem will include increased habitat volume, altered water chemistry, a reduction in diversity of the types of habitat available for fish and aquatic organisms, and changes to thermal regimes (BC Hydro EIS 2013). With moderate alkalinity, neutral to slightly basic pH, and moderate metal concentrations in the Peace River, available light and bio-available nutrients will be important drivers of productivity. The newly flooded reservoir will likely experience trophic upsurge that will taper off after an estimated 10 years, followed by trophic depression. The daily range in Site C Reservoir levels is expected to be 0.6 m with occasional fluctuations of >1.2 m. Littoral drawdown and turbidity from shoreline erosion will limit periphyton, aquatic macrophyte, and benthic invertebrate productivity in portions of the reservoir and likely result in pelagic-based phytoplankton and profundal food webs dominated by chironomids, oligochaetes, and zooplankton (BC Hydro EIS 2013).

The Halfway River flows into the Site C Reservoir approximately 46 km downstream of Peace Canyon Dam, while the smaller Moberly River flows into the Peace River less than 1 km upstream of the Project. These inflows can contribute higher concentrations of total phosphorus to the Peace River in summer compared to all other tributaries, which only contribute total phosphorus during freshet and stormflows. Except for the shallow 20 km downstream of Peace Canyon Dam, the Site C Reservoir is expected to develop a dimictic thermal structure, with maximum summer water surface temperatures of 16-21°C and bottom water temperatures ranging from only 9-11°C. The outlet of the Site C Reservoir will span depths between ~3 and 21 m, blending warm and cool water during summer stratified conditions (BC Hydro 2013).

Various hydrochemical changes are expected to occur in the Peace River downstream of the Project after reservoir filling. A smaller daily temperature range is expected, where outflows will be warmer than existing conditions from July to January and cooler from March to June. Also, the anticipated lower suspended sediment loads and turbidity, moderation of

flows, and reduced bed material mobility are expected to reduce the active channel width of the Peace River.

The minimum outflow requirement of the Project is 390 m³/s, with maximum discharges occurring during daylight hours. The range of operational releases will increase from 1,699 m³/s to ~2,130 m³/s with the Project. Consequently, the daily range of water levels is predicted to increase from 0.5 to 1.0 m in the dam tailrace, from 0.4 to 0.8 m near Taylor BC, and from 0.5 to 0.9 m near the Alces River confluence (BC Hydro 2013).

Baseline monitoring for Mon-6 and 7 was conducted in 2010 through 2012. Datasets from these years were combined with the 2017 and 2018 dataset and analysed for this report.

This report is organized by reservoir and riverine sites. Mon-6 and Mon-7 management questions are still considered separately. For Mon-17, a preliminary reach wide productivity model was generated and has been presented as a technical memorandum under separate cover. A conceptual model that describes key influences of flow alterations on physical processes is presented in Figure 1-1.

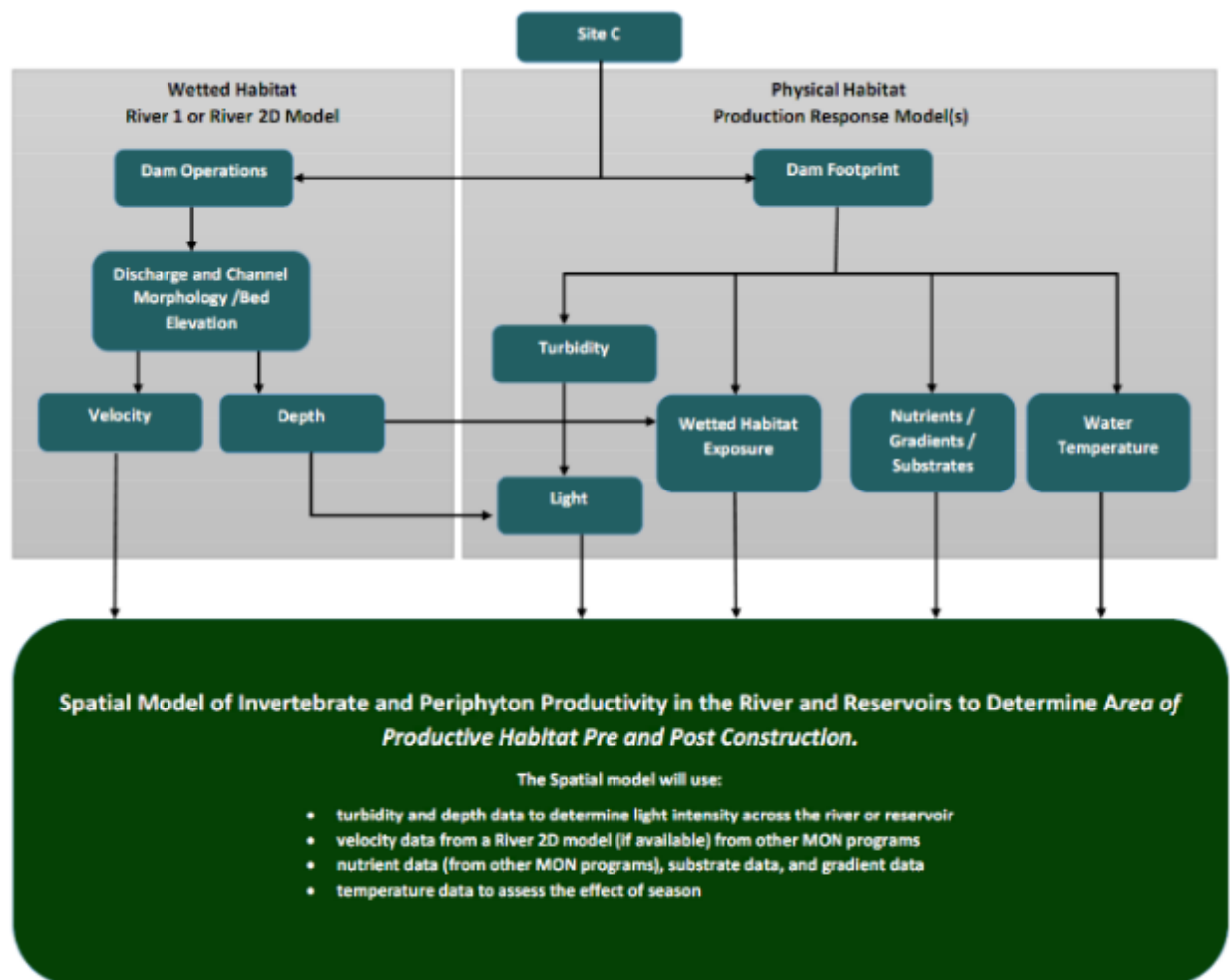


Figure 1-1: Conceptual model of fish food organism responses to habitat change associated with construction of Site C.

1.1 Mon-6 Management Questions

The purposes of the Mon-6 monitoring program is to: 1) understand and compare biomass and production of food for fish as well as the underlying processes that support benthos productivity in the Site C reach, pre- and post-flooding, and 2) to compare the Site C reach to reference sites in Williston and Dinosaur Reservoirs using a classic BACI design. The Mon-6 management questions are as follows:

- 1) What is the change in areal biomass (mass/m²) and reach-wide biomass (mass-km²/yr) of fish food organisms in the Site C reach between years before and after construction of the Project?
- 2) What is the change in production of fish food organisms in the Site C reach between years before and after construction of the Project?

The following are the management hypotheses for Mon-6:

H₁: Reach-wide biomass of invertebrates in the Site C reach will be the same between years before and after reservoir formation.

H₂: The production of fish food organisms in the Site C reach will be the same between years before and after reservoir formation.

1.2 Mon-7 Management Questions

The purpose of the Mon-7 monitoring program is to investigate the effects of dam construction and operations on the biomass and production of periphyton and invertebrate fish food organisms downstream of the Project Site to Many Islands in Alberta. The Mon-7 management questions are as follows:

- 1) What is the change in areal biomass of fish food organisms in the Peace River between years, before, during, and after construction of the Project?
- 2) What is the change in production of fish food organisms in the Peace River between years before, during, and after construction of the Project?

The following are the management hypotheses for Mon-7:

H₁: Reach-wide biomass of invertebrates in the Peace River between the Project and the Many Islands area in Alberta will remain the same over time before, during, and after the construction of the Project.

H₂: The production of fish food organisms in the Peace River between the Project and the Many Islands area in Alberta will remain the same over time before, during, and after the development of the Project.

1.3 Mon-17 Management Questions

This monitoring program investigates the effects of the timing and magnitude of water level fluctuations on benthos biomass and production from the Project to Many Islands in Alberta. The benthos components of the work program are intended to provide insight into the causal links between Project-related hydrological changes and any potential changes in productivity. Mon-17 utilized data from all relevant components of the Site C Fisheries and Aquatic Habitat Monitoring Follow-up Program (FAHMFP), and relied heavily on data

collected in Mon-6 and Mon-7 (this report), as well as other projects undertaken by BC Hydro such as CLBMON15b (Schleppe and Larratt 2016).

The Mon-17 management questions are as follows:

- 1) How do changes in the hydrologic regime affect estimates of catchability used in the Peace River Fish Community Monitoring Program (Mon-2)?
- 2) How do changes in the hydrological regime affect fish and fish habitat of the Peace River?

The following are the specific sub hypotheses to be addressed by this monitoring program:

H₂: Periphyton production among and within sites in the Peace River is independent of the magnitude and timing of flow fluctuations.

H₃: Biomass of invertebrates (benthos) among and within sites in the Peace River is independent of the magnitude and timing of flow fluctuations.

To help with Mon-17 management questions, a preliminary reach-wide productivity model (RWPM) that considered the timing and magnitude of flow regulation was prepared. The RWPM considered key physical processes identified in data collected in Mon-6 and Mon-7. The preliminary RWPM is presented in a technical memorandum (Schleppe et al. 2019).

2.0 METHODS

2.1 Study Area and Sampling Locations

The study area is in northeastern British Columbia on the Peace River, extending from the Williston Reservoir to immediately upstream of Many Islands, Alberta. There are several prominent tributaries including the Moberly and Halfway Rivers in the future Site C Reservoir footprint, and the Pine and Beaton Rivers downstream of the future reservoir (Figure 2-2). The study area is divided into three general areas: 1) Upstream control reservoirs including Williston and Dinosaur Reservoirs; 2) Site C reach from Peace Canyon Dam to the Project, and 3) Downstream of the Project to immediately upstream of Many Islands on the Peace River in Alberta. Table 2-1 and Table 2-2 provide the locations of the sites sampled in 2018 and Figure 2-1 provides a map of the general site locations. Detailed site maps are found in Appendix A.

Williston Reservoir is a large hydro reservoir with 2.2 years residence time that discharges at depth to Dinosaur Reservoir with only <5 days residence time. Dinosaur Reservoir discharges at depth to the current PR sites on the Peace River that will become Site C Reservoir. Site C reservoir will discharge to the Peace River PD sites (Figure 2-1; Figure 2-2).

Table 2-1: Mon-6 monitoring stations, sample types, UTM coordinates, and site description.

Site Name & Site Code	Pre Reservoir Sampling	Post Reservoir Sampling	UTM Coordinates (UTM 10)		Description
			Easting	Northing	
Williston (W1)	Pelagic	Pelagic	175783	6221552	Reference reservoir site
Dinosaur (D1)	Pelagic and Littoral	Pelagic and Littoral	187708	6214364	Reference reservoir site
Upper Site C Reservoir (PR1)	Lotic	Pelagic and Littoral	192170	6218363	Near the community of Hudson's Hope
Middle Site C Reservoir (PR2)	Lotic	Pelagic and Littoral	222732	6237370	Upstream of the Halfway River confluence
Lower Site C Reservoir (PR3)	Lotic	Pelagic and Littoral	255937	6236428	Upstream of the Moberly confluence
Halfway River Downstream (HD)	Lotic	Pelagic and Littoral	224666	6239272	After reservoir creation, this site will monitor water quality in the reservoir embayment created by the inundation of the Halfway River
Moberly River Downstream (MD)	Lotic	Pelagic and Littoral	256420	6235153	After reservoir creation, this site will monitor water quality in the reservoir embayment created by the inundation of the Moberly River

Table 2-2: Mon-7 Monitoring Stations, Sample Types, UTM Coordinates and Site Description.

Site Name & Site Code	Sampling Type	UTM Coordinates (UTM 10 and 11)		Description
		Easting	Northing	
Peace River Immediately Upstream of the Pine River (PD1)	Periphyton and Invertebrate Production	267672	6230284	Peace River upstream of the Pine River confluence on the left bank
Peace River immediately upstream of the Beatton River (PD2)	Periphyton and Invertebrate Production	288776	6222437	Peace River upstream of Beatton River on the left bank
Peace River immediately upstream of the Kiskatina River (PD3)	Benthic Drift	299341	6221976	Peace River upstream of the Kiskatina River on the right bank
Peace River immediately upstream of the Pouce Coupe River (PD4) ¹	Benthic Drift	317989	6225175	Peace River upstream of the Pouce Coupe River ¹ on the left bank
Peace River at Many Islands (PD5) ¹	Benthic Drift	364653	6242006	Upstream of the Moberly confluence ¹ on the left bank

1. 2017 was the first year these sites were sampled; both sites are in UTM 11.

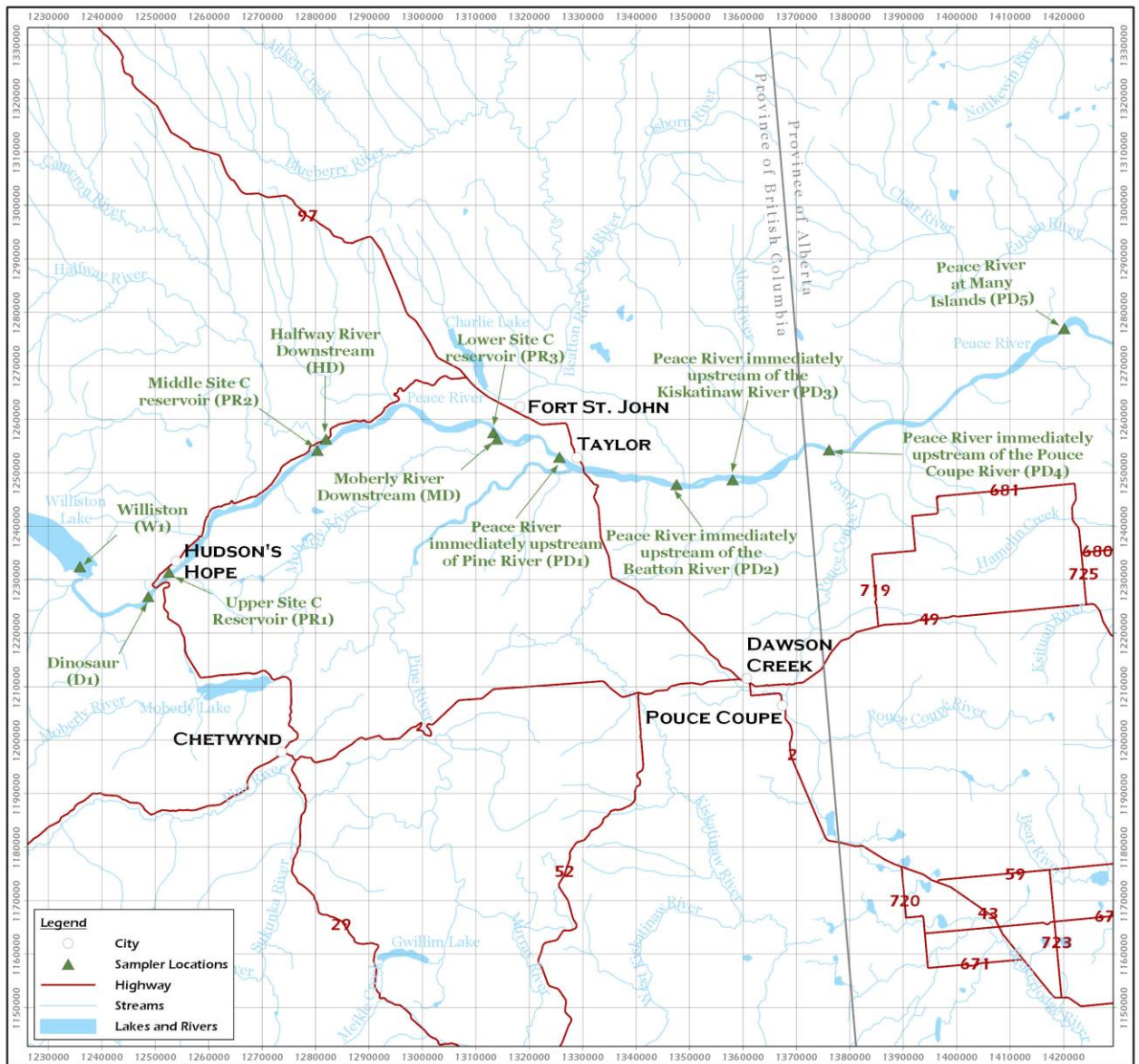


Figure 2-1: Map of the Peace River study area and sampling locations.

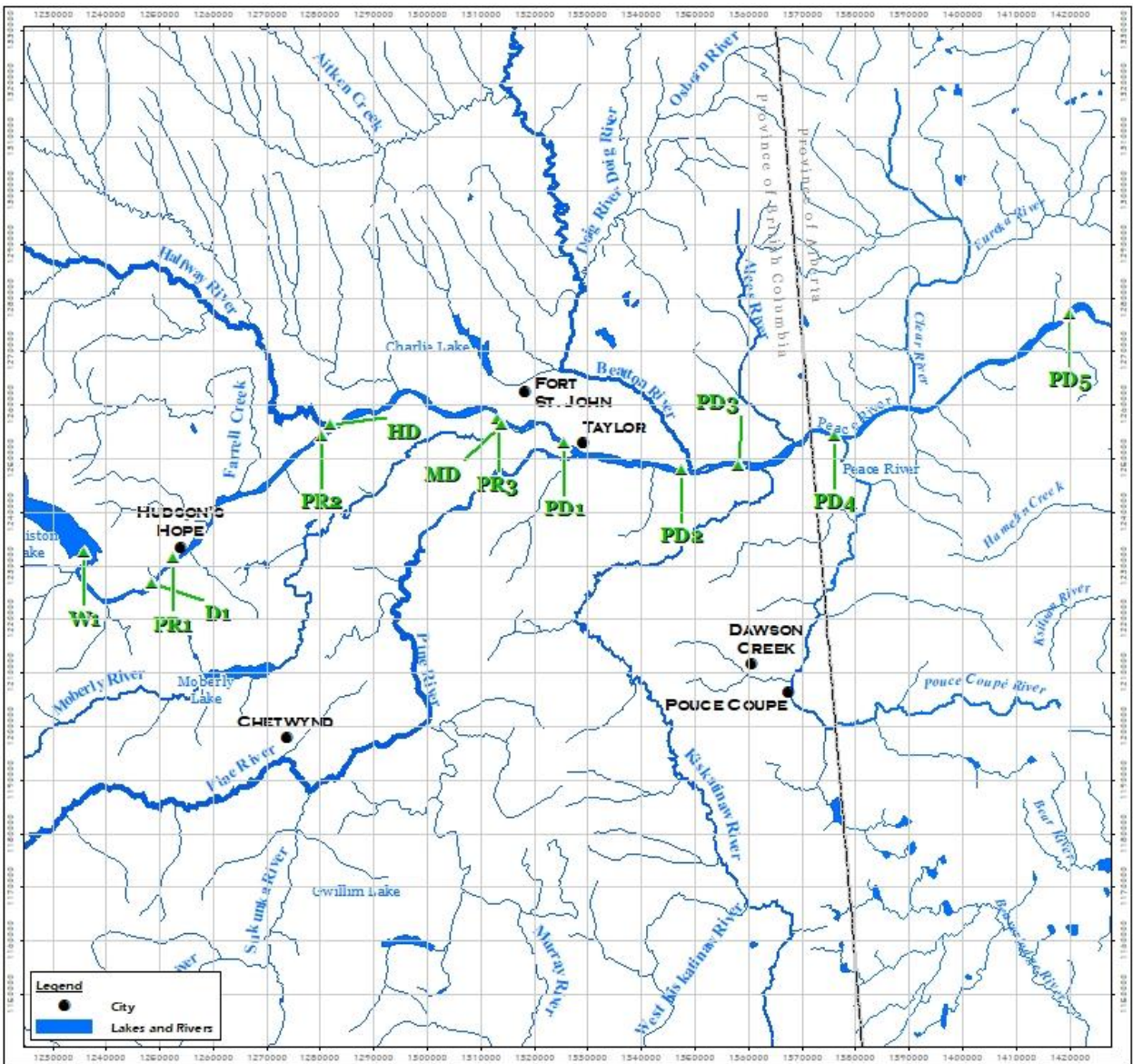


Figure 2-2: Map of the Peace River tributaries and sampling locations.

2.2 Site-level Water Elevation

River channel and bathymetric surveys were completed for each site. The upstream and downstream survey limits were set in the field to encompass the predetermined sampler placement and provide a detailed three-dimensional spatial understanding of the river channel.

The water surface profile, river banks, and bathymetric survey were completed using a real-time kinematic (RTK) survey instrument paired with a bathymetric sounder. Vertical and horizontal precisions were ± 0.02 m. This information was fundamental in understanding the relative position of each sampler in the river channel and their wetted depths over the deployment period (Appendix E).

With the primary setline anchored in place, the boat was positioned over the target sampler depth and the sampler was deployed. After deployment, the depth and location of each of the five samplers (along the setline) were surveyed using the RTK and sounder. A water level data logger (Onset® Hobo U20; Bourne, MA, USA) was securely fastened to the mid-depth sampler (permanently wetted - upper zone). The logger was configured to provide hourly water levels for the mid-depth sampler.

Hourly water depths were calculated from a combination of the bathymetric data, the hourly water levels at the mid-depth sampler, and the water depths recorded at deployment. Water levels at each site were plotted over the duration of the deployment period to understand the head of water above each sampler over time. The average depth at each transect sample was also considered to understand the submergence pattern at each site.

2.3 Productivity Sampling Program Overview

Productivity sampling was conducted using standard sampling methods for phytoplankton, zooplankton, periphyton, and benthic invertebrates. Detailed field methods for each technique are in Appendix B.

Plankton hauls/tows were conducted once a month from June through October 2018 to sample zooplankton and phytoplankton in the littoral and pelagic regions of Dinosaur Reservoir (D1) and a pelagic region in Williston Reservoir (W1). This method was also adapted to sample each of the Site C reach river monitoring sites to understand production associated with drift.

Periphyton growth was measured during two seasons in the Peace River and Dinosaur Reservoir using an artificial substrate (open-cell Styrofoam) that was deployed for 49 to 58 days in a transect with five samplers at different depths (Table 2-1 and Table 2-3). Each periphyton artificial substrate was mounted with a HOBO Pendant temperature/light logger that collected data every 30 min throughout each deployment session.

Benthic invertebrate community metrics and biomass was determined using artificial sampling substrates (rock baskets). Invertebrate samplers were placed at each of the sampling sites, with samplers in a transect that spanned the wetted depth range of the river (Table 2-3) or reservoir in the summer and fall field seasons (Table 2-1 and Table 2-4).

The periphyton and invertebrate artificial substrates were deployed across transects to sample different depths, from the upper varial zone to deeper river areas greater than 2 m (Table 2-2, Table 2-3). At each site, the depth of the samplers was collected using a HOBO level logger placed on the middle sampler of the transect. A bathymetric survey was used

to determine the water depth at each sampler and estimate the depth of each sampler in the transect over the duration of deployment. A sediment trap was also deployed at each river site with a level logger sensor. Continuous turbidity meters (YSI EXO5 w/ wiper) with hourly sampling intervals were also deployed at each downstream river site (PD1 through PD5).

Table 2-3: Naming Convention of Sampling Depths and Corresponding Depth Strata

Depth Label	Depth (alpha / numeric)	Depth Strata (m)	Periphyton (P) / Invertebrate Sample (B)
Upper Varial Zone	UV / (0)	0.3 – 0.8	P
Lower Varial Zone	LV / (1)	0.9 – 1.5	P / B
Permanent Wetted	PW / (2)	1.3 – 1.8	P / B
Upper Photic Zone	PM / (3)	1.5 – 2.6	P / B
Mid Photic Zone	PD / (4)	2.0 – 4.8	P / B

In addition to the artificial sampler, four samples from depositional areas in Dinosaur Reservoir (D1) and the Site C reach sites (PR1-PR3, HD, and MD) were collected using an Ekman dredge. Ekman dredges (species-level taxonomy and 200 µm mesh sieves) sample different benthic invertebrate communities than rock baskets, likely due to large differences in substrate size between the baskets and surrounding natural substrates (Beak 1995). Using both sampling techniques allowed comparison of the erosional and depositional habitat types pre- and post-flooding of the reservoir.

2.3.1 Artificial Sampling Design, Deployment, and Retrieval

In 2018, a single artificial sampler apparatus design was used for the summer and fall periods (Figure 2-3). All summer samplers were deployed from June 8 to August 1. Except for the sites/transects that were not retrieved after the usual summer deployment (Table 2-5), the fall samplers were deployed from August 1 to September 21. Artificial substrates were placed from depths of 0 m (partially exposed at some flows; photo-inhibition can occur) to 2.8 – 4.8 m (beyond expected limit of the riverine photic zone).

Table 2-4: Summary of lost samplers and delayed sampler retrieval during summer 2018 deployment.

Site	Transect Not Retrieved	Transects retrieved August 23 & 24
HD	T0 - T4	** none retrieved and no replacements deployed
MD	T1 - T4	
PR1	T4	T4
PD2	T2 - T4	T2
PD3	T1 - T4	T1 to T4
PD4	T4	
PD5	T2 - T4	T2

High flows and large sediment deposits prevented the retrieval of some samplers during the initial summer retrieval (July 29 to August 1), but there were some successful follow up attempts to retrieve samplers on August 23 and 24 (Table 2-4). The seven samples that were retrieved on August 23 and 24 had a longer deployment period of 75-76 days compared to previous summer deployments periods that were 44-63 days. For all samplers not retrieved on the first attempt (26% of total), replacements were deployed between August 23 and October 10, resulting in a similar duration (~50 days) but a different period than previous fall samples. No samplers were retrieved in the summer or redeployed at HD in the fall due to instability at the site. For specific deployment periods by sampler, see Appendix F.

After approximately seven to eight weeks of deployment, three periphyton Styrofoam punches were randomly collected from each sampler to assess the following metrics: 1) chlorophyll-a to give an estimate of only live autotrophic biomass; and 2) taxa and biovolume to give an accurate estimate of both live and dead cells. Styrofoam punches were placed in pre-labeled vials and stored on ice until further processing.

Benthic invertebrate baskets were retrieved following a similar protocol to the one described in Perrin and Chapman (2010). A 250 µm mesh net was placed beneath baskets while still in the water column to collect any invertebrates that could have been lost as baskets were lifted from the water. The net was inverted and any contents were rinsed into a labeled bucket with pre-filtered river water. The retrieved baskets were also placed in the labeled buckets until further field processing.

Individual rocks from each basket were scrubbed with a soft brush to release clinging invertebrates. Washed rocks were then rinsed in the sample water prior to being placed back in the basket and stored for re-use. The contents from each bucket were captured using a 250µm sieve, placed in pre-labeled containers, and fixed in an 80% ethanol solution.

Deployment at each site began with the establishment of a primary setline (Figure 2-3). A double anchor, with setline attached, was deployed in the river channel at the deepest point. The setline was then payed out and drawn shoreward and connected to a shore pin downgradient from the anchor point. The boat was then positioned on the setline and tie-in loops were established at the 5 target sampler depths along the gradient from shallow to deep. A 15 metre rope was connected, using a carabiner, to each tie-in along the setline and the sampler apparatus' were connected to the downstream ends and deployed at the target depth.

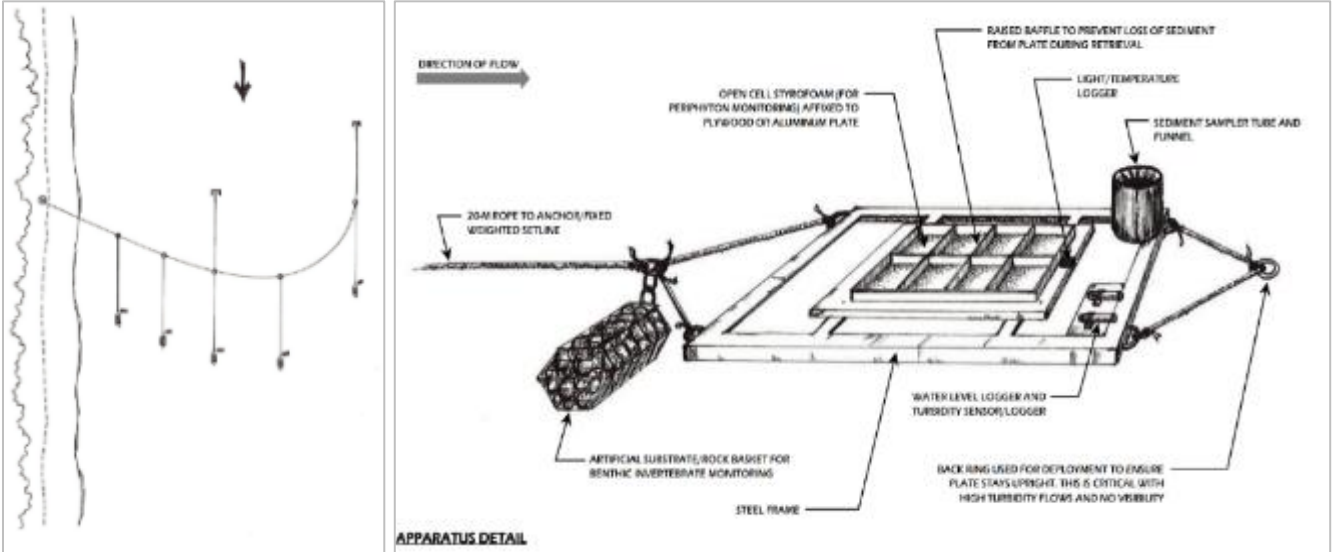


**Figure 2-3: The typical deployment (left) of the sampling apparatus (right) used.
Sampler designed by Ecoscape and illustrated by K. Hawes of Ecoscape**

2.3.2 Mon-6 and Mon-7 Sampling Program Summary

Table 2-5 summarizes the samplers deployed and retrieved for periphyton and benthic invertebrates to sample productivity in Mon-6 and 7 study areas.

Table 2-5: Artificial Sampler Deployment and Recovery Rates in 2018.

Season	Program	Site	Periphyton Samplers	Invertebrate Basket Samplers	Invertebrate Ekman Samplers
			#Retrieved / #Deployed	#Retrieved / #Deployed	# Sampled
Summer (Jun. 8 - Aug. 1) 53 - 76 days	Mon-6	D1	4/5*	5/5	5/5
		HD	0/5	0/4	4/4
		MD	1/5	0/4	4/4
		PR1	5/5	4/4	4/4
		PR2	5/5	4/4	4/4
		PR3	5/5	4/4	4/4
	Mon-7	PD1	5/5	4/4	
		PD2	3/5	2/4	
		PD3	4/5	3/4	0/0 (Not sampled)
		PD4	4/5	3/4	
PD5		3/5	2/4		
Fall (Jul. 31 - Sept 21) 44 - 51 days	Mon-6	D1	5/5	5/5	5/5
		HD	0/0	0/0	4/4
		MD	4/5	3/4	3/4
		PR1	5/5	4/4	4/4
		PR2	5/5	4/4	4/4
		PR3	5/5	4/4	4/4
	Mon-7	PD1	5/5	4/4	
		PD2	5/5	4/4	
		PD3	5/5	4/4	0/0 (Not sampled)
		PD4	5/5	4/4	
PD5		5/5	4/4		

2.3.3 Physical Habitat Parameters

A broader sampling transect was employed in 2017 and 2018 than in previous years to ensure better sampling coverage of the varial zone. Artificial substrates were placed at depths from 0 m (partially exposed at some flows; photo-inhibition can occur) to 2.8 – 4.8 m (beyond expected limit of the riverine photic zone). Key physical habitat conditions measured at the site and samplers are summarized below.

2.3.3.1 Sampler Submergence

Water and air temperature data obtained from the HOBO light/temperature loggers and hourly water depths were used as the primary dataset to determine the duration an artificial sampler was submerged. For 2017 and 2018, submergence or exposure of a sample was determined by using a combination of hourly temperature differences greater than $\pm 0.75^{\circ}\text{C}$, temperature differences greater than 1°C from permanently submerged samplers at the same site, water depths of less than 0.1 m, and high light intensity. Exposure was determined by using the two temperature rules and professional judgement for the 2010 and 2011 data because hourly depth and light was not available.

2.3.3.2 Suspended Sediments and Turbidity

The large suspended sediment load in the Peace River affects both water clarity and sedimentation rates. As sediment load in river water increases, the depth of light penetration decreases, with consequences for photosynthetic organisms. Light attenuates by a factor of four for every 5 m of depth in clean, oligotrophic waters. The depth of light penetration in the Peace River was considered using numerous metrics:

- Secchi depth $Z_{eu} \sim \sqrt{5 Z_s}$ Where Z_{eu} = euphotic zone; Z_s = Secchi depth in meters (Tilzer, 1988)
- Secchi depth x1.7
- 1% of incident light at water surface (standard limit for photosynthesis)
- PAR > 10 photons/m²/sec
- Turbidity (continuous and in situ)

The Secchi depth is reached when the reflectance equals the intensity of light back-scattered from the water.

In contrast to Secchi depth, which is not sensitive to light wavelengths, the light loggers mounted to each sampler plate measured visible light with wavelengths between 400 and 700 nm - the photosynthetically available radiation (PAR) used by phytoplankton for photosynthesis. Metrics using these measurements were used to determine the photic zones. The continuous light measurements from each sampler were compared with the ambient light conditions from a sensor mounted on shore at each site (with full exposure) above the river wetted level. A second light/temperature logger was installed on the mid-depth sampler for PD sites in order to quantify the effect of biofouling/sedimentation and attenuation of light on loggers' overtime. In addition, PAR profiles (ambient and through the water column) were measured to determine the continuous light attenuation coefficient based on in-situ turbidity.

2.3.3.3 Increased Resolution in Maximum Production Band

Data collection and analysis in 2017 identified that only a very narrow productive band existed along the shallow river margin because turbidity resulted in low light penetration. Increased production was identified in this narrow band; however, the standard sampler plates (generally spaced vertically greater than 0.50 m) did not adequately capture where peak production occurred. Therefore, chlorophyll-a samples were taken along a secondary linear Styrofoam strip that was mounted to an elongate metal frame and installed perpendicular to the river bank to span the depth between the standard sampler plates.

2.3.3.4 In-Reservoir Conditions

Dynamics of the reservoir photic zone, water layers, and light intensity were determined using logger lines, PAR meter (400-700 nm) and Tidbits (400-1000 nm). PAR helped define the depth of the photic zone and its lateral extent in the littoral zone, both of which are dynamic – expanding or contracting with changing turbidity and TSS. For example, light penetration of the Williston Reservoir water column was very low in June during freshet, measuring only 122 photons/m²/sec at 0.5 m depth. The Williston Reservoir summer thermocline was determined using multimeter profiles and thermistor data from 2017 and 2018.

2.3.4 Periphyton and Invertebrate Post Processing

2.3.4.1 Periphyton Post Processing

Of the three Styrofoam punches obtained from each artificial substrate, one was frozen and transported to ALS Environmental in Fort St. John, BC for the processing of low-detection limit fluorometric chlorophyll-a (chlorophyll-a) analysis. The remaining two punches were used for taxonomic identification. Fresh, chilled punches were examined for protozoa and other microflora that could not be reliably identified from preserved samples. Larratt Aquatic previously tested Lugol's solution compared to freezing the Styrofoam and determined that freezing provided enhanced long-term viability. Therefore, one of the two punches was frozen and stored until taxonomic identification and biovolume measurements could be undertaken. Species cell density and total biovolume were recorded for each sample. A photographic archive was also compiled. Detailed protocols on periphyton laboratory processing are available from Larratt Aquatic.

In 2017, 10% of randomly selected samples were re-read (QC) to calculate within-sample consistency. In 2018, five randomly selected samples were read from the duplicate punch (QA) to calculate variability among samples drawn from the same site and transect. The mean percent difference for total abundance of the duplicates was 19.0±10.3%. This is a reasonable result and reflects natural variation between samples drawn from the same site. Variations in the data smaller than ~20% may not be relevant.

2.3.4.2 Benthic Invertebrate Post Processing

Following retrieval, fixed benthic invertebrate samples were transported to Cordillera Consulting in Summerland, BC. Samples were sorted and identified to the genus-species level where possible. Benthic invertebrate identification and biomass calculations followed standard procedures. Briefly, field samples had organic portions removed and rough estimates of invertebrate density were calculated to determine if sub-sampling was required.

After samples were sorted, all macroinvertebrates were identified to species and all micro portions were identified following the Standard Taxonomic Effort lists compiled by the Xerces Society for Invertebrate Conservation for the Pacific Northwest (Richards and Rogers 2011). A reference sample was kept for each unique taxon found. A sampling efficiency of 95% was used for benthic invertebrate identification and was determined through independent sampling. Species abundance and biomass were determined for each sample. Digital biomass estimates were completed using standard regression from Benke (1999) for invertebrates and Smock (1980) for Oligochaetes. If samples were large, subsamples were processed following similar methods. Detailed protocols on invertebrate laboratory processing are in Appendix HH.

2.3.4.3 Fish Stomach Contents Post Processing

From August 27 to October 10, 2018, Golder collected fish stomachs by gastric lavage from Arctic Grayling (*Thymallus arcticus*), Mountain Whitefish (*Prosopium williamsoni*) and Rainbow Trout (*Oncorhynchus mykiss*). Detailed methods are described in Golder (2009b). The samples were preserved in 10% formalin and transported to Cordillera Consulting in Summerland, BC. The methods described in Appendix HH were used for benthic invertebrate identification at the family level. However, only invertebrate abundance was calculated.

2.4 Statistical Procedures

All statistical analyses and the creation of most figures were conducted in R (Version 3.5.1, R Development Core Team 2018) or ArcGIS Desktop 10.6 (ESRI, 2018). Statistical analyses were carried out using the comprehensive dataset (2010-2012, 2017-2018). Details related to specific data analysis tasks are provided below.

2.4.1 River and Reservoir Water Elevations

To understand the general hydraulic conditions at the Williston and Dinosaur Reservoirs and each riverine site, plots of the water elevations as well as the study period mean and standard deviation were created for May through October (Appendix D). See Table 2-6 for station (elevation) / site (our assessment) references.

Table 2-6: River Elevation Stations Graphed on the Peace River

Gauge Identifier	River Station Name	Closest Reference Site
07FD010	Peace River above Alces River	PD3
07FD010	Peace River above Alces River	PD4
07FD010	Peace River above Alces River	PD5
07FA004	Peace River above Pine River	PD1
07FA006	Halfway River near Farrell Creek	HD
07FB008	Moberly River near Ft. St. John	MD
07FD002	Peace River near Taylor	PD2

07EF001	Peace River at Hudson Hope	PR1
07EF001	Peace River at Hudson Hope	PR2
07EF001	Peace River at Hudson Hope	PR3

2.4.2 River and Reservoir Water Levels

No specific statistics were performed on river and reservoir water levels. The data from 2018 were, however, visually compared to the mean and standard deviation of all study years to understand how flows may have affected productivity in the study area.

2.4.1 Light Availability

Light availability at the riverbed is expected to strongly influence periphyton productivity in the Peace River. To better understand the effect of light attenuation in the river, light intensity, turbidity, and depth were all modelled using data from PD sites. Model parameters were estimated using Bayesian estimates that were produced using STAN (Carpenter et al. 2017). Refer to McElreath (2016) for additional information on Bayesian estimation.

Unless indicated otherwise, the Bayesian analyses used normal and uniform prior distributions that did not constrain the posterior distribution (Kery and Schaub 2011, 36). The posterior distributions were estimated from 1500 Markov Chain Monte Carlo (MCMC) samples thinned from the second halves of 3 chains (Kery and Schaub 2011, 38–40). Model convergence was confirmed by ensuring that the potential scale reduction factor $\hat{R} \leq 1.05$ (Kery and Schaub 2011, 40) and the effective sample size $ESS \geq 150$ (Brooks et al. 2011) for each of the monitored parameters (Kery and Schaub 2011, 61).

The parameters are summarized in terms of the point estimate, standard deviation (sd), the z-score, lower and upper 95% confidence/credible limits (CLs), and the p-value (Kery and Schaub 2011, 37, 42). The estimate is the median (50th percentile) of the MCMC samples, the z-score is mean/sd and the 95% CLs are the 2.5th and 97.5th percentiles. A p-value of 0.05 indicates that the lower or upper 95% CL crosses 0.

Model adequacy was confirmed by examination of residual plots for the full model(s).

The results were displayed graphically by plotting the modeled relationships between variables and the response(s) with the remaining variables held constant. In general, continuous and discrete fixed variables were held constant at their mean and first level values, respectively, while random variables were held constant at their typical values (expected values of the underlying hyperdistributions) (Kery and Schaub 2011, 77–82). When informative, the influence of variables was expressed in terms of the effect size (i.e., percent change in the response variable) with 95% confidence/credible intervals (CIs, Bradford, Korman, and Higgins 2005).

The analyses were implemented using R version 3.5.1 (R Core Team 2018) and the mbr family of packages.

2.4.1.1 Light Attenuation Model

The attenuation of light with water depth has been well-studied (Julian, Doyle, and Stanley 2008). The following equation captures the relationship between the irradiance at the surface (E_s) and the irradiance at depth (E_d)

$$E_d = E_0 \cdot \exp(-K_d \cdot y)$$

where E_0 is the initial irradiance, E_d is the irradiance at distance y and K_d is the diffuse attenuation coefficient (Julian, Doyle, and Stanley 2008).

Following Davies-Colley and Nagels (2008), the diffuse attenuation coefficient was assumed to vary with turbidity (T) according to the relationship

$$K_d = \exp(K_0 + K_T \cdot \log(T))$$

A K_d of 1 indicates that the light level decreases by 63% for every 1 m increase while a K_d of 2 indicates that the loss is 86% and a K_d of 3 indicates that the loss is 95%.

The above parameters were estimated from the monitored (fixed distance) and spot light readings. Refer to **Error! Reference source not found.** and **Error! Reference source not found.** for the full model description.

Key assumptions of the surface reflectance model include:

- There are no measurement errors in E_0 or T .
- The residual variation in E_d is log-normally distribution.

2.4.1 Periphyton and Invertebrate Community Responses

Non-metric multidimensional scaling (NMDS) was used to explore variation in benthic and periphyton community composition at the genus level. NMDS was conducted with abundance data from 2010 to 2012 and 2017 to 2018. A separate NMDS analysis was run for the benthic invertebrate basket and Ekman samplers. In addition, a family level NMDS for basket samplers was run for benthic invertebrate biomass on data from 2017 and 2018. The Bray-Curtis dissimilarity index was used for both NMDS analyzes. This index is sensitive to the variation of species that have smaller abundances (Clarke and Warwick 1998). To visually explore differences in community compositions, the NMDS scores for every sample from all study years were plotted using the R package ggplot2 (Wickham 2009).

A permutational multivariate analysis of variance (PERMANOVA) was used to determine if there were significant differences in community compositions according to season/year, reach, depth (transect), site, and reach. The amount of variability in community composition explained by each group, defined above, was determined by calculating the partial R^2 from a PERMANOVA. Both NMDS and PERMANOVAs do not make assumptions of the variable distributions and relationships (Anderson 2001; Clarke et al. 2006). The NMDS analysis and PERMANOVA used R package vegan (Oksanen et al. 2017). For both periphyton and invertebrates, the NMDS analysis was performed with rare taxa excluded. Rare taxa were defined as taxa that represented less than 5% of the total abundance of samples. To identify taxonomic differences between samples, taxa were related to the community differences by

fitting them to the ordination plot as factors using Envfit (Oksanen et al. 2017). Only the taxa that were significant ($p < 0.05$) with an R^2 greater than 0.1 were considered.

2.4.2 Periphyton and Invertebrate Productivity Responses

Exploratory analysis of production responses to predictors was completed for raw or log-transformed data using scatterplots for all response-predictor combinations. These plots were completed for summer and fall periods. The graphical representation of data was used as an initial assessment of the relationships between variables; it also helped gauge the applicability of potential explanatory variables prior to their inclusion in modelling of benthic invertebrate and periphyton community composition and productivity. Table 2-7 **Error! Reference source not found.** provides a description of the full suite of explanatory variables that were considered for both periphyton and benthic invertebrate models, where only bolded variables were used in the statistical models. Explanatory variables were selected for inclusion in statistical models based on literature and work from previous years.

Table 2-7: Explanatory Variables for for both Periphyton and Benthic Invertebrates, variables that were used in the mixed effects or random forest models are in bold.

Variable	Definition
Total Exposure Hours	Total time exposed (hrs) or time substrate is out of the water
Daily Average Exposure	The average number of hours spent out of the water each day
Maximum Cumulative Exposure Time	The longest period of continuous time the sampler was exposed.
Total Submergence Time	Total time spent submerged (hrs) in the water
Daily Average Submerged	The average number of hours spent submerged in water during each day
Average Light Intensity	The average daily light intensity over the duration of time deployed, regardless of submergence or exposure
Cumulative Light Intensity while submerged	Sum of the maximum observed light intensity each day over the duration of deployment while submerged
Average Daily Light Intensity while submerged	The average daily light intensity while submerged over the duration of deployment
Total Daytime Submergence	Total time (hrs) spent in the light and water
Total Submergence	Total time (hrs) spent in the water over the duration of deployment
Submergence Ratio	Total time submerged divided by duration of deployment
Mean Water Temperature While Submerged	Average temperature of the water the duration of deployment

Mean Water Temperature during exposure	Average temperature during periods when the sampler was exposed.
Water Velocity	The average velocity of two data points observed collected during either deployment, retrieval, or during sampler maintenance
Average turbidity over deployment	The average turbidity at submerged samplers over the duration of deployment.
Sediment Depositional Rate	The sediment depth measured in the sediment trap (cm/day)
Mean Depth over Deployment	The average depth (m) of the sampler over the duration of deployment
Total Hours over 10 Photons/m²/sec	The total time (hrs) that light intensity exceeded 10 Photons/m ²

A subset of the physical variables described in Table 2-7 were used as explanatory variables for the invertebrate and periphyton production models because they were identified as useful in similar models used for the Lower Columbia River (CLBMON144), Middle Columbia River (CLBMON15-b), and side channels of the Peace River (GMSMON-5). An indirect measure of water depth such as transect has been used as an explanatory variable in periphyton and benthic production models. However, this study was designed to explicitly measure water depth because of the importance of light availability, which is limited by high light attenuation in the turbid waters of the Peace River (Schleppe et al. 2014). Samplers that had a moderate mean depth (0.5-1.0 m) over the deployment period were expected to be the most productive because these samplers received adequate light and were submerged most of the time (Schleppe and Larratt, 2016). The mean water temperature over the deployment period were expected to be positively associated with invertebrate and periphyton production (Schleppe and Larratt, 2016).

Benthic and periphyton production are predicted to decrease with shorter submergence times. Frequent exposure of periphyton and invertebrate samplers results in the death of periphyton and a reduction in invertebrates, especially EPT taxa (Schleppe and Larratt, 2016; Kennedy et al. 2016). The biomass of EPT+D taxa, used as a fish food index, is also expected to change as a result of increased substrate dewatering. Samplers that are frequently dewatered are expected to have a less diverse community with more tolerant taxa such as chironomids and diatoms (Hawes et al. 2014; Plewes et al. 2017).

Light is the primary structuring mechanism for epipelton in lakes of all sizes (Vadeboncouer et al. 2014). The 10 photons/m²/sec light threshold was based on the known light tolerances of periphytic algae (Sigeo 2005). Periphyton productivity metrics are expected to increase with the total hours over 10 photons/m²/sec. This is roughly 2% of full sunlight striking the water surface (<1% is usually accepted as the photosynthetic limit) (Jassby and Platt 1976; Hill and Fanta 2008).

The effect of flow on invertebrate and periphyton production and community composition depends on velocity. Higher velocities cause a decrease in periphyton abundance and filamentous green taxa (Schleppe and Larratt, 2016). Moderate velocities provide ideal habitat for EPT taxa, and as a result, sites with higher velocities are often associated with higher invertebrate biomass and abundance (Schleppe et al. 2013; Hawes et al. 2014).

Deposition is expected to negatively impact local periphyton and invertebrate production metrics (Schleppe et al. 2014) and result in shifts in community composition. Areas that experience high sediment deposition have an invertebrate community with more chironomids and fewer EPT, and periphyton communities with more motile taxa such as myxotrophic flagellated algae (Schleppe et al. 2014).

Response variables for periphyton and benthic invertebrates were calculated to describe production and community composition. In 2018, only response variables that described fish food, benthic invertebrate and periphyton productivity were modelled using mixed effects and random forest models. All periphyton and benthic invertebrates response variables are described in Table 2-8 and Table 2-9. The dominant benthic invertebrate families and periphyton groups were graphically summarized to better understand the productivity of periphyton and benthic invertebrates in the Peace River and Dinosaur Reservoir.

Trait-based periphyton ecological guild analyses were undertaken in 2018 to help explain productivity along the river cross-sections. The method developed by Passy (2007a) and the planktic guild (PG) developed by Rimet & Bouchez (2011, 2012) were employed. We applied the diatom guild descriptions to non-diatom algae. The guild assignment of each taxa is recorded in the periphyton taxonomy table. Based on the literature, we expected: Low profile guild to dominate areas of turbulence, scour, and hydrologic disturbance; High Profile guild to do best in regions with stable flows; Motile guild to do best in silty areas and areas regularly exposed to variable water discharge, and; Planktic guild to do best immediately downstream of reservoir discharges (Passy 2007a; Rimet & Bouchez 2011, 2012; Stenger-Kovács et al. 2013). Use of the guild approach highlights large-scale changes and drivers as opposed to the more nuanced and complex approach of considering each taxa's distribution individually.

We used linear mixed-effects modeling (Zuur et al. 2009) and AICc model selection to evaluate the relative effects of the explanatory variables on each response variable. Methods described by Zuur et al. (2009) were employed to examine multi-collinearity among explanatory variables based on variance inflation factors (VIF) and correlation coefficients; none of the selected explanatory variables had $VIF > 3$. The MuMIn package in R (Barton 2012) was used to generate the model sets, rank them based on $\Delta AICc$ values and AICc weights (w_i), and to calculate multi-model averaged parameter estimates from 95% confidence sets for each response variable (Burnham and Anderson 2001; Grueber et al. 2011). Continuous explanatory variables were standardized to compare among all parameters and interpret the main effects in conjunction with interaction terms; standardization was achieved by subtracting global means from each value (centering) and dividing by two times the SD (scaling) (Gelman 2008; Schielzeth, 2010). We calculated relative variable importance (RVI), which is the sum of AICc weights from all models, that had an $\Delta AICc < 3$, containing the variable of interest with variables having RVI values above 0.55 and confidence intervals that did not span zero.

Mixed effect or linear regression statistical models were used to identify the physical factors (i.e. sediment deposition, velocity, flow fluctuations, light) that influenced the productivity of periphyton and benthic invertebrates in Dinosaur Reservoir, Site C reach, and downstream of the Project. The periphyton productivity metrics that were used as response variables in the statistical models included: Chlorophyll-a, total abundance, and total biovolume. Total abundance and total biomass were the benthic invertebrate productivity response variables used. The sum of biomass of Ephemeroptera/ Plecoptera /Trichoptera + Dipterans EPT+D

was also used as a response variable to serve as an index for the availability of fish food. All the above-mentioned response variables were natural log transformed to reduce heteroscedasticity and to further ensure that models met the assumption of normally distributed residuals. Cook's distance and residual plots were also examined.

A multiple linear regression model was used to model benthic invertebrate basket samplers and periphyton productivity in Dinosaur Reservoir. Regression was used instead of mixed effects models because year, season, and transect as random effects explained <1% variation in productivity metrics. However, the same process used to calculate multi-model averaged parameter estimates and scaling parameters was used for these regression models. The predictor variables of mean depth over deployment and hours of light over 10 photons were correlated. As a result, periphyton models included hours of light over 10 photons as a predictor, whereas benthic invertebrate models included mean depth over deployment as a predictor. Periphyton and benthic invertebrate productivity models from Dinosaur Reservoir included average water temperature while the sampler was submerged and total hours submerged as predictors.

Three different types of periphyton and benthic invertebrate models for the riverine sites were run. The mixed effects models for riverine sites all had a random effect of season:site:year. The first type of model included all 2017 and 2018 samples from the PR and PD sites. The HD and MD sites were not included in the models because of the high number of lost samplers at these sites. The second type of model included 2017 and 2018 samples that were permanently submerged with a submergence ratio of 0.95. Table 2-8 and Table 2-9 indicate the response variables considered. A detailed description of each explanatory variable is included in the methods (**Error! Reference source not found.**). The third type of model included all PR and PD sites from 2010-2011 and 2017-2018. Fall 2012 was not included in the model because temperature loggers were not deployed during this sampling session. There were a limited number of explanatory variables available for the 2010-2011 sampling session. Submergence metrics and average temperature submerged were considered for the invertebrate and periphyton production models for 2010-2011 and 2017-2018. However, linear mixed effects models only included total submergence time because there was limited variability in average temperature submerged between sampling sessions.

The explanatory variables in the full transect and permanently submerged benthic invertebrate models included water velocity, total submergence time, total hours of light over 10 photons, sediment depositional rate, and mean depth over deployment. The number of plausible benthic invertebrate models (those with an AICc<3.0) ranged from four to nine (Appendix DD and Appendix EE).

The explanatory variables in the full transect and permanently submerged periphyton models included water velocity, maximum cumulative hours submerged, hours of light over 10 photons, and sediment depositional rate. The permanently submerged periphyton models included all of the above explanatory variables except for total submergence time. Submergence ratio and average light intensity were also included in the permanently submerged models. The number of plausible periphyton models (those with an AICc<3.0) ranged from 4 to 11 (Appendix Z and Appendix AA).

To better understand threshold effects of physical parameters and interactions on periphyton and benthic invertebrate productivity, Random Forest (RF) models were used. RF models can accommodate categorical predictor variables, multi-collinearity among

predictors, and non-normal distributions (Read et al. 2015). The benthic invertebrate and periphyton RF models used the same productivity metrics as the dredge models. The explanatory variables used for the RF models included water velocity, maximum cumulative hours submerged, hours of light over 10 photons, season, transect, site, and mean depth over deployment. The benthic invertebrate RF models did not include any PR1-4 samplers because these samplers were much deeper than all other samplers.

RF models determine the importance of each predictor variable and the relationships between each predictor variable and response variable. The variable importance measure for each predictor is calculated as the mean decrease in prediction error (Mean Squared Error), if the predictor is dropped from the model (Liaw and Wiener, 2002). Predictor variables that have a strong relationship with the periphyton and invertebrate productivity response variable should have large variable importance. Dropping these predictors from the model causes a large increase in prediction error. Variable importance plots for all predictors included in each model were generated to help identify predictors associated with the productivity variables. Partial dependence plots were generated to better understand the effect of the top four predictors on each water quality variable. These partial dependence plots provide the relationship between the selected predictor and the response variable while considering the effects of the other variables in the RF model (Liaw and Wiener, 2002).

RF is a complex machine-learning algorithm that uses Classification and Regression Tree (CART) models as the base model. CART is a non-parametric tree-based method that splits data into separate groups based on the response variable (De'ath and Fabricus 2000; Jun 2013). CART initially partitions the data into two groups based on a split point and splitting variable that minimizes the sum of squares of the response variable of each group (De'ath and Fabricus 2000; Hastie et al. 2001). A recursive algorithm is used to search through every possible combination of explanatory variables and values to determine the best splitting variable and split point (Hastie et al. 2001). The CART algorithm continues to make binary splits at each tree node until a stopping criterion is reached (Jun, 2013).

RF builds different CART models by bagging, using a subset, the data and the explanatory variables tried at each split. Each CART model uses a random subset of the dataset and at each split in the tree a random subset of predictor variables is tried as a potential splitting variable (Jones and Linder, 2015). The default setting used in the R package randomForest were used for the water quality models (Liaw and Wiener, 2002). The RF models contain 500 trees (CART models) and in our case, two of the predictor variables were tried at each split (Liaw and Wiener, 2002).

Table 2-8: Responses for Periphyton, bolded variables were used in mixed effects and random forest models.

Variable	Description
Total Abundance	Total Abundance across all species
Total Biovolume	Total Biovolume across all species
Chlorophyll-a	Total Chlorophyll-a
Effective Number of Species	A measure of community diversity that is the e^S . S= Shannon-Wiener index.
Percent Motile	The percentage of motile taxa (resilient to deposition)
Percent from Reservoir	The percentage of taxa that originated from upstream lentic reservoir sources (imports)*

Species Richness	A count of the total number of unique species
Good Forage	The biomass of periphyton taxa considered to be good forage for invertebrates based upon cell size, cell structure
Percent High Profile Guild	Taxa of tall stature, including erect, filamentous, branched, chain-forming, tube-forming, stalked, and colonial centrals
Percent Low Profile Guild	Taxa of short stature, including prostrate, adnate, solitary centrals
Percent Motile Guild	Comparatively fast moving taxa, can avoid burial
Percent Planktonic Guild	Taxa originating from upstream lentic sources (imports)

Table 2-9: Responses for Benthic Invertebrates, bolded variables were used in mixed effects and random forest models.

Variable	Description
Total Abundance	Total Abundance across all species
Total Biomass	Total Biomass across all species
Effective Number of Species	A measure of community diversity that is the e^S . S= Shannon-Wiener index.
Percent EPT	The percentage of Ephemeroptera, Plecoptera, and Trichoptera based on biomass
Percent Chironomidae	The percentage of Chironomids based on biomass
Fish Food Biomass (Good Forage)	Calculated by summing the biomasses of Ephemeroptera, Trichoptera and Plecoptera, and Dipteran species, all considered good fish forage

2.4.3 Fish Stomach Contents

Stomach contents of fish sampled under Mon-2, Task 2a of the Site C FAHMFP (Peace River Large Fish Indexing Survey) were analyzed to better inform the testing of the availability of fish food organisms in the Peace River. The relative abundances of consumed fish forage were plotted for Arctic Grayling, Mountain Whitefish, and Rainbow Trout. Fish stomach content data were analyzed at the order level (i.e. EPT and D). NMDS at the family level was used to explore variation in benthic community composition in fish stomach contents collected from the Peace River. The same NMDS methods described in Section 2.4.1 were used for the fish stomach contents. A PERMANOVA was used to determine if there were significant differences in invertebrate community composition according to year, species, or site.

2.4.4 Zooplankton and Phytoplankton

Zooplankton and phytoplankton data for reservoirs were summarized according to dominant taxonomic group. Zooplankton densities for abundance and biomass were summarized and grouped by calanoid copepods, cyclopoid copepods, and Diplostraca, whereas phytoplankton biovolumes and abundances were summarized and grouped by cyanobacteria, diatoms, flagellates, dinoflagellates, and green algae.

2.5 Assumptions

Community losses along the edges of the artificial substrate were assumed to be negligible, as were the effects of edges of the sampler frame and the artificial Styrofoam sampling substrate. While our visual observations of periphyton growth on the samplers support this

assumption, we do not have empirical data to otherwise confirm it. We did not draw samples from the plate perimeters if possible; however, Styrofoam damage over the deployment occasionally necessitated collecting a sample near the edge.

The sampler frame was designed to trap deposited sediments so that we could sample the entire active benthic substrate. We assumed that sampler plates were not disproportionately affected by the retrieval and sample collection processes. It is possible that sampler plates retrieved from deeper areas may have experienced greater losses of sediment despite the baffle system, but this was not considered. Similarly, we assumed that previous sampling years did not have disproportionately greater sediment loss than 2018 due to slight variations in sampler design or retrieval method.

The effects of foraging invertebrates were assumed to be randomly distributed over the artificial substrate within and among sites. We acknowledge that invertebrates may spend more time foraging along the edges of substrata and therefore disproportionately affect productivity along the perimeter of artificial samplers. Therefore, we avoided collecting samples from substrate edges unless no other viable alternative was available. Foraging intensity on Peace River samples is likely a small effect, reducing any potential data-skewing. Further, it is probable that invertebrate distributions around plates were clumped, reducing the potential for effects across multiple replicates.

Our analysis assumed that artificial substrates did not bias results toward a given algal taxa nor did they bias towards those taxa actively immigrating at the time and location of the sampler submergence. Despite this assumption, the data suggests that artificial substrate types and natural substrates do respond differently (Schleppe et al, 2011). Future consideration may be required to accurately relate artificial samplers to natural substrates and determine if artificial substrates are indicative of actual riverine conditions. A direct comparison is currently not feasible.

Sampler assessments were not intended to address immigration, sloughing, or any other temporal aspect of the periphyton or invertebrate community. For invertebrate analyses, this means we have not considered emigration or immigration from within or between sites and that specific operational patterns have not unduly affected any one community by changing densities of invertebrates. Artificial substrate samples that were obviously biased due to sloughing from rock flipping, etc. were excluded from collection. In cases where periphyton artificial substrates were damaged but sufficient material was available for a sample, it was collected and treated the same as other samples. For invertebrates, damaged samplers were not analyzed as they were considered biased due to loss of rock within the basket. These field decisions were easy to make because large boulders rolling over artificial substrates, or those dragged upside down, left distinct trails of compressed Styrofoam or because sampling baskets were broken open. Despite a reduction in the available sample area, we do not suspect that it biased the results. We acknowledge that substrate mobility and periphyton sloughing/drift and invertebrate drift are important components of periphyton and invertebrate production in the Peace River.

Other assumptions for a particular analysis or concern may also be identified in appendices or elsewhere in the text.

3.0 RESULTS

3.1 River and Reservoir Water Elevations

Water elevations on the Peace River at Hudson's Hope (PR1, PR2 & PR3) within the Site C reach in 2018 were lower and less variable than 2010-2012 and 2017, except for high peak flows in August and notable low flows in September (Appendix D, Figure A15). Halfway River peaked (490 m³/s) in late June and was higher than the 2012-2018 normal (Appendix D, Figure A17). Moberly River freshet peaked earlier and higher in 2018 on May 11 (106 m³/s) compared to previous study years, with another peak observed in August (Appendix D, Figure A18). Downstream of the Project, the Peace River (PD1 through PD5) water elevations in 2018 were within the ranges observed over the study period (Appendix D).

Water elevations in Dinosaur Reservoir were consistent with previous study years, ranging between 500.6 and 502.8 masl. Water elevations in Williston Reservoir in 2018 were lower than the 2012-2018 normal, measuring around 657 masl and peaking to 667 masl in August.

3.2 Reservoir Physical Habitat Parameters

Water temperatures in the Williston Reservoir in 2018 were consistent with temperature measurements from previous studies on the Peace River system. The thermocline occurred near 10 m depth in July, 15 to 18 m in August, and descending to 17 to >20 m by mid-September (Appendix H). Peak surface water temperatures were 17 °C on August 4, 2017 and 19 °C on July 30, 2018. The average epilimnion temperature was 15.2 °C and 13.7 °C in 2017 and 2018, respectively.

Thermocline development was limited in Dinosaur Reservoir because of its brief residence time (<5 days, Appendix H). Thermal profiles identified a <2 °C difference in average temperatures between the surface and bottom water for most of the 2017 and 2018 growing seasons (May through Sept.). However, a shallow transient thermocline occurred near 4 m depth in early July 2017 and in late July 2018 during stable, hot weather. Surface water temperatures peaked at 16.6 °C and 14.3 °C in 2017 and 2018, respectively. In both years, the peak littoral temperature was >5 °C warmer than the peak pelagic temperature. The average of the upper 10 m of the water column was 12.4 °C in summer 2017 and 10.8 °C in summer 2018.

Pelagic PAR profiles and light logger data indicated that photic zone depth varied seasonally with water column turbidity (Appendix G). Using 10 photons/m²/sec in the PAR range as the minimum threshold for light required by most algae (Sigeo, 2005), the depth of light penetration defining the photic zone in freshet 2017 and 2018 was narrow in Dinosaur Reservoir (1.5 m), and more typical (4.5 – 7.5 m) in Williston Reservoir. The photic zones of both reservoirs expanded over the summer before tapering off again in October (Appendix G, Appendix F). The average depth of the photic zone during the growing season in Williston Reservoir was 6.1 m (range 4-9 m) in 2017 and 8.3 m (range 5-12 m) in 2018. The average depth of the photic zone in pelagic regions of Dinosaur Reservoir during the growing season was 6.3 m in 2017 (range 1.5 - 10 m) and 6.7 m (range 1.5 – 11 m) in 2018.

Contraction of the Dinosaur photic zone occurred when freshet or summer storms increased inflowing tributary turbidity. For example, a 52 mm rain event (July 20-22, 2018, Appendix I) raised turbidity between 5-20 NTU and temporarily reduced the depth of the littoral photic

zone from 7 m to 2 m. Multimeter turbidity profiles showed abrupt, elevated turbidity at variable depths including at the surface, 3 m, and mid-reservoir depths; this may be indicative of creek turbidity plumes travelling at discreet depths in Dinosaur Reservoir.

The average photic zone depth in Dinosaur Reservoir was 6.3 m and 6.7 m in 2017 and 2018 respectively. A 6.5 m depth provides a reasonable estimate of the littoral zone extent based on available light to support primary production (Appendix H). The photic zone estimate was confirmed by low periphyton growth on D1-5 positioned at 5–7 m. The photic zone only received enough light for photosynthesis for 16 hours (an average of 9 photons/m²/sec) in summer and 81 hours (an average of 14 photons/m²/sec) in the fall sample sessions, indicating D1-5 was nearing the limits of the photic zone in both seasons.

Although the Dinosaur Reservoir littoral samples were more productive and more diverse than the corresponding pelagic samples, draw-downs impacted productivity in the upper varial portion of the littoral zone. The Dinosaur Reservoir littoral samples from 2017 and 2018 had abundances of $3.21 \times 10^6 \pm 1.21 \times 10^6$ for periphyton and phytoplankton, whereas the pelagic samples had abundances of $2.98 \times 10^6 \pm 1.31 \times 10^6$. The Dinosaur pelagic and littoral samples had 42 and 92 unique taxa, respectively. Drawdowns of 2.8 and 2.2 m in the 2017 and 2018 deployments corresponded to contractions in the varial zone. (Appendix D).

The littoral zone of Dinosaur Reservoir is approximately 2.56 km² (based on depths of 4 to 6 m; Golder, 2012) and is ultimately determined by the turbidity, bathymetry, and light in the photic zone. During the critical growing season (June to October), the narrow littoral zone averaged 0.4 °C warmer (as much as 5°C warmer) than the pelagic zone.

Heavy freshets and intense summer storms increased total phosphorus (TP) supplies in the Williston and Dinosaur reservoirs in 2018. In the Dinosaur Reservoir, TP concentrations at 30 m depth increased from 1.0-12 ug/l prior to freshet to 3.0-21.2 ug/l as P during the freshet, a trend that has been consistent through all years of monitoring. TP in surface water increased from <2.0 -8.0 ug/l as P in the growing season to <2.0-14.3 ug/l as P during freshet. The 2018 P results classify Dinosaur and Williston reservoirs as intermediate between oligotrophic and ultra-oligotrophic (Table 3-1), which agrees with other studies (Golder 2012; Stockner et al., 2005).

The ash fall from wildfires in summer 2018 provided an unknown quantity of biologically available phosphorus (Hauer and Spencer 1998). Mon-8 of the Site C FAHMFP showed increased orthophosphate from <0.5 ug/L as P to >1.2 ug/L as P in 2018, and that would support the increased productivity observed in late summer 2018 in both reservoirs. Similarly, total dissolved P increased from a typical August range of 1 – 5.7 ug/L to 23.7 ug/L as P in August 2018.

Table 3-1: Reservoir / Lake Classification by Trophic Status

Trophic Status	chlorophyll-a ug/L chlorophyll-a	Total phosphorus ug/L as P	Total Nitrogen ug/L as N	Secchi disc m	Primary production mg Carbon/m ² /day	TSI Index
Ultra-oligotrophic	<0.95	<4	< 75	>10	> 50	<30
Oligotrophic (low nutrients)	1 – 2	4 – 10	<100	6 -12	50 - 300	30 - 40
Mesotrophic (moderate)	2 – 5	10 – 20	100 – 500	3 – 6	250 – 1 000	40 - 50
Meso-eutrophic	5 - 7	20 - 35	500 - 900	2 - 3		50 - 60
Eutrophic (high nutrients)	7 - 25	35 - 100	900-1500	1 - 2.5	>1 000	60 - 70
Hyper-eutrophic	>25	>100	>1500	<1		70 - 80+
Williston Reservoir Pelagic	0.81	6.2 - 7.4	57 - 62	too turbid	10 - 347	
Dinosaur Reservoir Pelagic	0.63	5.7 - 5.9	208 - 262	too turbid		
Dinosaur Reservoir Littoral	0.59	n/a	n/a	too turbid		

Stockner et al 2001; Harris et al 2005; Golder 2009a

(after Ashley 1983, Carlson 1983, Wetzel 2001, Carlson and Simpson 1996, Vollenweider and Kerekes, 1982, Kasprzac et al. 2008)

3.3 Reservoir Primary Productivity

Monthly photic zone samples during the 2017 and 2018 growing seasons confirmed previous results of low phytoplankton productivity in the pelagic regions of Williston Reservoir (Harris et al. 2005; Stockner et al. 2005) (Appendix L). Most of the phytoplankton taxa present in Williston Reservoir were also prevalent in Dinosaur Reservoir, in part from recruitment, even though flow releases from W.A.C Bennett Dam occurred from depths (44 and 78m below full pool¹) below the summer photic zone. Pelagic phytoplankton biomass in Dinosaur Reservoir was very low ($0.48 \pm 1.02 \mu\text{m/L}$), with brief pulses of greater diatom growth. Dinosaur Reservoir phytoplankton were dominated by pico-cyanobacteria and photosynthetic bacteria, together with the flagellated taxa that forage on them. This is consistent with previous studies that found extremely low productivity in Dinosaur Reservoir, driven by inputs from Williston Reservoir (Euchner 2011; Golder 2009a).

Phytoplankton abundance in the pelagic samples from 2017 was typical of historical averages, whereas 2018 was more productive. Abundance averaged 7425 in Williston Reservoir and 5642 cells/mL in Dinosaur Reservoir in 2018. Phytoplankton biovolume in Dinosaur Reservoir increased from $0.18 \pm 0.08 \mu\text{m/L}$ in 2017 to $1.87 \pm 1.93 \mu\text{m/L}$ in 2018. The

¹ Peace Project Water Use Plan Physical Works Terms of Reference • GMSWORKS-25 Williston Reservoir Bathymetry April 21, 2008 Available at:

https://www.bchydro.com/content/dam/hydro/medialib/internet/documents/environment/pdf/wup_-_peace_-_gmsworks-25.pdf

biovolume increase from 2017 to 2018 in Dinosaur Reservoir was related to diatom pulses that likely originated in Williston Reservoir from August to October when elevated soluble phosphorus (possibly from wildfire ash) was available.

Littoral zone phytoplankton samples from Dinosaur Reservoir in 2017 and 2018 captured taxa such as *Cladophora* that were likely torn off shoreline substrates by waves. Drawdowns can dislodge periphyton and cause them to temporarily join the phytoplankton as the zone affected by waves shifts up and down the varial zone.

3.4 Reservoir Zooplankton

Only minor differences were observed in zooplankton taxa in Williston and Dinosaur reservoirs between each study year the 2010-2012 and 2017-2018 datasets (Appendix Q). These minute grazers include large taxa that are food for fish such as *Daphnia*, and small members that are consumed by larger invertebrates such as rotifers. Each year, 13 to 17 zooplankton taxa were regularly captured in 150 µm plankton vertical hauls from Dinosaur D1-littoral, 14 to 16 taxa from D1-pelagic regions, and 15 to 21 taxa from W1-pelagic regions. Seventeen taxa have been observed in both reservoirs. In 2017 and 2018, zooplankton densities in D1 hauls were greater than those collected in D1-pelagic region, while the proportions of taxonomic classes were similar.

The 80 µm mesh zooplankton hauls collected in 2017 and 2018 from Williston and Dinosaur reservoirs were dominated by copepods. Abundance averaged 77-85% copepods, 9-17% rotifers, and 1-5% cladocerans in Dinosaur Reservoir littoral samples. Five rotifer taxa were identified from the 2017/2018 80 µm plankton tow samples. Although small rotifers can escape this fine net, these results indicate that the rotifer communities are important to invertebrate biomass production, particularly in the large pelagic regions.

The standard 150 µm hauls also demonstrated copepod dominance and very low cladoceran numbers. Abundance averaged >90% copepods and <10% cladocerans in annual averages from 2017 and 2018 in Dinosaur Reservoir littoral samples. The cladocerans such as *Daphnia* occurred in brief pulses, particularly in samples from Williston Reservoir. Grazing calanoid copepods were twice as abundant as the predatory cyclopoid copepods, indicating oligotrophy. However, Dinosaur Reservoir copepod biomass was more balanced, with a growing season standing crop calanoid:cyclopoid ratio of 127:117 (ug dry wt/L) in 2017 and 109:132 (ug dry wt/L) in 2018.

The standard hauls from Williston Reservoir W-1 pelagic zooplankton 2017/2018 samples averaged greater productivity at 13.29 ± 14.19 indiv/L than Dinosaur Reservoir at 4.87 ± 4.25 indiv/L. Dinosaur Reservoir littoral samples were double the pelagic zooplankton abundance at 9.72 ± 6.77 indiv/L. Similarly, littoral zooplankton biomass was twice the pelagic biomass/L in the 2018 growing season.

Total zooplankton biomass fluctuated with phytoplankton densities, both between seasons and among years. Peak abundance occurred in June 2018 at all reservoir sites in conjunction with freshet nutrient loading and high light intensities (Appendix Q, Table A9). Mean areal biomass estimates of zooplankton production ranged from 22.8 ± 20.1 ug dry wt/L at D1-P, 47.1 ± 35.4 ug dry wt/L at D1-L, to 89.6 ± 114 ug dry wt/L at W1-P in 2017 and 2018. Based on these averages, the standing crop of zooplankton for Dinosaur Reservoir is

roughly estimated at 735 kg dry wt in the littoral zone and 4856 kg dry wt in the larger pelagic zone.

No invasive mussel veligers were detected in the 2017 and 2018 zooplankton samples from reservoir sites.

3.5 Reservoir Periphyton

Dinosaur and Williston Reservoirs had similar periphyton community compositions and dominant taxa (Appendix N). As expected based on previous work, the periphytic communities in these reservoirs consisted of mostly diatoms and micro-flagellates (Golder 2012; Harris et al. 2005; Stockner et al. 2005). Dominance shifts occurred over the growing season in response to drawdowns and environmental conditions. In all sampling series, diatoms dominated Dinosaur Reservoir periphyton. Diatoms averaged 83% of biovolume in the upstream control reservoir sites, and increased to 88% in the Site C reach (PR) and to 90% in the Downstream Reach (PD). Conversely, cyanobacteria accounted for an average of 12% in the upstream samples, 6% at PR sites, and 4% at PD sites. Species richness was 10-32 taxa in D1 periphyton during both 2017 and 2018, very similar to earlier estimates (Golder 2009a). The effective number of species metric showed the Dinosaur periphyton community was diverse, with a mean of 7 – a similar value to the periphyton from downstream riverine sites.

Dinosaur Reservoir periphyton demonstrated the most growth on samplers D1-2 and D1-3 which were shallow, permanently water-covered plates (Appendix M). The upper varial zone (D1-1) experienced periodic substrate exposure and wave turbulence. Growth tapered off at the deepest D1-5 site in all years, indicating that 5-7m was approaching the limit of the photic zone. Dinosaur littoral samples occasionally included large filamentous green algae (e.g., *Cladophora* and *Mougeotia*), which increased the littoral surface area by up to 2000 times.

Dinosaur Reservoir periphyton biomass estimates were all substantially lower than estimates from downstream riverine reaches (Appendix M). For example, Dinosaur Reservoir periphyton chlorophyll-a was only one third of the periphyton chlorophyll-a generated at PR sites in 2017 and 2018 results.

Within the reservoir, littoral periphyton productivity increased with submergence time, time above a threshold light intensity of 10 photons/m²/sec PAR, and temperature (Appendix W). While there was high overall variability and low predictive capability in the dataset, these data agreed with other observational data in this study. This data indicates that light intensity and submergence time are important determinants of littoral zone productivity.

3.6 Reservoir Invertebrates

The Dinosaur Reservoir littoral zone was only sampled for invertebrates in fall 2010, 2017-2018 and summer 2017-2018. The Dinosaur Reservoir invertebrate community was mostly composed of chironomids, gastropods and oligochaetes (Figure A122). The taxa richness ranged from 6-15 (mean=11) in the fall D1 samples. Summer 2017-2018 D1 samples had taxa richness of 3-21 (mean=13). The shallowest samples (D1-1) had the lowest taxa richness (3-6) in summer sampling. Chironomids were the predominant invertebrate in the fall 2010 D1 littoral samples with a mean percent abundance of 81±12%. In fall 2017-2018,

chironomids had a lower mean percent abundance of $28\pm 19\%$. Gastropods had high mean percent abundances of $64\pm 26\%$ in summer 2017-2018 and $60\pm 24\%$ in fall 2017-2018.

Gastropods made large contributions to the invertebrate biomass with a mean percent biomass of $80\pm 30\%$ in summer and $73\pm 40\%$ in fall. Dinosaur Reservoir had low percentages of EPT taxa with a mean percent biomass of $8.2\pm 17\%$ and a mean percent abundance of $3.1\pm 6.6\%$. Chironomids and EPT contributed more to the biomass at the D1-1 samplers than the deeper depths in Dinosaur Reservoir. Percent biomass of chironomids were 12-68% in D1-1 samples in summer and fall. The D1-1 fall 2017-2018 samples had higher percent biomass of EPT, 37% in 2017 and 62% in 2018.

The dredge models for the invertebrate basket samplers from Dinosaur Reservoir explained 0-34% of the variation in fish food, 46-58% of the variation in invertebrate abundance and 46-49% invertebrate biomass. There was only one notable trend in Dinosaur Reservoir results; invertebrate biomass and abundance increased with water depth in rock basket samples (Appendix X). Depth had an RVI of 1 in the invertebrate abundance model and 0.85 in the invertebrate biomass model. In the littoral zone, densities and biomass increased up to and stabilized at 3 m depth and remained relatively constant to 6 m depth (Appendix X, Figure A166 & Figure A167). Invertebrate densities were highest from samplers D1-3 to D1-5 that had mean depths of 2 to 6 m during deployment. A peak density was not observed; however, sampling did not occur beyond the edge of the littoral zone.

At Dinosaur Reservoir, two Ekman samples were collected in fall 2010 and 2011, whereas five Ekman samples were collected in both summer and fall 2017 and 2018 (Figure A147). Chironomids were the dominant invertebrates in all Dinosaur Reservoir samples with mean percent abundances of $73\pm 16\%$ in summer and $72\pm 21\%$ in fall. Oligochaetes were also present in Dinosaur Reservoir Ekman samples with mean percent abundance of $8.3\pm 6.0\%$ in summer and $15\pm 11\%$ in fall. Nematodes had higher percent abundances of $23\pm 26\%$ in fall 2010 and 2011 samples compared to the other sampling sessions.

Invertebrate community biomass had high annual variation at Dinosaur Reservoir (Figure A153). In fall and summer 2018, percent gastropods were the highest with mean percent biomass of $58\pm 1.0\%$ and $58\pm 24\%$, respectively. Chironomids had a higher percent biomass in fall and summer 2018 of $72\pm 37\%$ and $77\pm 20\%$, compared to the 2017 sampling sessions. Fall 2010 and 2011 also had a higher percentage of chironomids ($75\pm 27\%$) compared to fall 2017 with mean percent biomass of $75\pm 27\%$.

3.7 Periphyton and Invertebrate Community Structure

3.7.1 Periphyton

Riverine periphyton responded to environmental factors that were highly variable between years (2010-2012, 2018-2019) and seasons sampled (series). NMDS and PERMANOVA revealed that year and/or season explained the majority (32%) of periphyton community variation at the genus level (Appendix S, Table A11). Site explained 12% of the periphyton community variation, whereas reach (Upstream Control, Site C Reach and Downstream) only explained 3% of periphyton community variation.

Percent ecological guild metrics identified that annual and seasonal periphyton community differences resulted from differences in flow and proximity to Dinosaur Reservoir. The

percentages of the high-profile guild (shear stress index) decreased during freshet seasons and increased during stable lower flows in the fall seasons (Appendix O, Figure A106). Peace River periphyton community structure was distinct from upstream reservoir periphyton (Appendix S, Figure A144). Despite high seasonal and annual variability, Dinosaur Reservoir had higher percentages of the planktonic guild that ranged from 2.7-67% (mean=23%) (Figure A109). The Site C reach periphyton had 0-61% (mean=11%) planktonic taxa that was higher than the percent planktonic of 0-30% (mean=6.3%) at downstream reach sites. For example, the percent planktonic guild was highest at D1 (41±22%) and PR1 (41±16%) in summer 2017 compared to all other sites and sampling sessions (Figure A109).

Differences in the percentage of motile taxa and *Didymosphenia geminata* (Didymo) were observed at PR and PD sites. In all studies years (2010-2012, 2017 and 2018), the mainstem PR periphyton biovolume was dominated by Didymo, and the cosmopolitan diatoms *Synedra*, *Diatoma*, *Nitzschia* and *Achnantheidium*. Because Didymo filaments increase the surface area available for adhesion by diatoms by at least an order of magnitude, Didymo often accounted for >20% of the total diatom biovolume and increased chlorophyll-a estimates at PR sites. Didymo was also detected at PD1, PD2 and PD3. PD4 and PD5 did not host Didymo but had the highest percent motile guild, indicated that PD sites had a higher silt deposition than PR sites. Silt deposition during the spring at PD sites caused burial of diatoms from upstream locations and induced vertical diatom migration of the motile guild (Appendix O, Figure A109).

3.7.2 Invertebrates

3.7.2.1 Ekman Samples

The NMDS for the Ekman samplers in Dinosaur Reservoir and the Peace River Site C reach indicated that site explained 22% of the invertebrate community composition at the genus level (PERMANOVA, Appendix U, Table A15), followed by series (season and year: 8%) and reach (7%). Invertebrate communities in Dinosaur Reservoir and PR1 were similar to PR2 and PR3 (Appendix U, Figure A146). There was a higher abundance of the snail taxa Valvatidae and Gastropoda at Dinosaur Reservoir compared to the other Site C reach sites.

Oligochaetes and chironomids were the most abundant invertebrate groups in fall and summer 2017 and 2018 samples from PR1, PR2 and PR3 (Appendix V). Gastropods had higher abundances at PR1 of 10±11% compared to <1% at PR2 and PR3. The PR3-1 samples from summer and fall 2017 were dominated by EPT and Springtails (Collembola), respectively.

The Site C Reach sites had the highest percent biomass of oligochaetes and chironomids. Oligochaetes and gastropods contributed the most to biomass in PR1 samples (mean biomass of 32±26% and 11±15%, respectively) in summer 2017 and 2018. The dominant invertebrate group in summer varied by sample at PR1 and was either gastropods or oligochaetes. In most PR1 fall samples, the dominant invertebrate groups were gastropods, oligochaetes and chironomids. The invertebrate community was more uniform in all sampling sessions at PR2, with oligochaetes and chironomids contributing the most to biomass (34±18% and 64±17%, respectively). Chironomids and oligochaetes also contributed the most to invertebrate biomass in most PR3 samples, contributing on average

a total of $28\pm 23\%$ and $65\pm 32\%$ biomass, respectively, for all sampling sessions. However, in PR3-1 samples from 2017 there were different dominant taxa. Trichoptera accounted for 71% of biomass in the fall 2017 PR3-1 samples, while Collembola accounted for 93% of biomass in the summer 2017 PR3-1 samples.

Oligochaetes and chironomids were the most abundant invertebrates in Halfway (HD) and Moberly (MD) Ekman samples in 2017 and 2018 (Appendix V). Summer HD samples had mean percent oligochaete and chironomid abundances of $45\pm 24\%$ and $45\pm 22\%$, respectively. However, in some summer 2018 HD samples, other dipterans were predominant with percent biomasses of 67-80%. Oligochaetes were dominant in Fall 2017 HD samples with mean percent abundance of $75\pm 14\%$, whereas chironomids were dominant in Fall 2018 HD samples with a mean percent abundance of $75\pm 14\%$. A higher percent biomass of $53\pm 44\%$ EPT taxa occurred in Fall 2018 MD samples compared to summer samples. In 2017 and 2018 summer MD samples, the mean percent oligochaetes and chironomid abundances were $20\pm 12\%$ and $51\pm 20\%$, respectively. Most fall MD samples had higher percent oligochaete abundance of $49\pm 11\%$ compared to summer MD samples. Unlike other MD and HD samples, the fall 2018 MD-3 sample had a high 67% abundance of EPT taxa. Dipterans not including chironomids were more abundant in MD summer samples with a mean percent abundance of $24\pm 17\%$, compared to fall samples with a mean percent abundance of $7.6\pm 4.2\%$.

3.7.2.2 Rock Basket Samples

NMDS analysis was performed on the invertebrate rock basket samples of D1, PR and PD sites for 2010-2012 and 2017-2018. NMDS analysis and PERMANOVA showed variations in benthic invertebrate community were most influenced by site (19%) as well as annual and seasonal differences (17%), followed by reach (7%) (PERMANOVA, Appendix T, Table A13). Dinosaur Reservoir had a distinct invertebrate community structure that was dominated by gastropods, Lymnaeidae (pond snails) and chironomids in summer and fall (Appendix T, Figure A145). In contrast, riverine sites (PR and PD) were dominated by chironomids and Naididae (oligochaetes) in summer deployment periods. During fall deployments, Brachycentridae (Trichoptera) became the dominant taxon at PR sites, but the PD sites showed greater dominance of EPT taxa including Taeniopterygidae (Plecoptera), Hydropsychidae (Trichoptera) and Brachycentridae (Trichoptera).

The Site C reach sites had high seasonal variation in percent EPT and high within site variation of invertebrate richness. The Site C Reach had invertebrate taxa richness that ranged from 4-37 in summer and 12-44 in fall. PR3 had higher taxa richness values than PR1 and PR2 (Table 3-2). The minimum taxa richness values were from summer 2011 which had high exposure ratios and high flows. The percent abundance of EPT was higher in fall than summer at all sites except MD. MD had higher percent EPT in summer compared to all other Site C reach sites.

Table 3-2: Summary of invertebrate taxa richness, percent EPT (abundance and biomass) for Site C reach invertebrate rock basket samplers 2010-2012 and 2017-2018.

Site	Taxa Richness Min-Max (Mean)		Percent Abundance EPT Min-Max (Mean)		Percent Biomass EPT Min-Max (Mean)	
	Summer	Fall	Summer	Fall	Summer	Fall
PR1	4-26 (17)	12-29 (22)	0-21% (3.2%)	1.4-55% (22%)	0-85% (21%)	1.5-99% (64%)
PR2	5-32 (21)	13-37 (25)	0.67-82% (18%)	1.6-92% (29%)	2.8-100% (60%)	1.7-100% (61%)
HD	12-20 (16)	8-29 (18)	18-81% (54%)	54-100% (82%)	57-99% (90%)	88-100% (98%)
MD	18-29 (25)	15-35 (26)	68-83% (74%)	22-98% (58%)	98-100% (99%)	81-100% (96%)
PR3	10-37 (24)	20-44 (29)	1.1-50% (18%)	0.81-70% (30%)	23-99% (76%)	8.6-99% (83%)

Chironomids and oligochaetes were predominant taxa in most summer sampling sessions at PR1 and PR2 (Figure A130 & Figure A131). Hydrozoans had higher percent abundances at PR1 compared to PR2. At PR1 hydrozoans had higher mean relative abundances of $62\pm 38\%$ in 2010-2012, compared to $16\pm 14\%$ in 2017-2018. Chironomids were dominant at PR1 in summer 2017-2018 with a mean percent abundance of $60\pm 13\%$. In most summer PR2 samples, chironomids were one of the dominant invertebrates with mean percent abundance of $24\pm 18\%$. Oligochaetes were more abundant in the summer 2017-2018 at PR1 with a mean percent of abundance of $16\pm 7.7\%$ compared to $0.1\pm 0.05\%$ in summer 2010-2012. At PR2, oligochaetes had higher percent abundances in summer 2017-2018 with a mean percent abundance of $37\pm 22\%$, compared to $16\pm 16\%$ from summer 2010-2011. Collembola and EPT taxa had higher percent abundances in summer 2011 samples relative to other summer sampling sessions.

There were differences in the dominant invertebrates at PR1 and PR2 in the fall sampling sessions. Hydrozoans and chironomids were the dominant invertebrates at PR1 in fall 2010-2012, whereas chironomids and oligochaetes were the dominant invertebrates at PR2 in fall 2010-2012. At PR1, there were higher EPT and chironomid abundances in fall 2017 and 2018 with mean percent abundances of $35\pm 15\%$ and $44\pm 17\%$, compared to fall 2010-2012 that had mean percent EPT and chironomid abundances of $13\pm 14\%$ and $13\pm 9.3\%$. The mean percent EPT in fall 2018 at PR2 was $69\pm 28\%$ which was much higher than the mean

percent EPT of $13\pm 13\%$ in fall 2017. Oligochaetes were the dominant invertebrate in PR2 fall 2017 samples with a mean percent abundance of $79\pm 13\%$.

At PR1 and PR2 the dominant invertebrates by biomass were highly variable in fall and summer between years. In summer sampling sessions, the percent biomass of EPT taxa were higher at PR2 compared to PR1. Oligochaetes and chironomids were the predominant invertebrate at PR1 in summer 2017-2018. The mean percent biomasses of oligochaetes and chironomids in summer 2017-2018 at PR1 were $58\pm 19\%$ and $41\pm 27\%$, respectively. The dominant invertebrates varied by PR1 sample in summer 2010-2011; dominant taxa in these samples included hydrozoans, nematodes, gastropods and chironomids. At PR2, the summer 2018 samples had a mean percent biomass of oligochaetes of $24\pm 16\%$ which was higher than the other summer sampling sessions. The percent EPT in summer PR2 samples was $60\pm 38\%$. The high variability in the percent biomass of EPT was a result of a few samples where gastropods and oligochaetes dominated. EPT were the dominant invertebrates in fall 2011-2012, and 2017-2018 with percent biomasses of $64\pm 34\%$ at PR1 and $61\pm 39\%$ at PR2. In fall 2017, oligochaetes had high percent biomasses ($>75\%$) at the PR2 shallow samples. Gastropods were dominant invertebrates in fall 2010 with mean percent biomasses of $71\pm 24\%$ at PR1 and $44\pm 25\%$ at PR2. Corixids also contributed to the biomass of invertebrates at PR2 with a mean percent abundance of $43\pm 27\%$ in fall 2010.

The Halfway (HD) and Moberley (MD) sites had a limited number of invertebrate samples in the summer sampling session because most of the samplers were lost to high flows. There were four samples retrieved in summer 2010 and two samples retrieved in summer 2017 at each site. The available samples showed MD had a higher mean taxa richness of 25 in summer compared to 17 at HD (Table 3-2). Chironomids and EPT were the dominant invertebrates in 2010 HD summer samples with a mean percent abundance for chironomids of $35\pm 18\%$, and EPT of $65\pm 18\%$. EPT were also dominant in MD summer 2010 samples with a mean percent abundance of $75\pm 7.3\%$. Other dipterans had higher abundances ($\sim 29\%$) in shallow MD 2010 samples, whereas in deeper samples chironomids had higher abundances ($\sim 19\%$). Summer 2017 had higher percent chironomids at both HD and MD compared to summer 2010 (Figure A123 & Figure A124). The percent abundance of chironomids were 36-71% at HD and 42-67% at MD.

In most fall sampling sessions at MD and HD, the taxa richness and percent EPT were higher compared to summer (Table 3-2). The fall taxa richness ranged from 15-35 at MD and 8-29 at HD. At MD, fall 2010 and 2018 had higher percent abundances of EPT compared to Fall 2011, 2012 and 2017. The percent abundances of EPT at MD in Fall 2010 and 2018 were $79\pm 9.4\%$ and $96\pm 1.9\%$, respectively. Chironomids had higher abundances in Fall 2011 and 2017 at MD, with percent mean abundances of $39\pm 4.1\%$ in Fall 2011 and $56\pm 11\%$ in fall 2017. MD samples from Fall 2012 had a mixture of chironomids ($31\pm 17\%$) and EPT ($58\pm 14\%$). HD had higher percent abundance of EPT in Fall 2010, 2012 and 2017 compared to Fall 2011. The mean percent abundances in Fall 2010, 2012 and 2017 were 87-89%, whereas the mean percent abundance in Fall 2017 was $65\pm 12\%$. Fall 2017 had higher percent abundances of chironomids ($30\pm 11\%$) than the other fall sampling sessions.

EPT taxa comprised a large percentage of the invertebrate biomass at HD and MD in all sampling sessions. The percent biomass of EPT at HD was $90\pm 17\%$ in summer and $98\pm 3.4\%$ in fall. At MD, the mean percent biomass of EPT in summer was $99\pm 0.5\%$ and the mean percent biomass in fall was $96\pm 5.6\%$.

Like PR1 and PR2, chironomids and oligochaetes were the most abundant invertebrates at PR3. In Summer 2010 and 2017-2018, the mean percent abundance of chironomids and oligochaetes were $36\pm 18\%$ and $27\pm 16\%$, respectively. Fall samples were also dominated by chironomids and oligochaetes. Annual differences in dominant invertebrates were observed from Fall 2010-2012 at PR3. Acariformes (mites) had a mean percent abundance of $42\pm 11\%$ in fall 2011 which was higher than the other fall samples sessions. EPT were more abundant in the fall 2010 PR3 samples with a mean percent abundance of $58\pm 12\%$. In Fall 2012, hydrozoans were the dominant invertebrate with a mean percent abundance of $42\pm 8\%$. Chironomids and oligochaetes were dominant invertebrates in Fall 2017 and 2018 samples, with mean percent abundances of $23\pm 16\%$ and $40\pm 13\%$, respectively.

EPT taxa made up a large proportion of the invertebrate biomass in summer and fall PR3 samples. The mean percent EPT was $92\pm 6\%$ in Fall 2010-2012 samples and was $70\pm 35\%$ in Fall 2017-2018. Some of the fall 2017-2018 samples had high percent biomasses from Coleoptera, chironomids and oligochaetes. EPT taxa were also predominant in Summer 2010 and 2017 with percent biomasses of $93\pm 3\%$ and $81\pm 24\%$, respectively. The percent biomass of EPT taxa was $67\pm 23\%$ in summer 2018 which was lower than other sampling sessions. Summer 2018 samples had higher contributions from chironomids than the other summer sampling sessions.

The five Downstream reach sites, PD1-PD5, had an invertebrate community that demonstrated high site and seasonal variation in taxa richness and percent EPT. The PD sites had a wide range (1-53) of invertebrate taxa richness in summer sampling sessions (Table 3-3). Invertebrate taxa richness increased to 9-44 in fall samples from the PD sites. The percent EPT biomass and abundance were higher at all PD sites in fall compared to summer.

Table 3-3: Summary of invertebrate taxa richness, percent EPT (abundance and biomass) for Downstream reach invertebrate rock basket samplers 2010-2012 and 2017-2018.

Site	Taxa Richness Min-Max (Mean)		Percent Abun EPT Min-Max (Mean)		Percent Biom EPT Min-Max (Mean)	
	Summer	Fall	Summer	Fall	Summer	Fall
PD1	5-39 (25)	19-45 (29)	0-49% (18%)	10-93% (61%)	0-98% (66%)	21-100% (89%)
PD2	4-51 (23)	21-39 (29)	0.91-64% (18%)	9.9-82% (45%)	1.1-98% (53%)	14-100% (83%)
PD3	1-32 (14)	19-34 (26)	0-41% (11%)	24-95% (64%)	0.48-100% (49%)	69-100% (97%)
PD4	7-44 (26)	9-35 (26) 16-44	6.9-43% (14%)	2.5-71% (31%)	1.3-99% (45%)	11-98% (69%)
PD5	8-53 (32)	(29)	1.4-46% (23%)	34-92% (64%)	16-96% (73%)	95-100% (98%)

Chironomids and oligochaetes were the dominant invertebrates at PD1 and PD2 in Summer 2010-2011 and 2017-2018 (Figure A125 & Figure A126). PD1 had a mean percent abundance of $45\pm 16\%$ for oligochaetes and $19\pm 10\%$ for chironomids, while PD-2 had a mean percent abundance of oligochaetes of $29\pm 19\%$ and a mean percent abundance of chironomids of $41\pm 19\%$. Acariformes had higher abundances in Summer 2010 at PD1, with a mean percent abundance of $19\pm 7\%$.

At PD1 and PD2, there was a higher percent abundance of EPT taxa in fall compared to summer (Table 3-3). However, fall 2012 and 2018 had higher percent abundances of EPT taxa. For example, fall 2012 samples had percent EPT of $72\pm 2.0\%$ at PD1 and $56\pm 8.5\%$ at PD2. In Fall 2018, the percent EPT was $80\pm 14\%$ at PD1 and $57\pm 25\%$ at PD2. Fall 2010 had the lowest percent EPT for all fall sampling sessions with $38\pm 20\%$ at PD1 and $39\pm 12\%$ at PD2. The predominant invertebrates at PD1 and PD2 in Fall 2010 were chironomids and oligochaetes. The mean percent abundance of EPT in Fall 2017 was $51\pm 29\%$ at PD1 and $54\pm 10\%$ at PD2.

The invertebrate that contributed most to biomass were variable in summer at PD1 and PD2. For example, percent biomass of EPT was $87\pm 10\%$ in summer 2017-2018 which was higher than $49\pm 39\%$ summer 2010-2011 at PD1. At PD1 and PD2, EPT taxa contributed a large percentage to the invertebrate biomass in fall. The percent biomass of EPT was $61\pm 23\%$ at PD1 and $45\pm 19\%$ at PD2 in all fall sampling sessions.

PD3 had a low mean taxa richness of 14 in summer compared to the other Downstream Reach sites (Table 3-3). The low mean taxa richness at PD3 was a result of low invertebrate taxa richness in summer 2011 when all PD3 samples were exposed for $>40\%$ of the deployment period. Chironomids and oligochaetes were the dominant benthic invertebrates at PD3 in summer 2010-2011 and 2018. Oligochaetes were the dominant invertebrate in summer 2011 and 2018 with percent mean abundances of $84\pm 19\%$ and $48\pm 40\%$. Chironomids were more abundant in summer 2010 with a mean percent abundance of $44\pm 30\%$.

Fall invertebrate taxa richness ranged from 19-34 at PD3. EPT were the dominant invertebrate group at PD3 in fall sampling sessions. Fall 2010, 2012 and 2018 had the highest percent EPT compared to the other fall sampling sessions. The percent mean abundance of EPT was $80\pm 4.1\%$ in fall 2010, $76\pm 2.3\%$ in fall 2012 and $85\pm 14\%$ in fall 2018. There were lower percentages of EPT in fall 2011 and 2017, and higher percent abundances of oligochaetes and chironomids. The percent mean abundance of oligochaetes was $20\pm 5.3\%$ in fall 2011 and $48\pm 16\%$ in fall 2017. In fall 2011, the mean percent abundance of chironomids was $20\pm 10\%$.

EPT taxa made large contributions to the biomass in all sampling sessions except summer 2011 at PD3 when oligochaetes dominated with a percent mean biomass of $78\pm 20\%$. EPT taxa contributed $56\pm 43\%$ of invertebrate biomass in Fall 2011 and $73\pm 29\%$ in Fall 2018. The shallowest sample (PD3-1) in Summer 2011 had a low percent of EPT taxa, while gastropods contributed 61% of biomass. All fall sampling sessions, 2010-2012 and 2017-2018, had a high percent biomass of EPT at $97\pm 7\%$.

The PD4 and PD5 sites were added to the MON-7 program in 2017 and 2018. Chironomids and oligochaetes were the dominant invertebrate taxa at PD4 with mean percent abundances of $45\pm 20\%$ and $28\pm 15\%$, respectively in Summer 2017 and 2018. Fall 2017 had a similar invertebrate community composition to the summer sampling sessions with a

high mean percent abundance of $35\pm 9\%$ for chironomids and $42\pm 10\%$ for oligochaetes. EPT taxa were more abundant in Fall 2018 compared to Fall 2017. The mean percent abundance of EPT was $49\pm 31\%$ in 2018 and $12\pm 10\%$ in 2017 at PD4. In fall, PD4 had the lowest percent EPT abundance compared to the other PD sites.

The invertebrates that contributed the most to biomass at PD4 had high seasonal and annual variation. The invertebrate groups of other dipterans, EPT and chironomids made up a large percentage of the biomass at PD4 in summer 2018. EPT had a percent mean percent biomass of $39\pm 18\%$ and other dipterans had a percent biomass of $31\pm 15\%$ in Summer 2018. EPT taxa contributed the most to biomass in Fall 2018 with a mean percent biomass of $78\pm 40\%$. The PD4-1 fall 2018 sample had a higher percent biomass for oligochaetes of 40% compared to other fall 2018 samples. In summer and fall 2017 the dominant invertebrate relative biomass varied by transect. EPT taxa contributed more biomass at some transects, while at other transects, chironomids and other aquatic insects (i.e. Collembola, Coleoptera) contributed more biomass. The PD4-1 sample from summer 2017 had a high percent biomass of Collembola and also had a low taxa richness of seven.

Chironomids, oligochaetes and hydrozoans were the most abundant invertebrate groups in summer 2017 at PD5. The mean percent abundances of chironomids, oligochaetes and hydrozoans were $20\pm 5\%$, $31\pm 13\%$ and $26\pm 26\%$, respectively. In Summer 2018 only two PD5 samplers were retrieved, and these samples were mostly composed of chironomids and EPT with percent abundances of 41-52% for chironomids and 20-37% for EPT. Like PD4, fall 2017 had a higher percent abundance of chironomids and oligochaetes compared to Fall 2018. The percent chironomids was $23\pm 7\%$ and percent oligochaetes were $42\pm 10\%$ in Fall 2017. Fall 2018 had higher abundances of EPT taxa with a mean percent abundance of $82\pm 12\%$ compared to $46\pm 11\%$ in Fall 2017.

EPT taxa contributed most the invertebrate biomass in summer and fall 2017-2018 at PD5. The percent biomass of EPT $73\pm 29\%$ was in summer and $98\pm 2\%$ in fall.

3.8 River Physical Habitat Parameters

3.8.1 Depth

At each river site, sampler elevations were set along a depth transect ranging from the upper varial zone (UV or transect position 0, partially exposed) down to 3 to 5 m deep (DP or deep photic zone) in ~ 0.5 m increments (Table 2-3; Appendix E). Thus, at lower varial or position 1, samplers were positioned between 0.8 and 1.5 m, with depth varying over time depending on river flows. Samplers at position 0 were exposed most frequently but were still submerged most of the time. The total time submerged varied between sites. Wetting frequency was also variable, and depended upon site, flows, and season.

3.8.2 Light

Light conditions were seasonally variable and dependent on turbidity and water depth. In the 2018 summer and fall deployment periods, most of the samplers at PR1 and PR2 had mean mid-day light intensities above 10 photons/m²/s (Appendix F). The summer and fall PR1-4 samplers had mean depths >6 m and as a result, received less light than all other PR1 and PR2 samplers. The summer "2-4" samplers at PR3, PD1, PD2, PD4 and PD5 had lower mean light intensities than in the fall, as a result of lower turbidities during the fall. The

very low light intensities at the PR3 summer samplers “2-4” were likely caused by sediment burial. PR3 is susceptible to sediment deposition because it has lower velocities.

PAR profiles for all Peace River sites indicated that photic zone depth varied seasonally with riverine water column turbidity (Appendix G). The depth of light penetration defining the photic zone in May 2018 ranged from ~0.1-0.95 m at the PR and PD sites. At the start of summer deployment, all sites that were downstream of major Peace River tributaries had photic zones of ~0.25-0.65 m. The two sites that were not influenced by major tributaries, PR1 and PR2, had wider photic zones compared to all other sites in June 2018. PR1 and PR2 had photic zones that exceeded 6 m and 2.8 m, respectively. The photic zones determined from the PAR profiles recorded at the start of fall deployment were sensitive to the day they were taken. The PD fall samplers that were deployed the latest, PD4 and PD5, had deeper photic zones (1-1.2 m) than the other PD sites (0.55 m). These deeper photic zones were a result of lower turbidity on August 3-4, 2018 compared to July 30-August 1, 2018. The PR sites had photic zones from 1 to 3 m at the beginning of fall deployment.

Turbidity and flows of the Peace River tributaries decreased in August resulting in deeper photic zones. For example, photic zones were deeper for most sites during the week of August 21st to 24th. For all PR sites, PD1, PD3 and PD5, the photic zone was deeper than the “4” sampler position. The photic zones of PD2 and PD4 were 1.3 to 1.6 m which were shallower compared to other sites. However, PD2 and PD4 still had deeper photic zones compared to earlier dates.

3.8.2.1 Light Modelling in Peace River and Reservoir

The diffuse light attenuation coefficient increased with increasing turbidity, meaning that light penetration to the Peace River streambed drops as turbidity increases (Figure 3-1, Appendix J). The analysis in 2018 improved light coefficients in models, and the light data collected fit well with modelled results. The light models demonstrate that the photic zone does not extend beyond 2 to 2.5 m during periods of turbidity of ~10 NTU and is dramatically reduced as turbidity increased beyond that point (Figure 3-1; Appendix J). During turbid conditions, *in situ* productivity in the Peace River was limited to areas receiving sufficient light, frequently in a band along the river margins and sandbars. As turbidity declined in clearer phases, the photic zone expanded to include larger portions of the riverbed.

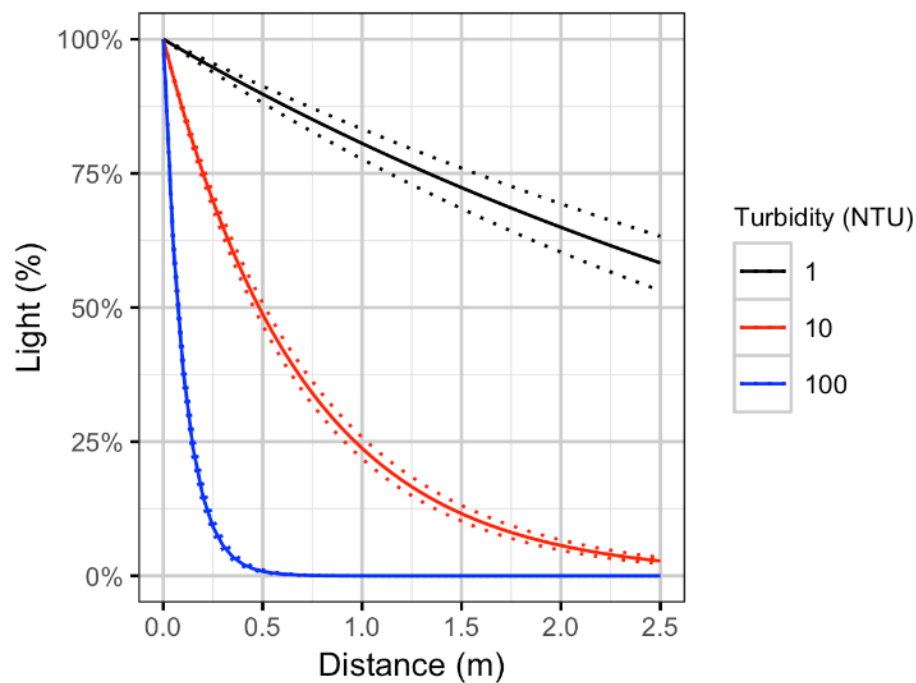


Figure 3-1: The relationship between the diffuse percentage of light transmission depth, under varying turbidity conditions. Dotted lines represented 95% Confidence Limits (CLs).

3.8.3 Turbidity

Mean daily turbidity measured by sensors at Peace River downstream sites was typically less than 100 FNU (Figure 3-2). The highest turbidity values of the summer and fall 2018 sampling periods occurred at the end of June 2018 after heavy rainfall.

PD2 located downstream of the Pine River had a smaller turbidity spike after the heavy rainfall compared to the other PD sites because the Pine River is the largest tributary along the PD reach and it does not experience the large changes in flow and turbidity after a storm event that the smaller Peace River tributaries do. Mean daily turbidity exceeded 1000 FNU at PD1, PD4, PD5 following the storm on June 25-26, 2018. Turbidity at PD3 approached 1000 FNU, while turbidity at PD2 showed a much lower storm response (Figure 3-2). Unlike the Pine River, the Pouce Coupe River is known to experience high flows after summer storm events (Foundry Spatial Ltd, 2011). The July 20 2018 storm caused increased flows and turbidity in the Pouce Coupe River and on July 22 and 23, mean daily turbidity values exceeded 1000 FNU at downstream PD5. Mon-9 data demonstrate that the Pouce Coupe River was a large source of suspended solids to the PD5 site following the heavy rainfall from July 22-23 when the turbidity of the Pouce Coupe River increased from 48.7 NTU on July 20 2018 to 1440 NTU on August 1 2018.

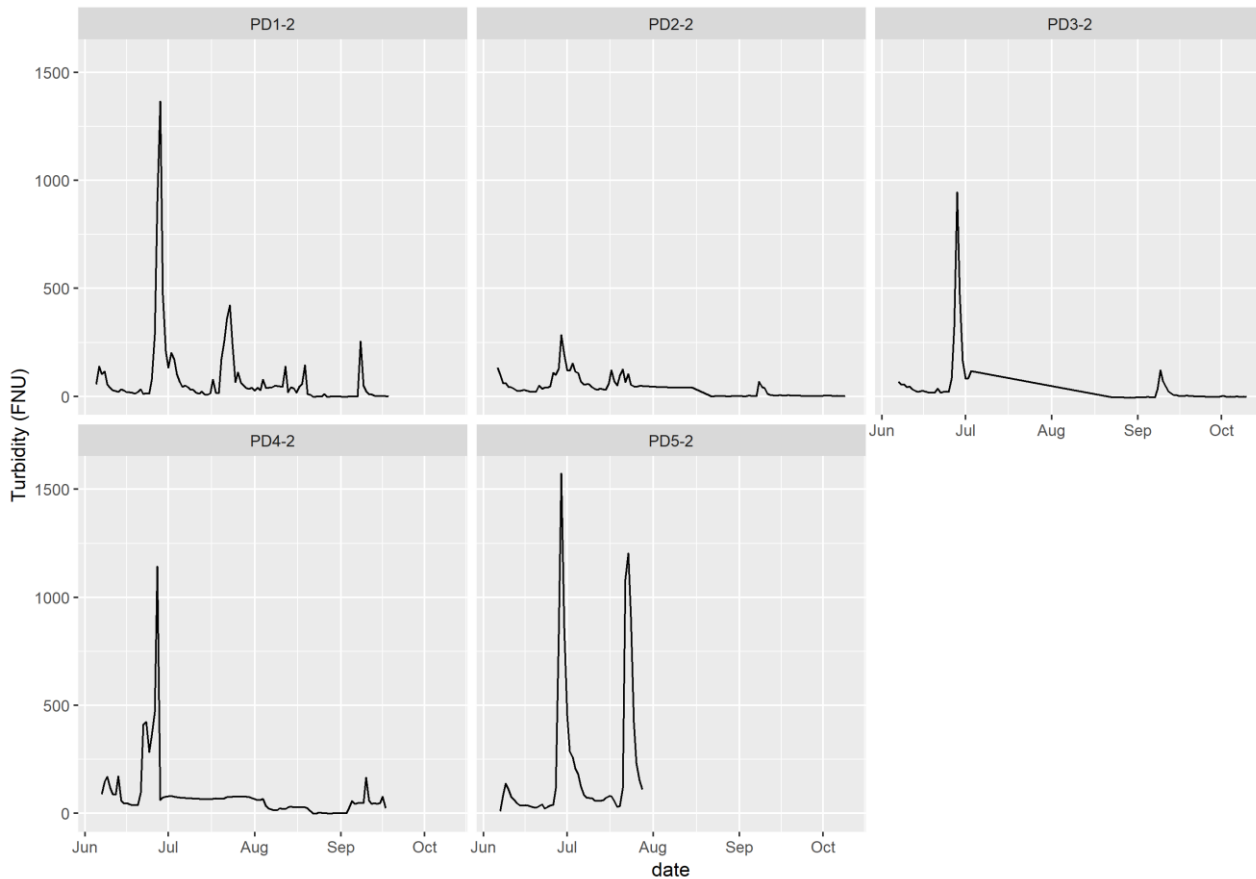


Figure 3-2: Average daily turbidity (FNU) at each downstream site in the Peace River over the duration of deployment in 2018.

3.8.4 Temperature

The water temperatures at each Peace River site ranged from 10 or 11 °C in June to a peak near 15 to 17 °C in August, before declining to 11 or 12 °C in October 2018 (Appendix K). Temperatures did not vary by transect, except during cases of exposure, but there was variation among sites. Factors such as tributary inflow were important determinants of site-specific temperatures. A slight trend of increasing temperature in downstream reaches was observed but not formally tested. The warmest sites were the downstream sites PD4 and PD5, while the coolest were immediately downstream of Dinosaur Reservoir (PR1 and PR2). A summary of mean daily temperatures is found in Appendix K.

3.9 Riverine Periphyton and Invertebrate Productivity

Since statistical modelling of multiple metrics across multiple scales is very complex, two statistical approaches were taken where feasible (Multi-Model Averaging or dredge and Random Forest (RF)). These techniques were used to better understand how key physical parameters affected productivity. The study design is well suited to understand broad spatial

patterns and changes over time but it increases the chances of pseudo-replication² because of complex interactions between year, reach, transect, season, and site. To simplify analyses, suites of similar predictors were used for a variety of responses, rather than determining a specific predictor suite for each response. This allowed efficient comparison of a broad range of responses and predictors but did not necessarily identify the optimal response / predictor combination.

3.9.1 Periphyton River Productivity

Peace River chlorophyll-a was strongly correlated with taxonomic estimates of abundance and biovolume in the Site C reach (PR) (Appendix M, Figure A87). The main producers of chlorophyll-a in the PR periphyton samples are living algae (plankton and periphyton), with a smaller contribution from other sources. In the downstream more depositional PD reach, a weaker correlation between chlorophyll-a and algal metrics occurred (Appendix M).

To improve text readability, full model summaries were placed in Appendix Y (2010-2011 and 2017 dredge), Appendix Z (Full transect dredge), Appendix AA (Submerge samples only dredge), and Appendix BB (Random Forest (RF) models).

In the RF models of periphyton productivity, seven explanatory variables explained 26% of the variation in total abundance variation and 33% of the variation in total biovolume, with top predictors of 1) season 2) site 3) maximum hours submerged and 4) hours >10 photos/m²/sec PAR. The RF model explained 21% of the variation of chl-a with the top predictors of 1) site, 2) maximum hours submerged, 3) hours >10 photos/m²/sec PAR and 4) site. These model outputs are described in more detail in the following section that presents explanatory variables in approximate order of importance.

3.9.1.1 Submergence

Submergence patterns define the upper bounds of the varial zone, while light penetration determines the lower bounds, resulting in a narrow band of peak periphyton production in turbid reaches (Schleppe and Larratt 2016).

Total submergence time explained limited variation in the periphyton production models for the 2010-2011 and 2017-2018 sampling sessions (Appendix Y). For each periphyton production metric, only one model that included total submergence time as a predictor had $\Delta AIC < 3$, as a result RVIs could not be calculated (Table A19). The random intercept of year, season and site explained 35% of the variation in chl-a. The addition of total submergence time as a predictor in the linear mixed effects models did not explain additional variation in chl-a ($R^2=0.35$). Similarly, the random intercept explained 46% of the variation in abundance, whereas total submergence time and the random intercept explained 47% of the variation in chl-a. The random intercept did not explain as much variation for total biovolume ($R^2=0.17$) and the addition of total submergence time resulted in 18% of the variation in biovolume explained.

Sampling in 2017 and 2018 spanned the entire photic zone, from its lower bounds (transect position 4) to the upper transitional edge of the varial zone (transect position 0). The shallowest samplers at transect 0 had the lowest periphyton production compared to all

² While we have attempted to account for pseudo-replication in analysis as much as possible, there still is some potential because of the complex interactions between site, reach, transect, year, and season that we may not be able to fully account for.

other transect positions. These samplers experienced frequent exposure and dewatering in 2017 and 2018. Periphyton productivity was greatest at the riverine sites in the permanently wetted upper varial zone (transect position 1), while production was lowest in the upper varial zone that experienced periodic substrate exposure (transect position 0).

When all sites, including samplers in the varial zone were compared, submergence time was a key factor determining periphyton productivity. In the RF models, maximum hours submerged was the second most important predictor of abundance with Variable Importance (VIMP) a 3.5×10^9 and the fourth most important chl-a predictor with VIMP of 0.93. The RF models also indicated that periphyton productivity (chlorophyll-a and abundance) increased from 0 to 200 hours of continuous submergence but abundance dropped after 1215 hours of continuous submergence (Appendix BB, Figure A182 & Figure A183). Interestingly, the dredge model for total abundance found cumulative time submerged was negatively associated with total abundance (Appendix AA, Figure A172). This negative association and lower total abundance occurred almost exclusively at deep sites, characterized by long periods of continuous submergence but low light intensity (Appendix Z, Figure A174). At these light-limited sites, productivity is a combination of settlement of upstream production and in situ growth of low light tolerant taxa.

Periphyton strip samplers were installed in 2018 to refine our understanding of periphyton production in the upper varial zone on a continuous gradient between T0 to T1 positions. The resulting strip chlorophyll-a measurements showed complex patterns that varied seasonally with flows (Appendix P). In high summer flows, PR1 and PD1 productivity increased along the T0 to T1 depth gradient, while PR2, PR3, PD2 showed an overall decrease with depth and PD3 PD4 PD5 showed very low productivity throughout this upper varial zone (Appendix P). In stable lower fall flows, PR1, PD1 and PD5 productivity increased along the depth gradient, while PR2 and PR3 showed an overall decrease and PD3 and PD4 showed low productivity throughout the T0 – T1 zone. These efforts demonstrated that upper varial zone productivity was highly variable due to substrate exposure.

3.9.1.2 Light

Light is a critical driver of periphyton productivity in the Peace River system. In the RF periphyton abundance models, the third most important predictor was *hours >10 photos/m²/sec PAR* with a VIMP of 2.43×10^9 . For the total biovolume RF model, the second most important predictor was *hours >10 photos/m²/sec PAR* with a VIMP of 209. Both the total biovolume and abundance RF models indicated that most of the periphyton growth occurs from ~0-150 hours of >10 photos/m²/sec PAR (Appendix BB, Figure A181 & Figure A182). Hours over 10 photos/m²/sec PAR was the third most important predictor of chl-a with a VIMP of 0.96.

The permanently submerged models explained more variation of periphyton production metrics than the full river transect models (Appendix AA). The submerged models explained 45-47% variation of chl-a, 49% variation of total abundance and 34% variation of total biovolume. The top predictor of chl-a and biovolume was *hours >10 photos/m²/sec PAR* in the permanently submerged dredge models (Figure A177). Hours over 10 photos/m²/sec PAR was positively associated with chl-a and biovolume with an RVI of 1 in both models. In the total abundance model, hours over 10 photos/m²/sec PAR and cumulative hours submerged both had RVIs of one. Cumulative hours submerged was the second most

important predictor of total biovolume with an RVI of 0.93. In total abundance and biovolume models, cumulative hours submerged had a negative association with productivity.

Periphyton samplers that were frequently beyond the limit of the riverine photic zone that received less than >10 photos/m²/sec PAR included PR3-4, PD4-3, PD5-4. These sites had markedly lower chl-a (42-77% less) compared to the shallower sampler that received sufficient light at each site (Appendix Z, Figure A175), and they had proportionately more motile diatoms confirming that settlement processes influence productivity at these sites. These depositional sites are likely driving the observed negative relationships with submergence in the dredge models mentioned earlier.

3.9.1.3 Velocity

The periphyton production models (chl-a, total biovolume, total abundance) for all Peace River 2017-2018 samples indicated relationships between physical variables and productivity were weak. The chl-a and total abundances models were the only models with significant associations (the 95% CI of the model coefficient did not cross zero). Velocity was positively associated with chl-a and had an RVI of 0.93. Maximum time submerged had a negative association with total abundance and an RVI of 0.97. The models explained 19% variation of chl-a and 32-35% variation in total abundance. There were no significant associations with the biovolume model and 17-22% of variation was explained.

Velocity, depositional rates and water depth were interrelated. The full transect dredge model (Appendix X) and RF models (Appendix BB) indicated that velocity likely plays a role in periphyton community development. The chlorophyll-a dredge model with all transects included was the only dredge model that had a positive association with velocity. The productivity at samplers with velocities below 0.5 m/s appeared to be influenced by other physical factors. The biovolume periphyton RF model was the only one that had velocity as a top predictor. The effect of velocity in these models is probably a result of site differences which are caused by the combined effects of deposition, light, and velocity. For example, PD4 had low velocity and low chlorophyll-a through the combined effects of deposition and turbidity shading.

3.9.1.4 Site

The RF model and the random effect used in the dredge model demonstrated site-level differences in periphyton productivity metrics (Appendix BB and Appendix X, respectively). These differences were expected, given the differing light, velocity, and substrate conditions between sites and transects. Site was the top predictor of chl-a with a VIMP of 1.27, PR1 had higher chl-a compared to the other sites and it was the fourth most important predictor for total biovolume and total abundance with VIMP of 186 and 2.39×10^9 , respectively. The 2017 and 2018 periphyton abundance and biovolume were generally greater at PD2 and PD3 than they were at PD4 and PD5 further downstream. PR1 and PR2 had the highest chlorophyll-a of all sites due to reservoir recruitment, *Didymo* proliferation, and higher light intensities when compared to downstream sites with more turbidity. These PR sites have shown high productivity across most years and most periphyton biomass metrics. *Didymo* growth at PR sites varied annually, but did best during controlled, moderate flows with high light conditions. It would be reasonable to expect similar *Didymo* densities downstream of Site C Reservoir.

Although most of the 2018 HD and MD samplers were lost to high flows, Halfway and Moberly rivers showed lower periphyton productivity relative to adjacent PR sites in the Peace River mainstem.

3.9.1.5 Season

The effects of season are a composite of flows, light and turbidity, water temperature, day length and weather. In the RF periphyton productivity models, season was an important predictor (Appendix BB, Figure A184). Season was the most important predictor of total abundance and biovolumes with VIMPs of 4.20×10^9 and 313, respectively. The season predictor showed that Fall had higher mean total abundances and biovolumes compared to Summer. Season was also the second most important chl-a predictor with VIMP of 1.08. Stable fall flows with greater light penetration due to lower overall turbidity resulted in higher productivity than during the high summer flow freshet period (Appendix BB). Periphyton abundance was lower at most riverine sites in the 2017 flood summer session (Jun-Aug) than in other sample sessions. Similarly, chlorophyll-a productivity in the early summer sessions was less than half of the fall sessions. Freshet processes increase water velocity, depth and turbidity, which all act to reduce light and increase scour on the river bottom.

3.9.1.6 Time to peak biomass

Time to peak biomass in the Peace River system is important to the assessment of reach-wide productivity, and can change through the creation of the Site C Reservoir. Peak production and the time required to achieve it has not been explicitly tested, however, samplers that were left in longer because they could not be retrieved due to higher flows in summer 2018 indicated that it took longer than the standard 6-7 week deployment to achieve peak biomass. These samplers remained deployed for 10-11 weeks in summer 2018 (PD2-2 PD3-2 PD3-3 PD3-4 PD5-2 PR1-4) and had 10 to 28% more biovolume than equivalent samples from the standard deployment.

3.9.1.7 Summary

In summary, key factors driving periphyton productivity metrics that can be directly affected by flow regulation were: 1) Submergence, 2) Light (turbidity), and 4) Site. These factors are followed by 4) Season and 5) Velocity, which varied more with annual physical patterns (e.g., depth and light) and site-level effects than they did with the timing or magnitude of flows.

3.9.2 Rock Basket River Samples

3.9.2.1 Site

Site was the most important predictor in the RF models for invertebrate abundance, the second most important predictor for good fish forage biomass (EPT+D) and the third most important predictor for invertebrate biomass. Site is itself a combination of flows, velocity, light and substrate. The Variable Importance (VIMP) for abundance, biomass and fish forage were 2.20×10^6 , 1.00×10^4 and 1.61×10^4 , respectively (Figure A200). The RF models explained more variation in biomass and good fish forage biomass than invertebrate abundance. The percent variation explained by the RF abundance model was 16%, whereas the invertebrate biomass and good fish forage biomass models explained 28% and

34%, respectively (Appendix FF). Interestingly, PR1 had very high invertebrate abundances, but biomass was lower compared to other sites. Summer 2017 and 2018 had high invertebrate abundances at PR1 that was a result of abundant chironomids. The RF models suggested that invertebrate densities do not vary significantly between the summer and fall sampling sessions (Appendix FF, Figure A197), but total and fish food (EPT+D) biomass increased as a year progressed (Appendix FF, Figure A198 and Figure A199). In 2017-2018, PD4-PD5 had lower invertebrate biomass and fish food compared to the upstream PD sites. The highest invertebrate biomass of all sampling sessions were at PD1 in fall 2018 and PD3 in fall 2017. Fall 2017 samples from PR1 and PR2 also had high invertebrate biomasses. Biomass trends were apparently driven by the less abundant, but high biomass EPT taxa. Elucidating the differences between site and physical characteristics like velocity are challenging because of the characteristically patchy distributions the EPT taxa.

3.9.2.2 Velocity

Velocity was the fourth most important predictor of invertebrate biomass with a VIMP of 8.4×10^4 and the fourth most important predictor of fish food with a VIMP of 1.06×10^4 . Invertebrate biomass and fish food were higher at sites with faster velocities. In some cases, it was difficult to separate the effects of velocity on invertebrate productivity from site-level differences and mean sampler depth. For example, the PD1 and PD3 sites had faster velocities and higher biomass compared to other sites (Figure A195). Depth was an important determinant of invertebrate biomass and food for fish biomass, and both of these metrics increased with depth (Appendix EE, Figure A193). The full transect models confirm that velocity was the most important determinant of biomass and biomass of fish food (EPT+D) along with depth (Figure A193), where biomass increased with increasing velocity and depth. The RVI of both depth and velocity in the fish model was 1, whereas the RVI of velocity and depth in the biomass model was 0.99. Samplers at transect positions "3"- "4" are closer to the middle of the river channel which results in higher velocities and less deposition. Invertebrate biomass and fish food biomass (EPT+D) were generally less in shallow, marginal regions of the river and greatest in areas with depths around 2 to 3 m and velocities above 1.0 m/s (Appendix FF, Figure A198 and Figure A199). EPT are the dominant taxa in terms of biomass at most Peace River sites. EPT taxa prefer higher velocities and predominantly cobble substrates (Pastuchova et al. 2008).

3.9.2.3 Season

Season was the most important predictor for the fish food RF and invertebrate biomass RF. Fall had higher fish food and invertebrate biomass compared to Summer. The VIMP for season in the fish food model was 2.83×10^4 and the invertebrate biomass model had a VIMP of 2.98×10^4 .

3.9.2.4 Submergence

Total submergence time explained 29-35% of the variation in the invertebrate production models for the 2010-2011 and 2017-2018 sampling sessions (Appendix CC). For each benthic invertebrate production metric, only one model that included total submergence time as a predictor had $\Delta AIC < 3$, as a result RVIs could not be calculated (Table A23). Total submergence time explained 29% of the variation in invertebrate abundance, 34% of the variation in invertebrate biomass and 35% of the variation in the fish food metric. The

association between submergence time and invertebrate production metrics was strongest from 0-1000 hours. Some samples in summer 2011 and 2017 had total submergence times less than 750 hours that were a result from frequent substrate dewatering. These samplers that experienced frequent dewatering also had lower biomass of EPT+D.

For the 2017-2018 RF models, maximum hours submerged was the fourth most important predictor of abundance with a VIMP of 2.94×10^4 . Invertebrate abundance was higher at sites that had maximum submergence times lower than 500 hours. Hours over 10 photos/m²/sec PAR and mean depth over deployment were the second and third most important predictors of invertebrate abundance. The VIMP for hours over 10 photos/m²/sec PAR and mean depth over deployment were 1.02×10^5 and 5.30×10^4 .

Rock basket samplers were analyzed in dredge models using the full sample transect (Appendix EE), and a subset consisting of only the samplers with a submergence ratio > 0.95 (Appendix DD) to reduce the strong influences of submergence from the models.

When considering the full sampler transect in dredge models, the fish food and invertebrate biomass models explained more variation than the invertebrate abundance model ($R^2=0.24-0.27$). The fish food and invertebrate biomass models explained 38-39% and 41-42% of the variation, respectively. The top predictors of invertebrate abundance were hours over 10 photos/m²/sec PAR (RVI=0.79) and average depth over deployment (RVI=0.76). Submergence is expected to be one of the most important factors affecting benthic abundance in the varial zone of flow regulated riverine areas. However, in this study only the lower varial zone was sampled. The lower varial zone samplers did not undergo frequent dewatering, except for the summer 2017 "1" sampler at PR2, PR3 and all PD sites during the summer 2017 sampling period.

Similar results occurred with dredge models that considered only those samplers submerged for >95% of the deployment period (Appendix DD). The top predictors of the invertebrate biomass and fish food models were average depth over deployment and velocity. Depth was the most important predictor of invertebrate fish food with an RVI of 0.99 and the second most important predictor of biomass with an RVI of 0.79. Velocity was the most important predictor of invertebrate biomass (RVI=0.98) and the second most important predictor of fish food with an RVI of 0.97. The invertebrate biomass model explained 31-38% of the variation, whereas the fish food model explained 31-34% of the variation. The mostly submerged invertebrate abundance model explained 27-28% of the variation and the top predictor was hours over 10 photos/m²/sec PAR (RVI=1). Samples that received more hours of light had higher invertebrate abundances. Thus, in these samples, benthic abundance increased with increasing light intensity and depth (Appendix DD, Figure A188). Invertebrate biomass also increased with depth and velocity.

3.9.2.5 Summary

In summary, based on statistical modelling, key factors under the influence of flow regulation that affected invertebrate abundance, biomass, and fish food biomass (EPT+D) were: 1) Submergence (or depth/light) and 2) Velocity, where both 3) Site and 4) Season were important but were less influenced by fluctuating flows from hydro operations than submergence and velocity.

3.10 Riverine Zooplankton

Some zooplankton were exported from Dinosaur Reservoir to the river and their numbers diminished from 3.14 ± 1.91 indiv/L at PR1, to 0.03 ± 0.03 indiv/L at PR2. Zooplankton density increased at PR3 to 0.12 ± 0.00 indiv/L, likely from zooplankters exported from Moberly Lake. In general, riverine sites are not suitable for zooplankton. Additionally, the pulses in Dinosaur Reservoir zooplankton density were mirrored in the exported zooplankton measured at the PR sites (Appendix Q). These pulses of recruitment would enhance zooplankton production in Site C Reservoir.

No invasive mussel veligers were detected in the 2017 and 2018 zooplankton or periphyton samples from Peace River samples.

3.11 Fish Stomachs

Analysis of the fish stomach contents was limited because invertebrate taxa were determined at the family level, but the propensity for invertebrates to enter drift is sometimes species-specific (Rader, 1997).

Ephemeroptera, Plecoptera, Trichoptera, and Dipterans (EPT+D) are important forage for fish and constituted at least 75% of the taxa in the stomach contents of Arctic Grayling, Mountain Whitefish, and Rainbow Trout (Figure 3-3). Fish stomach data from 2010-2012 and 2017-2018 indicated that Dipterans were important forage items in upstream reservoirs. Diptera provided a greater overall percentage of the Mountain Whitefish and Rainbow Trout forage than all other invertebrate taxa. More Ephemeroptera were consumed in Peace River than the upstream reservoir, where these taxa are much less abundant (Appendix R).

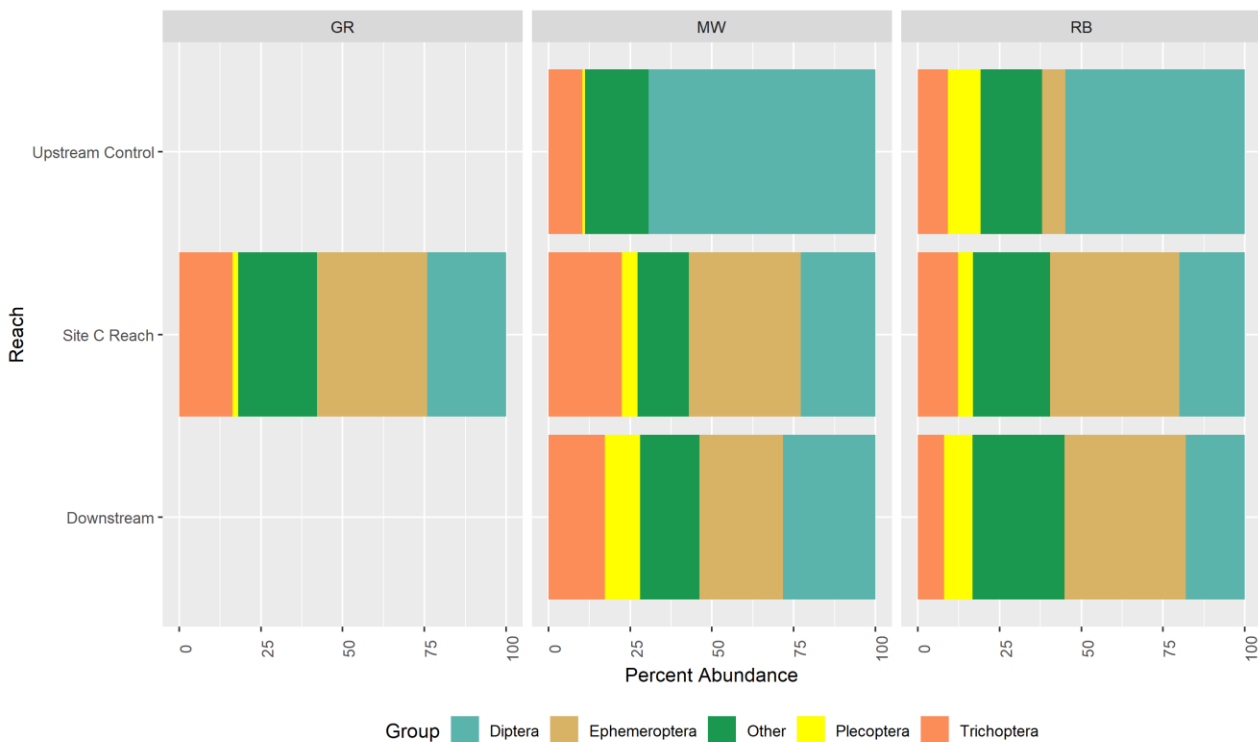


Figure 3-3: Relative abundance of Diptera, Ephemeroptera, Plecoptera, and Trichoptera in Arctic Grayling (GR), Mountain Whitefish (MW), and Rainbow Trout (RB).

Fish species explained 6% of the variation in the invertebrate community composition of fish stomachs (Appendix GG). Arctic Grayling and Rainbow Trout had similar invertebrate community composition, whereas Mountain Whitefish had a distinct community composition (Figure A201). The NMDS axis 1 that separated Rainbow Trout and Arctic Grayling from Mountain Whitefish was positively correlated with Corixidae (NMDS1=0.25, $R^2=0.1$). The Trichopteran families of Glossosomatidae (NMDS1=-0.31, $R^2=0.11$) and Hydropsychidae (NMDS1=-0.27, $R^2=0.09$) were negatively correlated with NMDS axis 1. NMDS axis 1 was also negatively associated with the Ephemeroptera family Heptageniidae (NMDS1=-0.22, $R^2=0.14$).

Ephemeroptera including the family Baetidae were more abundant in the fish stomachs of Rainbow Trout (RB) in the Peace River compared to Mountain Whitefish (MW) (Appendix GG). In the Site C reach, the percent abundance of Ephemeroptera was $51\pm 36\%$ in RB and $17\pm 28\%$ in MW. RB stomach samples had $68\pm 27\%$ Ephemeroptera in the Downstream reach compared to $14\pm 19\%$ in MW. Similarly, percent Baetidae was $5.8\pm 6.3\%$ in MW and $30\pm 36\%$ in RB in the Site C Reach. The Downstream reach had a higher percent Baetidae of $64\pm 35\%$ in RB stomachs compared to $9.4\pm 16\%$ in MW stomachs. Corixidae were only present in the fish stomachs of RB (Figure A205).

Glossosomatidae (Trichoptera) were more abundant in the MW stomach samples than RB stomach samples collected from the Peace River. In the Site C Reach, MW had a percent Glossosomatidae of $18\pm 23\%$ and RB had a percent Glossosomatidae of $4.3\pm 3.7\%$. Glossosomatidae were not present in any of the RB stomachs samples from Downstream reach. However, in the MW stomachs of the Downstream reach the percent Glossosomatidae was $36\pm 37\%$.

The percent abundance of chironomids had high variability in fish stomachs of Rainbow Trout and Mountain Whitefish collected from Dinosaur Reservoir and Site C reach (Figure A204). In the downstream reach, RB had a lower percent abundance of chironomids ($5.7\pm 5.4\%$) compared to MW ($26\pm 37\%$).

The nearest productivity sampling site that a fish was caught at explained 9% of the variation in the invertebrate community composition of fish stomachs, whereas reach explained 6% of the community variation. The fish stomachs collected from Dinosaur Reservoir had distinct invertebrate communities compared to the Peace River sites.

4.0 DISCUSSION

Many co-ordinating monitoring programs are needed to assess the influences of the Project on the Peace River. The objectives of the monitoring programs covered in this report are:

- Mon-6 was designed to understand phytoplankton, zooplankton, periphyton and invertebrate (food for fish) productivity and the underlying physical processes that support benthos productivity in the Site C reach, pre- and post-flooding. The Site C reach will be compared against reference sites in Williston and Dinosaur Reservoirs in a BACI style study design as part of a long-term monitoring program being conducted at a reach-wide scale on the Peace River.
- Mon-7 was designed to investigate the effects of Project construction, operation, and physical processes on periphyton and invertebrate production, including fish food organisms, downstream of the Project to Many Islands in Alberta. Physical processes that support benthos are considered in a BACI style study design that is part of a long-term, reach-wide scale monitoring program on the Peace River.

This discussion is based on Mon-6 and Mon-7 results; it considers only the periods prior to the inundation of the Site C reservoir, which is currently under construction. For this reason, the discussion focuses on physical mechanisms affecting productivity in both reservoir and riverine areas, and covers the following:

1. How the impact of physical reservoir processes on periphyton, invertebrates, phytoplankton, and zooplankton in the Williston and Dinosaur (control) reservoirs can help understand potential future Site C Reservoir conditions (Mon-6). Data from the Site C reach, which is currently riverine, is discussed with other riverine data in Mon-7 (Section 4.2) because productivity in the Site C reach and downstream areas are influenced by the same physical processes. Analyzing the pooled riverine data increases the statistical power of analyses.
2. The key physical processes that are influenced by flows or annual patterns that in turn, affect riverine periphyton and invertebrate densities and biomass (benthos productivity) (Mon-7). All data from the pre-inundation period collected in the Site C reach and downstream areas is considered.

4.1 Reservoir (Mon-6)

4.1.1 Physical Parameters

In addition to size, morphometry, and nutrient concentrations, thermal and light profiles are key for understanding reservoir primary productivity. Thermal layering affects water temperatures and directs inflow and outflow layers, while light penetration controls where primary productivity occurs. Thermocline depth in Summer 2017 and 2018 ranged from 10 to 15 m in Williston Reservoir. Only transient, shallow stratification was detected in Dinosaur Reservoir. This is consistent with all other studies (Golder 2012; Harris et al. 2005; Stockner et al. 2001). Previous year-round studies identified Williston Reservoir as dimictic, mixing from top to bottom in spring and fall (Harris et al. 2005). Dinosaur Reservoir is mixed year-round, likely resulting from the less than 5-day water residence time. Lack of stratification in

Dinosaur Reservoir increases its overall heat budget, while maintaining cooler surface water that slows primary production (Wetzel, 2001).

A reservoir photic zone is highly dynamic and depends upon light intensities at the surface, turbidity, water transparency, color, waves, and algal production. For example, the depth of the pelagic photic zone varied seasonally from 3.6 to 12 m (avg ~6 to 7 m) in Williston Reservoir and from 1.5 to 10 m (avg ~7 m) in Dinosaur Reservoir over the years of study. In littoral regions of Dinosaur Reservoir, the photic zone narrowed with increased turbidity to ~6.5 m. Site C Reservoir should also have a photic zone averaging ~6-7m and with an annual range of 1.5-10 m, after the initial flooding phase of one full water exchange to 10 years has passed.

Dinosaur Reservoir's narrow littoral zone was warmer than the larger pelagic zone during the growing season and that will maintain higher productivity than the same area with cooler water. The width of the littoral zone in Dinosaur Reservoir was previously defined to range from 3 to 6 m depth at high water (Blackman and Leering 2006; Harris et al., 2005; Golder 2009a; Golder 2012). Our results agree with the estimated maximal extent of the littoral zone of 6 to 6.5 m of water depth, since we have demonstrated periphyton growth and low but sufficient light to the substrates for primary production during most of the growing season at 6.5 m. Light models support these observations and confirm their suitability for estimating river or reservoir bed light intensities.

Using the available metrics and data collected to date (2010-2012, 2017 and 2018), both Williston and Dinosaur reservoir pelagic areas are classified as ultra-oligotrophic to oligotrophic, and their littoral areas as oligotrophic (AIM 2000, Stockner et al. 2001, 2005, Harris et al. 2005, Euchner 2011, Golder 2009a).

Nutrient sources are critical to productivity in Peace River reservoirs. Tributaries are key nutrient sources after the initial reservoir flooding nutrient surge has passed. Nutrients imported by tributaries, and their intrusion depth in each reservoir, are important to phytoplankton production (BC Hydro 2013). The ashfall from wildfires in summer 2018 likely provided biologically available phosphorus and contributed to a temporary increase in both the trophic status and productivity in late summer. A warming climate is predicted to cause increased intense wildfires (BC MoE 2019), and this intermittent nutrient source may be important to Site C Reservoir productivity.

4.1.2 Reservoir Phytoplankton

Phytoplankton samples from both Williston and Dinosaur reservoirs in 2017 and 2018 had similar communities that were numerically dominated by pico-cyanobacteria with brief pulses of diatoms, flagellates and green algae; productivity was, however, generally low. High diatom productivity in late summer 2018 resulted in unusually high productivity metrics that in turn, increased zooplankton metrics. Stockner et al. (2005) determined that most of the phytoplankton taxa in Dinosaur Reservoir were recruited from Williston Reservoir. Harris et al. (2005) determined that light and the major nutrients phosphorus and nitrogen co-limited Williston Reservoir. Data from 2017 and 2018 support this conclusion, but we could not explicitly test this because of pseudo-replication. The water quality sampling program only sampled at one location in the littoral zone for each sampling session. The water quality measurement is pseudo-replicated five times because there are five samples in the littoral zone. Littoral zone phytoplankton samples from Dinosaur Reservoir in 2017 and 2018 captured the influence of periphyton dislodged from shallow substrates by wave turbulence.

Dinosaur Reservoir littoral areal biomass production estimates of standing crop were calculated by taking the littoral area estimate of ~2.56 km² and multiplying by the average phytoplankton and periphyton chlorophyll-a for D1-L in 1 m depth increments to yield a rough estimate of ~26 metric tons (wet weight) standing crop during the growing season.

The CE-QUAL-W2 model (Vol 2, App P, Part I, BC Hydro 2013) forecasts seasonal algal biomass peaks in July through September forced almost exclusively by nutrient loadings from the tributaries. The 2017-2018 data also indicate low reservoir nutrient status, making nutrients imported by tributaries, and their intrusion depth in each reservoir, important to phytoplankton production. Although nutrients are lost from the reservoirs as plankton exports, plankton are important inputs downstream reservoirs and river reaches. Phytoplankton contributions to downstream periphyton abundance were greatest in the spring and ranged from 1 to 14% in 2010, 2017 and 2018 samples.

4.1.3 Reservoir Zooplankton

Total zooplankton biomass fluctuated with the phytoplankton densities they feed on, both between seasons and among years. Williston Reservoir generated higher zooplankton densities than Dinosaur Reservoir in 2017 and 2018, consistent with previous studies in 2010-2012 and earlier (Golder, 2012; Harris et al. 2005). In Dinosaur Reservoir, productivity in the narrow littoral zone was three times greater per unit area than productivity in the much larger pelagic zone. Littoral zooplankton benefit from the littoral zone periphyton. The Dinosaur Reservoir littoral zone is an important component of reservoir productivity despite its small area, as is often the case in oligotrophic lakes (Vadeboncoeur et al. 2014; Loeb et al. 1983).

Most zooplankton taxa were common to both reservoirs, because of donation and similar growing conditions. The grazing calanoid copepods abundances were usually greatest in both reservoirs, followed by predatory cyclopoid copepods, while the cladoceran abundance was low. These proportions and their low densities indicate oligotrophic conditions in Williston and Dinosaur reservoirs (Haberman and Haldna 2014; Stockner et al. 2005). The smaller micro-grazers such as ciliates and rotifers were common in the pelagic samples and they are consumed by larger zooplankton. This extra step in the food chain reduces the efficiency of the reservoir's food chain (Harris et al. 2005), but rotifers provide an important link between bacteria and predatory benthic invertebrates.

4.1.4 Reservoir Periphyton

Littoral zones provide a significant portion of the overall productivity in most lakes because of periphyton development on well-lit shallow substrates within its photic zone. This is especially true of oligotrophic reservoirs with large draw-downs where phytoplankton and aquatic macrophyte contributions are small such as reservoirs on the Peace River (Wetzel, 2001). Littoral productivity measurements to date for Williston and Dinosaur reservoirs confirm the importance of their littoral zones to overall reservoir productivity, despite >2 m water level fluctuations in the growing season and >10 m winter draw-downs in the Williston Reservoir (Harris et al. 2005). Littoral zone production is confined to a narrow band of substrates, but these can be "expanded" by large filamentous algae taxa (e.g., *Cladophora* and *Mougeotia*) that increase the littoral surface area by up to 2000 times. Dinosaur Reservoir periphyton showed similar diversity to downstream riverine sites, however areal productivity metrics were 2.5 to 4 times lower than the Peace River sites in all years of study.

The area of productive littoral habitat is constrained by light penetration to the reservoir bed at the deep, outer edge of the photic zone and by submergence times on the shoreward edge of the varial zone. Algal productivity will generally increase with temperature and nutrient concentrations in littoral areas. Periphyton nutrient supplies can cycle between littoral components and be augmented by shoreline detritus, making it less dependent upon the reservoir nutrient status than phytoplankton (Wetzel, 2001). The data collected in Mon-6 indicate that Site C Reservoir should behave similarly to Williston and Dinosaur reservoirs.

4.1.5 Reservoir Invertebrates

The Dinosaur Reservoir sample site had more chironomids and gastropods, but fewer EPT taxa compared to riverine sites in the Peace River; this finding was consistent with invertebrate habitat preferences. Fish stomach data from 2010-2012 and 2017- 2018 indicated that Dipterans were important forage items in Williston and Dinosaur reservoirs. Chironomids are pioneer species that have short life cycles and can quickly establish after a flood or other disturbance (DeWalt and Olive, 1988; McEwen and Bulter, 2010). With flooding of the future Site C Reservoir, we anticipate a reduction in the EPT populations and greater predominance of chironomids and gastropods.

Littoral zones usually have the highest invertebrate productivity within a reservoir. Littoral taxa rely on periphyton for forage and are expected to be confined to the littoral zone. The productivity of invertebrates in the littoral zone of Dinosaur Reservoir was highest when depths were ~2 to 6 m. Less wave action and smaller temperature fluctuations in littoral zones facilitated the establishment of gastropods in Dinosaur Reservoir (McEwen and Butler, 2010; Poznanska et al. 2009). Furthermore, high productivity samples obtained at 6 m depth from summer and fall of 2017 and 2018 in the Dinosaur Reservoir indicated measurable productivity beyond the photic littoral zone. The pelagic zone of reservoirs is known to support chironomids that can utilize the deep profundal substrates (Wagner et al. 2012). Addition of chironomid production in the Dinosaur pelagic region would better estimate its invertebrate productivity and inform forecasts of Site C Reservoir productivity.

4.2 River (Mon-7)

4.2.1 Physical Habitat Parameters

The 2017 and 2018 monitoring showed that temporal and spatial (site) variabilities in incident light, water depth, and turbidity affected submergence patterns and light intensities along the riverbed. These factors influenced productivity of periphyton and invertebrates in the riverine photic zone. Sediment loads originating from tributary plumes or localized deposition processes impacted site turbidity and therefore light conditions. These changes in nearshore light conditions were important because active periphyton growth occurred in bands confined by light penetration (turbidity) on the lower bound and submergence on the upper bound. Growing season temperatures influenced the benthos community composition and reproduction rates (Wetzel, 2001). Understanding the wetted history, as well as light and temperature conditions at each site is necessary to understand both peak biomass growth and total benthic productivity.

4.2.1 River Phytoplankton

Williston and Dinosaur reservoirs were important sources of algal organic material to the downstream Peace River, particularly to sites immediately downstream of a reservoir.

Zooplankton and phytoplankton drift from Dinosaur Reservoir and possibly from Moberly Lake represent taxa and nutrient imports to the Site C reach. Some consideration should be given to reservoir imports in productivity modeling, particularly in areas immediately downstream of dams. Further, *Didymo* growth at PR sites varied annually, but did best during controlled, moderate flows with high light conditions. It would be reasonable to expect similar *Didymo* densities downstream of Site C Reservoir.

4.2.2 River Periphyton

The main producers of chlorophyll-a in the Peace River periphyton were algae. Other primary producers such as photosynthetic bacteria and terrestrial detritus made smaller contributions in the Site C reach and were more important at the downstream PD sites.

Taxonomic indices of shear, depositional rates, and reservoir recruitment indicated that the Peace River is a turbid, dynamic system subject to high flows and highly variable light and submergence conditions. The key factors that influenced riverine periphyton productivity – substrate submergence, light, velocity, reservoir exports – are discussed below in order of importance.

Modelling of the 2010-2011 and 2017-2018 determined annual, seasonal and site variability were more important determinants of periphyton productivity in riverine areas than substrate submergence. However, when only the 2017-2018 periphyton data was considered included samples that were in the upper varial zone, abundance and chl-a increased with longer durations of substrate submergence. Periods of periphyton growth and death in the varial zone were attributed to changes in water level and wetting/drying cycles created by operations and major tributary inflows (Halfway, Moberly, Pine, Beaton, Kiskatinaw, Alces, Pouce Coupe, Clear). Numerous sampling efforts demonstrated that upper varial zone productivity was highly variable due to substrate exposure.

Light is often identified as a critical determinant of periphyton productivity in riverine ecosystems (Schleppe et al. 2013; Harris et al. 2005). Sampling in 2017-2018 indicate that a minimum of 40 hours of >10 photons/m²/s is needed to support optimal growth. While submergence patterns defined the upper bounds of the varial zone, light penetration determines its lower bounds (Schleppe and Larratt 2016). Light penetration is limited by turbidity; hence, only a narrow band of peak periphyton production is expected in turbid reaches (PD sites and some PR3). In shallow sand bar habitats and PR sites where, upstream reservoirs have reduced turbidity, the photic zones were wider. Turbidity was frequently high enough to reduce light penetration to the riverbed, and ultimately this reduced production from primary producers in deep water. For example, periphyton samplers that were frequently beyond the limit of the riverine photic zone based on light data (PR3-4, PD4-3 and PD5-4) had markedly lower productivity and diversity but proportionately more motile diatoms than sites with more light. Freshet and intense summer storms increased turbidity and decreased periphyton productivity particularly at sites affected by tributaries. At light-limited sites, productivity was determined by a combination of settlement of upstream production and in situ growth of low light-tolerant taxa. An increase in available light is expected downstream of Site C Reservoir after its construction is complete.

These two physical factors, substrate submergence and turbidity, combine to limit the spatial extent of areas where new periphyton growth can occur. In contrast, deposition resulting

from scour in upstream areas or from immigration from reservoir phytoplankton is controlled by deposition patterns, not submergence or turbidity. It was less important than in situ periphyton growth, but was significant, accounting for 3.3-61% of abundance at PR1. Reservoir exports of phytoplankton/periphyton contributed to the overall productivity of PR1 and PR2. In regulated rivers, the contribution to river periphyton production made by imported reservoir algae is often significant (Larratt et al. 2013).

Although velocity is a well-known driver of periphyton production in many large rivers, the statistical models identified that velocity has only a minor influence at the Peace River sites. The maximum velocity of the samplers in the PR and PD reaches (2.09 m/s at PD3-4) was lower than the velocity where scour is known to occur (Flinders and Hartz 2009; Luce et al. 2010; Schleppe and Larratt, 2016). At velocities below 0.5 m/s, biomass was more variable because settlement of algae originating from upstream areas augmented productivity in low velocity depositional areas of the river (Schleppe et al. 2014).

Areas with high depositional rates had less diverse periphyton communities because these areas favor taxa that are motile and tolerant of low light (Schleppe et al. 2014). High periphyton biovolume occurred in areas where light penetration was low because deposition of algae cells from upstream areas augmented and local growth of low light-tolerant motile taxa and cyanobacteria.

In summary, data from Mon-6 and Mon-7 indicate that the time substrates spent submerged in water with adequate light is likely the most important determinant of areas contributing new productivity in the Peace River, as it is in other hydro-influenced systems (Schleppe et al. 2011; Jones, 2011; Perrin and Bennet 2013). Bands of periphyton production occurred along the river margins and bars. Productivity in these bands was usually limited by submergence at the upper boundary and light penetration to the substrates at the lower boundary, with turbidity being the most important factor governing light penetration. Sediment deposition rates were also important to periphyton production metrics, with greater periphyton biovolume likely in areas where deposition is high.

Table 4-1: Riverine Periphyton Comparison

Metric	Oligotrophic or stressed	Typical large rivers*	Eutrophic or productive	PR Site C Reach	PD down stream
Taxa richness(live & dead)	<20 – 40	25 – 60	variable	17 - 21	8 – 20
Chlorophyll-a ug/cm ²	<2	2 – 5	>5–10 (30+)	2.0 – 3.6	1.4 – 3.8
Algae density cells/cm ²	<0.2 x10 ⁶	1 - 4 x10 ⁶	>10 x10 ⁶	0.9– 1.8 x10 ⁶	0.2–1.5 x10 ⁶
Algae biovolume cm ³ /m ²	<0.5	0.5 – 5	20 - 80	2.9 - 6.7	3.0 – 6.5
Diatom density frustules/cm ²	<0.15 x10 ⁶	1 – 2-5 x10 ⁶	>10 x10 ⁶	0.0032-6.95x10 ⁶	0.037-6.75x10 ⁶
Biomass – AFDW mg/cm ²	<0.5	0.5 – 2	>3	n/a	n/a

Biomass –dry wt mg/cm ²	<1	1 – 5	>10	n/a	n/a
Bacteria count, HTPC CFU/cm ²	<4 -10 x10 ⁶	0.4–50 x10 ⁶	>50x10 ⁶ – >10 ¹⁰	n/a	n/a
Accrual chlorophyll-a	<0.1	0.1 – 0.6	>0.6	n/a	n/a

Comparison data obtained from Flinders and Hartz 2009; Biggs 1996; Peterson and Porter 2002; Freese et al. 2006; Durr and Thomason 2009; Romani 2001; Biggs and Close 1989. (ug/cm²= 0.1 x mg/m²)

*Rivers include Jackson River, Colorado; New Zealand Rivers (Canterbury); Yellowstone River; River Warnow, Germany; Riera Major, northeastern Spain

4.2.3 Invertebrates

The Peace River is a turbid, dynamic system subject to high flows and variable light and submergence conditions. The key factors that influence riverine invertebrate productivity are all influenced by fluctuating flows. They are presented in order of importance – substrate submergence, velocity and depth, site, and seasonal differences.

Substrate dewatering was a key factor determining benthic invertebrate productivity in the upper varial zone (Schleppe et al. 2018) because the substrate submergence regime defined the upper edge of productive habitat in the Peace River. Extended periods of substrate dewatering reduced invertebrate productivity and altered invertebrate community composition in 2010-2011 and 2017-2018. Submergence times less than 1000 hours, which occurred most often in Summer 2011 and 2017, resulted in lower biomass of EPT+D and invertebrate abundance. The abundance and richness of EPT taxa also decreased after extended periods of dewatering. The invertebrate taxa that have higher resistance to desiccation such as oligochaetes, gastropods and chironomids became the dominant taxa in the upper varial zone (Calapez et al. 2014; Jones 2013). The duration of dewatering in the upper varial zone was an important determinant of the availability of fish food because the higher biomass EPT were less prevalent in these varial zone areas.

The combined effects of velocity and depth were an important factor determining the invertebrate biomass and biomass of EPT+D at PR and PD sites. Densities of Trichopteran and Dipterans have been shown to increase with depth and velocity in other regulated river systems (Jones 2013). The Trichopteran families of Hydropsychidae and Brachycentridae make up a large proportion of the total biomass at the PD sites. Hydropsychidae are known to prefer sites with higher velocities (Georgian and Thorp 1992). Invertebrate biomass and fish food biomass (EPT+D) were generally less in shallow, marginal regions of the river and greatest in areas with depths around 2 to 3 m and velocities above 1.0 m/s. The Middle Columbia River demonstrated a similar interaction between depth and invertebrate biomass and percent Chironomidae in the varial zone (Schleppe et al. 2018). These physical processes determined the deposition rates and invertebrate drift rates that together affect the settlement of invertebrates and their availability as fish forage.

Site differences in invertebrate production and community composition were driven by local velocity, light and sediment deposition rates. They were most evident at PR1 and PD4. PR1 had the greatest biovolume and abundance of Didymo which can influence the distribution of EPT (high individual biomass, low abundance) and Dipteran taxa (low individual biomass, high abundance) (Ladrera 2018). Didymo may have contributed to low summer EPT

abundance but high biovolume at PR1 compared to all other sites. PD4 was turbid and depositional, conditions that caused its low invertebrate biomass and fish food availability compared to PD1-PD3. Depositional conditions at PD4 hindered EPT taxa because they cannot withstand sediment burial and it also lowered their periphyton forage. Low EPT abundances also occurred at PR1 and PR2 in part because there were no adjacent upstream tributaries that could act as a source of invertebrate drift. PR3 did not have favorable conditions for EPT with velocity less than 0.6 m/s and fine substrates.

Seasonal variations in invertebrate community composition and productivity are universal. In the Peace River, the invertebrate biomass and the biomass of EPT+D taxa were higher in the fall than the summer (**Error! Reference source not found.** and **Error! Reference source not found.**). Statistical models and community analyses indicate that there was more fish food in late summer/early fall because of a higher abundance of EPT taxa. Higher fall biomasses were a result of greater EPT abundance and these are shredders and filterers. Higher densities of shredders and filterers in late summer/early fall have been reported in natural river systems (Giller and Twomey 1993). In regulated river systems, Hydropsychidae are more abundant downstream of dams and in warmer months (Plewes et al. 2017). During the summer sampling period, the Peace River had a higher abundance of oligochaetes. The higher abundance of oligochaetes during periods of higher flows has been reported elsewhere because oligochaetes can withstand habitats that have high sediment deposition and high turbidity (Donohue and Irvine 2004; Kang et al 2017; Boulton et al 1992).

Data on the availability of fish food organisms in the Peace River was influenced by seasonal differences and by benthic invertebrate sampling method. Basket samplers (2010-2012 and 2017-2018) capture more EPT taxa compared to Ekman samplers (2017-2018) because the Ekman samplers capture sediment-dwelling taxa such oligochaetes and chironomids. However, the basket samplers may be more representative of the available food for fish because many fish are known to forage on invertebrate drift (Cochran-Biederman and Vondracek, 2017).

Ephemeroptera, Plecoptera, Trichoptera, and Dipterans (EPT+D) were important forage for fish and constituted at least 75% of the taxa in the stomach contents of Arctic Grayling, Mountain Whitefish, and Rainbow Trout collected in this study. However, Rainbow Trout and Mountain Whitefish stomach contents demonstrated their different feeding styles. The Rainbow Trout fish stomachs collected from the Downstream Reach indicated Rainbow Trout were preferentially feeding on invertebrates available in drift such as Ephemeroptera including Baetidae (Rader 1997), while the Mountain Whitefish fed on Glossosomatidae and chironomids that are found near the riverbed (Scott and Crossman 1973). For example, at PD sites in Fall, stomach samples from Rainbow Trout contained 68±27% Ephemeroptera; 0% Trichoptera; 5.7±5.4% chironomids while Mountain Whitefish stomach samples contained 14±19% E; 36±37% T; 26±37% chironomids. These results partially reflect the invertebrates that were available to the fish at the time of sampling. The most abundant invertebrate families at PD1-PD3 in Fall were Brachycentridae, Hydropsychidae, Taeniopterygidae, and Chironomidae in rock basket samplers. Chironomidae and some species of Hydropsychidae have a lower propensity to drift compared to Ephemeroptera families such as Baetidae (Rader 1997).

Because the fish stomach samples collected from Dinosaur Reservoir had distinct invertebrate taxa compared to the Peace River samples, it is reasonable to expect altered fish foraging after Site C is flooded.

Analysis of the fish stomach contents was limited because invertebrate taxa were determined at the family level, but the propensity for invertebrates to enter drift is sometimes species-specific (Rader 1997). Further, the timing of stomach sample collections may also be important when evaluating the importance of fish forage. Consideration of drift guilds identified in Rader (1997) would provide further insights regarding the importance of different invertebrate species as fish forage and their specific availability as forage for fish in the Peace River.

In summary, data from Mon-6 and Mon-7 indicate that the timing and magnitude of flow fluctuations are important factors influencing invertebrate productivity in the Peace River. In varial zone areas, submergence was the most important determinant of productivity. Within permanently submerged areas, physical processes such as velocity were important to invertebrate productivity.

Periphyton productivity was usually greatest in the permanently wetted shallows while invertebrate biomass was generally less in shallow, marginal regions of the river and greatest in areas with depths around 2 to 3 m and velocities above 1.0 m/s. Peak forage and peak invertebrate biomass was separated laterally at some sites, suggesting that drift and deposition of upstream forage can be important to invertebrates in the Peace River.

5.0 REFERENCES

- Adboller M. 2013. Hydrologic stochasticity and biodiversity of biofilm algae. 1–41. Master Thesis. University of Vienna. URL <http://othes.univie.ac.at/30022/>.
- AIM Ecological Consultants Ltd. 2000. Dinosaur Lake aquatic plant enhancement potential. Peace/Williston Fish and Wildlife Compensation Program Report No. 259. 26pp plus appendices.
- Anderson, M. J. 2001. A new method for non-parametric multivariate analysis of variance. *Austral ecology*, 26(1), 32-46.
- Ashley K.I. 1983. Hypolimnetic aeration of a naturally eutrophic lake: Physical and chemical effects. *Can J Fish Aquat Sci* 40 1343-1359.
- Ateia, M.M., Nasr., A. Ikeda, H. Okada, M. Fujii, M. Natsuike, and C. Yoshimura. 2016. Nonlinear relationship of near-bed velocity and growth of riverbed periphyton. *Water*. 8(10):461.
- Barton, K., 2012. MuMIn: Multi-model inference. R package version 1.7. 7.
- BC Hydro 2013. Environmental Impact Statement – Site C Clean Energy Project <http://www.ceaa-acee.gc.ca/050/document-eng.cfm?document=85328>
- BC Hydro. 2015. Fisheries and Aquatic Habitat Monitoring and Follow-up Program Site C Clean Energy Project. <https://www.sitecproject.com/sites/default/files/Fisheries%20and%20Aquatic%20Habitat%20Monitoring%20and%20Follow-up%20Program.pdf>
- BC MoE (2019) Impacts of Climate Change. <https://www2.gov.bc.ca/gov/content/environment/climate-change/adaptation/impacts>
- Beak Consultants – CANMET. 1995. Field Evaluation of Aquatic Effects Monitoring Methods Pilot Study Volume 1 - Report Sponsored by Canada Centre for Mineral and Energy Technology (CANMET) Mining Association of Canada on Behalf of: Aquatic Effects Technology Evaluation (AETE).
- Benke, A. C., Huryn, A. D., Smock, L. A., & Wallace, J. B. 1999. Length-mass relationships for freshwater macroinvertebrates in North America with particular reference to the southeastern United States. *Journal of the North American Benthological Society*, 18(3), 308–343. doi:10.2307/1468447.
- Blackman, B.G. and D.M. Cowie. 2005. 2004 Assessment of Habitat Improvements in Dinosaur Reservoir. Peace/Williston Fish and Wildlife Compensation Program Report No. 299. 9 pp.
- Blackman, B.G. and G. Leering. 2006. Dinosaur Reservoir Strategic Implementation Plan: Dinosaur Reservoir 2006 Five Year Action Plan.
- Bradford, Michael J, Josh Korman, and Paul S Higgins. 2005. “Using Confidence Intervals to Estimate the Response of Salmon Populations (*Oncorhynchus* Spp.) to Experimental Habitat Alterations.” *Canadian Journal of Fisheries and Aquatic Sciences* 62 (12):2716–26. <https://doi.org/10.1139/f05-179>.

- Biggs, B. J. F., & Close, M. E. (1989). Periphyton biomass dynamics in gravel bed rivers: the relative effects of flows and nutrients. *Freshwater Biology*, 22(2), 209–231. doi:10.1111/j.1365-2427.1989.tb01096.x.
- Biggs, B. (1996). Hydraulic disturbance as a determinant of periphyton development in stream ecosystems. University of Canterbury. Retrieved from <http://ir.canterbury.ac.nz/handle/10092/4891>.
- Bothwell, Max L. 1988. "Growth Rate Responses of Lotic Periphytic Diatoms to Experimental Phosphorus Enrichment: The Influence of Temperature and Light." *Canadian Journal of Fisheries and Aquatic Sciences* 45 (2): 261–70. <https://doi.org/10.1139/f88-031>.
- Boulton, A. J., & Lake, P. S. (1992). Benthic organic matter and detritivorous macroinvertebrates in two intermittent streams in south-eastern Australia. *Hydrobiologia*, 241(2), 107-118.
- Burnham, K. P., & Anderson, D. R. (2002). Model selection and multimodel inference: a practical information-theoretic approach. (Springer-Verlag, Ed.) *Ecological Modeling* (Vol. 172, p. 488). Springer. doi:10.1016/j.ecolmodel.2003.11.004.
- Calapez, A. R., Elias, C. L., Almeida, S. F., & Feio, M. J. (2014). Extreme drought effects and recovery patterns in the benthic communities of temperate streams. *Limnetica*, 33(2), 281-296.
- Carpenter, Bob, Andrew Gelman, Matthew D. Hoffman, Daniel Lee, Ben Goodrich, Michael Betancourt, Marcus Brubaker, Jiqiang Guo, Peter Li, and Allen Riddell. 2017. "Stan: A Probabilistic Programming Language." *Journal of Statistical Software* 76 (1). <https://doi.org/10.18637/jss.v076.i01>.
- Carlson, R.E. 1983. Discussion on "Using differences among Carlson's trophic state index values in regional water quality assessment," by Richard A. Osgood. *Water Resources Bulletin*. 19:307-309.
- Carlson R.E., Simpson J. 1996, Coordinator's Guide to Volunteer Lake Monitoring Methods, North American Lake Management Society, <http://dipin.kent.edu/tsi.htm>.
- Ceola S., Hödl I., Adlboller M., Singer G., Bertuzzo E., Mari L. 2013. Hydrologic variability affects invertebrate grazing on phototrophic biofilms in stream microcosms. *PLoS ONE* 8: e60629.
- Clarke, K., Chapman, M., Somerfield, P., and Needham, H. 2006. Dispersion-based weighting of species counts in assemblage analyses. *Marine Ecology Progress Series*, 320(1), 11–27. doi:10.3354/meps320011
- Clarke, K. R., & Warwick, R. M. 1998. Quantifying structural redundancy in ecological communities. *Oecologia*, 113(2), 278-289.
- Cochran-Biederman, J. L., & Vondracek, B. (2017). Seasonal feeding selectivity of brown trout *Salmo trutta* in five groundwater-dominated streams. *Journal of Freshwater Ecology*, 32(1), 653-673.
- Crossman, E. J., & Scott, W. B. (1973). *Freshwater fishes of Canada*. Ottawa: Fisheries Research Board of Canada.

- Davies-Colley, R.J., and John W. Nagels. 2008. "Predicting Light Penetration into River Waters." *Journal of Geophysical Research* 113 (G3). <https://doi.org/10.1029/2008JG000722>.
- De'ath, G., & Fabricius, K. E. (2000). Classification and regression trees: a powerful yet simple technique for ecological data analysis. *Ecology*, 81(11), 3178-3192.
- Depew, D.C. 2009. *Cladophora growth in littoral environments of Large Lakes: Spatial complexity and ecological interpretations* A thesis presented to the University of Waterloo in fulfillment of the thesis requirement for the degree of Doctor of Philosophy in Biology Waterloo, Ontario, Canada.
- DeWalt, R. E., & Olive, J. H. (1988). Effects of eroding glacial silt on the benthic insects of Silver Creek, Portage County, Ohio.
- Donohue, I., & Irvine, K. (2004). Seasonal patterns of sediment loading and benthic invertebrate community dynamics in Lake Tanganyika, Africa. *Freshwater biology*, 49(3), 320-331.
- Dürr, S., & Thomason, J.C. 2009. *Biofouling*. ISBN: 978-1-405-16926-4 Dec 2009, Wiley-Blackwell 456 pages.
- EBA 2012. *SITE C CLEAN ENERGY PROJECT VOLUME 2 APPENDIX H TECHNICAL DATA REPORT: RESERVOIR WATER TEMPERATURE AND ICE REGIME* Prepared for BC Hydro Power and Authority. Lead Author: Justin Rogers, M.Sc. and James Stronach Ph.D., P.Eng.
- ESSA, Limnotek, and Golder 2012. *Future Aquatic Conditions in the Peace River. Site C Clean Energy Project, BC Hydro. Environmental Impact Assessment. Volume 2 Aquatic Productivity Reports, Part 3 Future Aquatic Conditions in the Peace River.* Prepared for BC Hydro. October 10, 2012. 131 p. + 6 app.
- ESRI. (2018). *Release 10.6: ArcGIS Desktop*. Redlands, CA: Environmental Systems Research Institute.
- Euchner, T. 2011. *Dinosaur Reservoir Sampling and Literature Review* Prepared by Diversified Environmental Services. www.sitecproject.com/sites/default/files/2010-dinosaur-reservoir-sampling-literature-review.pdf
- Foundry Spatial Ltd, 2011. <https://foundryspatial.com/>
- Freese, H. M., Karsten, U., & Schumann, R. (2006). Bacterial abundance, activity, and viability in the eutrophic River Warnow, northeast Germany. *Microbial Ecology*, 51(1), 117–127. Retrieved from <http://www.ncbi.nlm.nih.gov/pubmed/16395540>.
- Gelman, A. (2008). Scaling regression inputs by dividing by two standard deviations. *Statistics in Medicine*, 27(October 2007), 2865–2873. doi:10.1002/sim
- Georgian, T., & Thorp, J. H. (1992). Effects of microhabitat selection on feeding rates of net-spinning caddisfly larvae. *Ecology*, 73(1), 229-240.
- Giller, P. S., & Twomey, H. (1993, November). Benthic macroinvertebrate community organisation in two contrasting rivers: between-site differences and seasonal patterns. In *Biology and Environment: Proceedings of the Royal Irish Academy* (pp. 115-126). Royal Irish Academy.

- Golder Associates Ltd. 2009a. Baseline data collection: Peace River watershed water quality and Dinosaur Lake limnology sampling – 2008. Prepared for BC Hydro, Vancouver, BC. 87pp.
- Golder Associates Ltd. 2009b. Large River Fish Indexing Program – Lower Columbia River 2008 Phase 8 Investigations. Report prepared for BC Hydro, Castlegar, B.C. Golder Report No. 08-1480-0046F: 58 p. + 6 app.
- Golder Associates Ltd. 2012. Hydrodynamic, Water Quality and Productivity Modelling for the Site C Project. Site C Clean Energy Project, BC Hydro. Environmental Impact Statement. Volume 2 Appendix P Aquatic Productivity Reports, Part 2 Hydrodynamic, Water Quality and Productivity Modelling for the Site C Project. Prepared for BC Hydro. December 3, 2012. 121 p. + 5 app.
- Grueber, C. E., Nakagawa, S., Laws, R. J., & Jamieson, I. G. 2011. Multimodel inference in ecology and evolution: challenges and solutions. *Journal of Evolutionary Biology*, 24(4), 699–711. doi:10.1111/j.
- Haberman, J. and M. Haldna 2014. Indices of Zooplankton Community as Valuable Tools in Assessing the Trophic State and Water Quality of Eutrophic Lakes: Long Term Study of Lake Vörtsjärv. DOI: 10.4081/jlimnol.2014.828
- Harris, S.L., A.R. Langston, J.G. Stockner and L. Vidmanic 2005. A Limnological Assessment of Four Williston Reservoir Embayments, 2004. Peace/Williston Fish and Wildlife Compensation Program Report No. 305. 48pp. plus appendices.
- Hastie, T., Tibshirani, R., & Friedman, J. (2001). The elements of statistical learning: data mining, inference and prediction. New York: Springer-Verlag, 1(8), 371-406.
- Hauer, F.R. and C.N. Spencer, 1998. Phosphorus and Nitrogen Dynamics in Streams Associated with Wildfire: A Study of Immediate and Long-term Effects. *Int. J. Wildland Fire* 8(4): 183-198, 1998 IAWF.
- Hawes, K., H. Larratt, and N. Swain. 2014. Lower Columbia River Aquatic Receiving Environment Monitoring Program for the Teck Metals Ltd. Trail Smelter – Annual Data Collection and Interpretation Report. Ecoscape Environmental Consultants Ltd. 148pp.
- Hill, W.R. and S.E. Fanta, 2008. Phosphorus and light colimit periphyton growth at subsaturating irradiances *Freshwater Biology* (2008) 53, 215–225.
- Hillebrand, H. G. de Montpellier and A. Liess, 2004. Effects of Macrograzers and Light on Periphyton Stoichiometry. *Oikos* Vol. 106, No. 1 (Jul., 2004), pp. 93-104.
- Jassby A.D. & Platt T. (1976) Mathematical formulation of the relationship between photosynthesis and light for phytoplankton. *Limnology and Oceanography*, 21, 540–547.
- Jones, N.E. 2011. Benthic Sampling in Natural and Regulated Rivers. Sampling Methodologies for Ontario's Flowing Waters. Ontario Ministry of Natural Resources, Aquatic Research and Development Section, River and Stream Ecology Lab, Aquatic Research Series 2011-05 .
- Jones, N. E. (2013). Spatial patterns of benthic invertebrates in regulated and natural rivers. *River Research and Applications*, 29(3), 343-351.

- Jones, Z., & Linder, F. (2015, April). Exploratory data analysis using random forests. In Prepared for the 73rd annual MPSA conference.
- Julian, J. P., M. W. Doyle, and E. H. Stanley. 2008. "Empirical Modeling of Light Availability in Rivers." *Journal of Geophysical Research* 113 (G3). <https://doi.org/10.1029/2007JG000601>.
- Jun, S. (2013). Boosted regression trees and random forests. (Statistical Consulting Report). Vancouver, BC: Department of Statistics, UBC.
- Kang, H., Bae, M. J., Lee, D. S., Hwang, S. J., Moon, J. S., & Park, Y. S. (2017). Distribution Patterns of the Freshwater Oligochaete *Limnodrilus hoffmeisteri* Influenced by Environmental Factors in Streams on a Korean Nationwide Scale. *Water*, 9(12), 921.
- Kasprzak, Peter & Padisak, Judit & Koschel, Rainer & Krienitz, Lothar & Gervais, Frank. (2008). Chlorophyll a concentration across a trophic gradient of lakes: An estimator of phytoplankton biomass?. *Limnologica - Ecology and Management of Inland Waters*. 38. 327-338. 10.1016/j.limno.2008.07.002.
- Kery, M., and M. Schaub. 2011. Bayesian Population Analysis Using WinBUGS : A Hierarchical Perspective. Boston: Academic Press. <http://www.vogelwarte.ch/bpa.html>.
- Kilroy C. and M.L. Bothwell, 2011. *Didymosphenia geminata* growth rates and bloom formation in relation to ambient dissolved phosphorus concentration. IN *Freshwater Biology 2012 vol 57 pg 641-653*.
- Kennedy, T. A., Muehlbauer, J. D., Yackulic, C. B., Lytle, D. A., Miller, S. W., Dibble, K. L., and Baxter, C. V. (2016). Flow management for hydropower extirpates aquatic insects, undermining river food webs. *BioScience*, biw059.
- Ladrera, R. 2018. Effects of *Didymosphenia geminata* massive growth on stream communities: Smaller organisms and simplified food web structure. *PLoS One*. 2018; 13(3): e0193545. doi: 10.1371/journal.pone.0193545
- Larratt, H., J., Schleppe, M.A., Olson-Russello, and N. Swain. (2013). Monitoring Study No. CLBMON-44 (Year 5) Lower Columbia River Physical Habitat and Ecological Productivity, Study Period: 2012. Report Prepared for BC Hydro, Castlegar, British Columbia. 97 p. Report Prepared by Ecoscape Environmental Consultants Ltd.
- Liaw, A., & Wiener, M. (2002). Classification and regression by randomForest. *R news*, 2(3), 18-22.
- Limnoteck and Golder. 2012. Site C Clean Energy Project: EIS Technical Appendix: Baseline Aquatic Productivity. Volume 2; Appendix P Part 1. Prepared for BC Hydro.
- Loeb S.L., Reuter J.E., Goldman C.R., 1983. Littoral zone production of oligotrophic lakes. In: Wetzel R.G. (eds) *Periphyton of Freshwater Ecosystems*. Developments in Hydrobiology, vol 17. Springer, Dordrecht
- Luce, J. J., Cattaneo, A., & Lapointe, M. F. (2010). Spatial patterns in periphyton biomass after low-magnitude flow spates: geomorphic factors affecting patchiness across gravel-cobble riffles. *Journal of the North American Benthological Society*. doi:10.1899/09-059.1

- May L, O'Hare M., 2005. Changes in rotifer species composition and abundance along a trophic gradient in loch Lomond, Scotland, UK. *Hydrobiologia*. 2005;54:397–404.
- McElreath, Richard. 2016. *Statistical Rethinking: A Bayesian Course with Examples in R and Stan*. Chapman & Hall/CRC Texts in Statistical Science Series 122. Boca Raton: CRC Press/Taylor & Francis Group.
- McEwen, D. C., & Butler, M. G. (2010). The effects of water-level manipulation on the benthic invertebrates of a managed reservoir. *Freshwater Biology*, 55(5), 1086-1101.
- Mulholland, P.J., E.R. Marzolf, S.P. Hendricks, R.V. Wilkerson, and A.K. Baybayan 1995. Longitudinal Patterns of Nutrient Cycling and Periphyton Characteristics in Streams: A Test of Upstream-Downstream Linkage. *FreshWater Science* Volume 14, Number 3 | Sep., 1995.
- Oksanen, J., Blanchet, F. G., Friendly, M., Kindt, R., Legendre, P., McGlin, D., & Solymos, P. (2017). *vegan: Community Ecology Package*. R package version 2.4-3. 2017 [accessed 2016 Jan 1].
- Pastuchova, Z., M. Lehotsky, A. Greskova. 2008. Influence of morphohydraulic habitat structure on invertebrate communities (Ephemeroptera, Plecoptera, and Trichoptera). *Biologia*. Vol. 63. 720-729.
- Passy, S. I. (2007). Diatom ecological guilds display distinct and predictable behavior along nutrient and disturbance gradients in running waters. *Aquatic botany*, 86(2), 171-178.
- Perrin, C.J. and B. Chapman, 2010. Middle Columbia River Ecological Productivity Monitoring, 2009. Report Prepared by Golder Associates Ltd. And Limnotek Research and Development Inc. for BC Hydro. 52 pPerrin, C. and B. Chapman. 2010. Columbia River Project Water Use Plan: Middle Columbia River Ecological Productivity Monitoring. Golder Associates. Report No. 09-1480-0036. 54 pp. Study Period: 2009.
- Perrin, C.J. and S.A. Bennett. 2013. Aberfeldie water use plan: Primary and secondary productivity monitoring. Report prepared by Limnotek Research and Development Inc. for BC Hydro. 52p.
- Peterson, D. A., & Porter, S. D. (2002). Biological and chemical indicators of eutrophication in the Yellowstone River and major tributaries during August 2000. National Water Quality Monitoring Council.
- Plewes, R., H. Larratt, M.A. Olson-Russello. 2017. Monitoring Study No. CLBMON-44 (Year 9) Lower Columbia River Physical Habitat and Ecological Productivity, Study Period: 2016. Prepared for BC Hydro, Castlegar, British Columbia. 62 pgs + Appendices. Prepared by: Ecoscape Environmental Consultants Ltd.
- Poznańska, M., Kobak, J., Wolnomiejski, N., & Kakareko, T. (2009). Shallow-water benthic macroinvertebrate community of the limnic part of a lowland Polish dam reservoir. *Limnologia*, 39(2), 163-176.
- R Core Team. 2018. "R: A Language and Environment for Statistical Computing." Vienna, Austria: R Foundation for Statistical Computing. <http://www.R-project.org/>.

- Rader, R.B. 1997. A functional classification of drift: traits that influence invertebrate availability to salmonids. *CJFAS* 54: 1211-1234.
- Richards, A. B., & Rogers, D. C. 2011. Southwest association of freshwater invertebrate taxonomists (SAFIT), list of freshwater macroinvertebrate taxa from California and adjacent states including standard taxonomic effort levels. March 2011.
- Rimet, F., & Bouchez, A. (2011). Use of diatom life-forms and ecological guilds to assess pesticide contamination in rivers: lotic mesocosm approaches. *Ecological indicators*, 11(2), 489-499.
- Rimet, F., & Bouchez, A. (2012). Life-forms, cell-sizes and ecological guilds of diatoms in European rivers. *Knowledge and management of Aquatic Ecosystems*, (406), 01.
- Romani A.M., and Sabater S. 1999. Epilithic ectoenzyme activity in a nutrient-rich Mediterranean river. *Aquatic Sci* 61: 122–132.
- Romaní, A. M., & Sabater, S. 2001. Structure and activity of rock and sand biofilms in a Mediterranean stream. *Ecology*, 82(11), 3232-3245.
- Romani A.M., Guasch H., Munoz I., Ruana J., Vilalta E., Schwartz T. 2004. Biofilm structure and function and possible implications for riverine DOC dynamics. *Microb Ecol* 47: 316–328.
- Sanderson, B.L., H.J. Coe, C.D. Tran, K.H. Macneale, D.L. Harstad, and A.B. Goodwin, 2009. Nutrient limitation of periphyton in Idaho streams: results from nutrient diffusing substrate experiments. *Journal of the North American Benthological Society* 28(4), (29 September 2009).<https://doi.org/10.1899/09-072.1>
- Schielzeth, H. 2010. Simple means to improve the interpretability of regression coefficients. *Methods in Ecology and Evolution*, 1(2), 103-113.
- Schleppe, J., H. Larratt, and M.A. Olson-Russello. 2011. CLBMON-15b Middle Columbia River Ecological Productivity Monitoring, Annual Report 2010. Ecoscape Environmental Consultants Ltd. & Larratt Aquatic Consulting Ltd. Ecoscape File No. 10-599 Kelowna, BC.
- Schleppe, J., H. Larratt, A. Cormano, and N. Swain. 2013. Peace River Water Use Plan GSMON5 Peace River Productivity Monitoring, Year 1 Report, 2013. Prepared for BC Hydro. Prepared by Ecoscape Environmental Consultants Ltd. and Larratt Aquatic. Ecoscape File No. 13-1107. Kelowna, BC.
- Schleppe, J., H. Larratt, A. Cormano 2014. Peace Project Water Use Plan GSMON5 Peace River Productivity Monitoring, Year 2 Report, 2014. Prepared for BC Hydro. Prepared by Ecoscape Environmental Consultants Ltd. and Larratt Aquatic Consulting Ltd. Ecoscape File No. 13-1107. Kelowna, BC.
- Schleppe, J., Wagner, R. Robertson, C., Plewes, R. and Olson-Russello, M.A. 2015. Spatial model of benthic productivity for the Brilliant Expansion Project. Prepared for Columbia Power Corporation (CPC), Castlegar, British Columbia. Prepared by Ecoscape Environmental Consultants Ltd. Pg. 42.
- Schleppe, J., and H. Larratt. 2016. CLBMON-15b Middle Columbia River Ecological Productivity Monitoring, Annual Report 2015. Okanagan Nation Alliance with Ecoscape Environmental Consultants Ltd. & Larratt Aquatic Consulting Ltd. 108 pp.

- Shortreed; K R S and J G Stockner, 1981. Limnological results from the 1979 British Columbia lake enrichment program. Dept. of Fisheries and Oceans, Resource Services Branch, West Vancouver Laboratory. Series: Canadian technical report of fisheries and aquatic sciences, no. 995. Stockner J.G 1981.
- Sigee, David C. 2005. *Freshwater Microbiology: Biodiversity and Dynamic Interactions of Microorganisms in the Aquatic Environment*. John Wiley & Sons, Ltd. ISBN: 9780471485292. Online ISBN: 9780470011256. DOI: 10.1002/0470011254
- Smock, L.A. 1980. Relationships between body size and biomass of aquatic insects. *Freshwater Biology* 10: 375-383.
- Stanley, Emily H., Stuart G. Fisher, and Jeremy B. Jones Jr. 2004. "Effects of Water Loss on Primary Production: A Landscape-Scale Model." *Aquatic Sciences - Research Across Boundaries* 66 (1): 130–38. <https://doi.org/10.1007/s00027-003-0646-9>
- Stenger-Kovács, C., E.Lengyel, L.O.Crossetti, V.Üveges and J.Padisák 2013. Diatom ecological guilds as indicators of temporally changing stressors and disturbances in the small Torna-stream, Hungary. *Ecological Indicators* Vol.24 pages 138-147.
- Stockner, J. G., A. R. Langston, and G. A. Wilson. 2001. The limnology of Williston Reservoir. Peace/Williston Fish and Wildlife Compensation Program Report No. 242. 51pp plus appendices.
- Stockner, J.G., A. Langston, D. Sebastian and G. Wilson. 2005. *The Limnology of Williston Reservoir: British Columbia's Largest Lacustrine Ecosystem*. *Water Quality Research Journal of Canada* 40(1) January 2005.
- Trábert, Z., Tihamér Kiss, K., Várbíró, G., Dobosy, P., Grigorszky, I., & Ács, É. (2017). Comparison of the utility of a frequently used diatom index (IPS) and the diatom ecological guilds in the ecological status assessment of large rivers. *Fundamental and Applied Limnology/Archiv für Hydrobiologie*, 189(2), 87-103.
- Tilzer, M.M. 1988. Secchi disk – chlorophyll relationships in a lake with highly variable phytoplankton biomass. *Hydrobiologia* Vol. 162:2 pp 163-171.
- Vadeboncoeur, Y., Devlin, S. P., McIntyre, P. B., & Vander Zanden, M. J. (2014). Is there light after depth? Distribution of periphyton chlorophyll and productivity in lake littoral zones. *Freshwater Science*, 33(2), 524-536.
- Vollenweider, R. A. & J. Kerekes, 1982. *Eutrophication of Waters-Monitoring, Assessment and Control*. Organisation for Economic Co-Operation and Development, Paris, 154 pp.
- Wagner, A., S. Volkmann and P.M.A. Dettinger-Klemm, 2012. Benthic–pelagic coupling in lake ecosystems: the key role of chironomid pupae as prey of pelagic fish IN *Ecosphere* Vol.3 Issue 2.
- Wetzel, R. 2001. *Limnology: lake and river ecosystems*. New York: Academic Press.
- Wickham, H. 2009. *ggplot2: elegant graphics for data analysis* Springer.

- Yoshida T, Urabe J, Elser JJ., 2003. Assessment of 'top-down' and 'bottom-up' forces as determinants of rotifer distribution among lakes in Ontario, Canada. *Ecological Research*. 2003;18:639–650. doi: 10.1111/j.1440-1703.2003.00596
- Zuur, A., Leno, E.N., Walker, N., Saveliev, A.A. and Smith, G.M. 2009. *Mixed effects models and extensions in Ecology with R*. Springer Science+Business Media, LLC. New York, New York, USA.

Appendix A Detailed Site Maps



Figure A1 Detailed Williston Site Location Map.

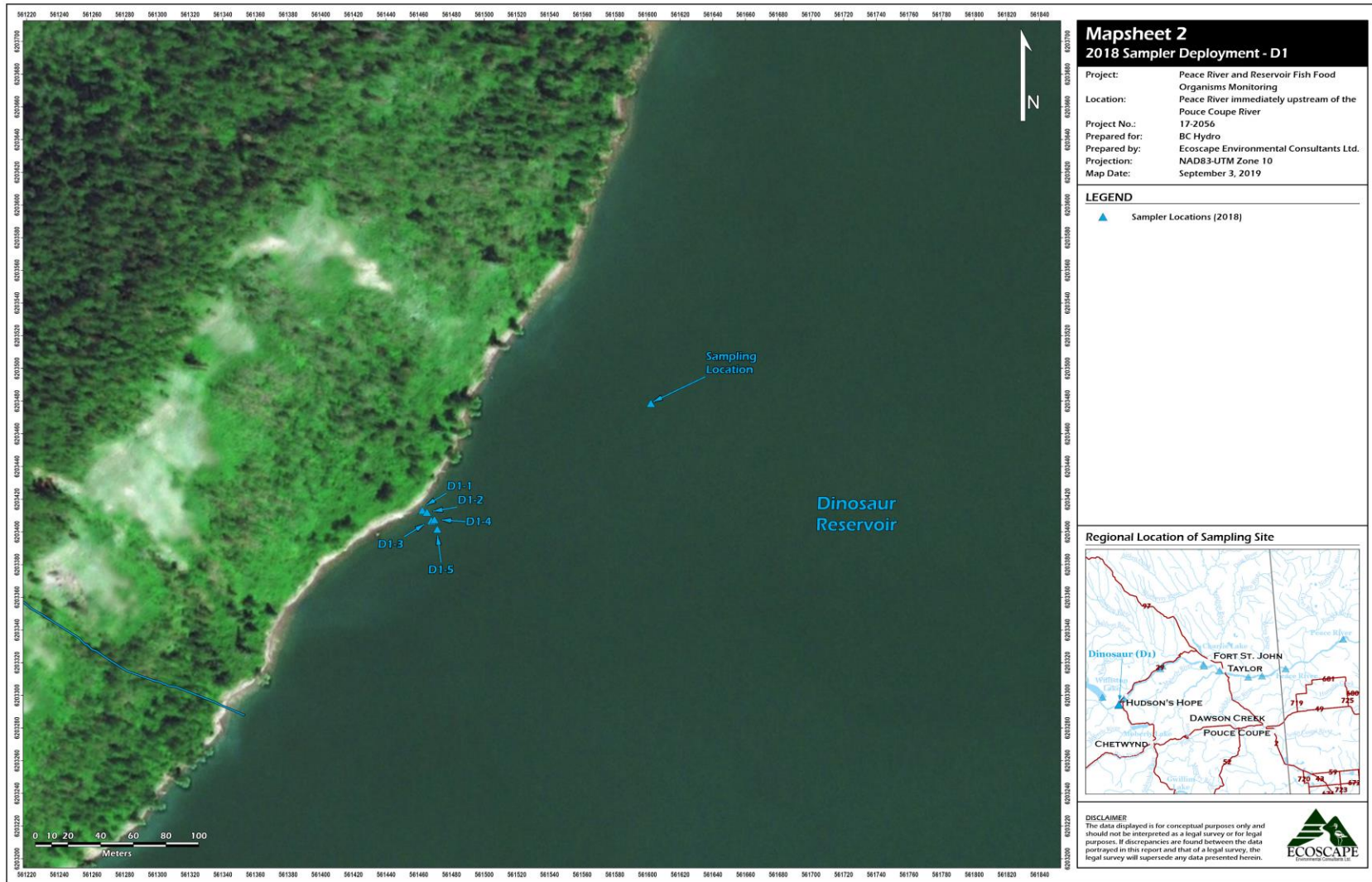


Figure A2 Detailed Dinosaur Site Location Map.

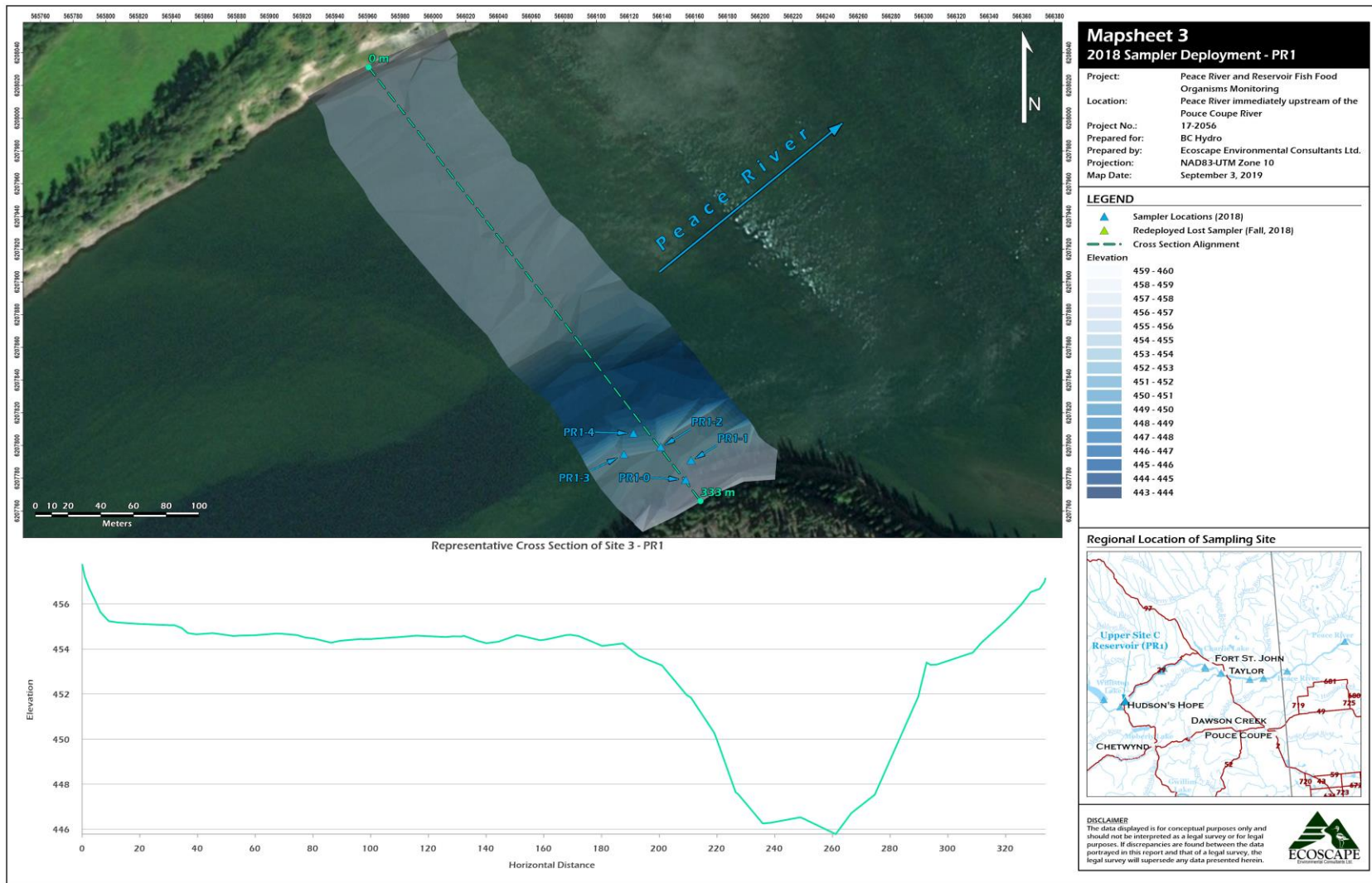


Figure A3 Detailed PR1 Site Location Map.

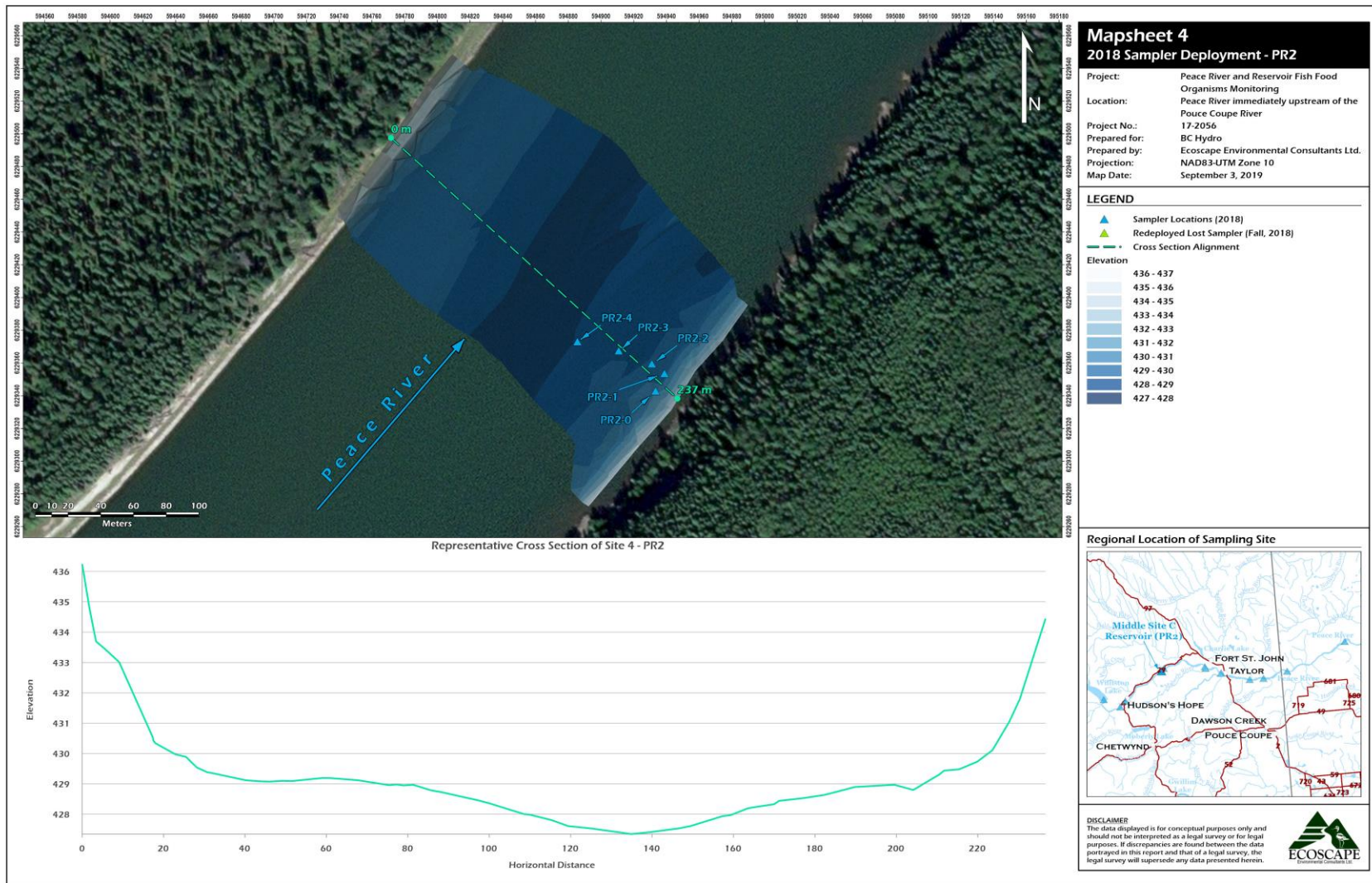


Figure A4 Detailed PR2 Site Location Map.

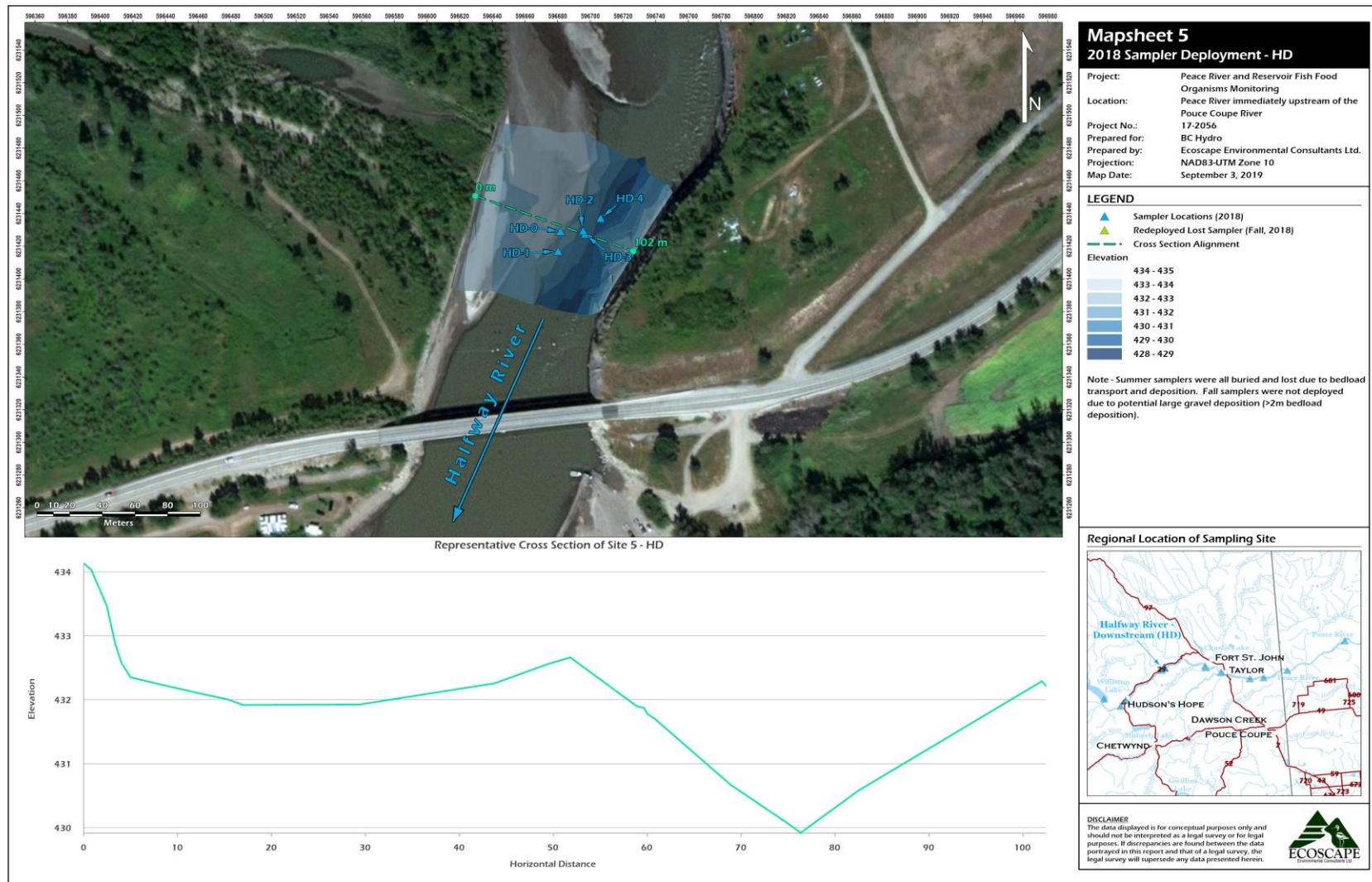


Figure A5 Detailed HD Site Location Map.

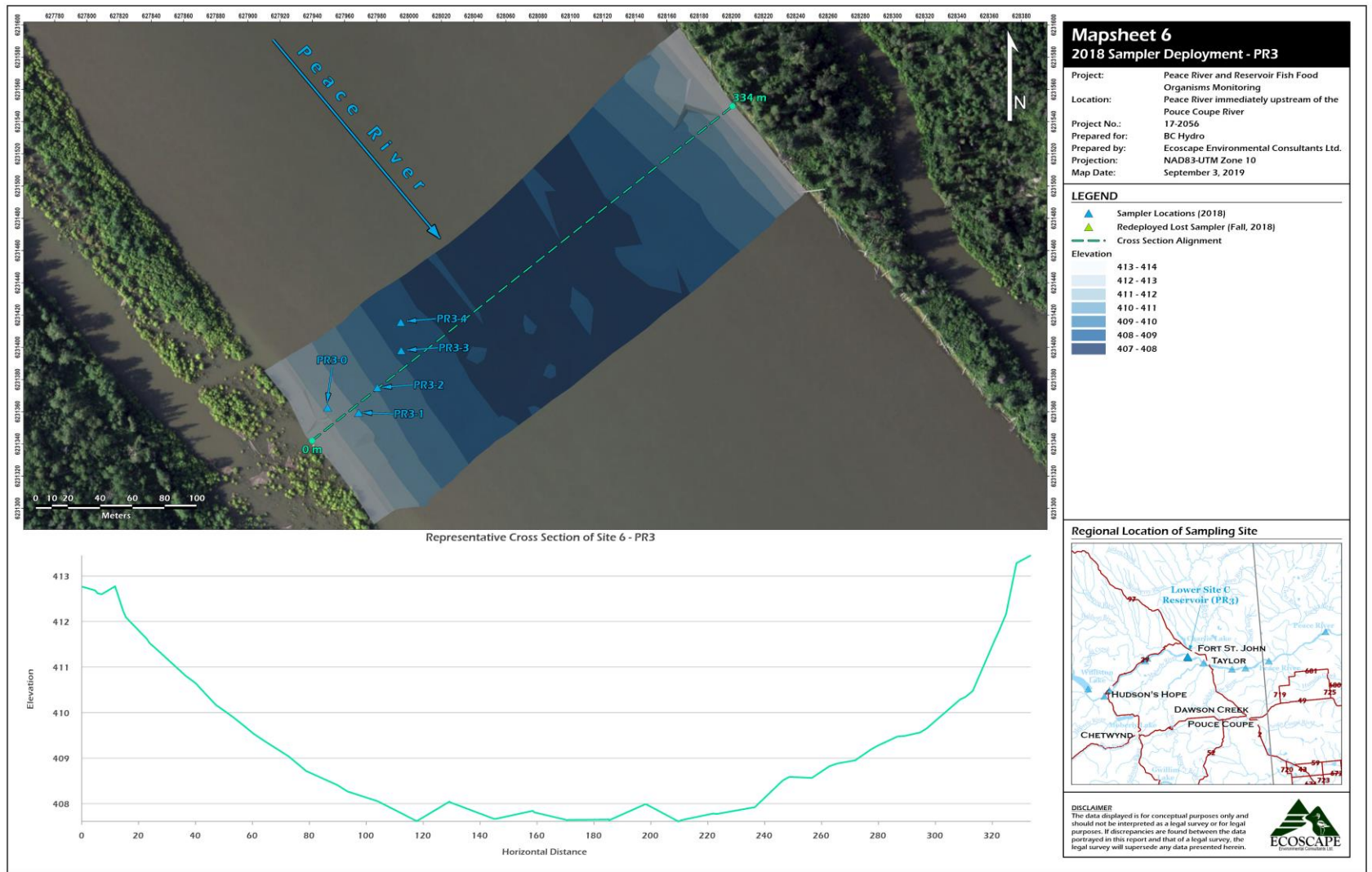


Figure A6 Detailed PR3 Site Location Map.

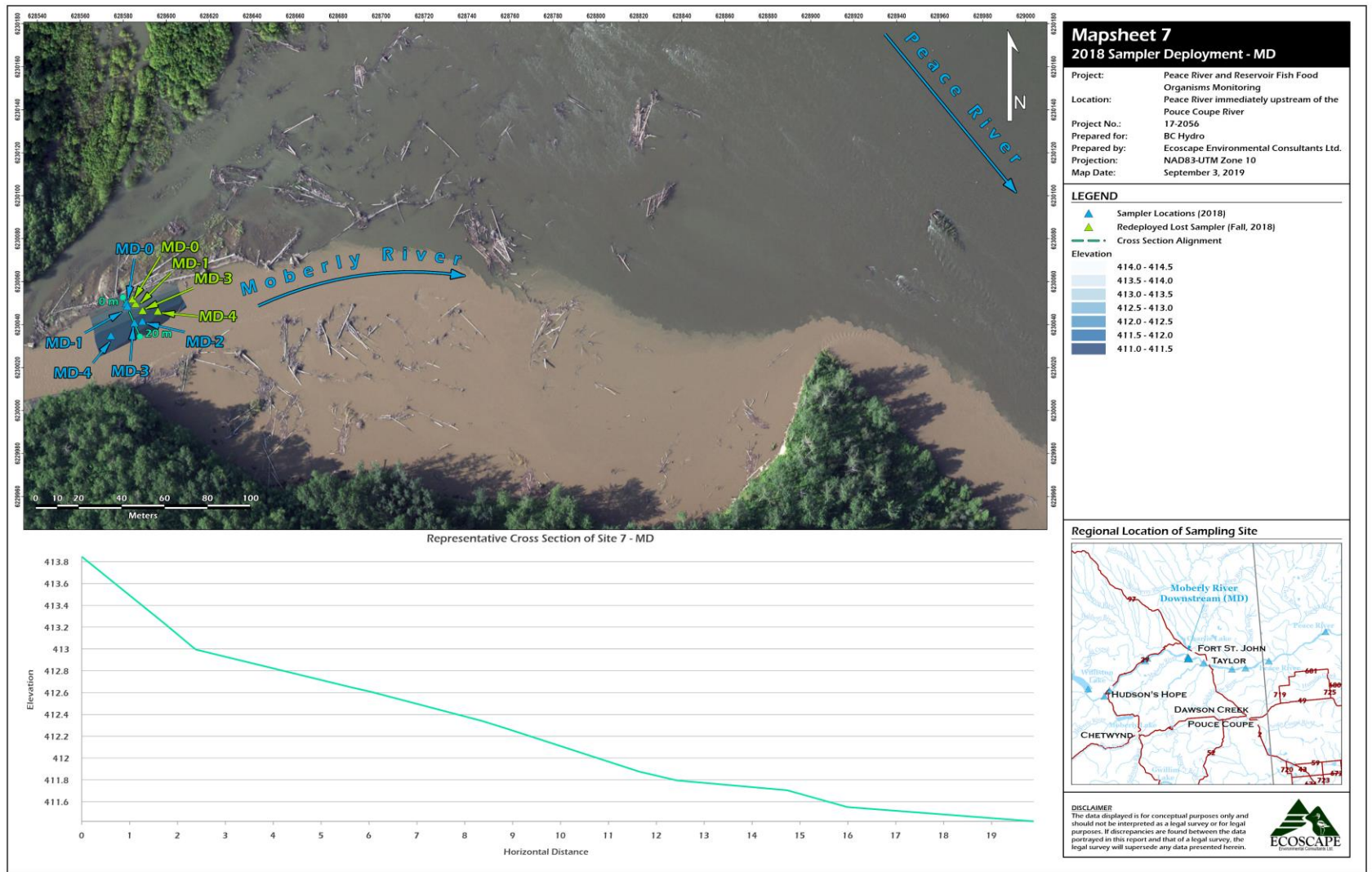


Figure A7 Detailed MD Site Location Map.

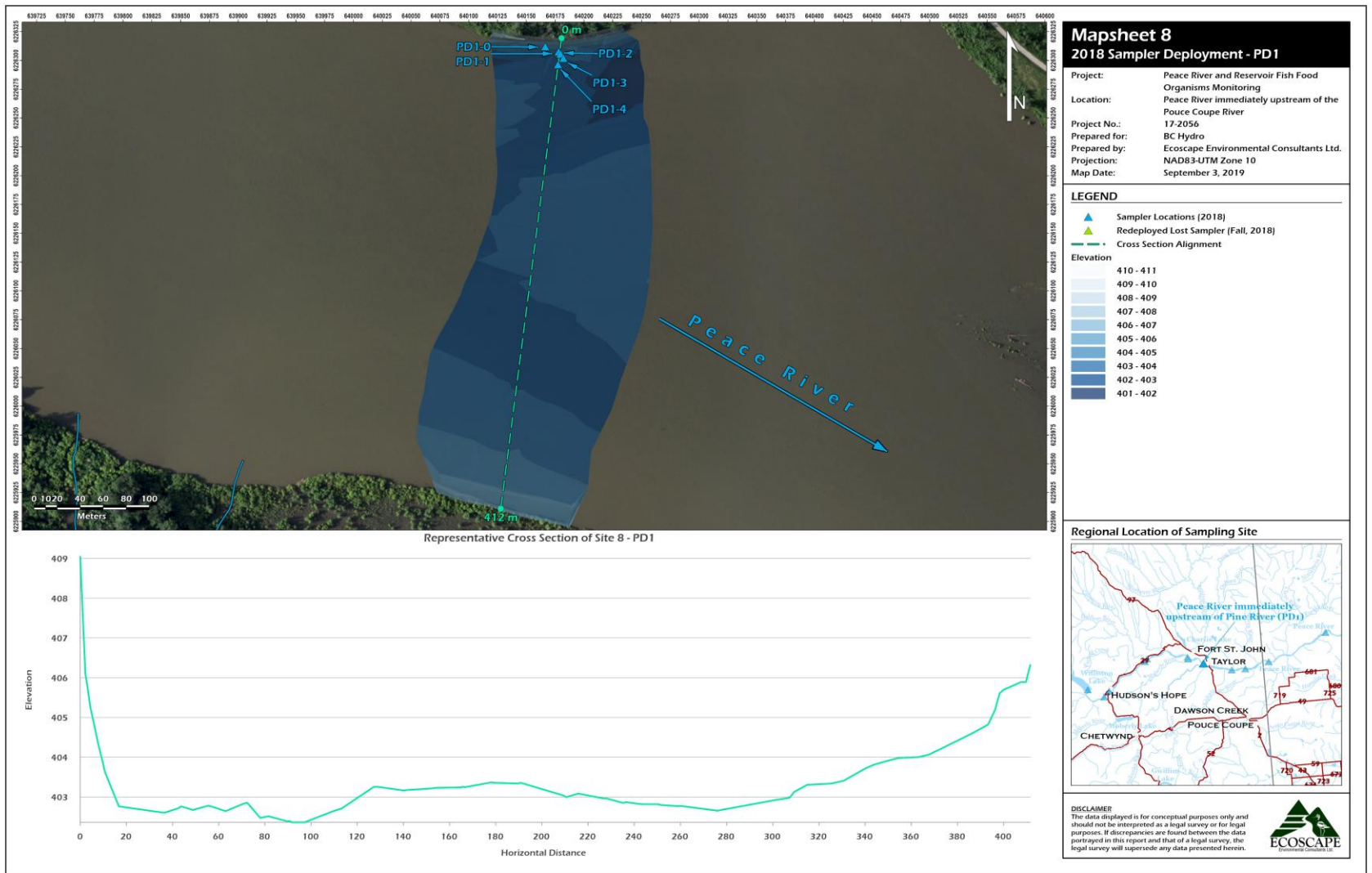


Figure A8 Detailed PD1 Site Location Map.

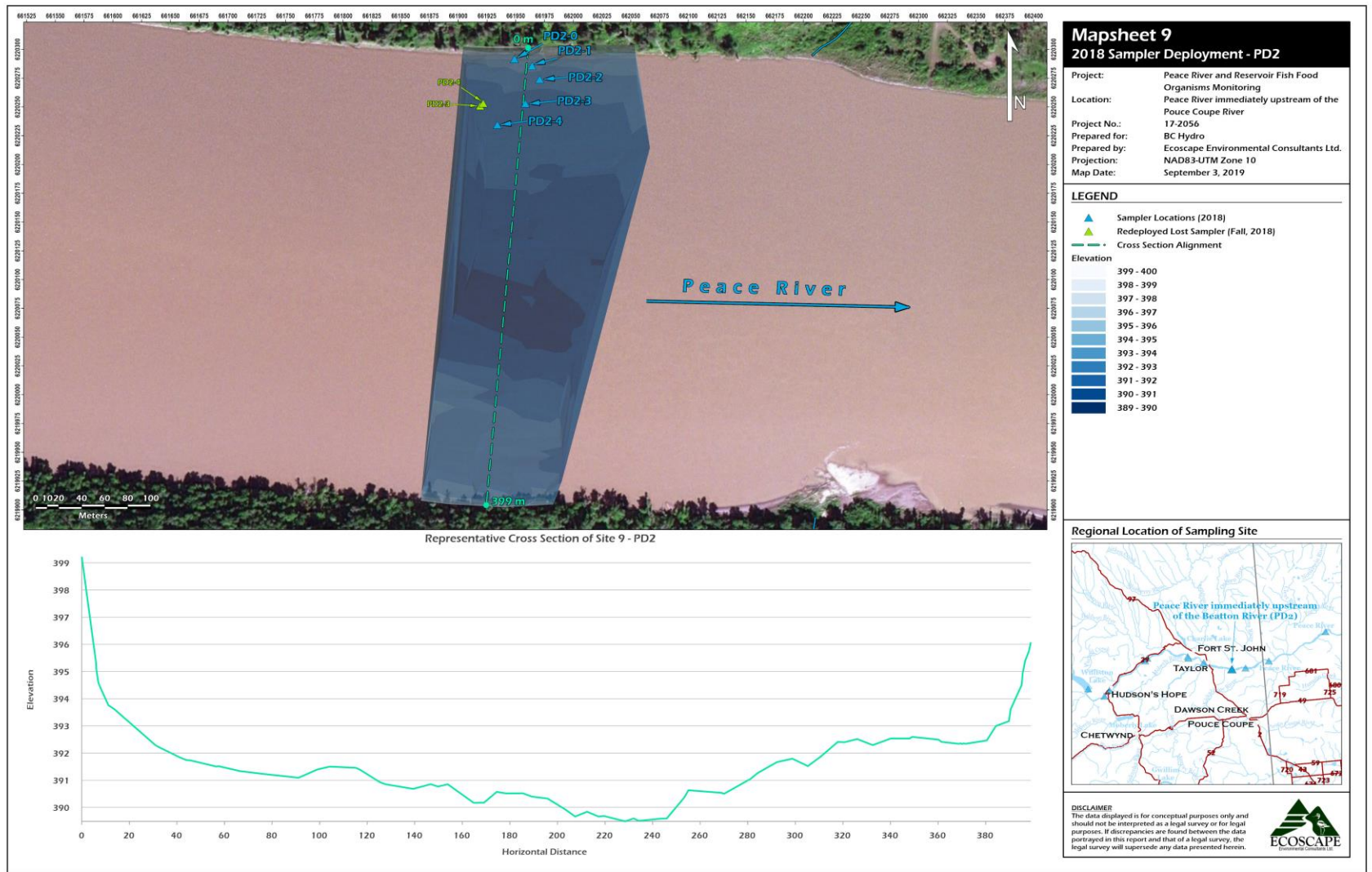


Figure A9 Detailed PD2 Site Location Map.

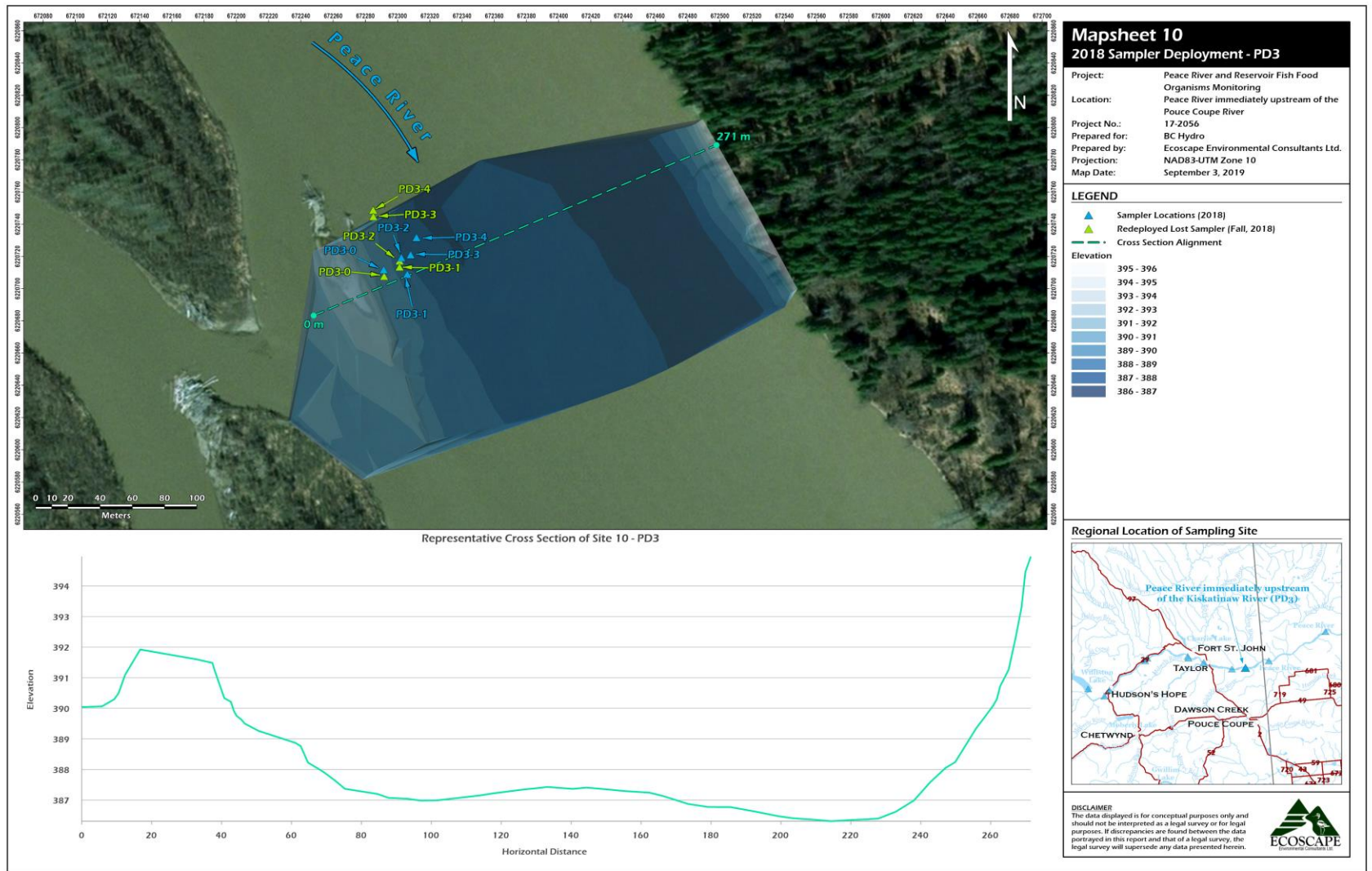


Figure A10 Detailed PD3 Site Location Map.

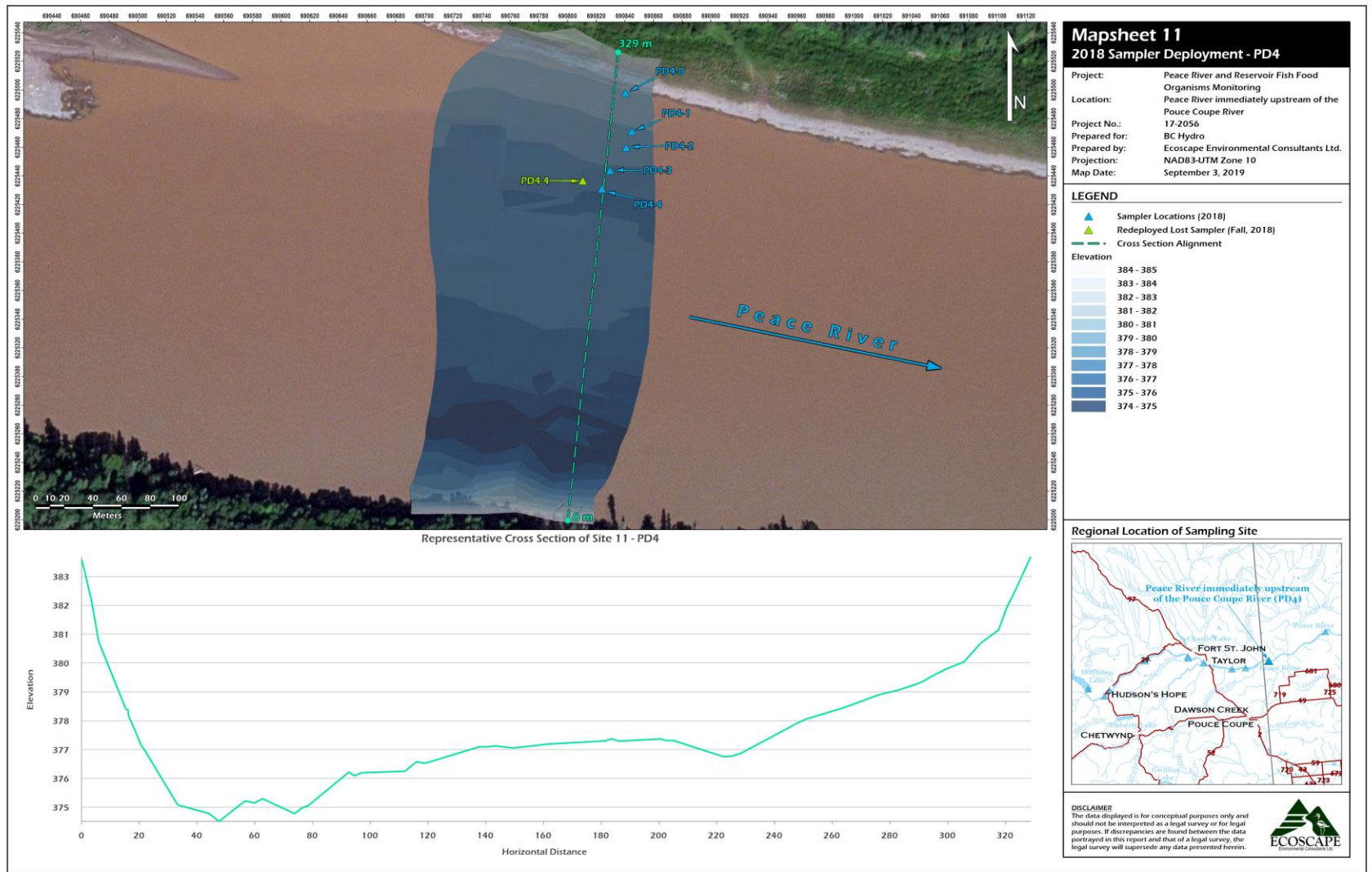


Figure A11 Detailed PD4 Site Location Map.

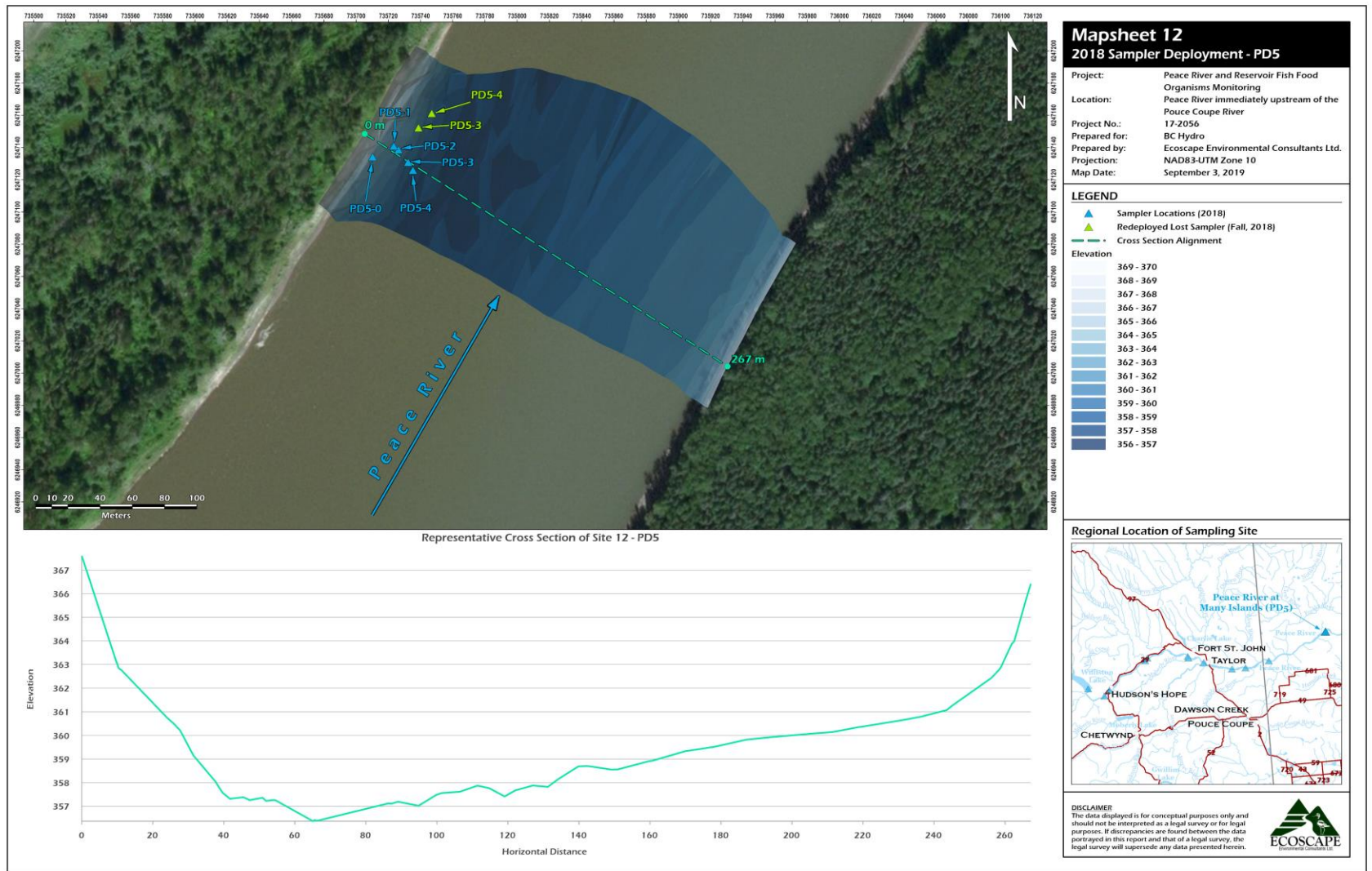


Figure A12 Detailed PD5 Site Location Map.

Appendix B Detailed Sampling Methods

Phytoplankton Sampling (Taxonomy and Chlorophyll-a)

A preferred method of determining reservoir productivity involves collecting a composite sample with a Van Dorn water sampler. Water samples were collected from three depths above the thermocline at the pelagic site in Willison Reservoir and at both the littoral and pelagic sites in Dinosaur Reservoir. Composite samples were collected from each site monthly between June and October 2017. The Van Dorn was used to collect three water samples from (1) 1 m depth, (2) the lower extent of the photic zone (field estimated as 1.7 times the Secchi depth) and (3) mid-way between these depths. These three samples were evenly (by volume) combined and mixed in a 4 L plastic bottle that was pre-marked to delineate the three volumes. Once the three samples were combined, the 4 L bottle was capped and inverted several times to thoroughly mix the water. One (1) litre of the sample was subsequently poured off into a 1 L plastic bottle for analysis. The bottle was labelled with the site name and date of collection. It was stored in the dark and chilled on ice until the end of the field day, when approximately half of the sample was filtered through a 0.45µm nitrocellulose filter. The volume of the filtered sample was recorded and the filter was folded into an aluminum foil cover to exclude light and stored on ice until submission to the laboratory for chlorophyll-a analysis. The remainder of the 1 L sample was fixed with Lugal's solution prior to storage at 4°C until it could be delivered to Larratt Aquatic for taxonomic identification, and biovolume / density determination.

Phytoplankton Vertical Hauls (Taxonomy)

Reservoir productivity was also determined using phytoplankton vertical hauls. Composite samples were collected from the pelagic site in Willison Reservoir and at both the littoral and pelagic sites in Dinosaur Reservoir monthly between June and October 2017. A 80 µm phytoplankton net was lowered to 1.7times the Secchi depth and pulled through the water at a speed of less than 1 m/second. The contents of the net were then rinsed into a 300 mL plastic container. The phytoplankton haul was repeated two more times with the contents of the additional pulls placed in the same container. The composite sample was fixed with Lugal's solution prior to storage at 4°C until it could be delivered to Larratt Aquatic for taxonomic identification, and biovolume / density determination. The phytoplankton hauls were useful to determine rare species and were also used as a backup for zooplankton taxonomy.

Zooplankton Vertical Hauls (Taxonomy and Biomass)

Reservoir zooplankton communities were sampled using a plankton net with a 500 mm diameter frame opening and a mesh size of 153 µm. Composite samples were collected from the pelagic site in Willison Reservoir and at both the littoral and pelagic sites in Dinosaur Reservoir monthly between June and October 2017. The wetted depth at each sample location was determined using the on-board depth sounder. The zooplankton net was then lowered to 2 m above the reservoir bed and slowly pulled vertically through the water column at a rate of 0.5 m/second. The contents of the net were placed into a 1 L plastic bottle. Three hauls were collected at each site and the contents combined as a composite. Once all three hauls were complete, the sample was fixed with 70% reagent alcohol. Organisms/m³ was subsequently calculated (*total depth of the hauls • area of frame opening mouth*).

Artificial Substrates (Rock Baskets) for Benthic Invertebrate Community Analysis and Biomass

Benthic invertebrate communities were assessed using artificial substrate samplers (rock baskets). Rock baskets (planar area = 0.038m²) were filled with pebble-sized rock (32-64 mm). Samplers were deployed for between 49 to 54 days in the summer and 52 to 58 days in the fall. Upon retrieval, the rock baskets were transferred immediately into a pre-labelled bucket of clean filtered river water. The baskets were opened in the bucket and all the rocks were individually scrubbed using a soft bristle brush to release clinging invertebrates. Washed rocks were then rinsed in the sample water and placed back in the basket and stored for future use. The contents from each bucket were captured on a 397 µm sieve, and rinsed into pre-labeled 500 mL plastic containers and preserved in 70% reagent alcohol prior to transport to Cordillera Consulting for taxonomic identification and community metrics.

Natural Substrate Sampling (Benthic Invertebrate Taxonomy and Biomass)

Natural depositional substrates were sampled using an Ekman dredge. This was done to allow consistent and paired sampling of riverine and future Site C reservoir conditions at sites PR1, PR2, PR3, HD, and MD. Samples were also collected from D1 littoral areas for comparison. Where possible, a composite of three sub-samples was batched into every sample analyzed, to account for variable sample size due to small sample volumes. The invertebrate samples were sieved in a wash bucket with a 250 micron mesh and transferred to a labeled sample bottle and preserved with 70% reagent alcohol.

Turbidity and Total Suspended Solids (TSS)

Turbidity loggers (YSI EXO Sonde by Xylem (Yellow Springs, OH, USA)) were deployed on the mid-depth samplers at the five sites downstream of the Project. Data were downloaded from loggers during the mid-deployment maintenance schedule, and the sondes/sensors were cleaned of sediment and recalibrated using turbidity standards. In-situ turbidity was also measured, using a Hach 2100P Turbidimeter (Loveland, CO, USA), at mid-sampler depth locations at all the riverine sites as well as in Williston and Dinosaur reservoir pelagic and littoral sites. Furthermore, turbidity was measured from cross-channel composite samples to compare spatial differences in turbidity across the river. The cross channel composite water sample was also retained (1 L) and submitted for analysis of total suspended solids (TSS).

Reservoir PAR Profiles

Photosynthetically active radiation was profiled in the pelagic and littoral reservoir sites as well as the thalweg of the Peace River at each of the riverine sample sites. The sensor was affixed to a cannonball and downrigger containing a fin to maintain the vertical aspect of the sensor in current and drift. In the reservoir, PAR readings were measured at the water surface and at 1 m depth intervals whereas 0.5 m intervals were measured in the river.

Reservoir Temperature Thermistor Profiles

Two thermistor lines with six light/temperature loggers each were constructed to inform the temperature/light profiles of the Williston and Dinosaur reservoirs. Each thermistor line was deployed in approximately 20 m depth and constantly they recorded data from June through October. The thermistors were concentrated in the photic zone depths, with one thermistor at mid-depth and one near the 20 m depth on each line.

Detailed Classification of Reservoirs

The following table provides an overview of ranges in productivity for comparison of the upstream control reservoirs and for the future Site C reservoir, in relation to other BC lakes.

Table A1 General Estimates of reservoir annual primary productivity	
Trophic status productivity	Production of organic carbon
Productive – eutrophic cold	0.15 – 0.5 kg C/m²/yr (1500 – 5000 kg C/ha/yr)
phytoplankton	200 - 2000 kg C/ha/yr
periphyton	20 - 1000 kg C/ha/yr
aquatic macrophytes	1170 kg C/ha/yr
riparian vegetation	not available
Mesotrophic - typical BC lake	0.05 - 0.15 kg C/m²/yr (500 - 1500 kg C/ha/yr)
phytoplankton	100 - 400 kg C/ha/yr
periphyton	1000 kg C/ha/yr
aquatic macrophytes	500 kg C/ha/yr
riparian vegetation	not available
Oligotrophic – D1 W1 sites	0.01 – 0.05 kg C/m²/yr (100 – 500 kg C/ha/yr)
phytoplankton	47 - 80 kg C/ha/yr
periphyton	400 kg C/ha/yr
aquatic macrophytes	180 kg C/ha/yr
riparian vegetation	not available

Wetzel 2001, Table 19-7 – 10 convert kg C to kg organic matter (OM = 46.5% C)

Appendix C Reservoir Station Elevation Plots

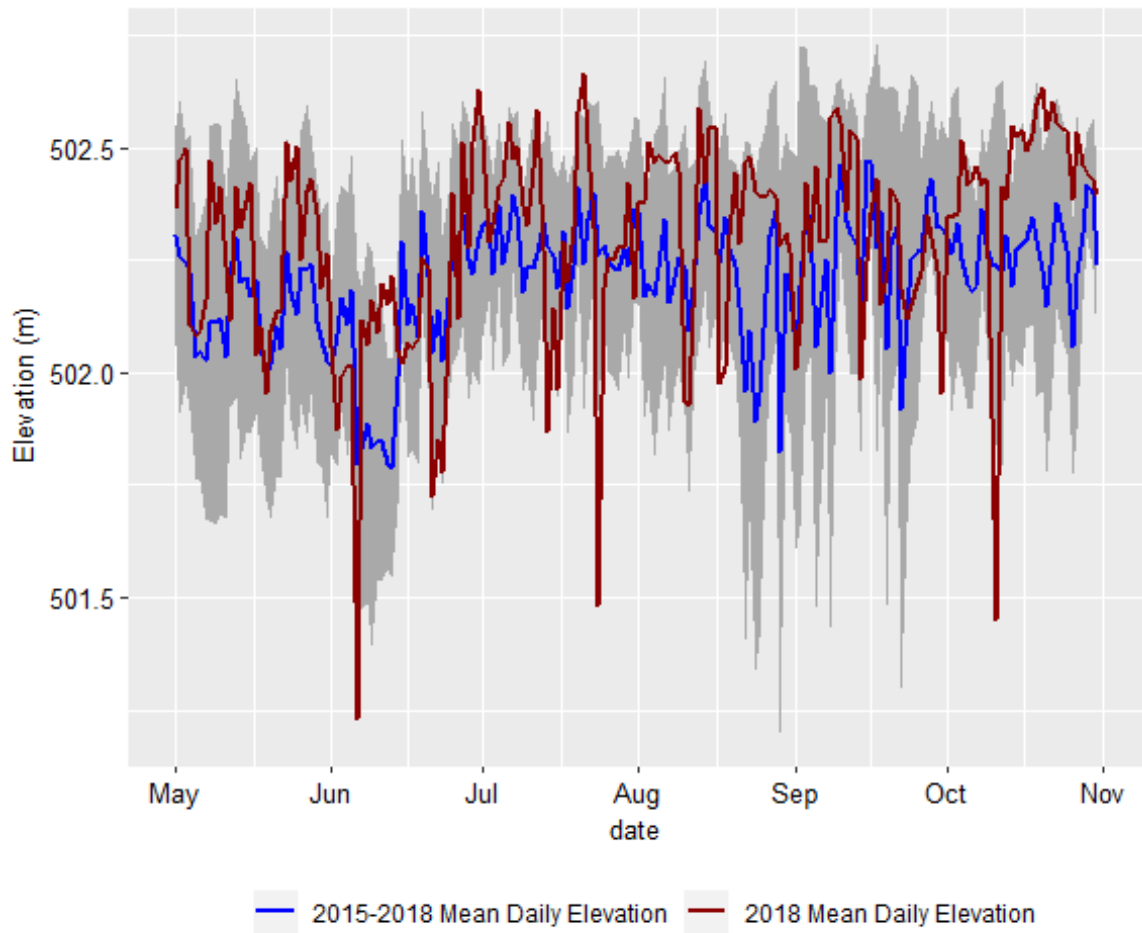


Figure A13 Water Elevations in Dinosaur Reservoir at Dam Forebay

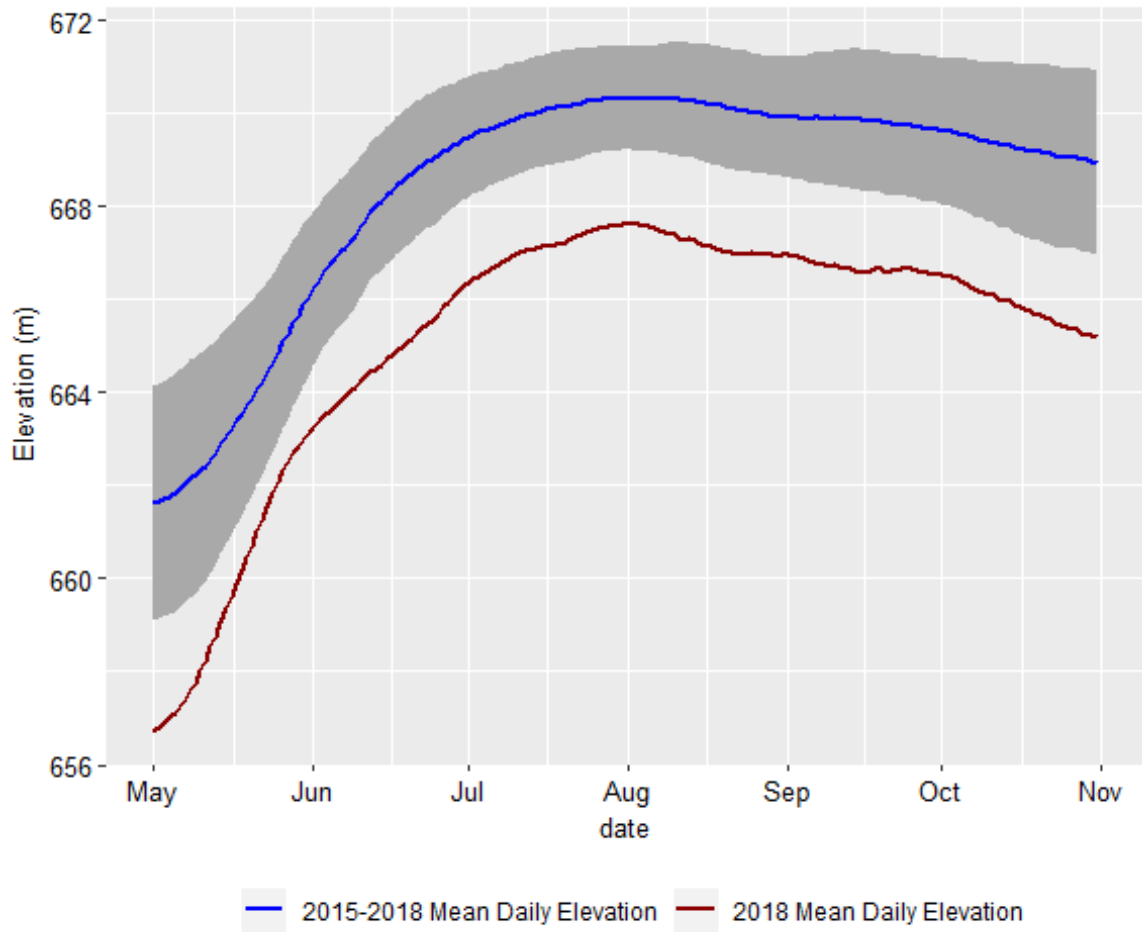


Figure A14 Water Elevations in Williston Reservoir at Williston Forebay 1

Appendix D River Station Elevation Plots

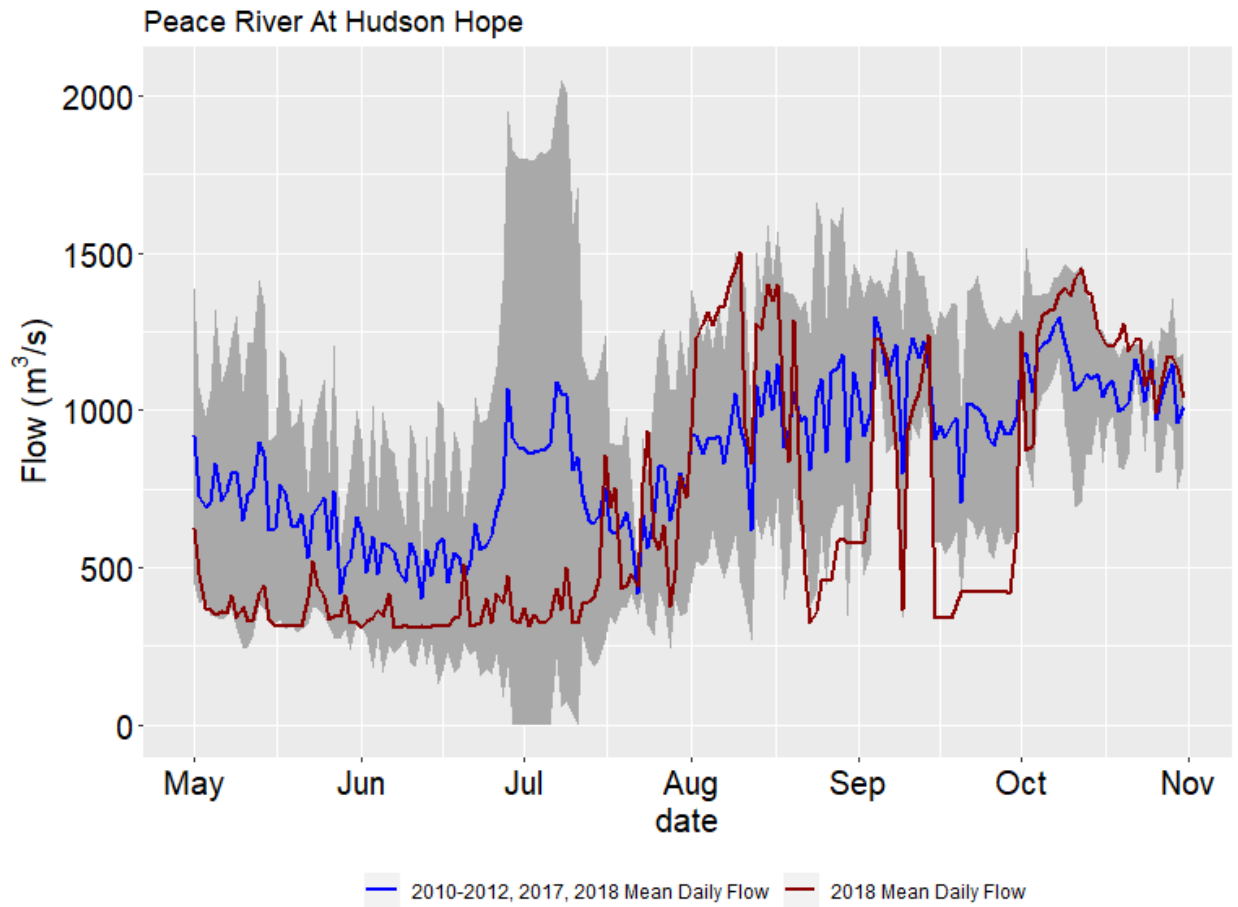


Figure A15 Flow at Peace River At Hudson Hope (07EF001)

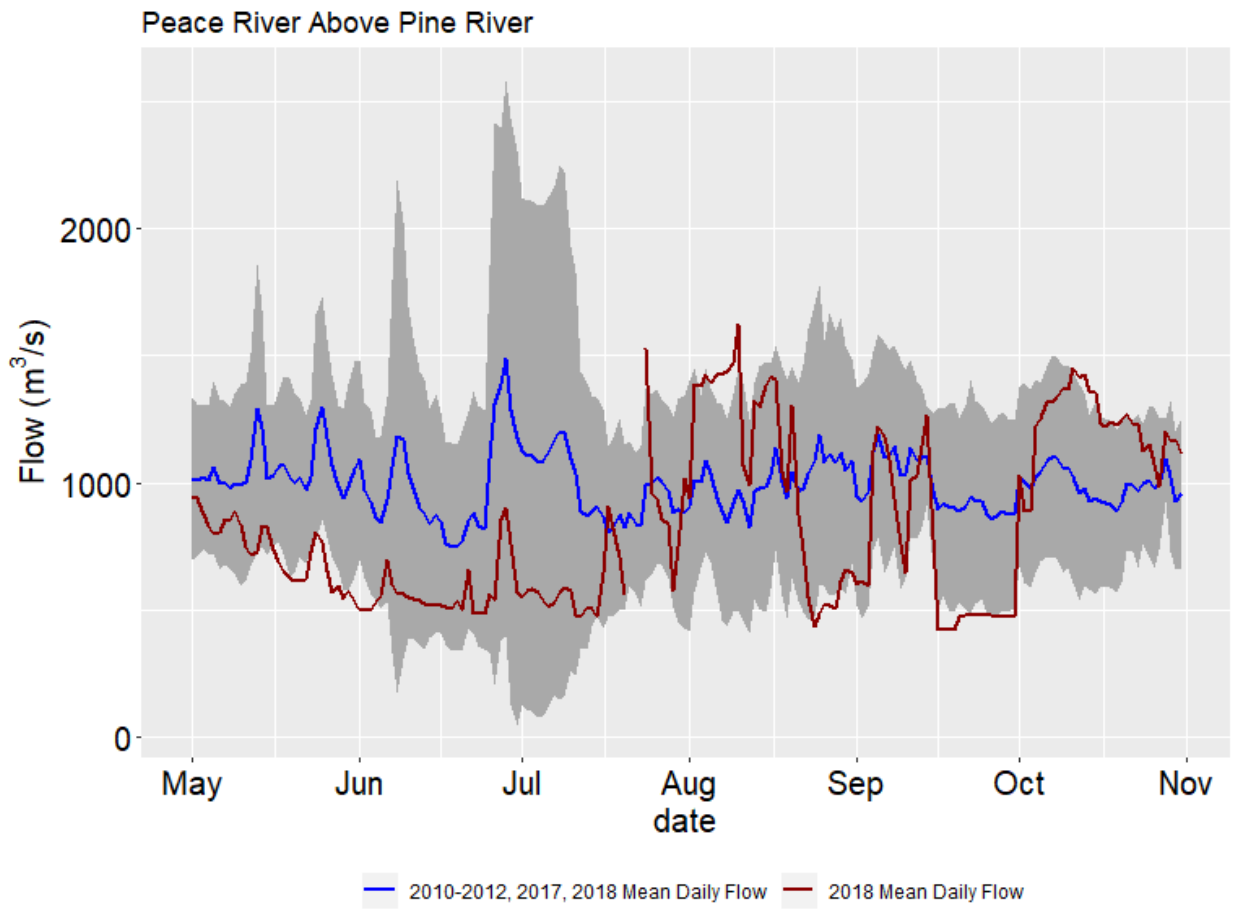


Figure A16 Flow at Peace River Above Pine River (07FA004)

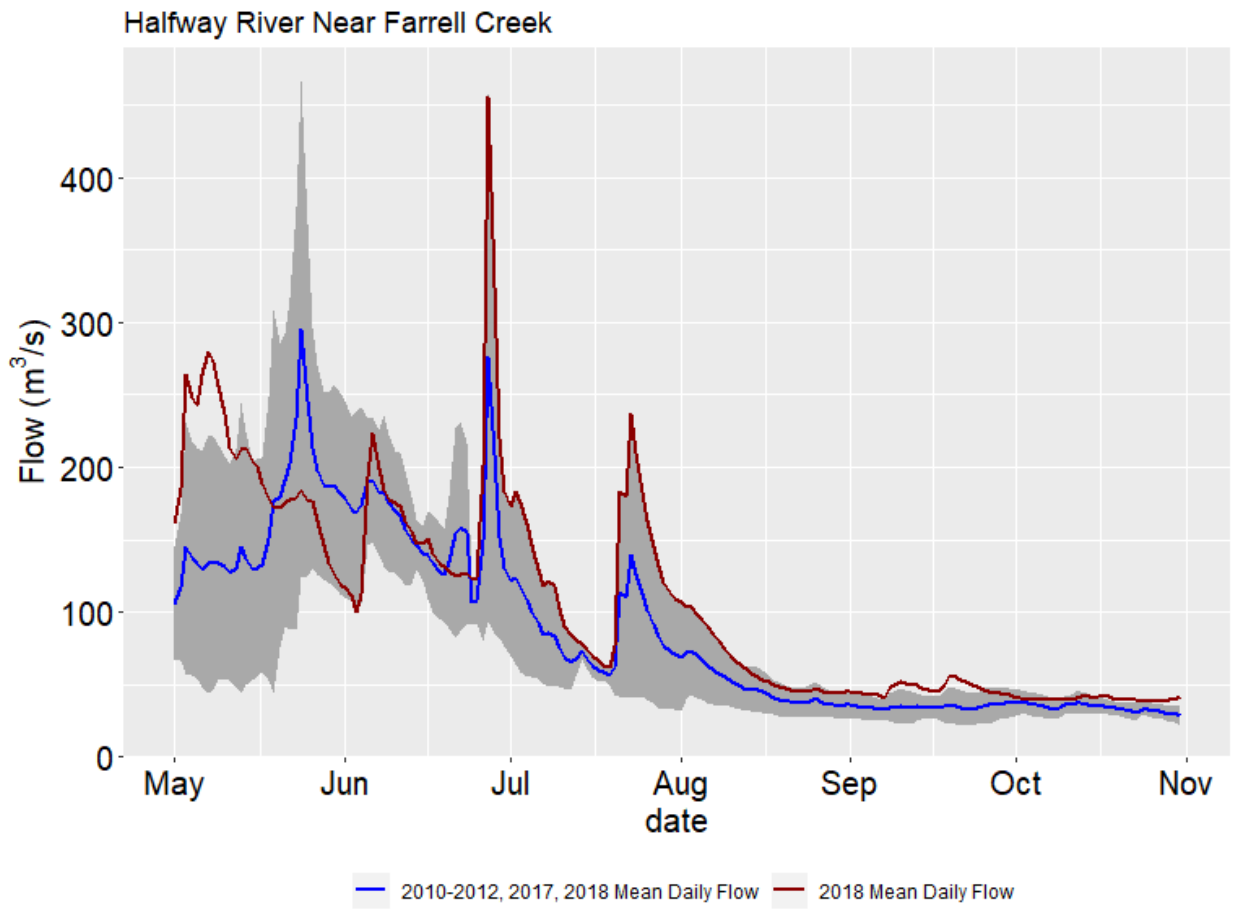


Figure A17 Flow at Halfway River Near Farrell Creek (07FA006)

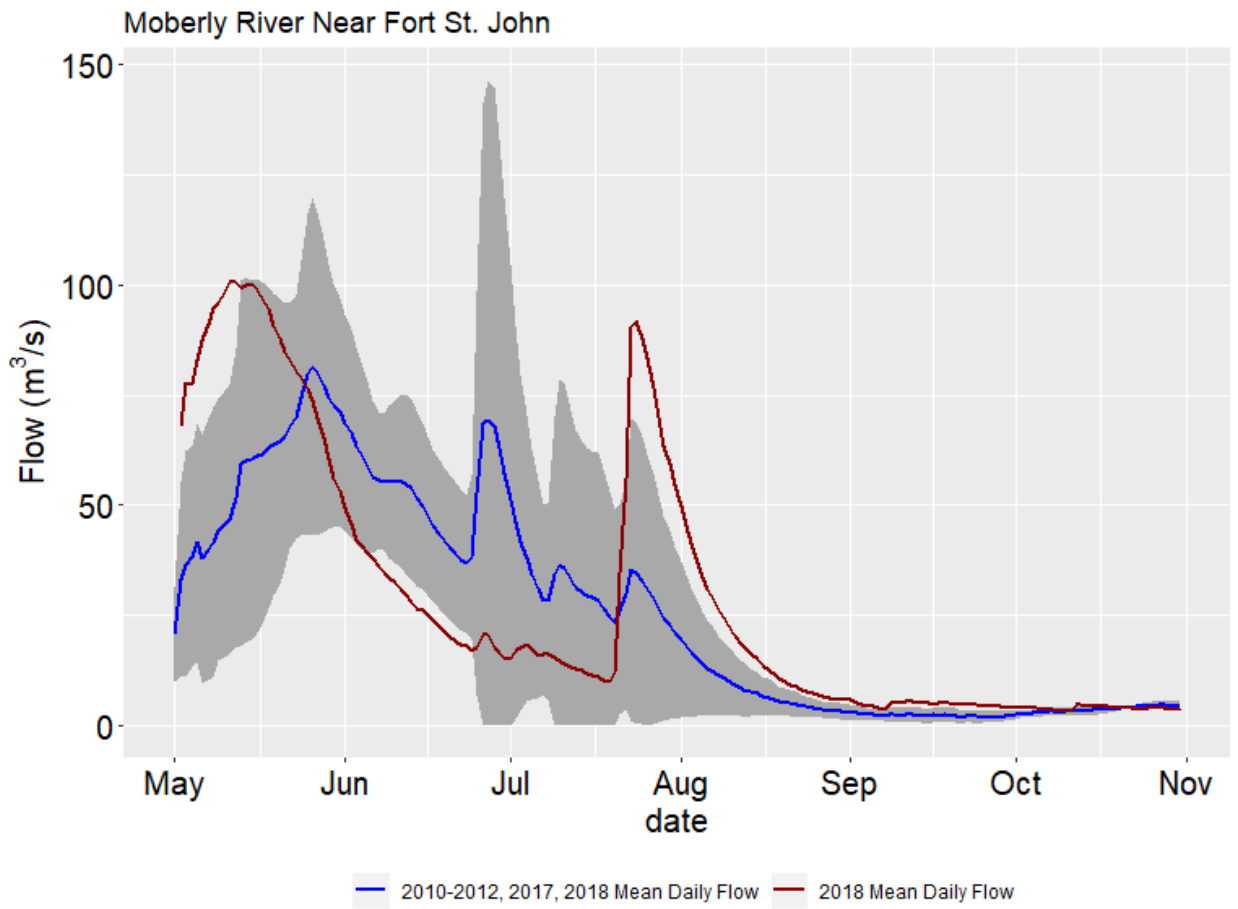


Figure A18 Flow at Moberly River Near Fort St. John (07FB008)

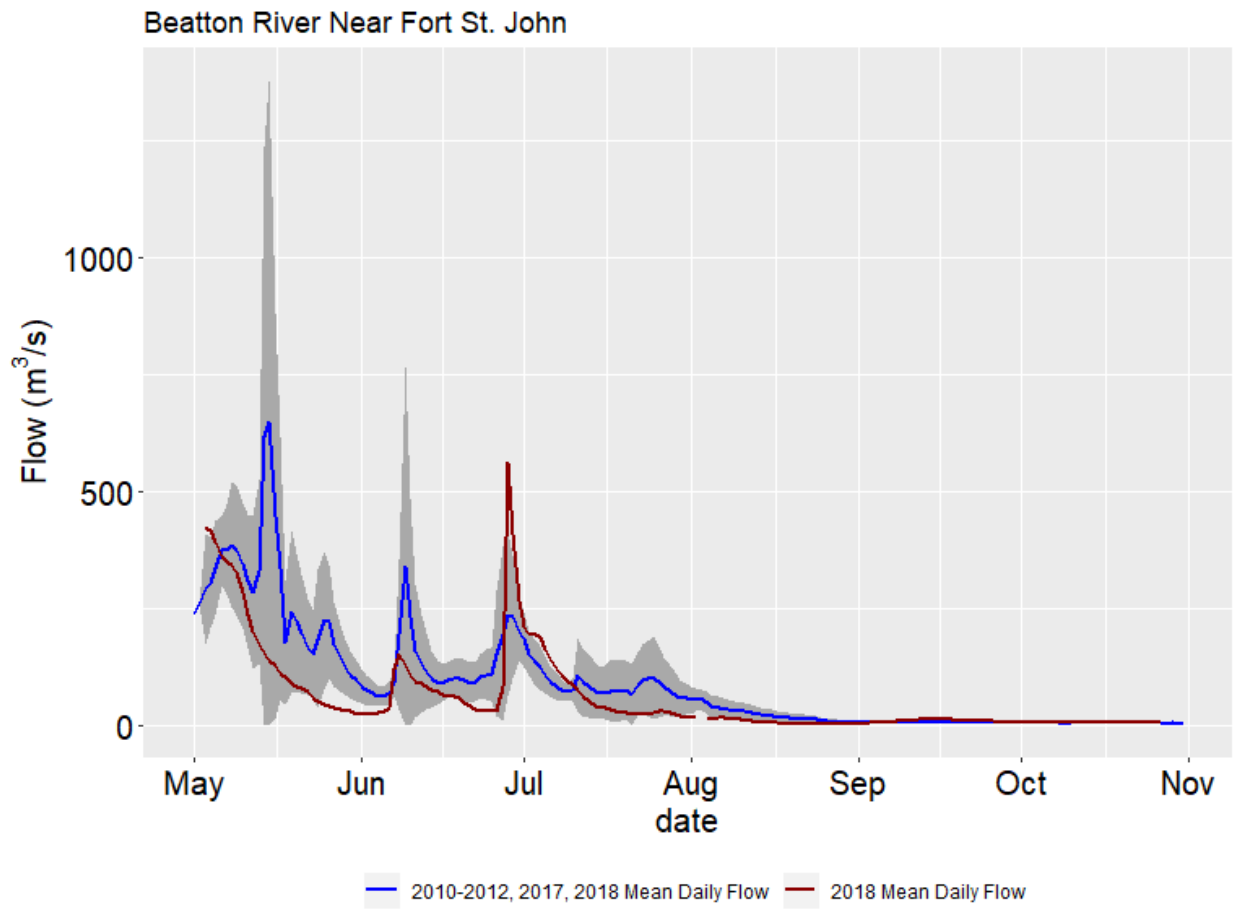


Figure A19 Flow at Beatton River Near Fort St. John (07FC001)

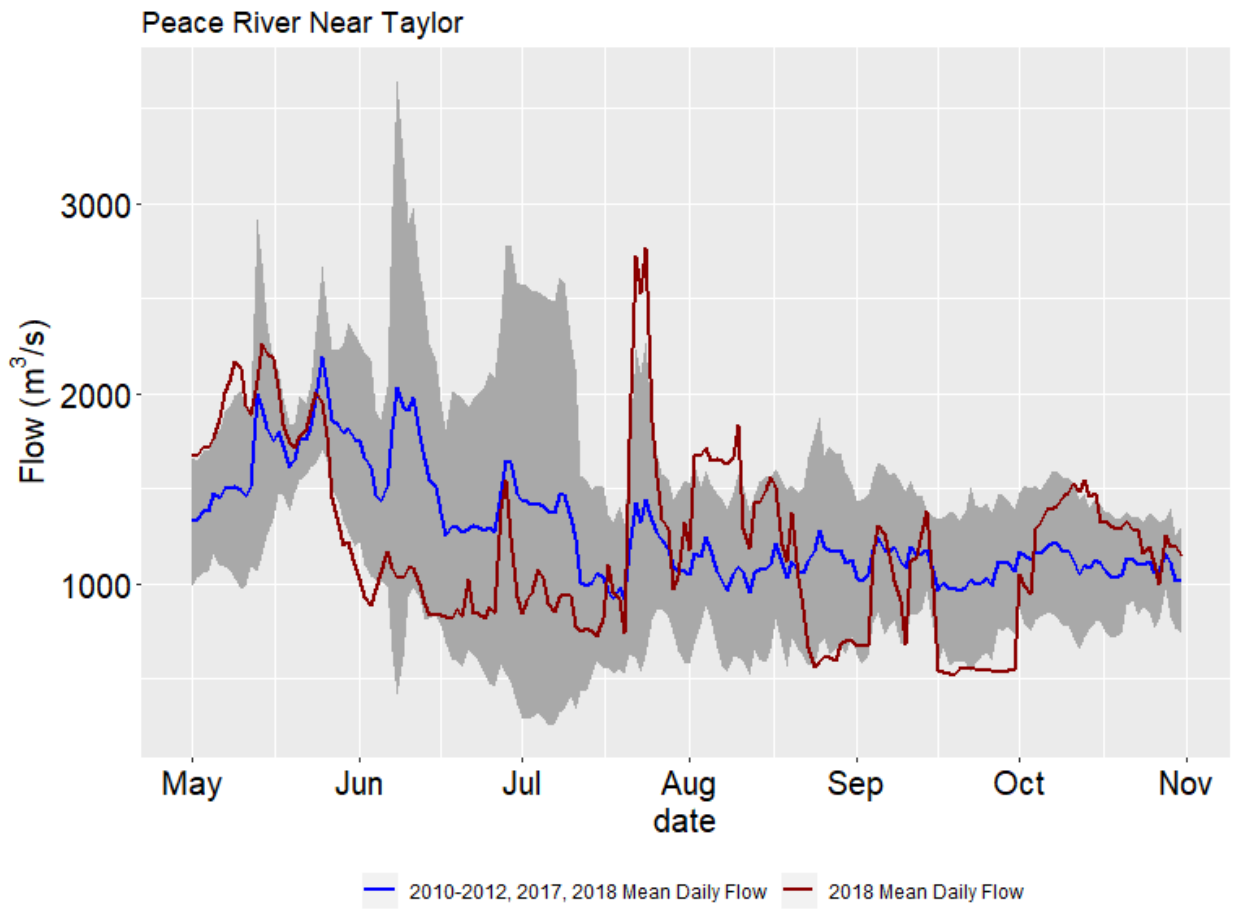


Figure A20 Flow at Peace River Near Taylor (07FD002)

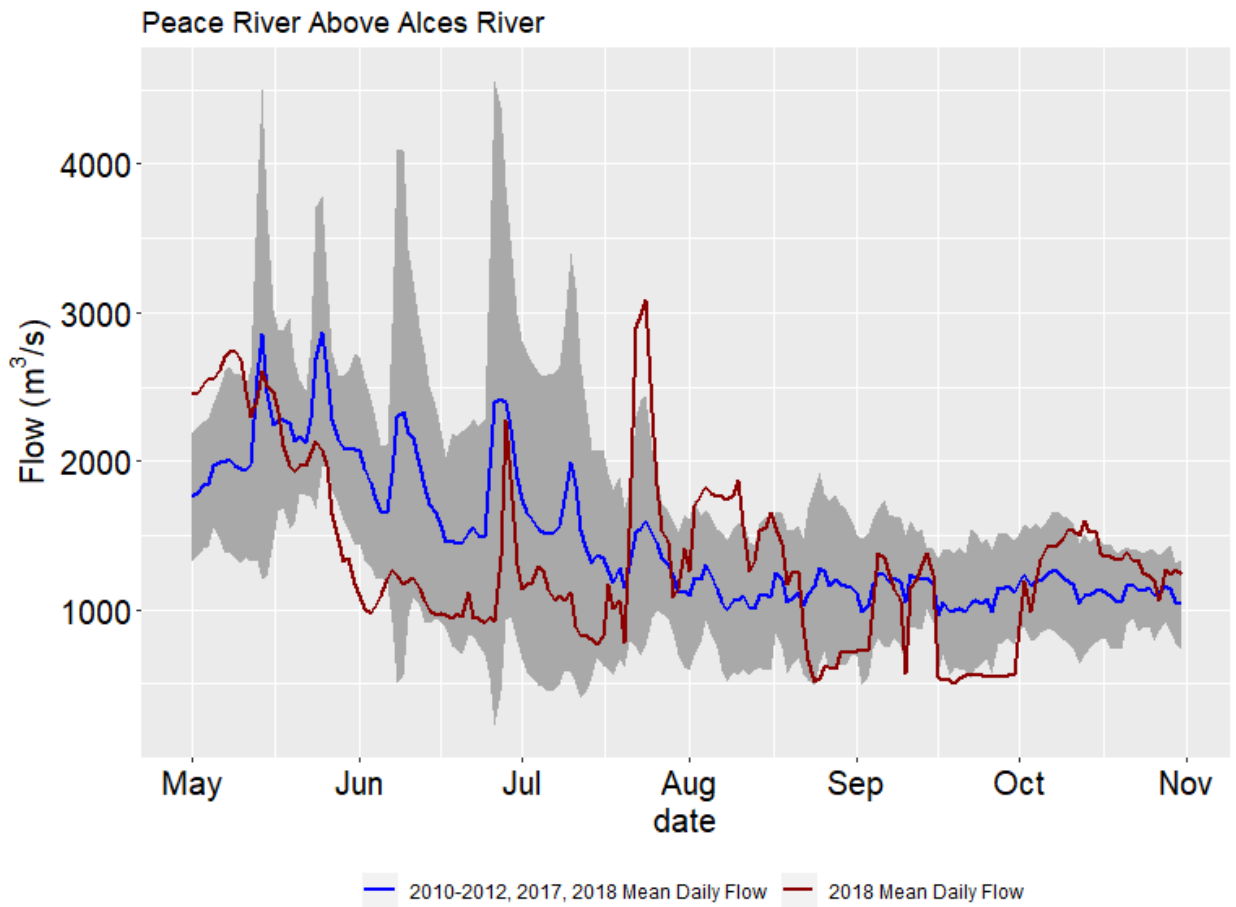


Figure A21 Flow at Peace River Above Alces River (07FD010)

Appendix E Site Depth Plots

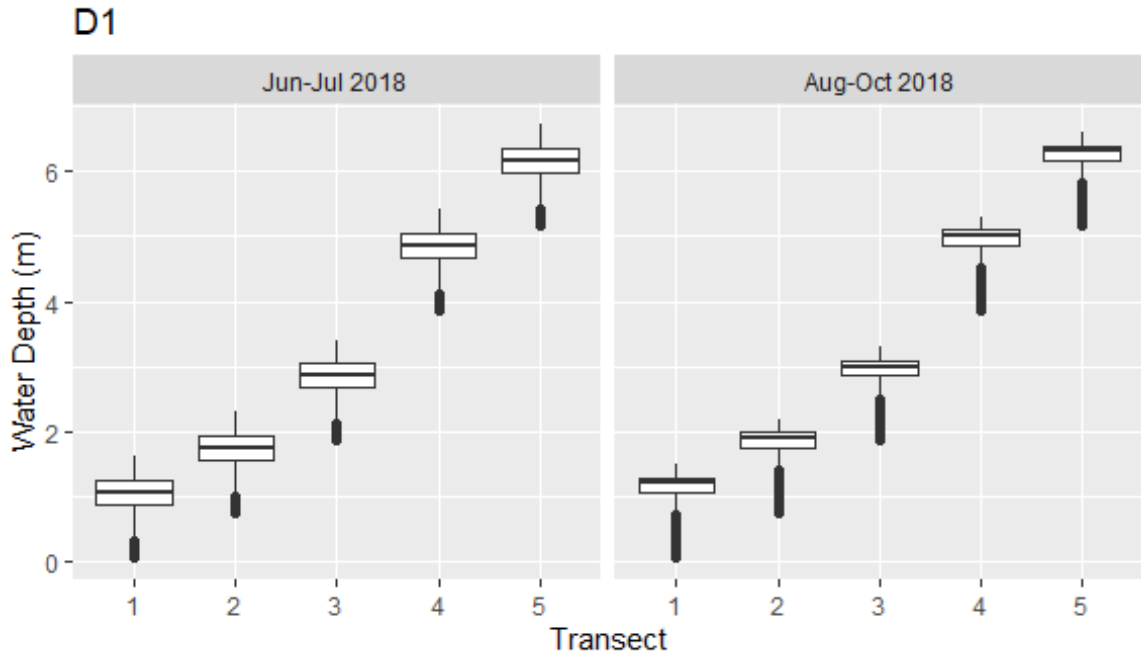


Figure A22 Boxplots of mean daily water depth for summer and fall 2018 sampling periods at each transect position in D1

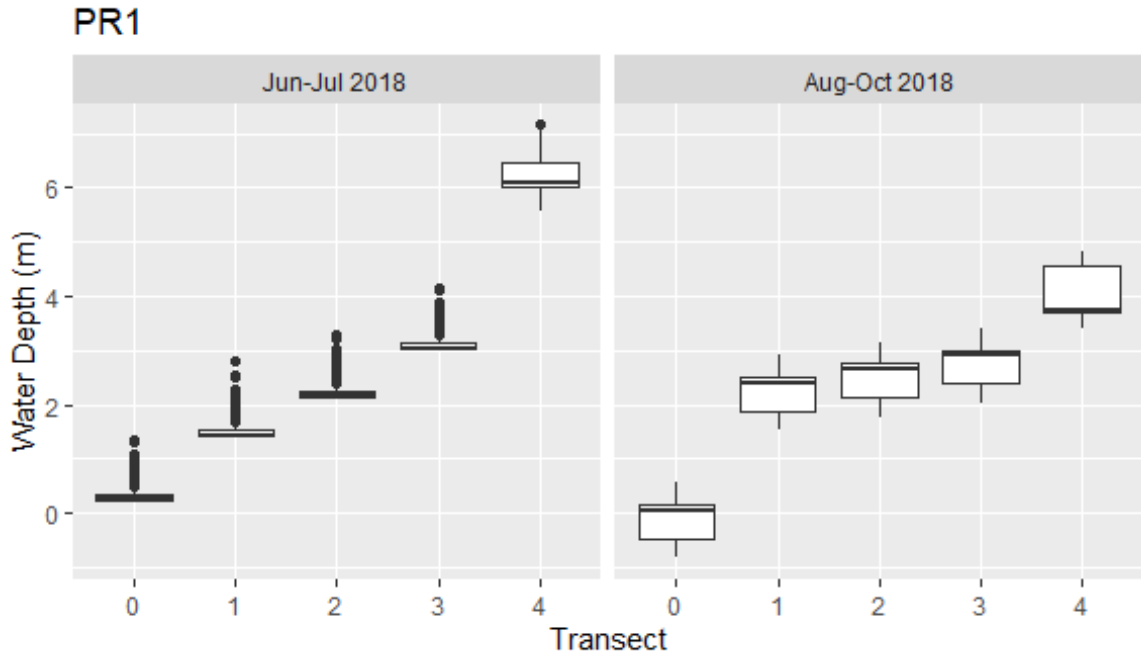


Figure A23 Boxplots of mean daily water depth for summer and fall 2018 sampling periods at each transect position in PR1

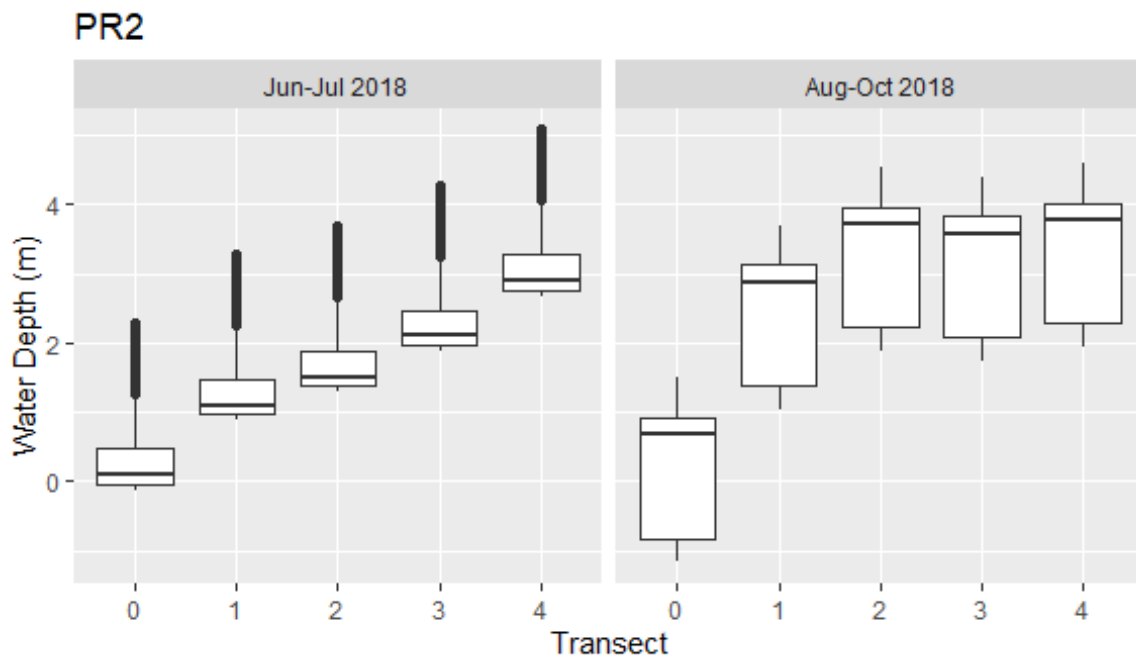


Figure A24 Boxplots of mean daily water depth for summer and fall 2018 sampling periods at each transect position in PR2

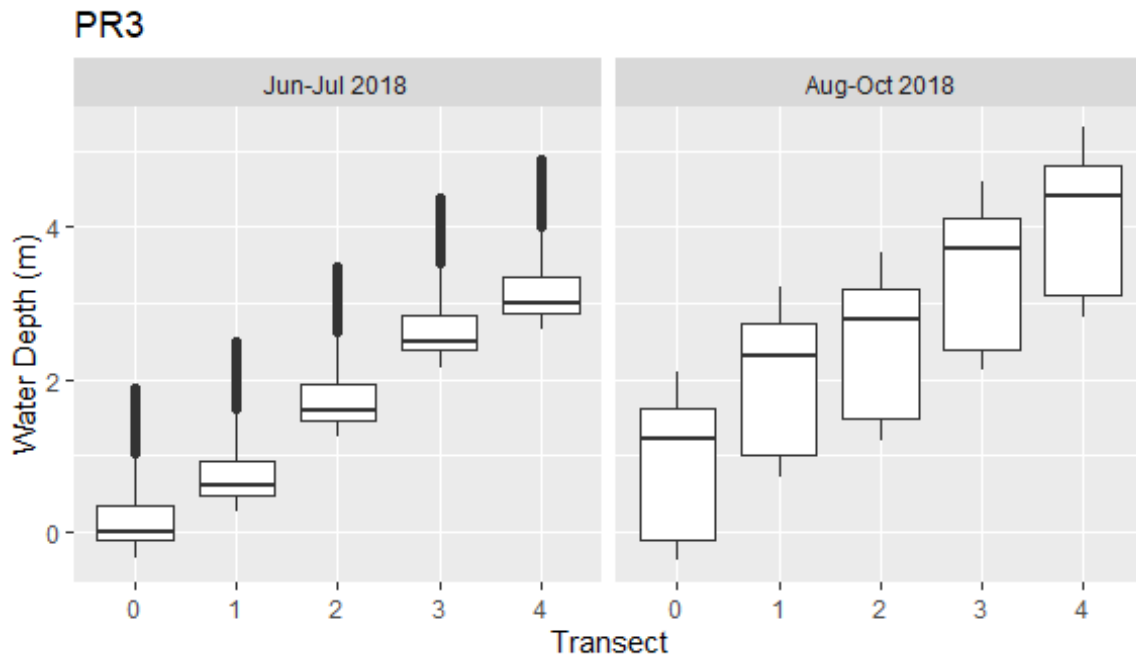


Figure A25 Boxplots of mean daily water depth for summer and fall 2018 sampling periods at each transect position in PR3

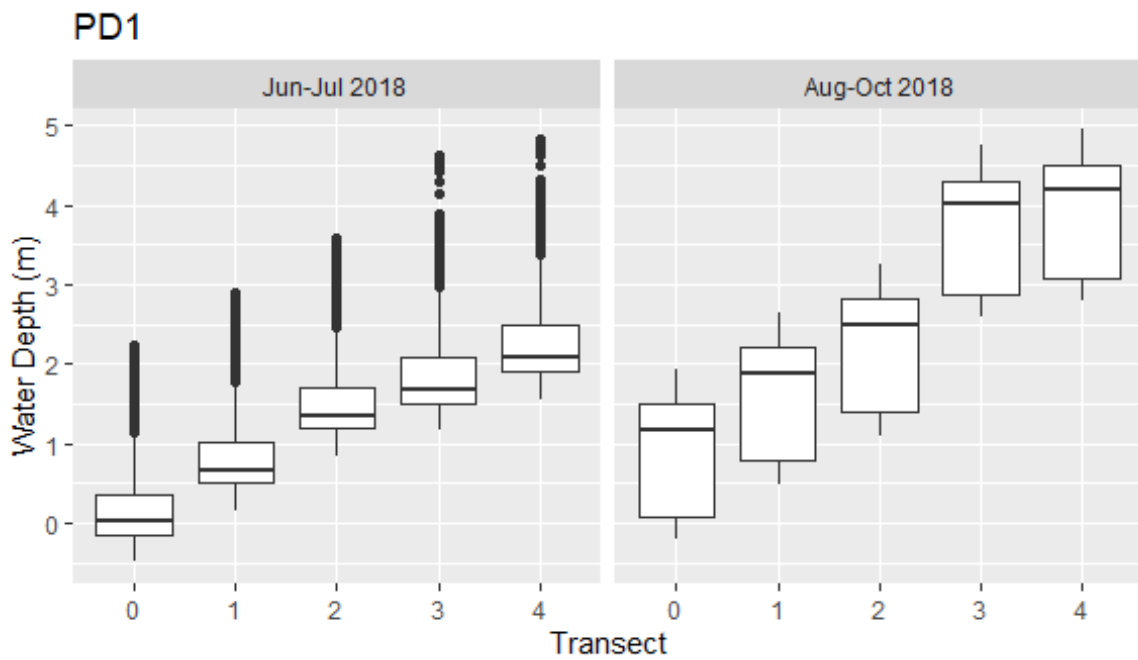


Figure A26 Boxplots of mean daily water depth for summer and fall 2018 sampling periods at each transect position in PD1

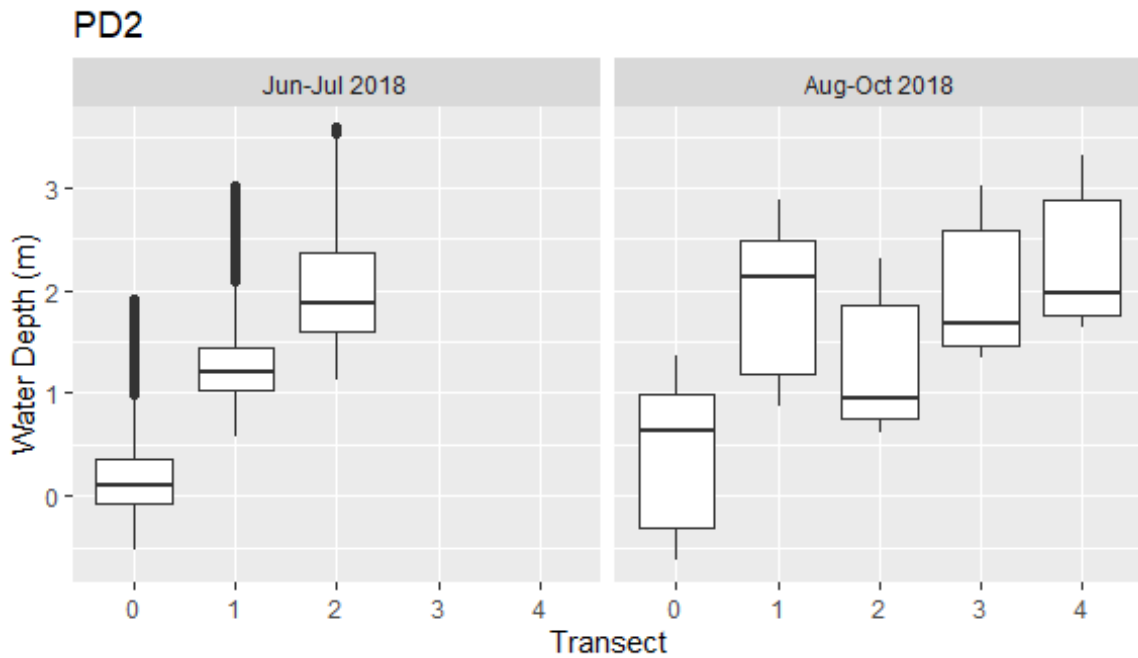


Figure A27 Boxplots of mean daily water depth for summer and fall 2018 sampling periods at each transect position in PD2

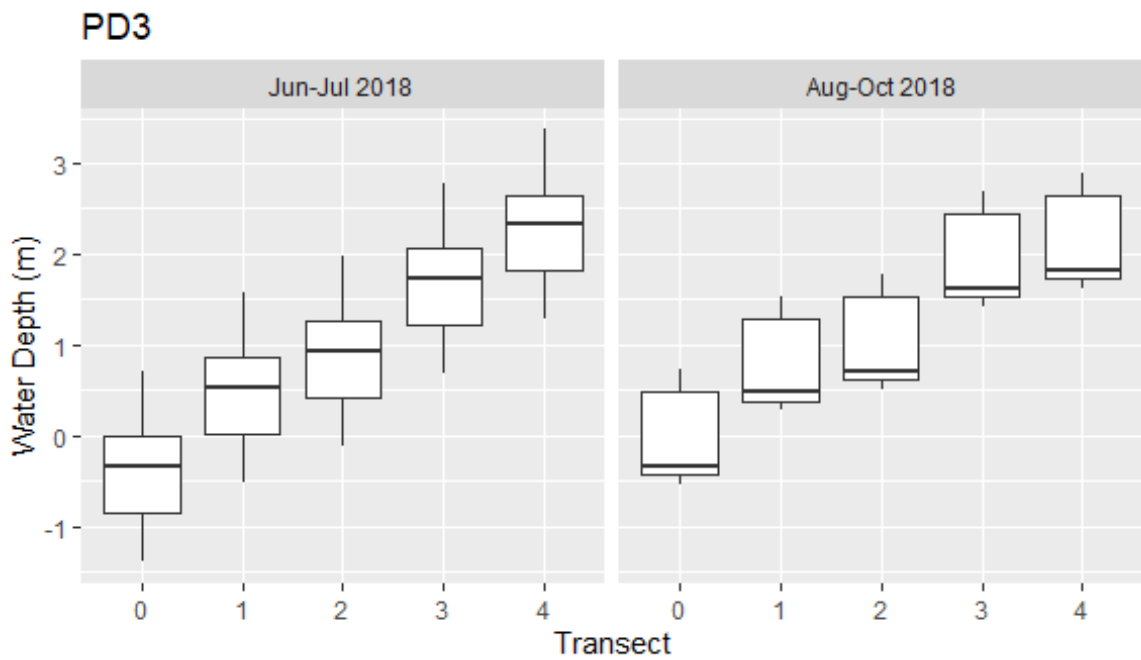


Figure A28 Boxplots of mean daily water depth for summer and fall 2018 sampling periods at each transect position in PD3

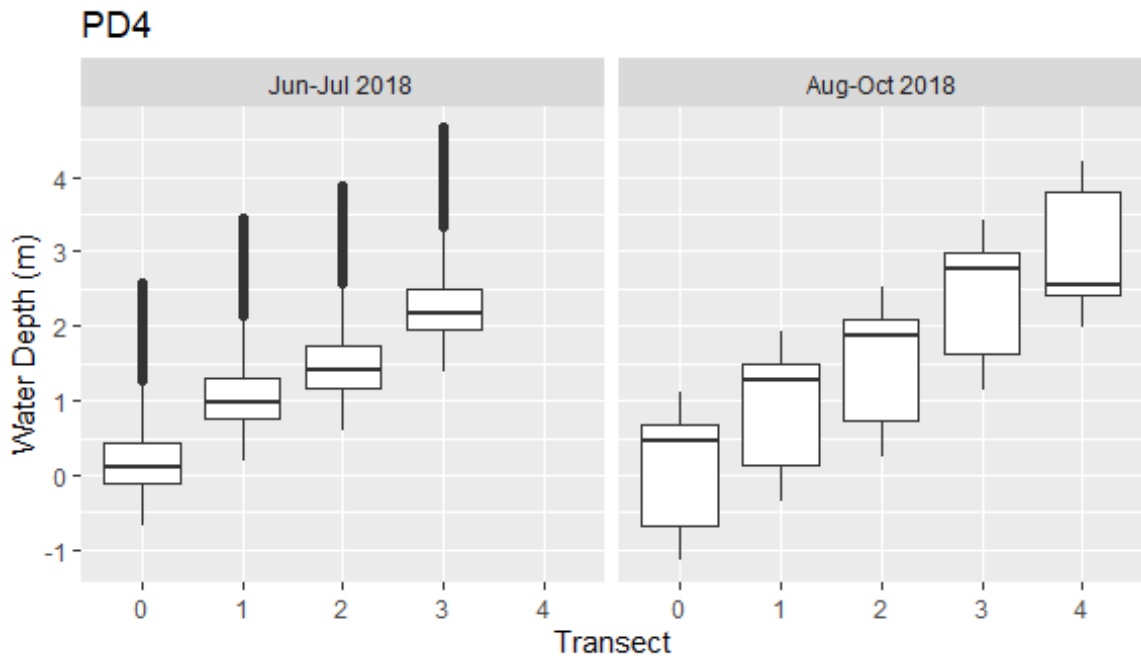


Figure A29 Boxplots of mean daily water depth for summer and fall 2018 sampling periods at each transect position in PD4

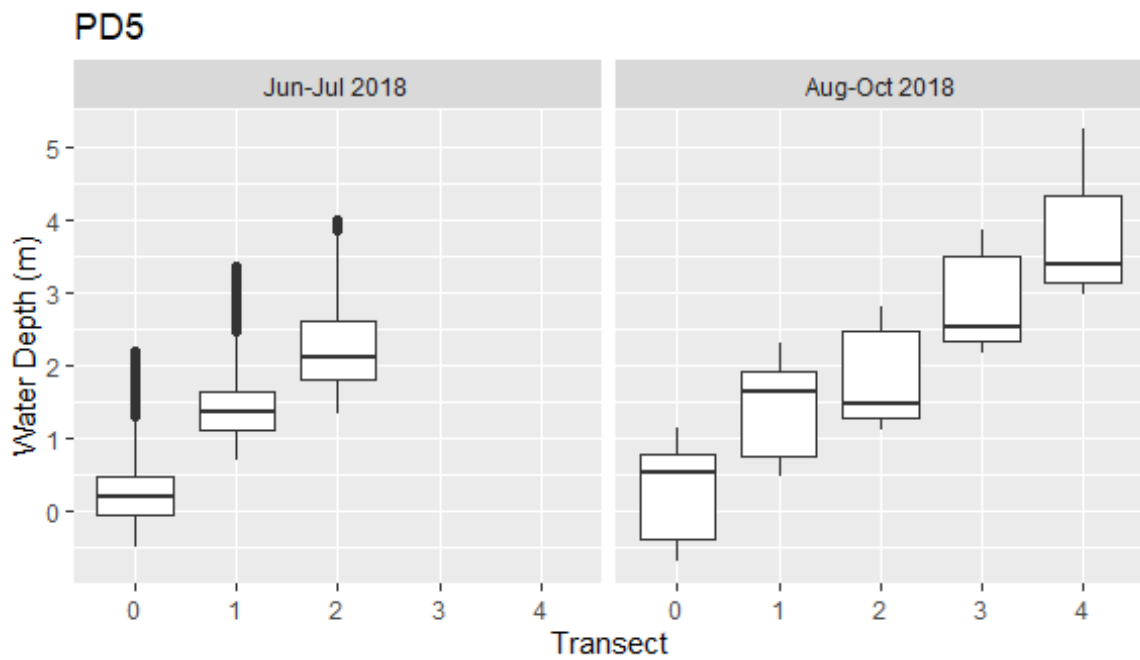


Figure A30 Boxplots of mean daily water depth for summer and fall 2018 sampling periods at each transect position in PD5

Appendix F Site Light Plots

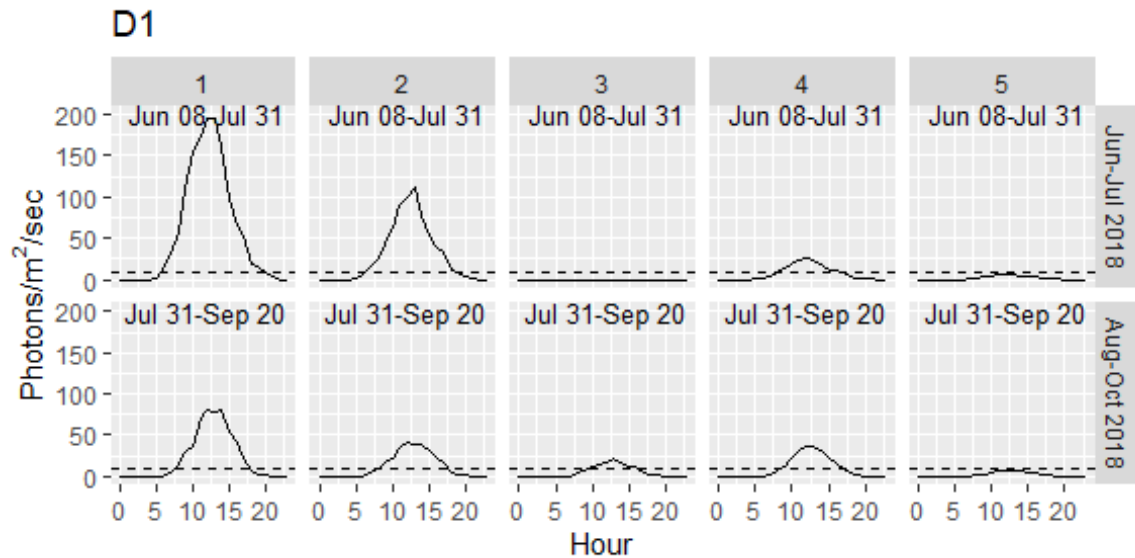


Figure A32 Average daily light intensity when samplers are submerged by transect (1-5) at D1 over the duration of deployment. The date range of deployment for 2018 is indicated, note the range is based on when samplers are submerged. Dashed line represents 10 photons, which delineates the lower extent of the photic zone.

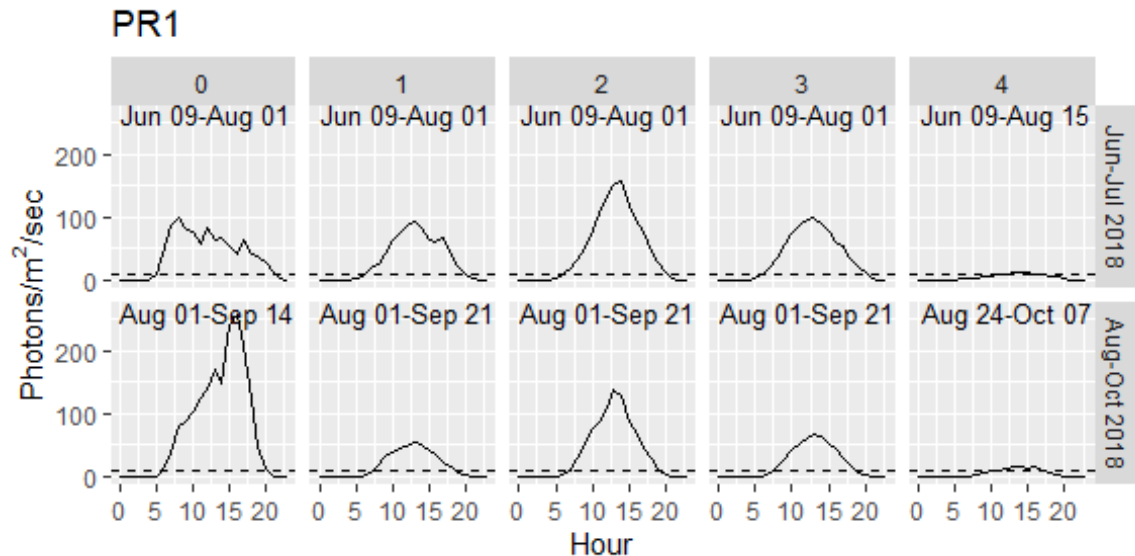


Figure A33 Average daily light intensity when samplers are submerged by transect (0-4) at PR1 over the duration of deployment. The date range of deployment for 2018 is indicated, note the range is based on when samplers are submerged. Dashed line represents 10 photons, which delineates the lower extent of the photic zone.

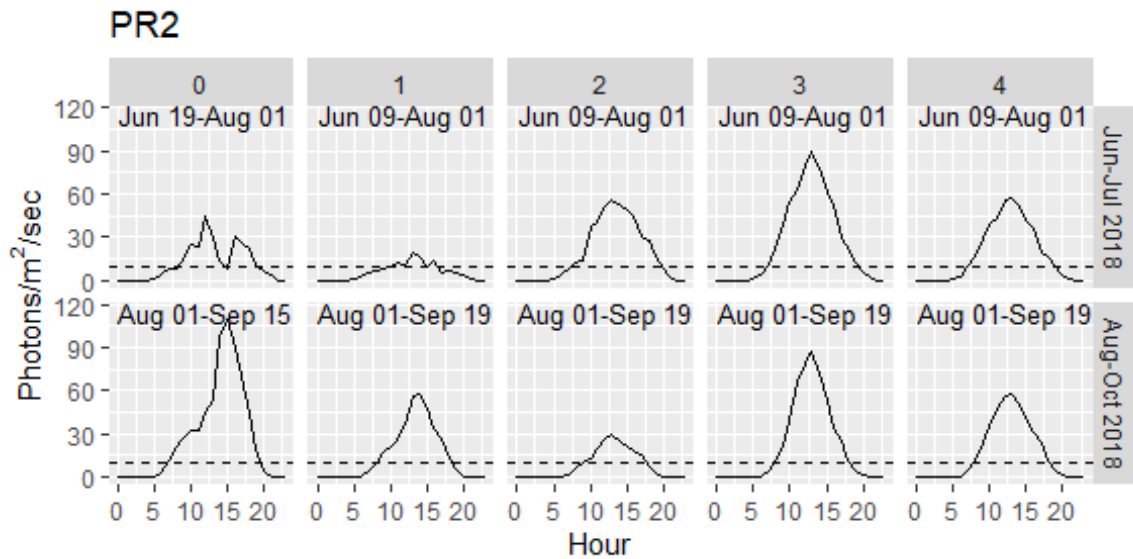


Figure A34 Average daily light intensity when samplers are submerged by transect (0-4) at PR2 over the duration of deployment. The date range of deployment for 2018 is indicated, note the range is based on when samplers are submerged. Dashed line represents 10 photons, which delineates the lower extent of the photic zone.

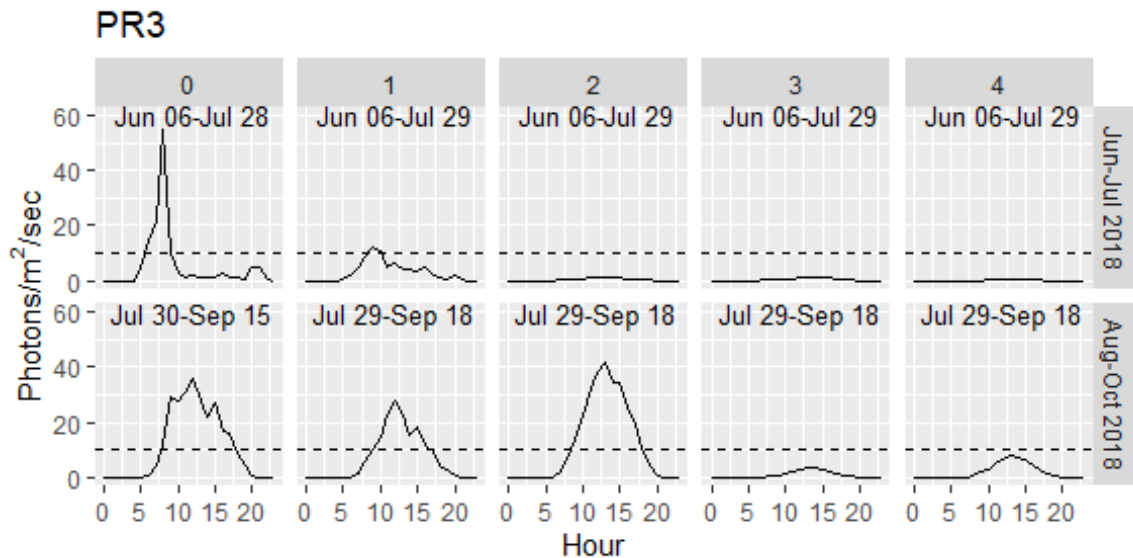


Figure A35 Average daily light intensity when samplers are submerged by transect (0-4) at PR3 over the duration of deployment. The date range of deployment for 2018 is indicated, note the range is based on when samplers are submerged. Dashed line represents 10 photons, which delineates the lower extent of the photic zone.

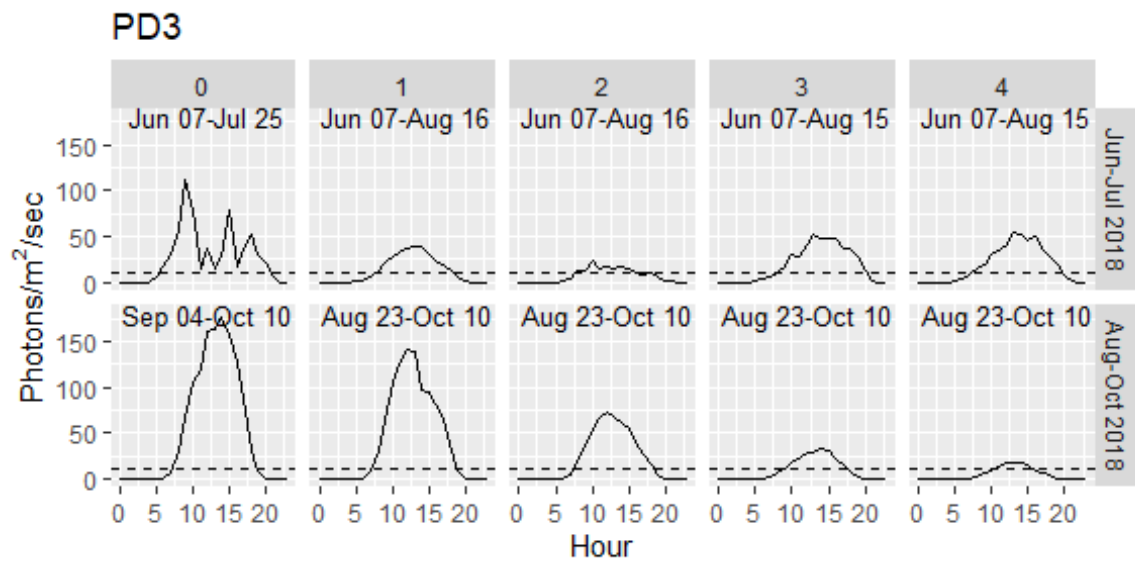


Figure A38 Average daily light intensity when samplers are submerged by transect (0-4) at PD3 over the duration of deployment. The date range of deployment for 2018 is indicated, note the range is based on when samplers are submerged. Dashed line represents 10 photons, which delineates the lower extent of the photic zone.

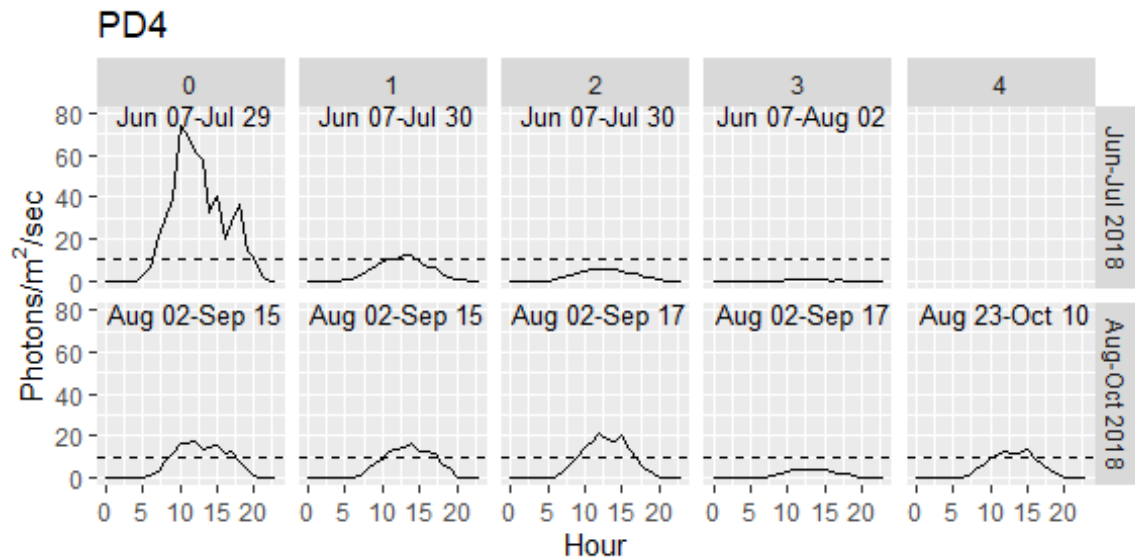


Figure A39 Average daily light intensity when samplers are submerged by transect (0-4) at PD4 over the duration of deployment. The date range of deployment for 2018 is indicated, note the range is based on when samplers are submerged. Dashed line represents 10 photons, which delineates the lower extent of the photic zone.

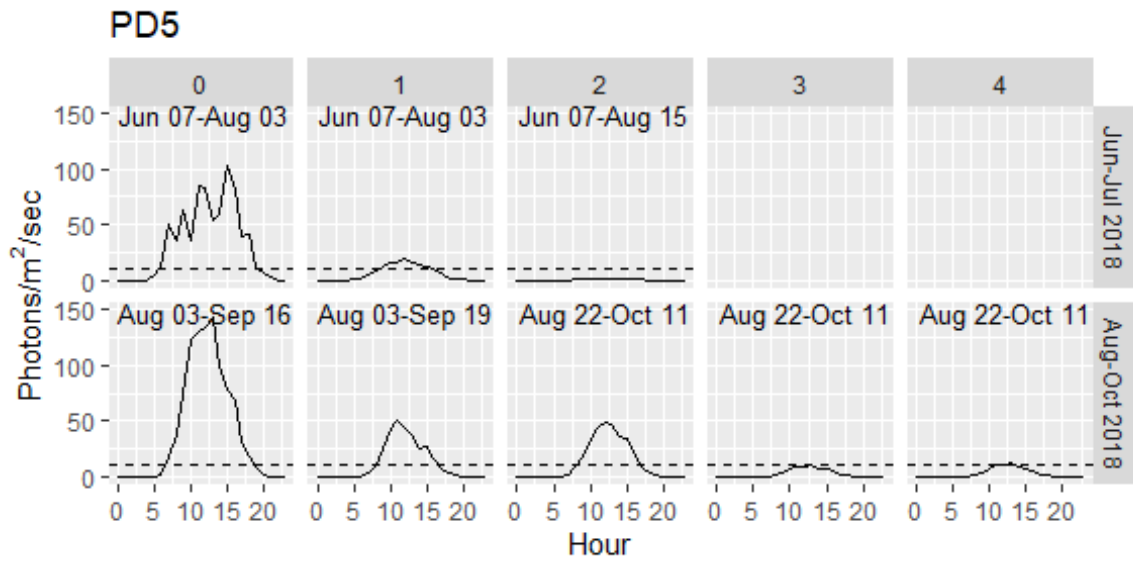


Figure A40 Average daily light intensity when samplers are submerged by transect (0-4) at PD5 over the duration of deployment. The date range of deployment for 2018 is indicated, note the range is based on when samplers are submerged. Dashed line represents 10 photons, which delineates the lower extent of the photic zone.

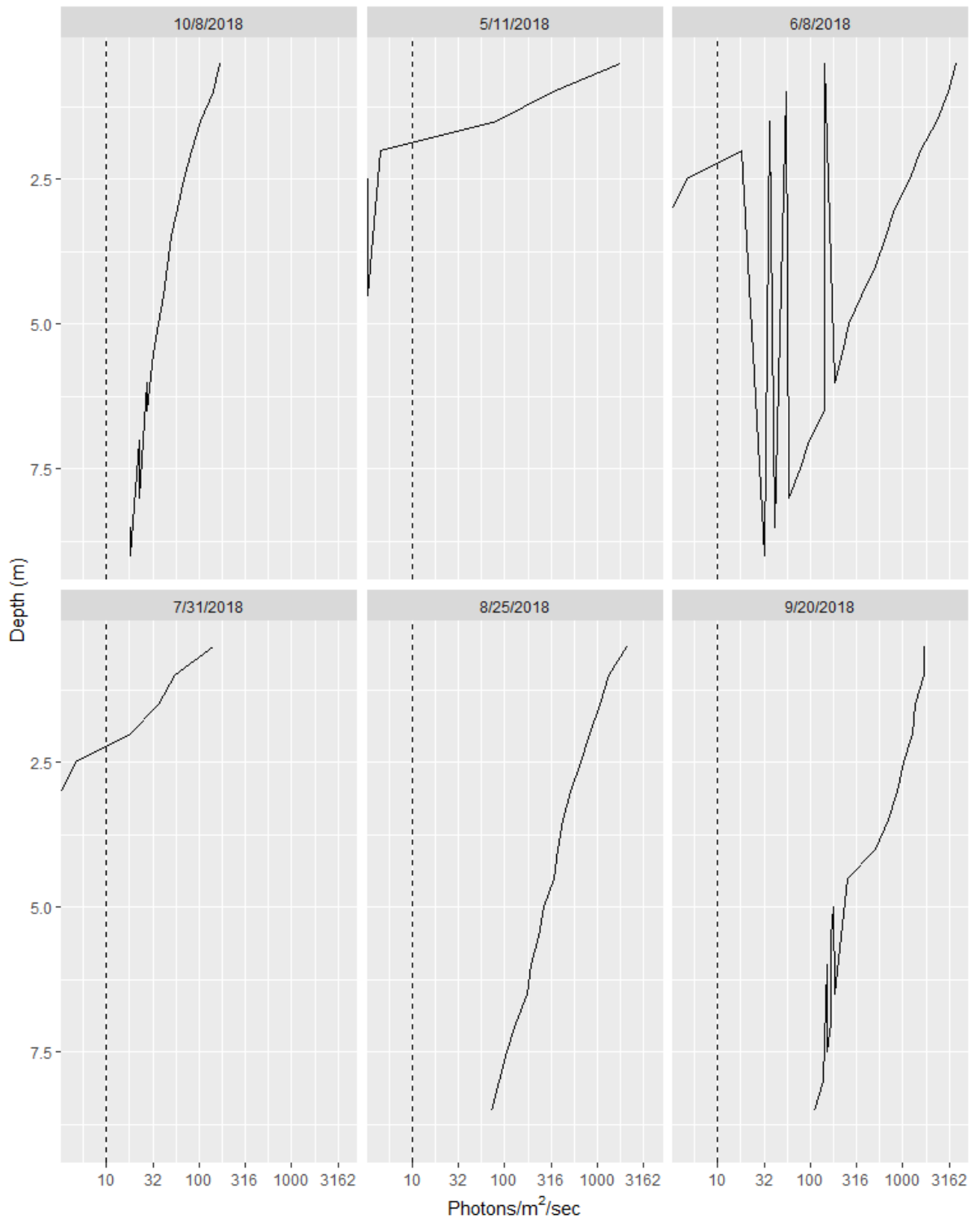
Appendix G Reservoir and Riverine PAR Profiles

Figure A41 PAR profiles for 2018 Dinosaur Pelagic ,10 photons delineates the lower extent of the photic zone.

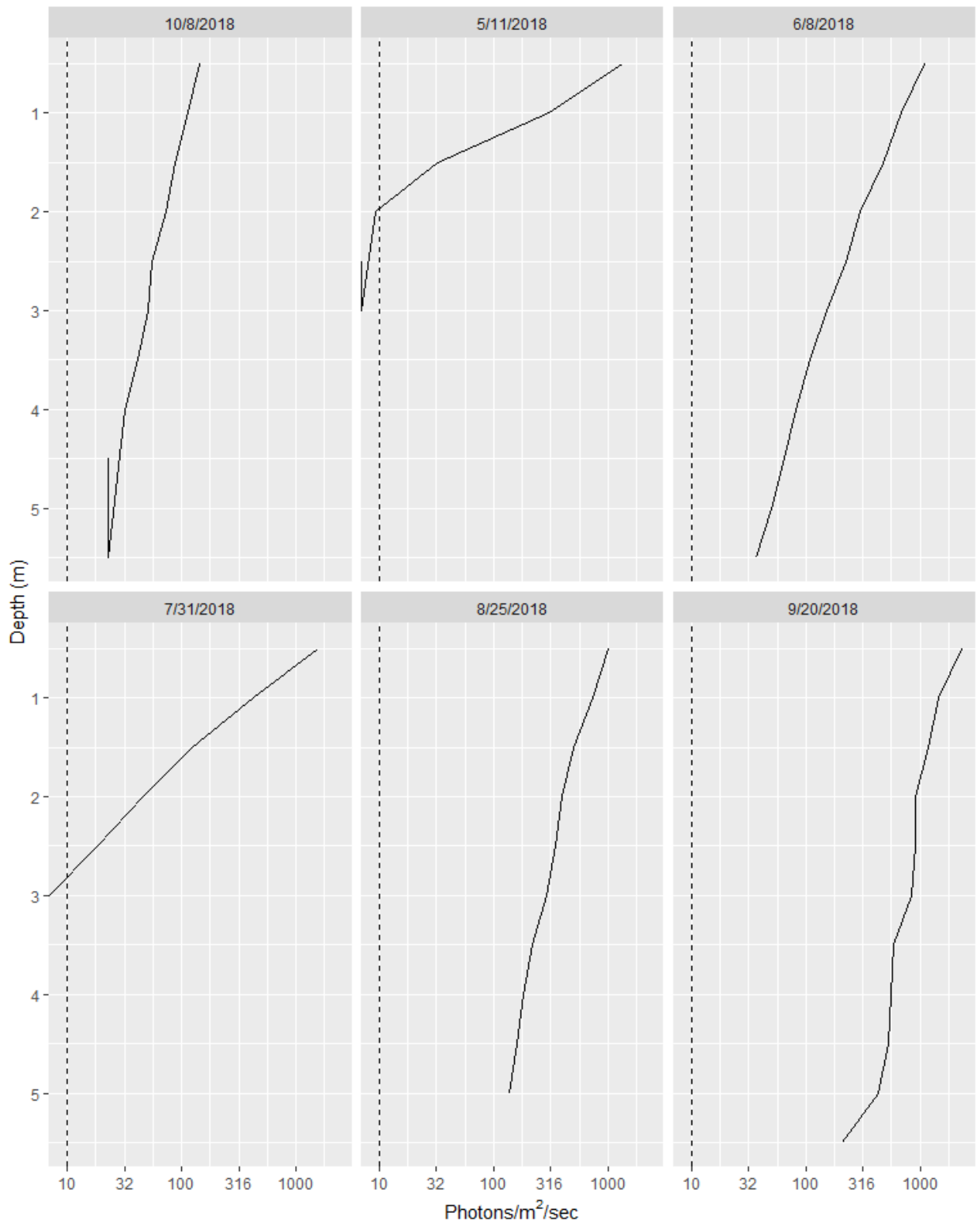


Figure A42 PAR profiles for 2018 Dinosaur Littoral, 10 photons delineates the lower extent of the photic zone.

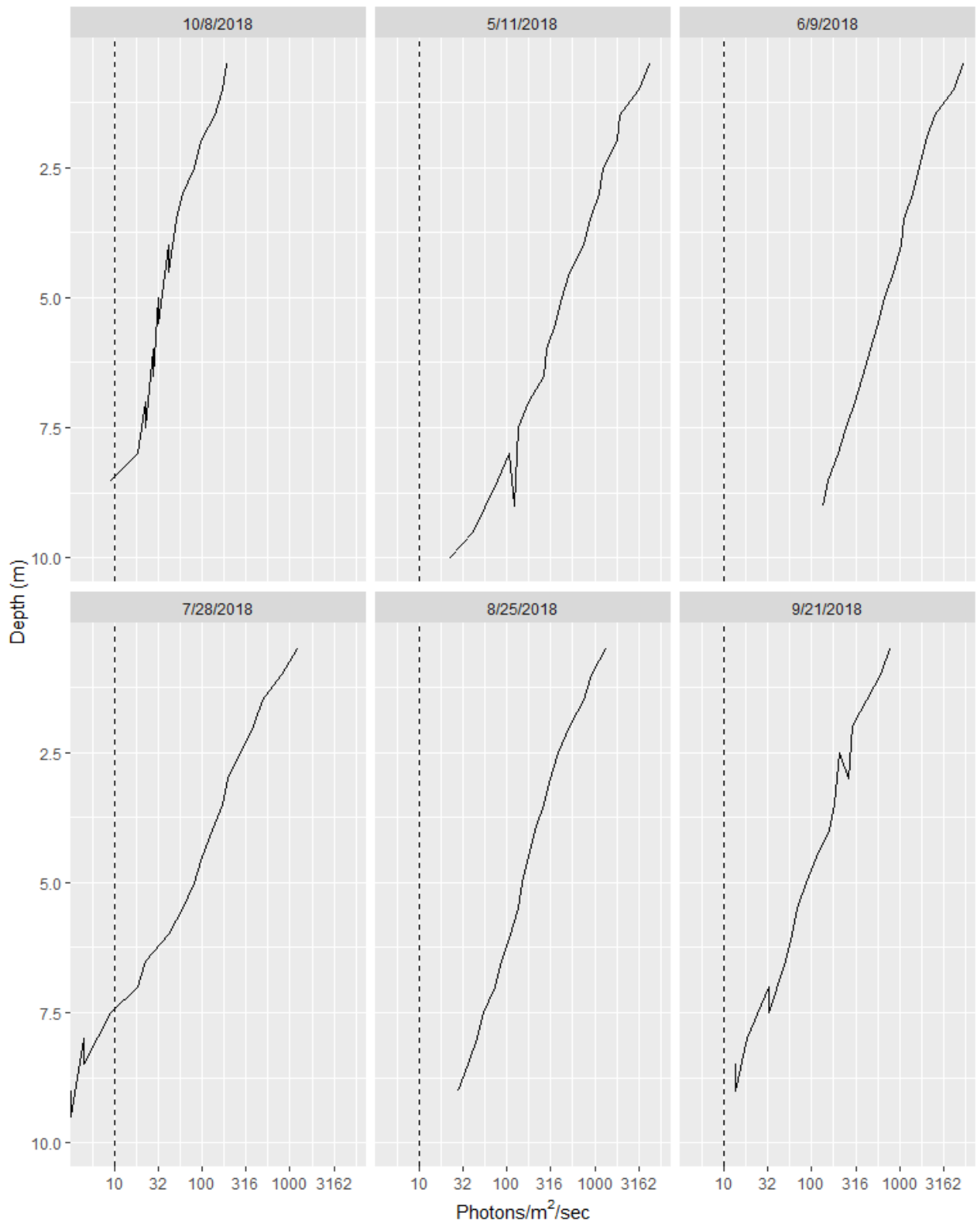


Figure A43 PAR profiles for 2018 Williston Pelagic, 10 photons delineates the lower extent of the photic zone.

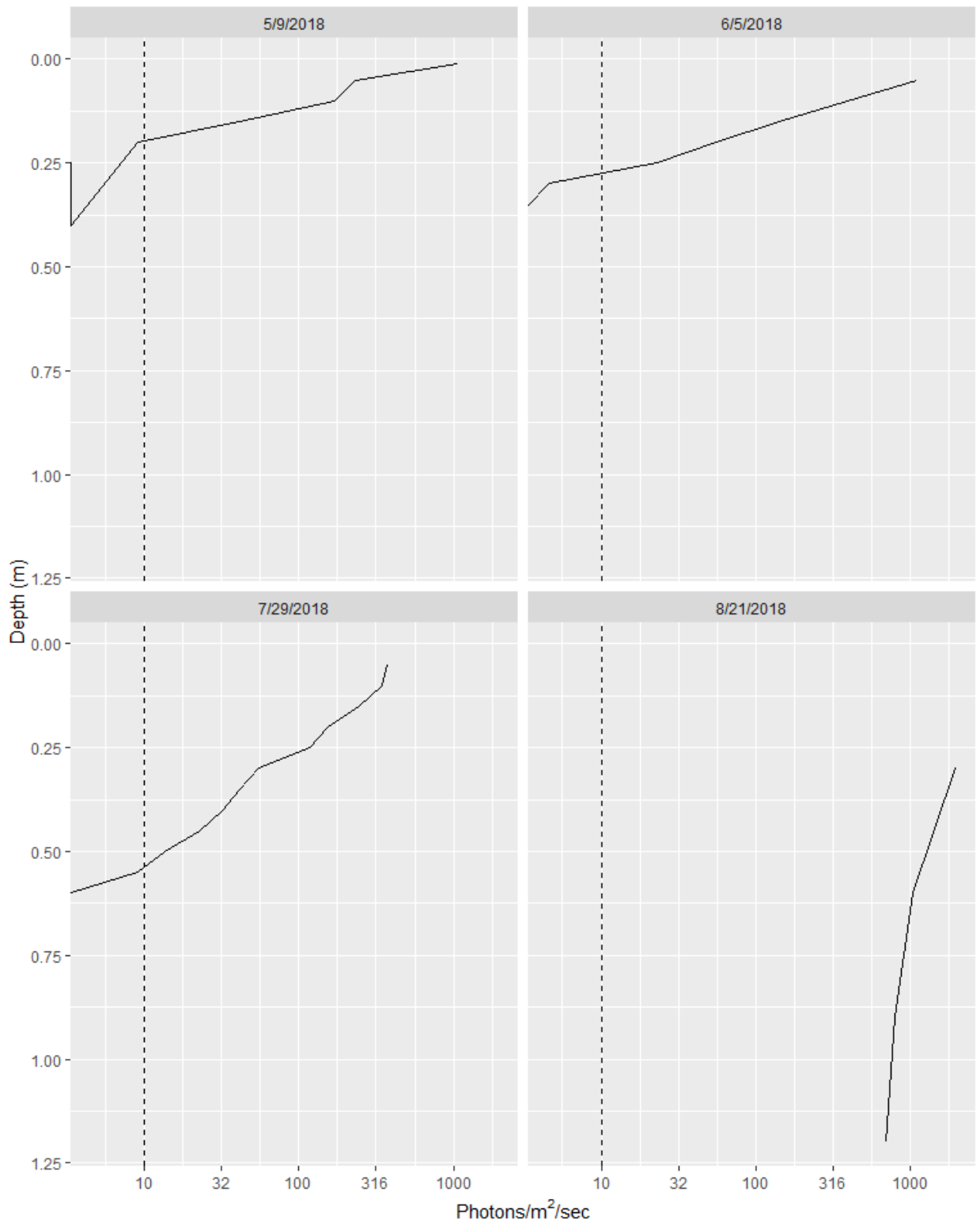


Figure A44 PAR profiles for 2018 PD1 ,10 photons delineates the lower extent of the photic zone.

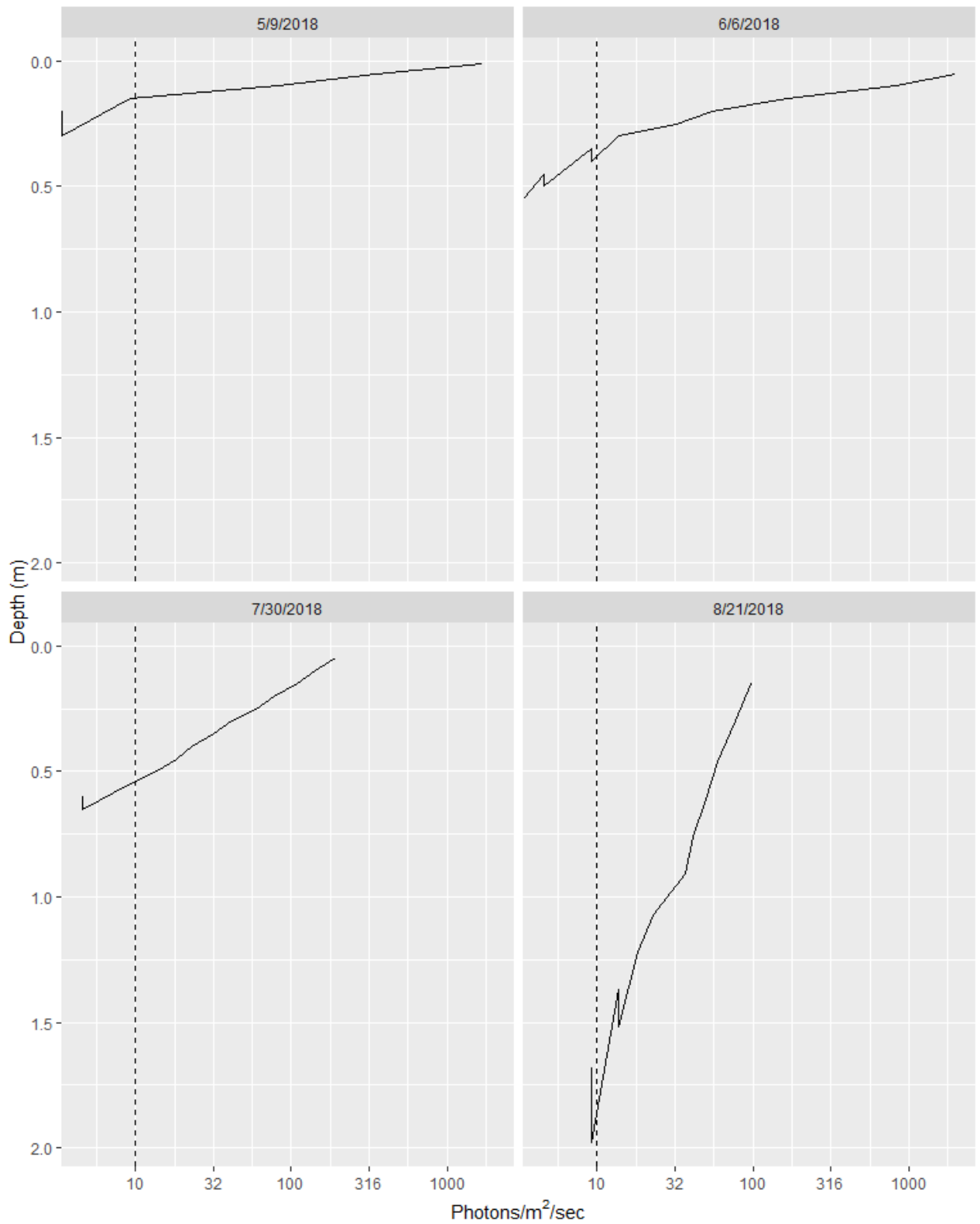


Figure A45 PAR profiles for 2018 PD2 ,10 photons delineates the lower extent of the photic zone.

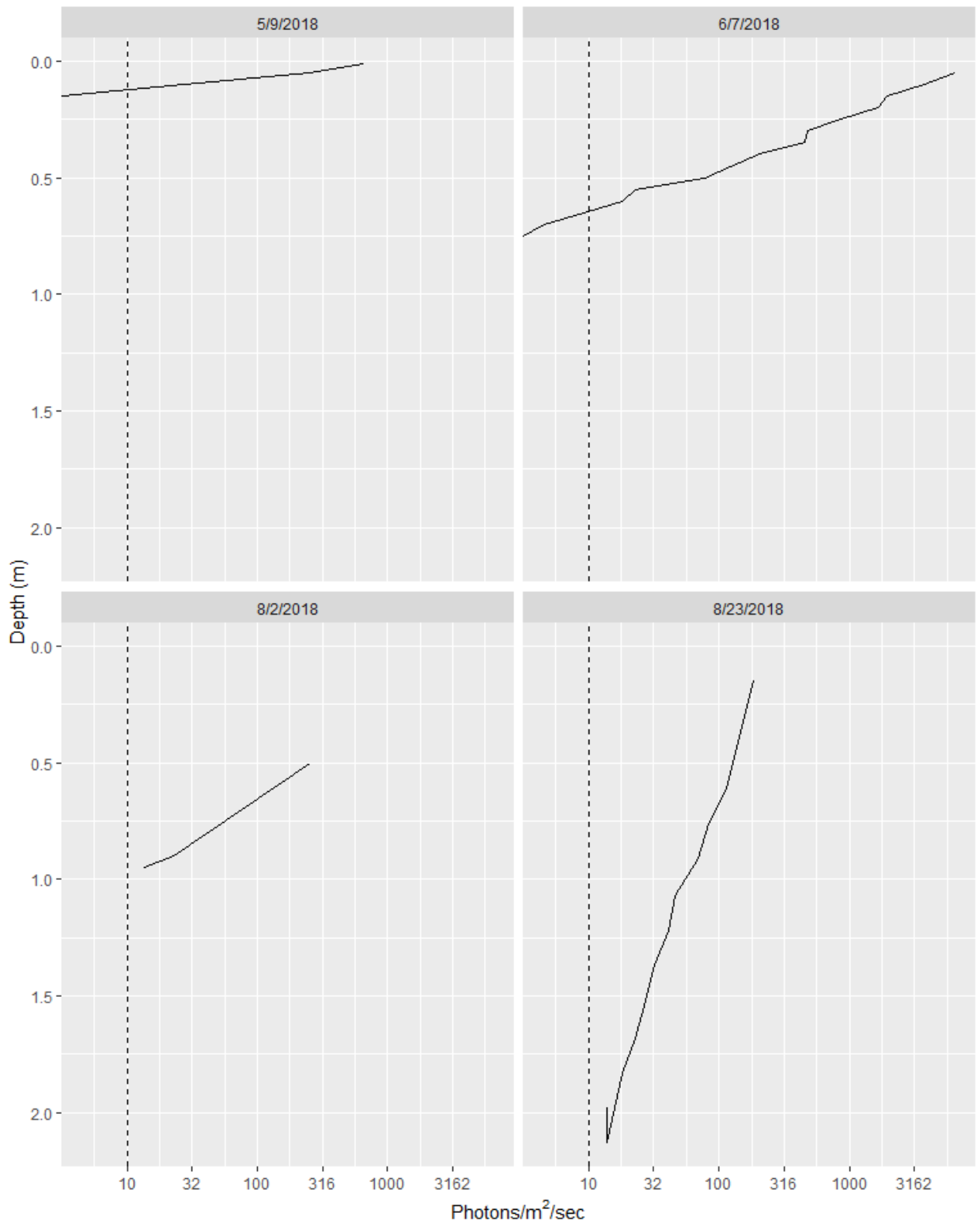


Figure A46 PAR profiles for 2018 PD3 ,10 photons delineates the lower extent of the photic zone.

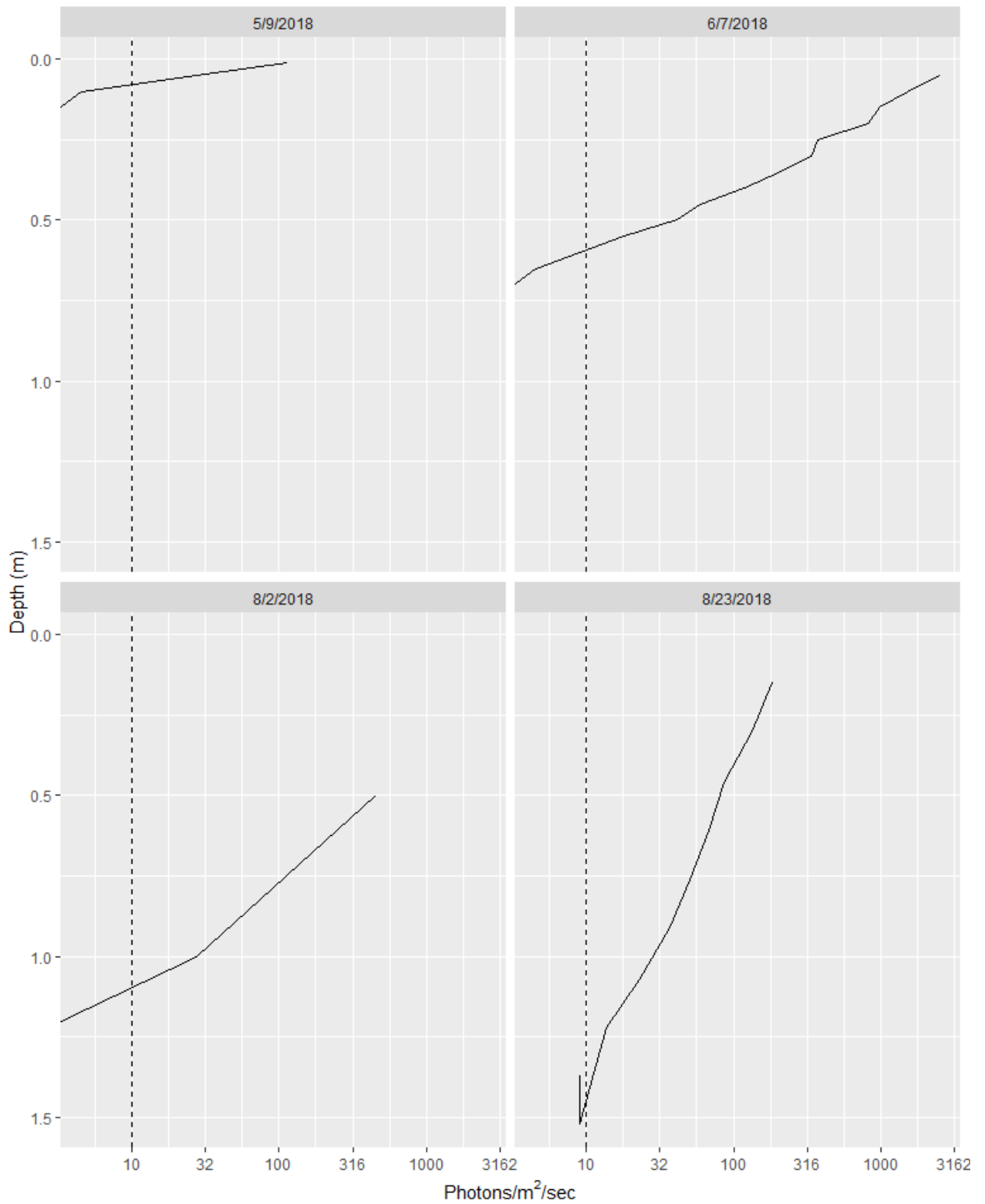


Figure A47 PAR profiles for 2018 PD4 ,10 photons delineates the lower extent of the photic zone.

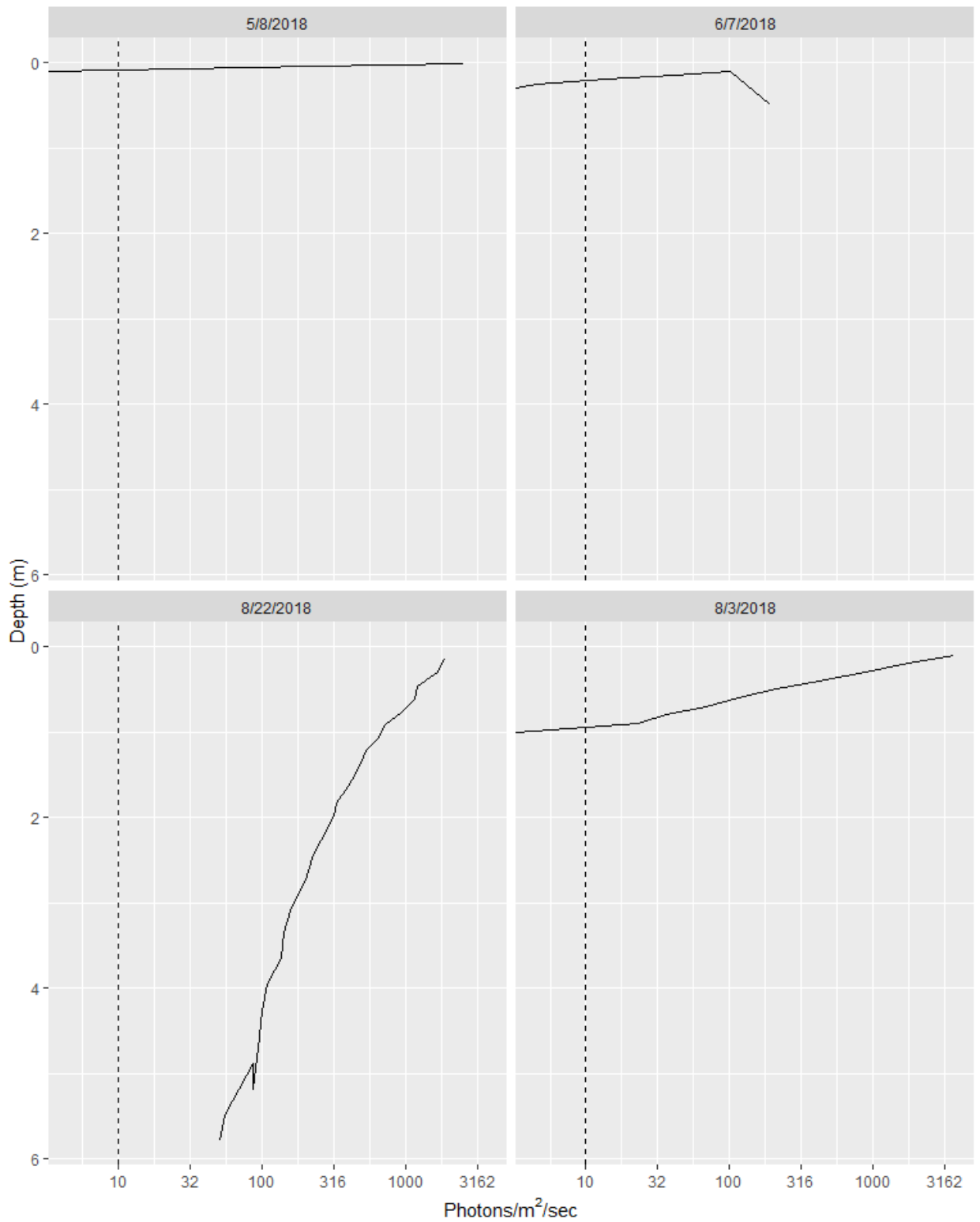


Figure A48 PAR profiles for 2018 PD5 ,10 photons delineates the lower extent of the photic zone.

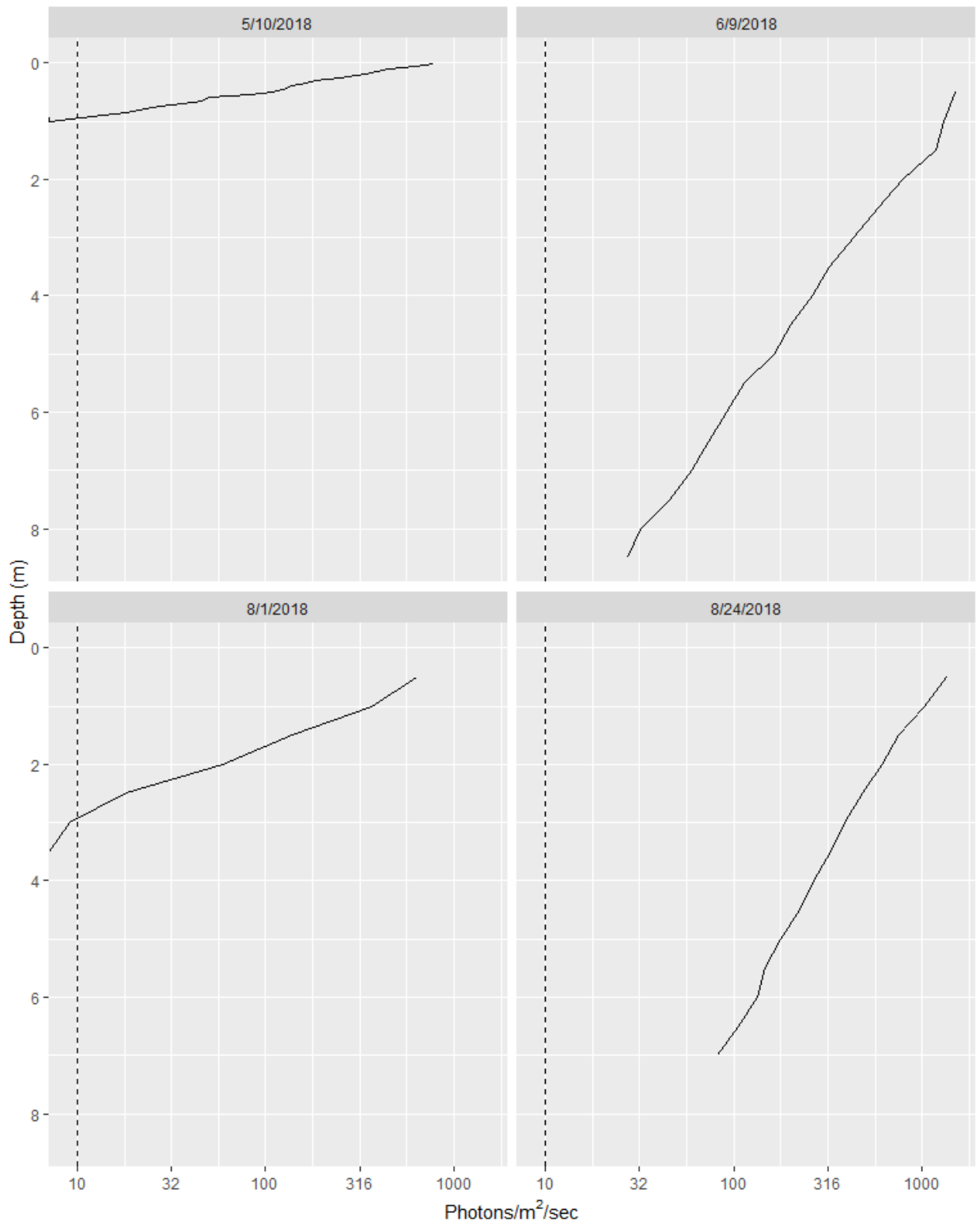


Figure A49 PAR profiles for 2018 PR1 ,10 photons delineates the lower extent of the photic zone.

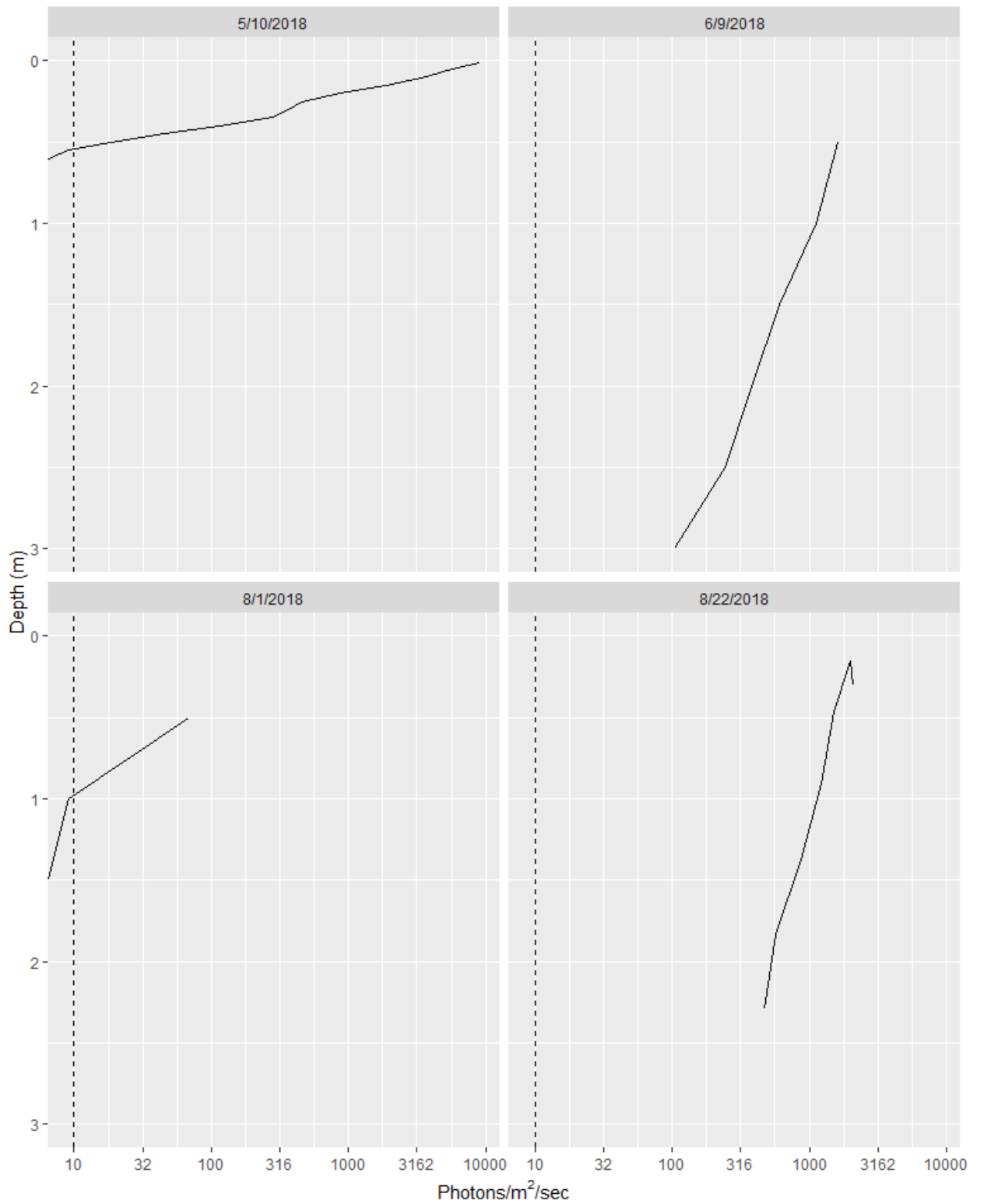


Figure A50 PAR profiles for 2018 PR2 ,10 photons delineates the lower extent of the photic zone.

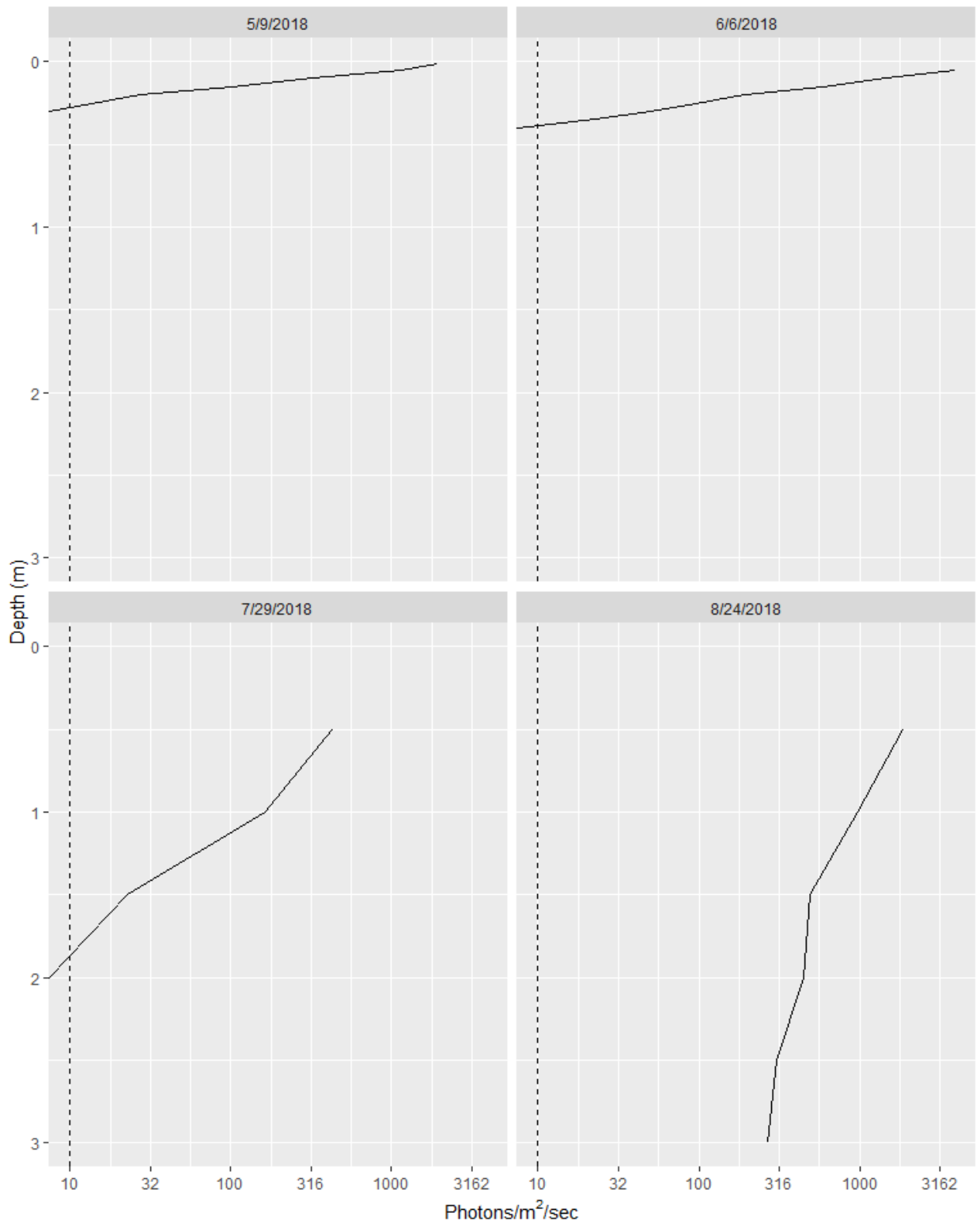


Figure A51 PAR profiles for 2018 PR3 ,10 photons delineates the lower extent of the photic zone.

Appendix H Reservoir Multimeter Temperature / Turbidity Profiles

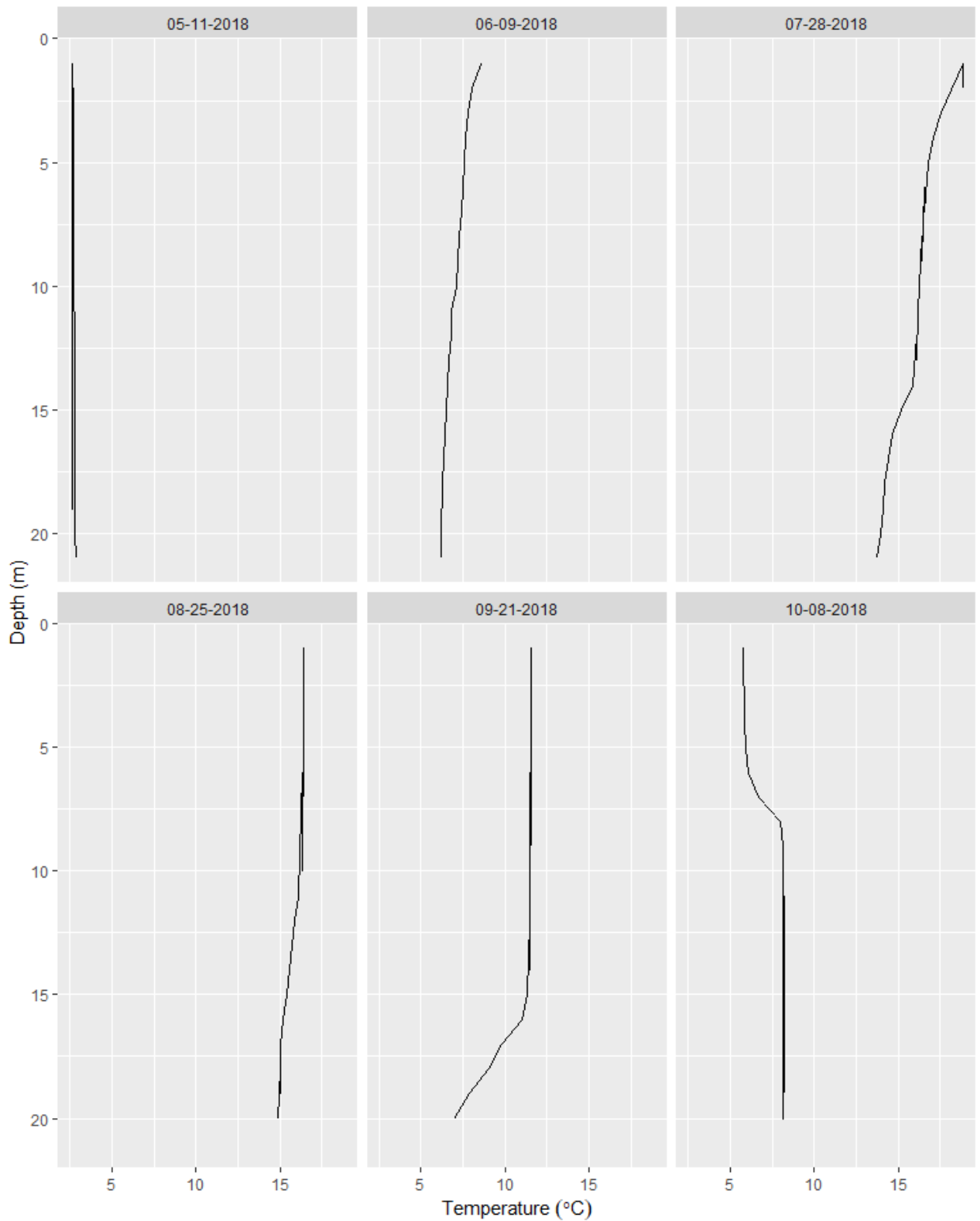


Figure A52 Multimeter depth and temperature profiles for 2018 W1 .

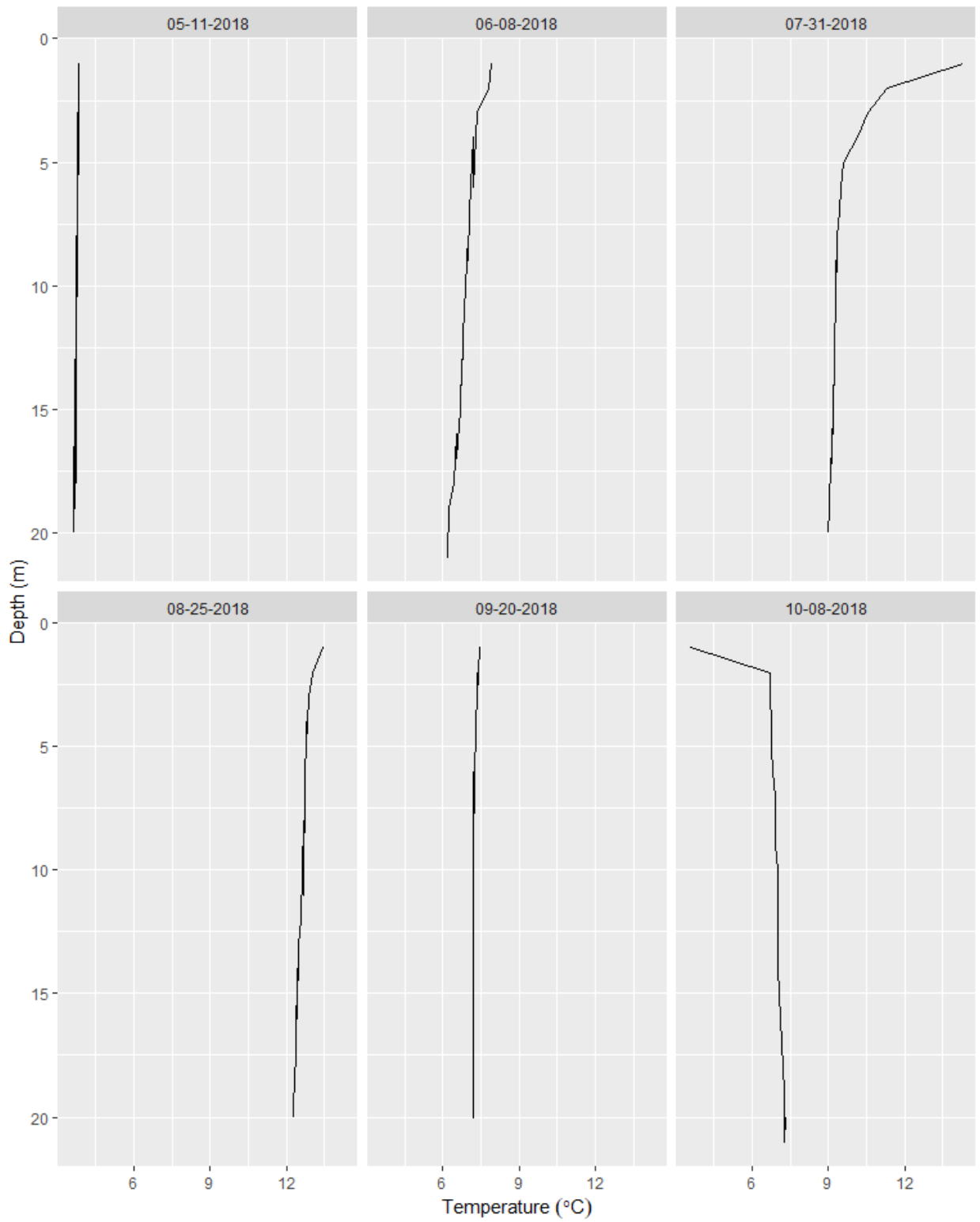


Figure A53 Multimeter depth and temperature profiles for 2018 D1-P .

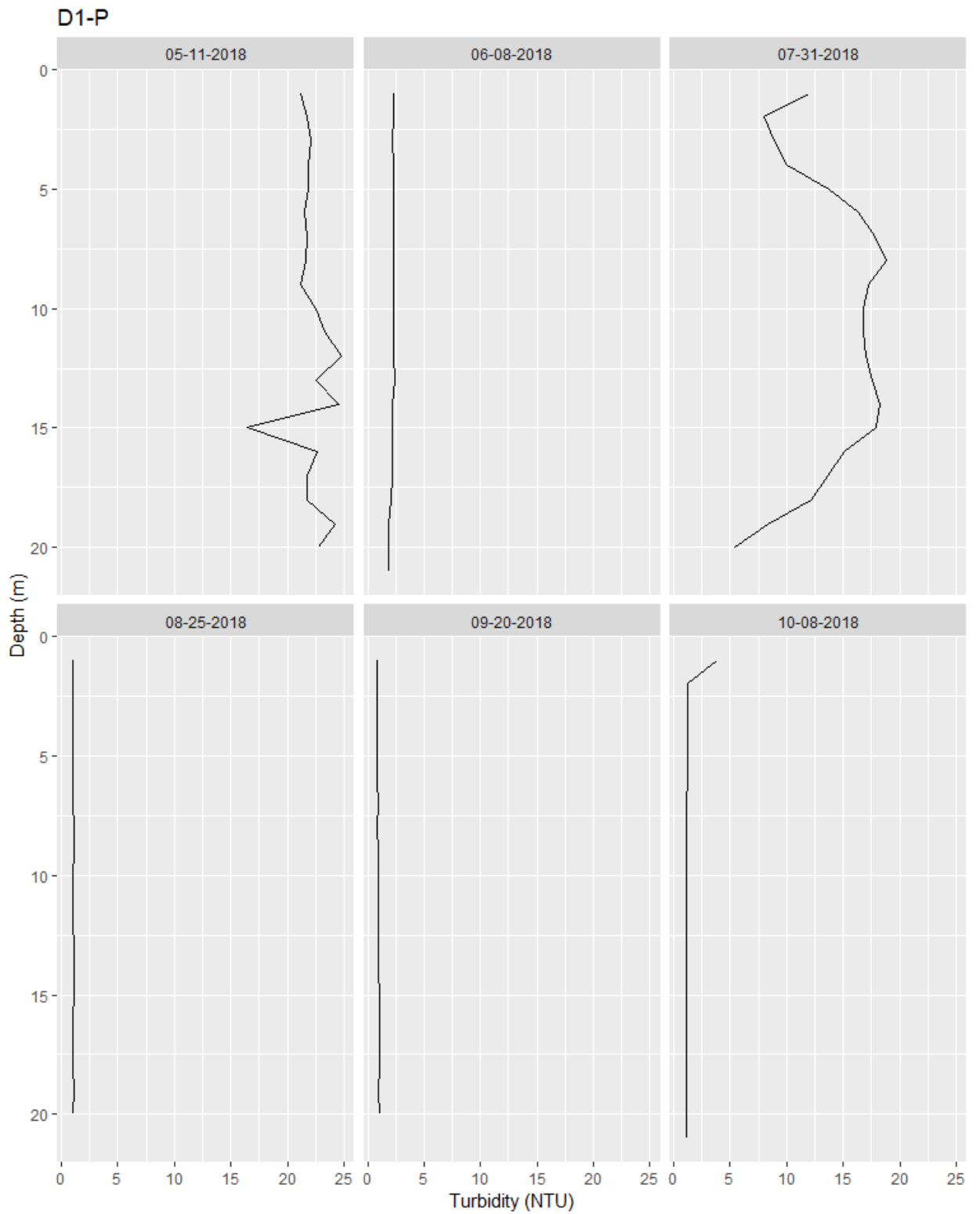


Figure A54 Multimeter depth and turbidity profiles for 2018 at D1-P .

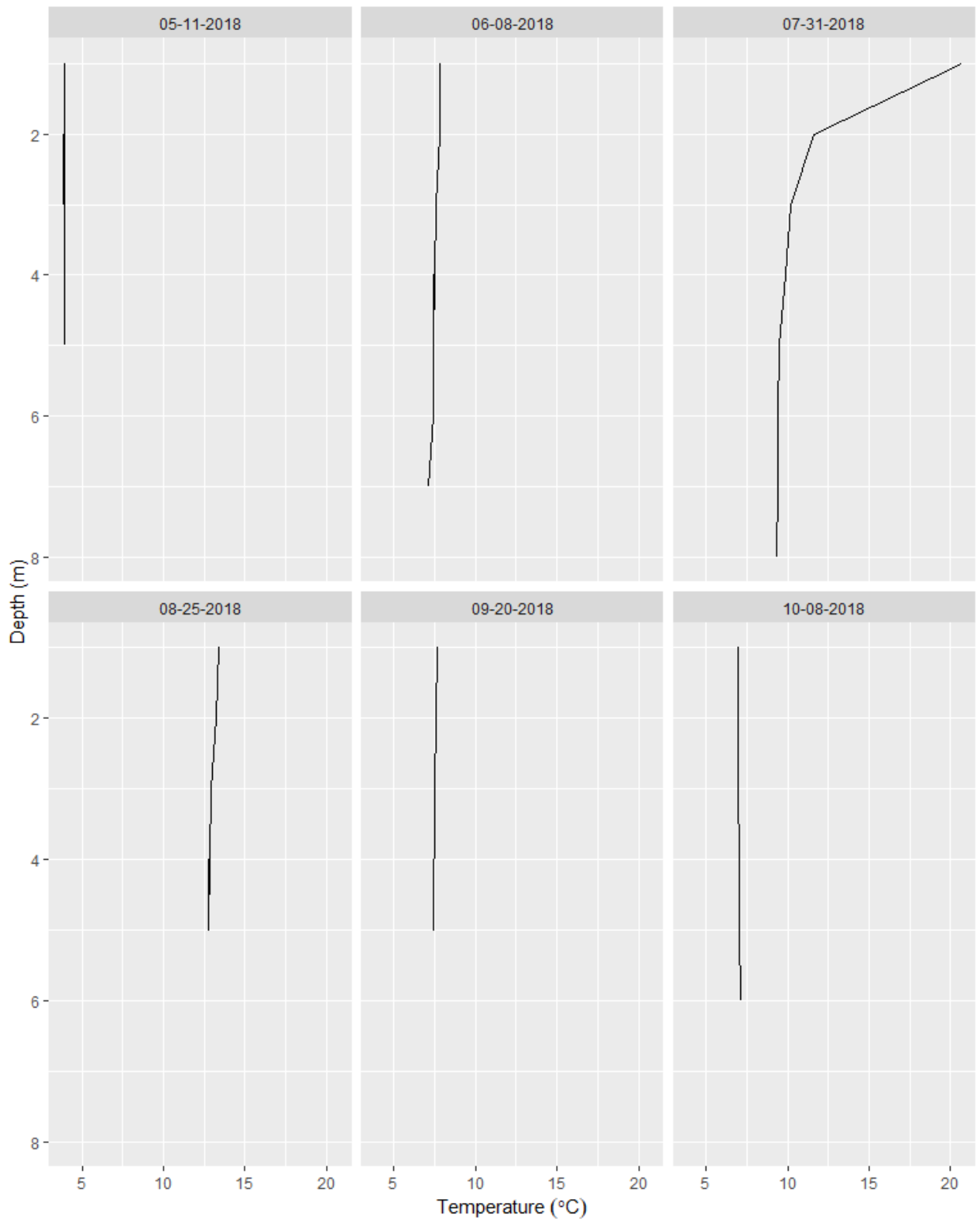


Figure A55 Multimeter depth and temperature profiles for 2018 D1-L .

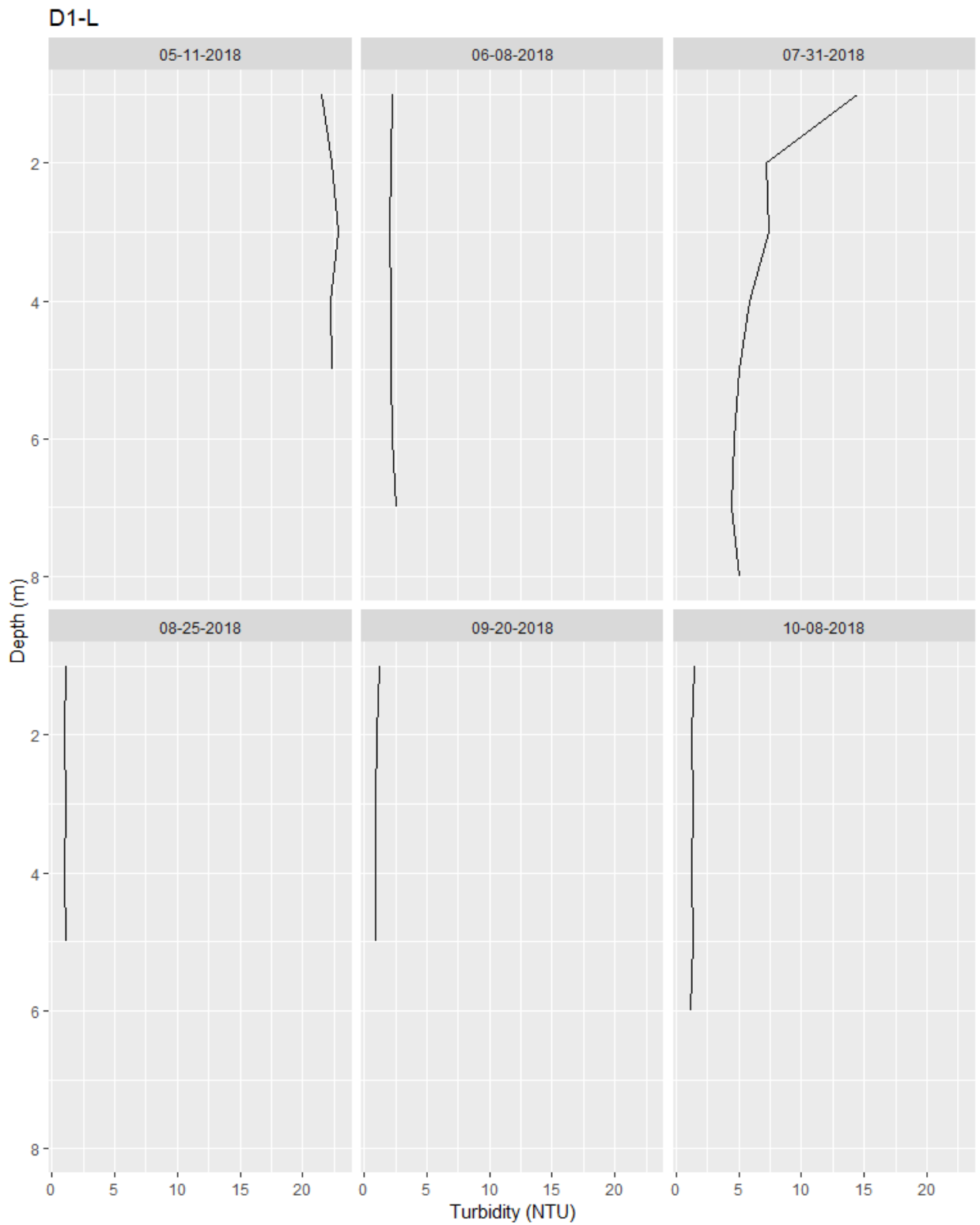


Figure A56 Multimeter depth and turbidity profiles for 2018 at D1-L .

Appendix I Fort St. John Weather Results

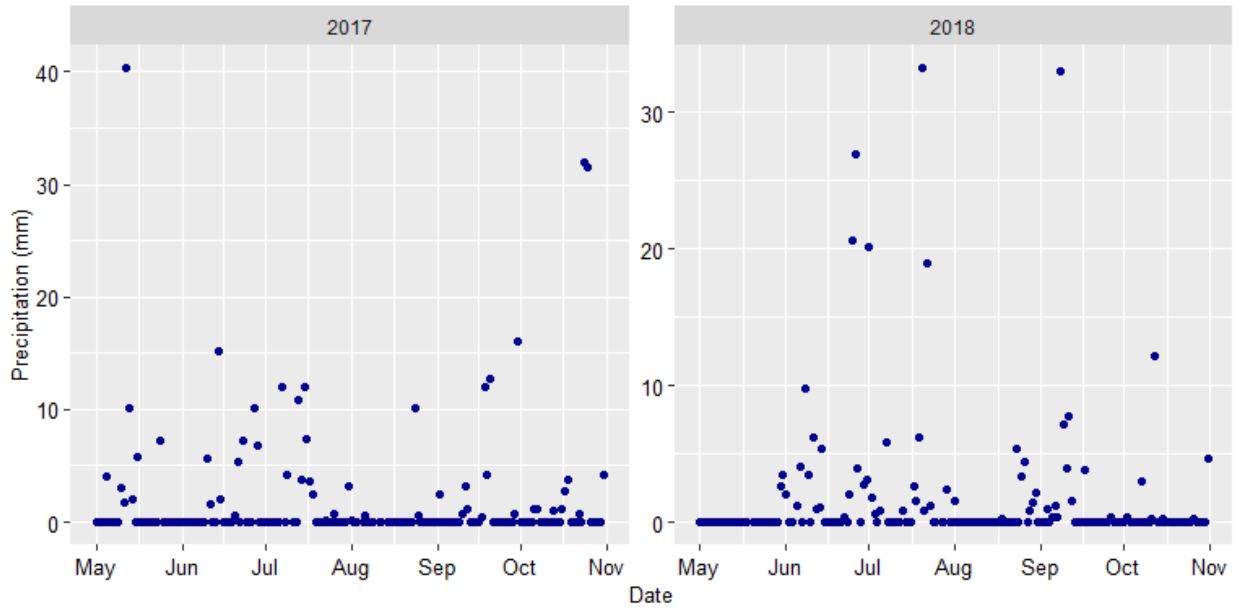


Figure A57 Average Daily Precipitation (mm) between May and October by Year

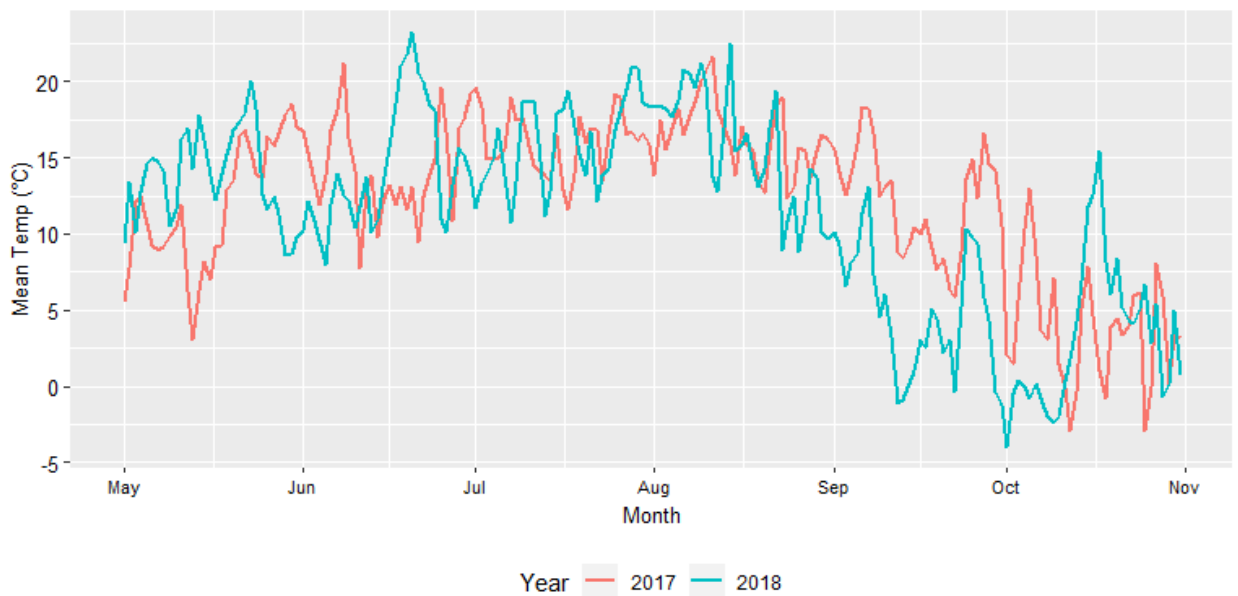


Figure A58 Average Daily Air Temperature (°C) between May and October by Year

Appendix J Light Model Results

Site C Light Attenuation Analysis 2018

Thorley, J.L.

Draft: 2018-09-28 17:34:02

The suggested citation for this [analytic report](#) is:

Thorley, J.L. (2018) Site C Light Attenuation Analysis 2018. A Poisson Consulting Analysis Report. URL: <http://www.poissonconsulting.ca/f/1021989194>.

Background

The primary goal of the analysis is to address the following question:

How is light attenuation in the Peace River influenced by depth and turbidity?

Methods

Data Collection

In 2018, Ecoscape deployed light loggers a fixed distance apart at various sites. They also deployed turbidity loggers at a subset of sites and took spot light readings at the surface, 0.01 m below the surface and at increasing depths together with spot turbidity measurements.

The data were provided as csv files.

Data Preparation

The data were prepared for analysis using R version 3.5.1 (R Core Team 2018).

Statistical Analysis

Model parameters were estimated using Bayesian methods. The Bayesian estimates were produced using JAGS (Plummer 2015). For additional information on Bayesian estimation the reader is referred to McElreath (2016).

Unless indicated otherwise, the Bayesian analyses used normal and uniform prior distributions that were vague in the sense that they did not constrain the posteriors (Kery and Schaub 2011, 36). The posterior distributions were estimated from 1500 Markov Chain Monte Carlo (MCMC) samples thinned from the second halves of 3 chains (Kery and Schaub 2011, 38–40). Model convergence was confirmed by ensuring that the potential scale reduction factor $\hat{R} \leq 1.05$ (Kery and Schaub 2011, 40) and the effective sample size (Brooks et al. 2011) $ESS \geq 150$ for each of the monitored parameters (Kery and Schaub 2011, 61).

The parameters are summarized in terms of the point *estimate*, standard deviation (*sd*), the *z-score*, *lower* and *upper* 95% confidence/credible limits (CLs) and the *p-value* (Kery and Schaub 2011, 37, 42). The estimate is the median (50th percentile) of the MCMC samples, the z-score is mean/sd and the 95% CLs are the 2.5th and 97.5th percentiles. A p-value of 0.05 indicates that the lower or upper 95% CL is 0.

Model adequacy was confirmed by examination of residual plots for the full model(s).

The results are displayed graphically by plotting the modeled relationships between variables and the response(s) with the remaining variables held constant. In general, continuous and discrete fixed variables are held constant at their mean and first level values, respectively, while random variables are held constant at their typical values (expected values of the underlying hyperdistributions) (Kery and Schaub 2011, 77–82). When informative, the influence of particular variables is expressed in terms of the *effect size* (i.e., percent change in the response variable) with 95% confidence/credible intervals (CIs, Bradford, Korman, and Higgins 2005).

The analyses were implemented using R version 3.5.1 (R Core Team 2018) and the [mbr](#) family of packages.

Model Descriptions

Light Attenuation

The following equation describes how light attenuates in water

$$E_d = E_0 \cdot \exp(-K_d \cdot y)$$

where E_0 is the initial irradiance, E_d is the irradiance at distance y and K_d is the diffuse attenuation coefficient (Julian, Doyle, and Stanley 2008).

Following Davies-Colley and Nagels (2008), the diffuse attenuation coefficient was assumed to vary with turbidity (T) according to the relationship

$$K_d = \exp(K_0 + K_T \cdot \log(T))$$

The above parameters were estimated from the monitored (fixed distance) and spot light readings.

Key assumptions of the surface reflectance model include:

- There are no measurement errors in E_0 or T .
- The residual variation in E_d is log-normally distribution.

Surface Reflectance

The relationship between the irradiance at the surface (E_s) and the irradiance 0.01 m below the surface (E_0) was modelled from the spot readings using the relationship

$$E_0 = E_s \cdot r \cdot \exp(-K_d \cdot 0.01)$$

where r is the reflection coefficient (Julian, Doyle, and Stanley 2008) and K_d was estimated using the coefficients from the spot light attenuation model.

Key assumptions of the surface reflectance model include:

- There are no measurement errors in E_s and T .
- The residual variation in E_0 is log-normally distributed.

Model Templates

Light Attenuation

```
model{
  Kd ~ dnorm(0, 5^-2)
  KdTurbidity ~ dnorm(0, 5^-2)
  sLight2 ~ dunif(0, 5)
```

```

for (i in 1:length(Light2)) {
  eKd[i] <- exp(Kd + KdTurbidity * log(Turbidity[i]))
  eLight2[i] <- Light[i] * exp(-eKd[i] * Distance[i])

  Light2[i] ~ dlnorm(log(eLight2[i]), sLight2^-2)
}
..

```

Template 1. The model description.

Surface Reflectance

```

model{
  rho ~ dunif(0, 1)
  sLight2 ~ dunif(0, 1)

  for (i in 1:length(Light2)) {
    eKd[i] <- exp(-1.1 + 0.62 * log(Turbidity[i]))
    eLight2[i] <- Light[i] * exp(-eKd[i] * 0.01) * rho
    Light2[i] ~ dlnorm(log(eLight2[i]), sLight2^-2)
  }
..

```

Template 2. The model description.

Results

Tables

Light Attenuation

Table A2 **Parameter Descriptions**

Parameter	Description
Distance	The distance (y) in m
eLight2	Expected Light2
Kd	The diffuse attenuation coefficient (K_d) at a Turbidity of 1 in m^{-1}
KdTurbidity	The effect of $\log(\text{Turbidity})$ on Kd
Light	The initial irradiance (E_0) in lx
Light2	The irradiance at distance (E_d) in lx
sLight2	SD of measurement error in Light2
Turbidity	The turbidity (T) in FNU

Light Attenuation - Loggers**Table A3 Model Coefficients**

term	estimate	sd	zscore	lower	upper	pvalue
Kd	-1.5336286	0.0812006	-18.88243	-1.6977924	-1.3754048	7e-04
KdTurbidity	0.8236869	0.0231275	35.59723	0.7767276	0.8701156	7e-04
sLight2	0.3110752	0.0078679	39.52462	0.2961205	0.3264704	7e-04

Table 3. Model summary.

n	K	nchains	niters	nthin	ess	rhat	converged
778	3	3	500	20	246	1.007	TRUE

Light Attenuation - Spot**Table A4 Model Coefficients**

term	estimate	sd	zscore	lower	upper	pvalue
Kd	-1.0875706	0.1221675	-8.91312	-1.3330729	-0.8570062	7e-04
KdTurbidity	0.6221436	0.0595476	10.42037	0.4989131	0.7352343	7e-04
sLight2	0.1434442	0.0142492	10.15262	0.1207312	0.1748792	7e-04

Table 5. Model summary.

n	K	nchains	niters	nthin	ess	rhat	converged
55	3	3	500	20	1113	0.999	TRUE

Surface Reflectance**Table A5 Parameter Descriptions**

Parameter	Description
Light	The irradiance at the surface (E_s) in lx
Light2	The irradiance just below the surface (E_0) in lx
rho	Reflection coefficient (r)
sLight2	SD of measurement error in Light2

Surface Reflectance - Raw**Table A6 Model Coefficients**

term	estimate	sd	zscore	lower	upper	pvalue
rho	0.6161369	0.0254178	24.273512	0.5678476	0.6696888	7e-04
sLight2	0.2175829	0.0319357	6.909297	0.1687282	0.2897639	7e-04

Table 8. Model summary.

n	K	nchains	niters	nthin	ess	rhat	converged
29	2	3	500	1	586	1.003	TRUE

Surface Reflectance - Shrouded**Table A7 Model Coefficients**

term	estimate	sd	zscore	lower	upper	pvalue
rho	0.6831169	0.0113113	60.34804	0.6605476	0.7062941	7e-04
sLight2	0.1383633	0.0112515	12.35628	0.1189482	0.1622706	7e-04

Table 10. Model summary.

n	K	nchains	niters	nthin	ess	rhat	converged
76	2	3	500	1	867	1.002	TRUE

Figures
Physical Parameters

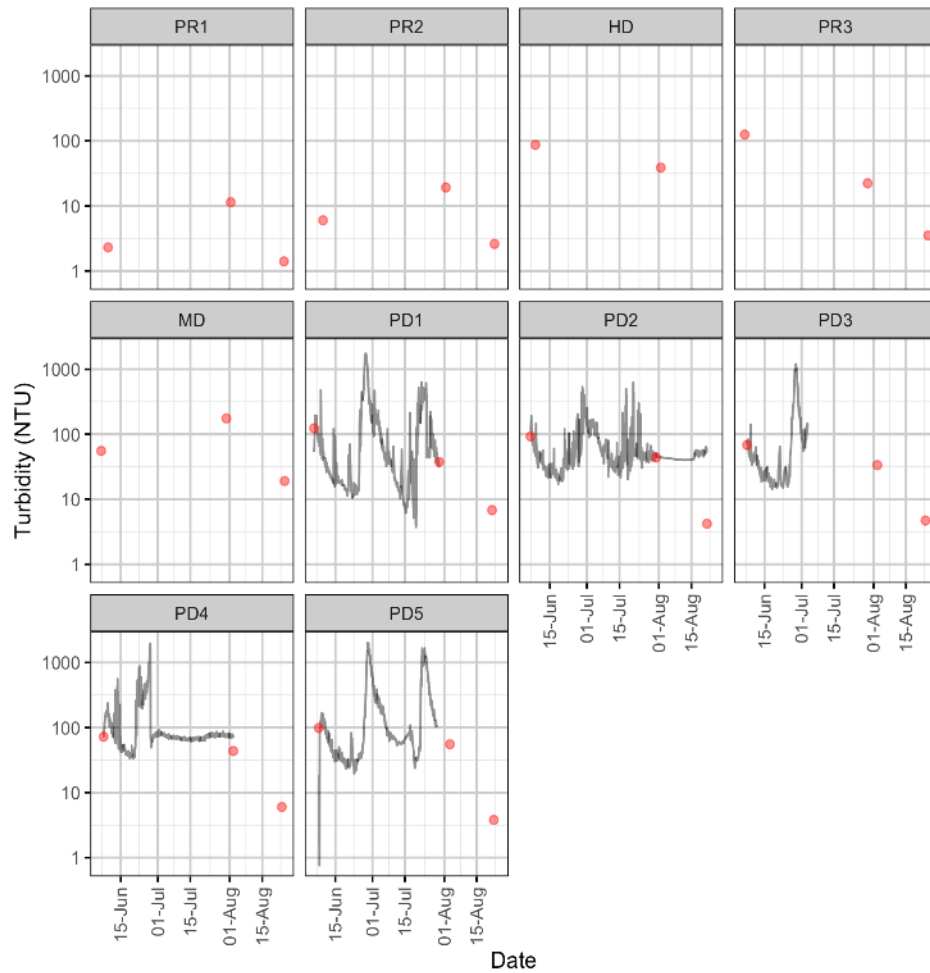


Figure A59 The logged (black lines) and spot (red points) turbidity by date and site.

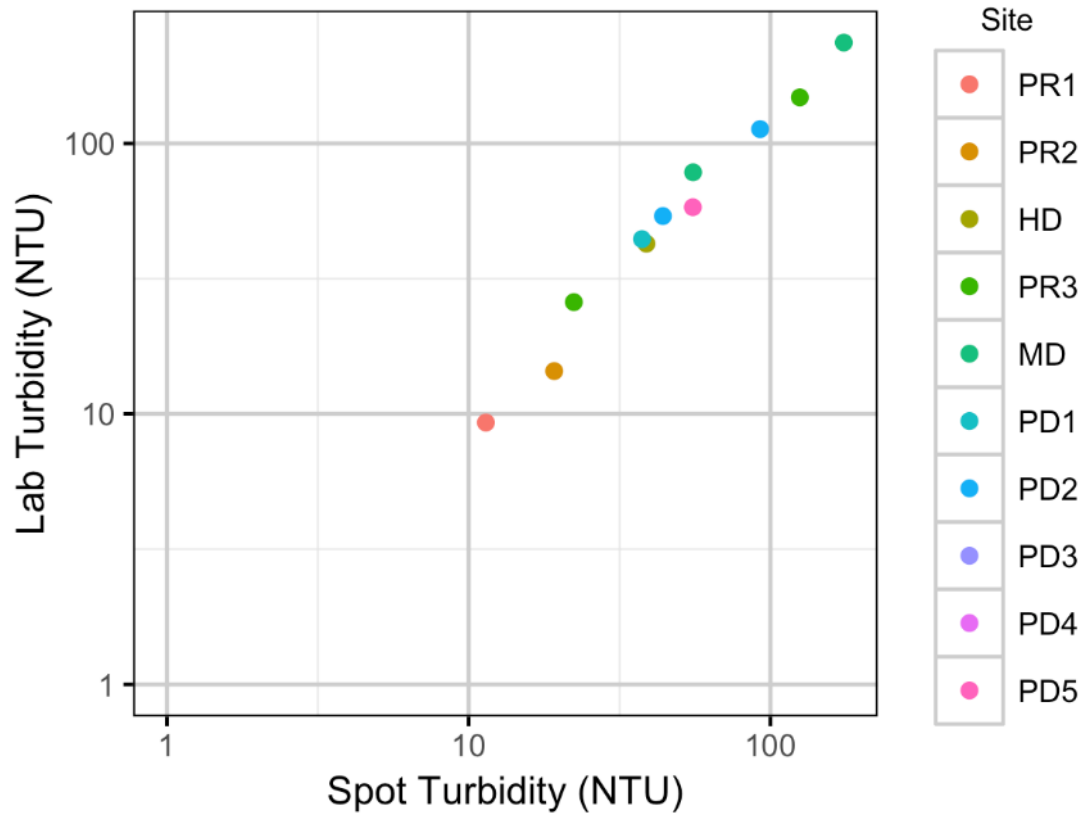


Figure A60 The lab by spot turbidity by site.

Figure 2. The lab by spot turbidity by site.

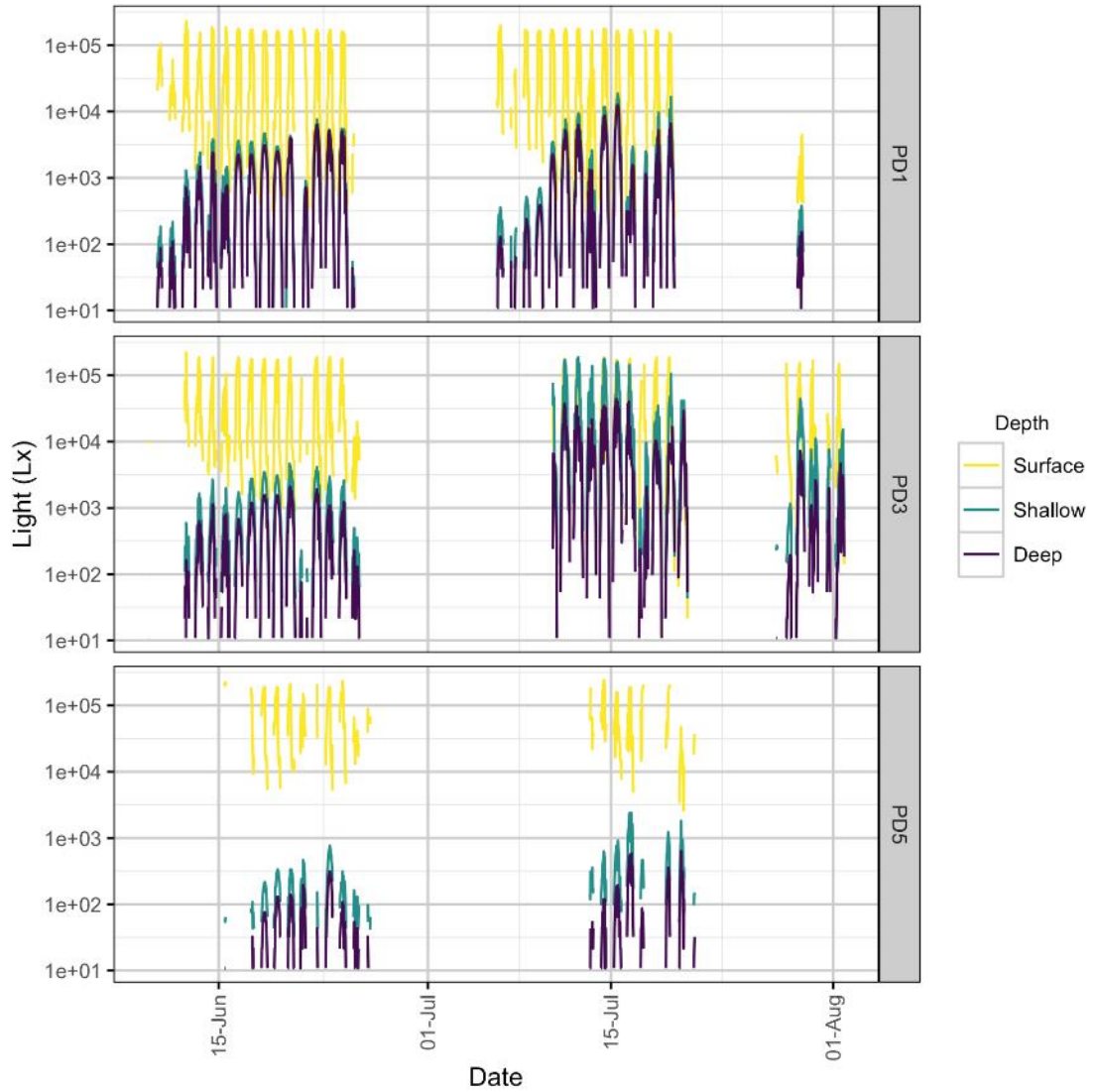


Figure A61 The logged light by date, site and depth.

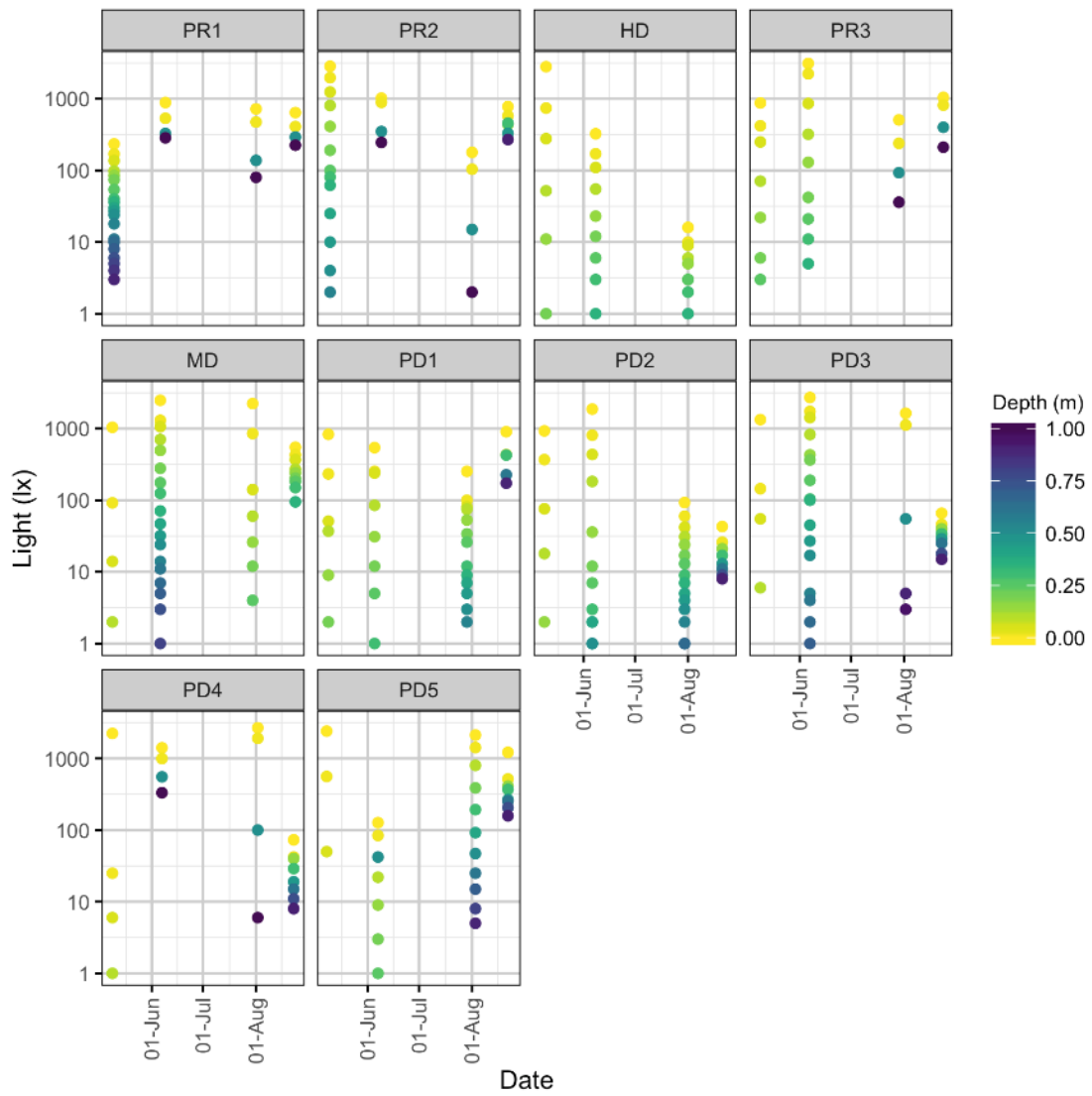


Figure A62 The light spot readings by date, site and depth.

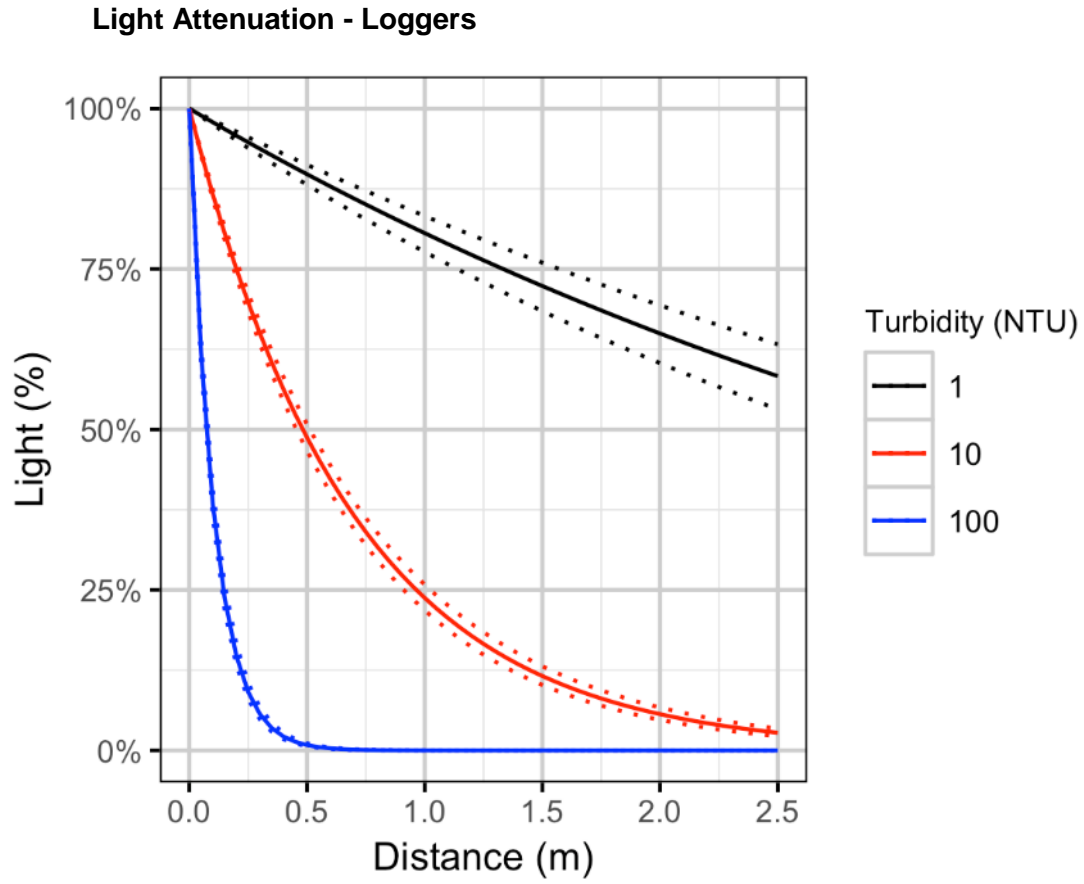


Figure A63 Light attenuation by distance and turbidity.

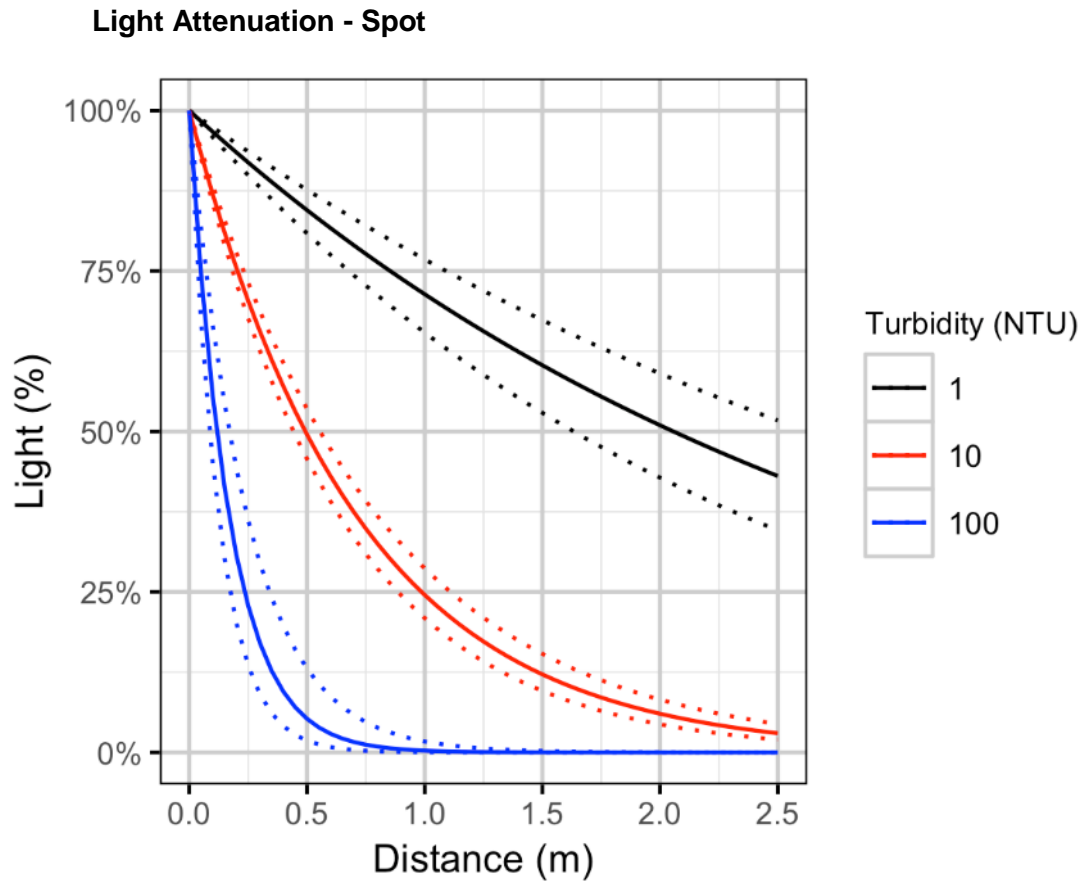


Figure A64 Light attenuation by distance and turbidity.

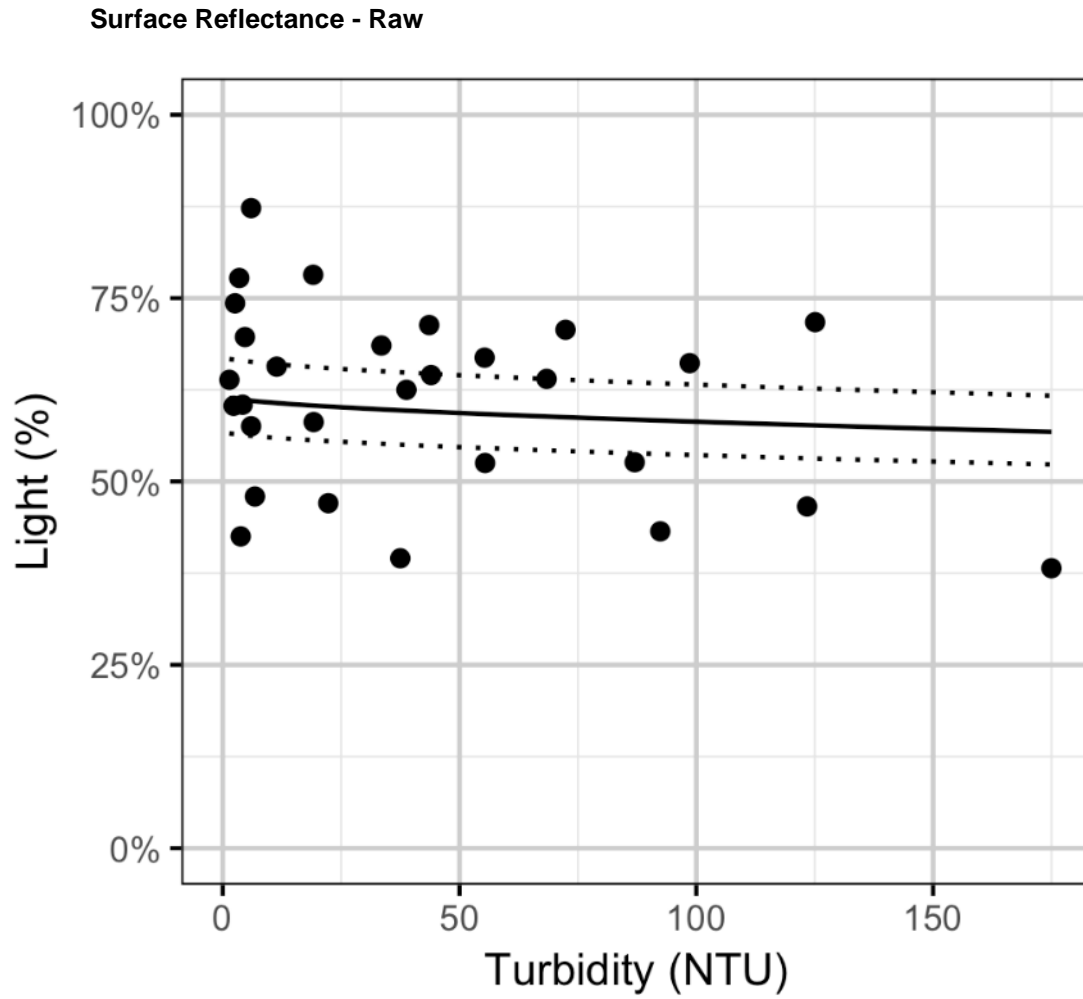


Figure A65 The predicted loss at 0.01 m by turbidity.

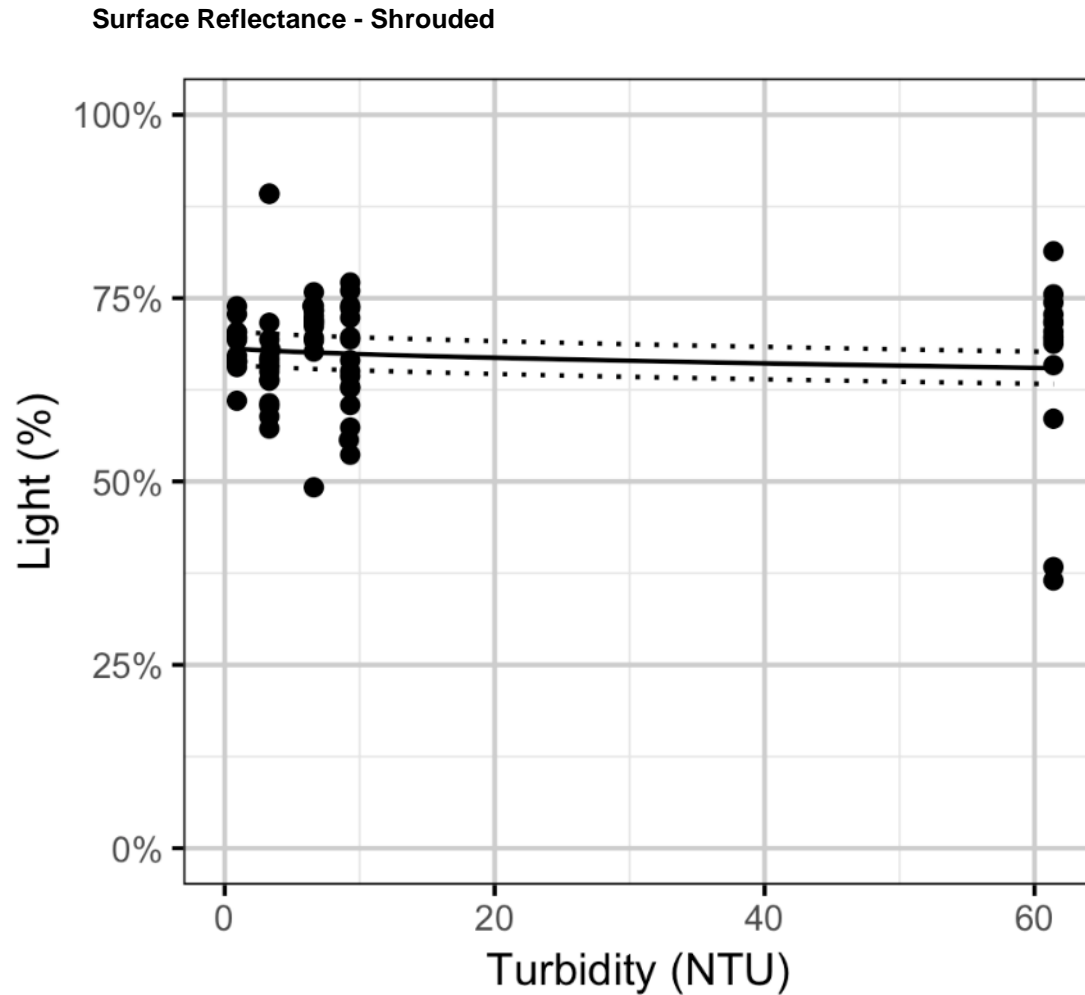


Figure A66 The predicted loss at 0.01 m by turbidity.

Acknowledgements

The organisations and individuals whose contributions have made this analysis report possible include:

BC Hydro

Ecoscape

Jason Schleppe

Mary Ann Olson-Russello

Rachel Plewes

References

- Bradford, Michael J, Josh Korman, and Paul S Higgins. 2005. "Using Confidence Intervals to Estimate the Response of Salmon Populations (*Oncorhynchus* Spp.) to Experimental Habitat Alterations." *Canadian Journal of Fisheries and Aquatic Sciences* 62 (12): 2716–26. <https://doi.org/10.1139/f05-179>.
- Brooks, Steve, Andrew Gelman, Galin L. Jones, and Xiao-Li Meng, eds. 2011. *Handbook for Markov Chain Monte Carlo*. Boca Raton: Taylor & Francis.
- Davies-Colley, Robert J., and John W. Nagels. 2008. "Predicting Light Penetration into River Waters." *Journal of Geophysical Research* 113 (G3). <https://doi.org/10.1029/2008JG000722>.
- Julian, J. P., M. W. Doyle, and E. H. Stanley. 2008. "Empirical Modeling of Light Availability in Rivers." *Journal of Geophysical Research* 113 (G3). <https://doi.org/10.1029/2007JG000601>.
- Kery, Marc, and Michael Schaub. 2011. *Bayesian Population Analysis Using WinBUGS : A Hierarchical Perspective*. Boston: Academic Press. <http://www.vogelwarte.ch/bpa.html>.
- McElreath, Richard. 2016. *Statistical Rethinking: A Bayesian Course with Examples in R and Stan*. Chapman & Hall/CRC Texts in Statistical Science Series 122. Boca Raton: CRC Press/Taylor & Francis Group.
- Plummer, Martyn. 2015. "JAGS Version 4.0.1 User Manual." <http://sourceforge.net/projects/mcmc-jags/files/Manuals/4.x/>.
- R Core Team. 2018. *R: A Language and Environment for Statistical Computing*. Vienna, Austria: R Foundation for Statistical Computing. <https://www.R-project.org/>.

Appendix K Temperature Plots

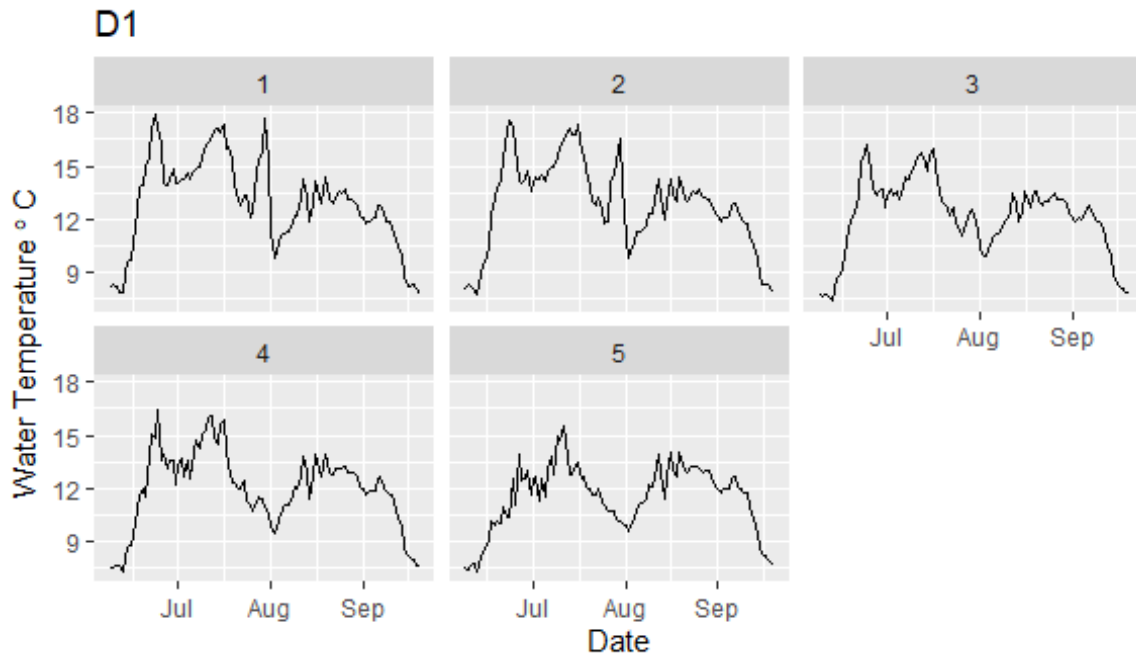


Figure A67 Average daily water temperature by transect (1-5) at D1 over the duration of deployment in 2018.

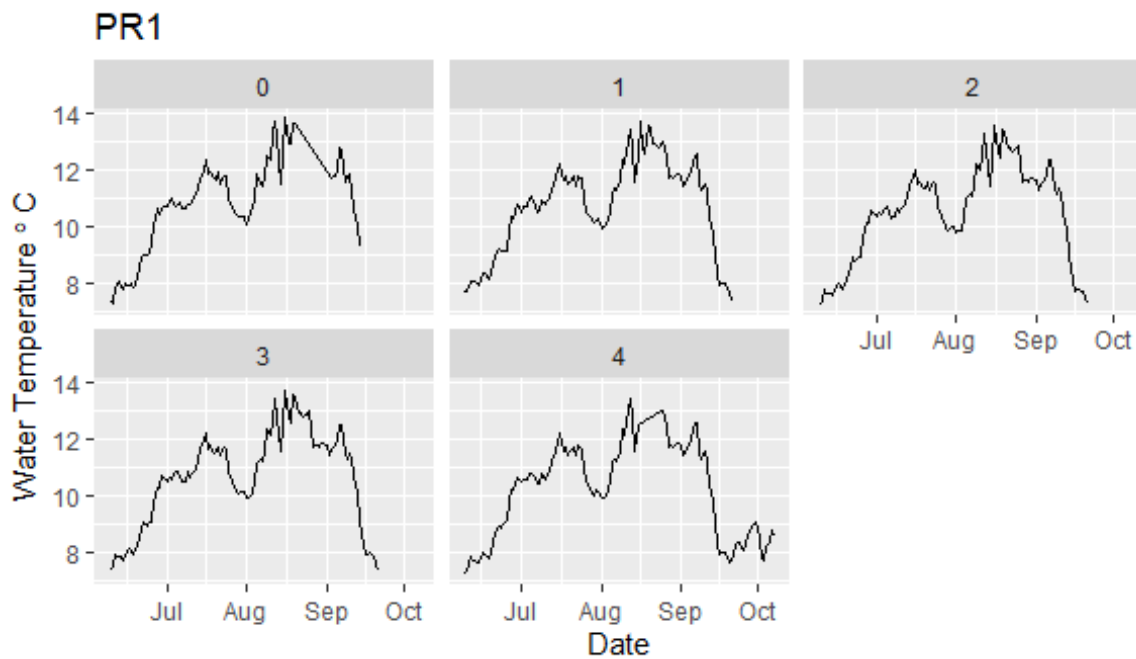


Figure A68 Average daily water temperature by transect (0-4) at PR1 over the duration of deployment in 2018.

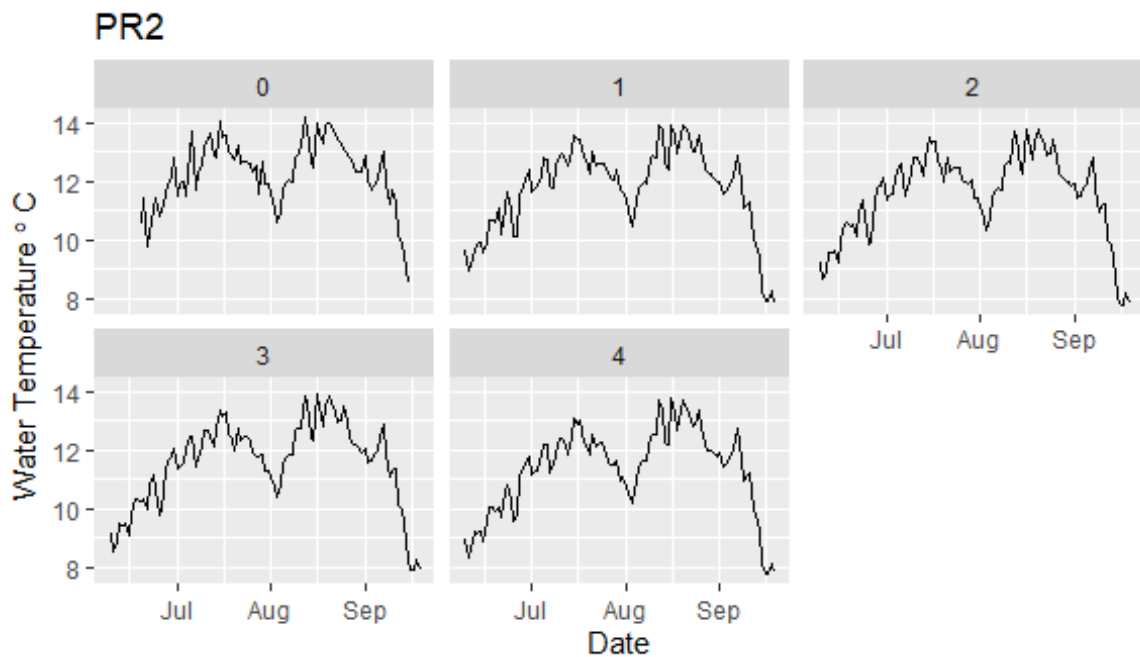


Figure A69 Average daily water temperature by transect (0-4) at PR2 over the duration of deployment in 2018.

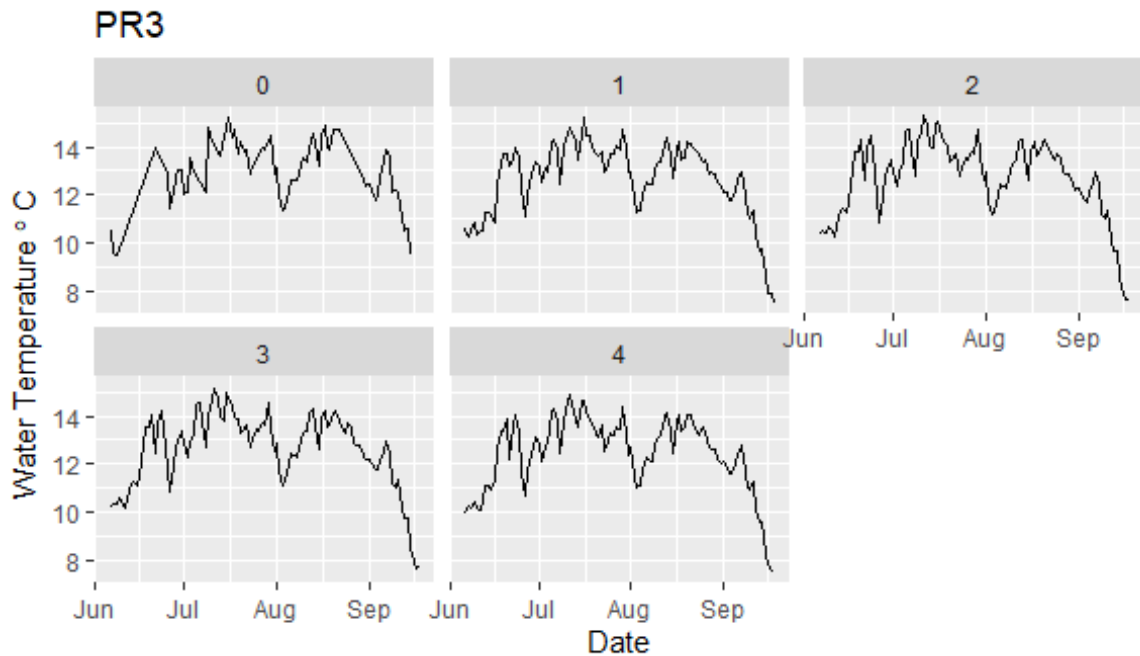


Figure A70 Average daily water temperature by transect (0-4) at PR3 over the duration of deployment in 2018.

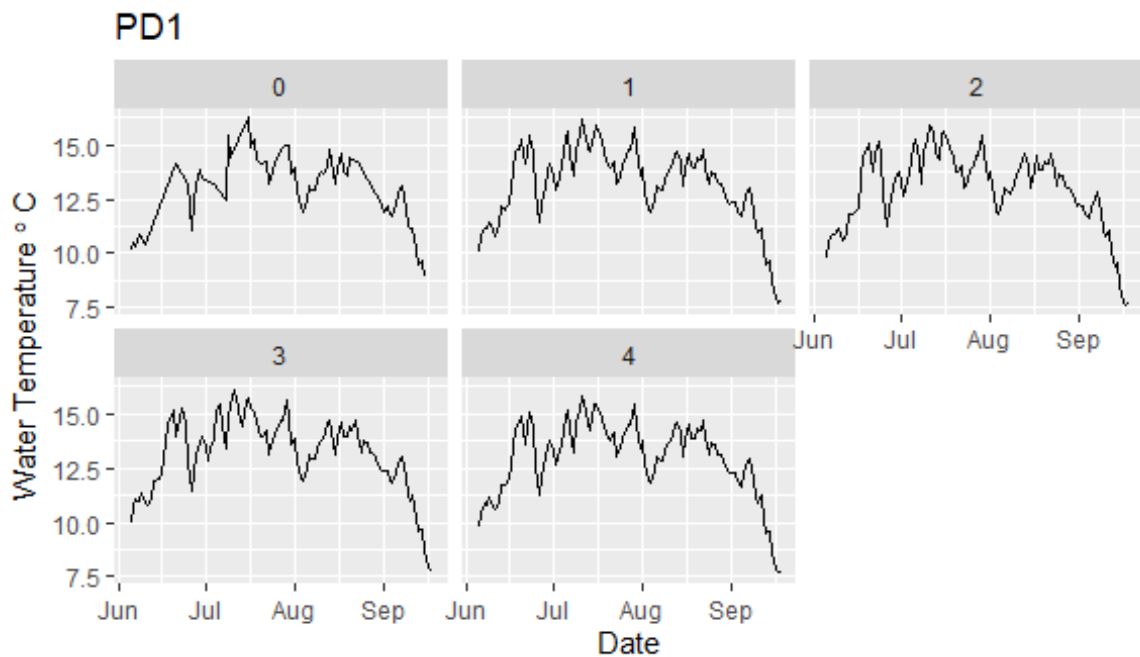


Figure A71 Average daily water temperature by transect (0-4) at PD1 over the duration of deployment in 2018.

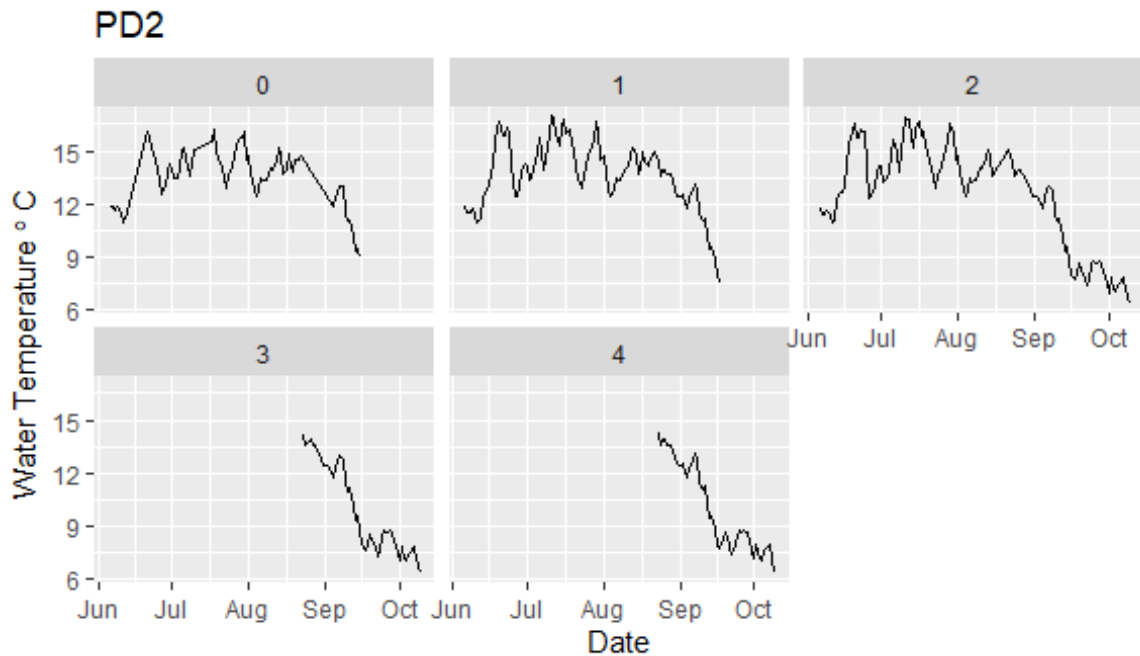


Figure A72 Average daily water temperature by transect (0-4) at PD2 over the duration of deployment in 2018.

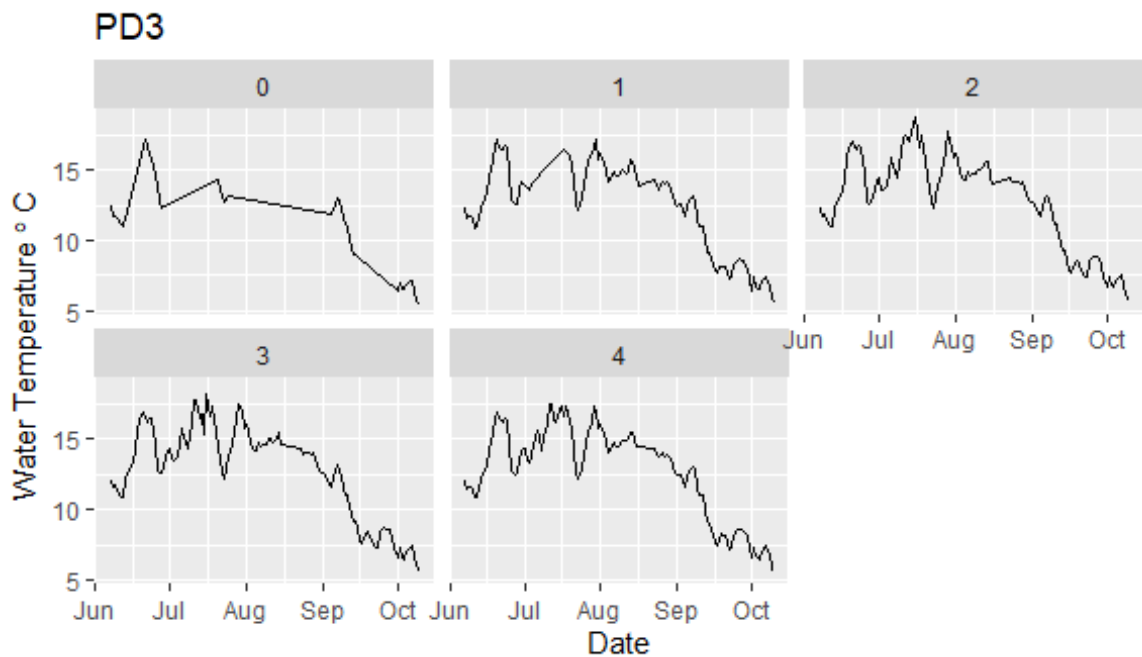


Figure A73 Average daily water temperature by transect (0-4) at PD3 over the duration of deployment in 2018.

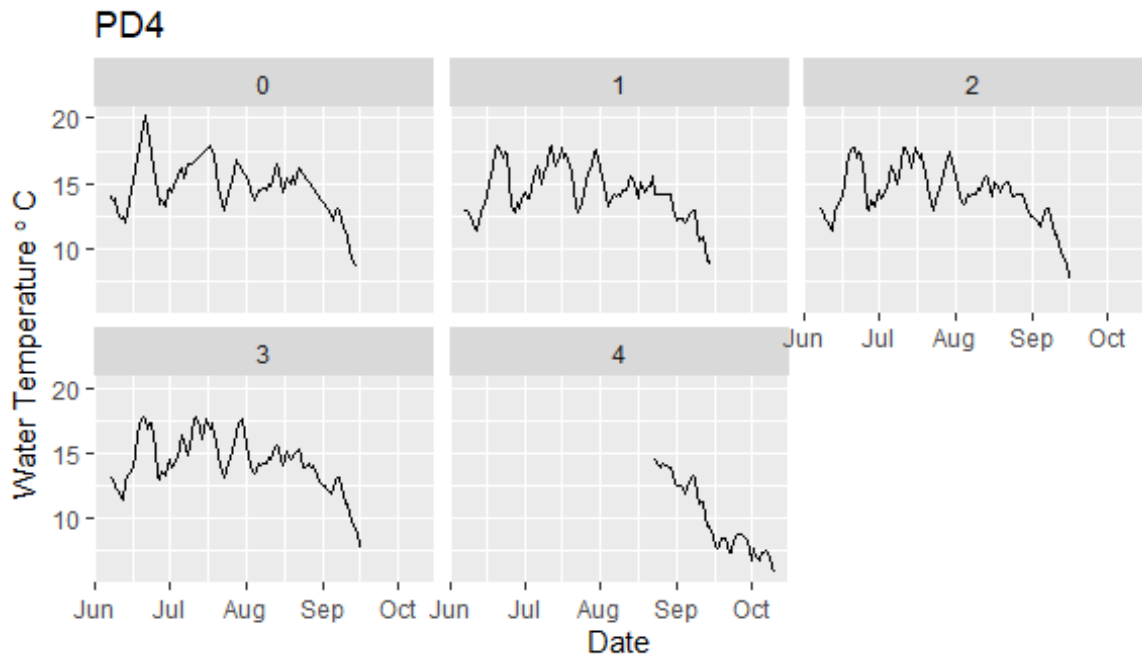


Figure A74 Average daily water temperature by transect (0-4) at PD4 over the duration of deployment in 2018.

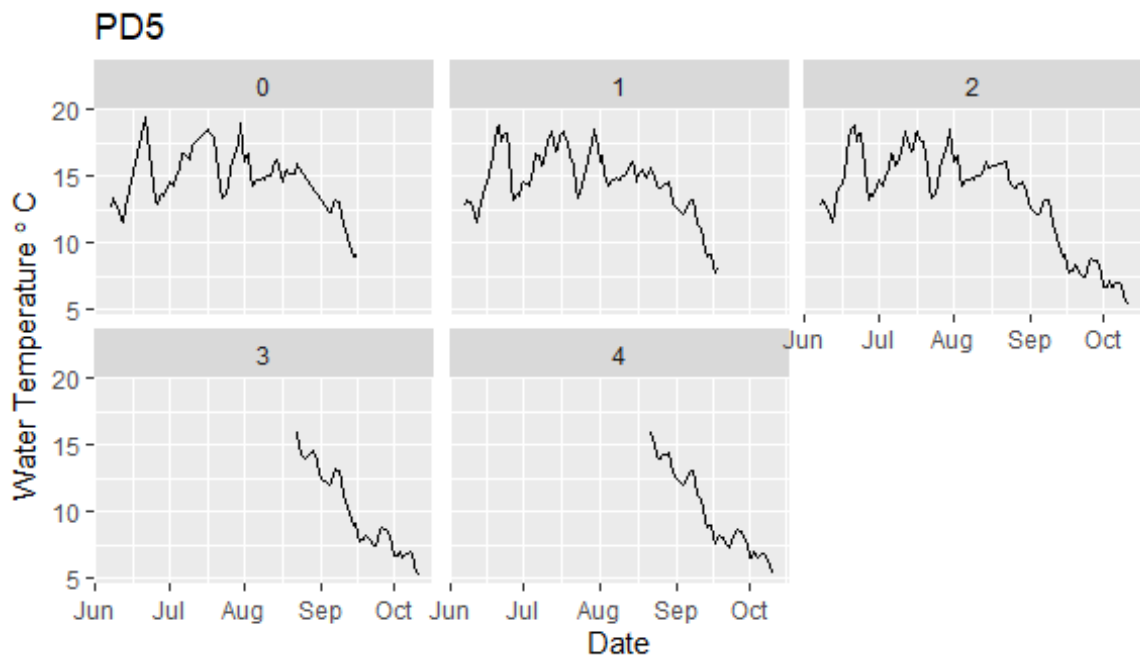


Figure A75 Average daily water temperature by transect (0-4) at PD5 over the duration of deployment in 2018.

Appendix L Phytoplankton Summary Stats

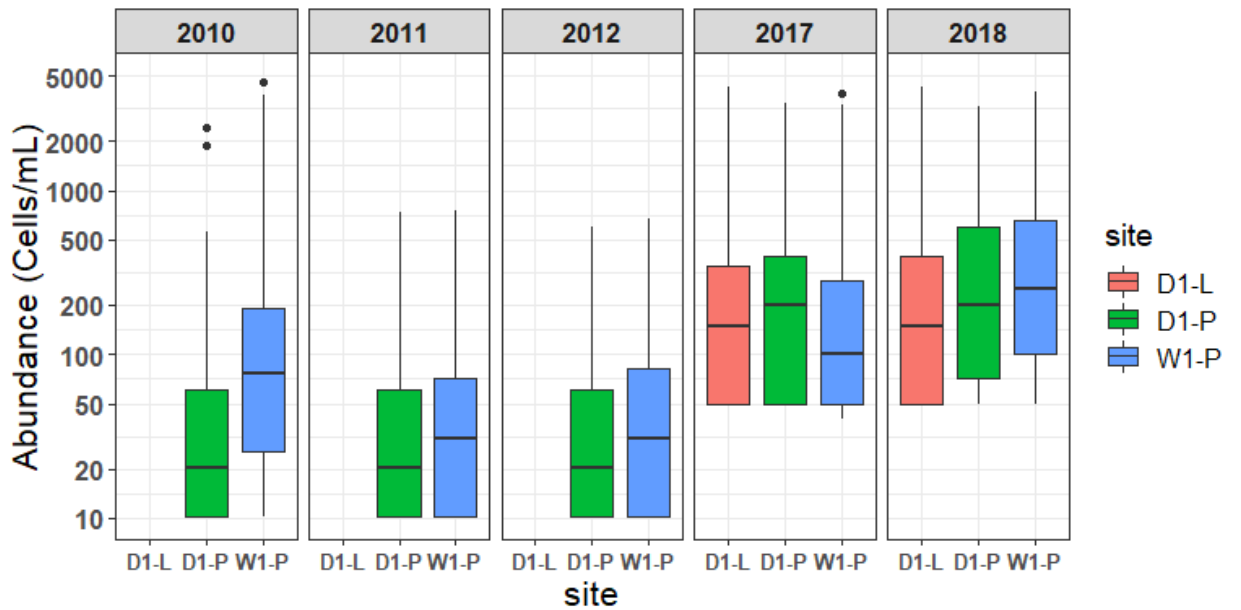


Figure A76 Phytoplankton Abundance by Year for Reservoir Sites

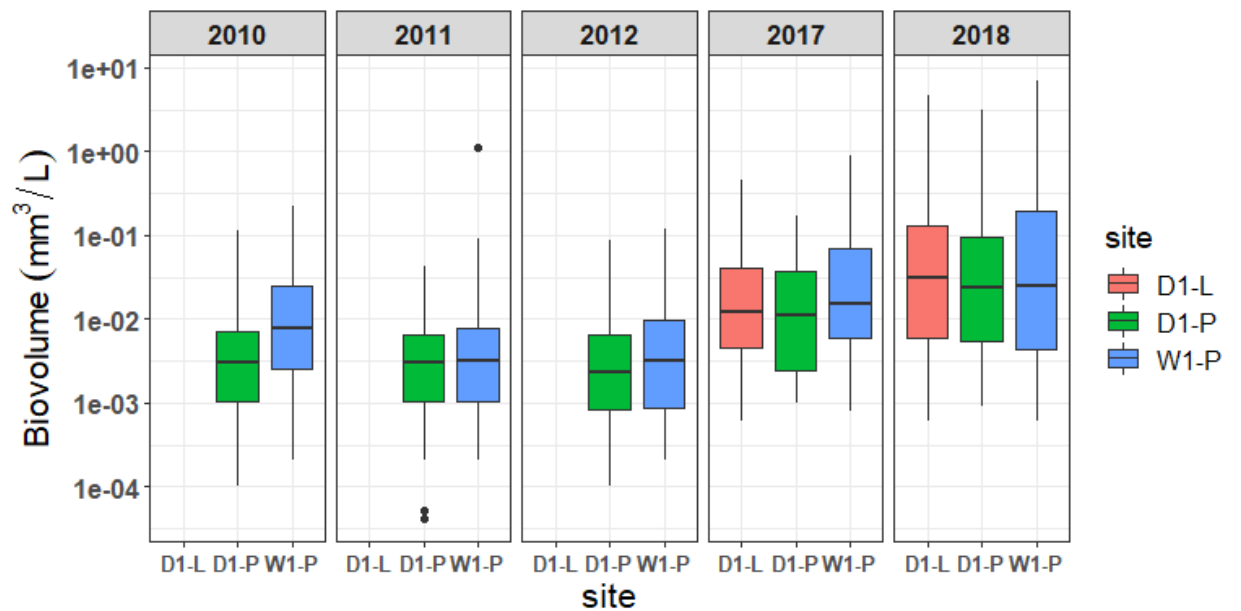


Figure A77 Phytoplankton Biovolume by Year for Reservoir Sites

Appendix M Periphyton Response Summary Stats

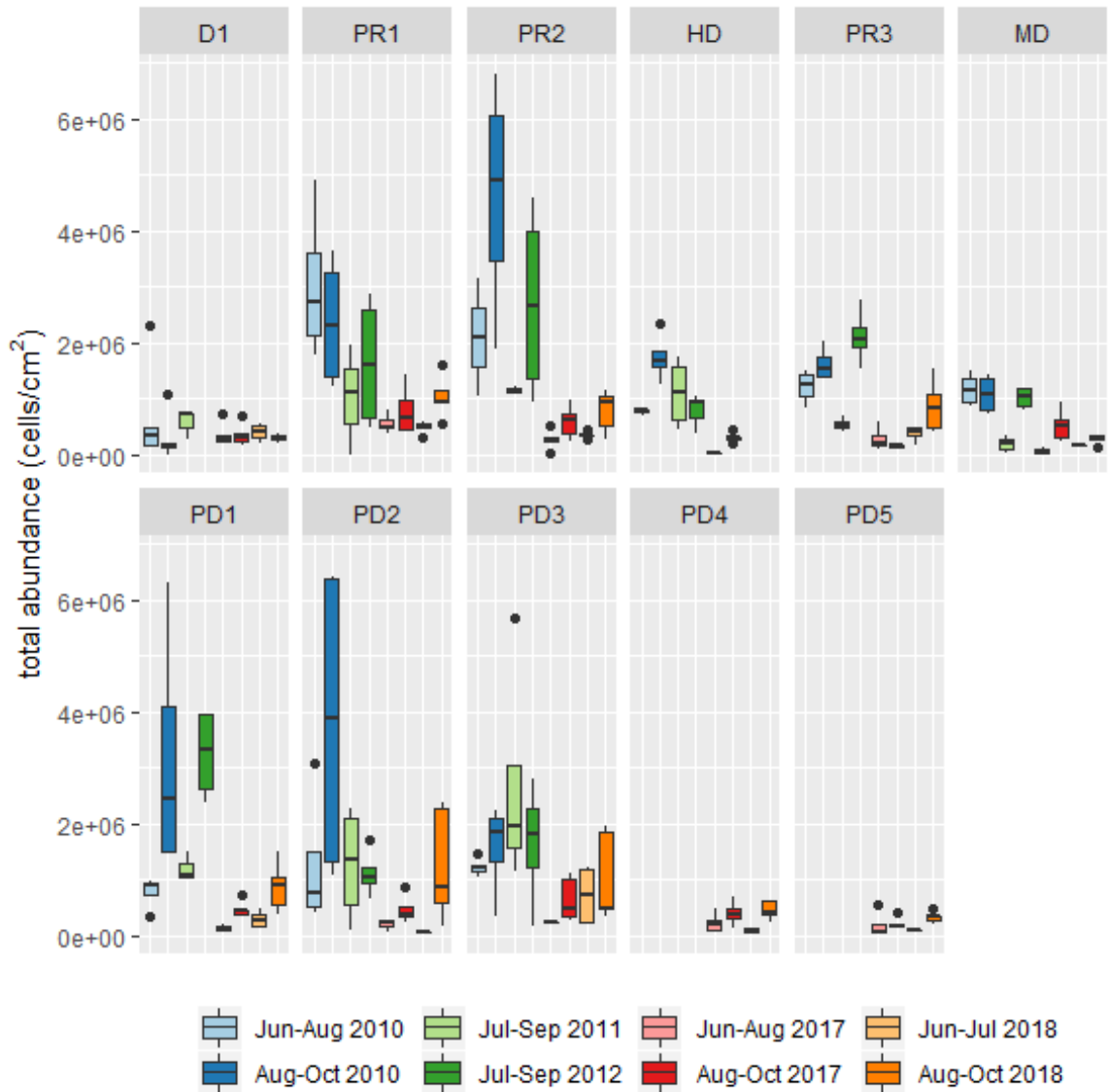


Figure A78 Boxplot of total abundance by site and series.

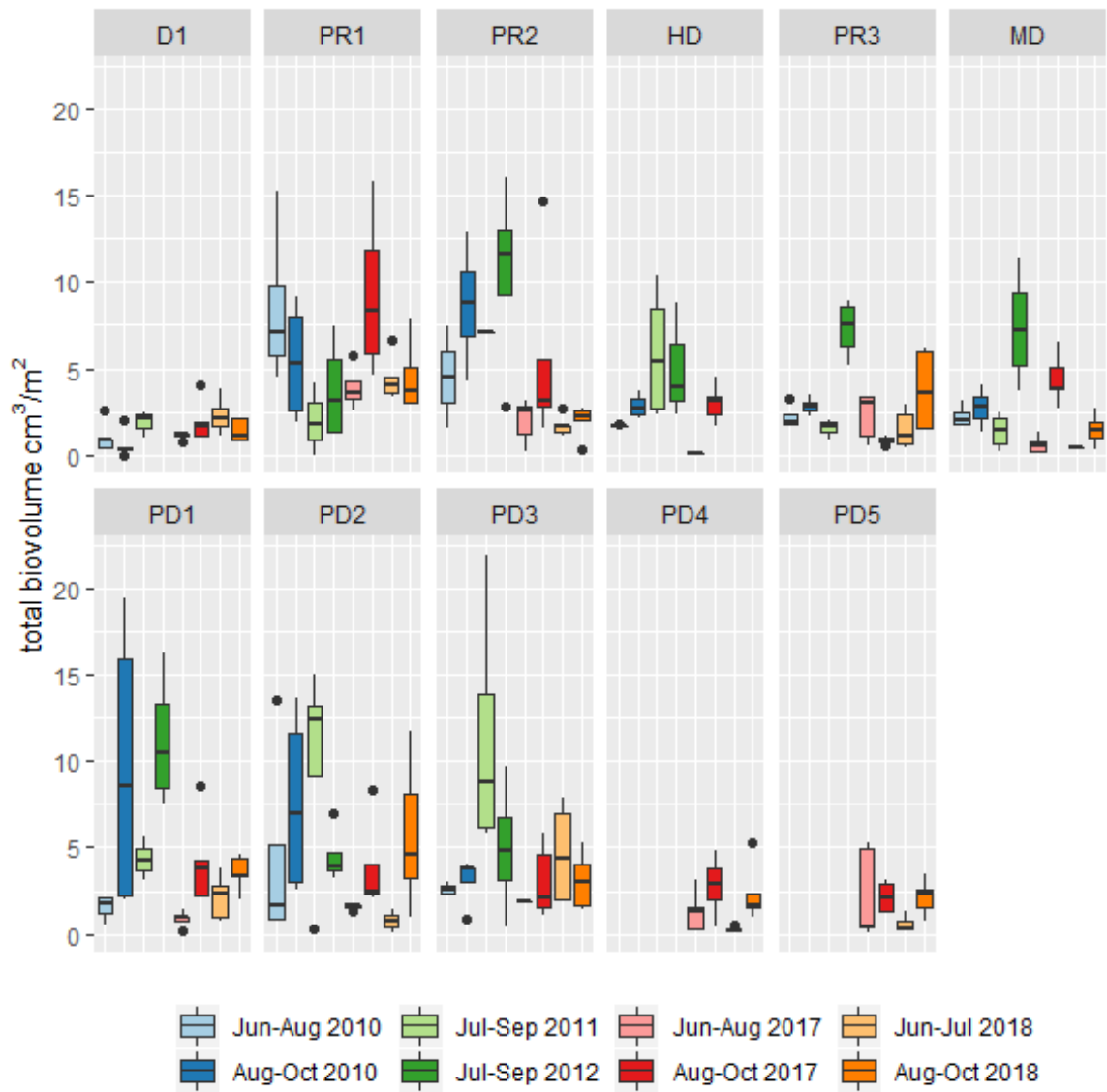


Figure A79 Boxplot of total biovolume by site and series.

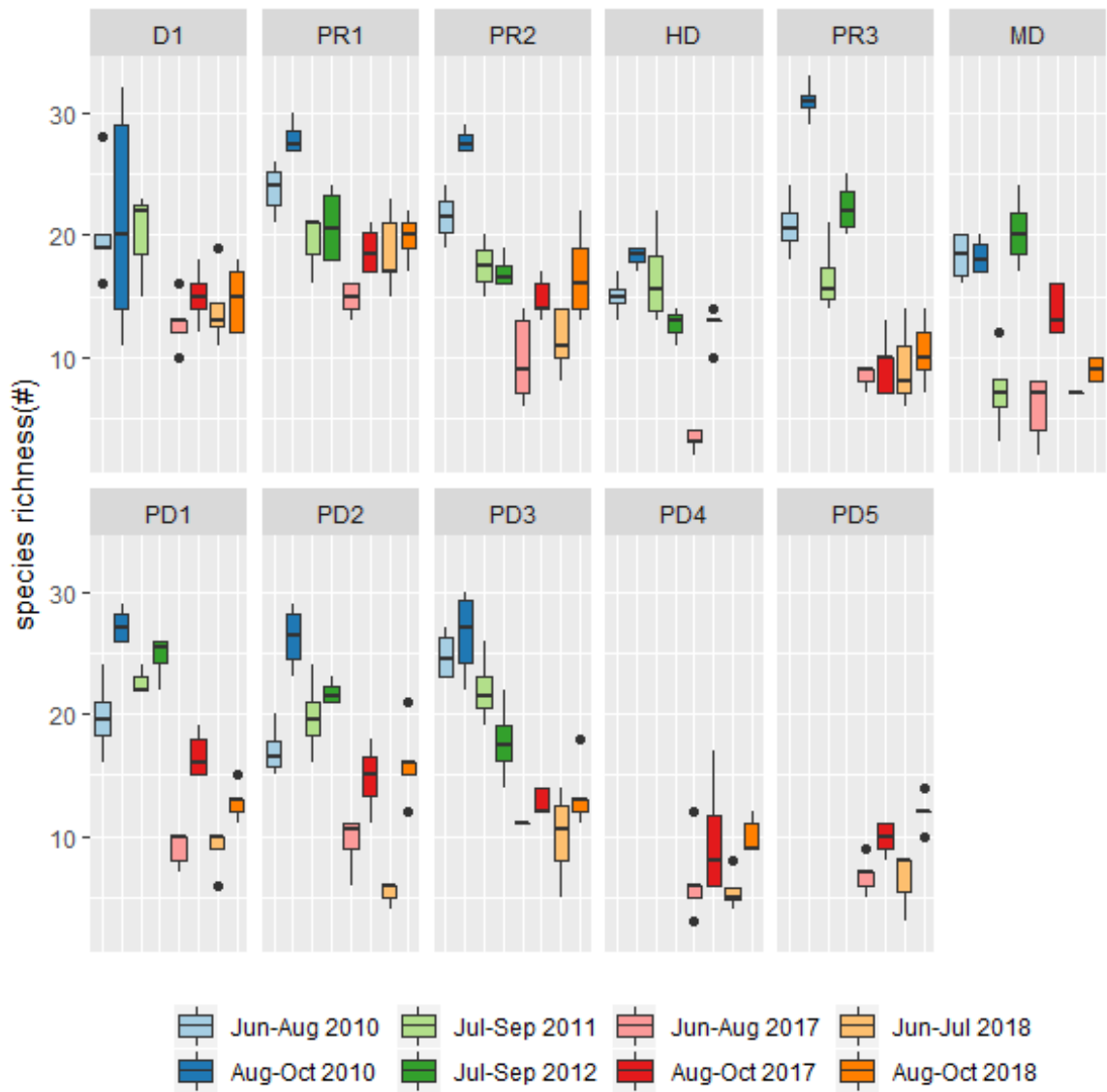


Figure A80 Boxplot of species richness by site and series.

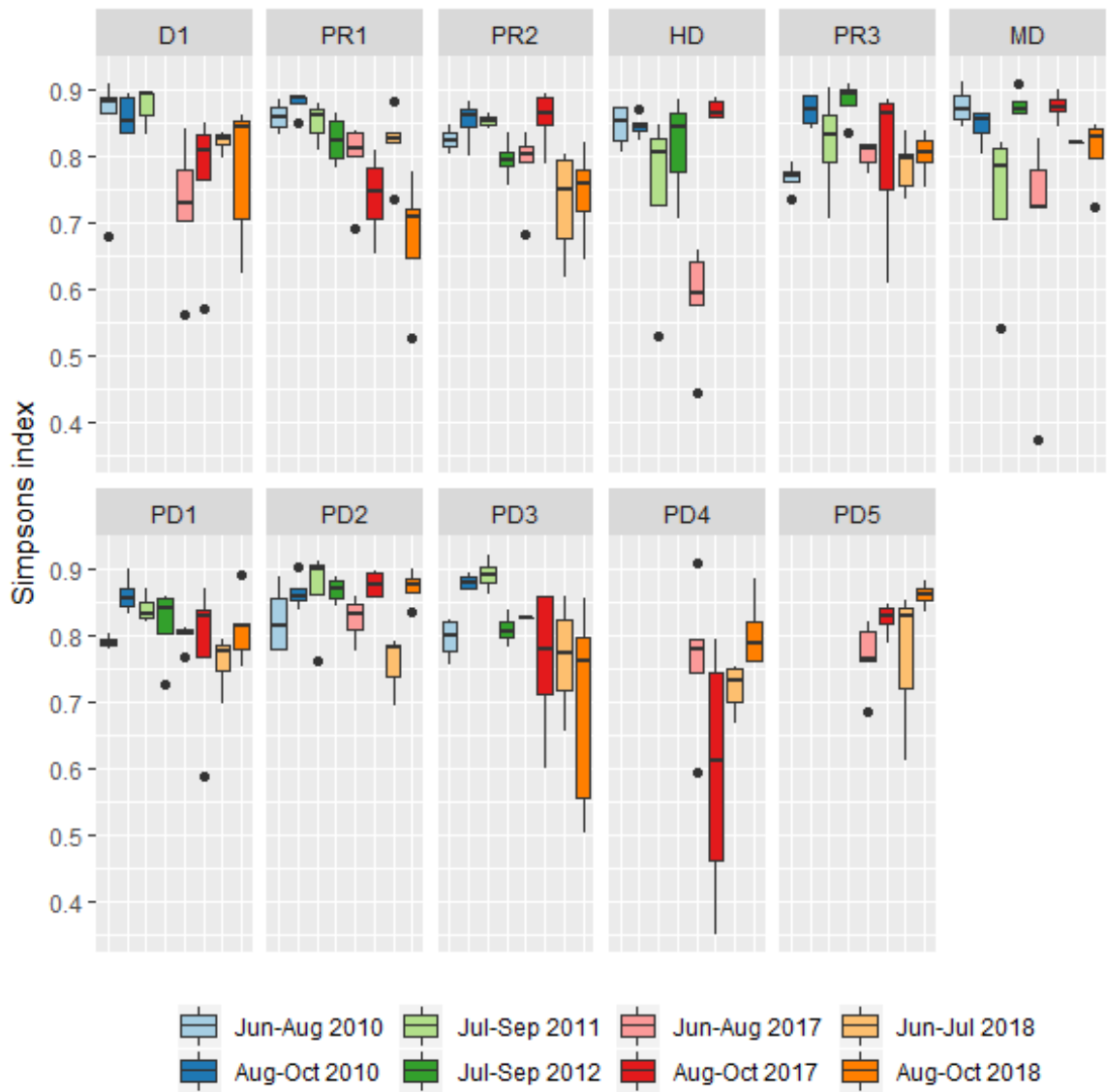


Figure A81 Boxplot of Simpsons index by site and series.

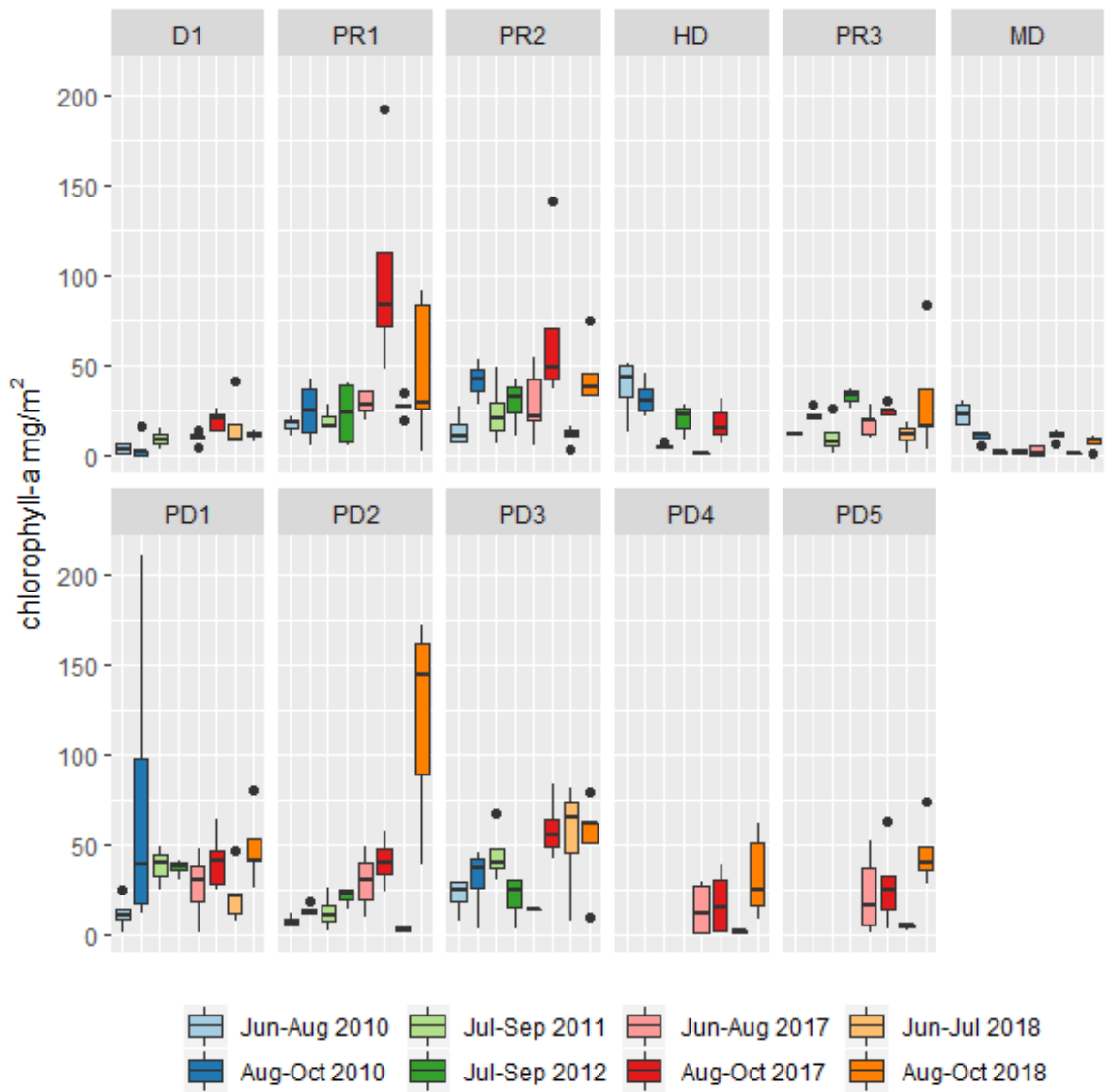


Figure A82 **Boxplot of chlorophyll-a by site and series.**

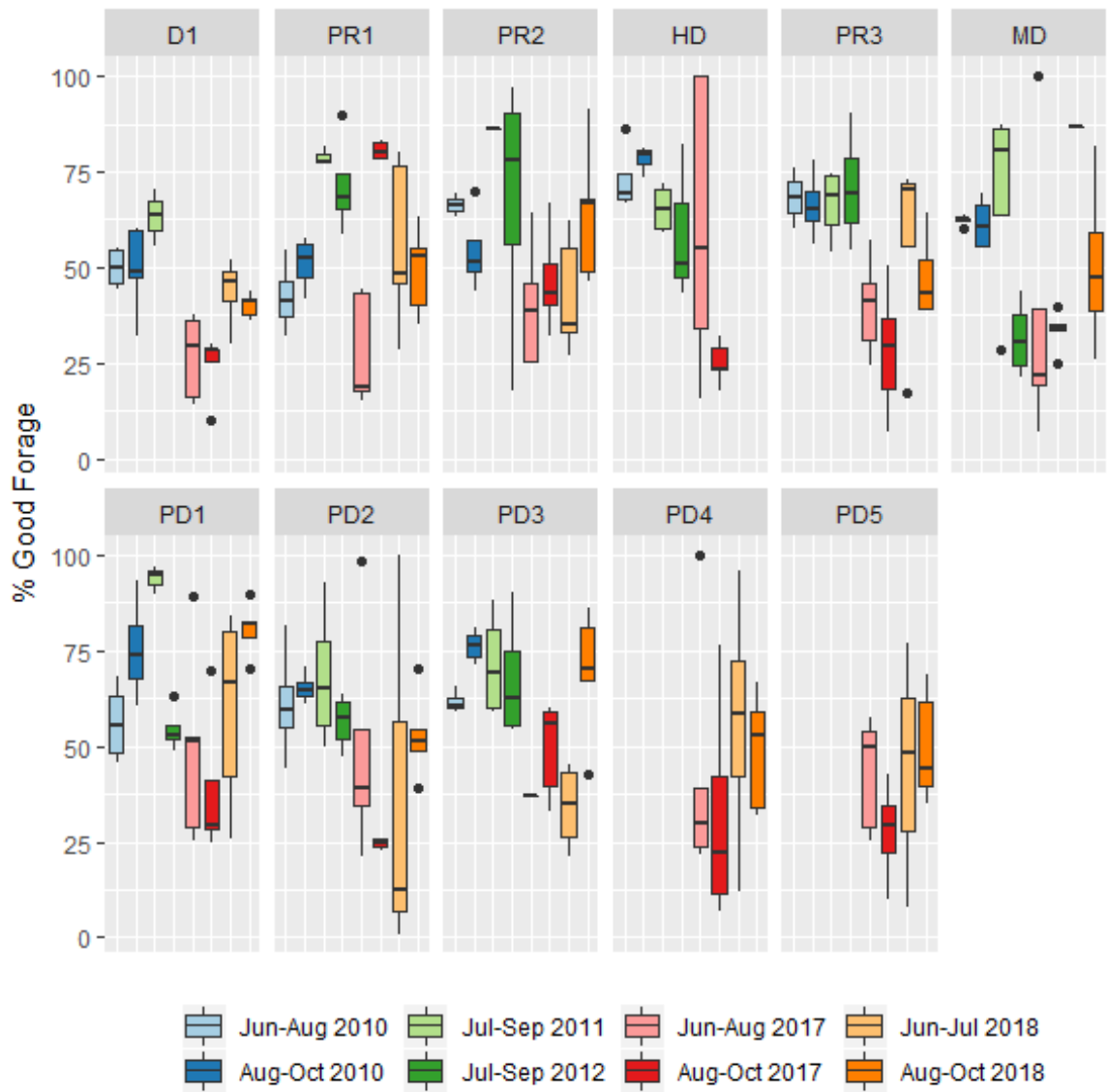


Figure A83 Boxplot of % Good Forage by site and series.

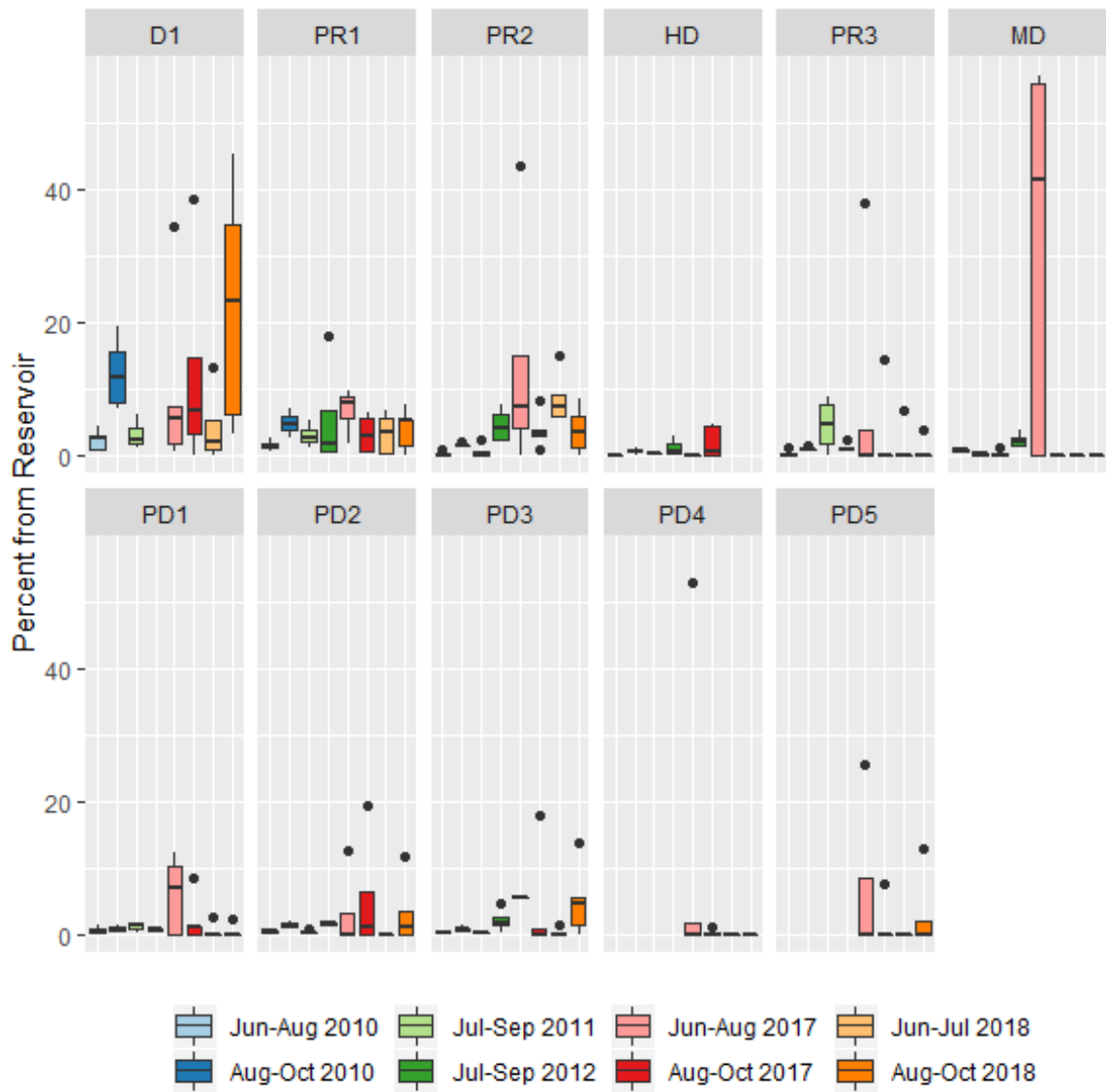


Figure A84 Boxplot of Percent from Reservoir by site and series.

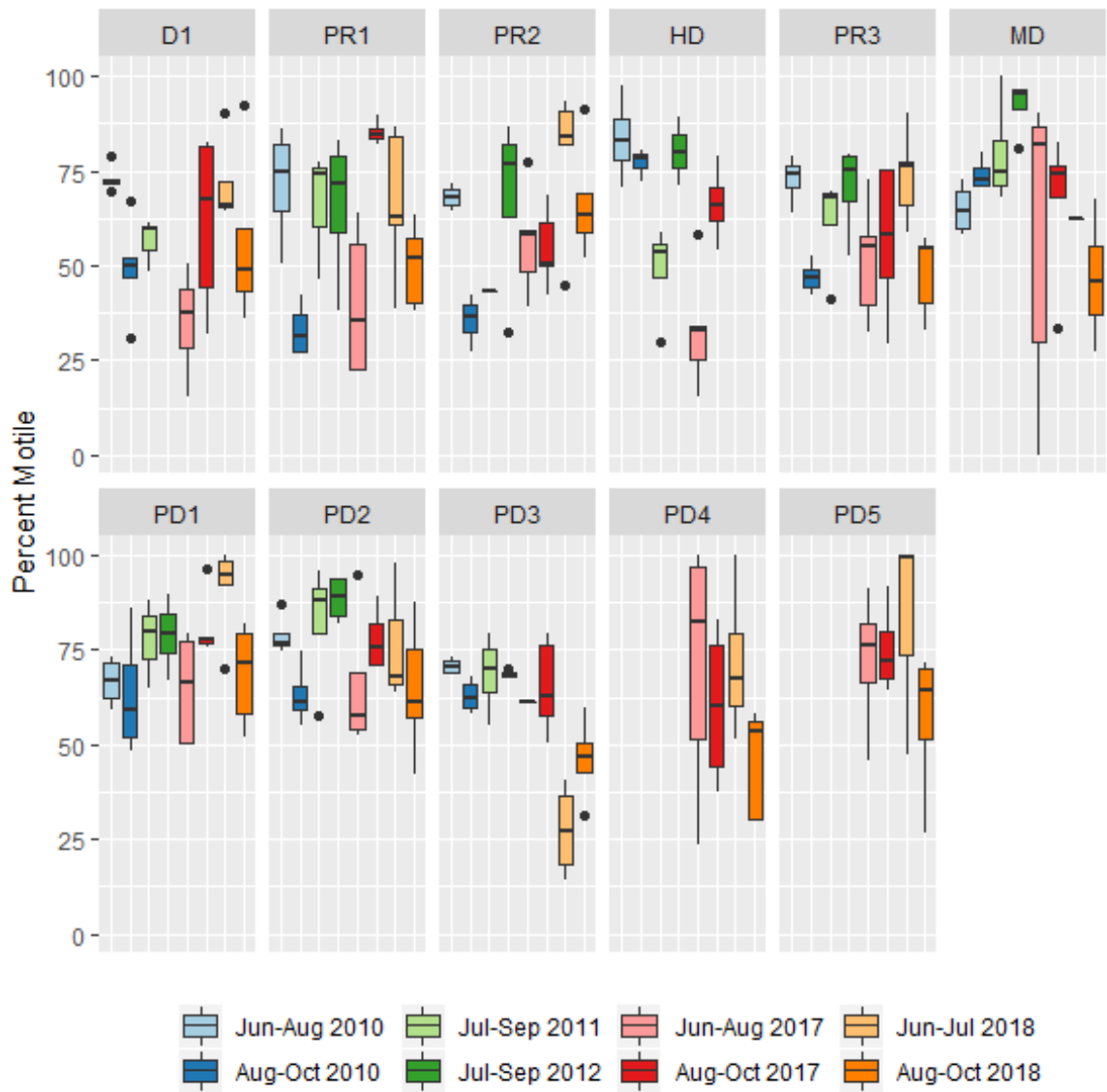


Figure A85 Boxplot of Percent Motile by site and series.

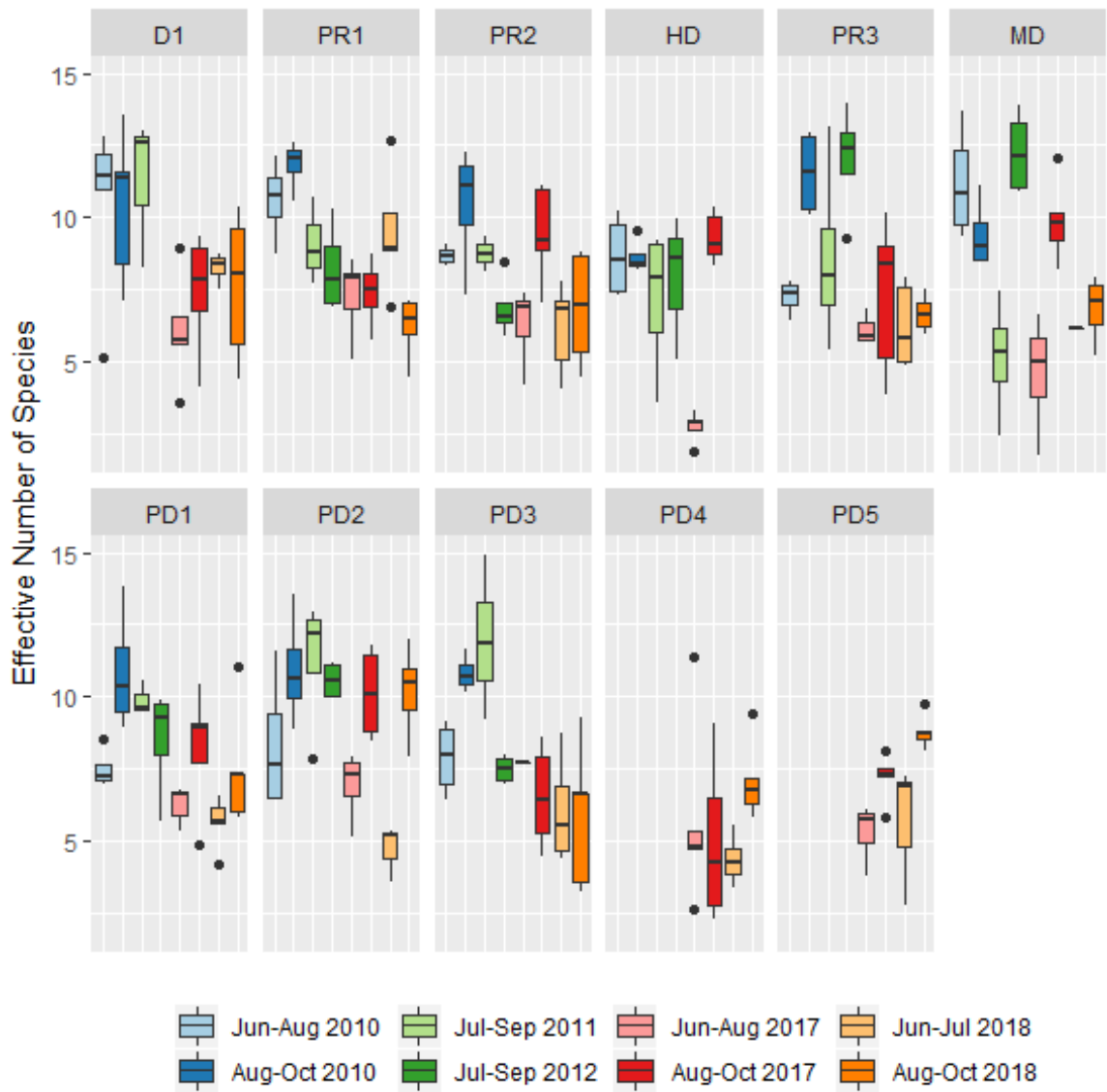


Figure A86 Boxplot of Effective Number of Species by site and series.

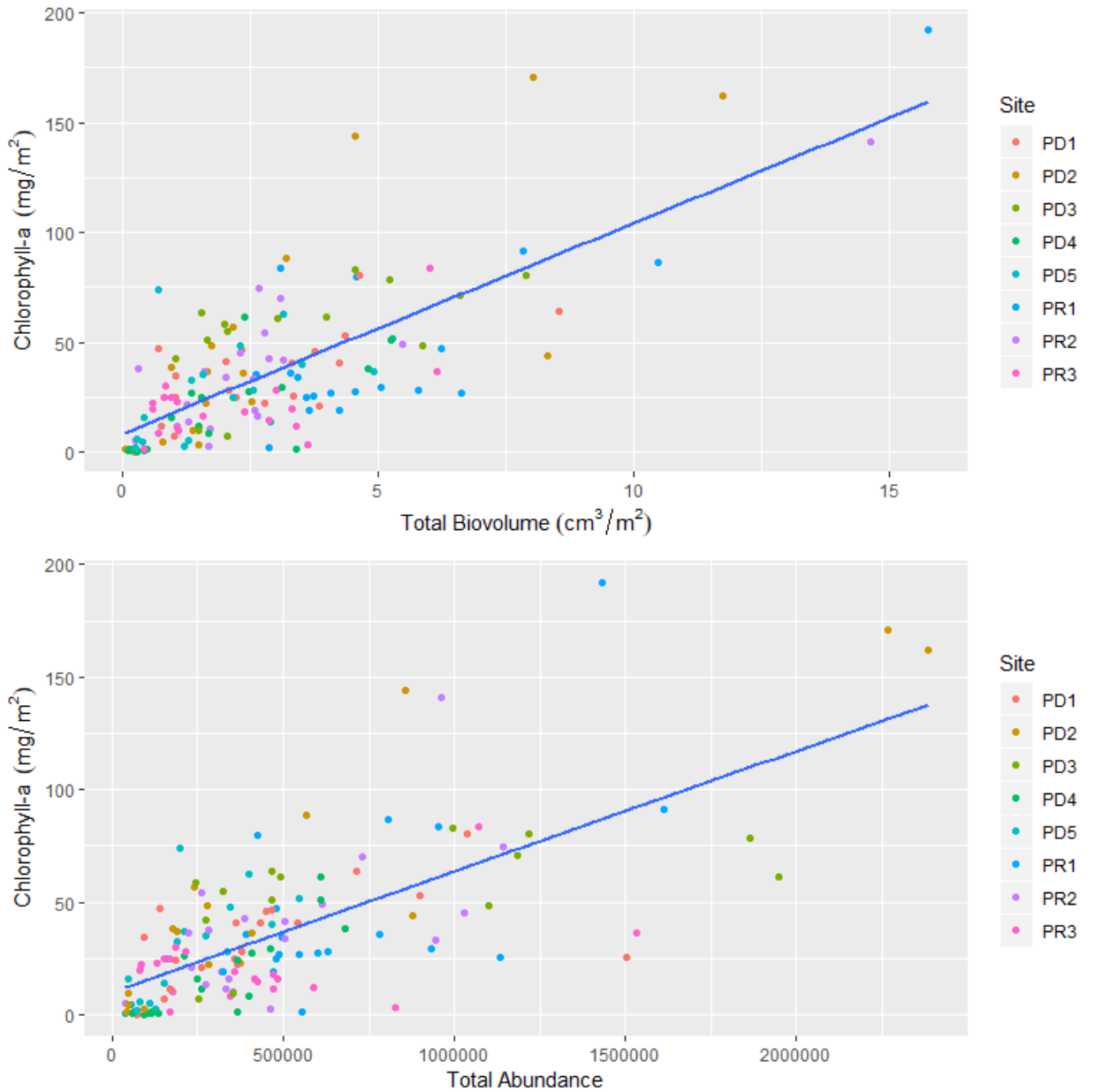


Figure A87 Regression of Chlorophyll-a vs. Total Biovolume and Chlorophyll-a vs Total Abundance for all samples from 2017 and 2018.

Table A8 Summary statistics for regression of Chlorophyll-a with total biovolume ($R^2=0.50$, $p<0.001$) and total abundance ($R^2=0.55$, $p<0.001$).

Term	Estimate	Std.error	Statistic	P-value
(Intercept)	3.83	4.88	0.78	0.44
Total Biovolume	11.65	1.36	8.59	<0.001
(Intercept)	6.44	4.51	1.43	0.16
Total Abundance	0.000050	0.000006	8.90	<0.001

Appendix N Periphyton Broad Group Summary Stas

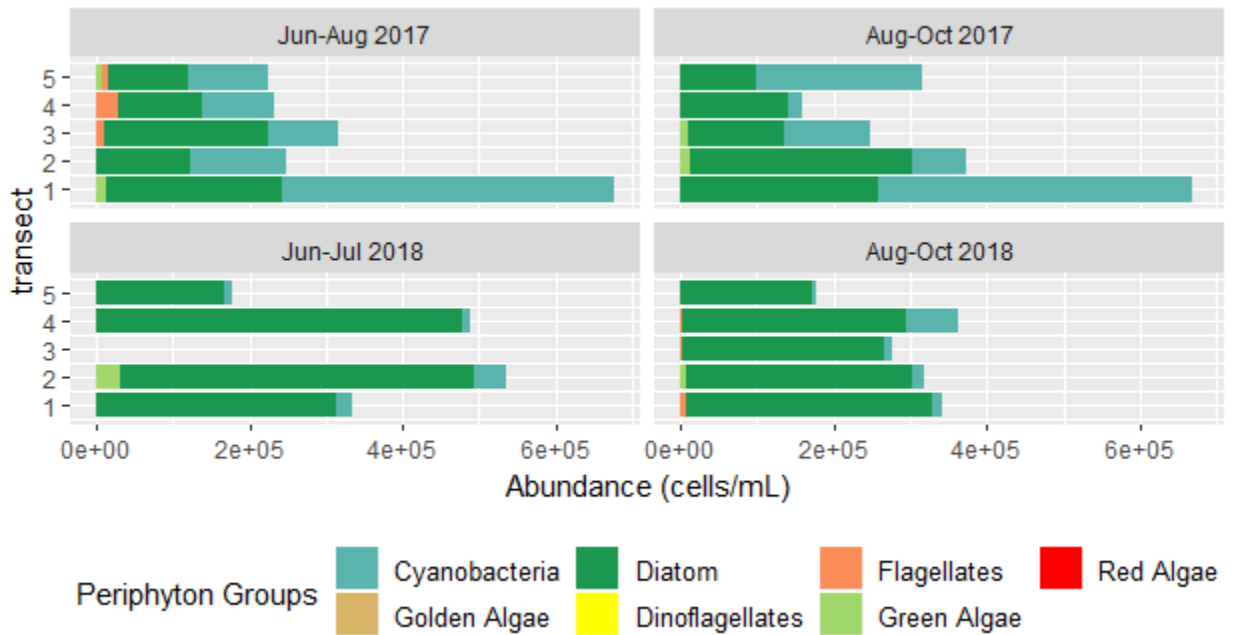


Figure A88 Abundance by Periphyton Group at D1 .

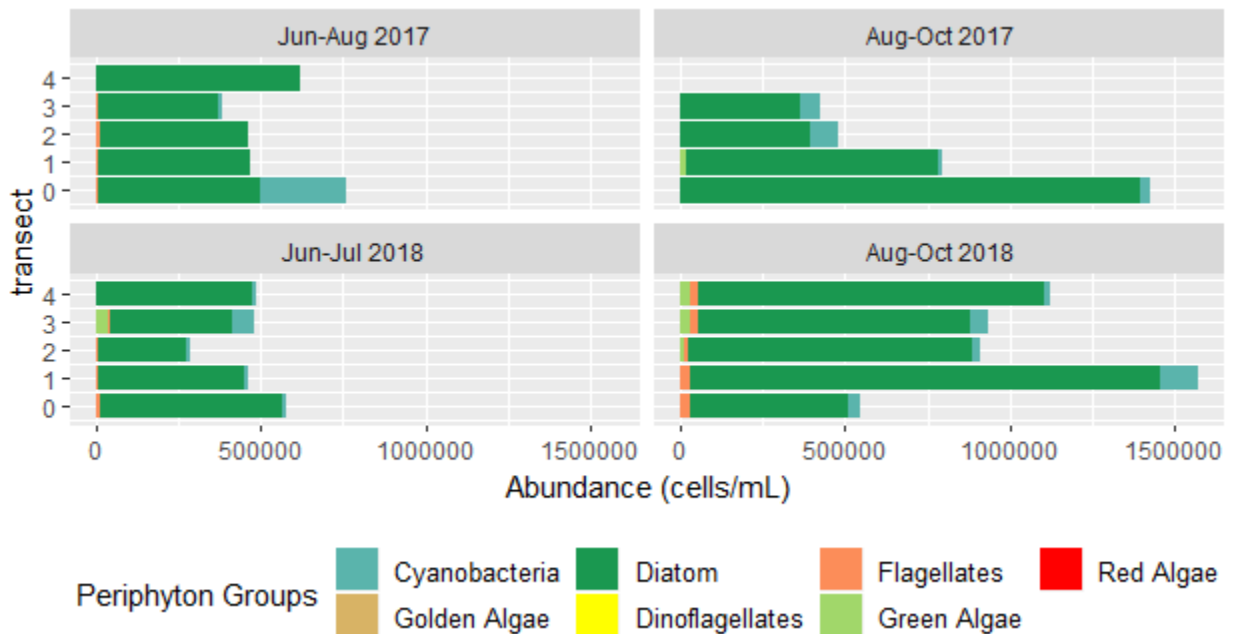


Figure A89 Abundance by Periphyton Group at PR1 .

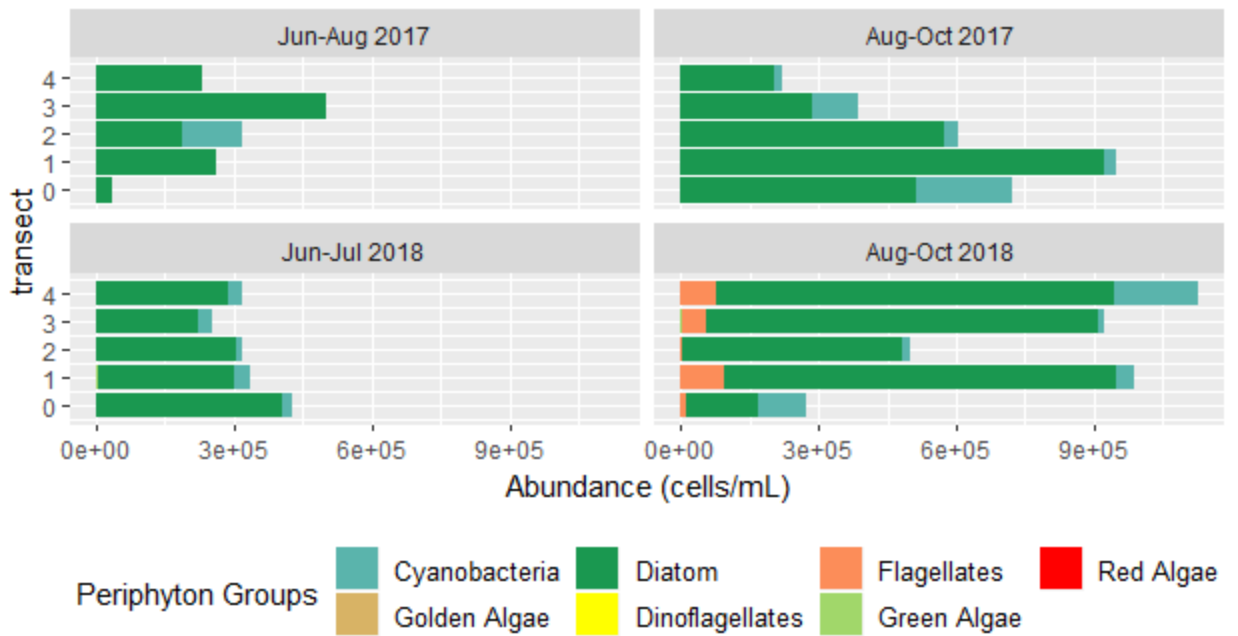


Figure A90 Abundance by Periphyton Group at PR2 .

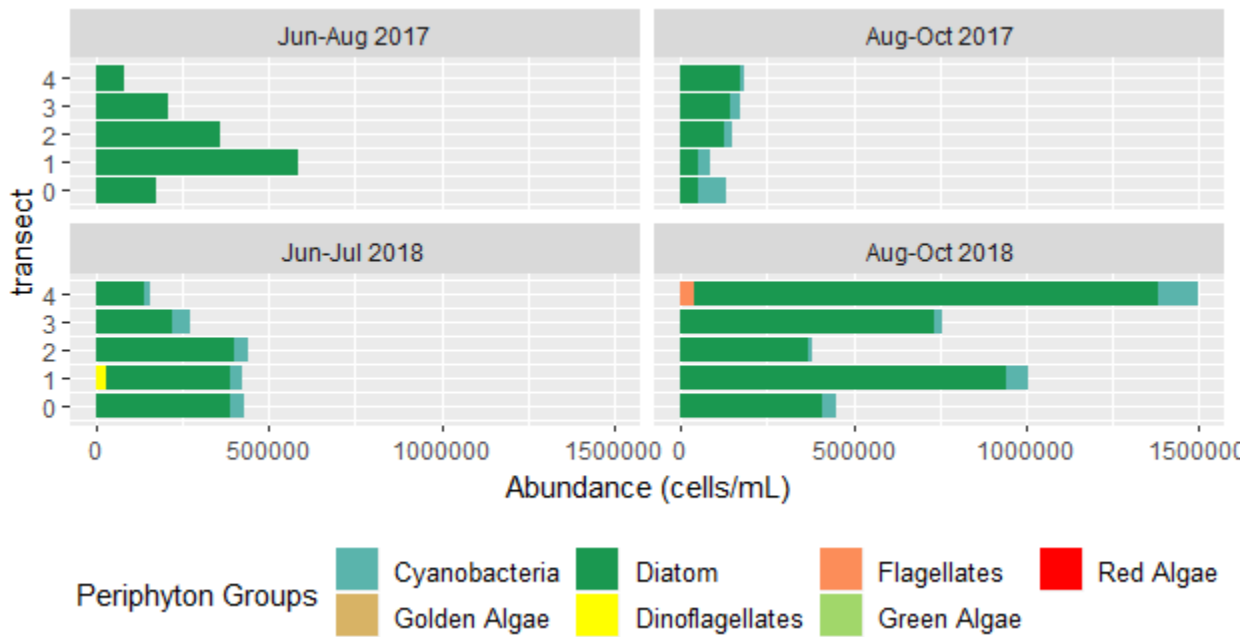


Figure A91 Abundance by Periphyton Group at PR3 .

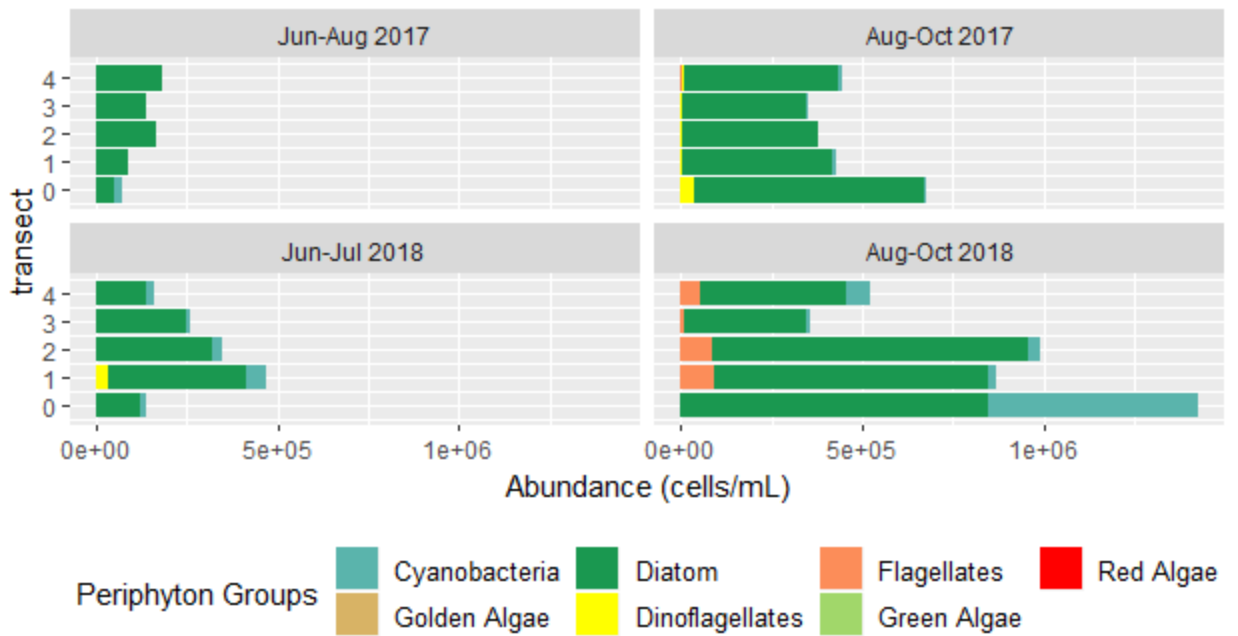


Figure A92 Abundance by Periphyton Group at PD1 .

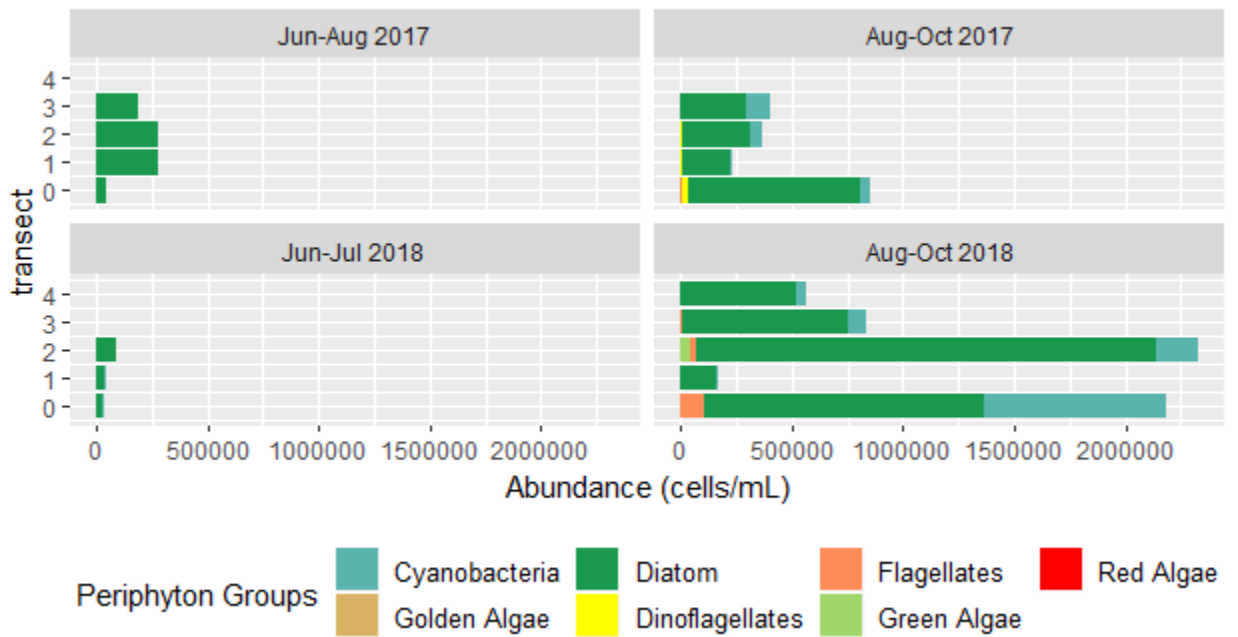


Figure A93 Abundance by Periphyton Group at PD2 .

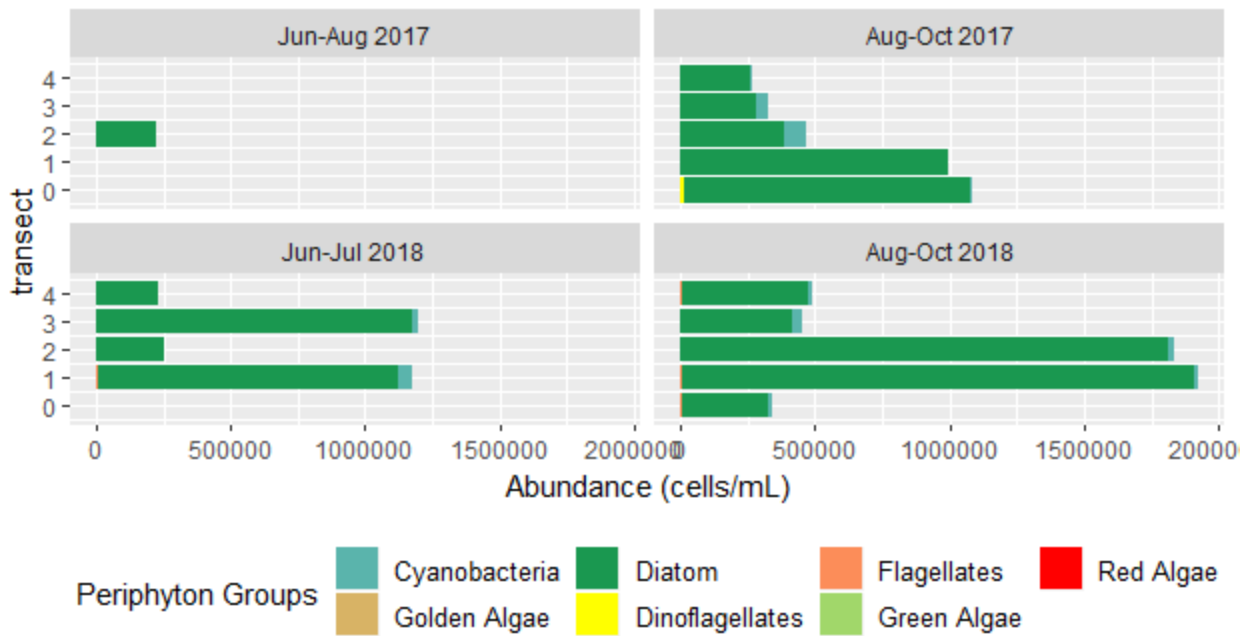


Figure A94 Abundance by Periphyton Group at PD3 .

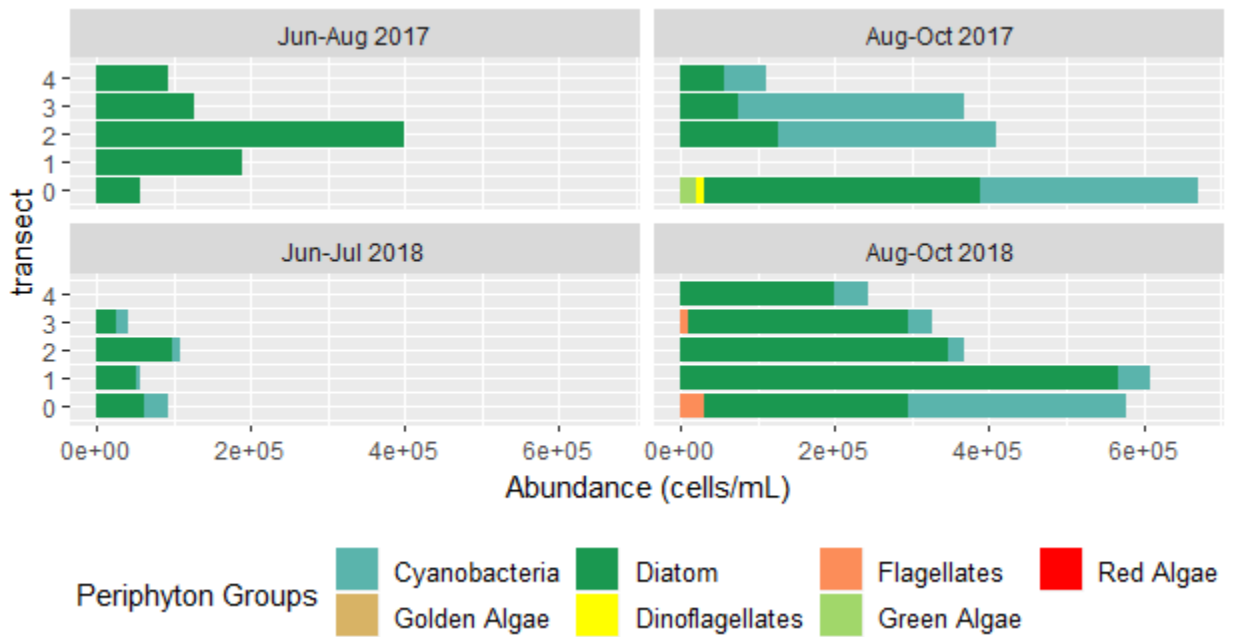


Figure A95 Abundance by Periphyton Group at PD4 .

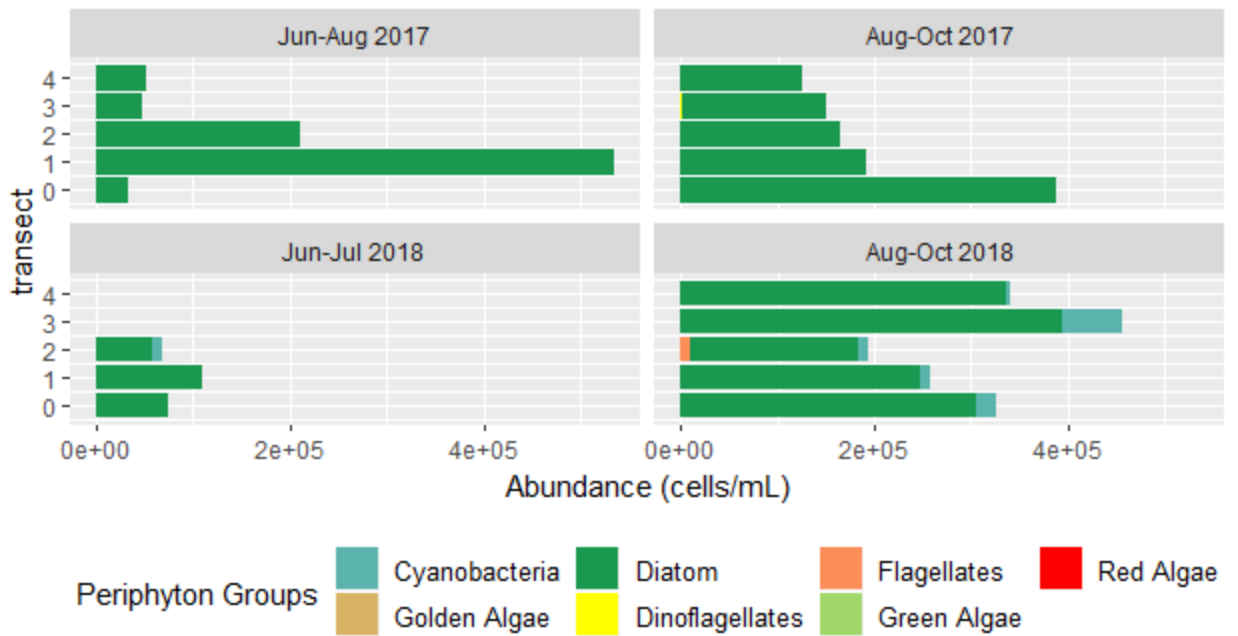


Figure A96 Abundance by Periphyton Group at PD5 .

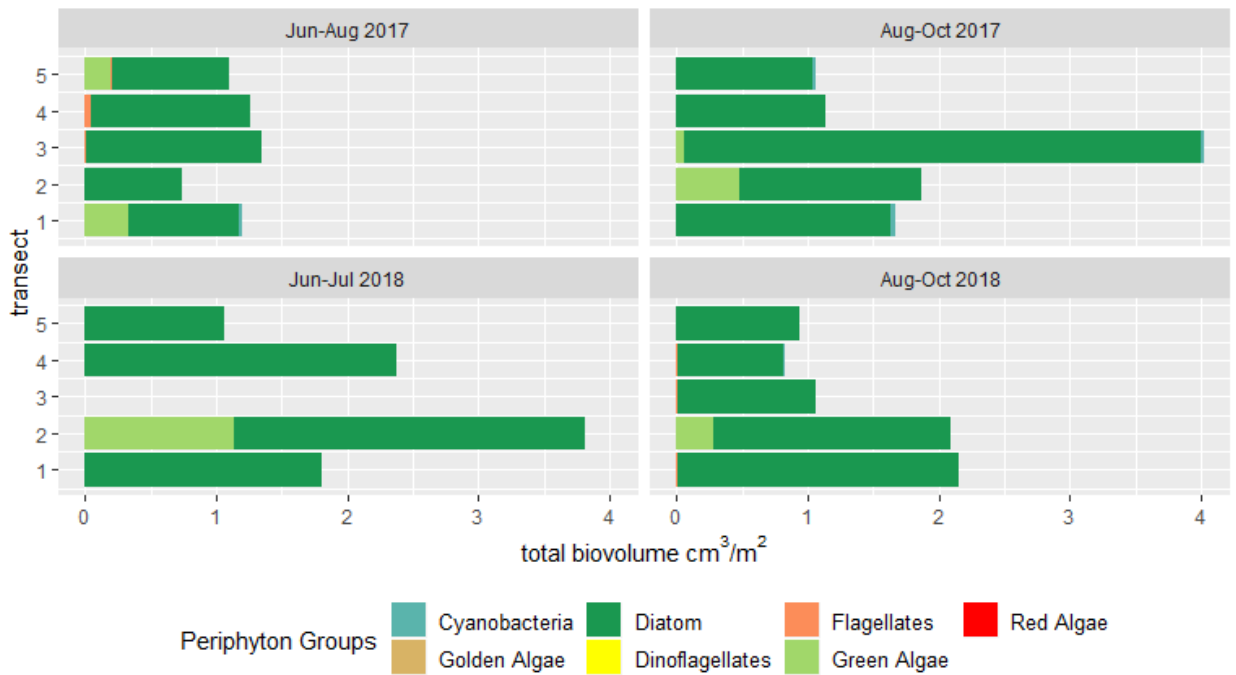


Figure A97 Biovolume by Periphyton Group at D1 .

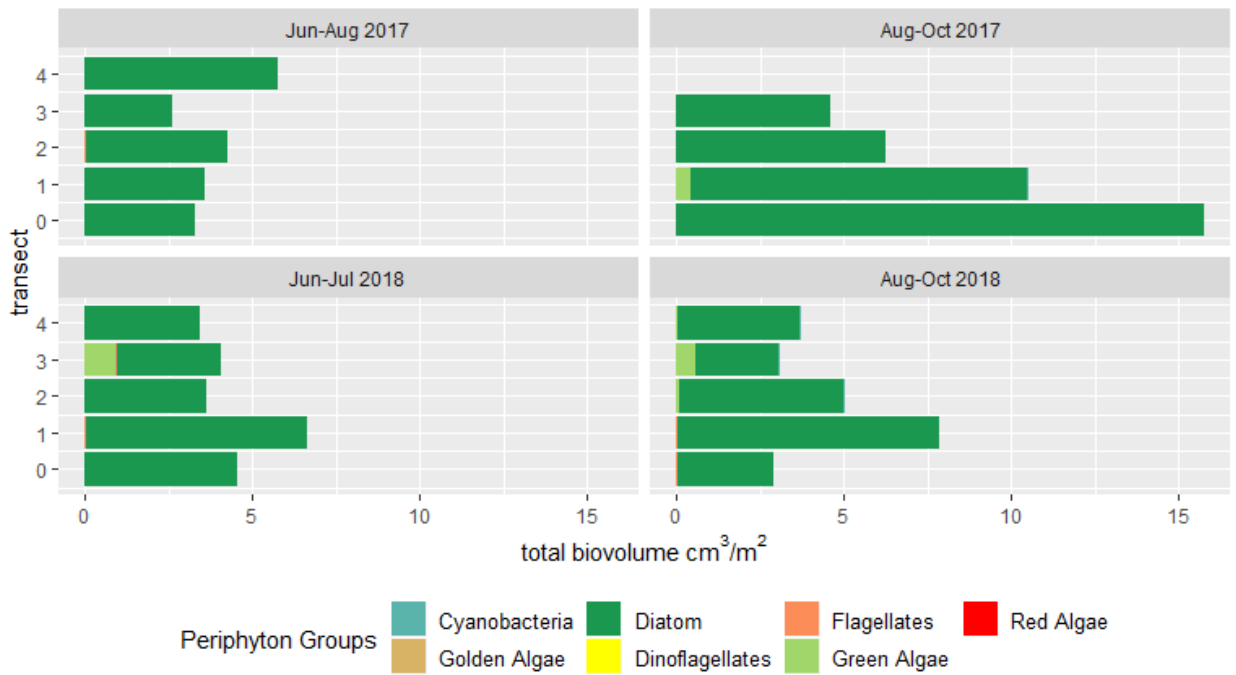


Figure A98 Biovolume by Periphyton Group at PR1 .

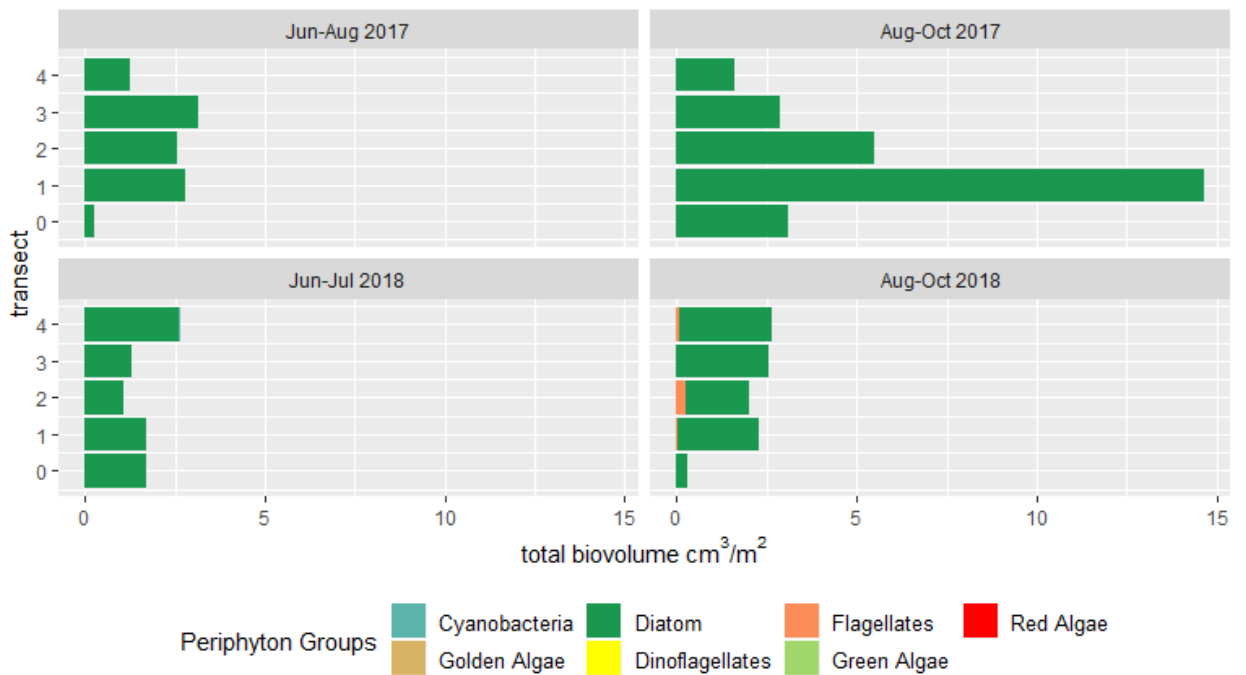


Figure A99 Biovolume by Periphyton Group at PR2 .

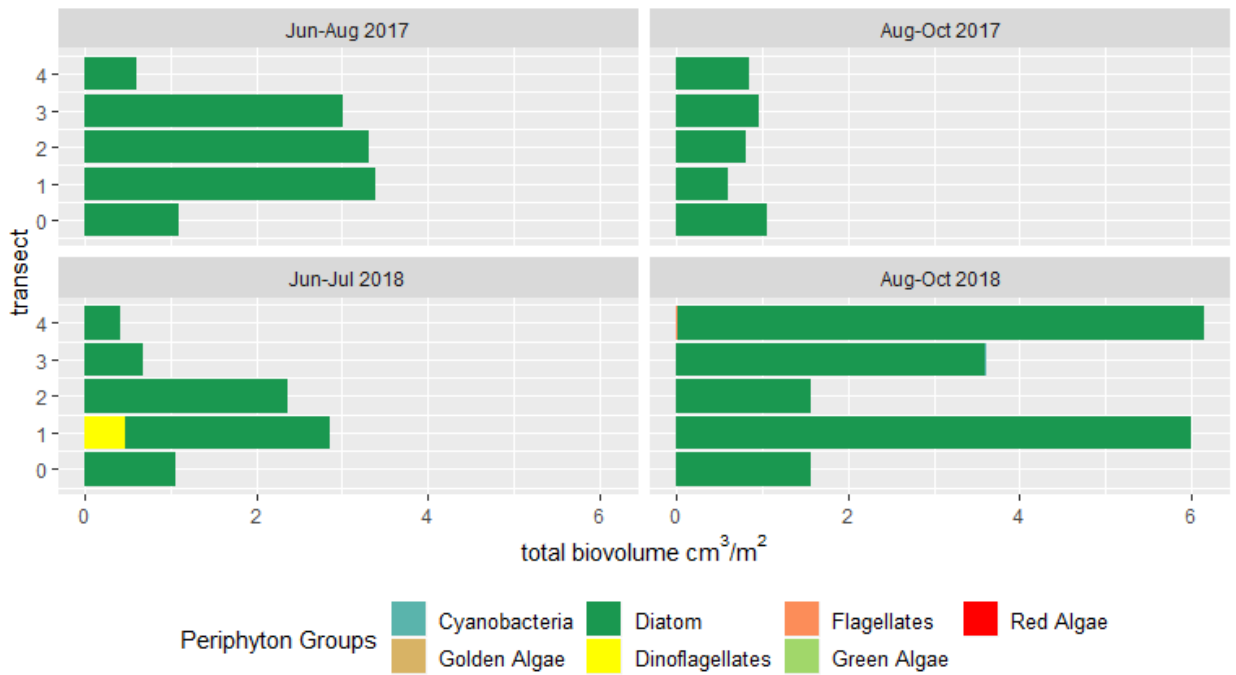


Figure A100 Biovolume by Periphyton Group at PR3 .

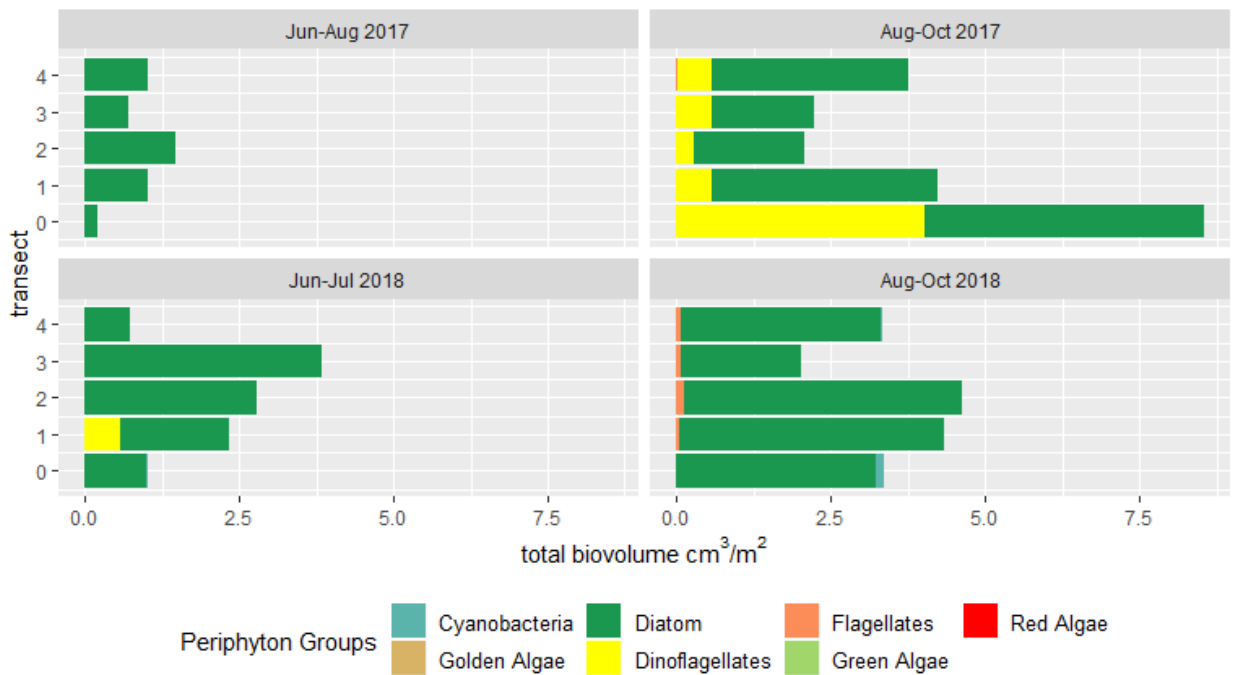


Figure A101 Biovolume by Periphyton Group at PD1 .

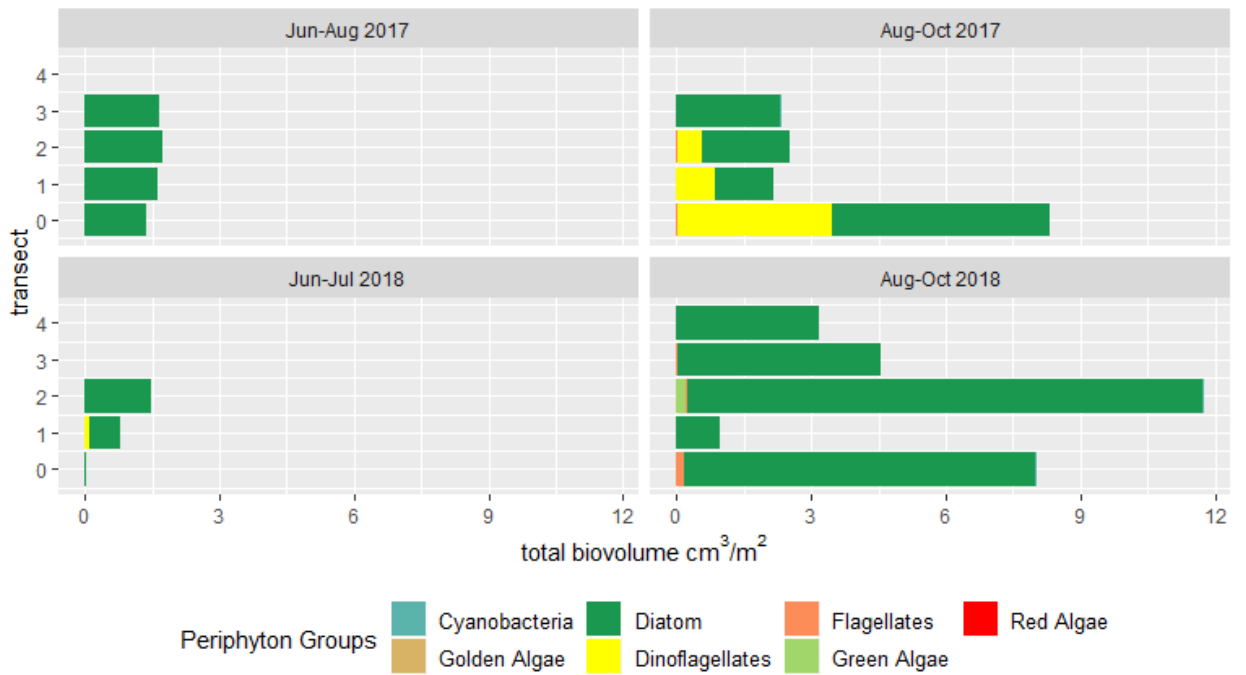


Figure A102 Biovolume by Periphyton Group at PD2 .

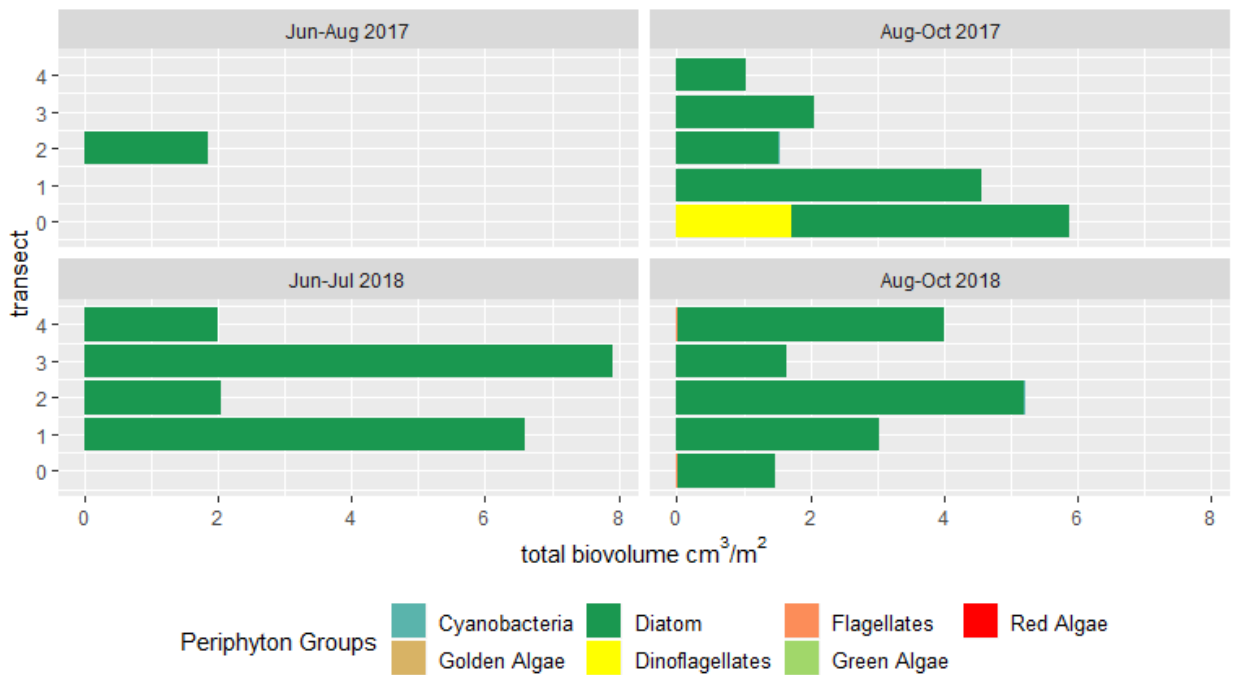


Figure A103 Biovolume by Periphyton Group at PD3 .

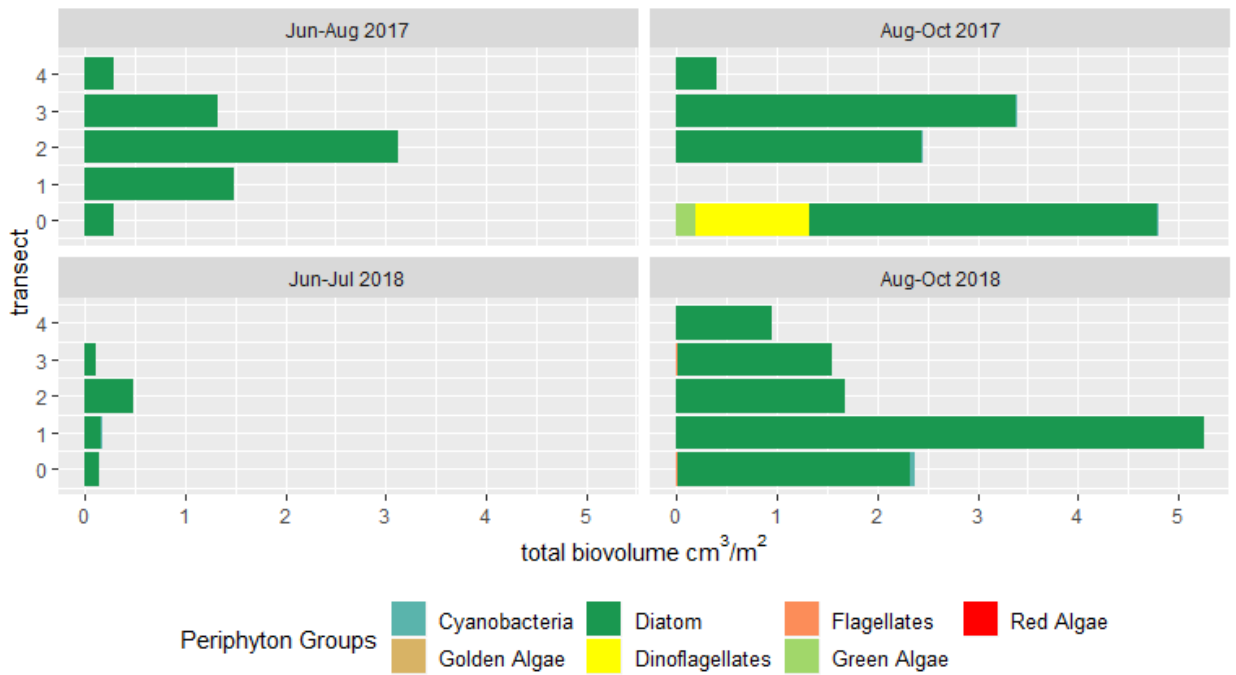


Figure A104 Biovolume by Periphyton Group at PD4 .

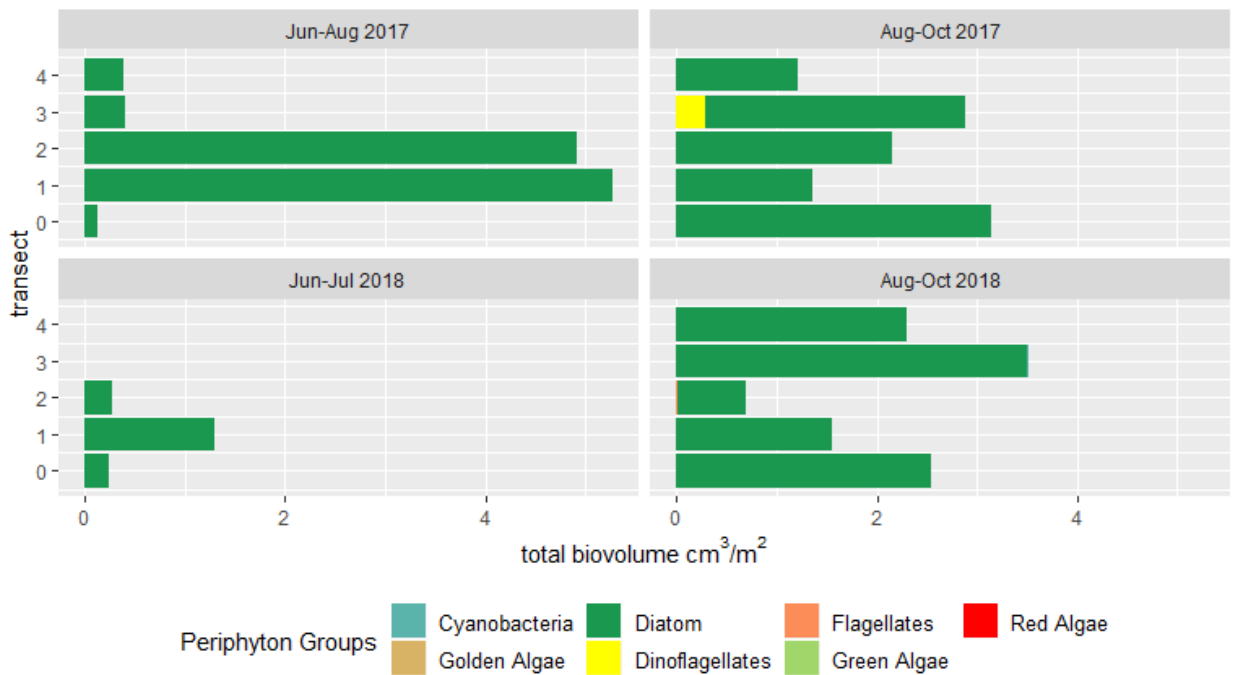


Figure A105 Biovolume by Periphyton Group at PD5 .

Appendix O Periphyton Ecological-Guild Summary Stats

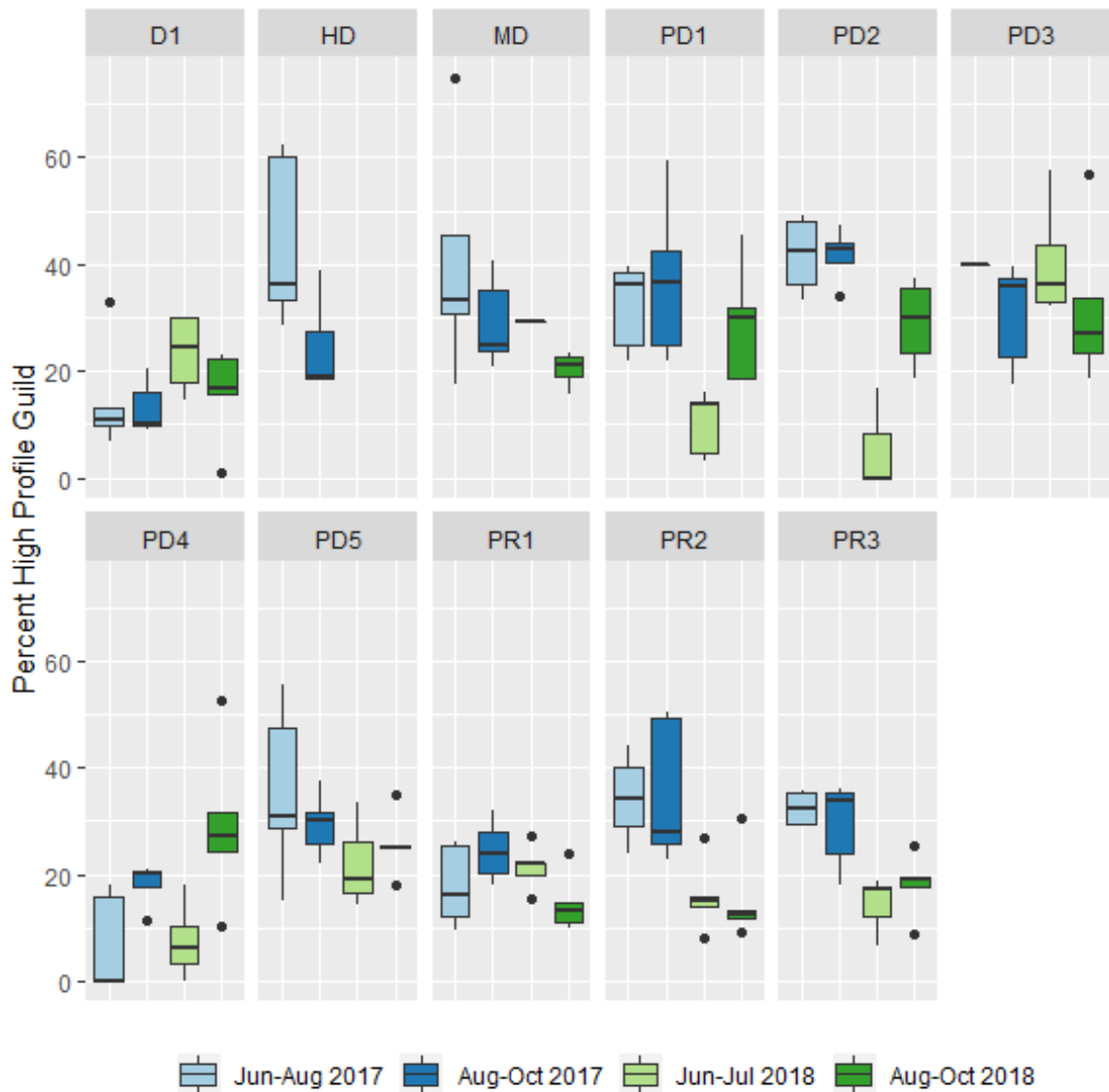


Figure A106 Boxplot of Percent High Profile Guild by site and series.

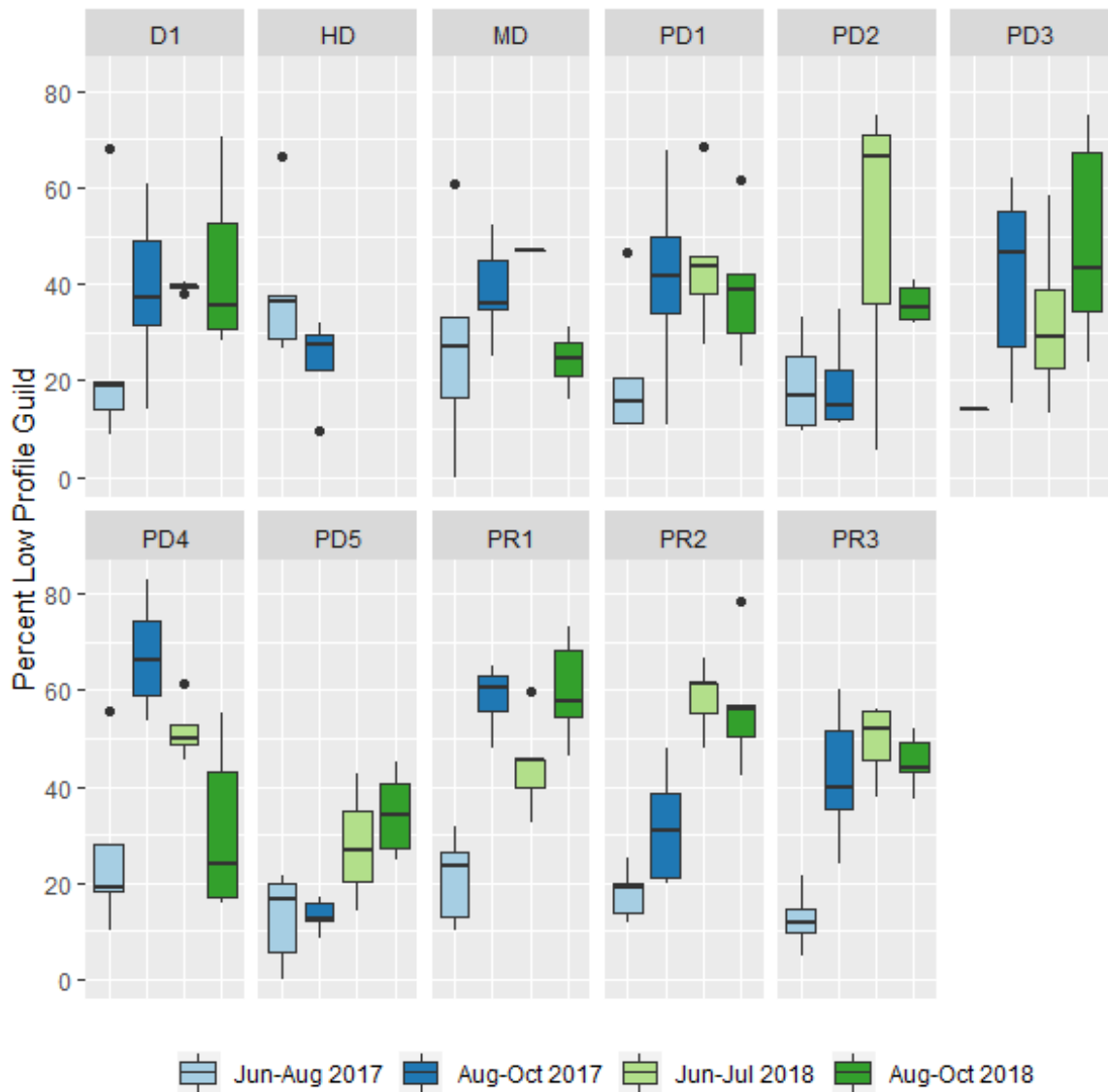


Figure A107 Boxplot of Percent Low Profile Guild by site and series.

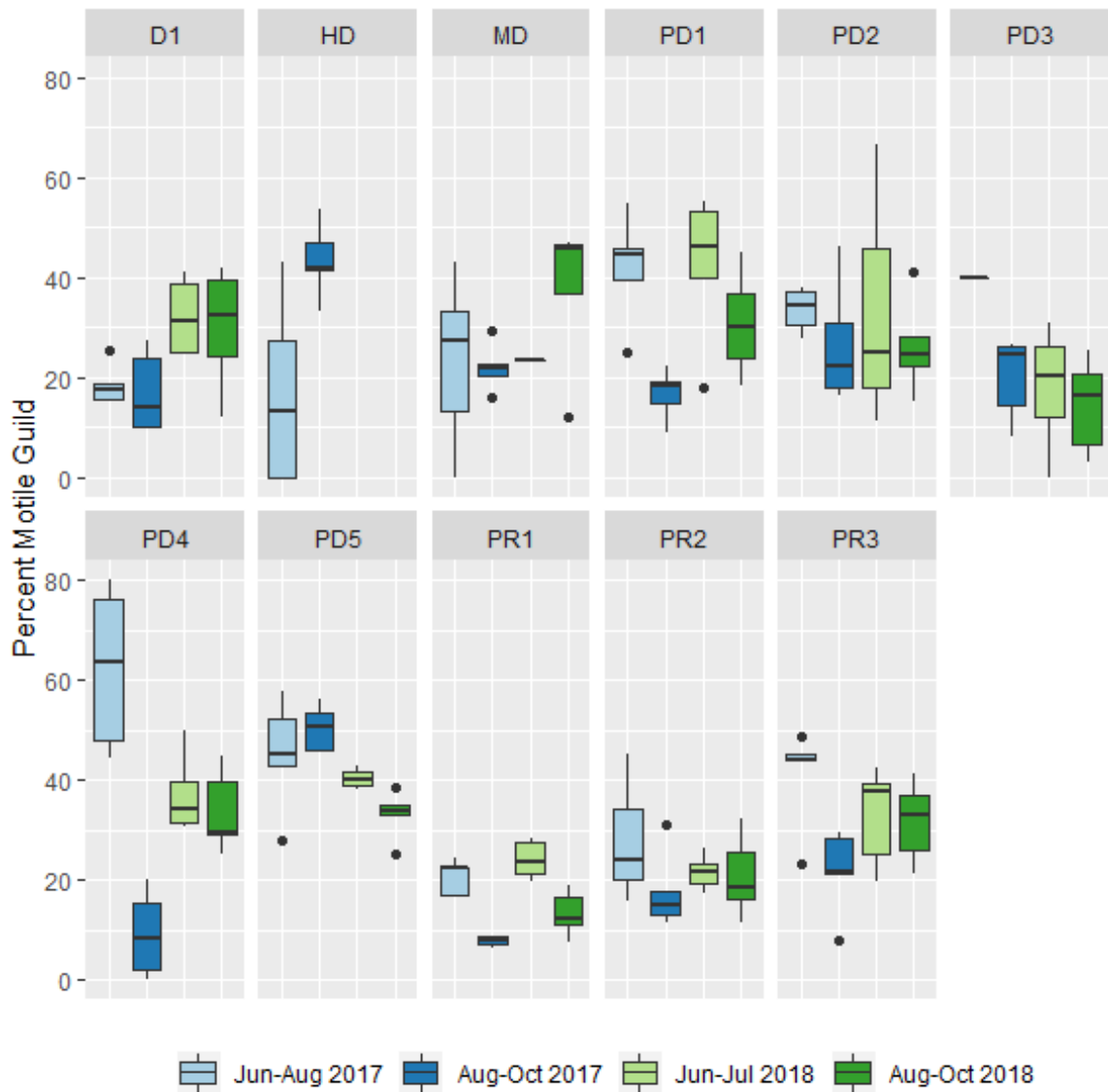


Figure A108 Boxplot of Percent Motile Guild by site and series.

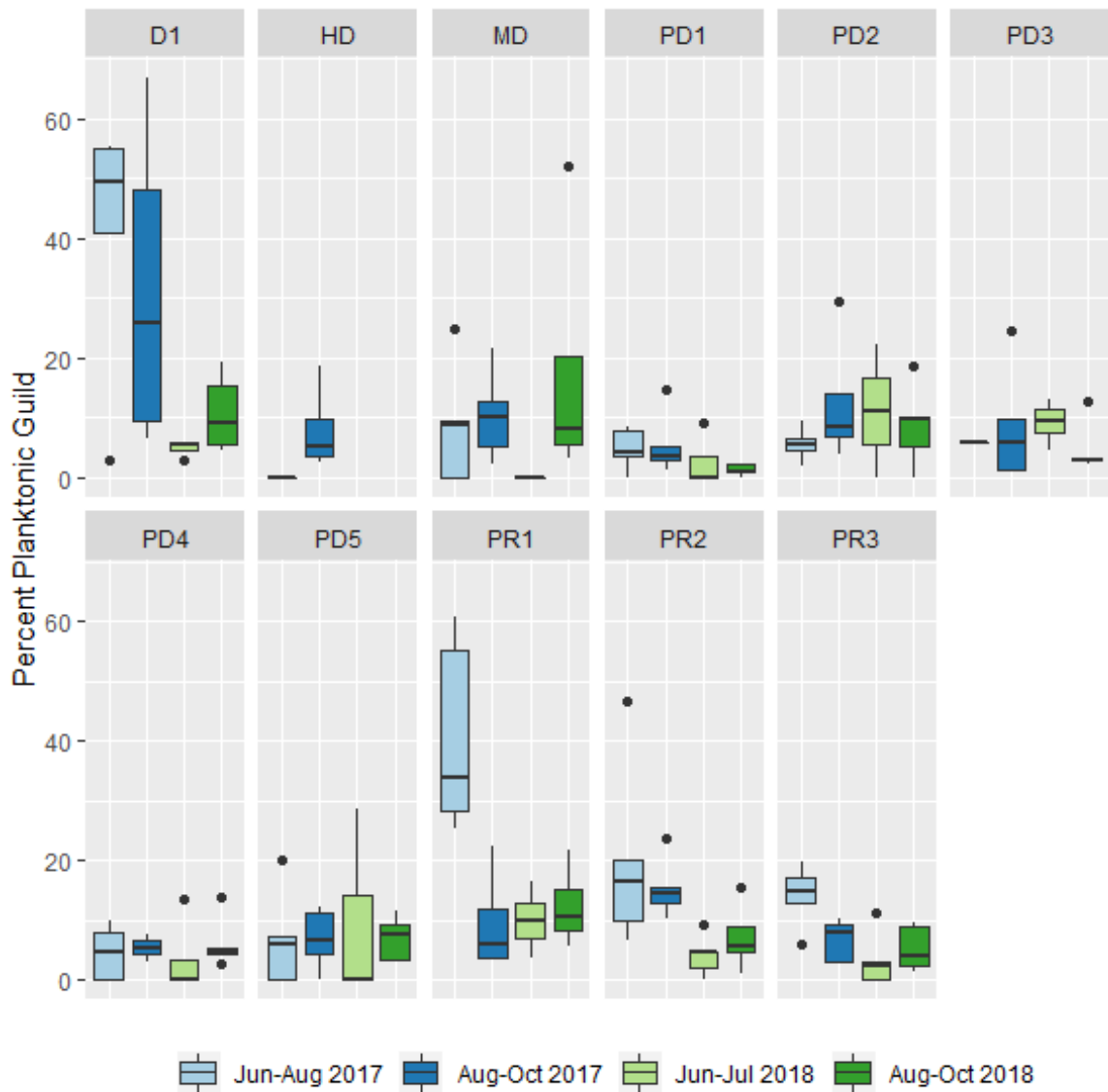


Figure A109 Boxplot of Percent Planktonic Guild by site and series.

Appendix P Periphyton Shallow Water Strip Productivity Results and Correlations

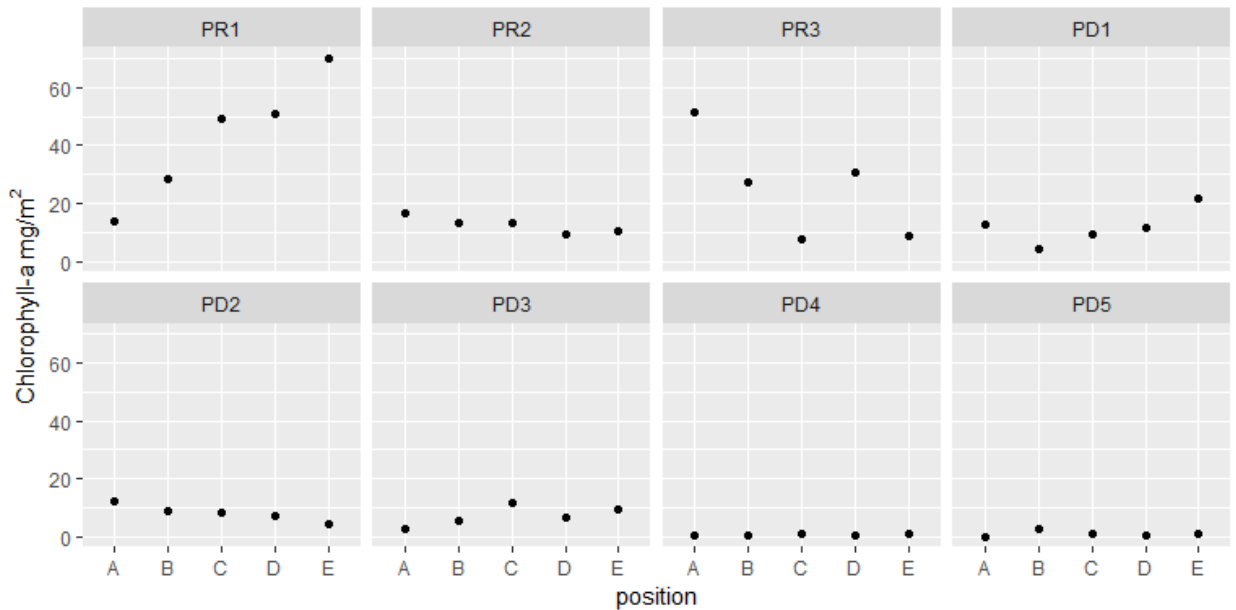


Figure A110 Periphyton strip samplers from Summer 2018, A position is closest sampler 0 and E is closest to sampler 1. When the PR2 strip was retrieved it was upside down.

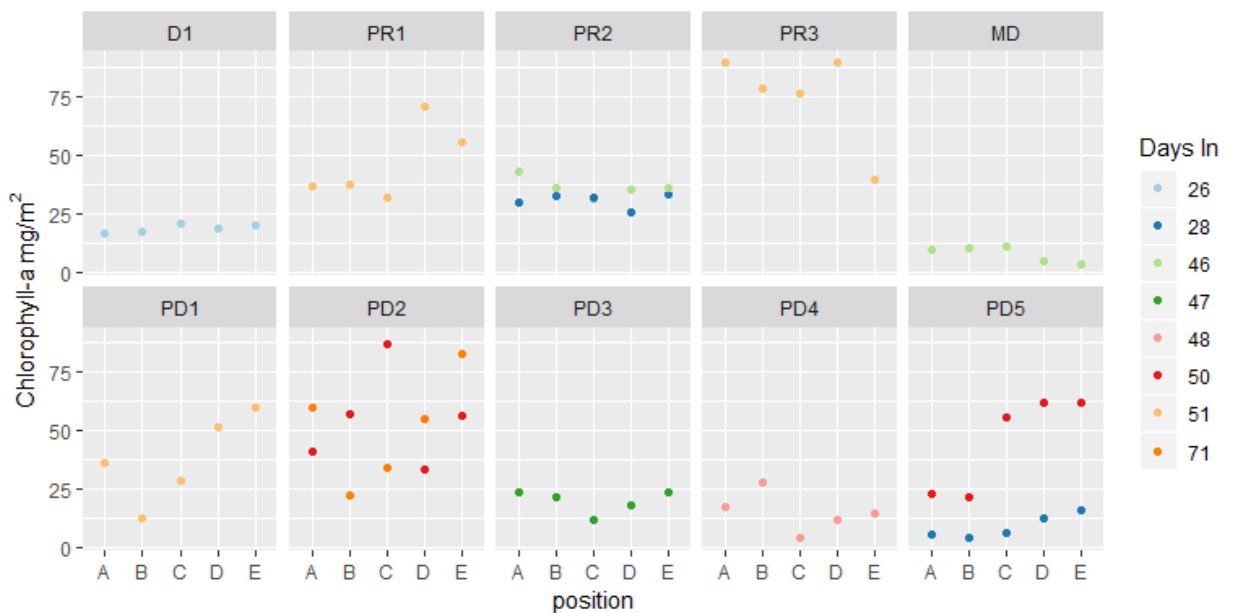


Figure A111 Periphyton strip samplers from Fall 2018, A position is closest sampler 0 and E is closest to sampler 1.

Appendix Q Reservoir Zooplankton Summary

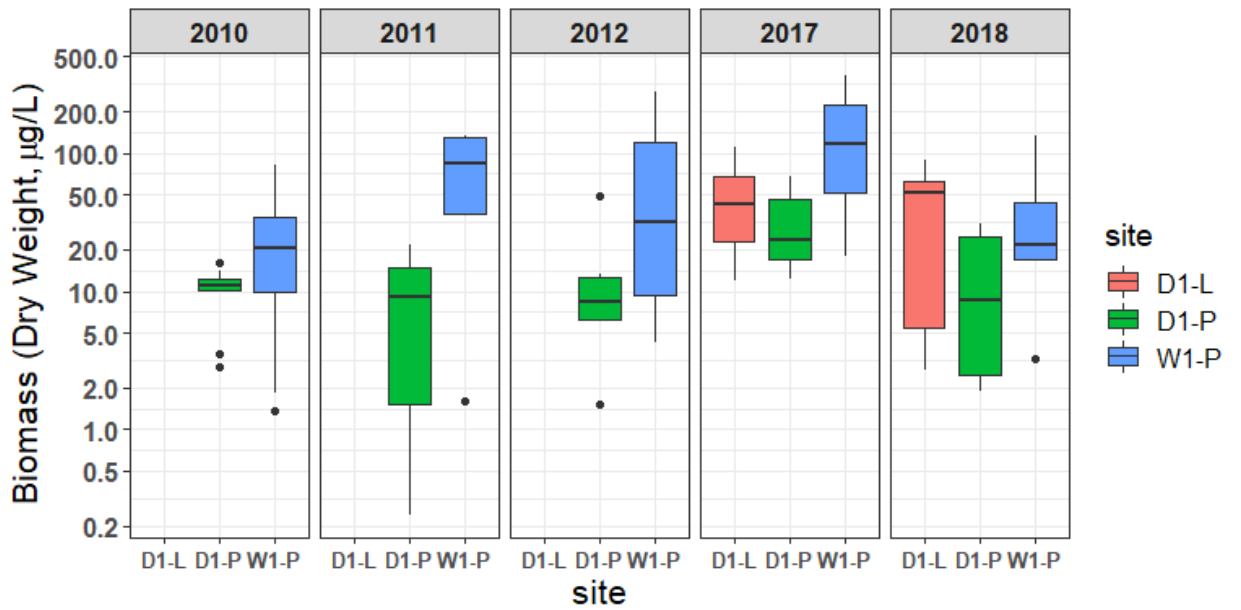


Figure A112 Zooplankton Biomass by Year for Reservoir Sites

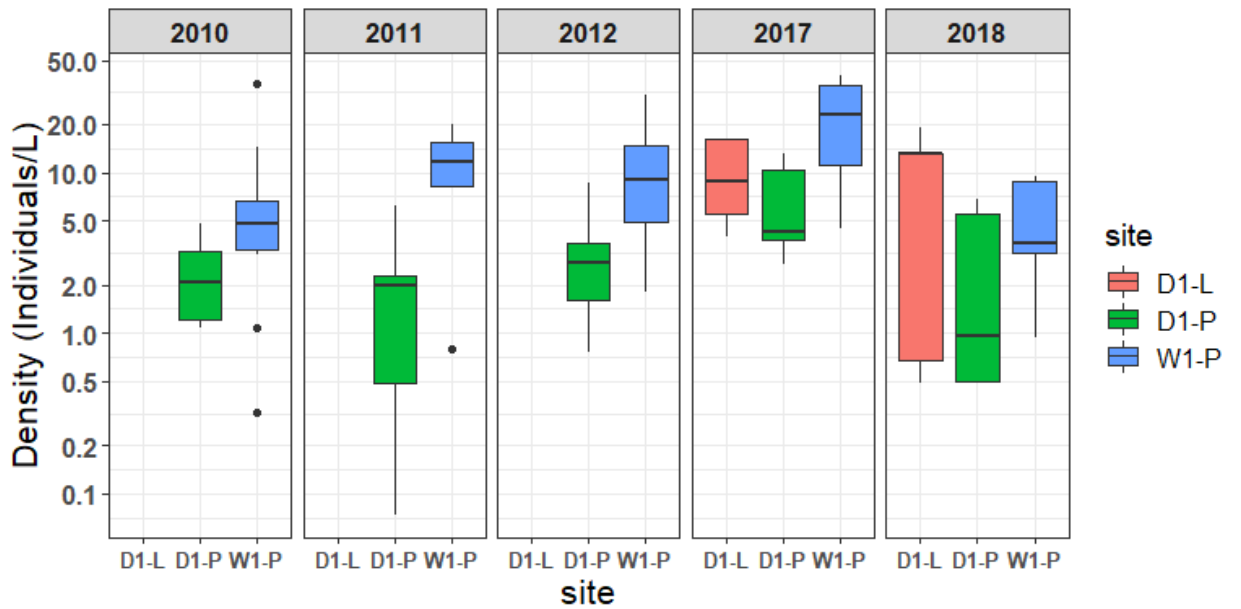


Figure A113 Zooplankton Density by Year for Reservoir Sites



Table A9 Total Biomass by month and site in 2018.

month	D1-L	D1-P	W1-P	HD	MD	PR1	PR2	PR3
May	2.740	2.030	3.200					
June	88.200	30.800	26.400					
July	61.000	27.300	133.000					0.115
August	43.200	17.800	52.900	0.298	0.000	1.790	0.049	
Sept	2.700	4.240	16.800	0.007	0.016	4.500	0.006	0.119
Oct	62.800	1.880	17.400					

Table A10 Total Density by month and site in 2018.

month	D1-L	D1-P	W1-P	HD	MD	PR1	PR2	PR3
May	0.673	0.491	0.937					
June	19.200	6.870	8.780					
July	13.300	5.580	9.360					0.041
August				0.064		0.459	0.015	
Sept	0.485	0.956	3.140	0.001	0.004	1.130	0.002	0.020
Oct	13.100	0.501	3.620					



Appendix R Invertebrate Response Summary Stats

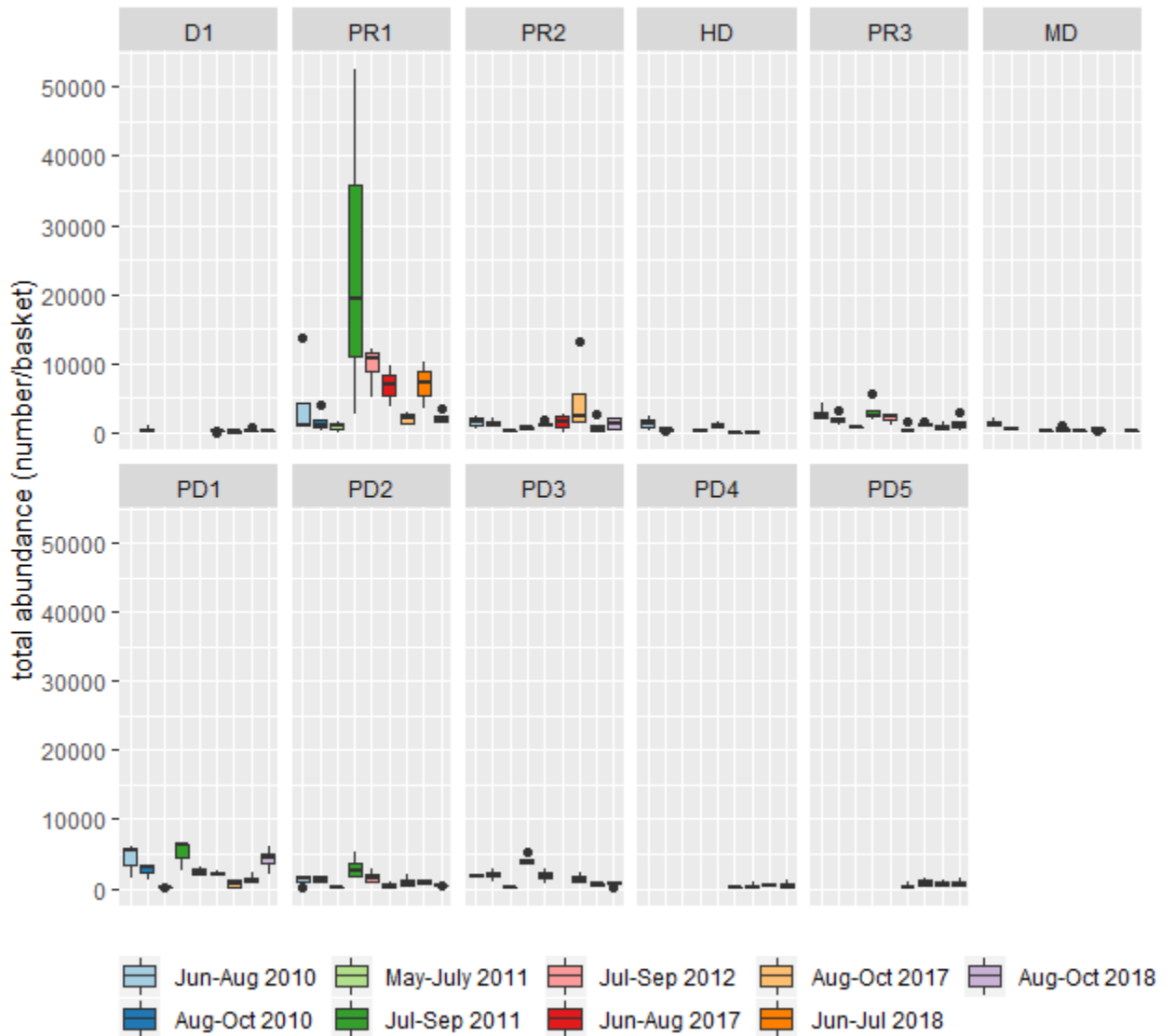


Figure A114 Boxplot of total abundance (number/basket) by site and series.



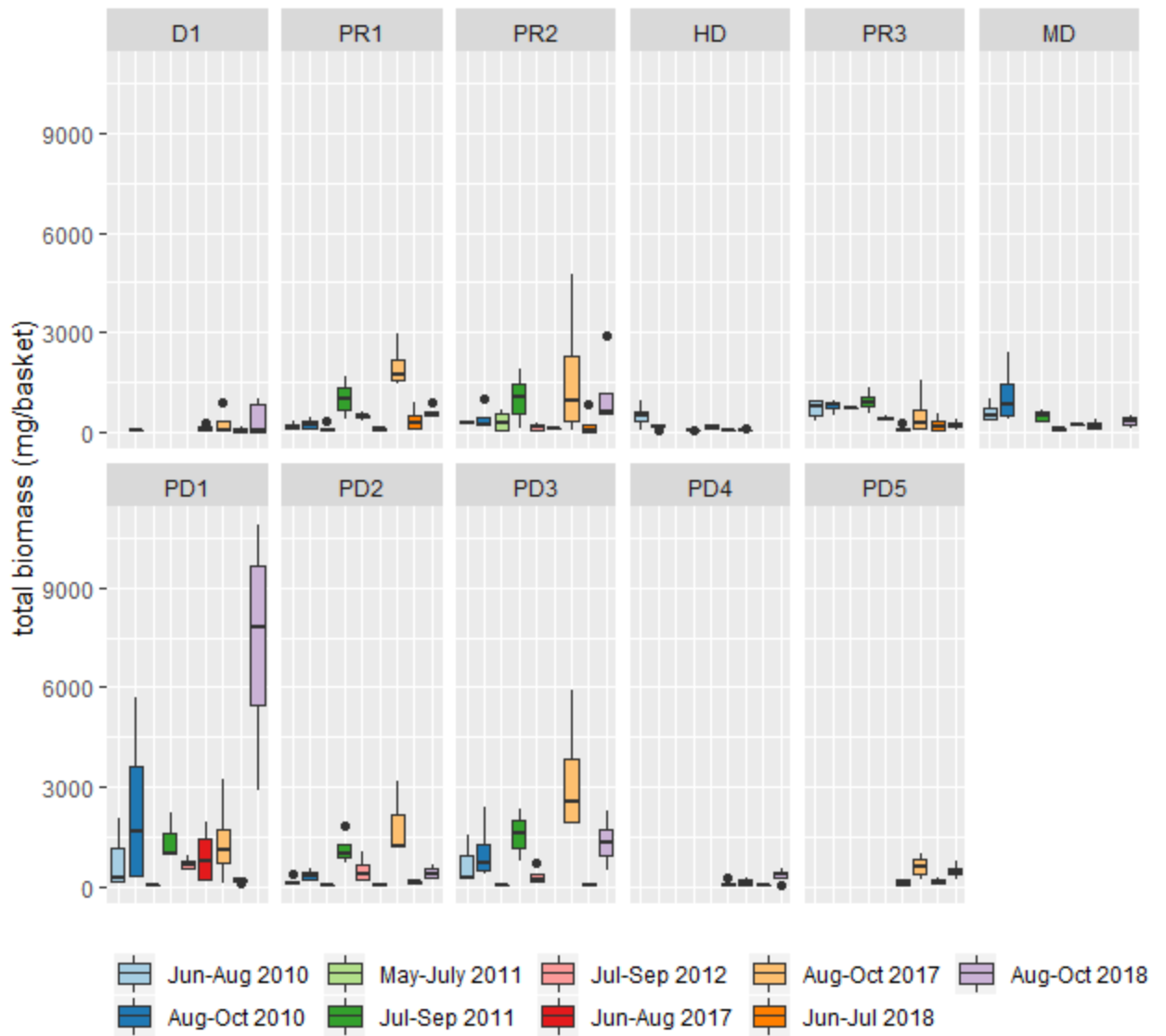


Figure A115 Boxplot of total biomass (mg/basket) by site and series.



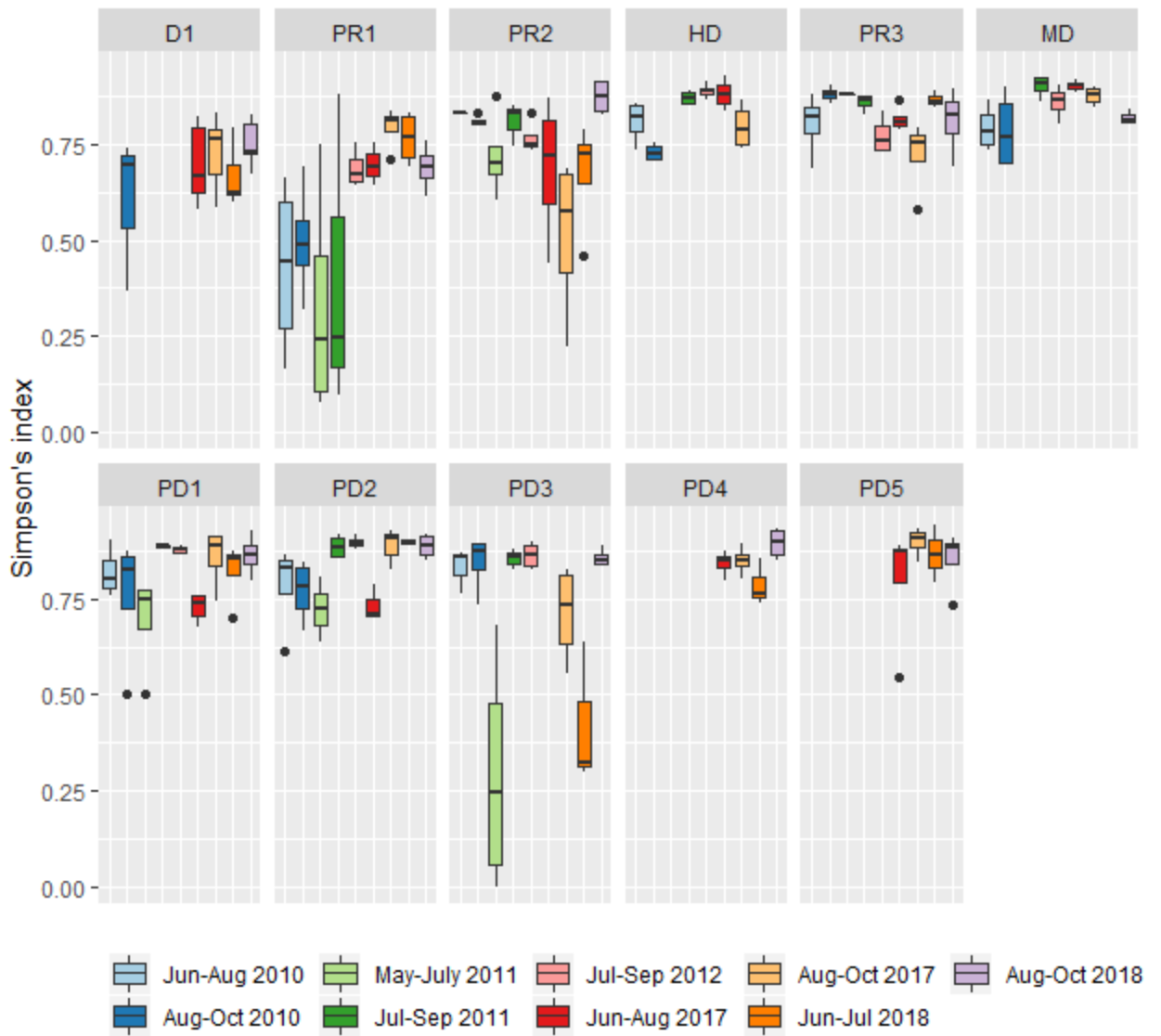


Figure A116 Boxplot of Simpson's index by site and series.



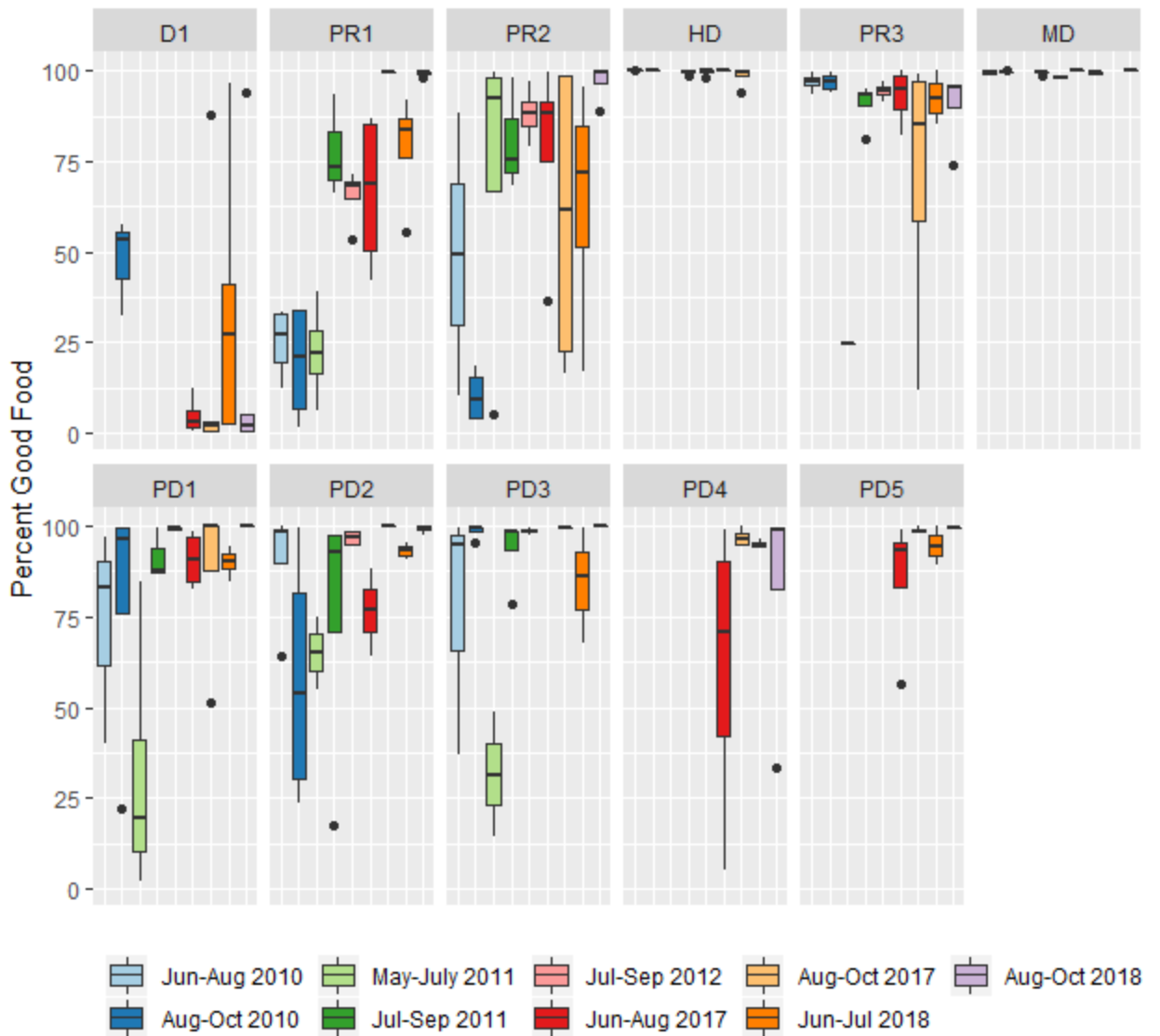


Figure A117 Boxplot of Percent Good Food by site and series.



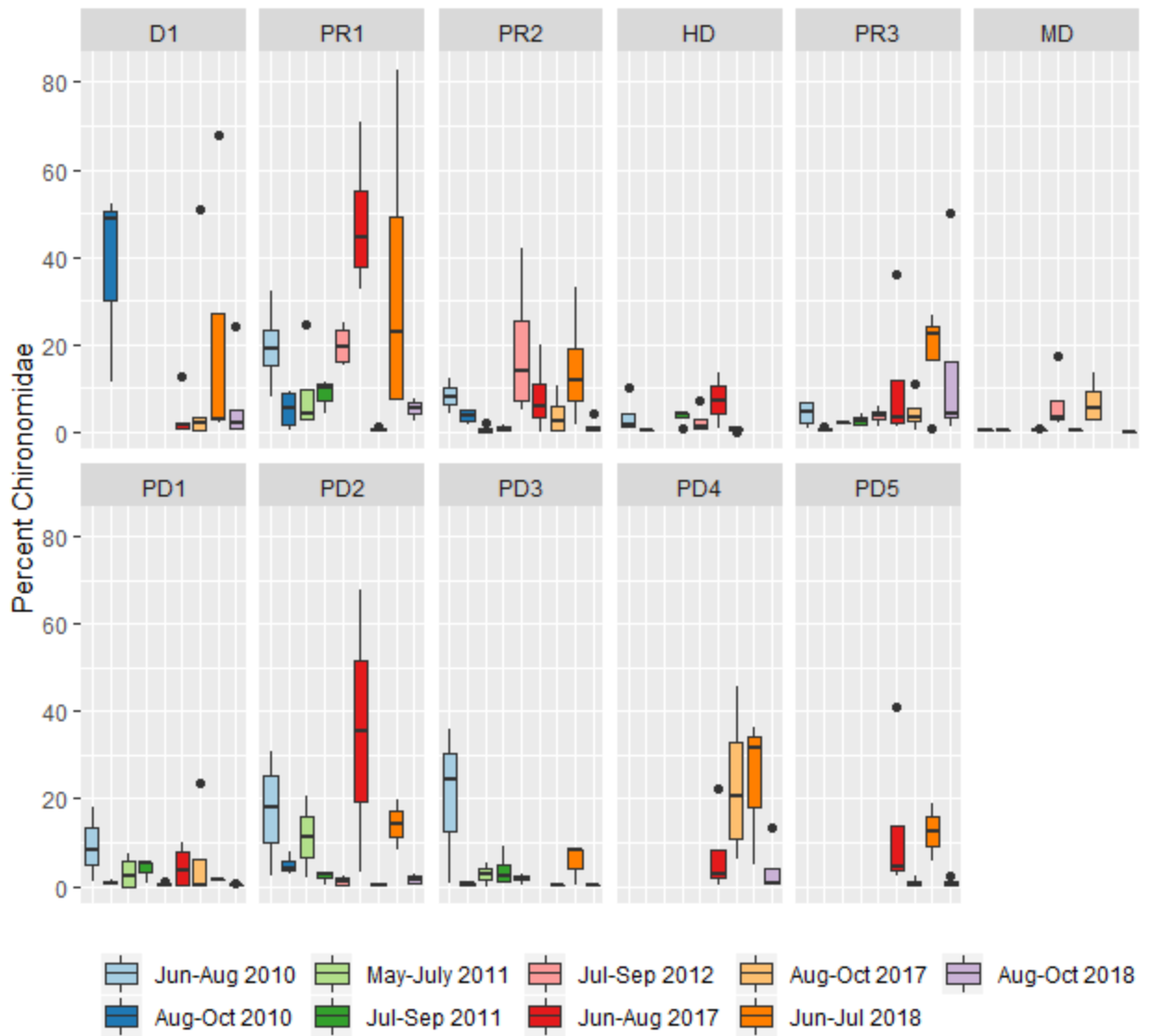


Figure A118 Boxplot of Percent Chironomidae by site and series.



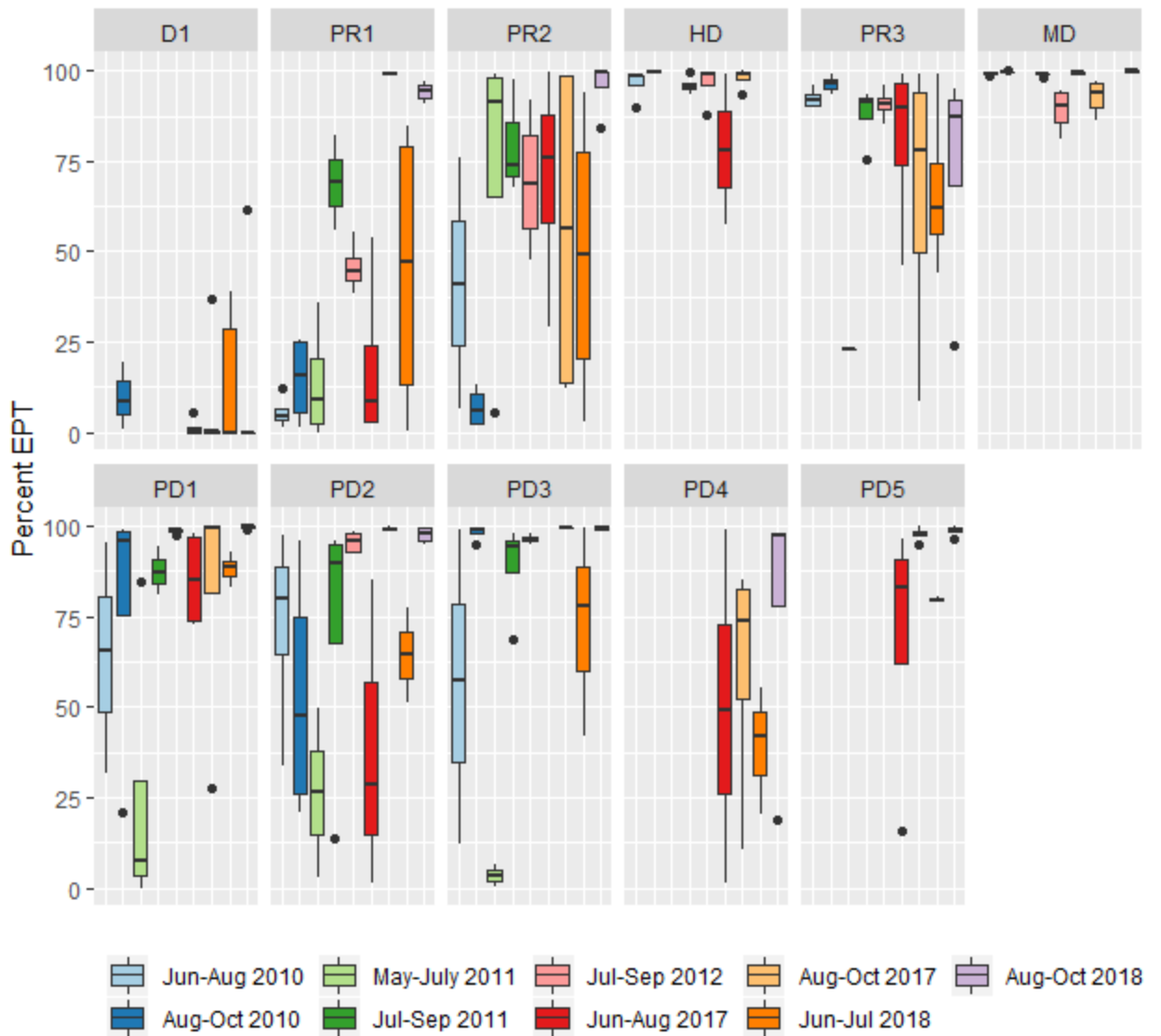


Figure A119 Boxplot of Percent EPT by site and series.



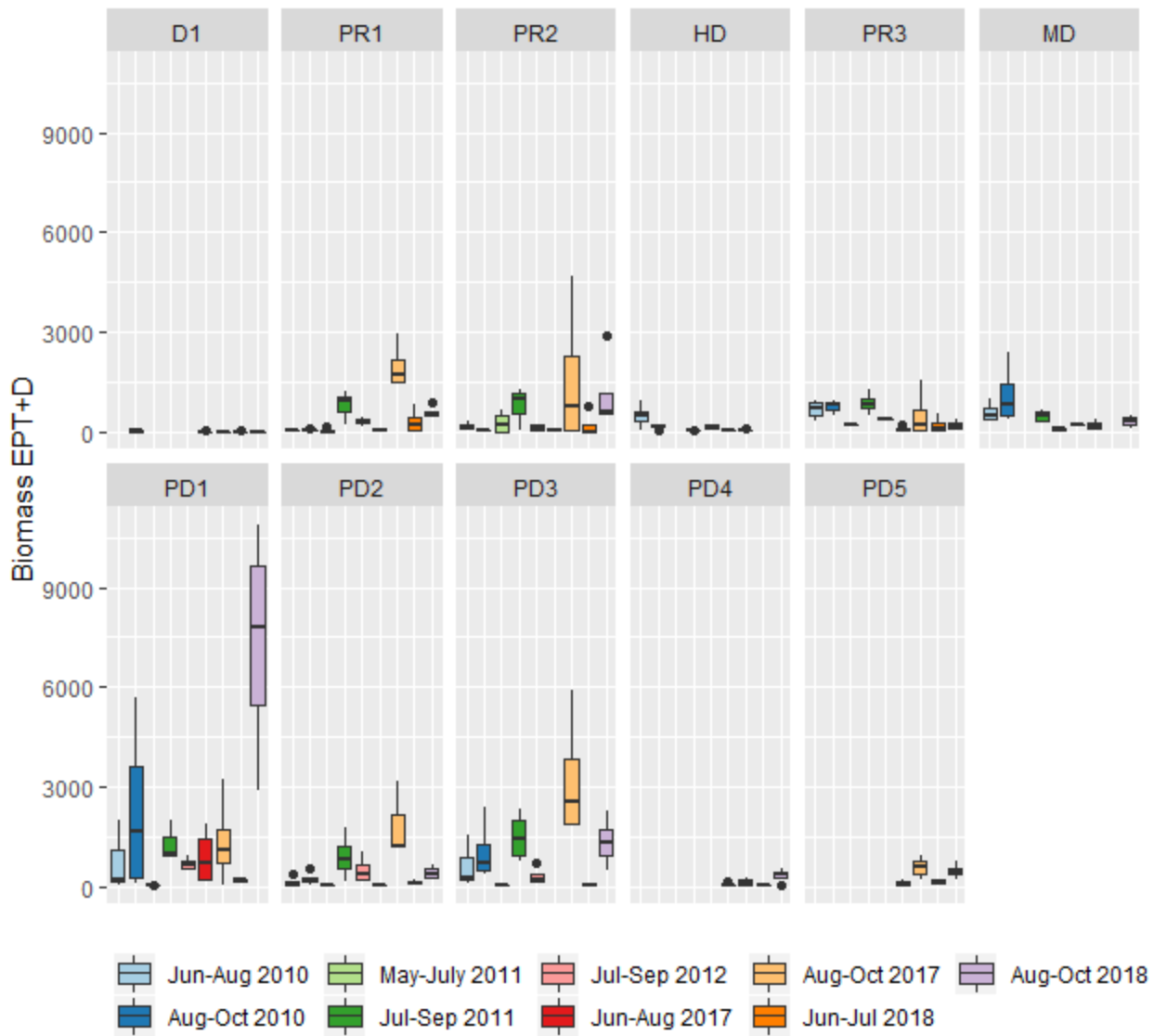


Figure A120 Boxplot of Biomass EPT+D by site and series.



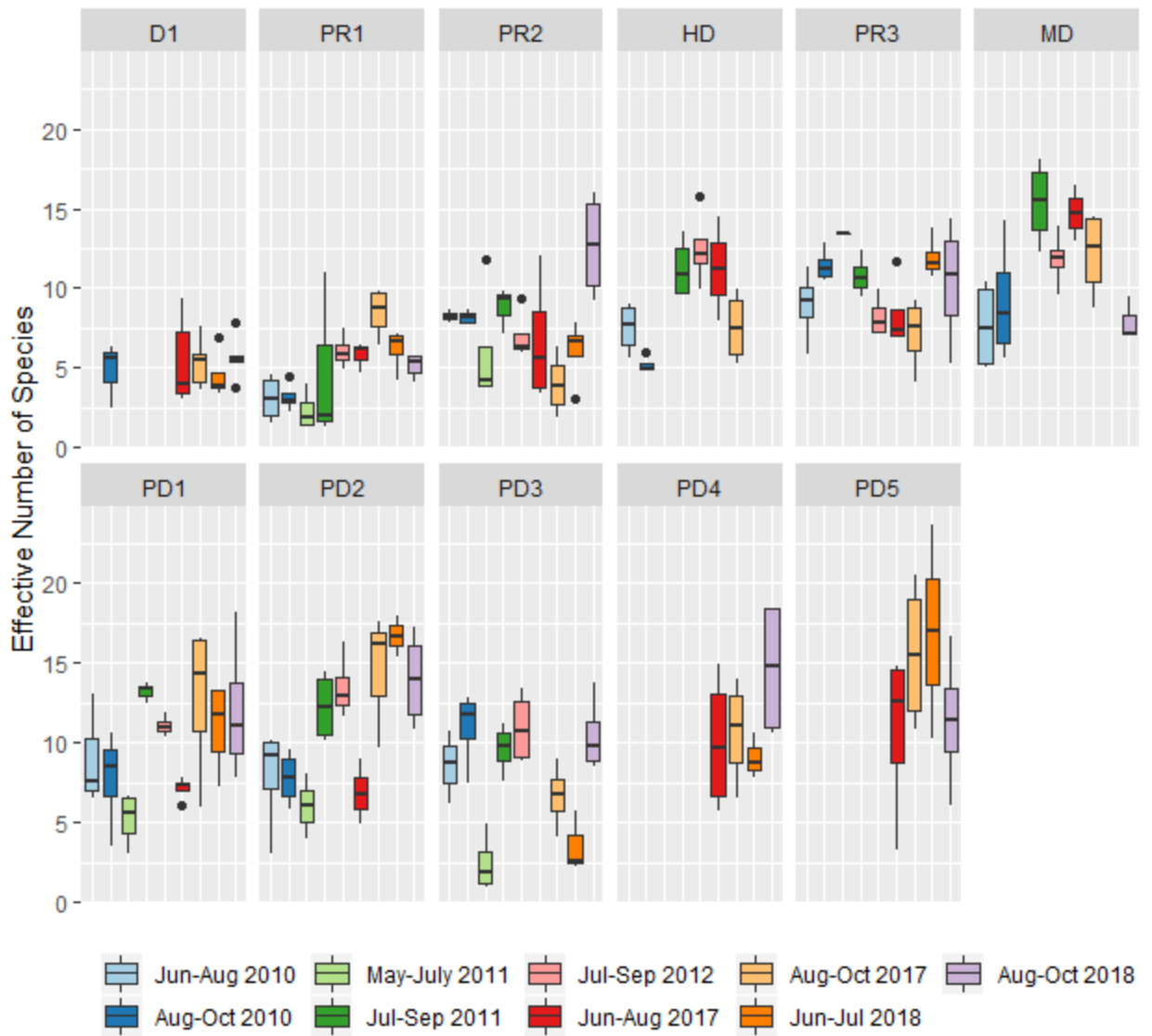


Figure A121 Boxplot of Effective Number of Species by site and series.



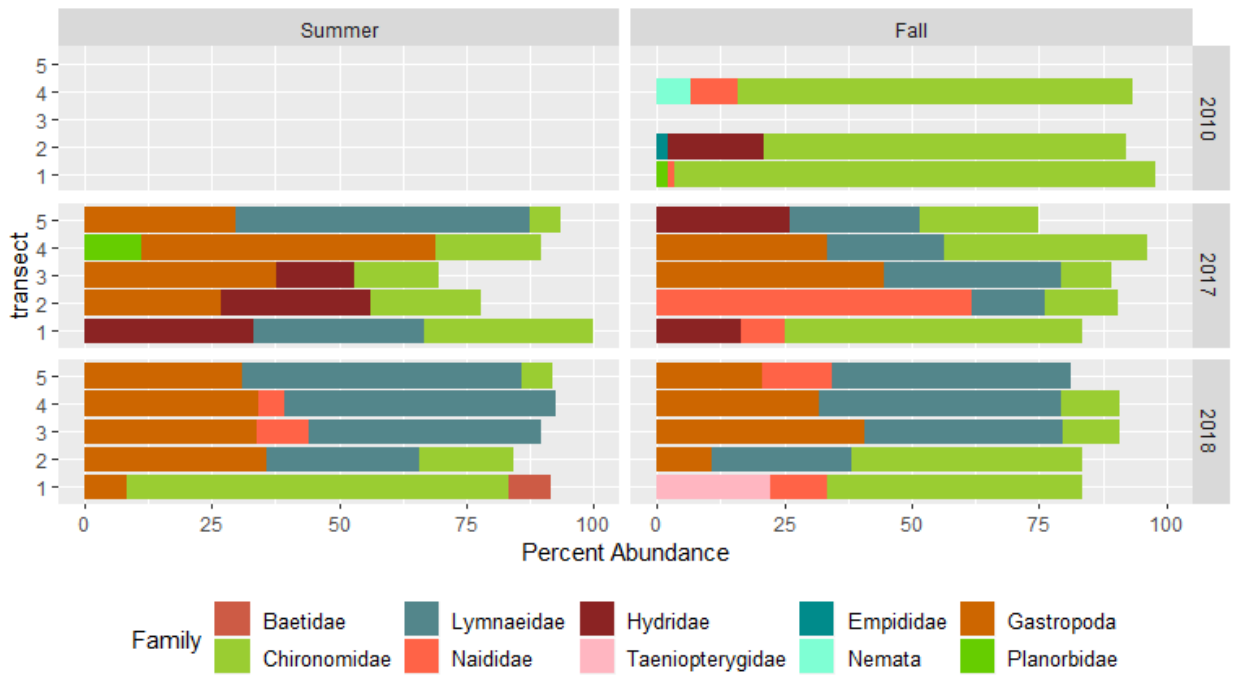


Figure A122 Benthic Percent Abundance by Family Level at D1 .

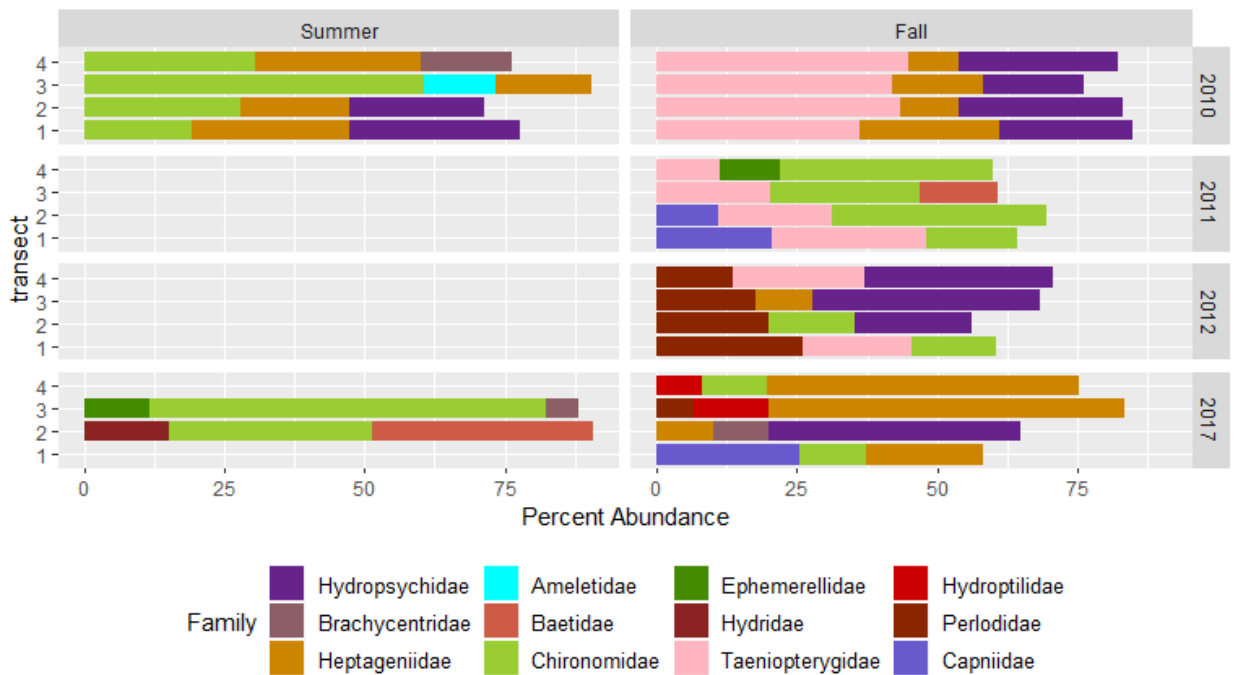


Figure A123 Benthic Percent Abundance by Family Level at HD .



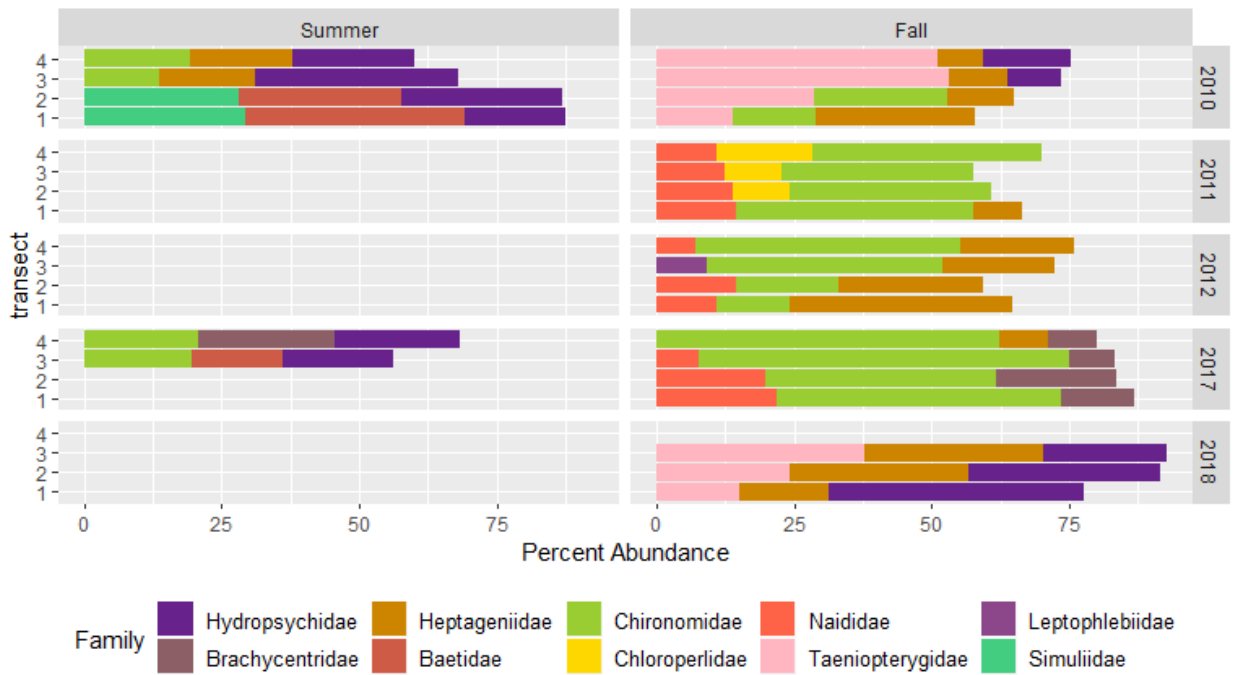


Figure A124 Benthic Percent Abundance by Family Level at MD .

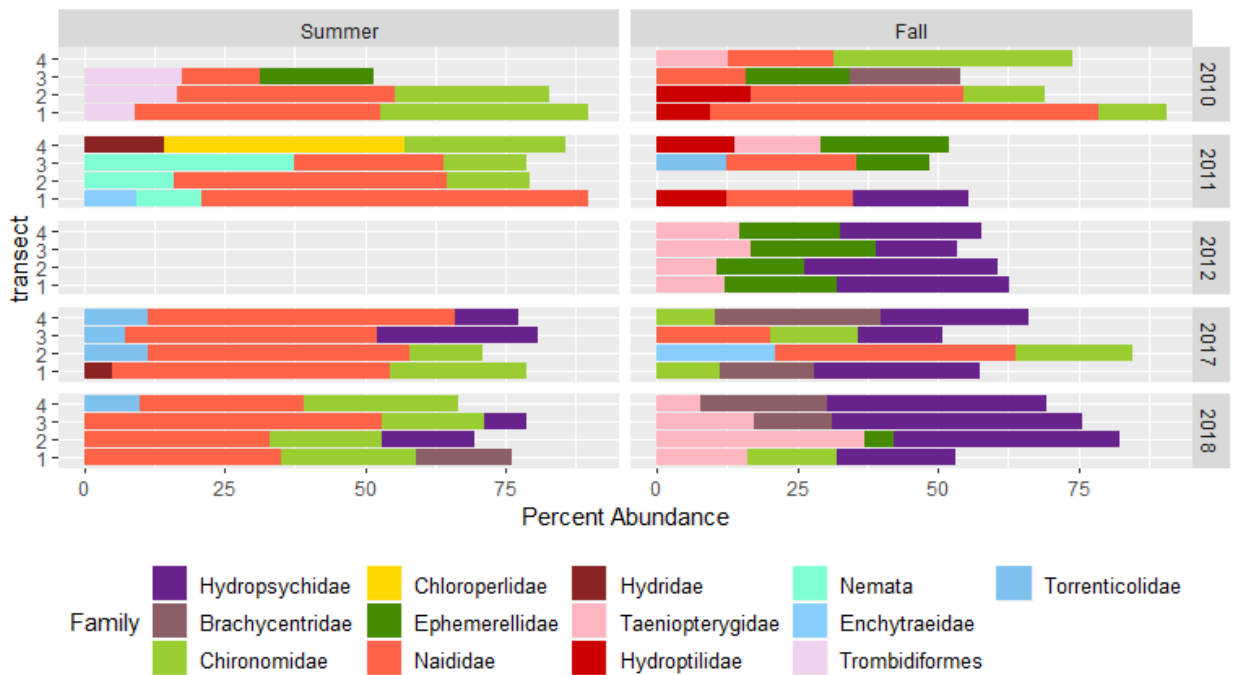


Figure A125 Benthic Percent Abundance by Family Level at PD1 .



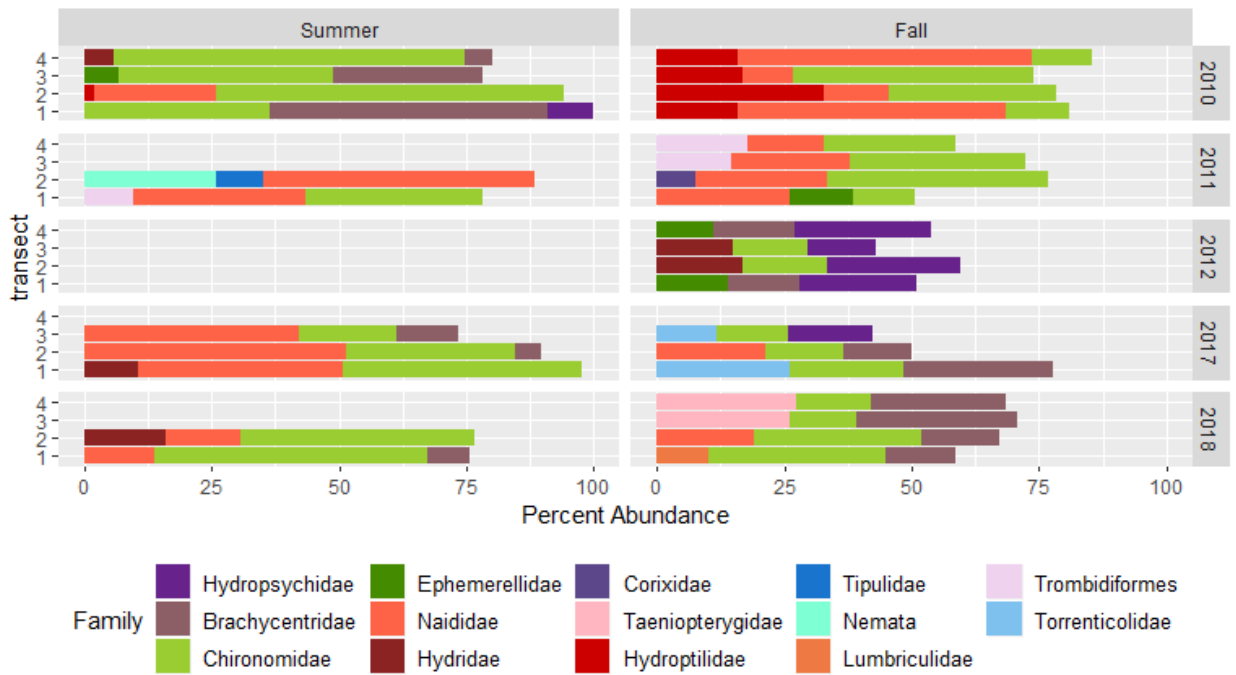


Figure A126 Benthic Percent Abundance by Family Level at PD2 .

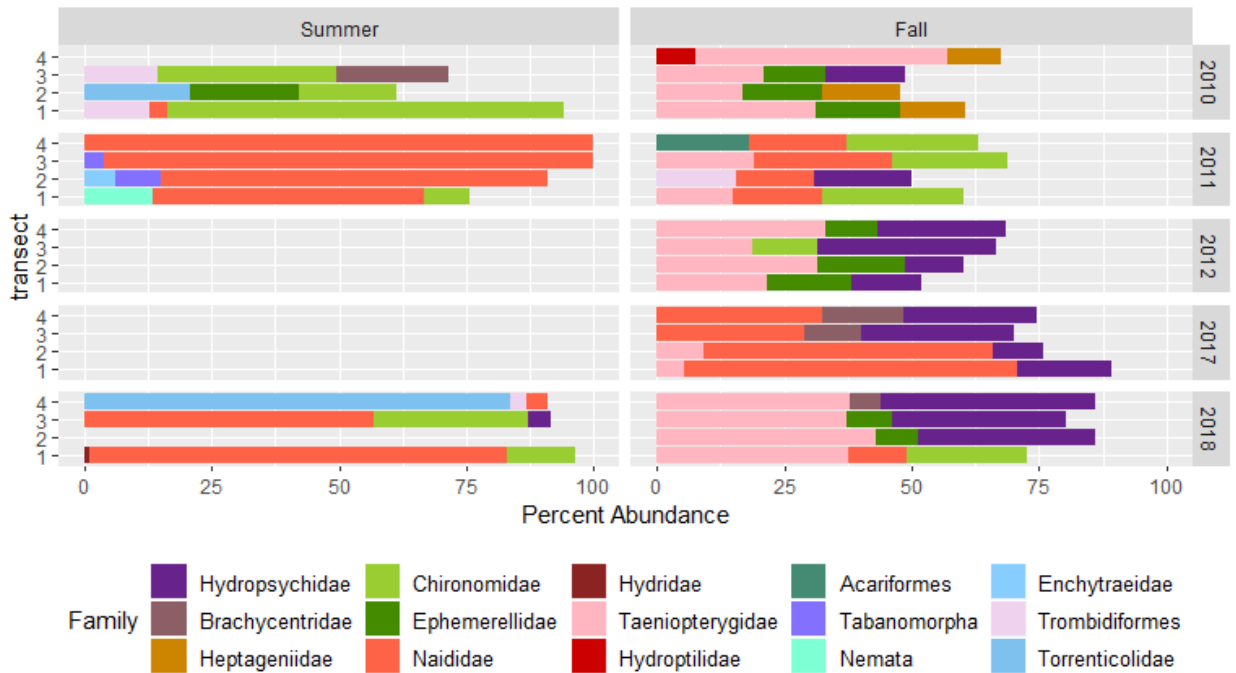


Figure A127 Benthic Percent Abundance by Family Level at PD3 .



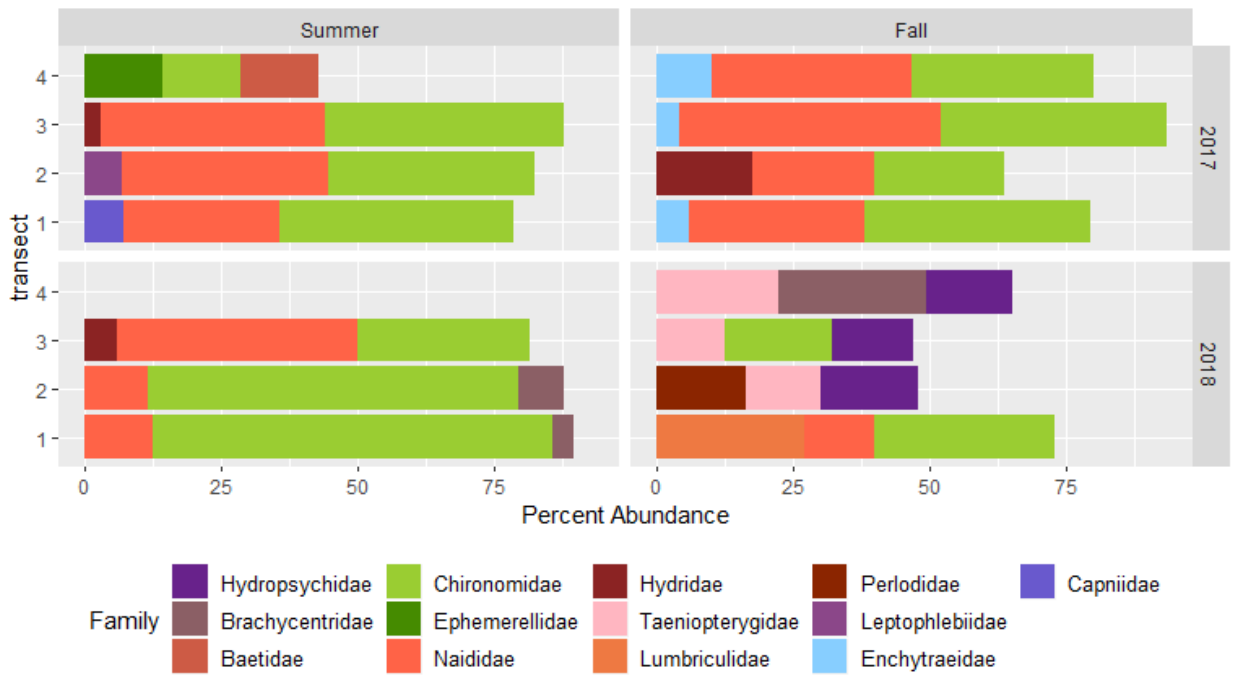


Figure A128 Benthic Percent Abundance by Family Level at PD4 .

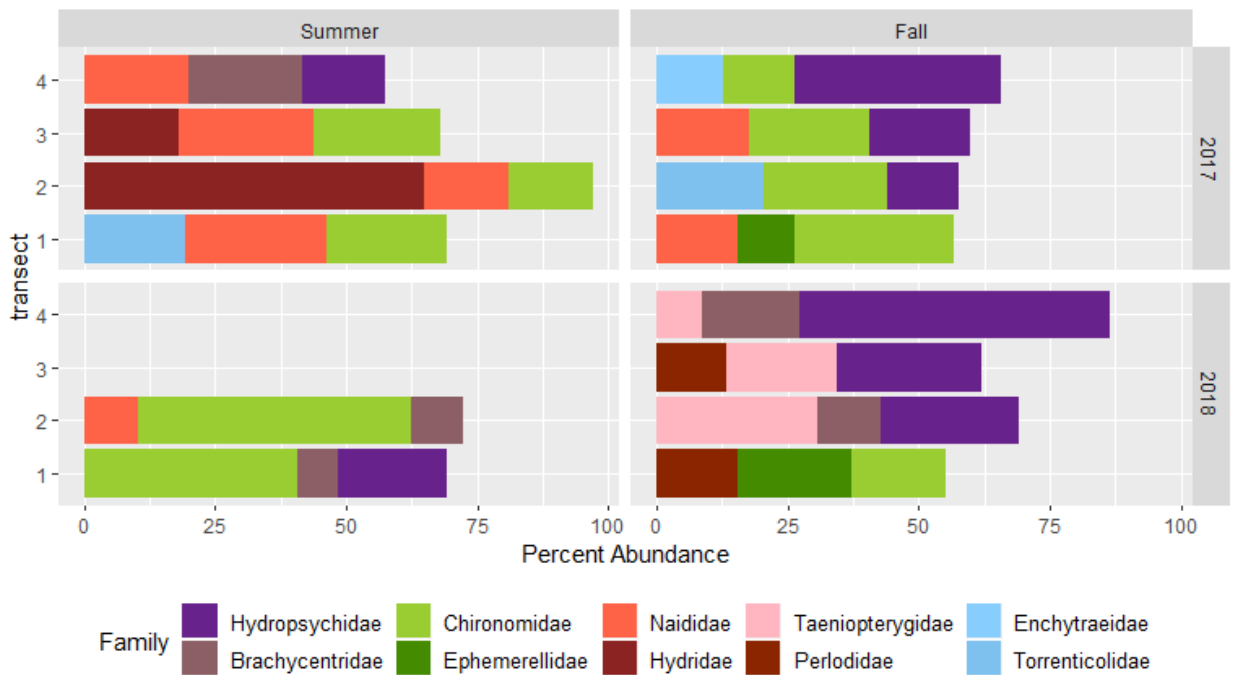


Figure A129 Benthic Percent Abundance by Family Level at PD5 .



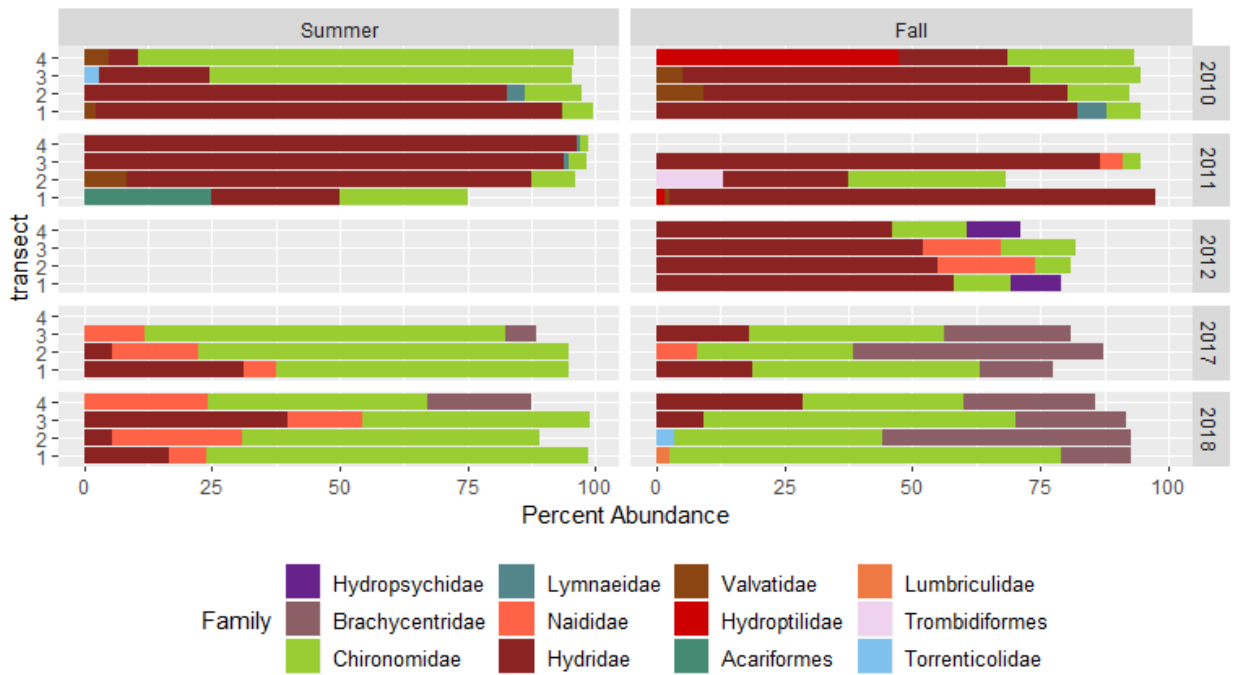


Figure A130 Benthic Percent Abundance by Family Level at PR1 .

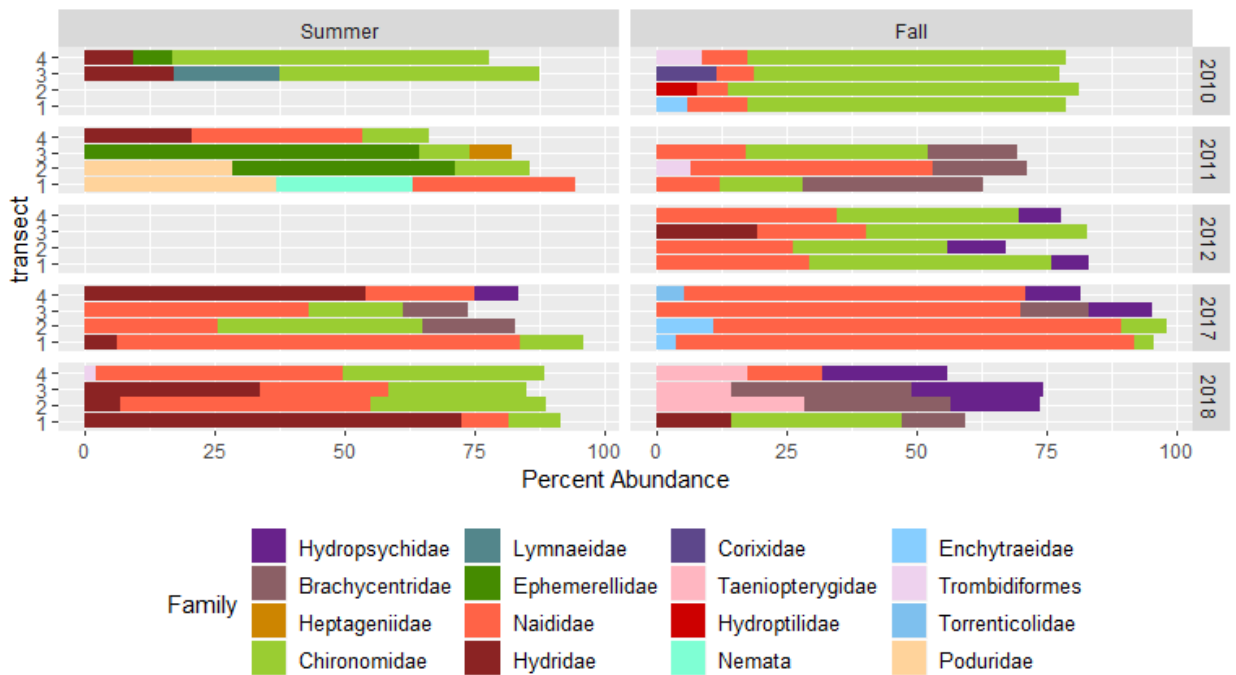


Figure A131 Benthic Percent Abundance by Family Level at PR2 .



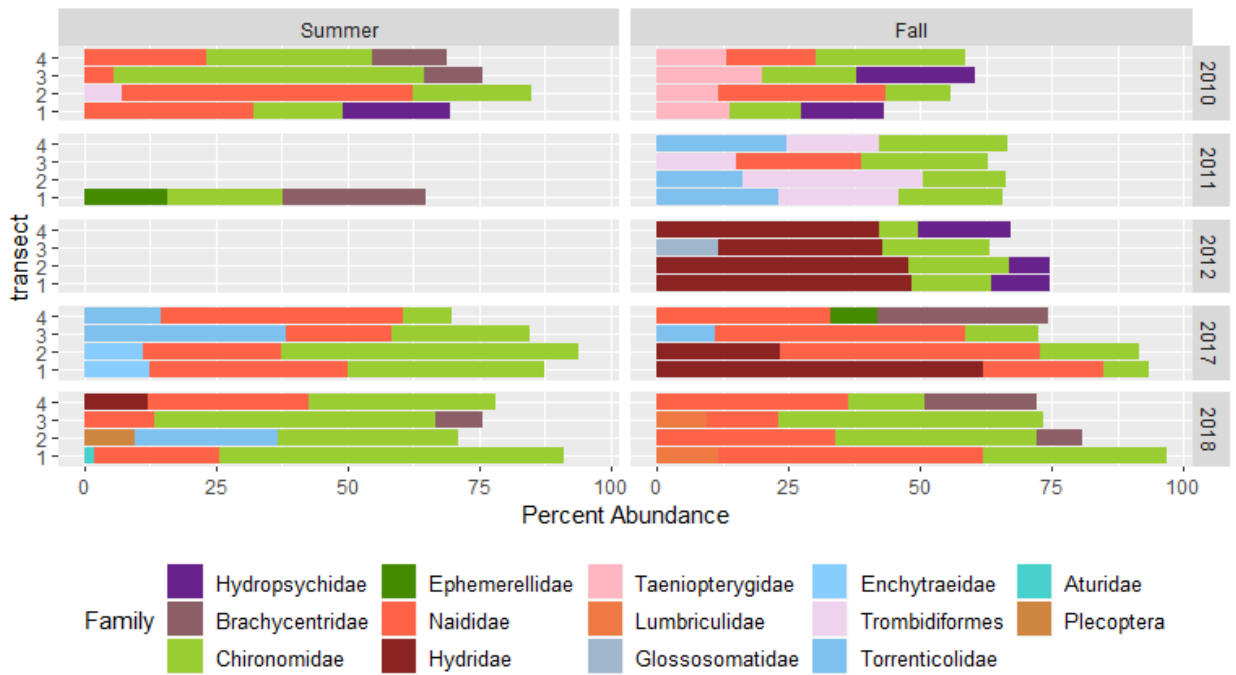


Figure A132 Benthic Percent Abundance by Family Level at PR3 .

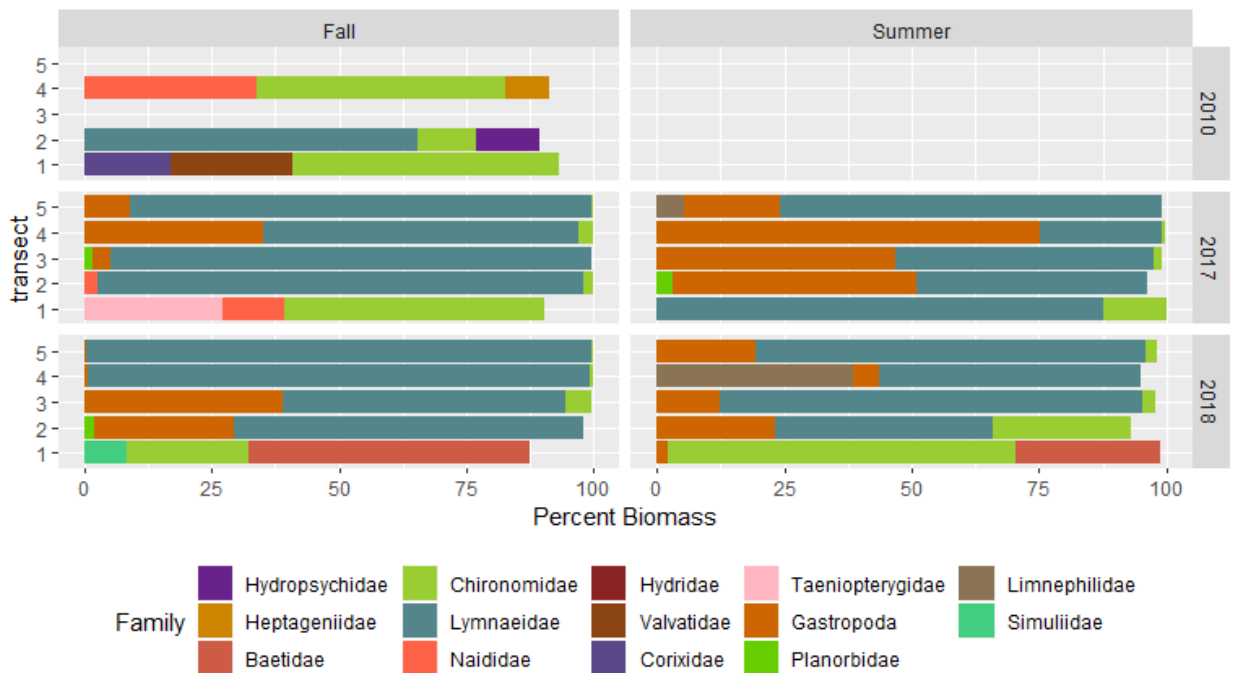


Figure A133 Benthic Percent Total Biomass by Family Level at D1 .



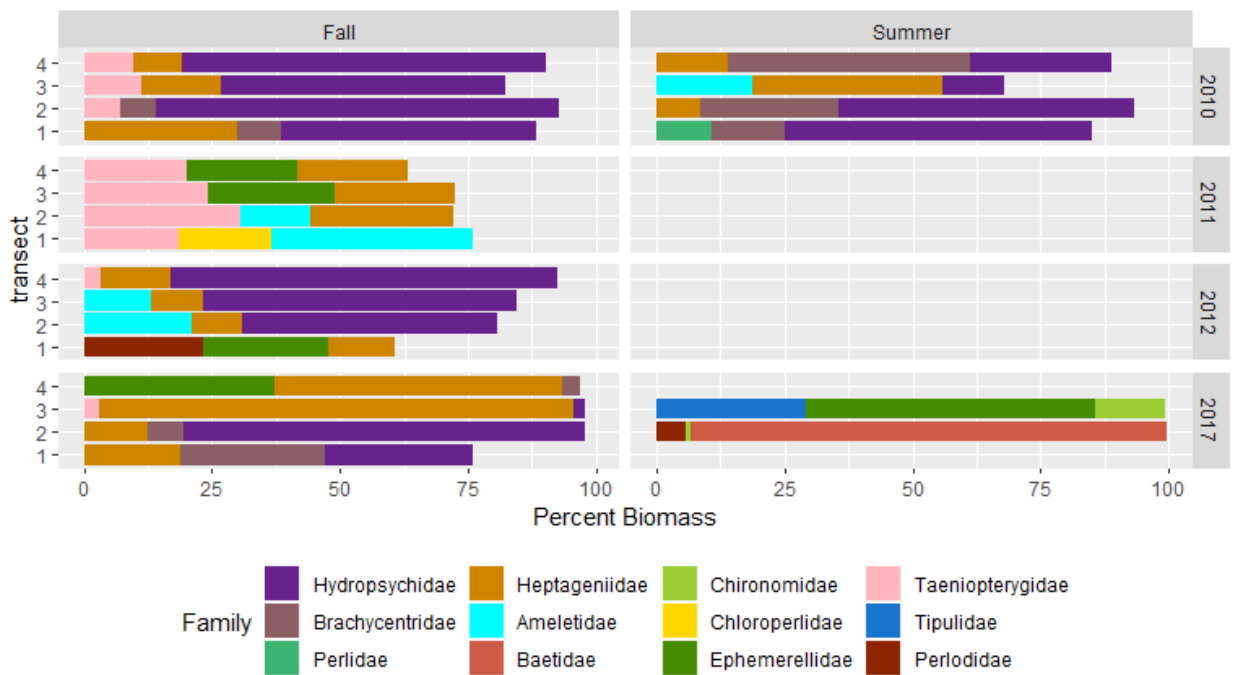


Figure A134 Benthic Percent Total Biomass by Family Level at HD .

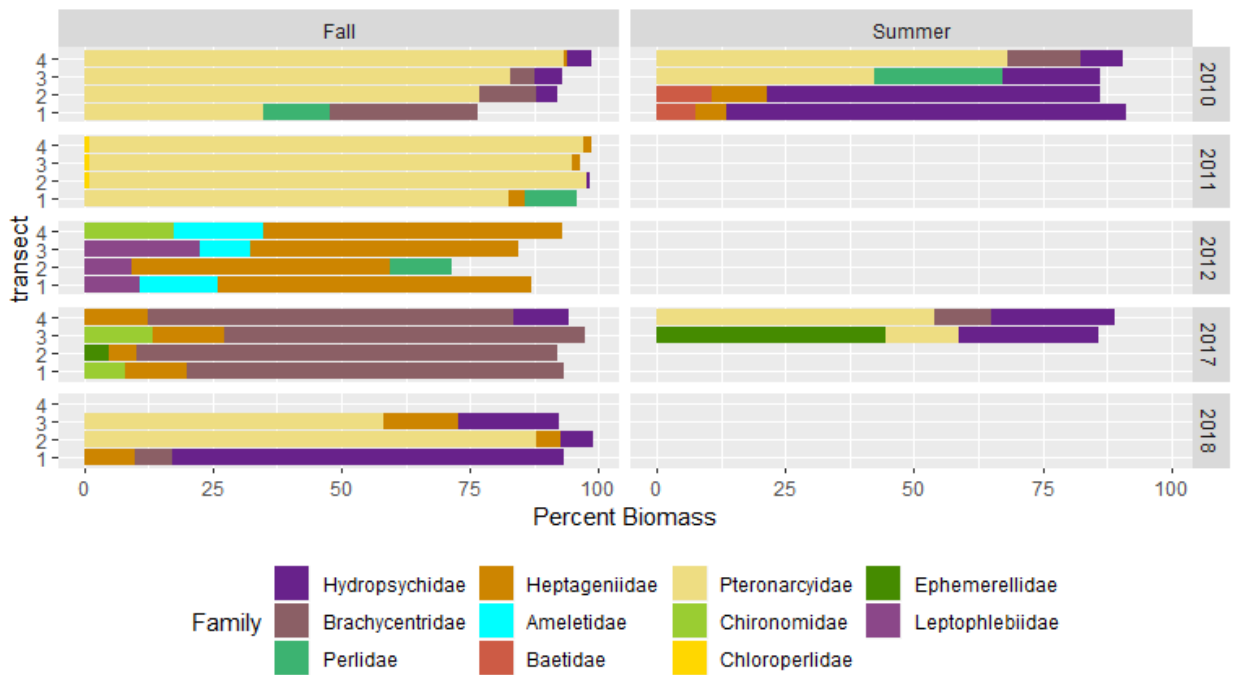


Figure A135 Benthic Percent Total Biomass by Family Level at MD .



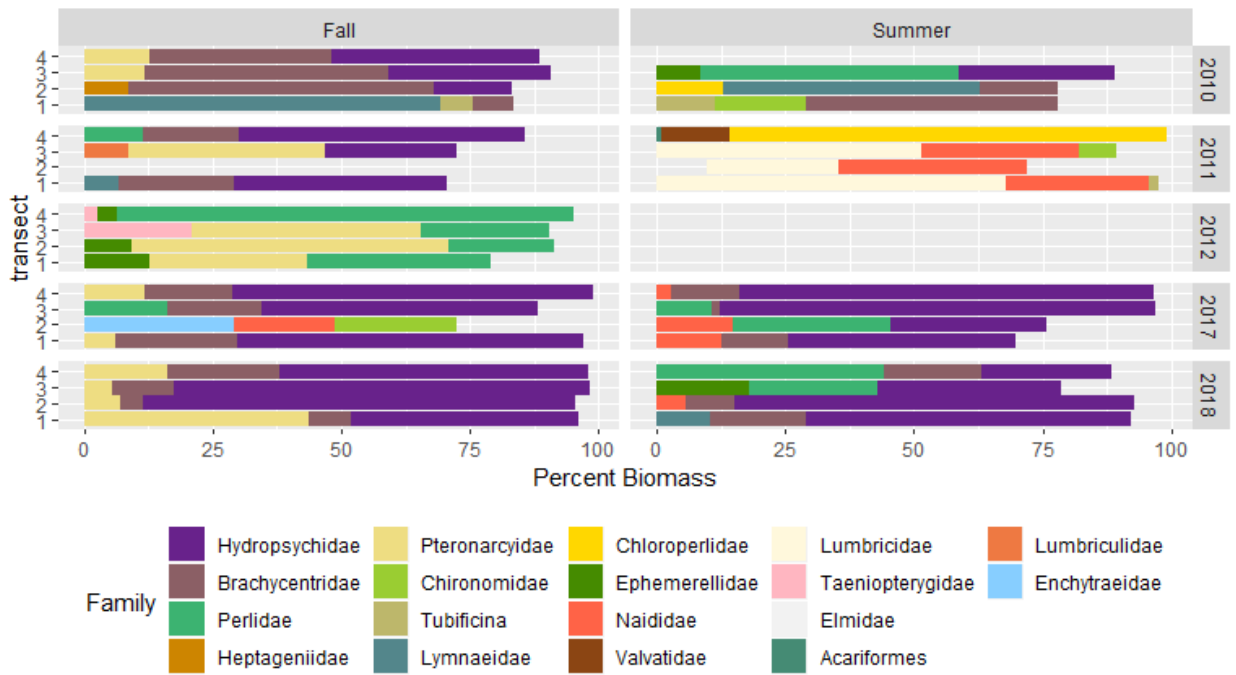


Figure A136 Benthic Percent Total Biomass by Family Level at PD1 .

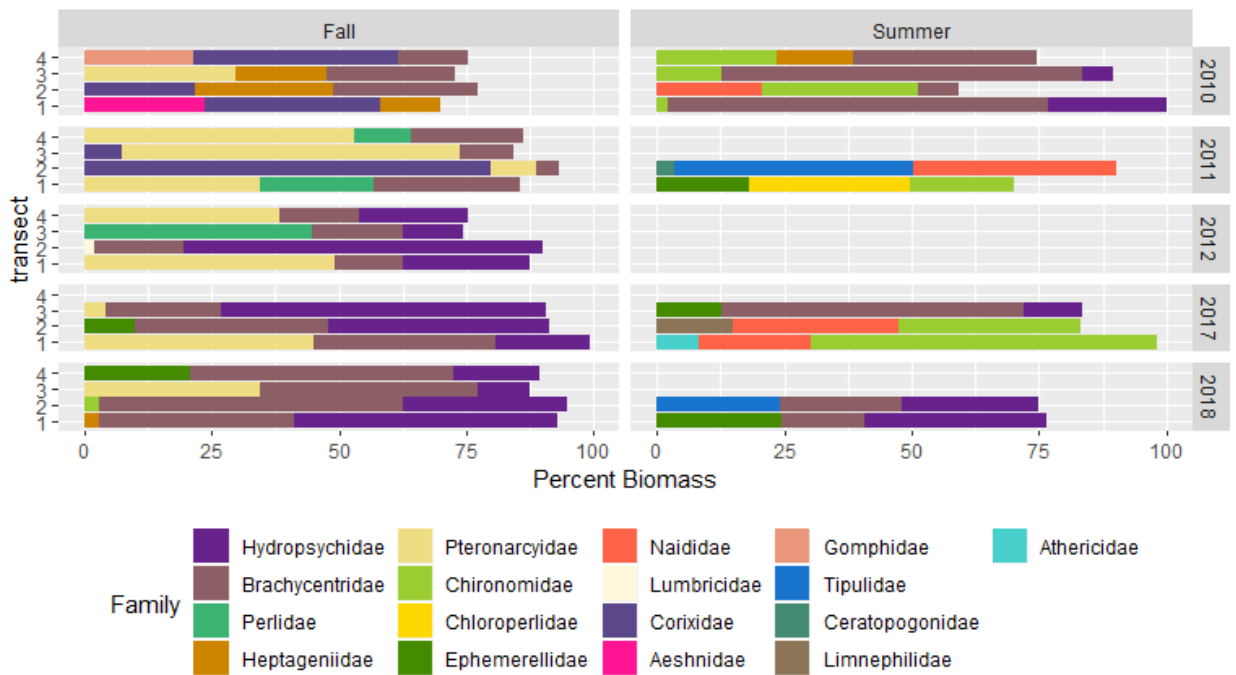


Figure A137 Benthic Percent Total Biomass by Family Level at PD2 .



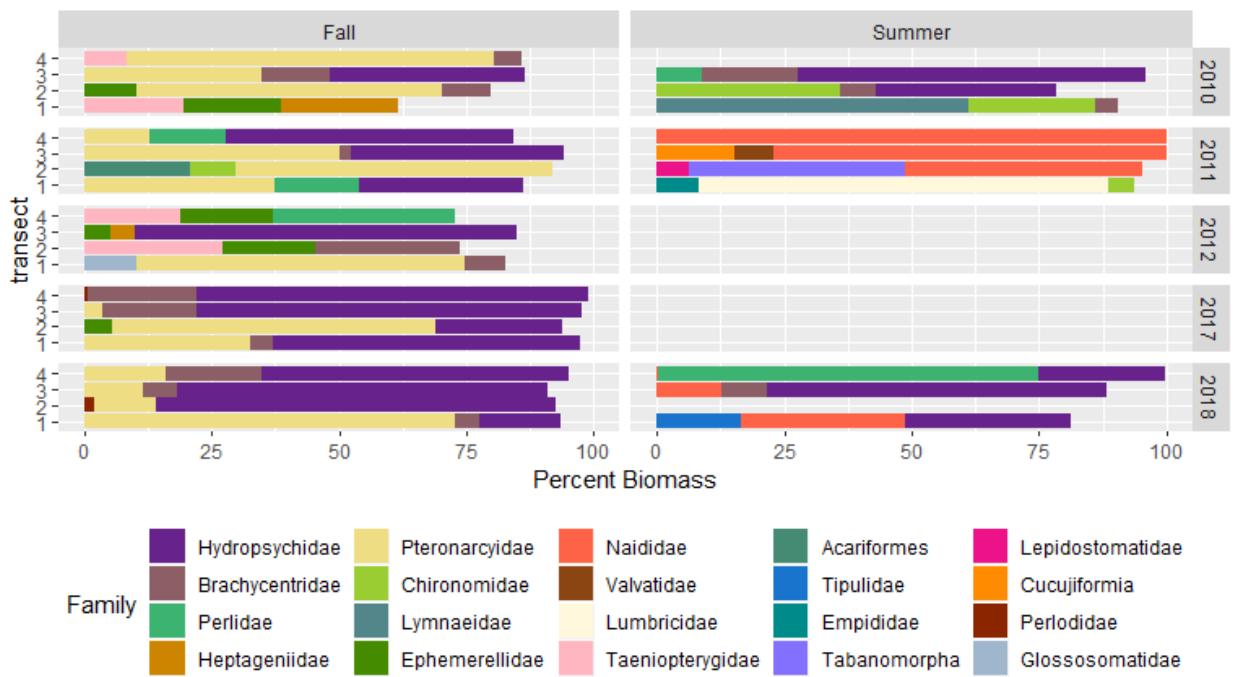


Figure A138 Benthic Percent Total Biomass by Family Level at PD3 .

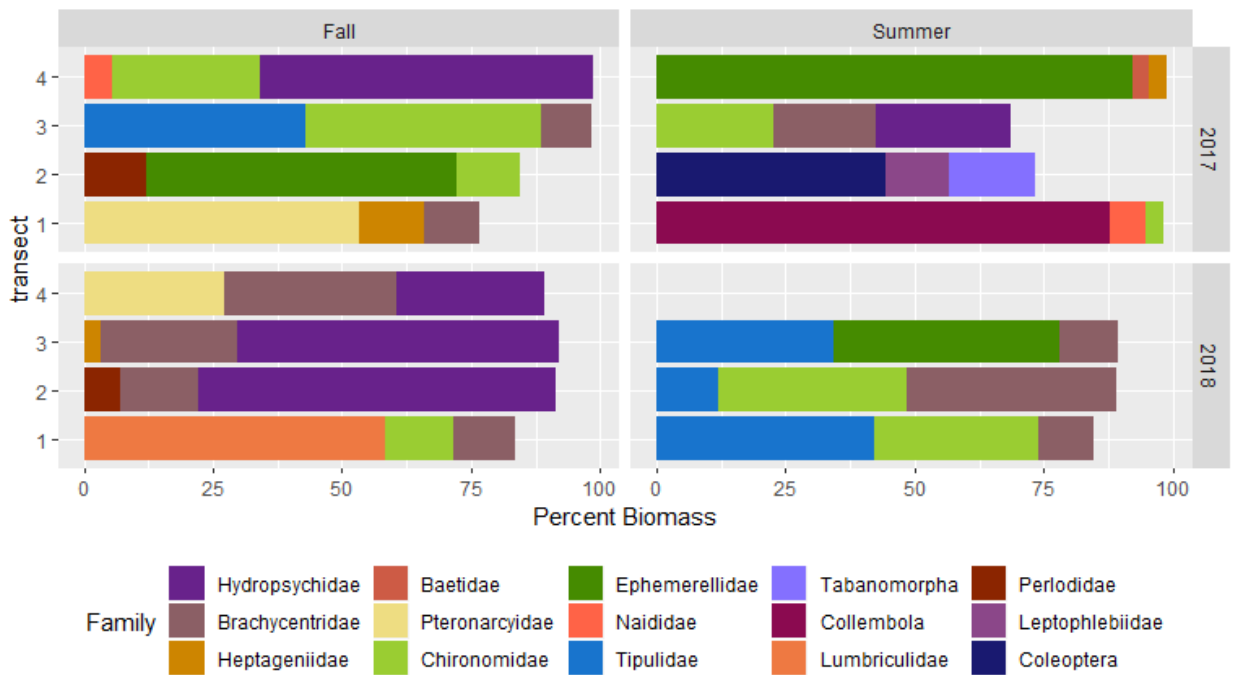


Figure A139 Benthic Percent Total Biomass by Family Level at PD4 .



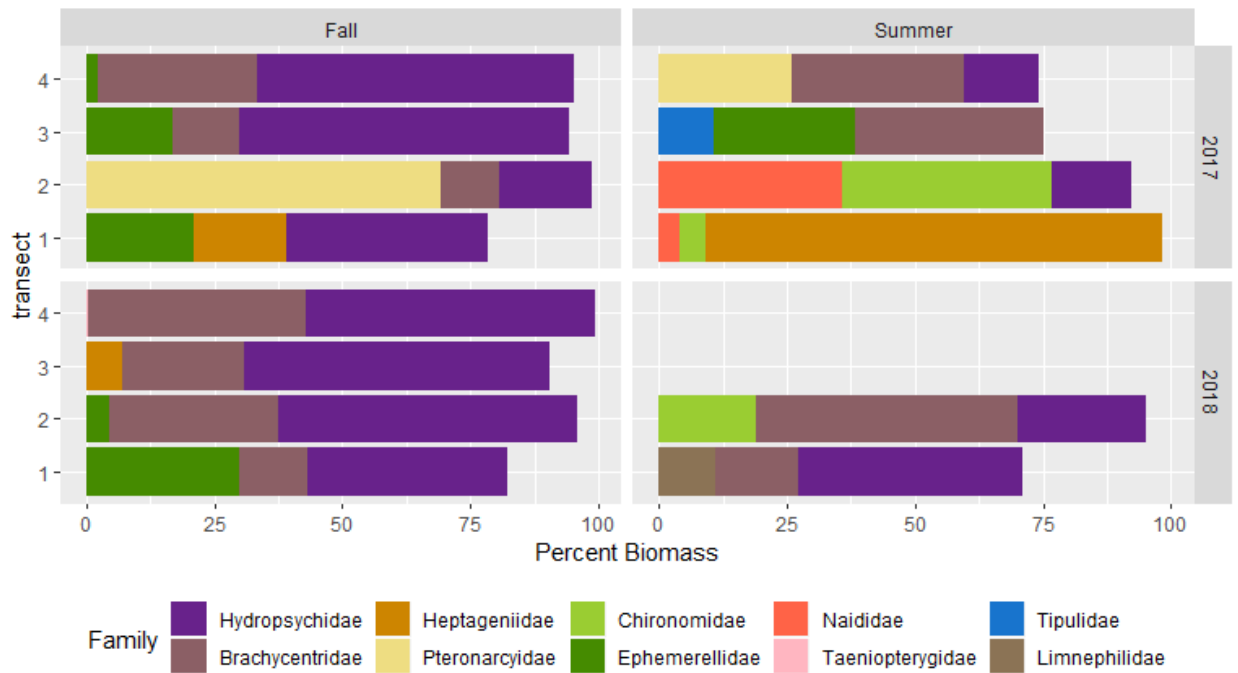


Figure A140 Benthic Percent Total Biomass by Family Level at PD5 .

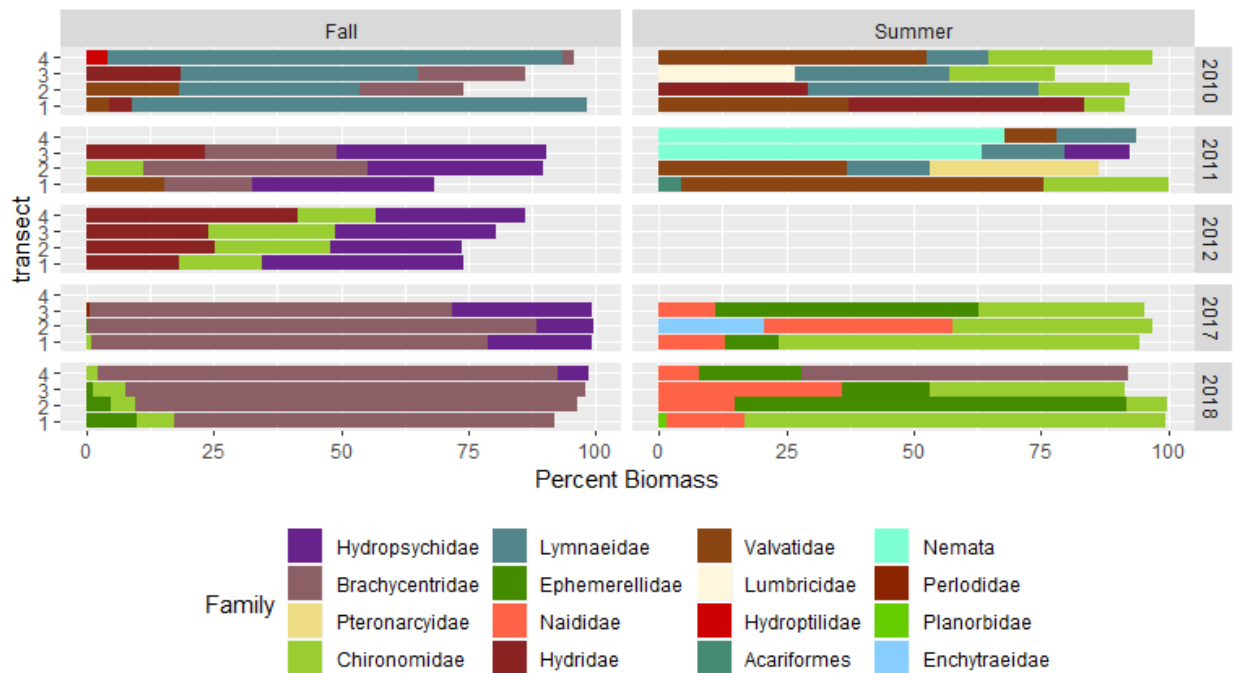


Figure A141 Benthic Percent Total Biomass by Family Level at PR1 .



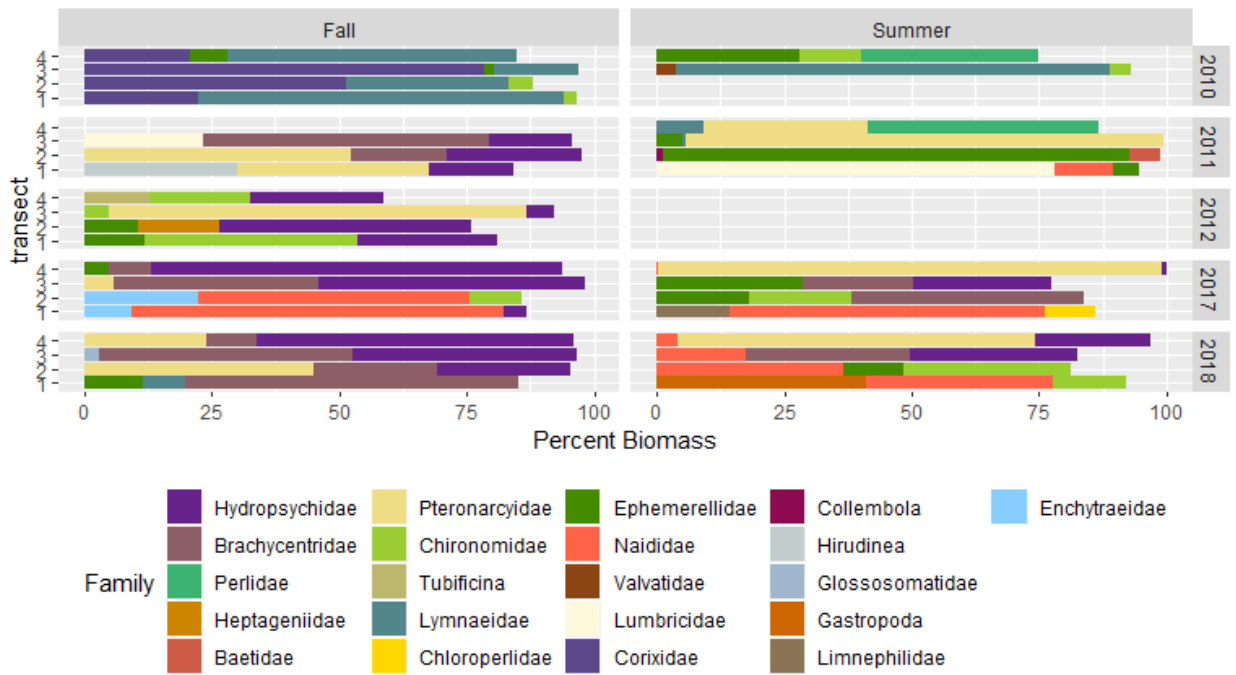


Figure A142 Benthic Percent Total Biomass by Family Level at PR2 .

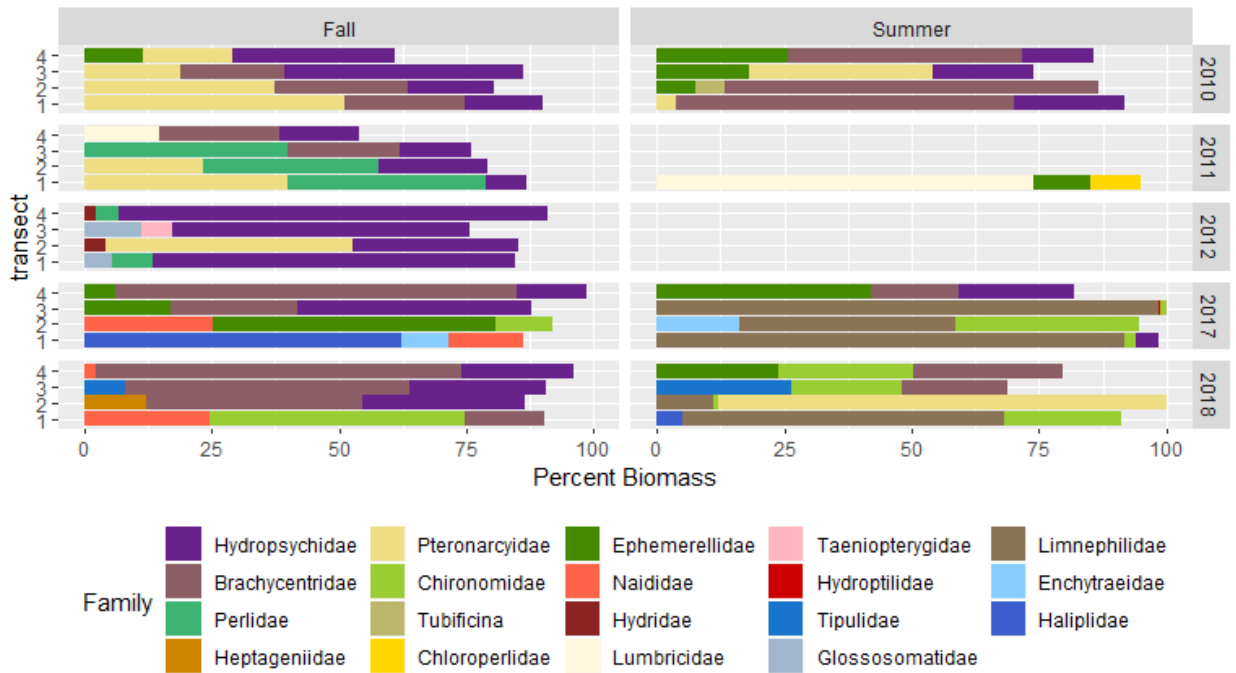


Figure A143 Benthic Percent Total Biomass by Family Level at PR3 .



Appendix S Periphyton Community Analysis using NMDS

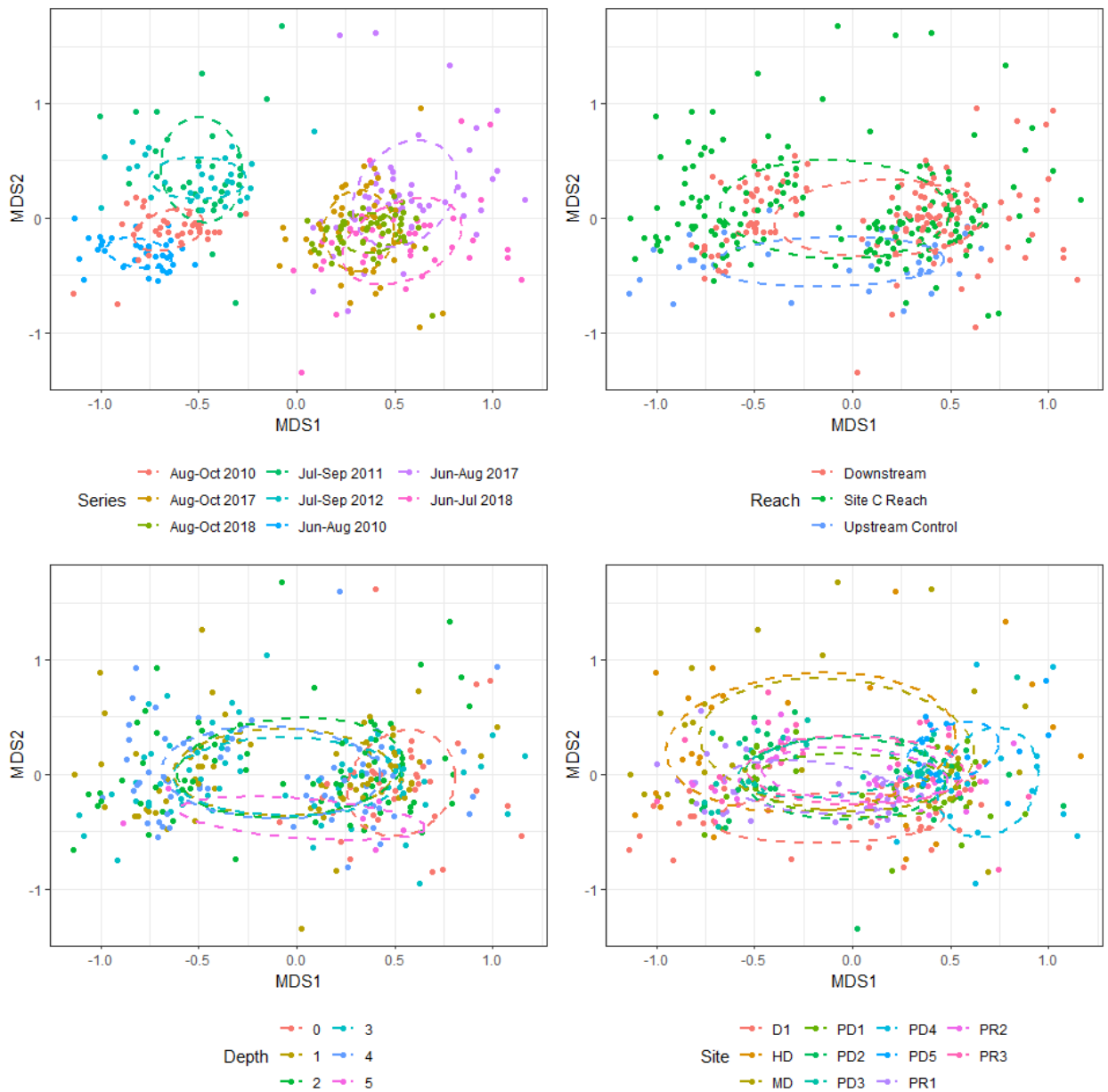


Figure A144 NMDS plots of periphyton (at Genus level) sampled in upstream reservoirs, Site C Reach, and downstream areas with a stress index of 0.2 . Data is considered by Reach, Site, Depth, and Series.



Table A11 PERMANOVA results for periphyton at Genus level.

group	R_stat	Fstat	p_val
series	0.320	21.120	<0.001
reach	0.030	4.990	<0.001
depth	0.010	2.200	0.021
site	0.120	4.410	<0.001

Table A12 Taxa scores for NMDS axes with p-value and R2.

Species	NMDS1	NMDS2	pval	r2
Achnanthydium	-0.310	-0.190	0.000	0.130
Anabaena	-0.320	0.100	0.000	0.110
Ankistrodesmus	-0.420	0.170	0.000	0.210
Asterionella	-0.300	-0.100	0.000	0.100
Chilomonas	-0.360	0.210	0.000	0.170
Chroomonas	-0.460	-0.120	0.000	0.220
Cryptomonas	-0.340	0.240	0.000	0.170
Encyonema	-0.360	0.150	0.000	0.150
Eucoconeis	-0.360	-0.280	0.000	0.200
Eunotia	-0.370	0.140	0.000	0.150
Heteroleibleinia	0.390	-0.270	0.000	0.230
Peridinium	-0.290	-0.200	0.000	0.120
Pseudanabaena	-0.410	0.150	0.000	0.190
Staurisira	-0.380	-0.120	0.000	0.150
Synechocystis	0.220	-0.230	0.000	0.100
Synedra	-0.360	-0.030	0.000	0.130



Appendix T Invertebrate Community Analysis from Rock baskets using NMDS

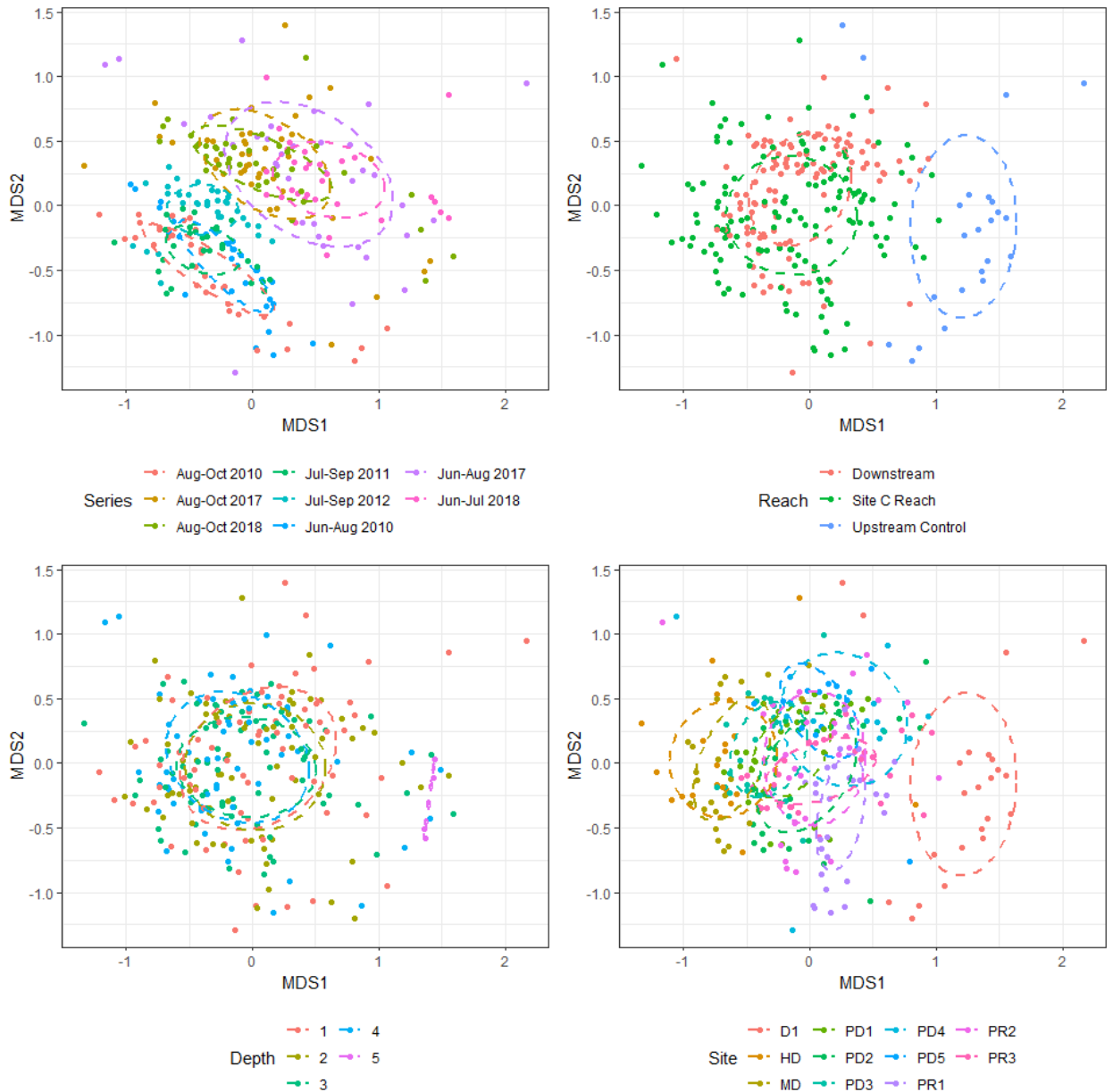


Figure A145 NMDS plots of benthic invertebrates (at Genus level) sampled using baskets in upstream reservoirs, Site C Reach, and downstream areas with a stress index of 0.23 . Data is considered by Reach, Site, Depth, and Series.



Table A13 PERMANOVA results for benthic invertebrates basket samplers at Genus level.

group	R_stat	Fstat	p_val
series	0.170	7.620	<0.001
reach	0.070	9.470	<0.001
depth	0.020	1.550	0.002
site	0.190	6.020	<0.001

Table A14 Taxa scores for NMDS axes with p-value and R2.

Species	NMDS1	NMDS2	pval	r2
Capniidae	-0.290	-0.140	0.000	0.100
Gastropoda	0.400	-0.080	0.000	0.160
Pteronarcys	-0.330	-0.040	0.000	0.110
Rhithrogena	-0.370	-0.150	0.000	0.160
Taenionema	-0.330	-0.060	0.000	0.110
Tanypodinae	-0.060	-0.360	0.000	0.130
Tanytarsini	-0.080	-0.410	0.000	0.180



Appendix U Invertebrate Community Analysis in Eckman Dredge using NMDS Invertebrate Results

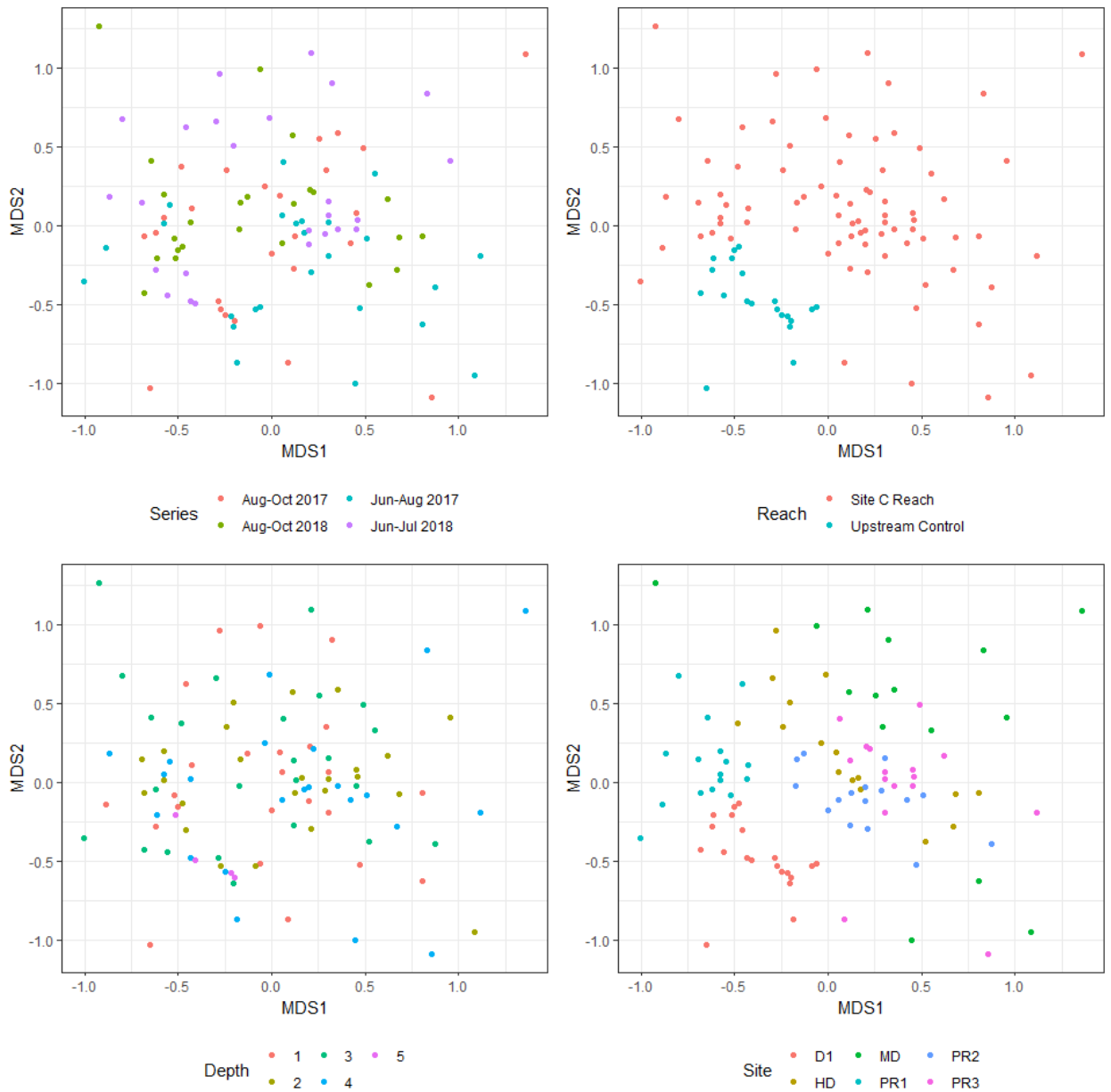


Figure A146 NMDS plots of benthic invertebrate (at Genus level) Ekman samples in upstream reservoirs and Site C Reach with a stress index of 0.24 . Data is considered by Reach, Site, Depth, and Series.



Table A15 PERMANOVA results for Ekman benthic invertebrates at Genus level.

group	R_stat	Fstat	p_val
series	0.080	2.700	<0.001
reach	0.070	6.820	<0.001
depth	0.040	0.870	0.722
site	0.220	5.220	<0.001

Table A16 Taxa scores for NMDS axes with p-value and R2.

Species	NMDS1	NMDS2	pval	r2
Dolichopodidae	-0.170	0.330	0.000	0.140
Empididae	-0.150	-0.310	0.000	0.120
Gastropoda	-0.380	-0.170	0.000	0.170
Gyraulus	-0.310	-0.140	0.010	0.110
Heterotrissocladius	-0.110	-0.320	0.000	0.120
Micropsectra	-0.270	-0.170	0.010	0.100
Physidae	-0.320	-0.120	0.000	0.120
Pisidiidae	-0.390	-0.110	0.000	0.160
Pisidium	-0.440	-0.160	0.000	0.220
Procladius	-0.370	-0.230	0.000	0.190
Protanypus	-0.080	-0.310	0.010	0.100
Tanytarsus	-0.140	-0.340	0.000	0.130
Valvata	-0.380	-0.090	0.000	0.150



Appendix V Ekman Samples Invertebrate Dominant Taxa by Family

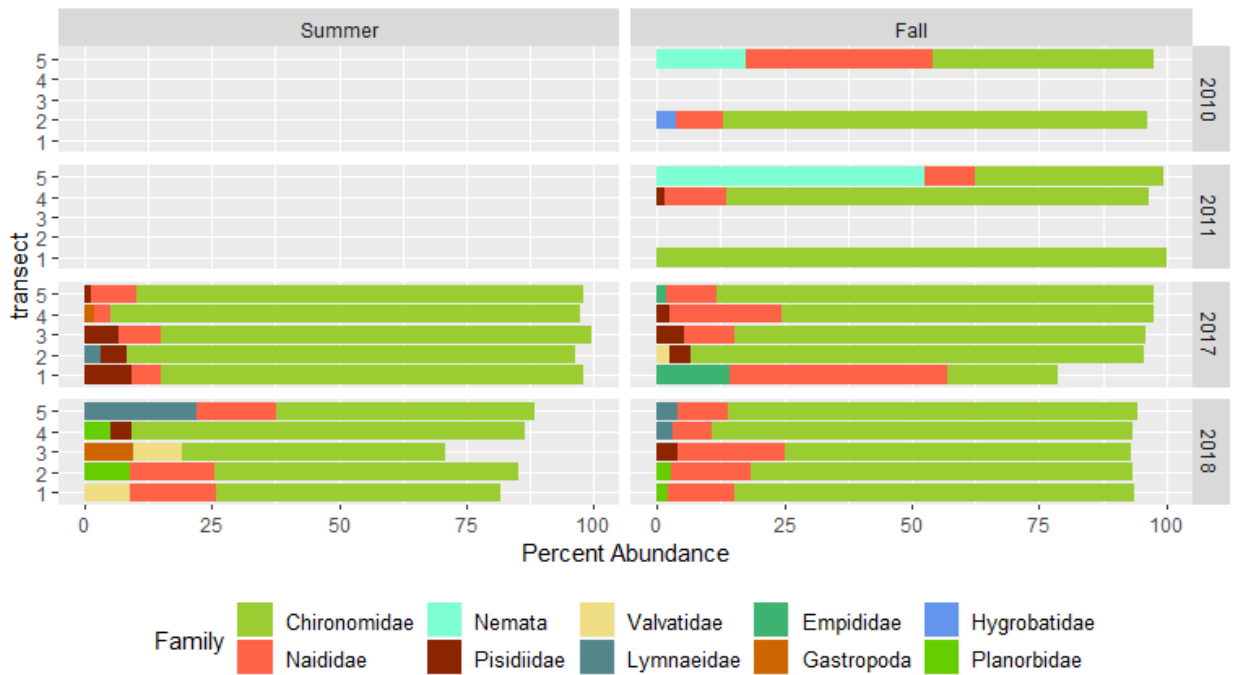


Figure A147 Benthic Percent Abundance by Family Level at D1 for Ekman Samples.

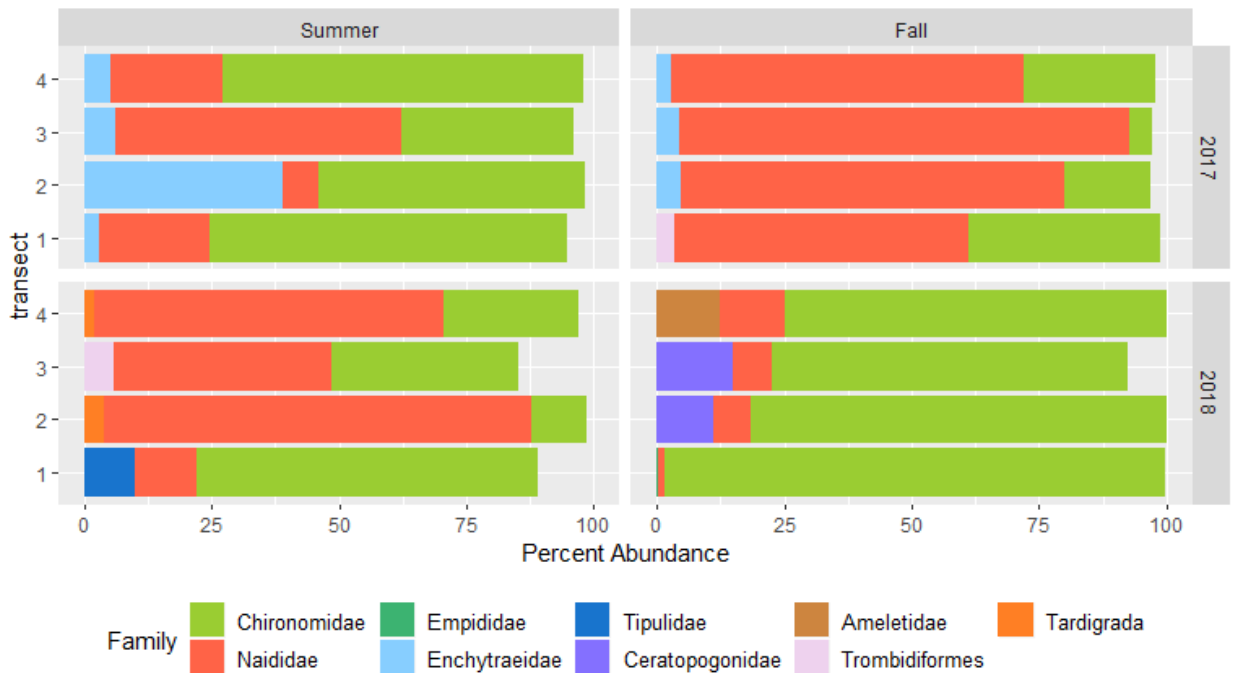


Figure A148 Benthic Percent Abundance by Family Level at HD for Ekman Samples.



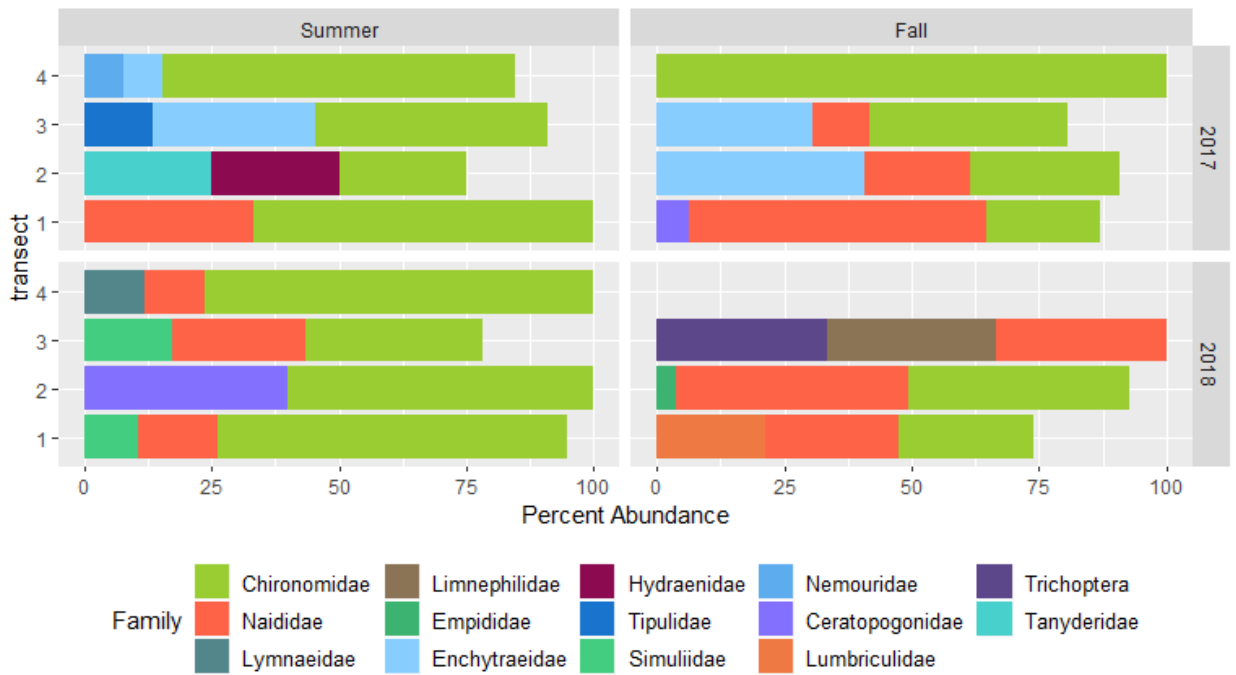


Figure A149 Benthic Percent Abundance by Family Level at MD for Ekman Samples.

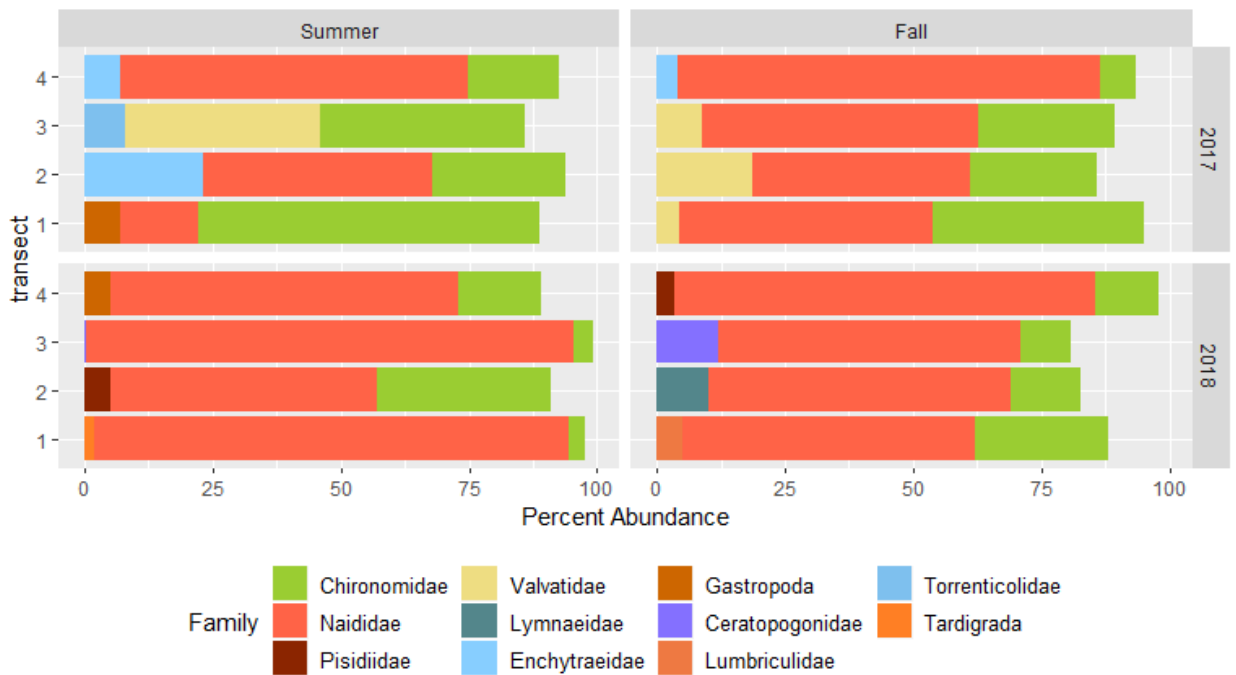


Figure A150 Benthic Percent Abundance by Family Level at PR1 for Ekman Samples.



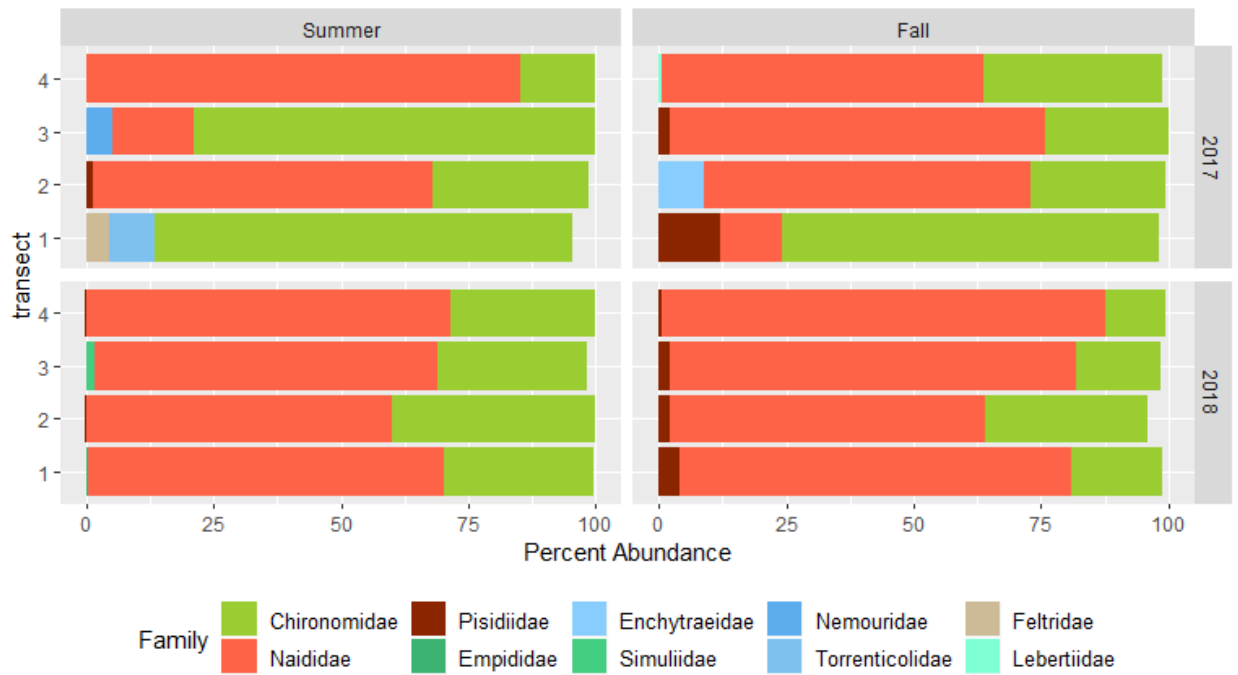


Figure A151 Benthic Percent Abundance by Family Level at PR2 for Ekman Samples.

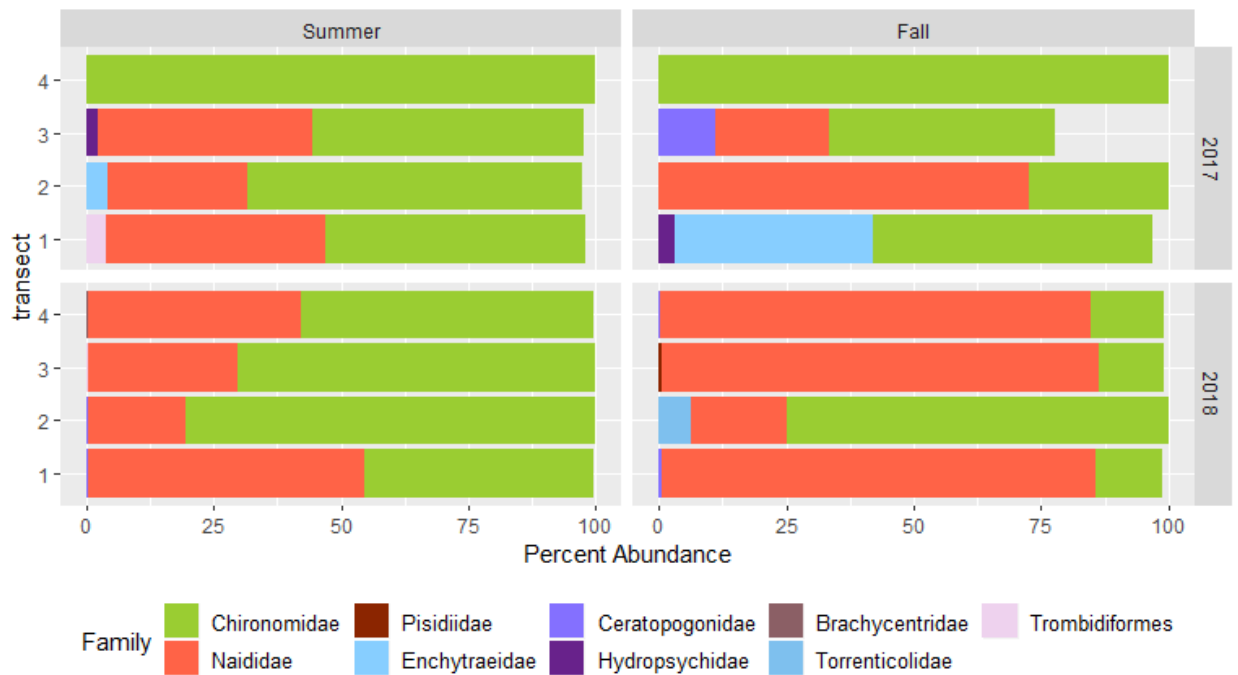


Figure A152 Benthic Percent Abundance by Family Level at PR3 for Ekman Samples.



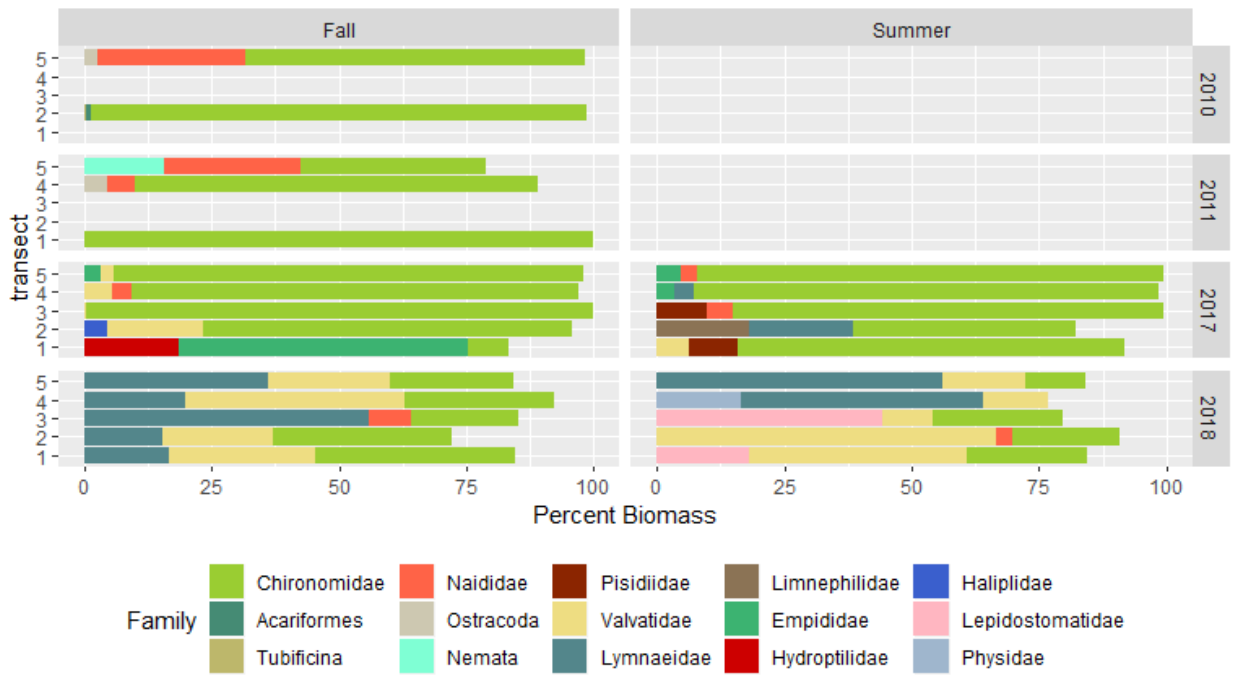


Figure A153 Benthic Percent Total Biomass by Family Level at D1 for Ekman Samples.

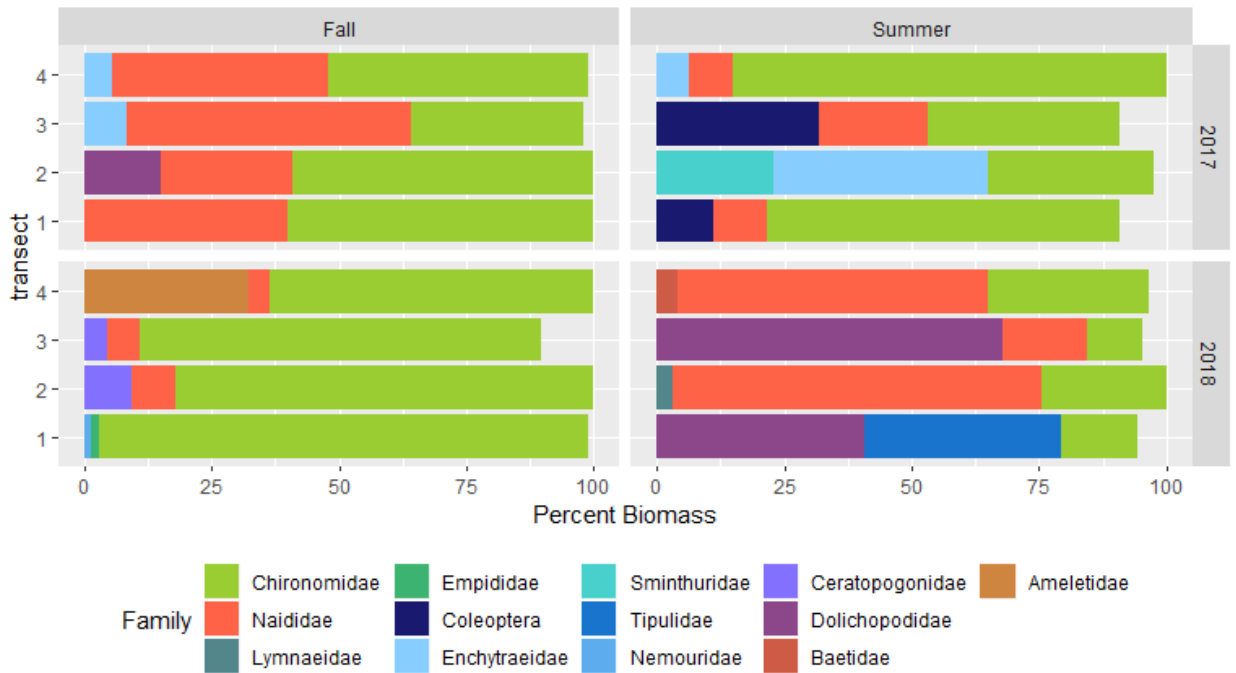


Figure A154 Benthic Percent Total Biomass by Family Level at HD for Ekman Samples.



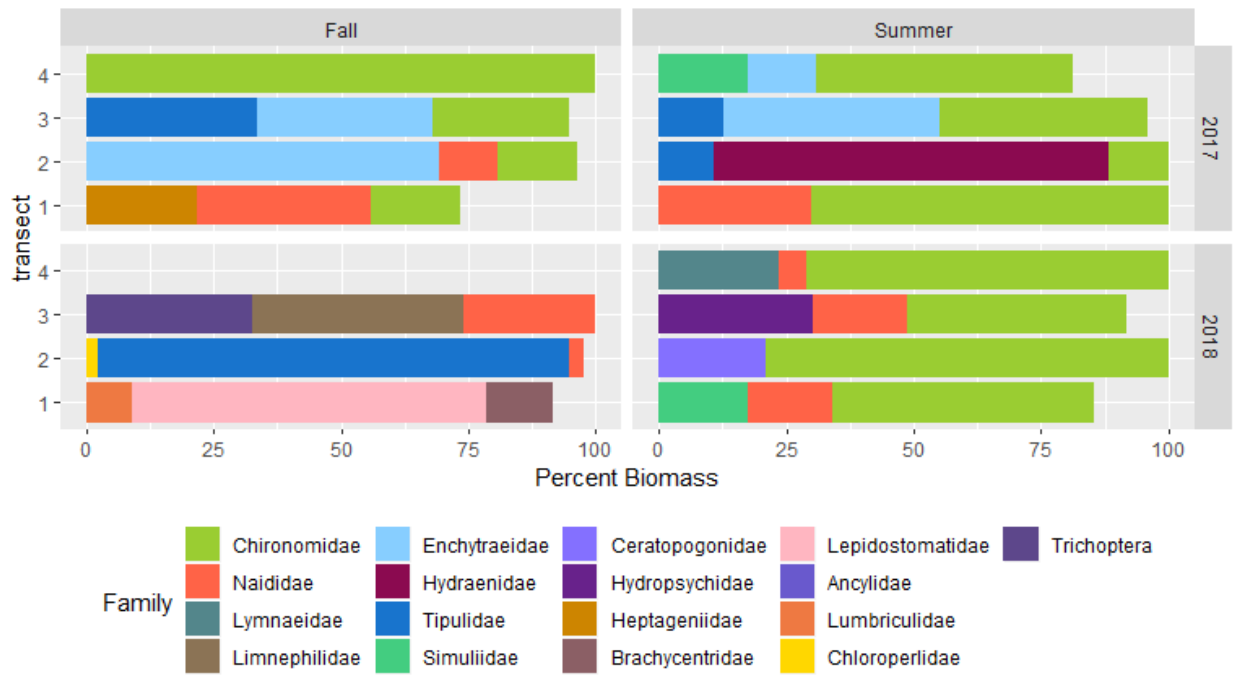


Figure A155 Benthic Percent Total Biomass by Family Level at MD for Ekman Samples.

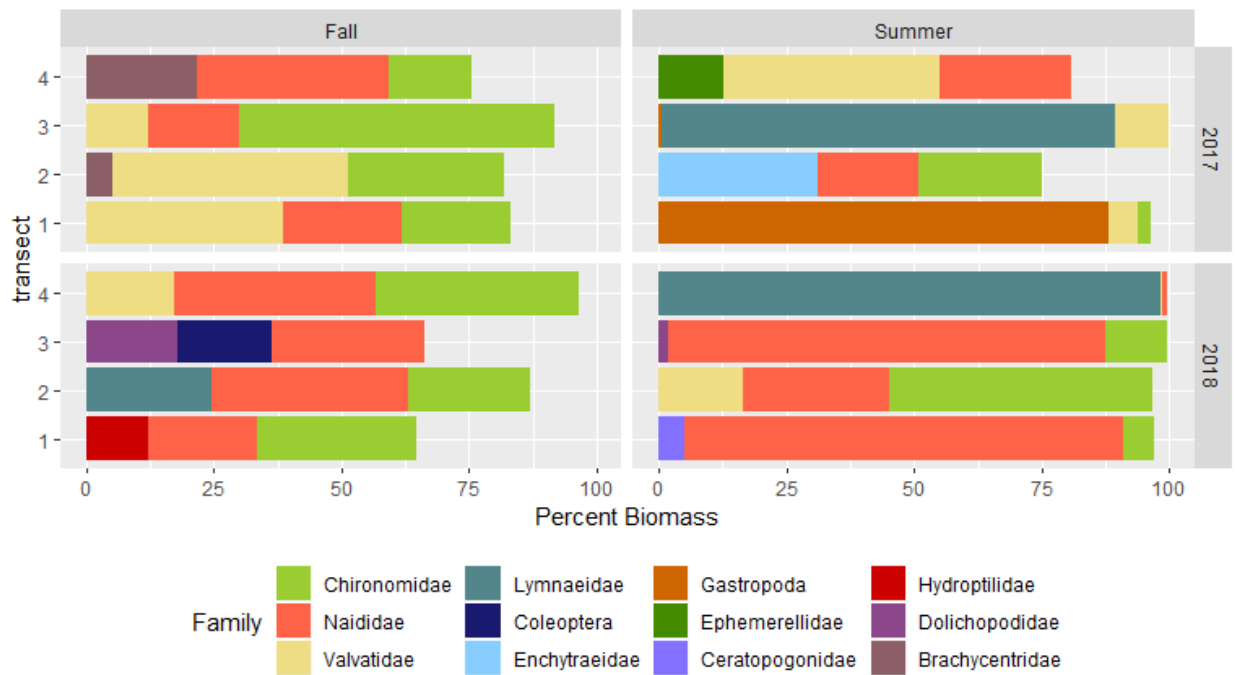


Figure A156 Benthic Percent Total Biomass by Family Level at PR1 for Ekman Samples.



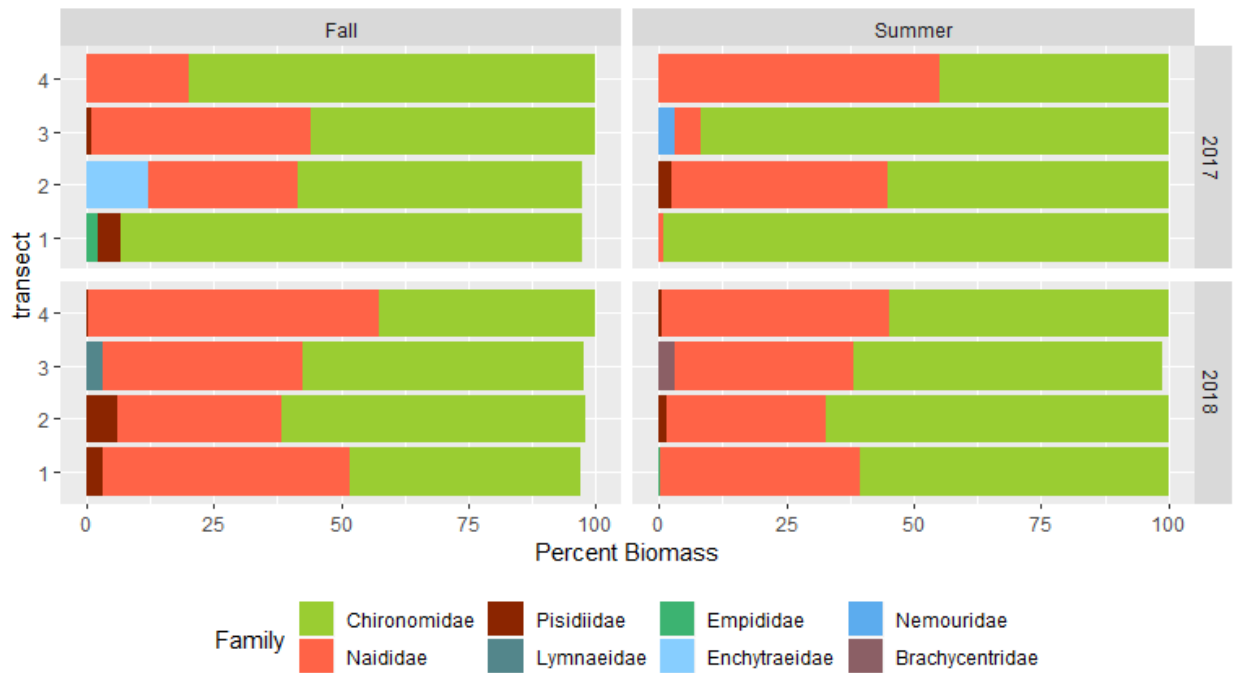


Figure A157 Benthic Percent Total Biomass by Family Level at PR2 for Ekman Samples.

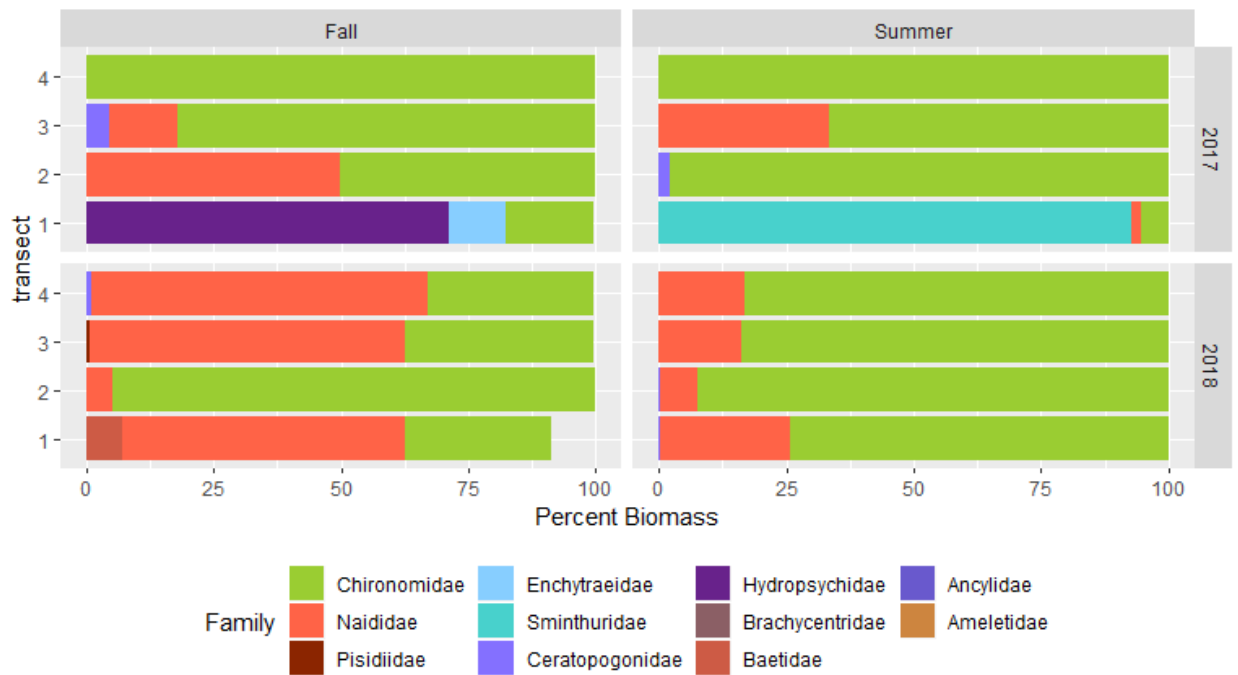


Figure A158 Benthic Percent Total Biomass by Family Level at PR3 for Ekman Samples.



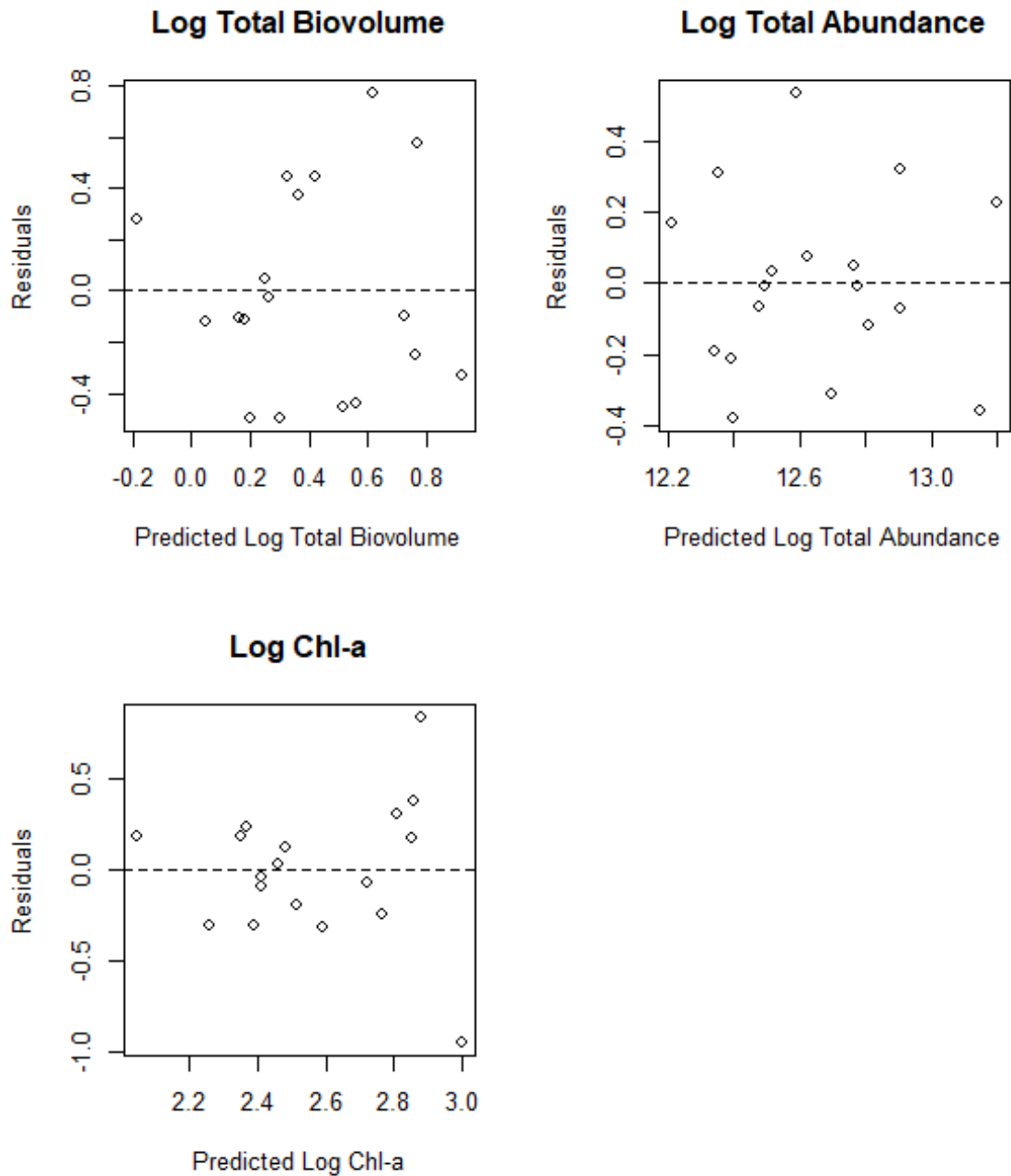
Appendix W Reservoir Periphyton Model Results**Figure A159 Residual Plots for Reservoir Periphyton Models**

Table A17 Summary of plausible periphyton models for Site C Dinosaur Reservoir identified using model averaging (those with a delta AIC <3) with pseudo-R2 values and coefficients.

Response	X.Intercept.	Total Submergence Time (Hours)	Hours over 10 Photons	Mean Temperature Submerged	R.2	df	AICc	delta	weight
Log Chl-a	2.560		0.366	0.428	0.301	4.000	26.400	0.000	0.214
Log Chl-a	2.560				0.000	2.000	26.600	0.167	0.197
Log Chl-a	2.560			0.350	0.147	3.000	26.700	0.216	0.192
Log Chl-a	2.560	0.299		0.370	0.254	4.000	27.600	1.170	0.119
Log Chl-a	2.560		0.275		0.091	3.000	27.800	1.370	0.108
Log Chl-a	2.560	0.275			0.091	3.000	27.800	1.370	0.108
Log Total Abundance	12.600		0.550		0.540	3.000	8.430	0.000	0.682
Log Total Abundance	12.600		0.568	0.084	0.552	4.000	11.300	2.880	0.161
Log Total Biovolume	0.401		0.451	0.439	0.326	4.000	28.200	0.000	0.256
Log Total Biovolume	0.401				0.000	2.000	29.000	0.836	0.168
Log Total Biovolume	0.401		0.357		0.133	3.000	29.400	1.170	0.142
Log Total Biovolume	0.401			0.343	0.123	3.000	29.600	1.380	0.128
Log Total Biovolume	0.401	0.333			0.116	3.000	29.700	1.530	0.119
Log Total Biovolume	0.401	0.357		0.366	0.256	4.000	30.000	1.790	0.105



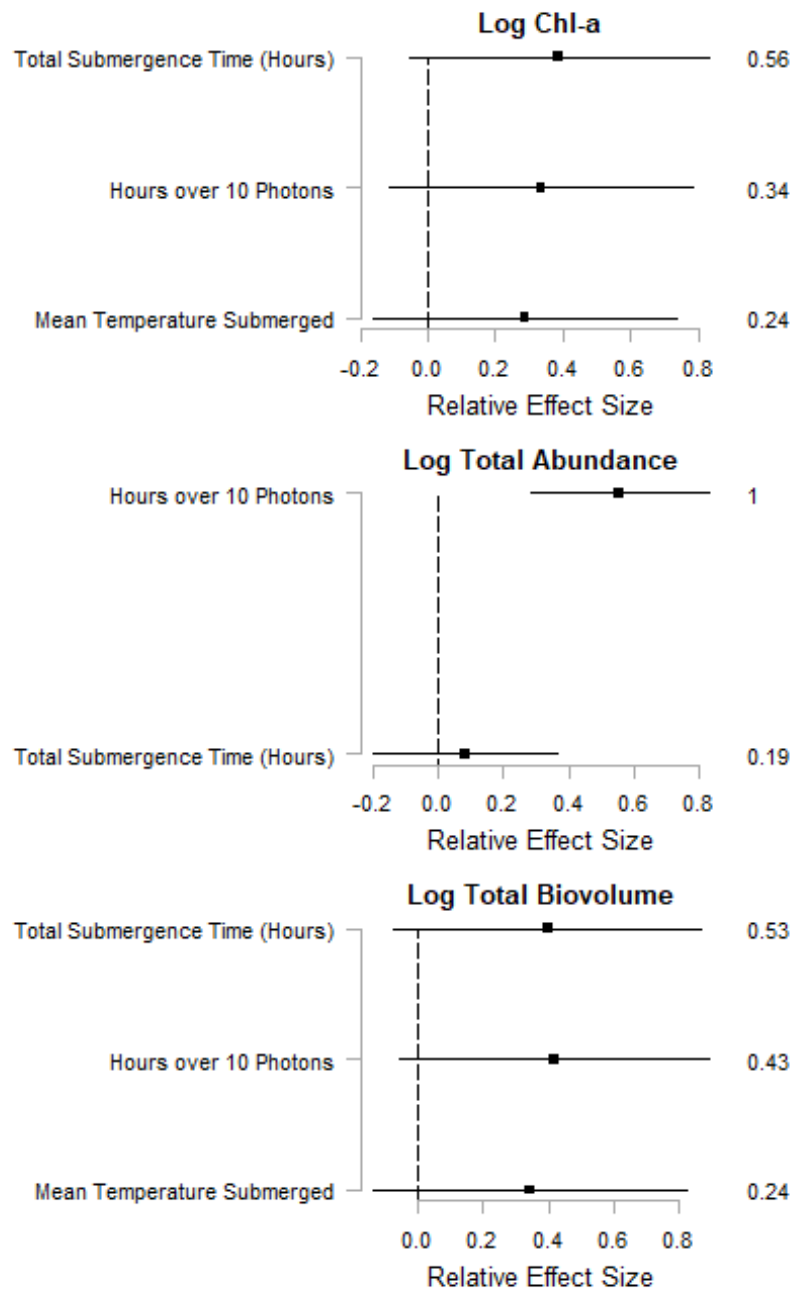


Figure A160 The coefficients and their 95% CLs of standardized explanatory variables of periphyton production in Dinosaur Reservoir. Periphyton responses included abundance, chl-a and biovolume. Explanatory variables included total hours over 10 photons, average water temperature and total submergence time. Coefficients were standardized to allow comparisons of the direction and size of effects, noting that variables with CLs that do not cross zero have an effect on the response variable. Key explanatory variables are those that have a relative variable importance (RVI) of greater than 0.6-0.7 and the RVI is shown on the right-hand side of each figure.



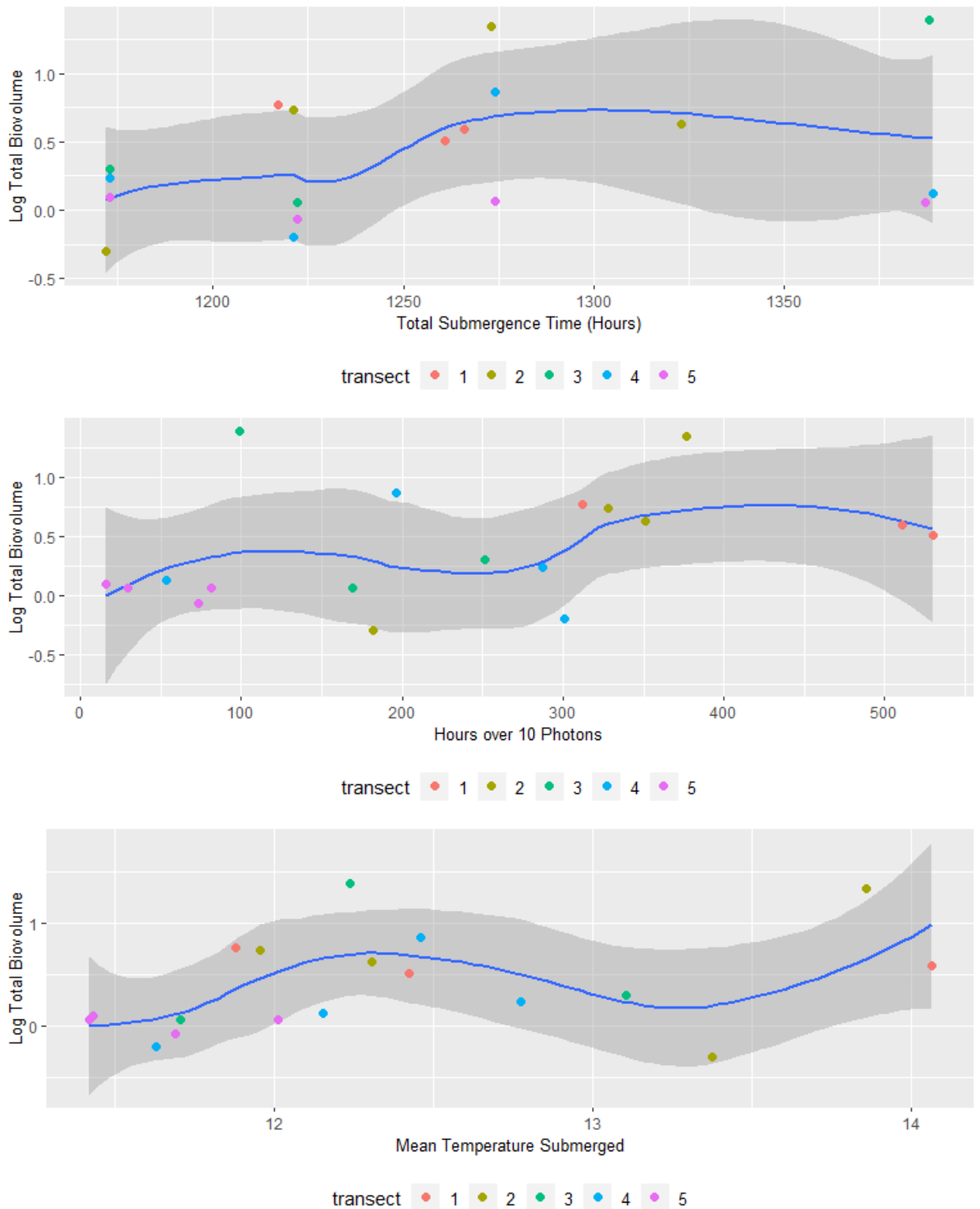


Figure A161 Explanatory variables and Log Total Biovolume grouped by transect for Dinosaur Reservoir.



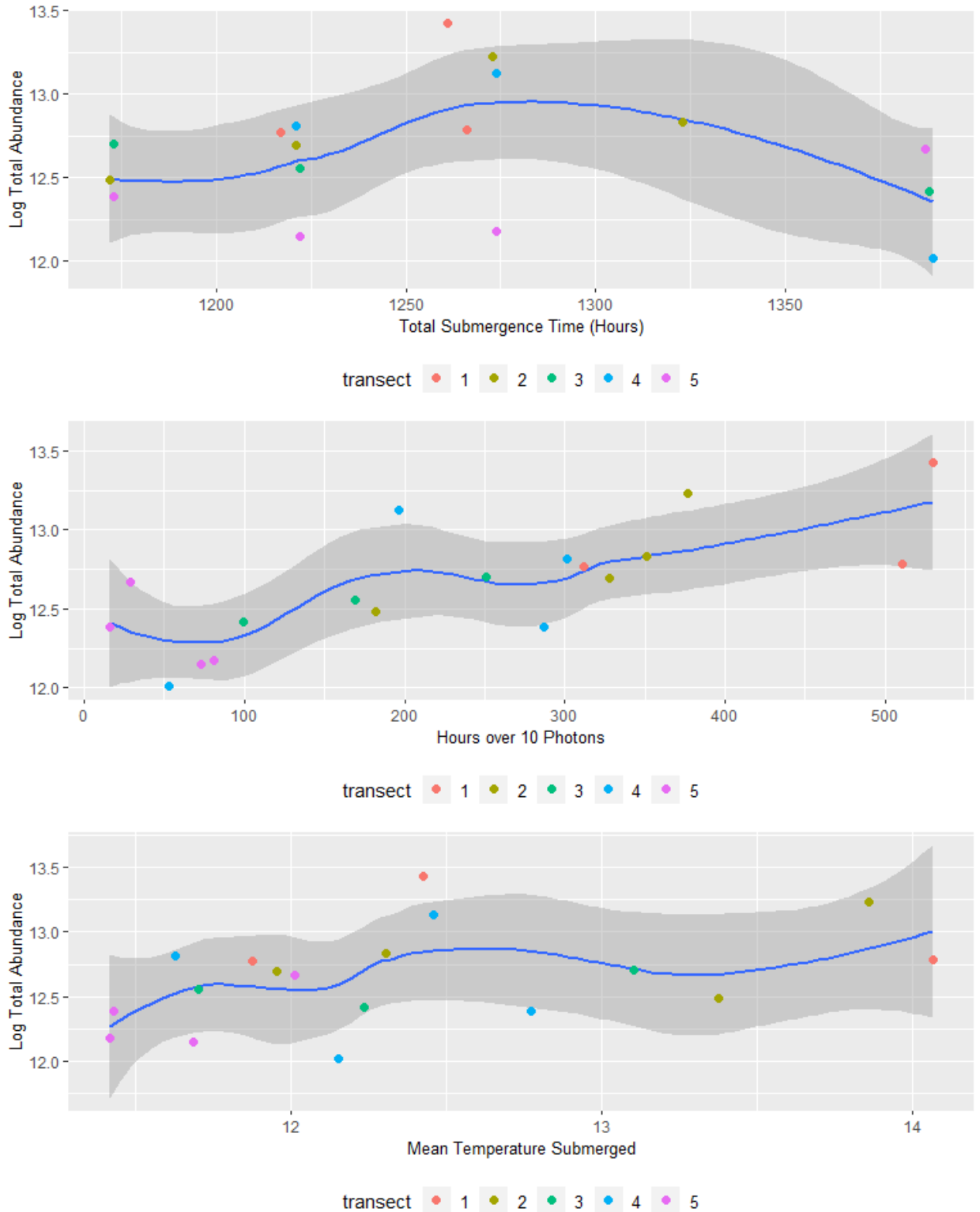


Figure A162 Explanatory variables and Log Total Abundance grouped by transect for Dinosaur Reservoir.



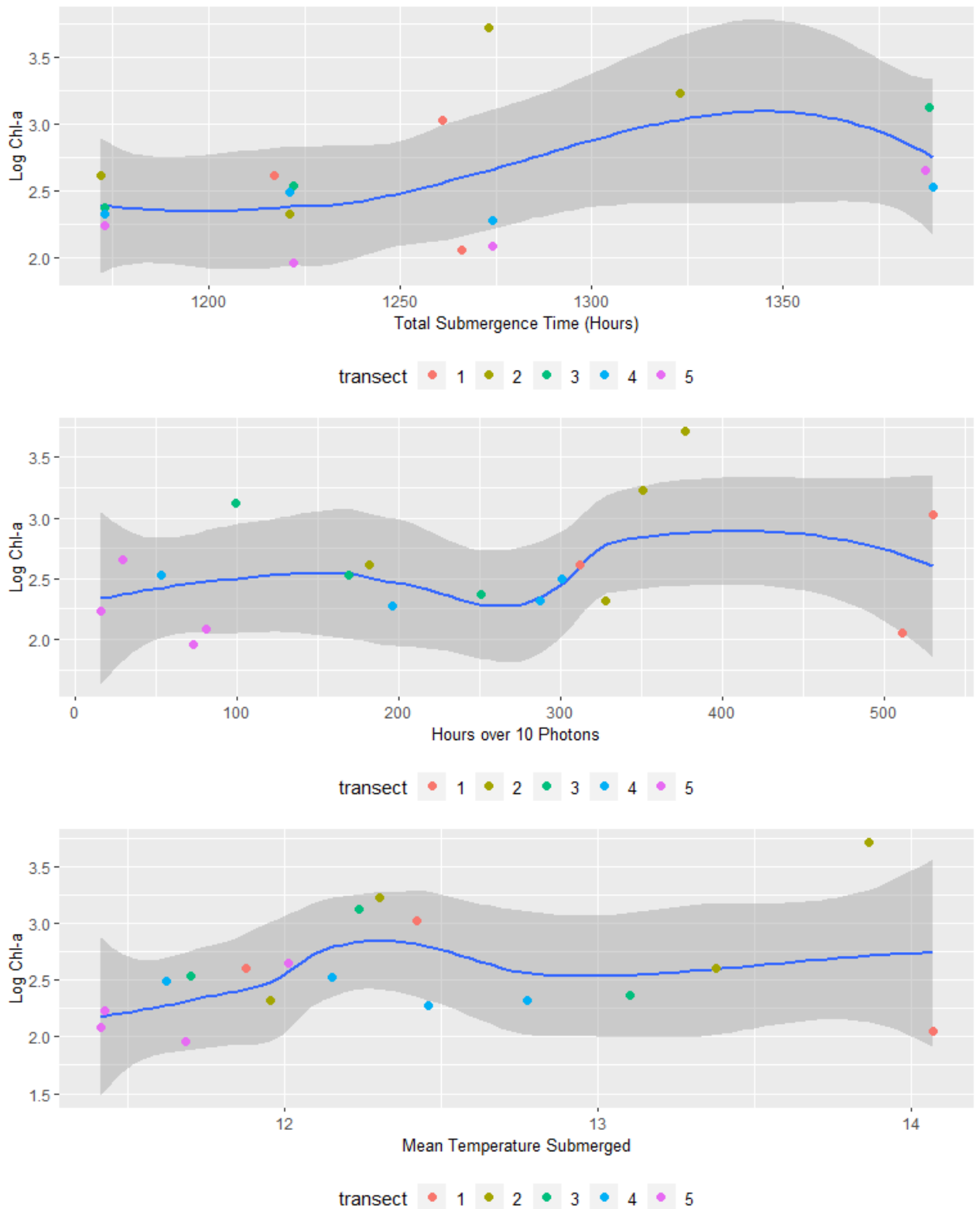


Figure A163 Explanatory variables and Log Chl-a grouped by transect for Dinosaur Reservoir.



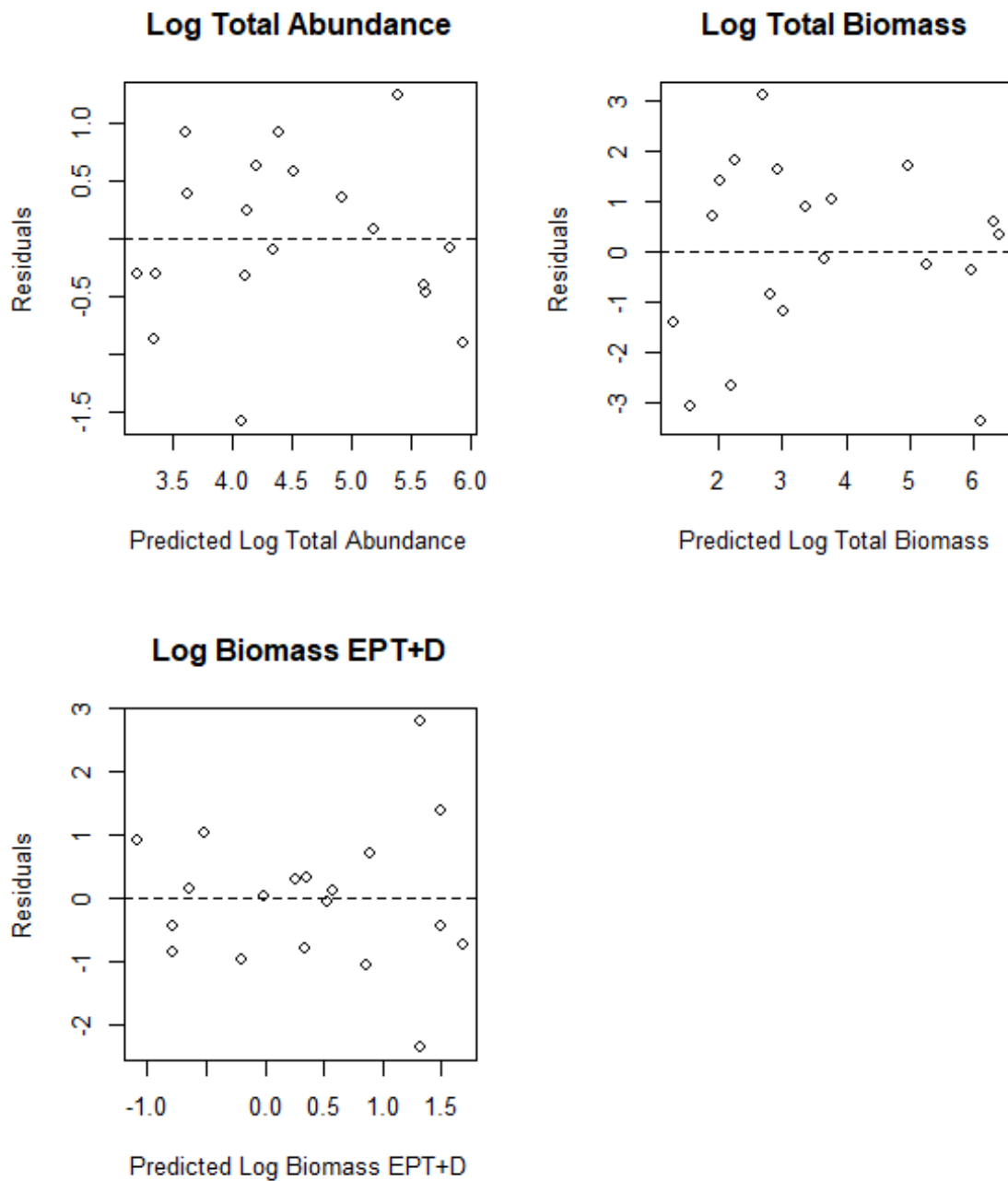
Appendix X Reservoir Invertebrate Rock Basket Productivity Model Results**Figure A164 Residual Plots for Dinosaur Reservoir Invertebrate Models**

Table A18 Summary of plausible benthic invertebrate models for Site C Dinosaur Basket samples identified using model averaging (those with a delta AIC <3) with pseudo-R2 values and coefficients.

Response	X.Intercept.	Average Temperature (Submergence)	Average Depth (m)	Total Submergence Time (Hours)	R.2	df	AICc	delta	weight
Log Biomass EPT+D	0.374		1.470		0.269	3.000	67.700	0.000	0.401
Log Biomass EPT+D	0.374	1.130	2.160		0.368	4.000	68.200	0.495	0.313
Log Biomass EPT+D	0.374		1.490	-0.338	0.283	4.000	70.600	2.890	0.095
Log Total Abundance	4.500		1.630		0.515	3.000	51.700	0.000	0.413
Log Total Abundance	4.500	0.758	2.100		0.583	4.000	52.100	0.360	0.345
Log Total Abundance	4.500		1.660	-0.382	0.543	4.000	53.800	2.130	0.143
Log Total Abundance	4.500	0.745	2.120	-0.367	0.609	5.000	54.600	2.900	0.097
Log Total Biomass	3.610		3.390		0.477	3.000	82.300	0.000	0.666
Log Total Biomass	3.610	0.704	3.820		0.490	4.000	85.000	2.790	0.165



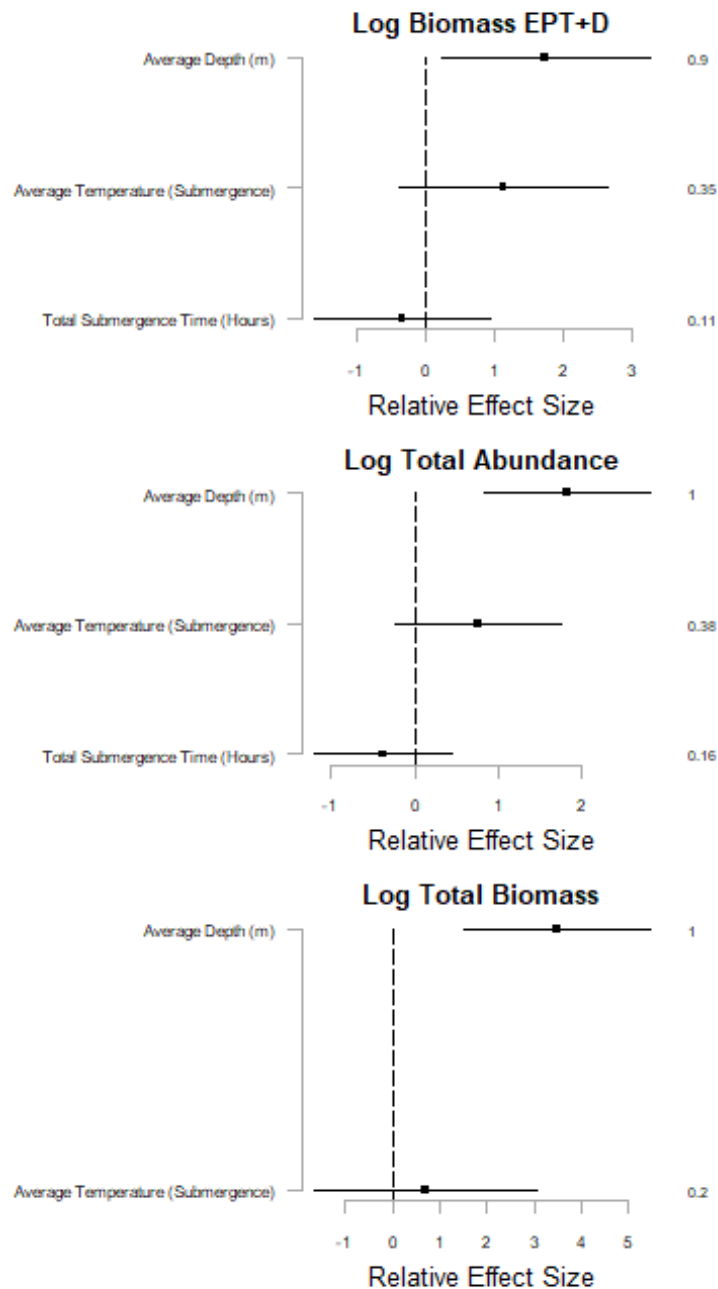


Figure A165 The coefficients and their 95% CLs of standardized explanatory variables of benthic invertebrates in Dinosaur Reservoir. Benthic invertebrates responses included abundance, biomass, and biomass of EPT+D. Explanatory variables included mean water temperature submerged, mean depth over deployment and total hours submerged. Coefficients were standardized to allow comparisons of the direction and size of effects, noting that variables with CLs that do not cross zero have an effect on the response variable. Key explanatory variables are those that have a relative variable importance (RVI) of greater than 0.6-0.7 and the RVI is shown on the right-hand side of each figure.



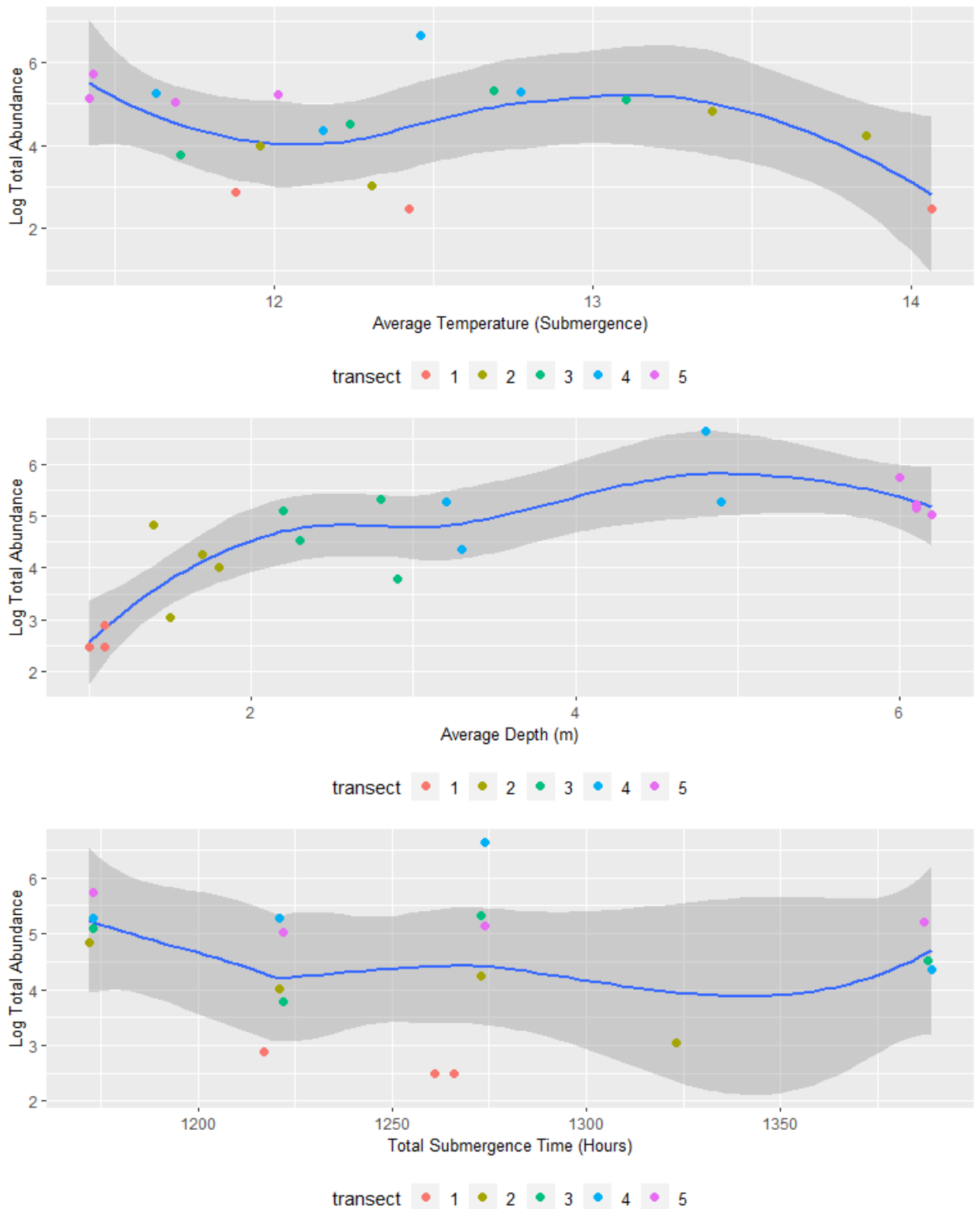


Figure A166 Explanatory variables and Log Total Abundance grouped by transect for Dinosaur Reservoir.



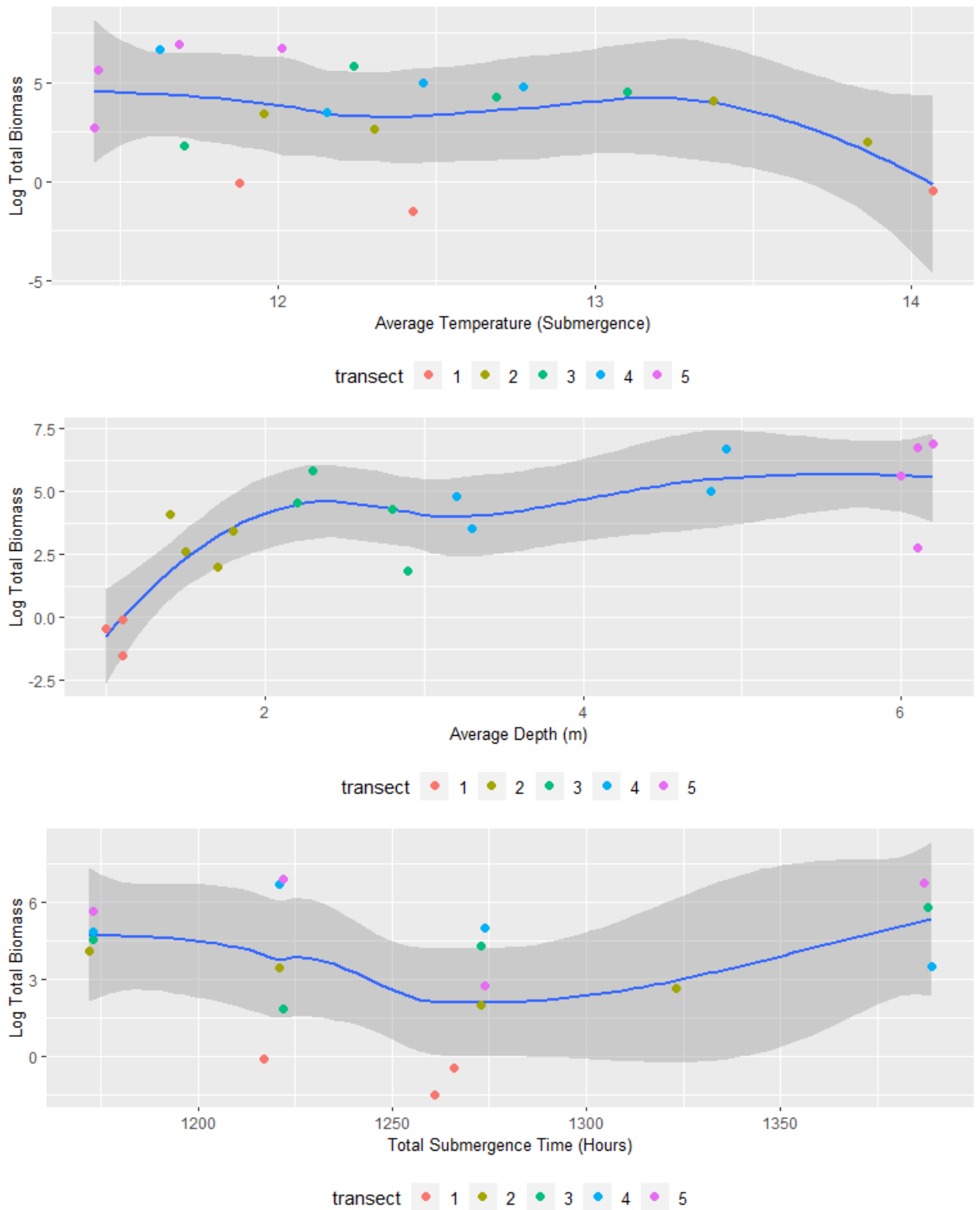


Figure A167 Explanatory variables and Log Total Biomass grouped by transect for Dinosaur Reservoir.



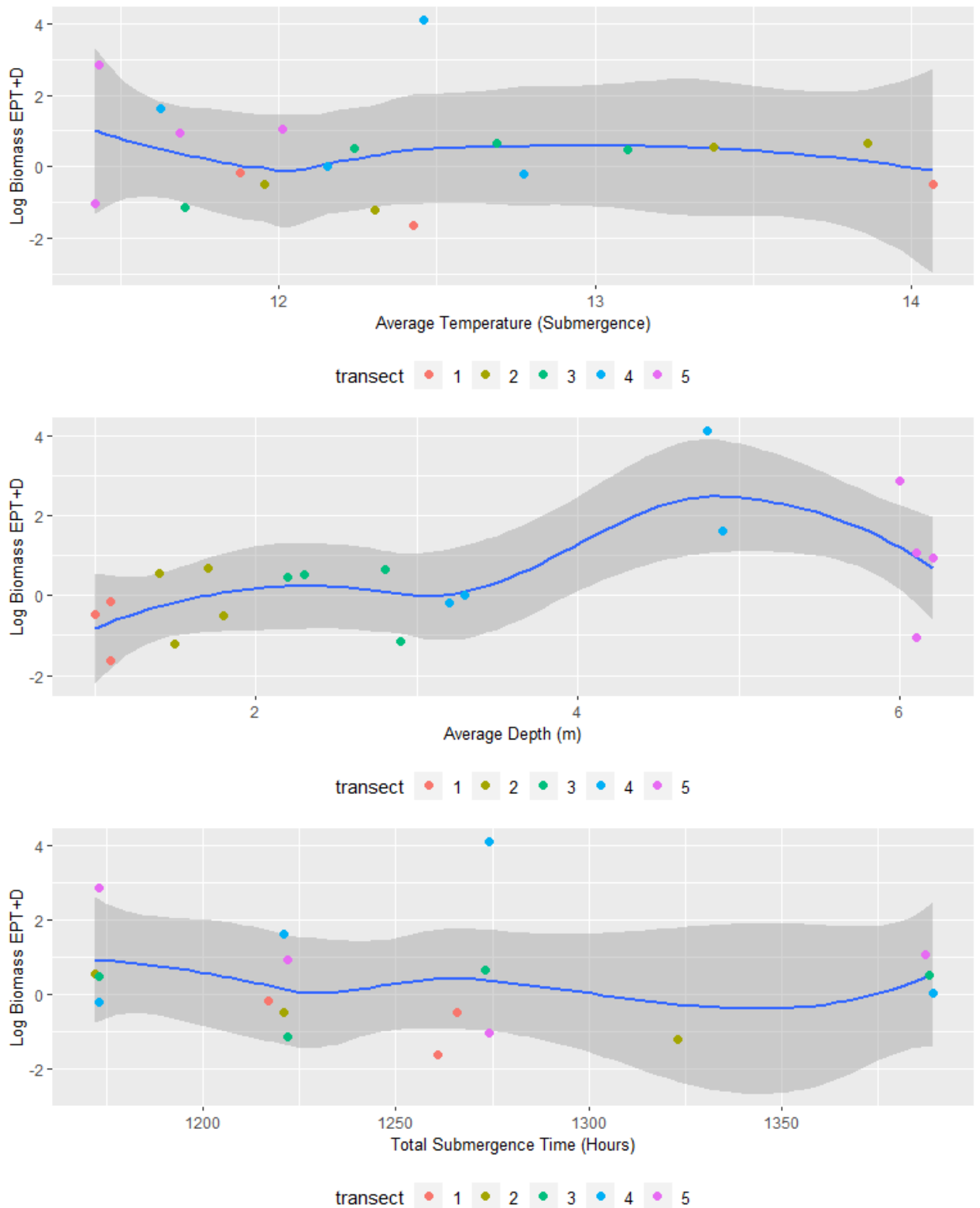


Figure A168 Explanatory variables and Log Biomass EPT+D grouped by transect for Dinosaur Reservoir.



Appendix Y Periphyton 2010-2011 and 2017-2018 Riverine Sites Dredge Results

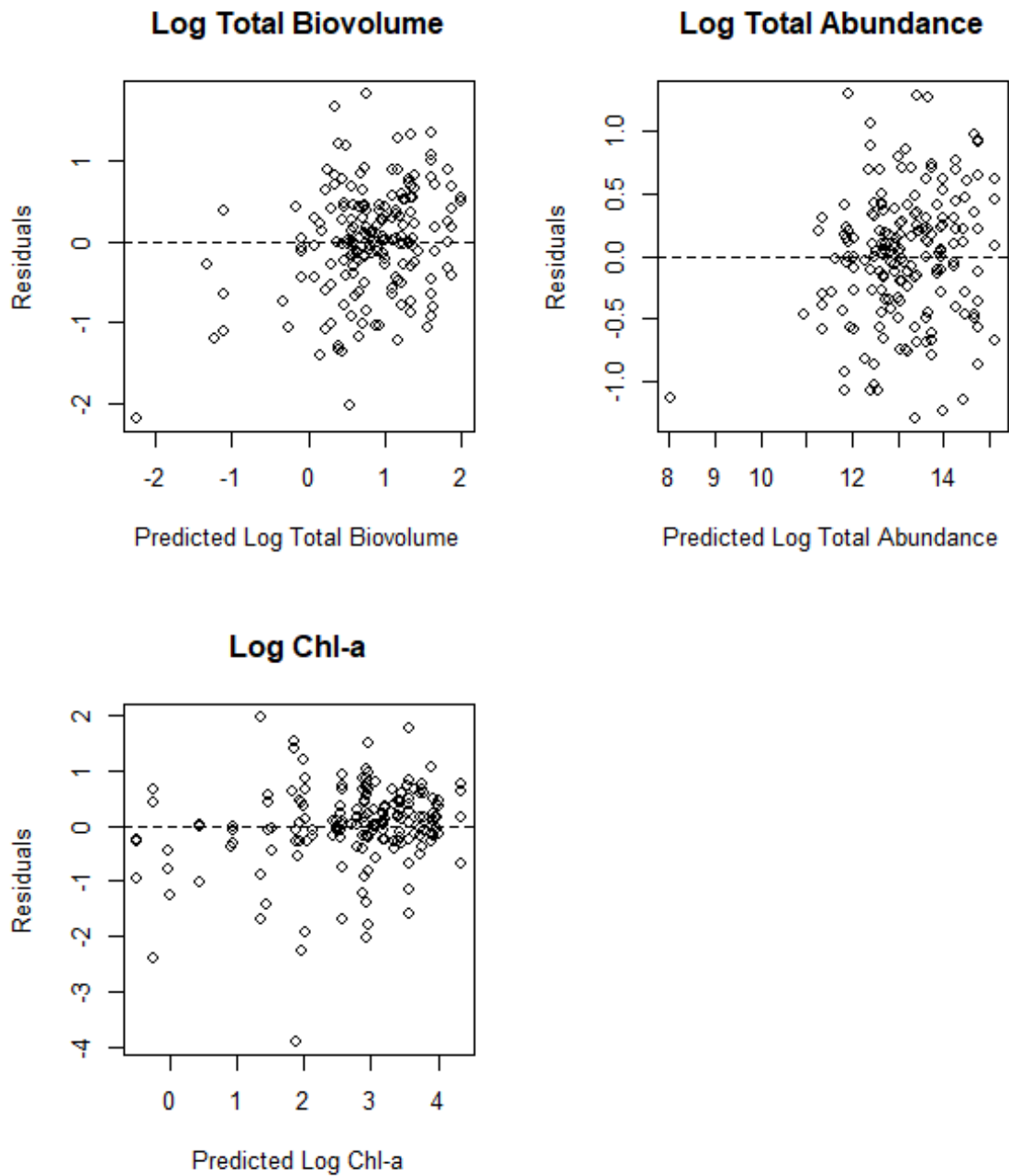


Figure A169 Residual Plots for Periphyton Models



Table A19 Summary of plausible models identified using model averaging (those with a delta AIC <3) with pseudo-R2 values and coefficients for all riverine samples 2010-2011 and 2017-2018 except MD and HD.

Response	X.Intercept.	Total Submergence Time (Hours)	R.2	df	AICc	delta	weight
Log Chl-a	2.610		0.351	3.000	579.000	0.000	0.739
Log Chl-a	2.610	0.017	0.351	4.000	581.000	2.080	0.261
Log Total Abundance	13.000		0.464	3.000	467.000	0.000	0.677
Log Total Abundance	13.000	-0.103	0.466	4.000	468.000	1.480	0.323
Log Total Biovolume	0.729		0.171	3.000	496.000	0.000	0.651
Log Total Biovolume	0.740	-0.144	0.175	4.000	497.000	1.250	0.349



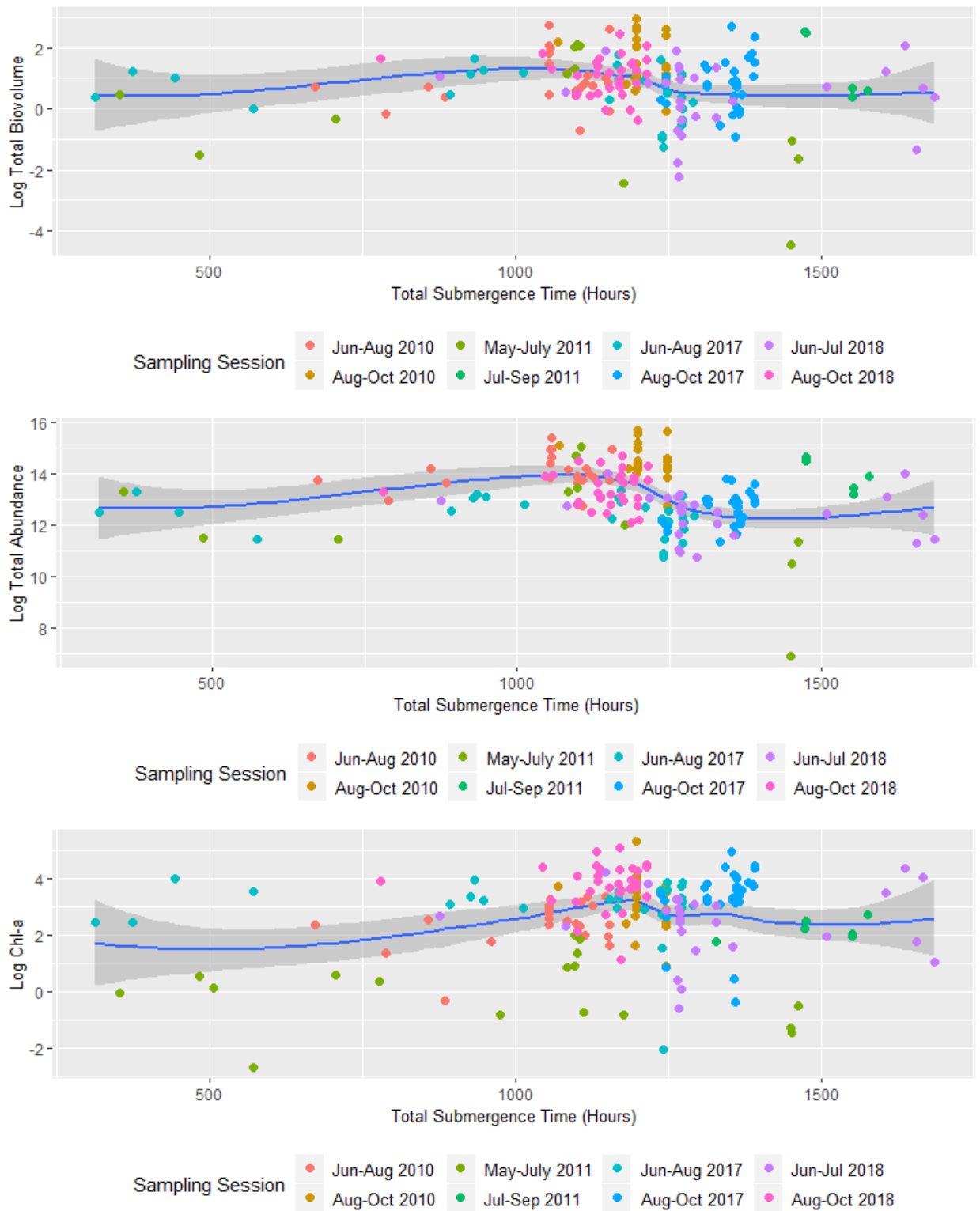


Figure A170 Explanatory variables and Periphyton responses grouped by site for riverine samplers.



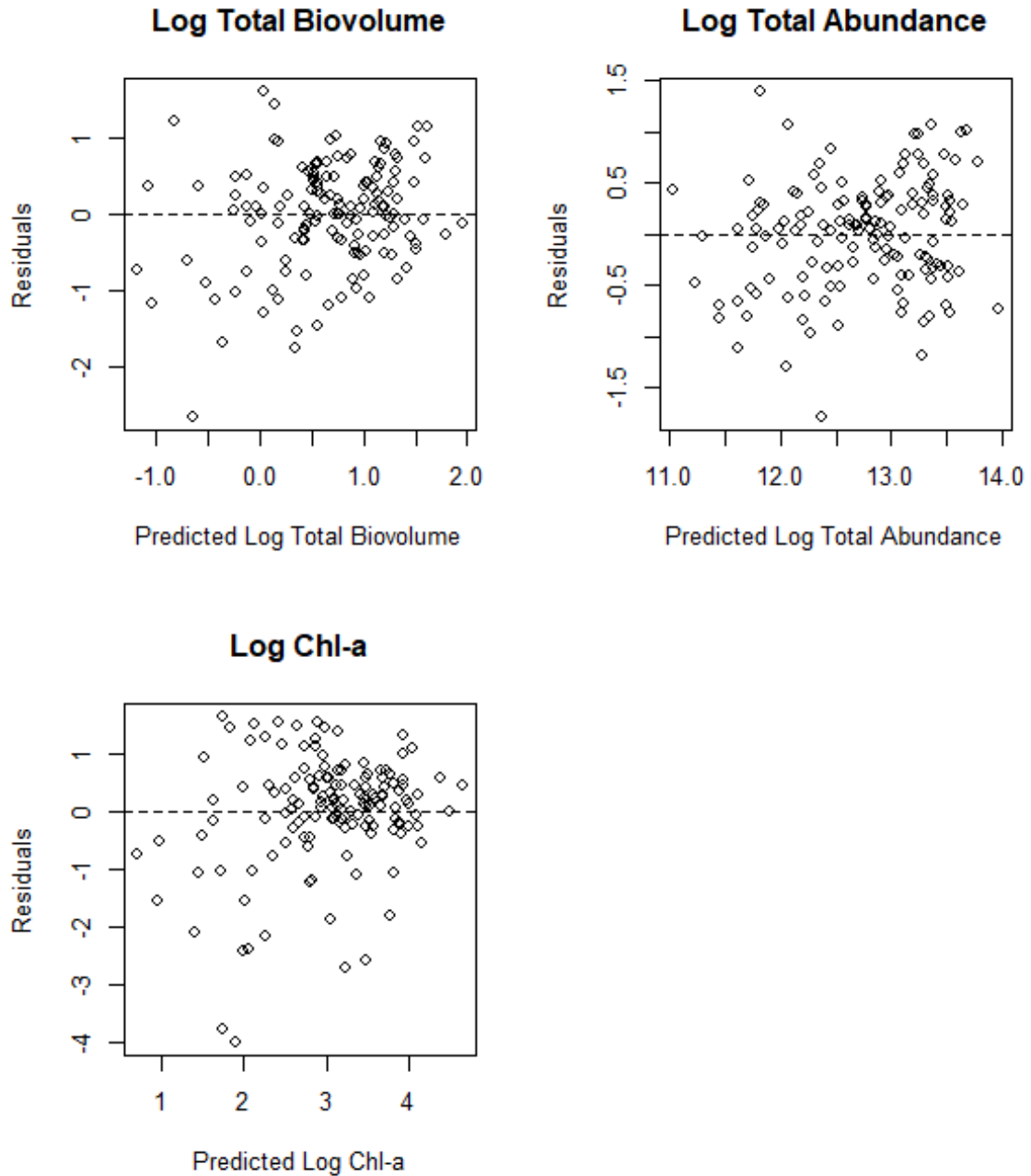
Appendix Z River Periphyton Full Transect Model Results**Figure A171 Residual Plots for Full Transect Periphyton Models**

Table A20 Summary of plausible models identified using model averaging (those with a delta AIC <3) with pseudo-R2 values and coefficients for all riverine samples except MD and HD.

Response	X-Intercept.	Depositional Rate (cm/day)	Velocity	Cumulative Submergence Time (Hours)	Hours over 10 Photons	R-2	df	AICc	delta	weight
Log Chl-a	2.980				0.610	0.187	4.000	473.000	0.000	0.298
Log Chl-a	2.980			-0.217	0.776	0.191	5.000	474.000	1.340	0.153
Log Chl-a	2.980	-0.234			0.626	0.189	5.000	475.000	1.730	0.125
Log Chl-a	2.980		0.000		0.610	0.187	5.000	475.000	2.150	0.102
Log Chl-a	2.990	-0.268		-0.235	0.811	0.194	6.000	476.000	2.960	0.068
Log Total Abundance	12.700			-0.417	0.407	0.341	5.000	328.000	0.000	0.309
Log Total Abundance	12.700	-0.265		-0.429	0.430	0.345	6.000	329.000	1.190	0.170
Log Total Abundance	12.700		-0.141	-0.499	0.390	0.344	6.000	330.000	1.490	0.147
Log Total Abundance	12.700	-0.307	-0.168	-0.528	0.413	0.350	7.000	331.000	2.430	0.092
Log Total Abundance	12.700			-0.221		0.318	4.000	331.000	2.620	0.083
Log Total Biovolume	0.625		-0.342	-0.508	0.464	0.204	6.000	395.000	0.000	0.137
Log Total Biovolume	0.627			-0.302	0.491	0.190	5.000	395.000	0.236	0.122
Log Total Biovolume	0.630	-0.423	-0.391	-0.558	0.504	0.215	7.000	395.000	0.259	0.120
Log Total Biovolume	0.624					0.163	3.000	395.000	0.690	0.097
Log Total Biovolume	0.625				0.251	0.175	4.000	396.000	0.857	0.089
Log Total Biovolume	0.630	-0.320		-0.321	0.529	0.197	6.000	396.000	1.170	0.076
Log Total Biovolume	0.622		-0.380	-0.306		0.181	5.000	397.000	1.860	0.054
Log Total Biovolume	0.622		-0.142			0.168	4.000	397.000	1.990	0.050
Log Total Biovolume	0.627	-0.273			0.270	0.180	5.000	397.000	2.090	0.048
Log Total Biovolume	0.626	-0.226				0.167	4.000	397.000	2.220	0.045
Log Total Biovolume	0.624			-0.061		0.165	4.000	397.000	2.620	0.037



Response	X-Intercept.	Depositional Rate (cm/day)	Velocity	Cumulative Submergence Time (Hours)	Hours over 10 Photons	R.2	df	AICc	delta	weight
Log Total Biovolume	0.626	-0.343	-0.425	-0.335		0.188	6.000	397.000	2.830	0.033
Log Total Biovolume	0.624		-0.049		0.223	0.175	5.000	398.000	2.940	0.032



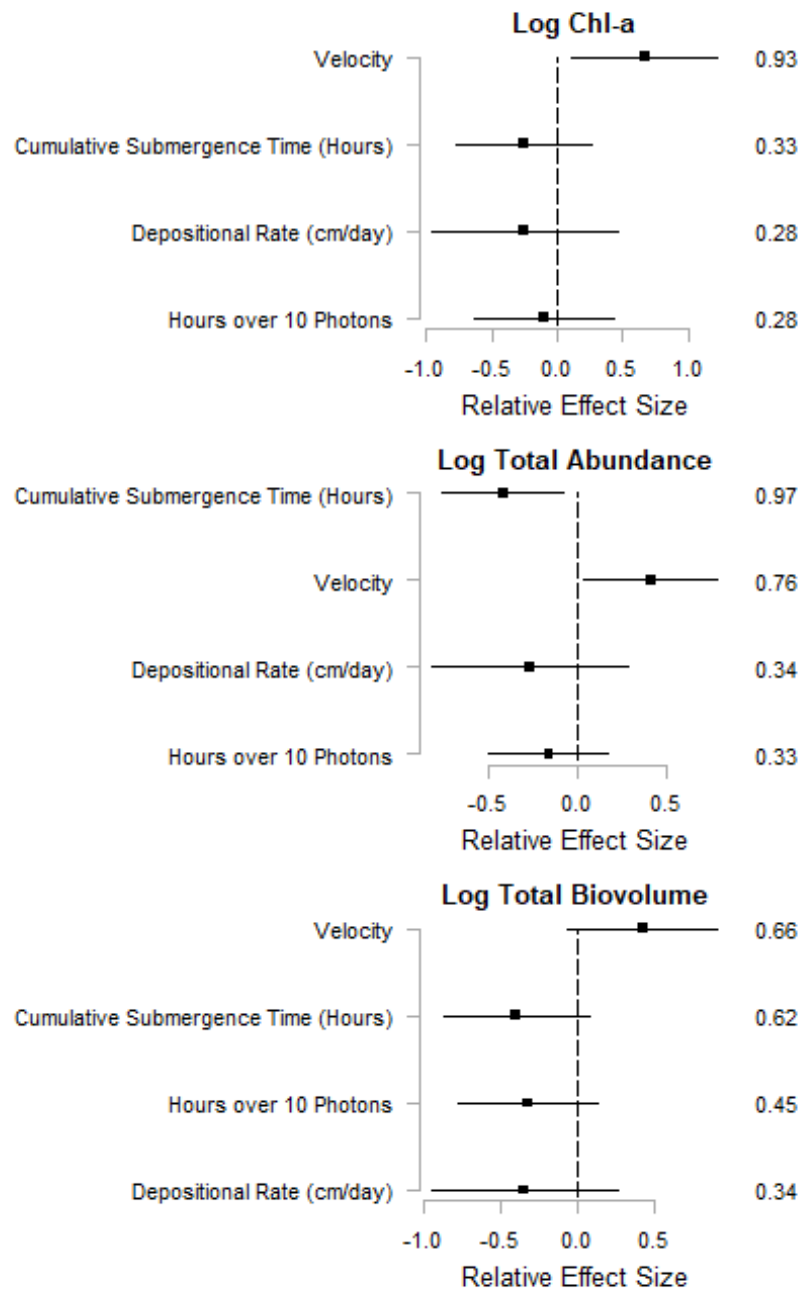


Figure A172 The coefficients and their 95% CLs of standardized explanatory variables of periphyton production for all riverine samplers except MD and HD. Periphyton responses included abundance, chl-a and biovolume. Explanatory variables included total hours over 10 photons, velocity, depositional rate and cumulative submergence time. Coefficients were standardized to allow comparisons of the direction and size of effects, noting that variables with CLs that do not cross zero have an effect on the response variable. Key explanatory variables are those that have a relative variable importance (RVI) of greater than 0.6-0.7 and the RVI is shown on the right-hand side of each figure.



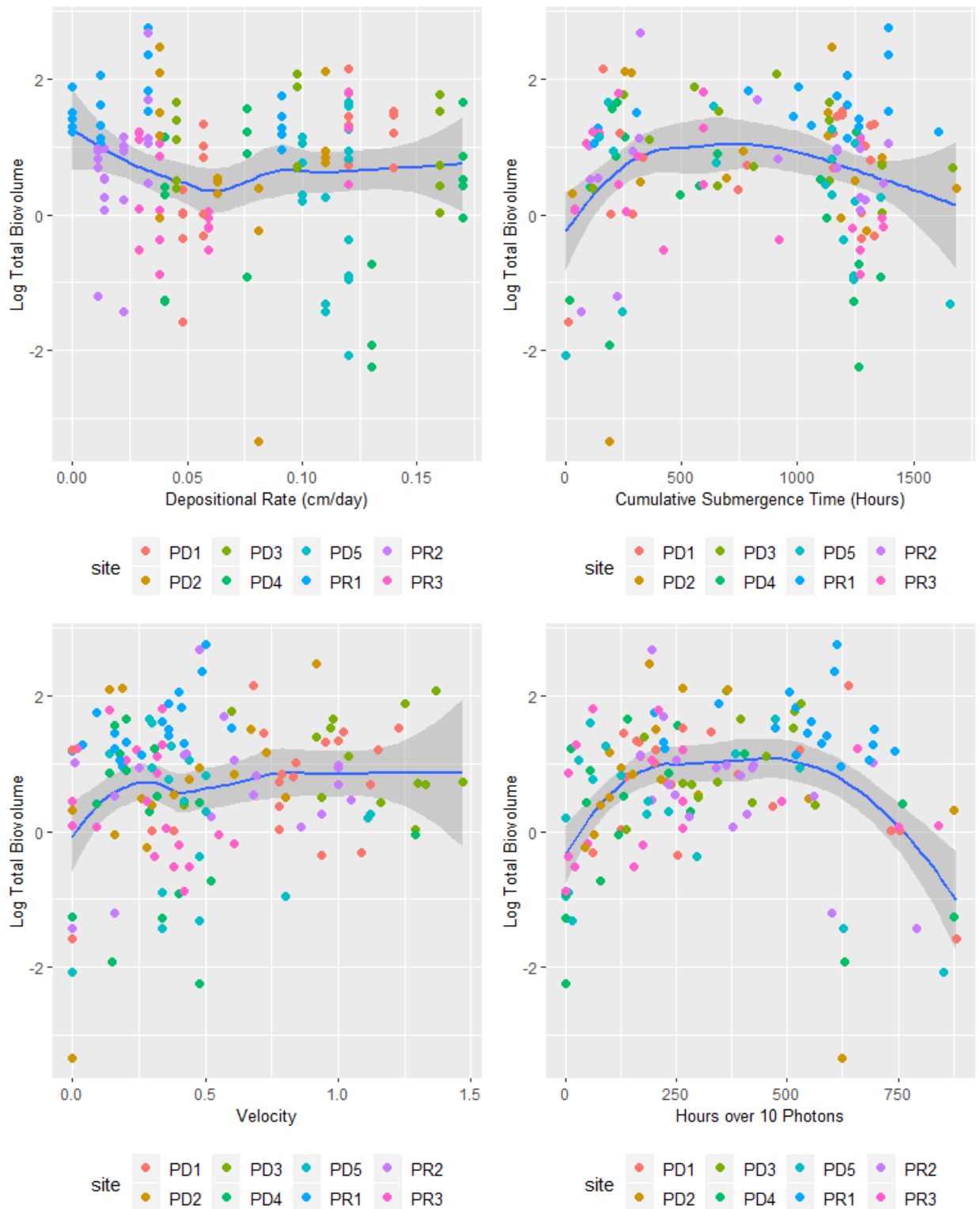


Figure A173 Explanatory variables and Log Total Biovolume grouped by site for riverine samplers.



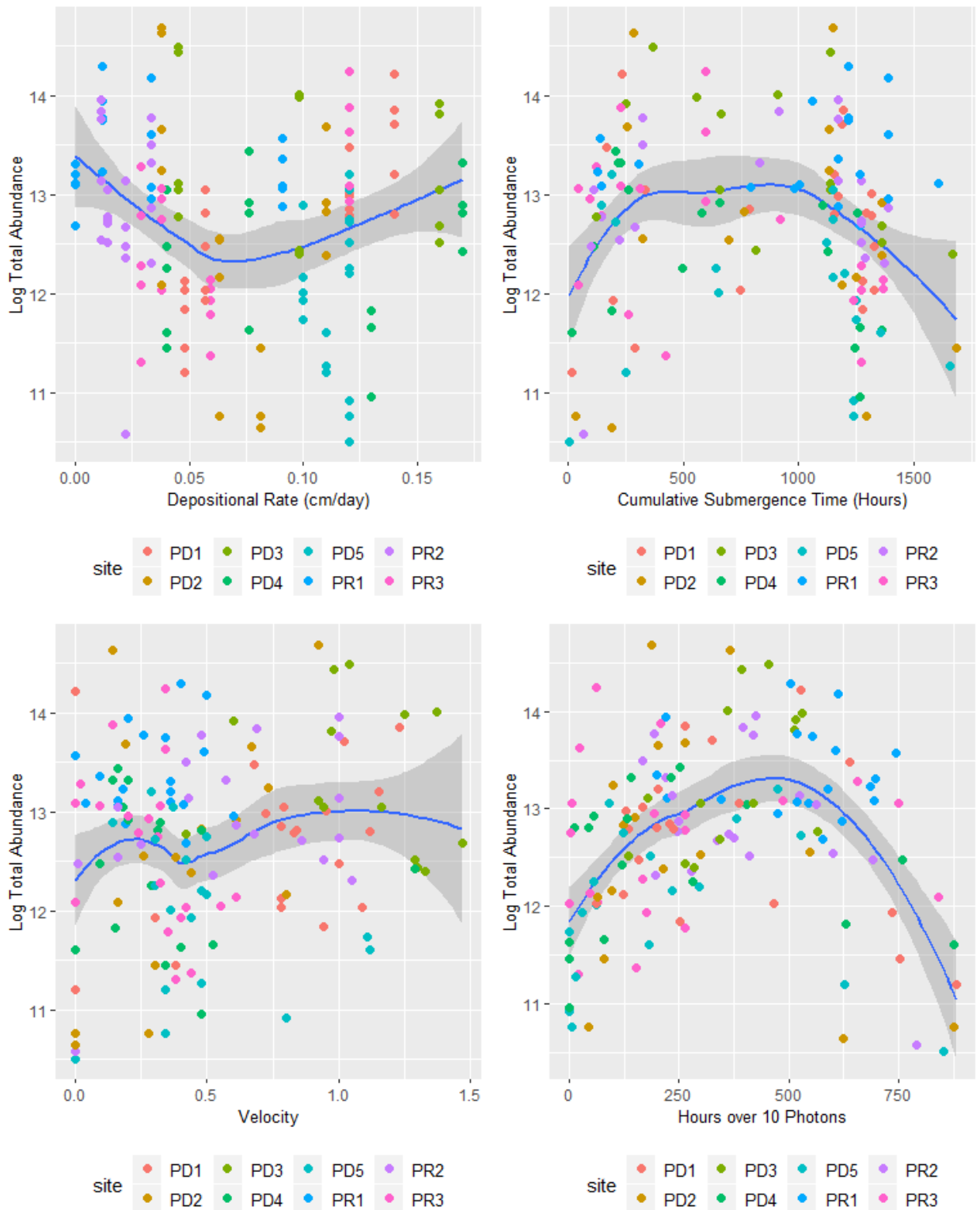


Figure A174 Explanatory variables and Log Total Abundance grouped by site for riverine samplers.



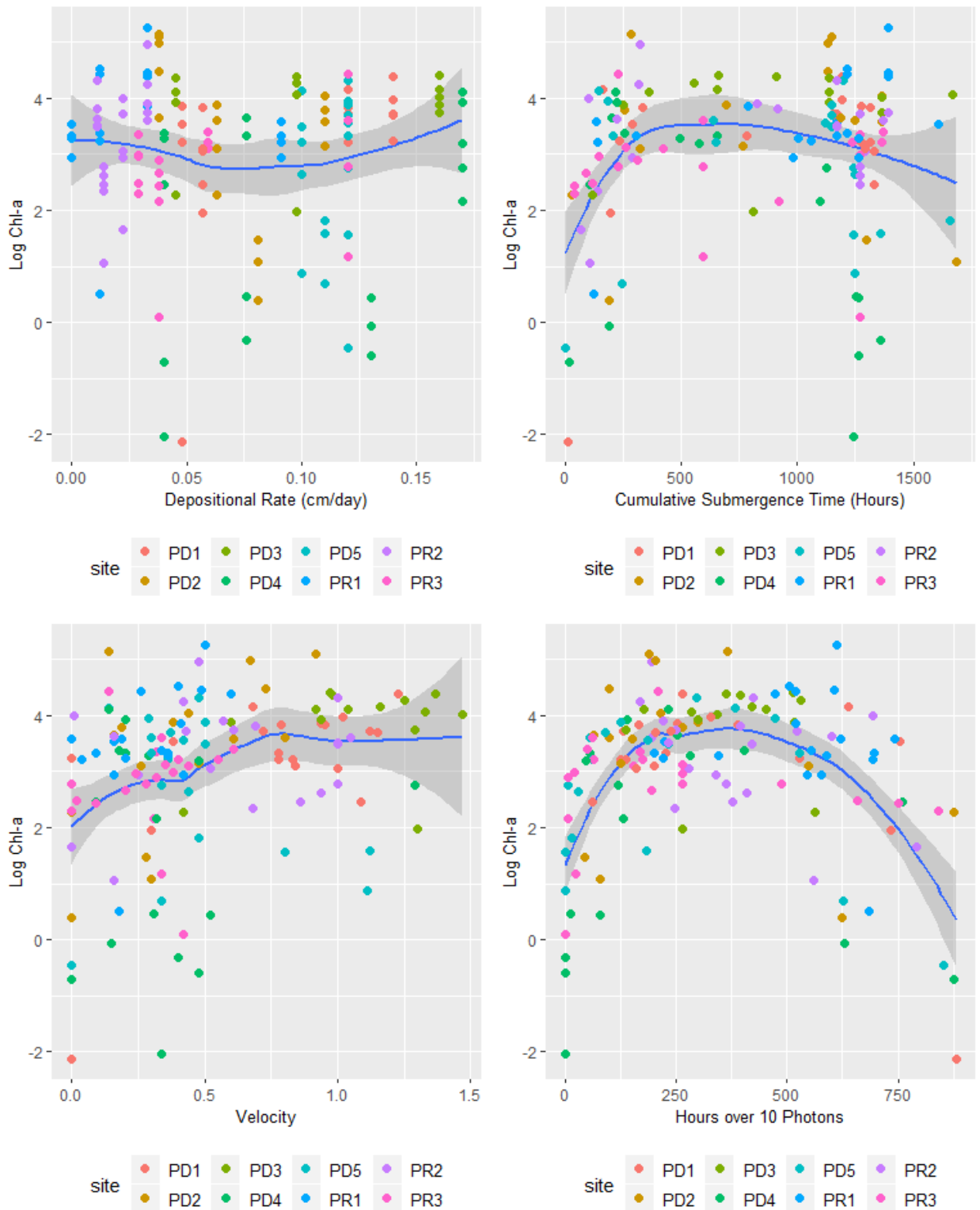


Figure A175 Explanatory variables and Log Chl-a grouped by site for riverine samplers.



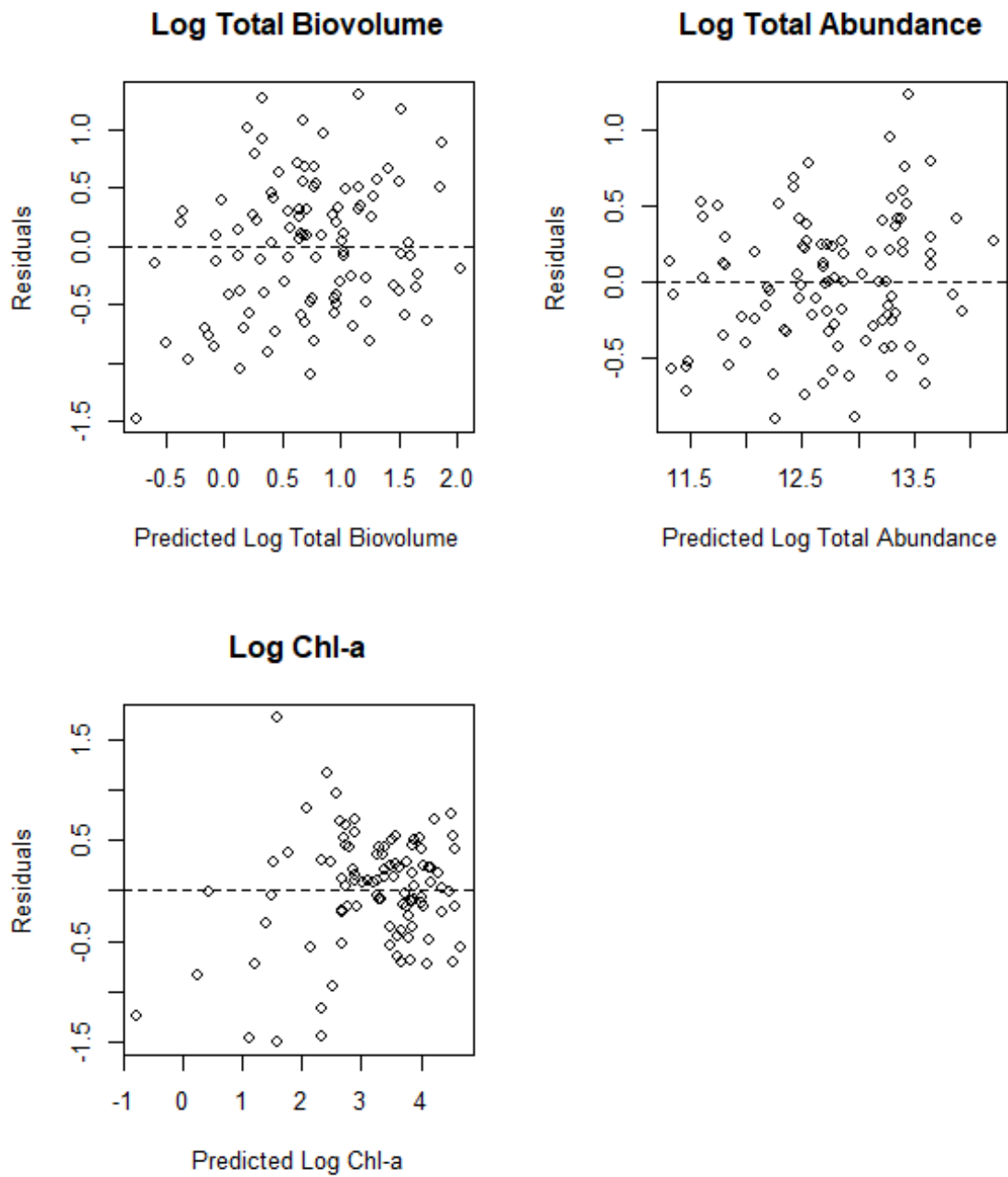
Appendix AA River Periphyton Fully Submerged Sites Model Results**Figure A176 Residual Plots for Mostly Submerged Periphyton Models**

Table A21 Model average summaries of periphyton models for mostly submerged samplers for Riverine sites not including MD and HD. The explanatory variables have standardized coefficients with 95% CLs.

Response	X-Intercept.	Depositional Rate (cm/day)	Velocity	Cumulative Submergence Time (Hours)	Hours over 10 Photons	R.2	df	AICc	delta	weight
Log Chl-a	3.040		0.888	-0.308		0.474	5.000	271.000	0.000	0.389
Log Chl-a	3.040		0.974			0.453	4.000	272.000	1.610	0.174
Log Chl-a	3.050		0.890	-0.324	0.073	0.474	6.000	273.000	2.180	0.131
Log Chl-a	3.040	0.005	0.877	-0.308		0.473	6.000	273.000	2.300	0.123
Log Total Abundance	12.700		0.638	-0.317		0.483	5.000	197.000	0.000	0.420
Log Total Abundance	12.700		0.625	-0.358	0.180	0.489	6.000	198.000	1.060	0.248
Log Total Abundance	12.700	-0.142	0.607	-0.320		0.485	6.000	199.000	1.920	0.161
Log Total Abundance	12.700	-0.202	0.581	-0.371	0.211	0.493	7.000	200.000	2.610	0.114
Log Total Biovolume	0.693		0.778	-0.359		0.342	5.000	231.000	0.000	0.477
Log Total Biovolume	0.691	-0.122	0.737	-0.366		0.344	6.000	233.000	2.000	0.175
Log Total Biovolume	0.692		0.765	-0.372	0.059	0.343	6.000	233.000	2.190	0.160



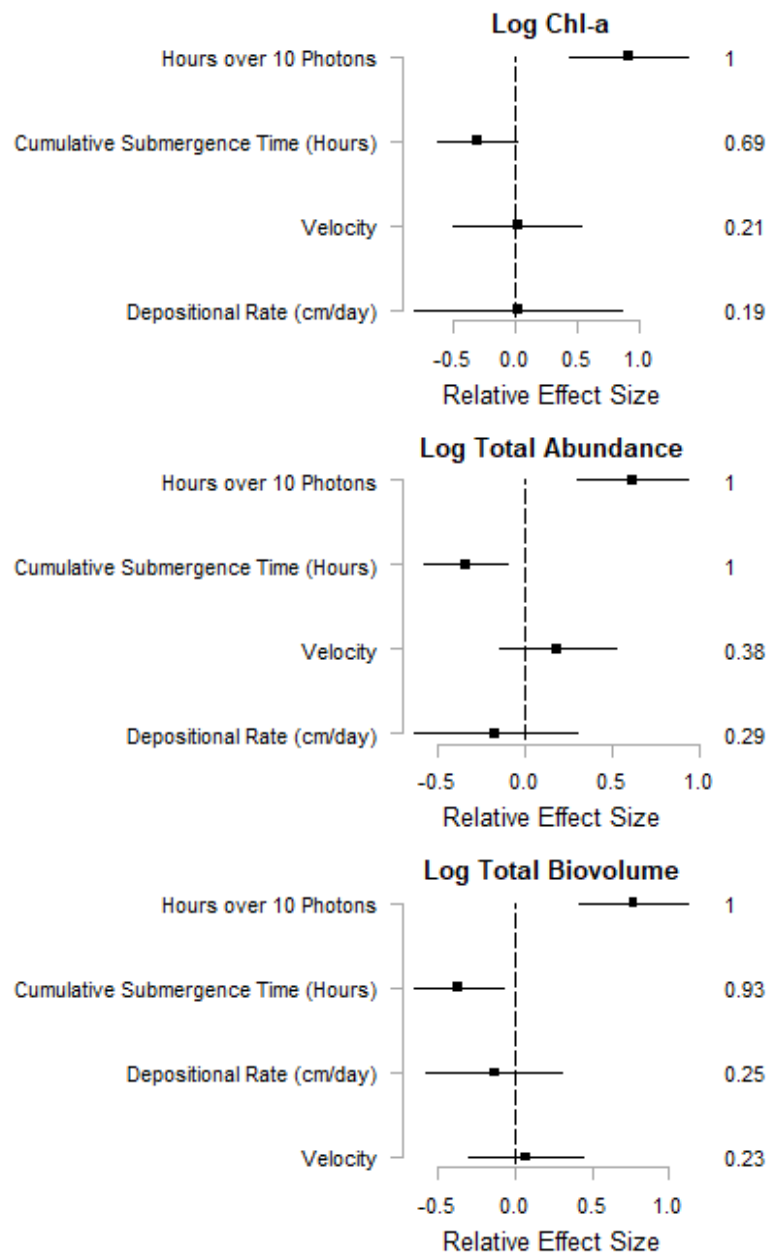


Figure A177 The coefficients and their 95% CLs of standardized explanatory variables of periphyton production for mostly submerged riverine samplers except MD and HD. Periphyton responses included abundance, chl-a and biovolume. Explanatory variables included total hours over 10 photons, velocity, depositional rate and cumulative submergence time. Coefficients were standardized to allow comparisons of the direction and size of effects, noting that variables with CLs that do not cross zero have an effect on the response variable. Key explanatory variables are those that have a relative variable importance (RVI) of greater than 0.6-0.7 and the RVI is shown on the right-hand side of each figure.



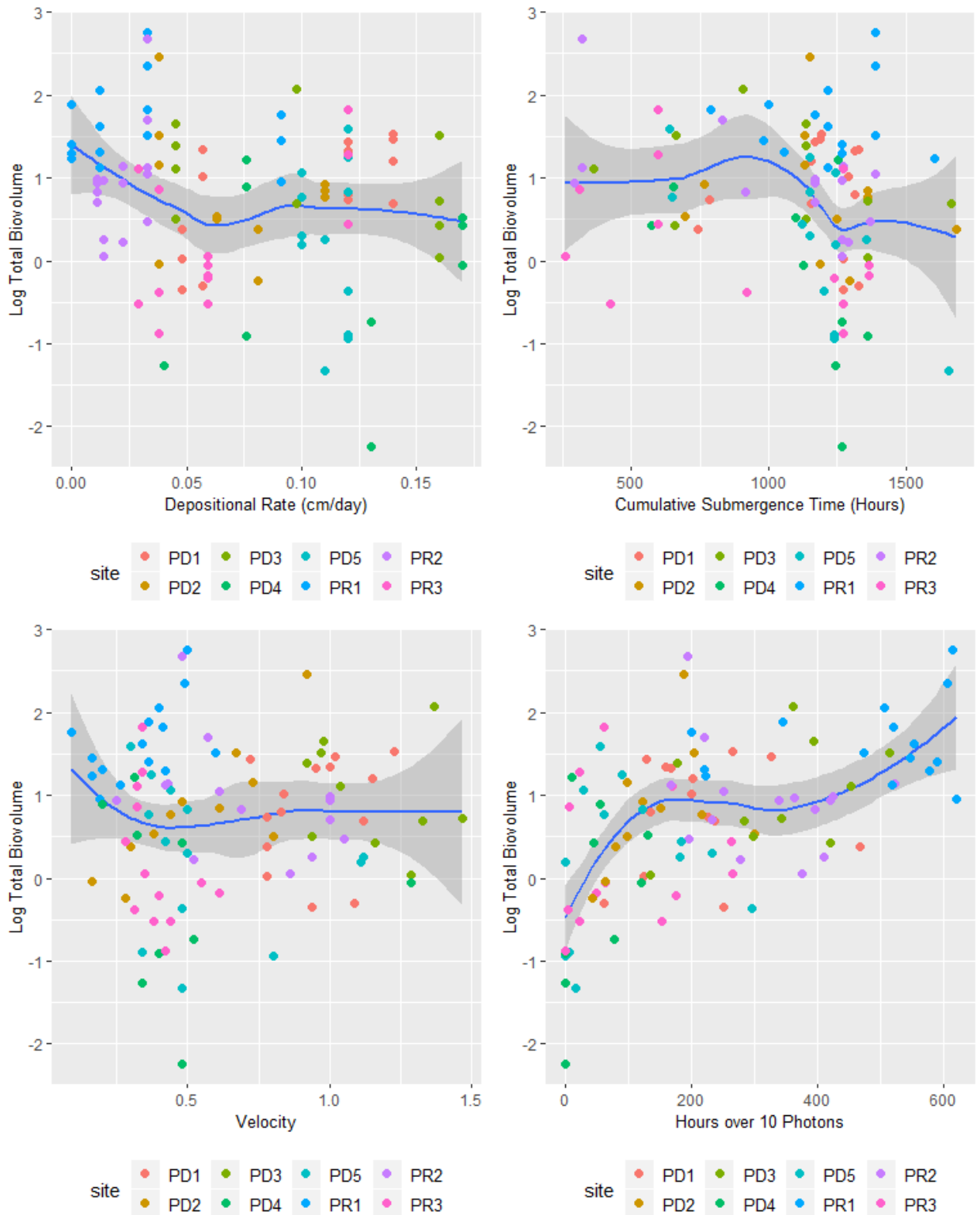


Figure A178 Explanatory variables and Log Total Biovolume grouped by site for riverine samplers.



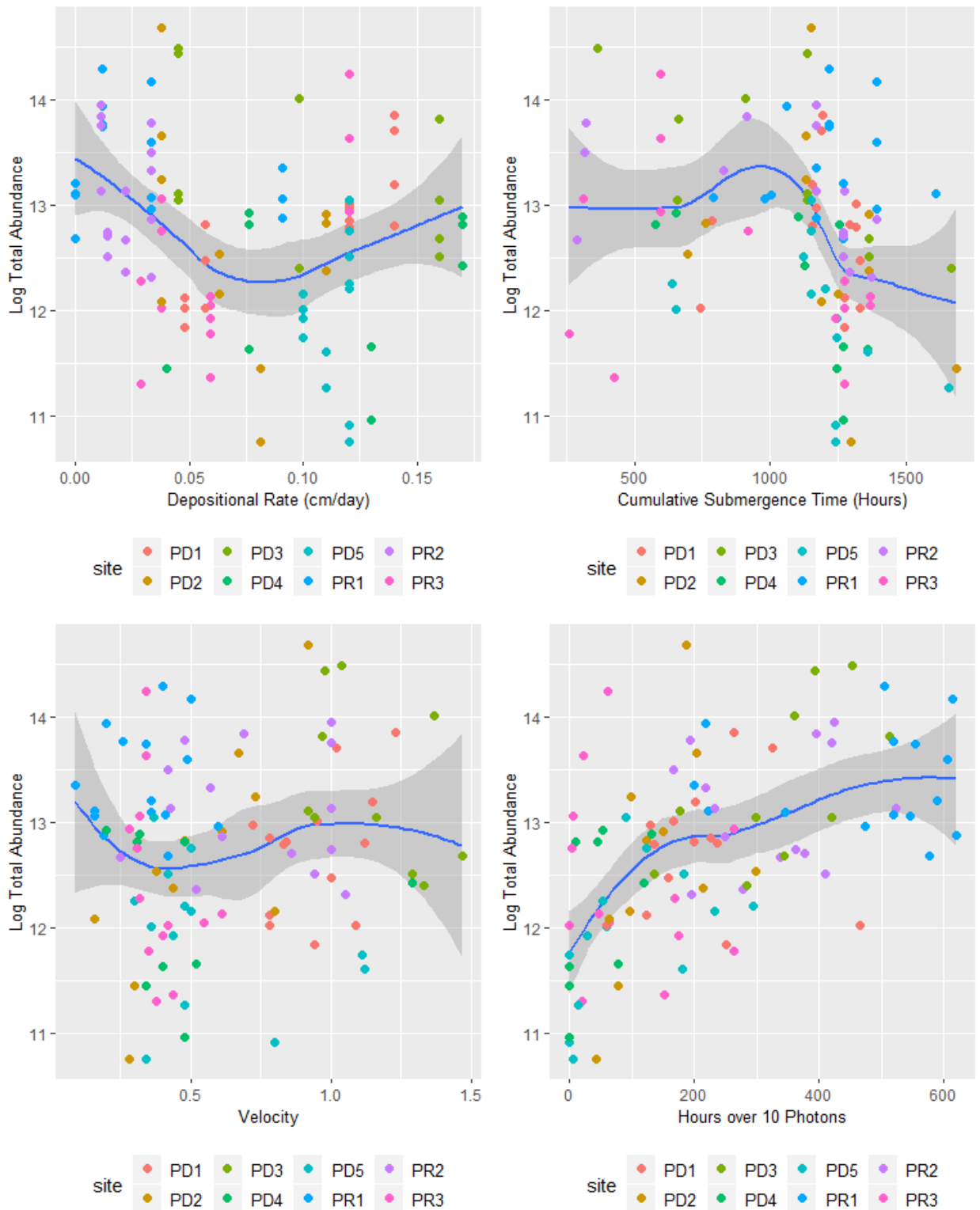


Figure A179 Explanatory variables and Log Total Abundance grouped by site for riverine samplers.



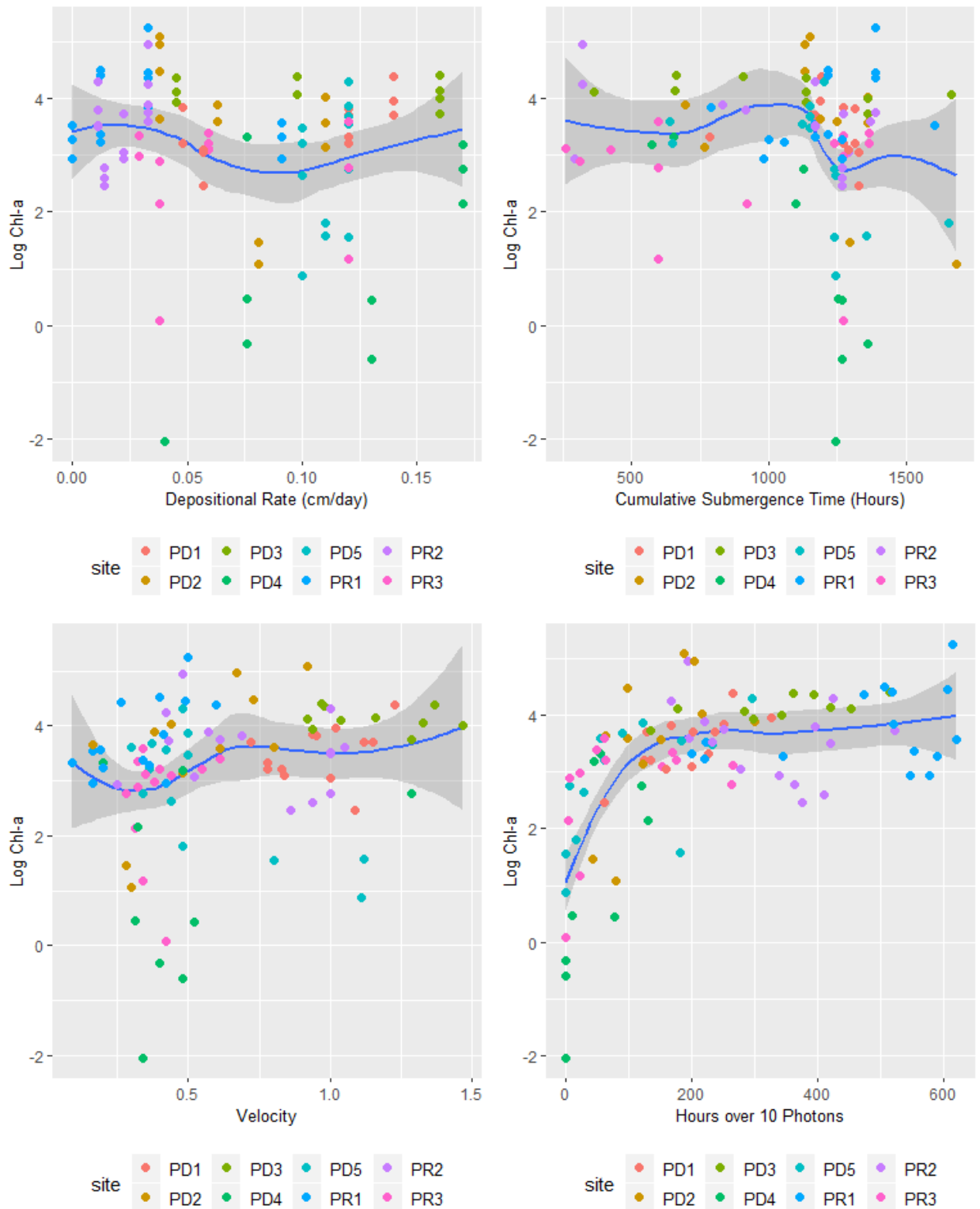


Figure A180 Explanatory variables and Log Chl-a grouped by site for riverine samplers.



Appendix BB River Periphyton Random Forest Results

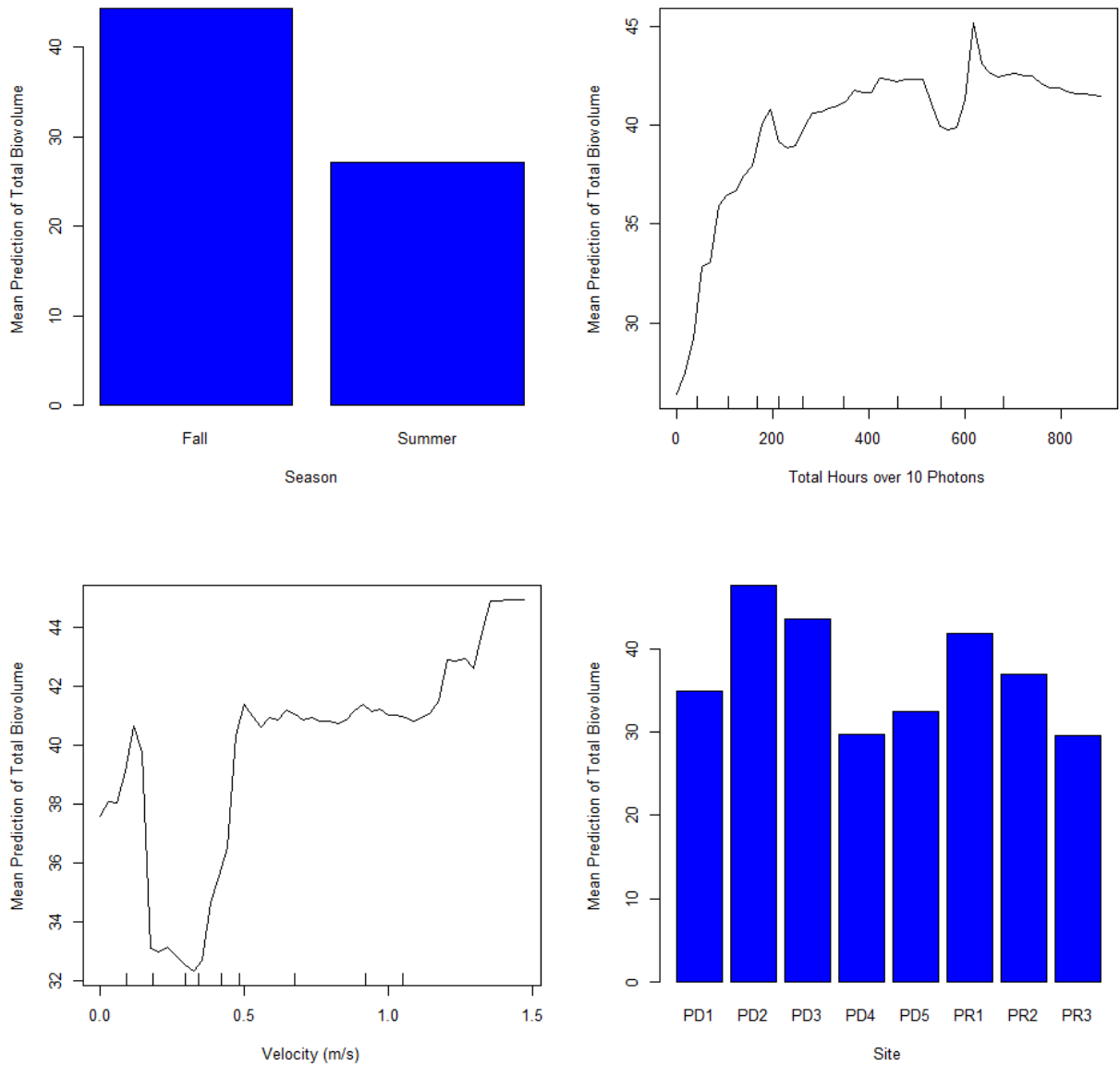


Figure A181 Partial dependence plots for the top four explanatory variables for Total Biovolume Random Forest Model.



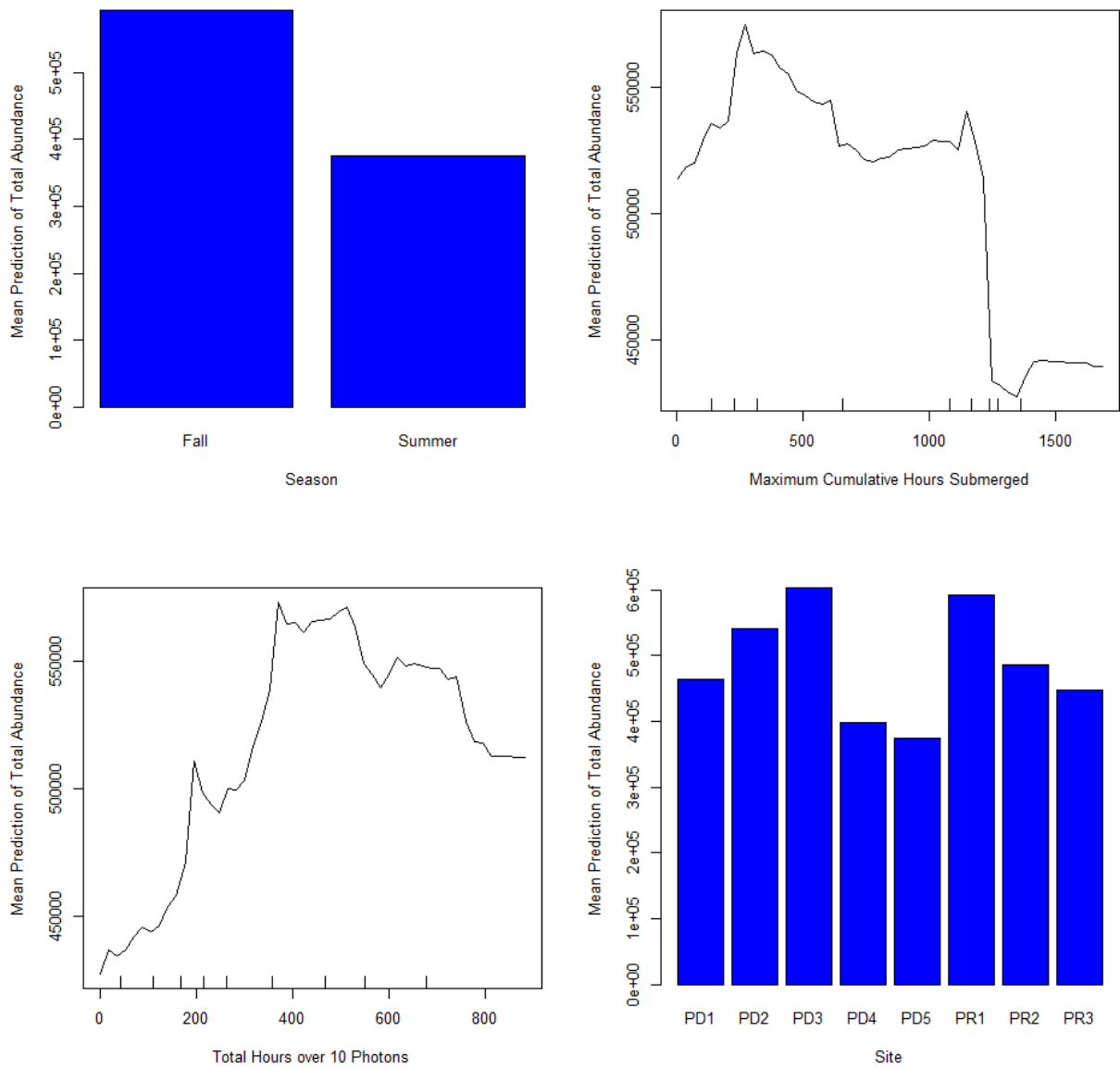


Figure A182 Partial dependence plots for the top four explanatory variables for Total Abundance Random Forest Model.



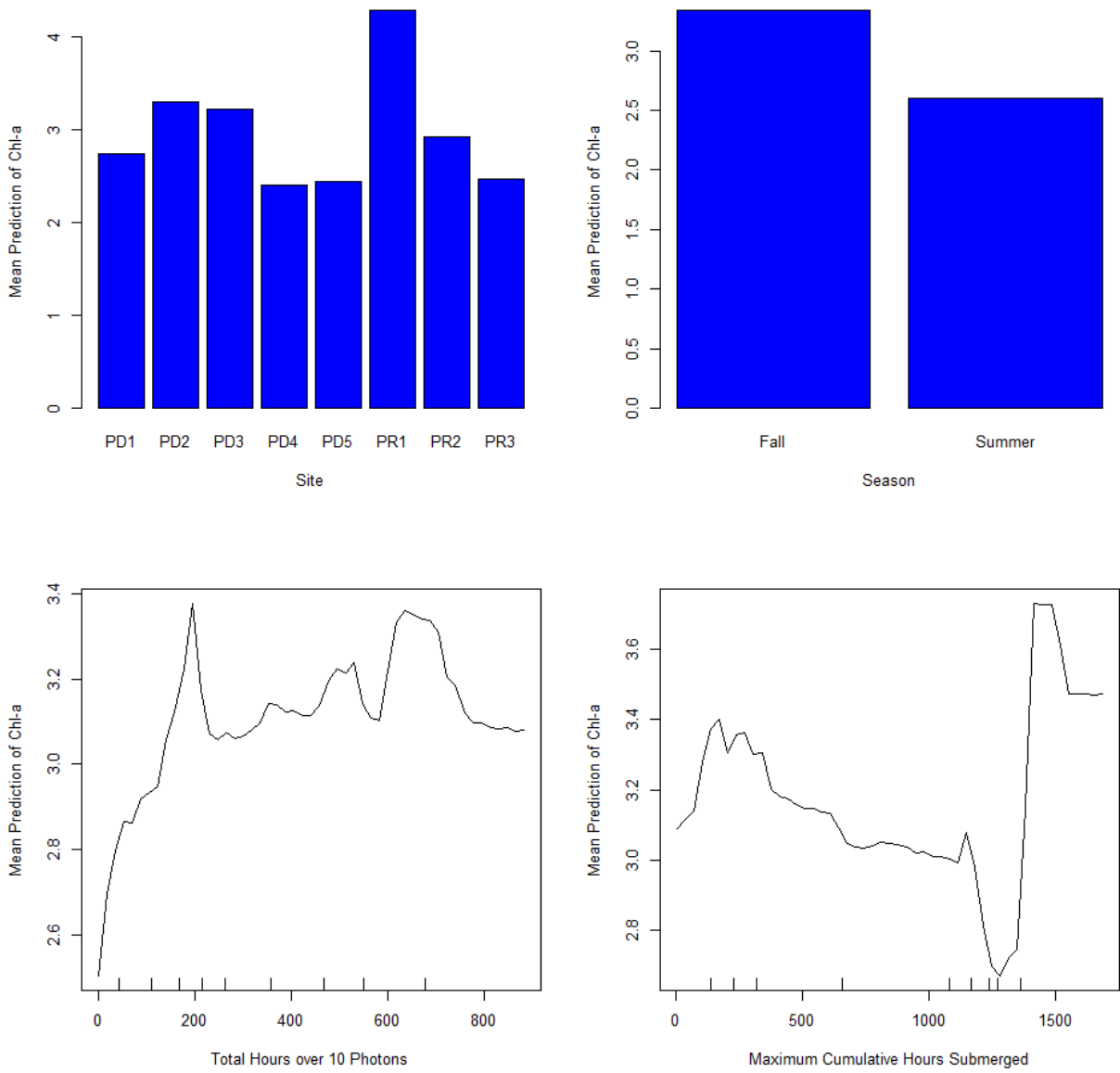


Figure A183 Partial dependence plots for the top four explanatory variables for Chl-a Random Forest Model.



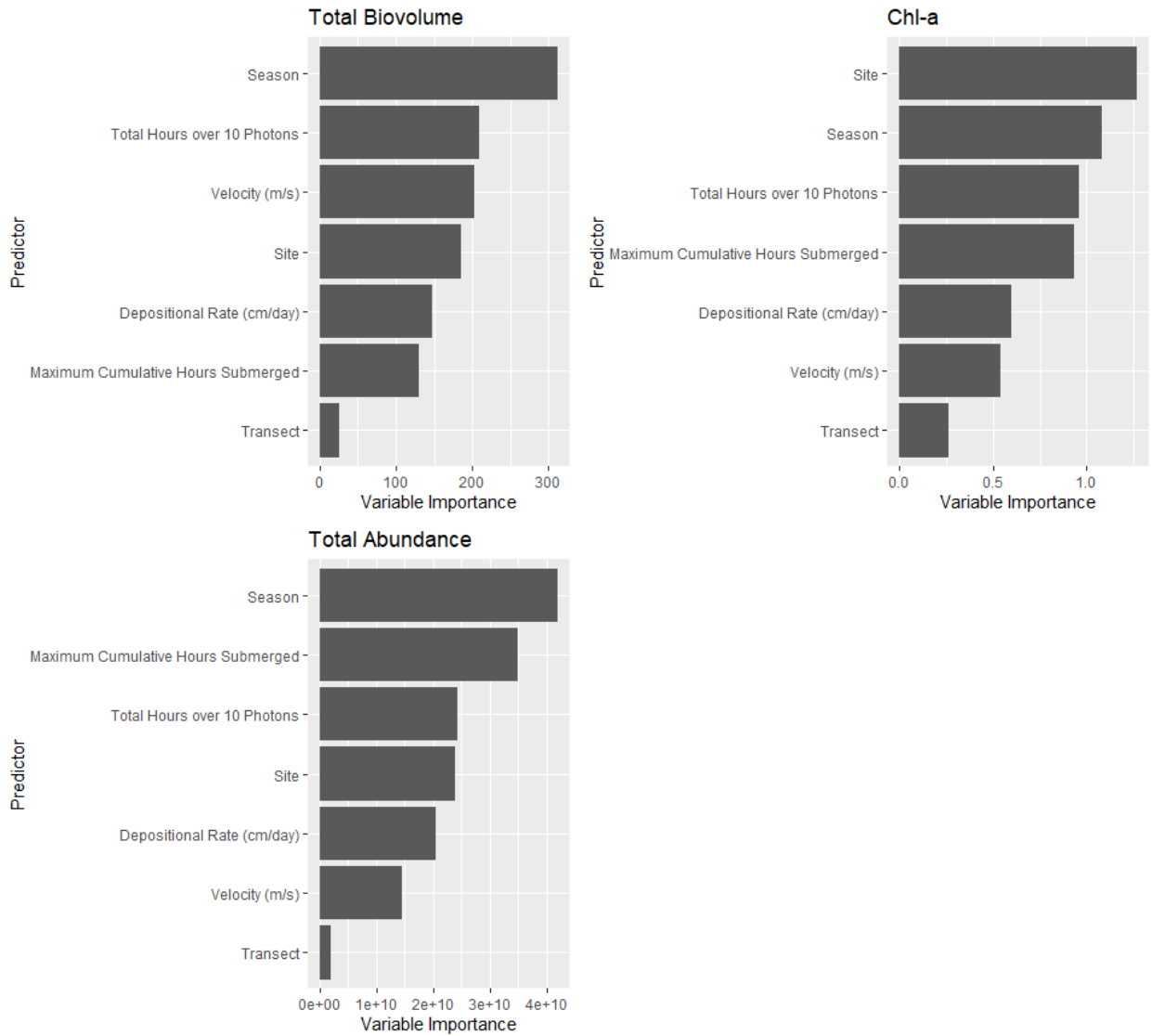


Figure A184 Random Forest variable importance plots for periphyton models.

Table A22 Summary of periphyton Random Forest Models mse=Mean Squared Error, resp=response variable and rsq=model R2.

mse	resp	rsq
726.690	Total Biovolume	0.350
137341379503.070	Total Abundance	0.270
5.310	Chl-a	0.210



Appendix CC Invertebrate 2010-2011 and 2017-2018 Riverine Sites Dredge Results

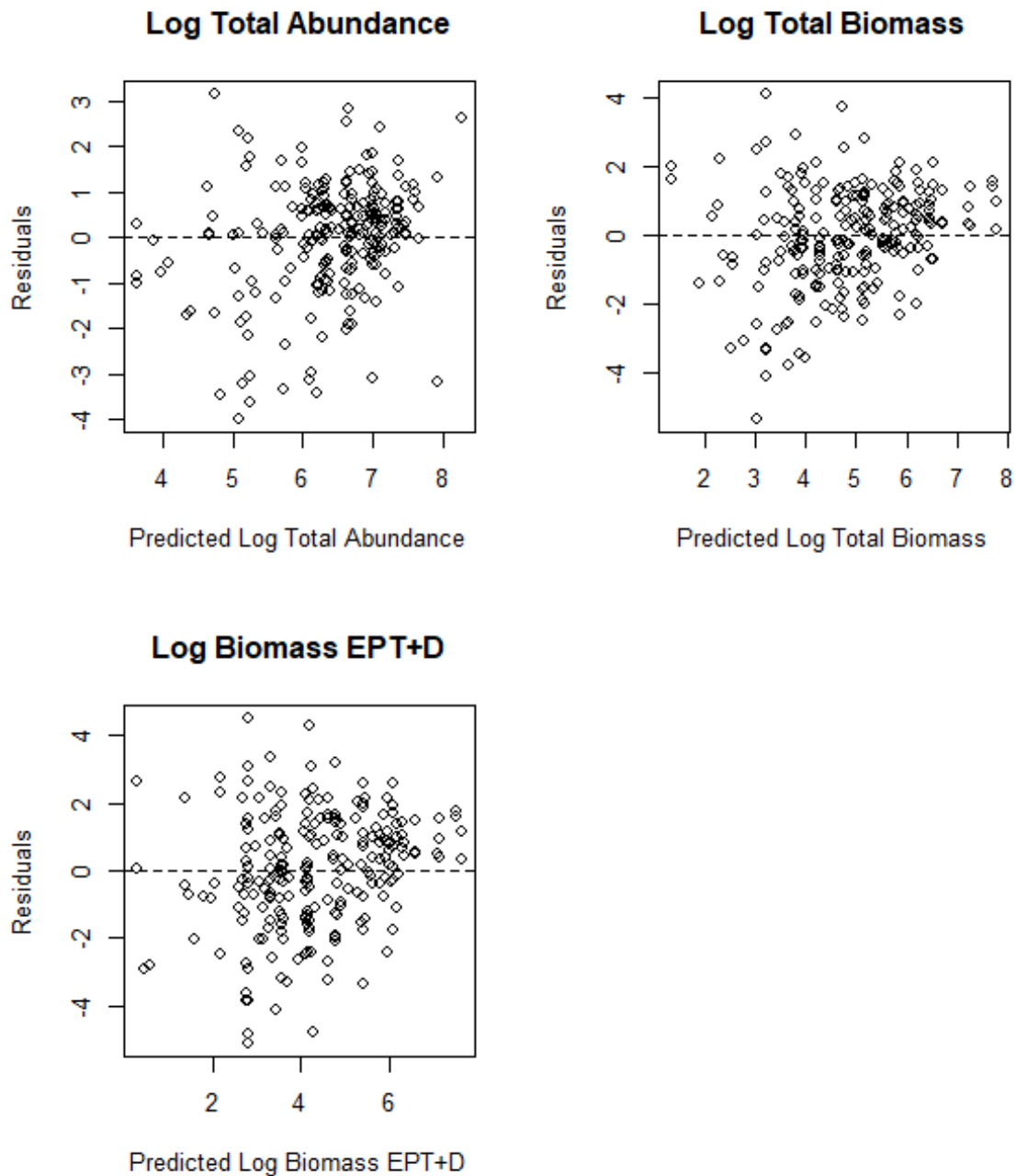


Figure A185 Residual Plots for Benthic Invertebrate Models



Table A23 Summary of plausible models identified using model averaging (those with a delta AIC <3) with pseudo-R2 values and coefficients for all rock basket invertebrate riverine samples 2010-2011 and 2017-2018 except MD and HD.

Response	X.Intercept.	Total Submergence Time (Hours)	R.2	df	AICc	delta	weight
Log Biomass EPT+D	4.840	1.700	0.354	4.000	732.000	0.000	1.000
Log Total Abundance	6.630	0.904	0.291	4.000	622.000	0.000	0.999
Log Total Biomass	5.300	1.210	0.339	4.000	686.000	0.000	1.000



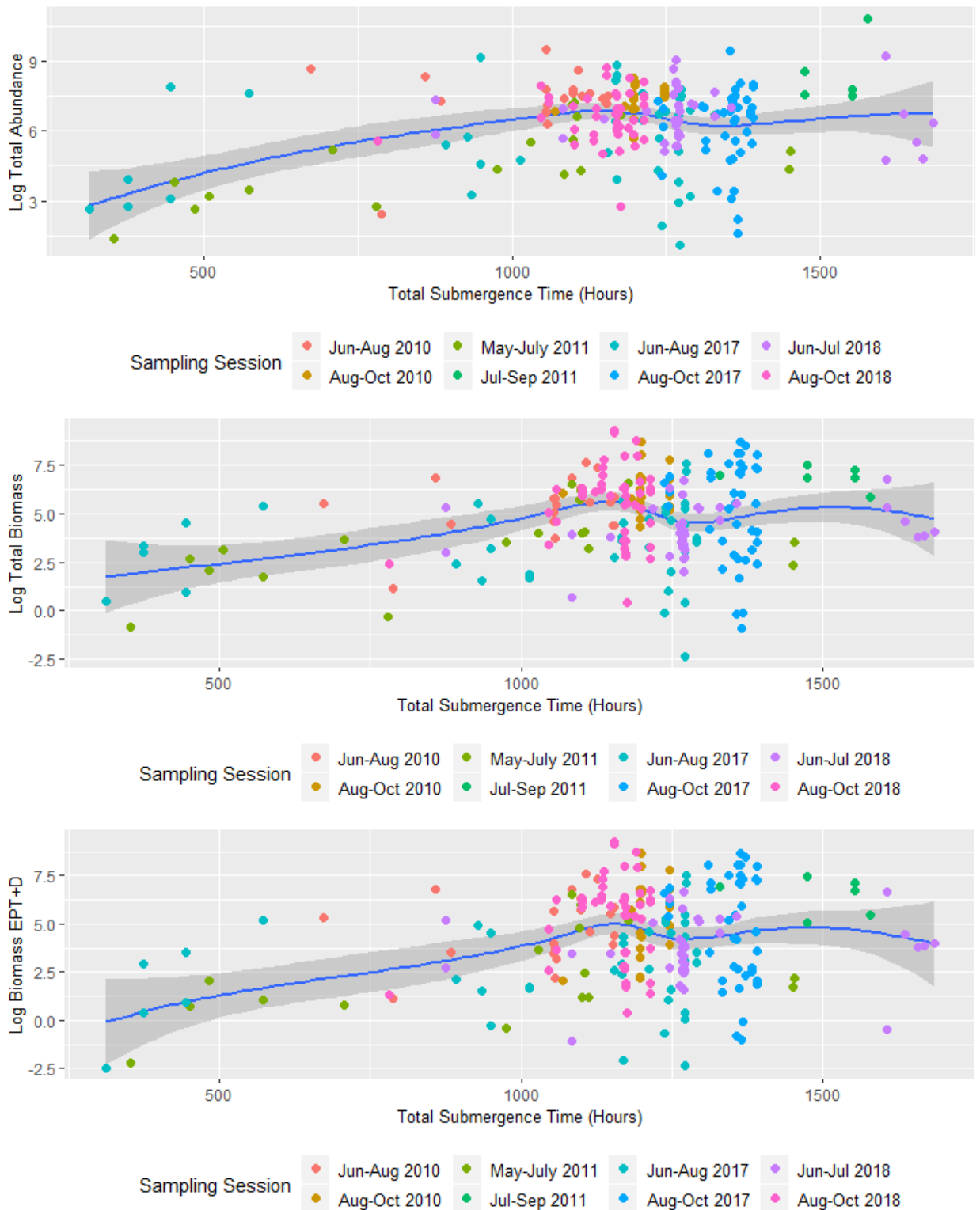


Figure A186 Explanatory variables and benthic invertebrate responses grouped by site for riverine samplers.



Appendix DD River Model Invertebrate Results for Mostly Submerged Rock Baskets

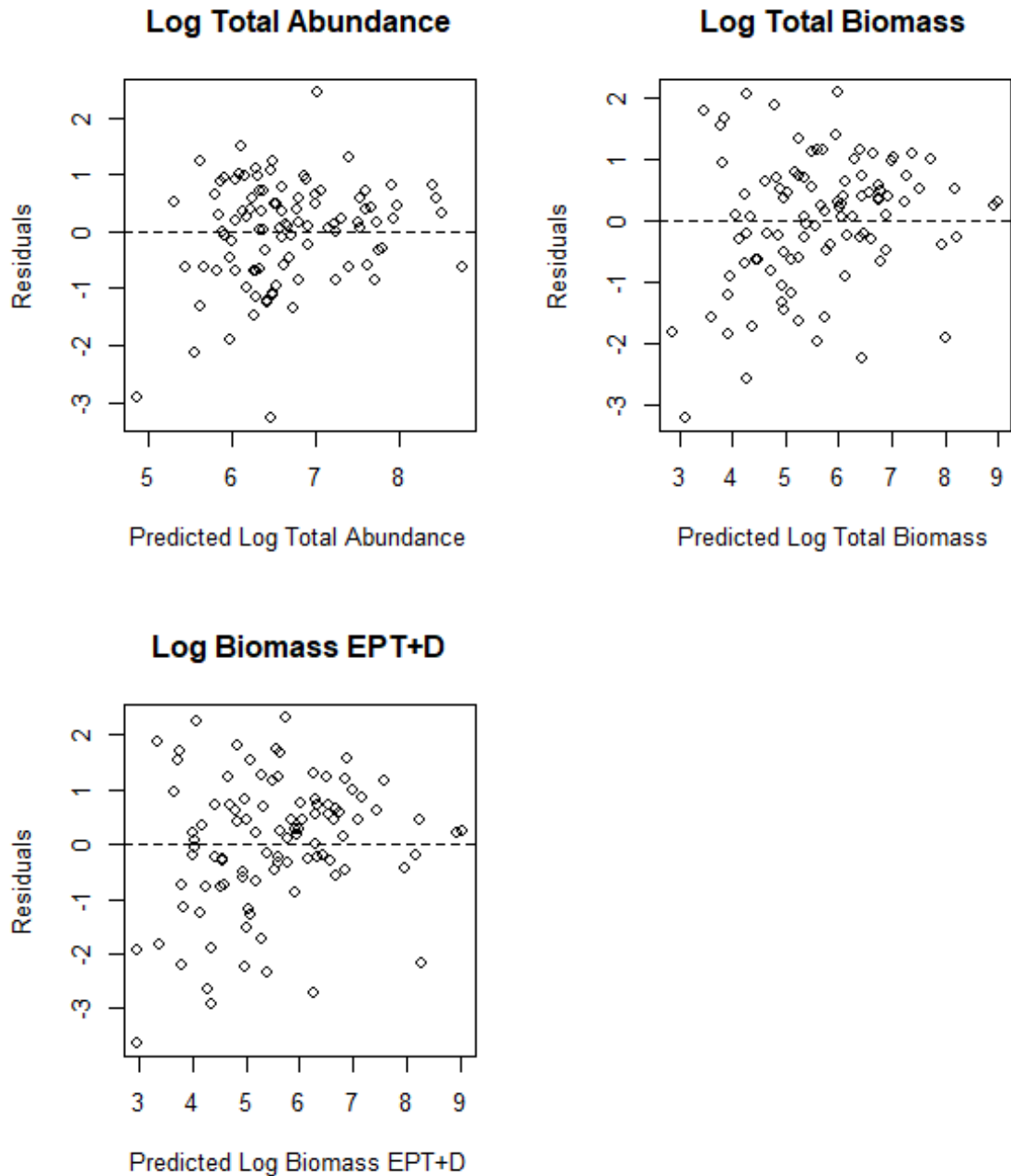


Figure A187 Residual Plots for Mostly Submerged Benthic Invertebrate Models



Table A24 Summary of plausible benthic invertebrate models identified using model averaging (those with a delta AIC <3) with pseudo-R2 values and coefficients for all mostly submerged samplers at Riverine sites not including MD and HD.

Response	X.Intercept.	Average Depth (m)	Total Submergence Time (Hours)	Depositional Rate (cm/day)	Velocity (m/s)	Hours over 10 Photons	R.2	df	AICc	delta	weight
Log Biomass EPT+D	5.380			0.941		1.250	0.305	5.000	383.000	0.000	0.177
Log Biomass EPT+D	5.400			1.000	-0.553	1.280	0.318	6.000	384.000	0.436	0.143
Log Biomass EPT+D	5.380	0.655		1.010		1.150	0.316	6.000	384.000	0.763	0.121
Log Biomass EPT+D	5.390	0.936	0.653	1.190		1.050	0.331	7.000	384.000	0.841	0.116
Log Biomass EPT+D	5.400	0.667		1.080	-0.566	1.180	0.330	7.000	384.000	1.090	0.103
Log Biomass EPT+D	5.410	0.937	0.630	1.250	-0.544	1.080	0.344	8.000	385.000	1.270	0.094
Log Biomass EPT+D	5.390		0.376	1.030		1.210	0.311	6.000	385.000	1.470	0.085
Log Biomass EPT+D	5.410		0.349	1.080	-0.534	1.250	0.323	7.000	385.000	2.040	0.064
Log Total Abundance	6.640		1.120	0.610			0.274	5.000	308.000	0.000	0.369
Log Total Abundance	6.640	0.197	1.180	0.648			0.277	6.000	310.000	1.900	0.143
Log Total Abundance	6.640		1.110	0.617	-0.100		0.274	6.000	310.000	2.200	0.123
Log Total Abundance	6.640		1.130	0.615		-0.083	0.274	6.000	310.000	2.220	0.121
Log Total Biomass	5.500			0.712	-0.767	1.180	0.356	6.000	359.000	0.000	0.168
Log Total Biomass	5.480			0.695		1.120	0.334	5.000	360.000	0.935	0.106
Log Total Biomass	5.500	0.579		0.768	-0.777	1.100	0.365	7.000	360.000	1.060	0.099
Log Total Biomass	5.510	0.833	0.598	0.924	-0.720	1.020	0.379	8.000	360.000	1.250	0.090



Response	X.Intercept.	Average Depth (m)	Total Submergence Time (Hours)	Depositional Rate (cm/day)	Velocity (m/s)	Hours over 10 Photons	R.2	df	AICc	delta	weight
Log Total Biomass	5.510		0.358	0.792	-0.732	1.150	0.362	7.000	360.000	1.480	0.080
Log Total Biomass	5.490	0.844	0.658	0.923		0.966	0.359	7.000	360.000	1.880	0.066
Log Total Biomass	5.490				-0.739	1.370	0.327	5.000	361.000	2.000	0.062
Log Total Biomass	5.480	0.562		0.748		1.040	0.342	6.000	361.000	2.070	0.060
Log Total Biomass	5.490		0.415	0.789		1.100	0.342	6.000	361.000	2.120	0.058
Log Total Biomass	5.470					1.310	0.306	4.000	361.000	2.710	0.043



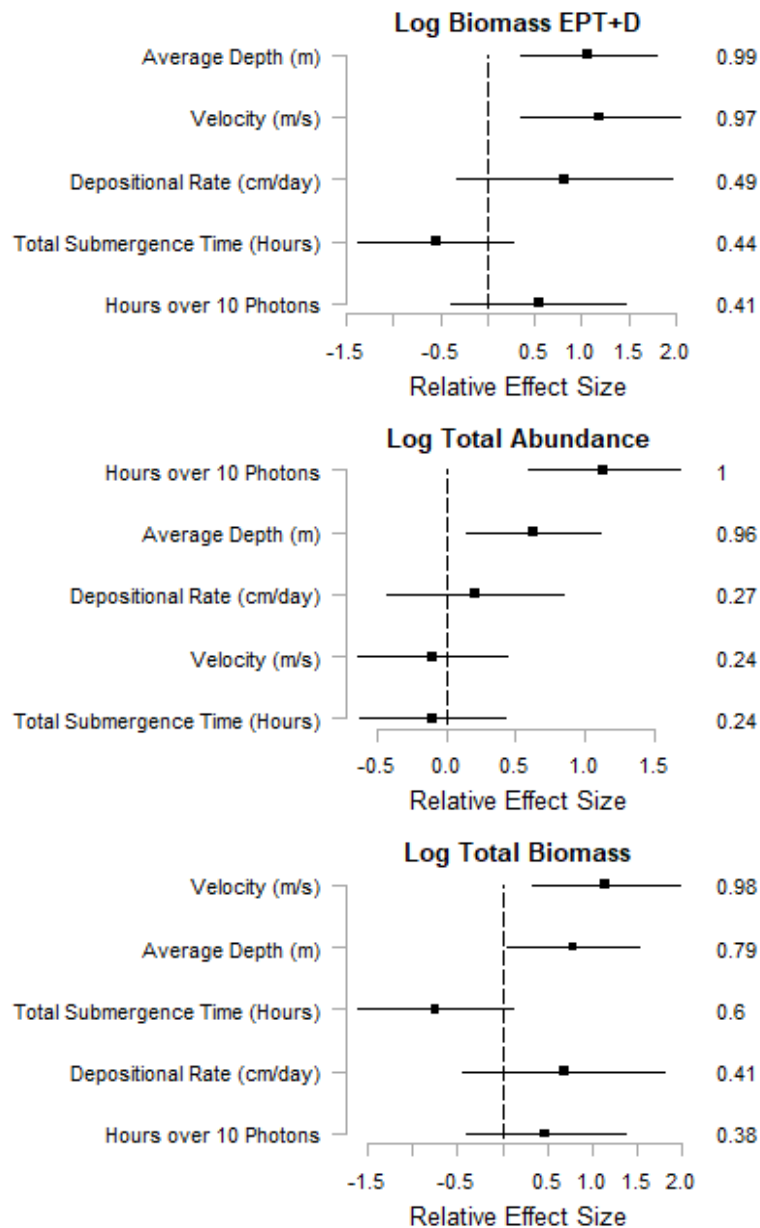


Figure A188 The coefficients and their 95% CLs of standardized explanatory variables of benthic invertebrates for mostly submerged riverine samplers. Benthic invertebrates responses included abundance, biomass EPT+D and biomass. Explanatory variables included mean depth over deployment, total hours submerged, velocity, total hours over 10 photons and depositional rate. Coefficients were standardized to allow comparisons of the direction and size of effects, noting that variables with CLs that do not cross zero have an effect on the response variable. Key explanatory variables are those that have a relative variable importance (RVI) of greater than 0.6-0.7 and the RVI is shown on the right-hand side of each figure.



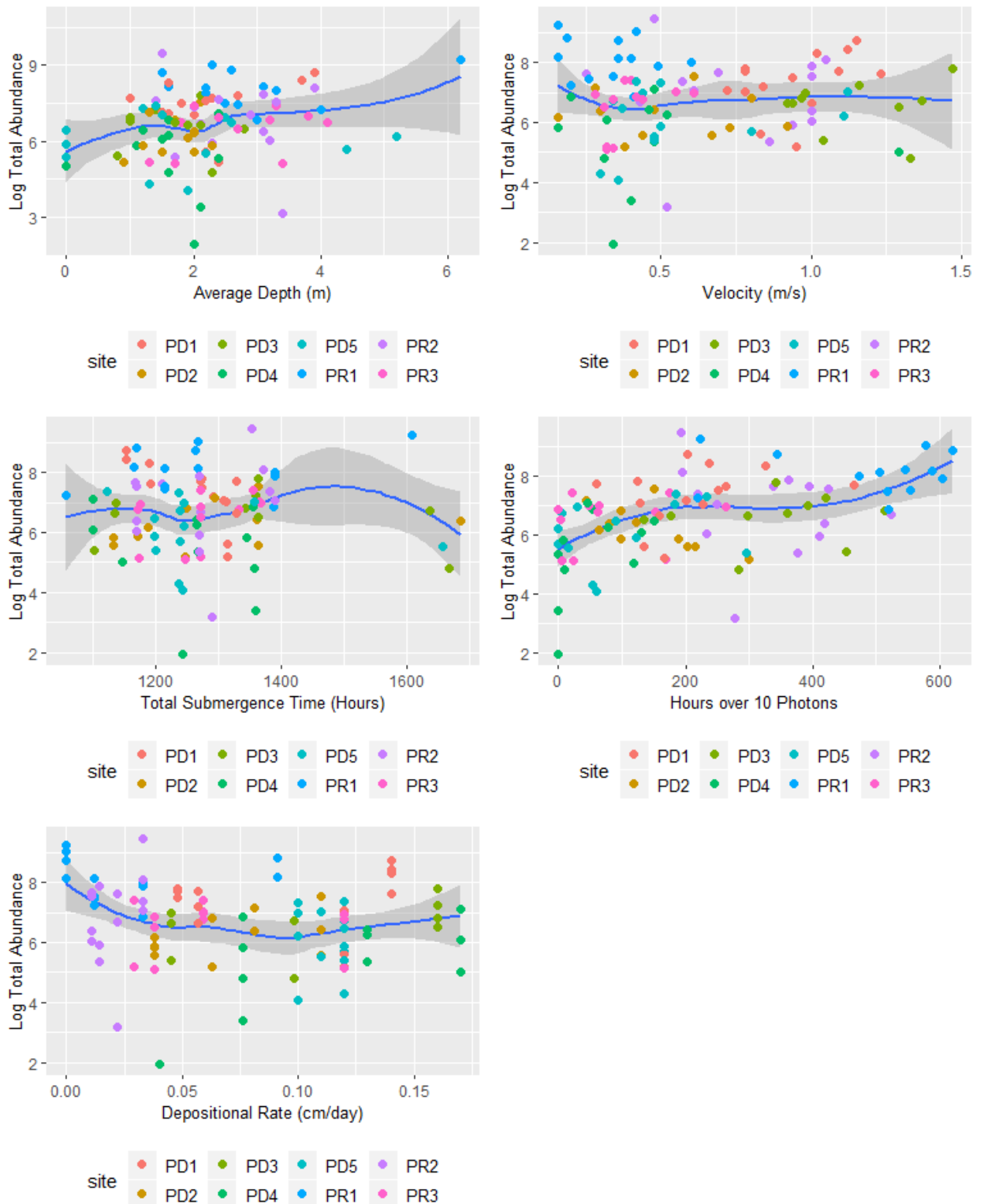


Figure A189 Explanatory variables and Log Total Abundance grouped by site for all mostly submerged Riverine Samplers.



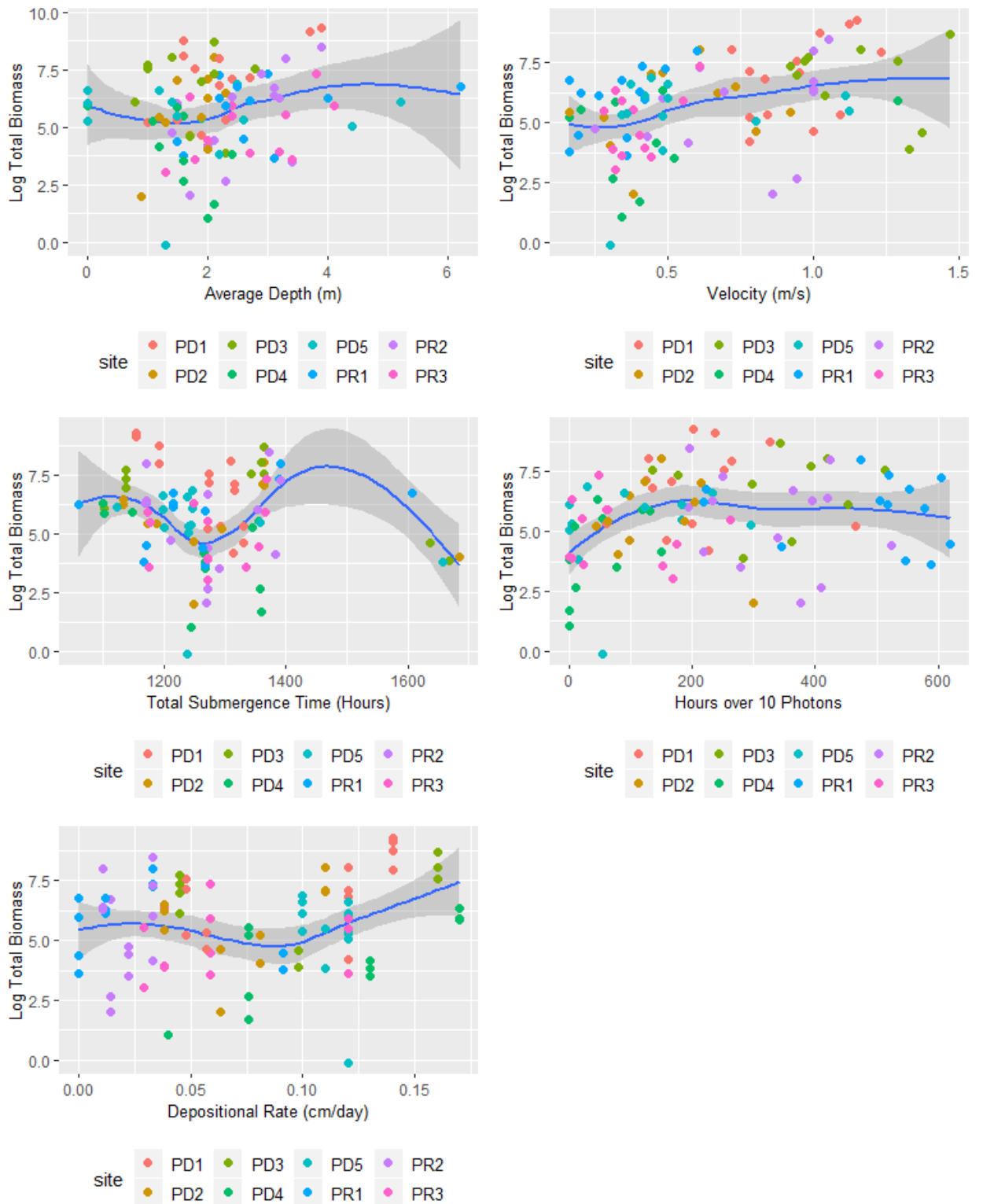


Figure A190 Explanatory variables and Log Total Biomass grouped by site for all mostly submerged Riverine Samplers.



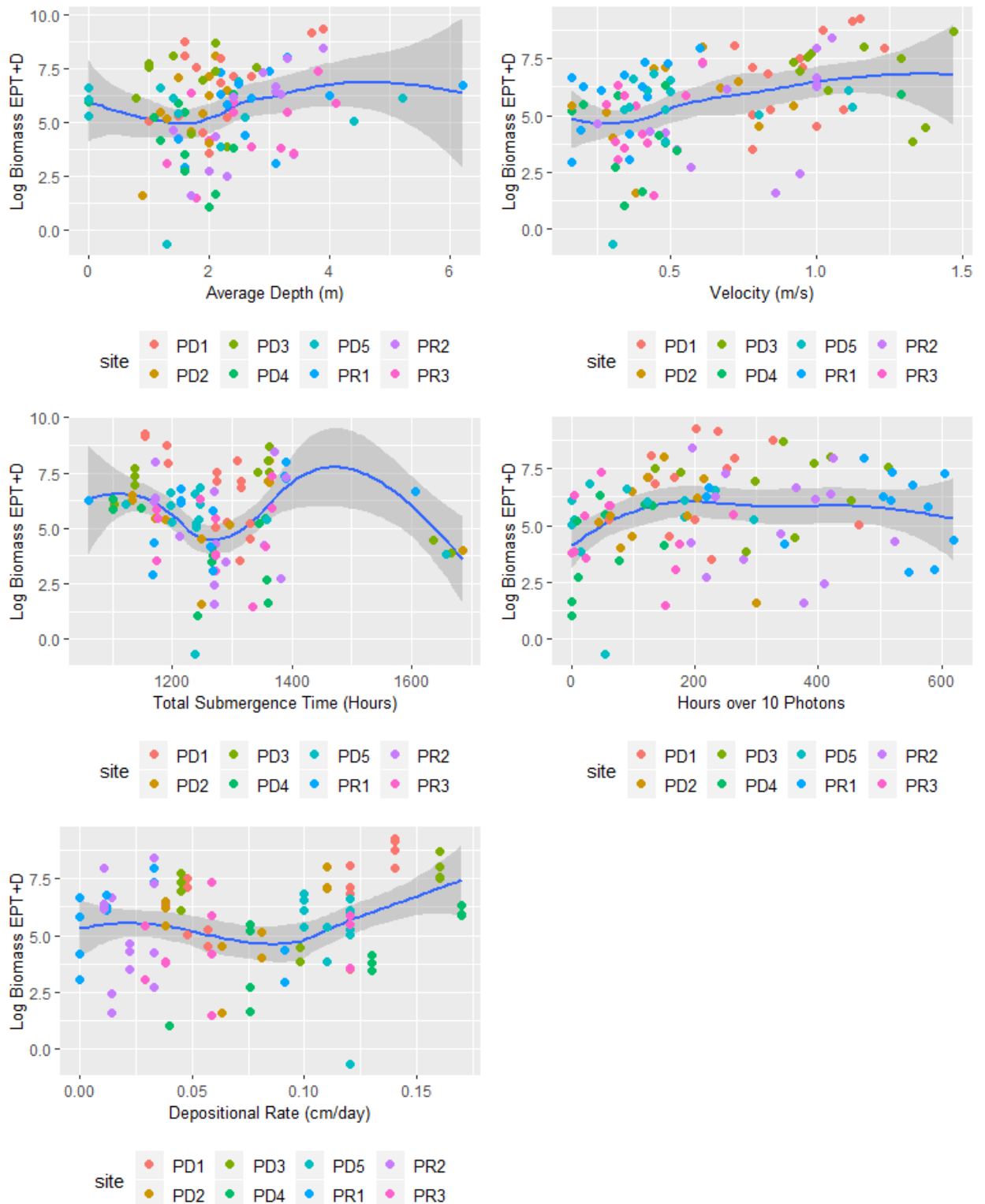


Figure A191 Explanatory variables and Log Biomass EPT+D grouped by site for all mostly submerged Riverine Samplers.



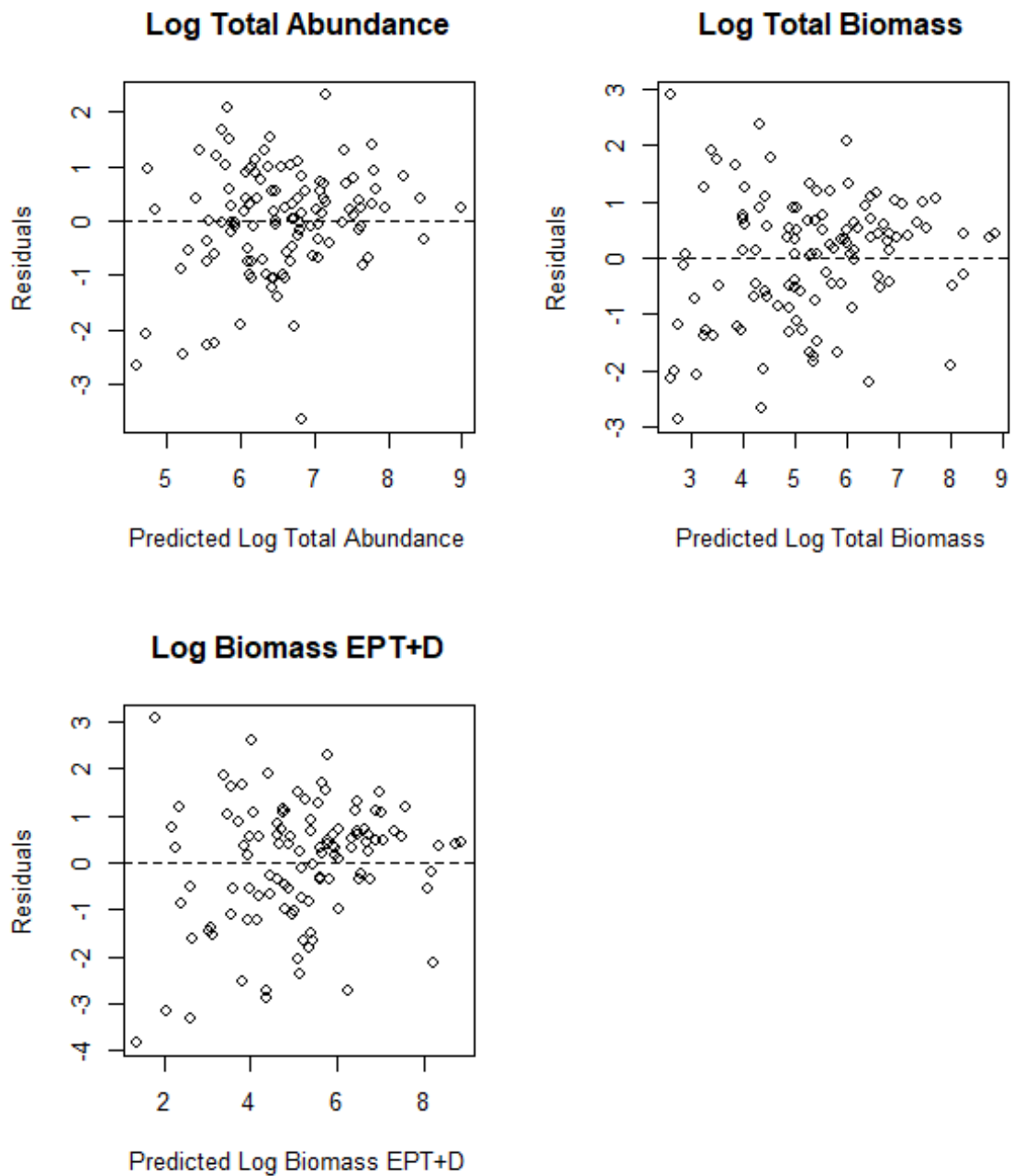
Appendix EE River Model Results for All Rock Baskets**Figure A192 Residual Plots for Full Transect Benthic Invertebrate Models**

Table A25 Summary of plausible benthic invertebrate models identified using model averaging (those with a delta AIC <3) with pseudo-R2 values and coefficients for all riverine samplers except for MD and HD.

Response	X.Intercept.	Average Depth (m)	Total Submergence Time (Hours)	Depositional Rate (cm/day)	Velocity (m/s)	Hours over 10 Photons	R.2	df	AICc	delta	weight
Log Biomass EPT+D	5.140			1.100		1.480	0.384	5.000	458.000	0.000	0.299
Log Biomass EPT+D	5.130	0.584		1.150		1.380	0.391	6.000	459.000	1.050	0.177
Log Biomass EPT+D	5.130			0.998	0.258	1.400	0.387	6.000	460.000	1.780	0.123
Log Biomass EPT+D	5.140		0.151	1.160		1.480	0.385	6.000	460.000	2.100	0.105
Log Biomass EPT+D	5.130	0.719	0.323	1.300		1.380	0.394	7.000	461.000	2.720	0.077
Log Biomass EPT+D	5.130	0.562		1.060	0.231	1.310	0.393	7.000	461.000	2.970	0.068
Log Total Abundance	6.560		0.935	0.603	0.581		0.268	6.000	380.000	0.000	0.245
Log Total Abundance	6.570		0.612	0.695			0.243	5.000	381.000	1.610	0.110
Log Total Abundance	6.560	0.104	0.960	0.619	0.579		0.269	7.000	382.000	2.200	0.082
Log Total Abundance	6.560		0.935	0.605	0.597	-0.069	0.268	7.000	382.000	2.250	0.080
Log Total Abundance	6.560		0.693		0.694		0.236	5.000	382.000	2.640	0.066
Log Total Biomass	5.320			0.854		1.210	0.410	5.000	427.000	0.000	0.303
Log Total Biomass	5.320	0.456		0.891		1.140	0.414	6.000	428.000	1.430	0.149
Log Total Biomass	5.320		0.305	0.984		1.230	0.413	6.000	429.000	1.510	0.143
Log Total Biomass	5.320			0.871	-0.045	1.220	0.410	6.000	429.000	2.210	0.101
Log Total Biomass	5.320	0.640	0.444	1.100		1.140	0.421	7.000	429.000	2.240	0.099



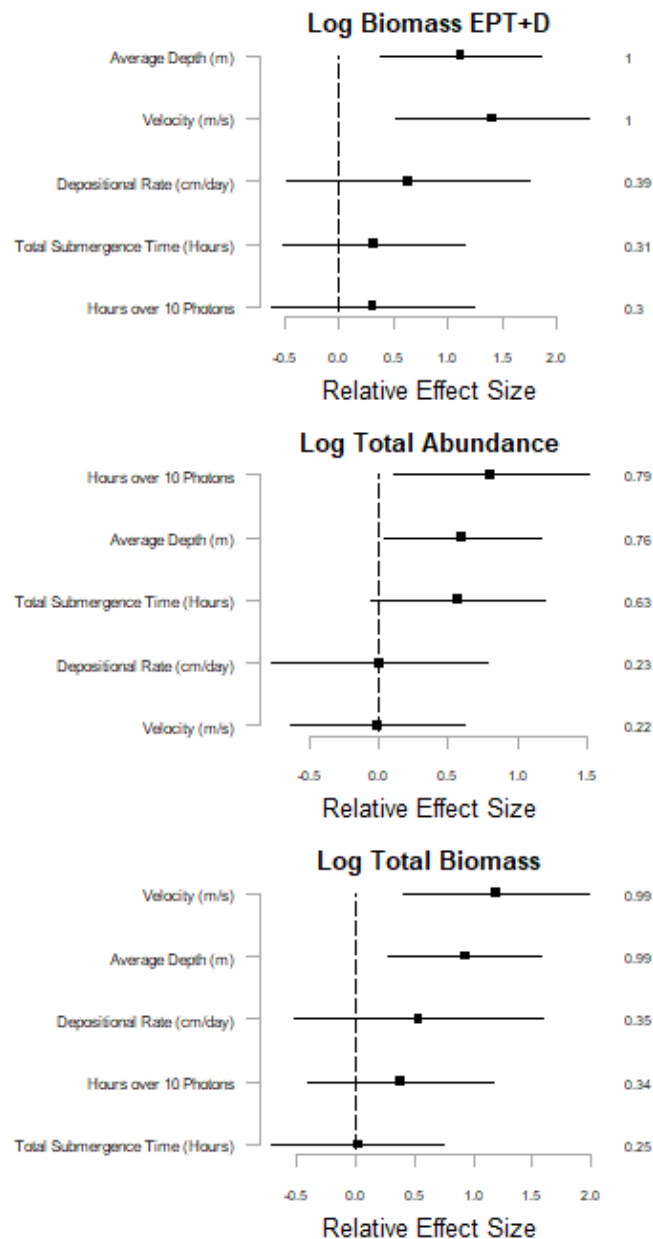


Figure A193 The coefficients and their 95% CLs of standardized explanatory variables of benthic invertebrates for all riverine samplers except MD and HD. Benthic invertebrates responses included abundance, biomass and biomass of EPT+D. Explanatory variables included mean depth over deployment, total hours submerged, velocity, total hours over 10 photons and depositional rate. Coefficients were standardized to allow comparisons of the direction and size of effects, noting that variables with CLs that do not cross zero have an effect on the response variable. Key explanatory variables are those that have a relative variable importance (RVI) of greater than 0.6-0.7 and the RVI is shown on the right-hand side of each figure.



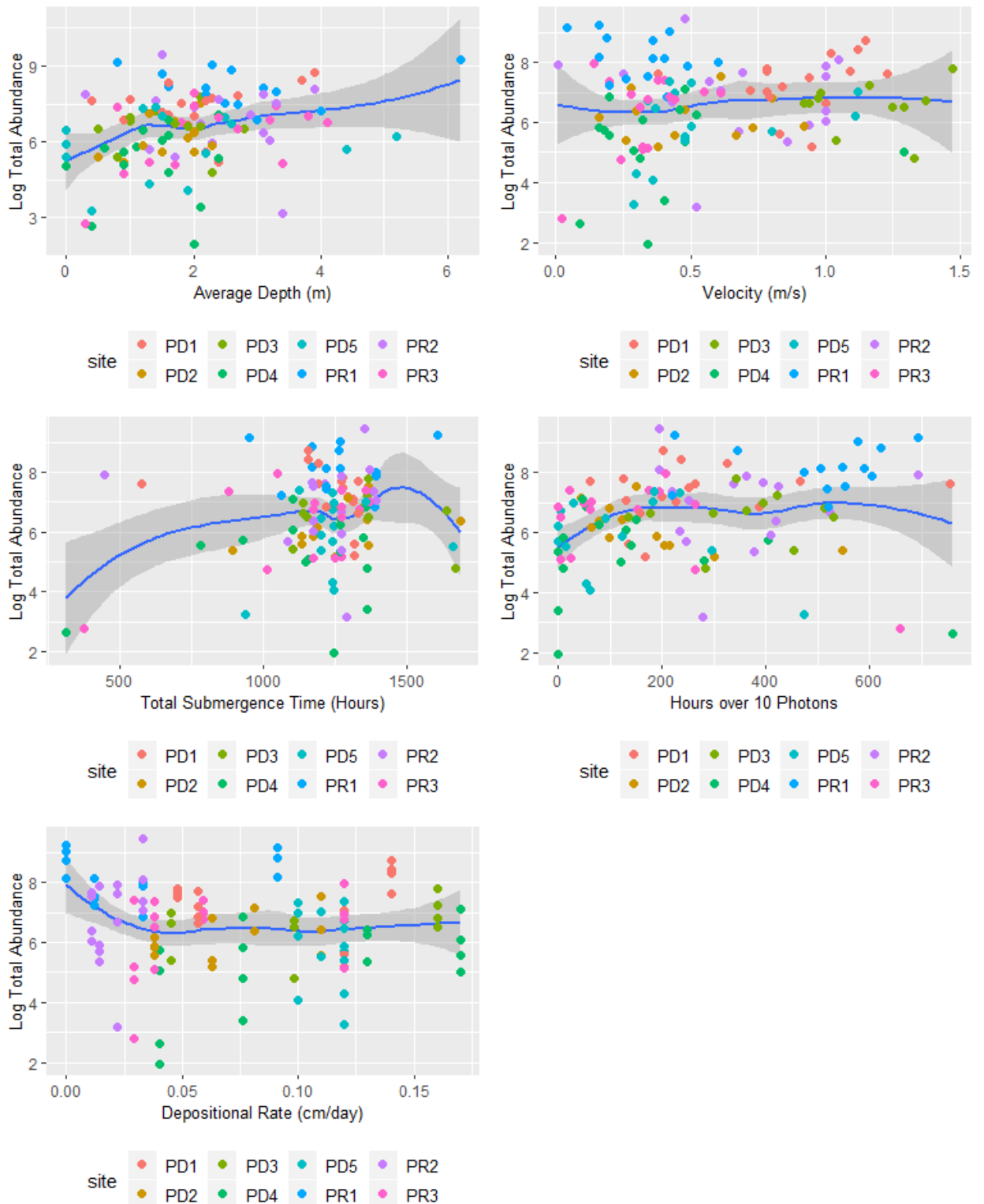


Figure A194 Explanatory variables and Log Total Abundance grouped by site for riverine samplers.



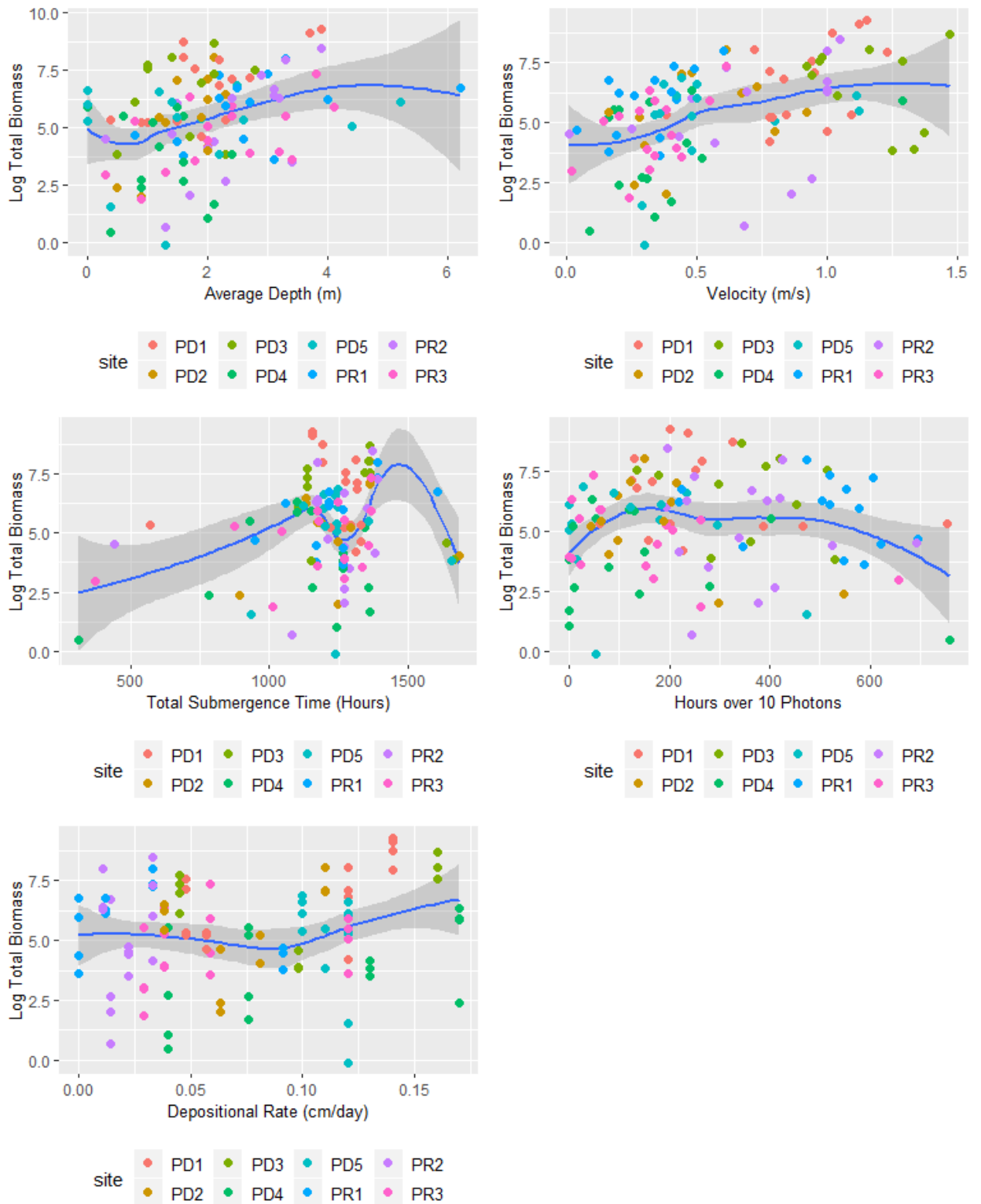


Figure A195 Explanatory variables and Log Total Biomass grouped by site for riverine samplers.



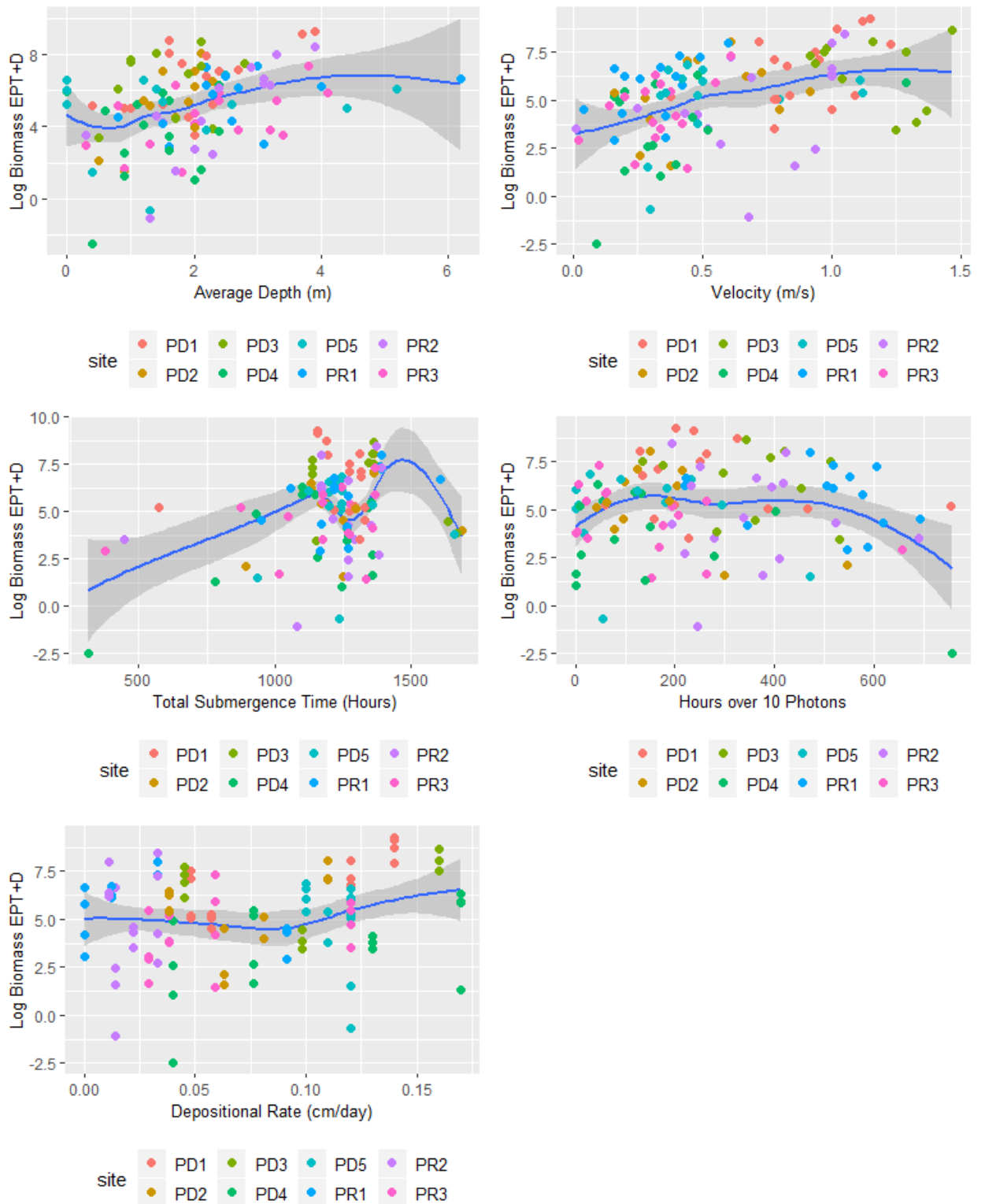


Figure A196 Explanatory variables and Log Biomass EPT+D grouped by site for riverine samplers.



Appendix FF River Benthic invertebrates Random Forest Results

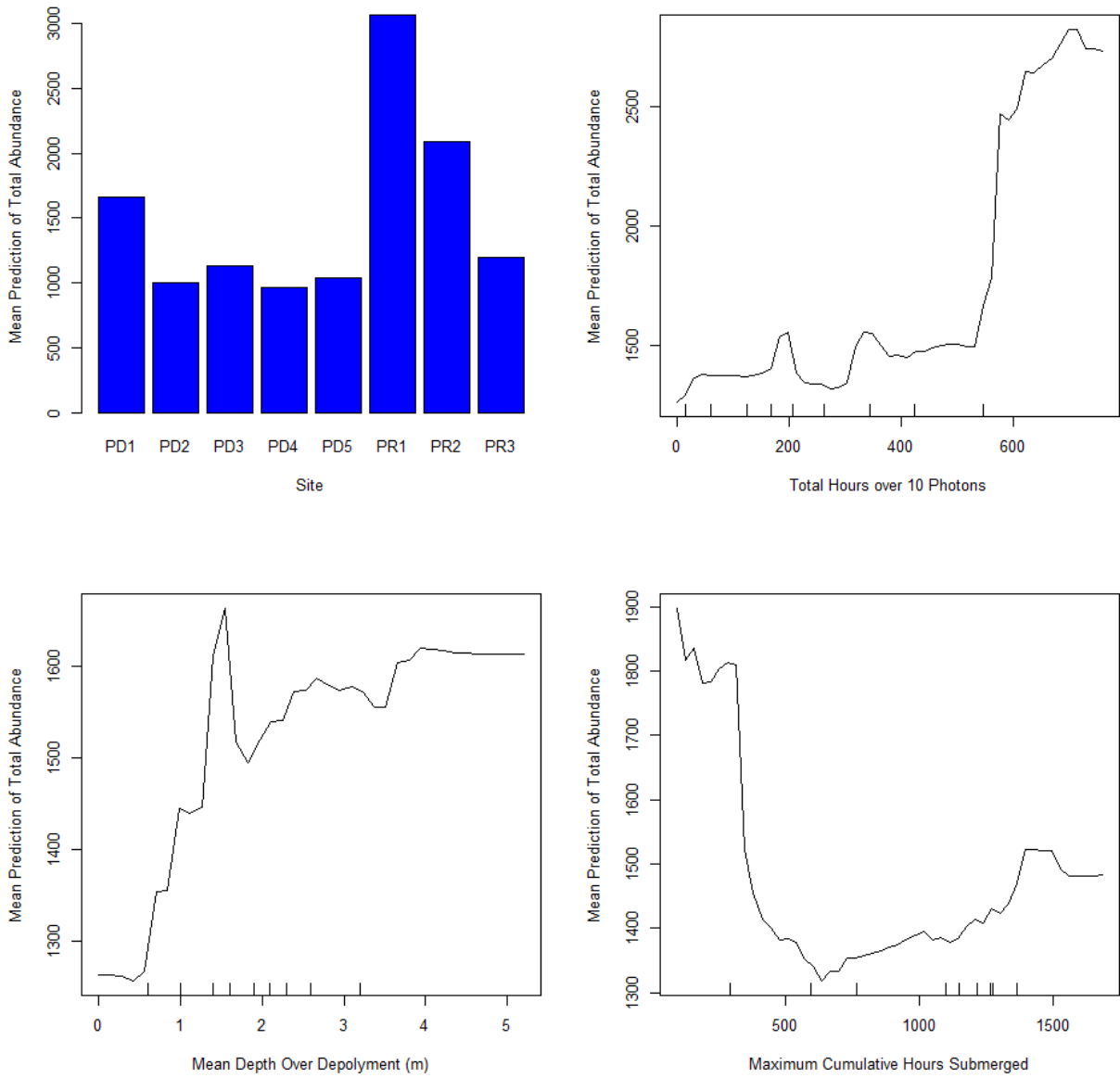


Figure A197 Partial dependence plots for the top four explanatory variables for Total Abundance Random Forest Model.



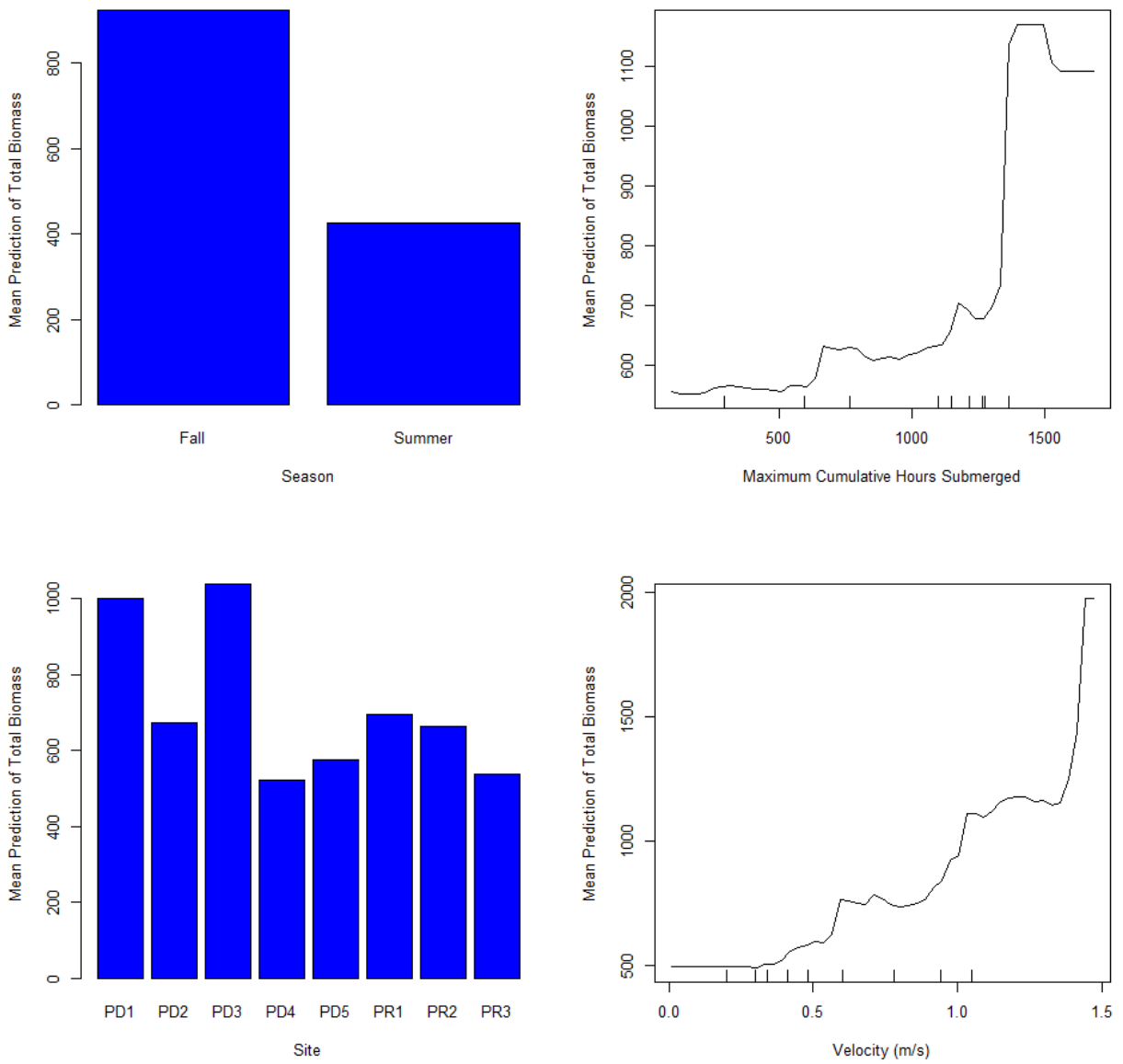


Figure A198 Partial dependence plots for the top four explanatory variables for Total Biomass Random Forest Model.



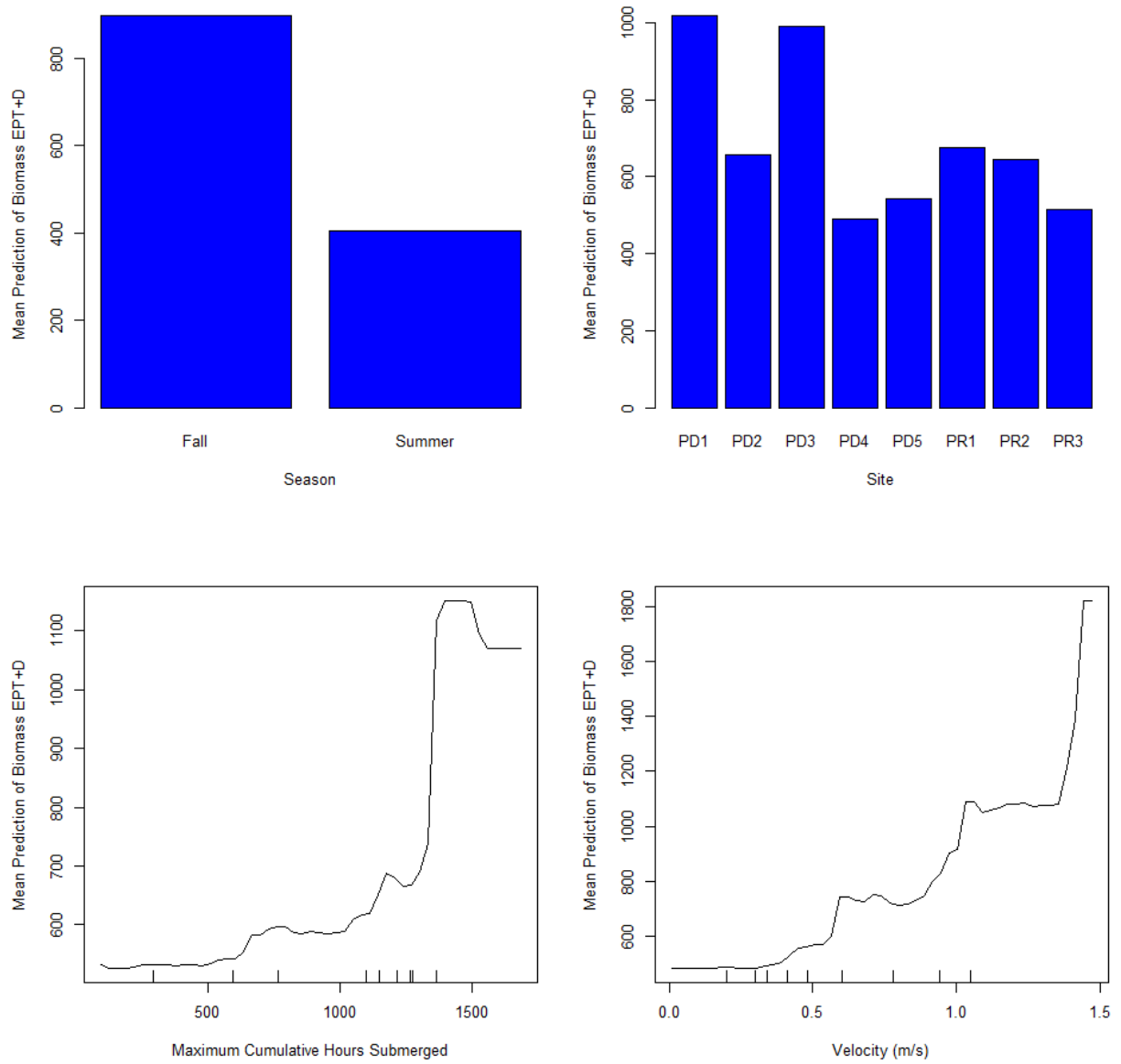


Figure A199 Partial dependence plots for the top four explanatory variables for Biomass EPT+D Random Forest Model.



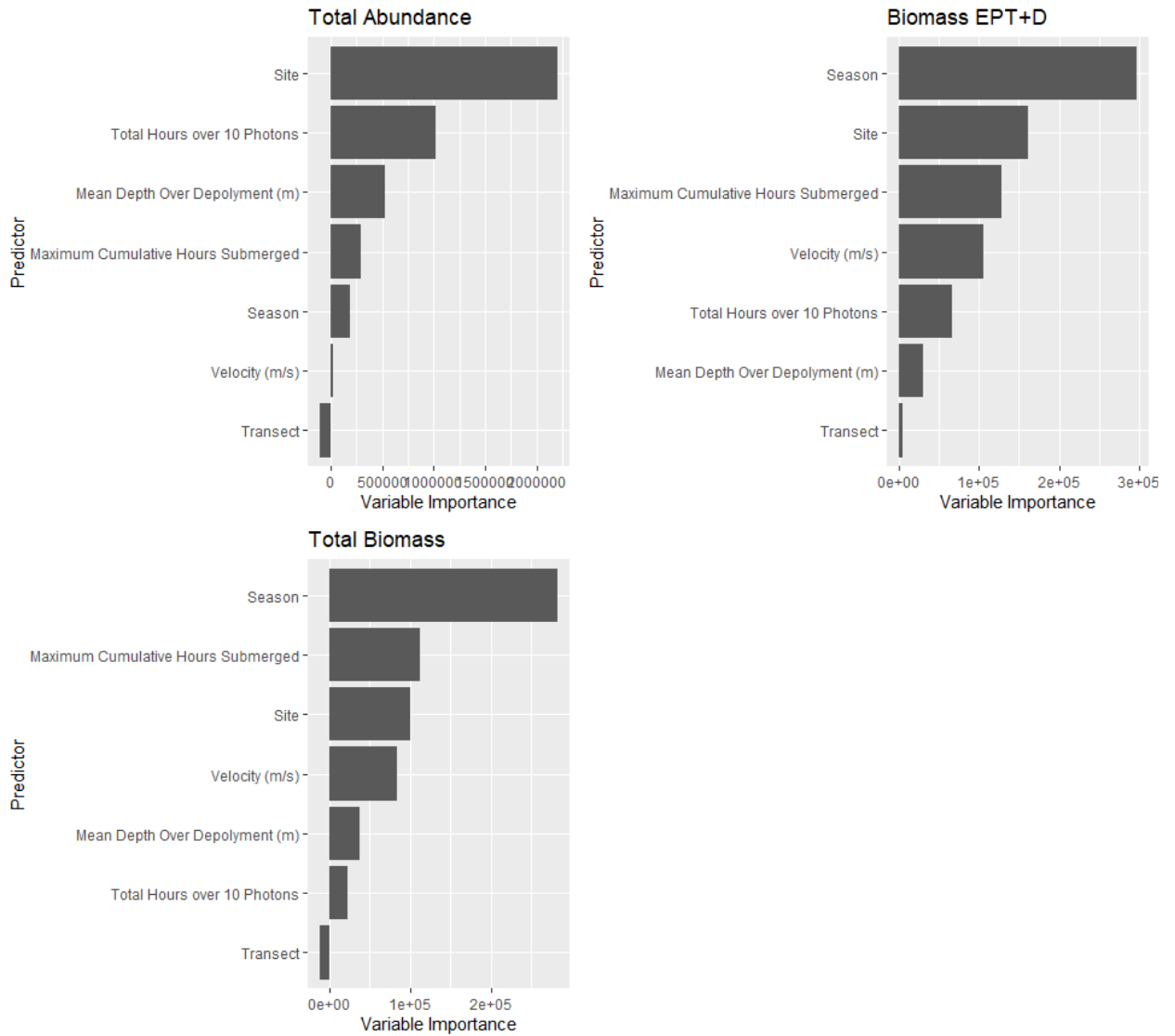


Figure A200 Random Forest variable importance plots for benthic invertebrate models.

Table A26 Summary of Benthic Invertebrate Random Forest Models mse=Mean Squared Error, resp=response variable and rsq=model R2.

mse	resp	rsq
3099618.150	Total Abundance	0.160
937567.520	Total Biomass	0.280
859250.680	Biomass EPT+D	0.340



Appendix GG Fish Stomach NMDS Analysis and Percent Abundance

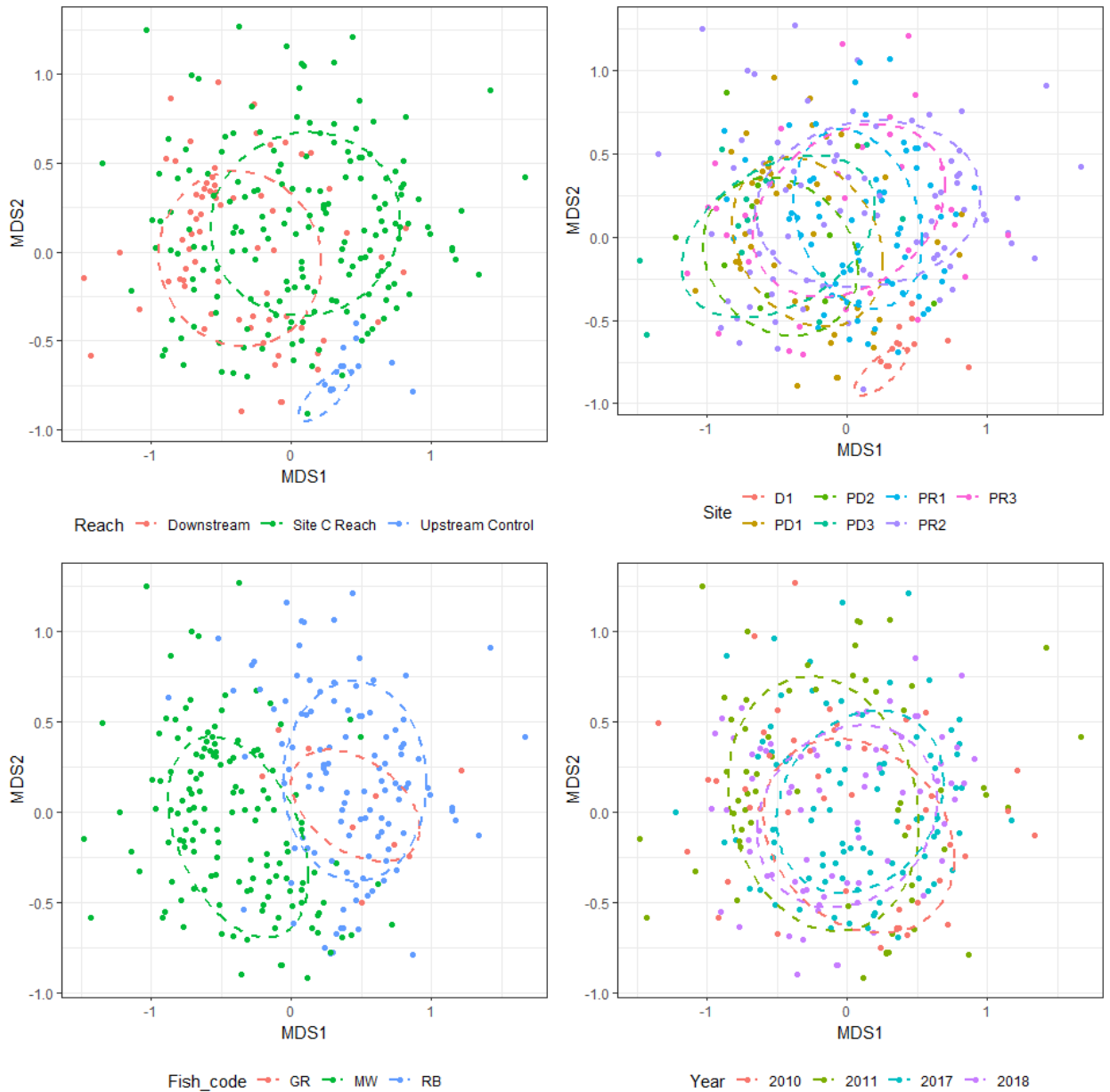


Figure A201 NMDS plots of benthic invertebrates consumed by fish in upstream reservoirs, Site C Reach, and downstream areas with a stress index of 0.21 . Data is considered by Reach, Site, Species, and Year. GR= Arctic Grayling, MW= Mountain Whitefish, and RB= Rainbow Trout.



Table A1 PERMANOVA results for fish stomachs at family level.

group	R_stat	Fstat	p_val
reach	0.060	10.850	<0.001
site	0.090	5.200	<0.001
fish_code	0.060	9.590	<0.001
year	0.020	6.700	<0.001

Table A2 Taxa scores for NMDS axes with p-value and R2.

Species	NMDS1	NMDS2	pval	r2
Baetidae	0.040	0.180	0.000	0.030
Brachycentridae	-0.130	0.040	0.040	0.020
Chironomidae	0.040	-0.400	0.000	0.160
Chloroperlidae	-0.190	0.160	0.000	0.060
Corixidae	0.250	0.190	0.000	0.100
Ephemerellidae	-0.010	0.130	0.060	0.020
Ephemeroptera	0.160	0.070	0.000	0.030
Glossosomatidae	-0.310	-0.110	0.000	0.110
Heptageniidae	-0.220	0.300	0.000	0.140
Hydropsychidae	-0.270	0.120	0.000	0.090
Perlodidae	-0.070	0.070	0.200	0.010
Plecoptera	0.080	0.000	0.300	0.010
Trichoptera	0.040	0.130	0.020	0.020



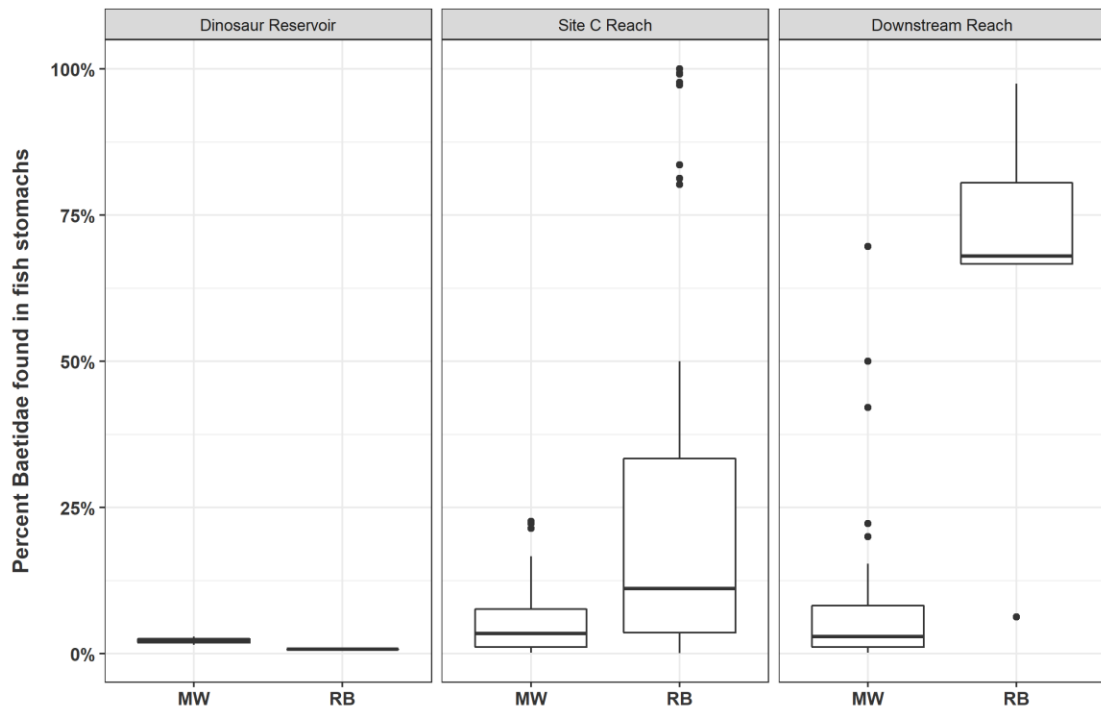


Figure A202 Percentage of Baetidae found in fish stomachs in the Dinosaur Reservoir, Site C Reach, and Downstream Reach

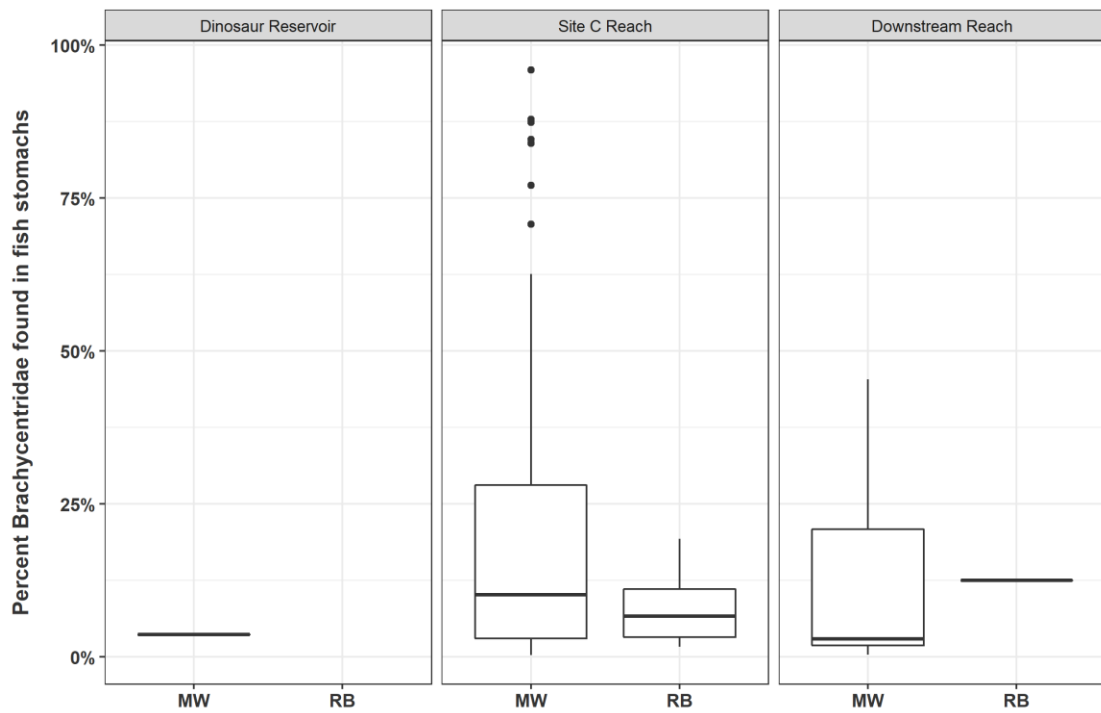


Figure A203 Percentage of Brachycentridae found in fish stomachs in the Dinosaur Reservoir, Site C Reach, and Downstream Reach



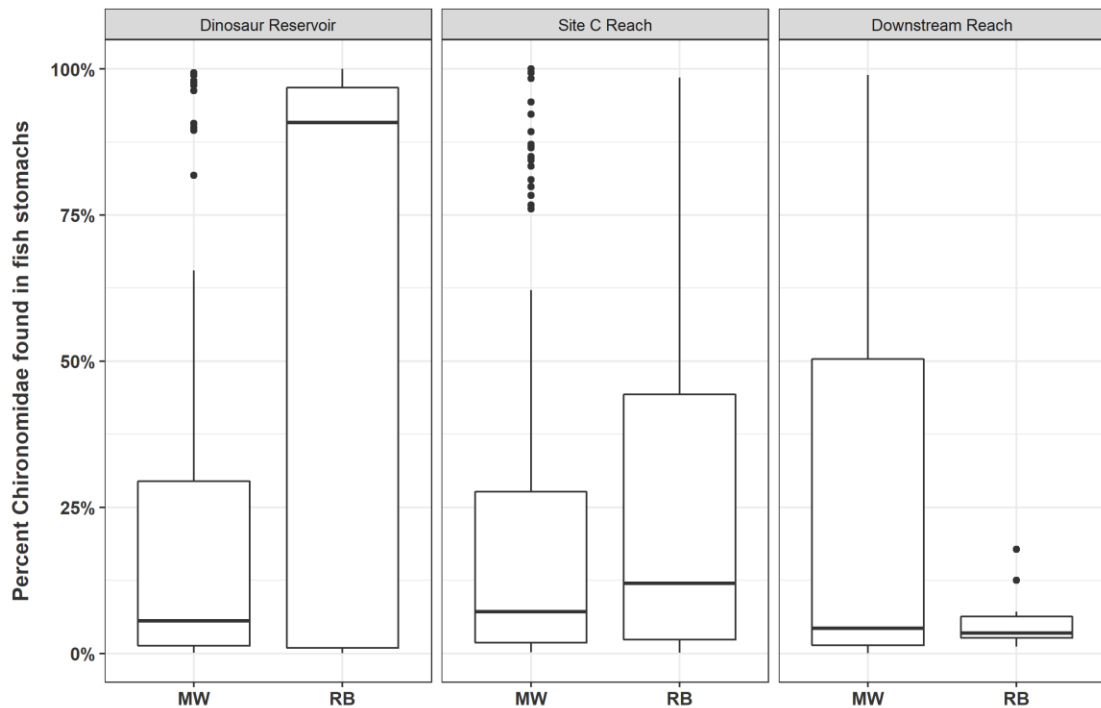


Figure A204 Percentage of Chironomidae found in fish stomachs in the Dinosaur Reservoir, Site C Reach, and Downstream Reach

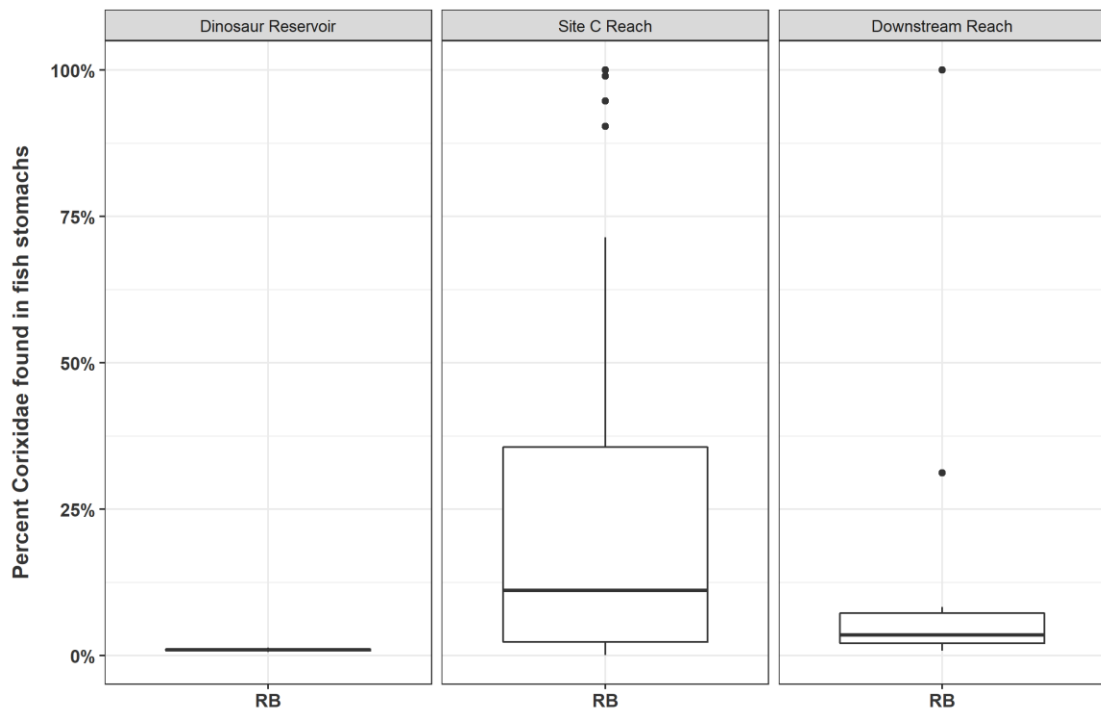


Figure A205 Percentage of Corixidae found in fish stomachs in the Dinosaur Reservoir, Site C Reach, and Downstream Reach



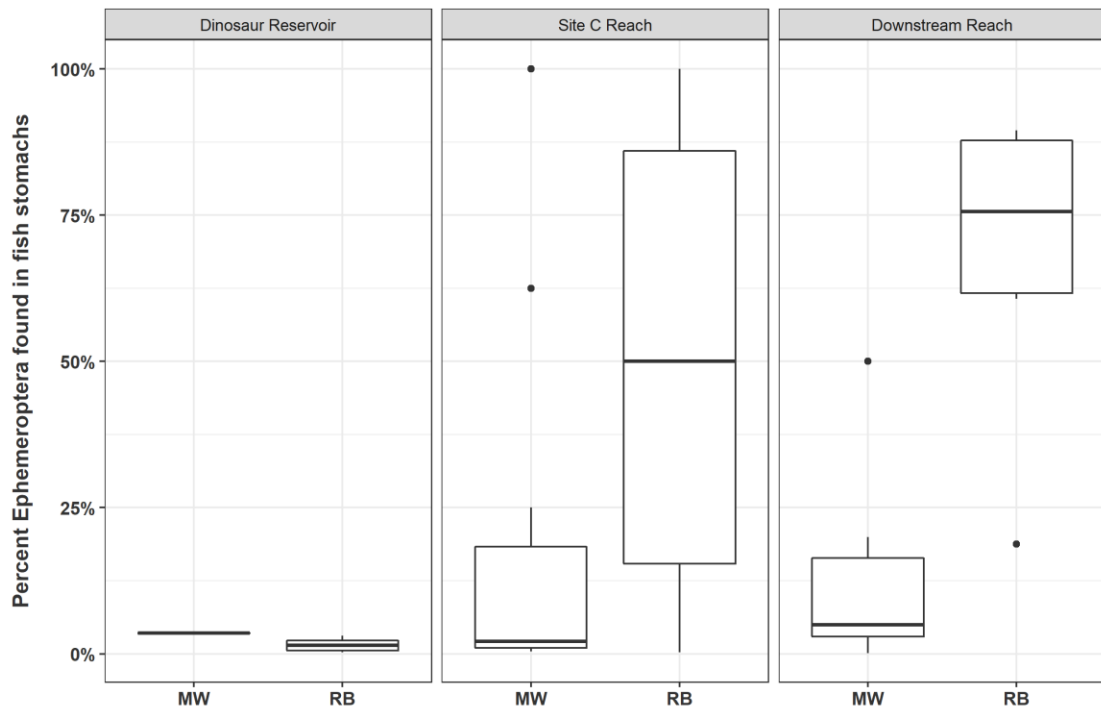


Figure A206 Percentage of Ephemeroptera found in fish stomachs in the Dinosaur Reservoir, Site C Reach, and Downstream Reach

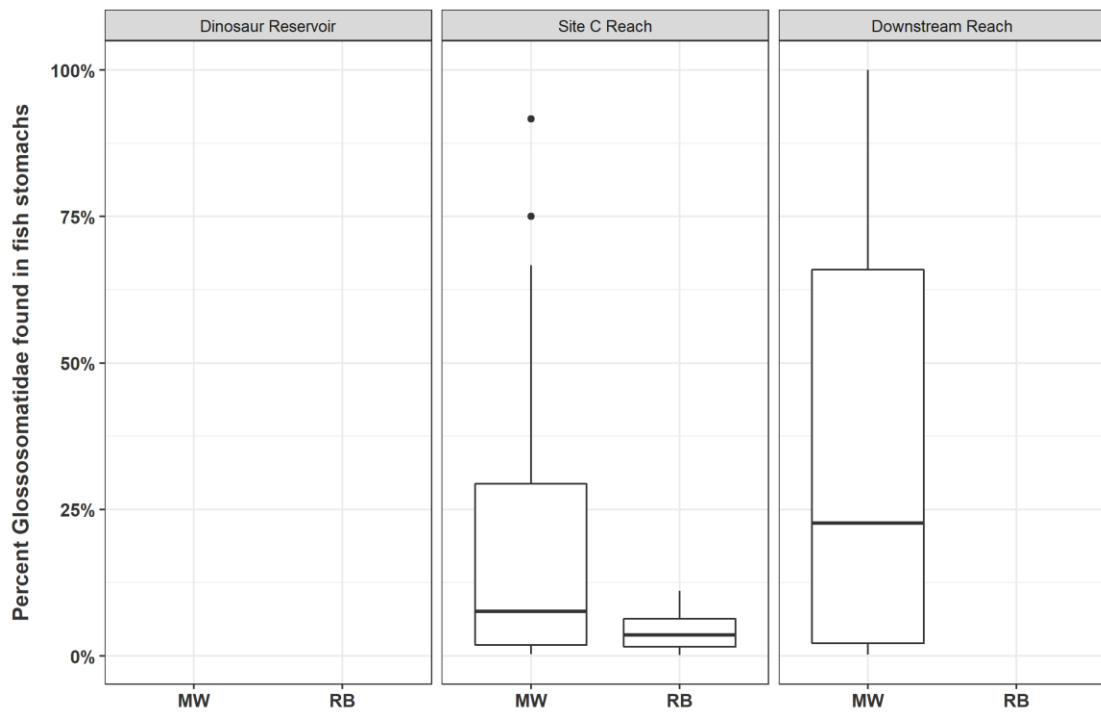


Figure A207 Percentage of Glossosomatidae found in fish stomachs in the Dinosaur Reservoir, Site C Reach, and Downstream Reach



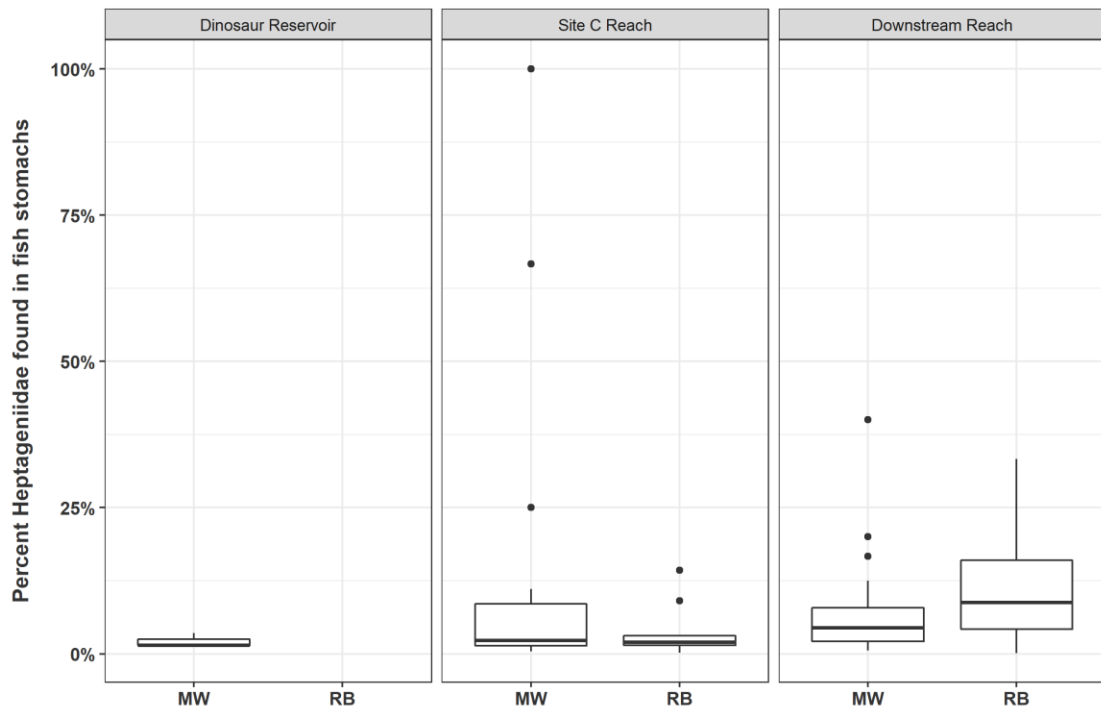


Figure A208 Percentage of Heptageniidae found in fish stomachs in the Dinosaur Reservoir, Site C Reach, and Downstream Reach

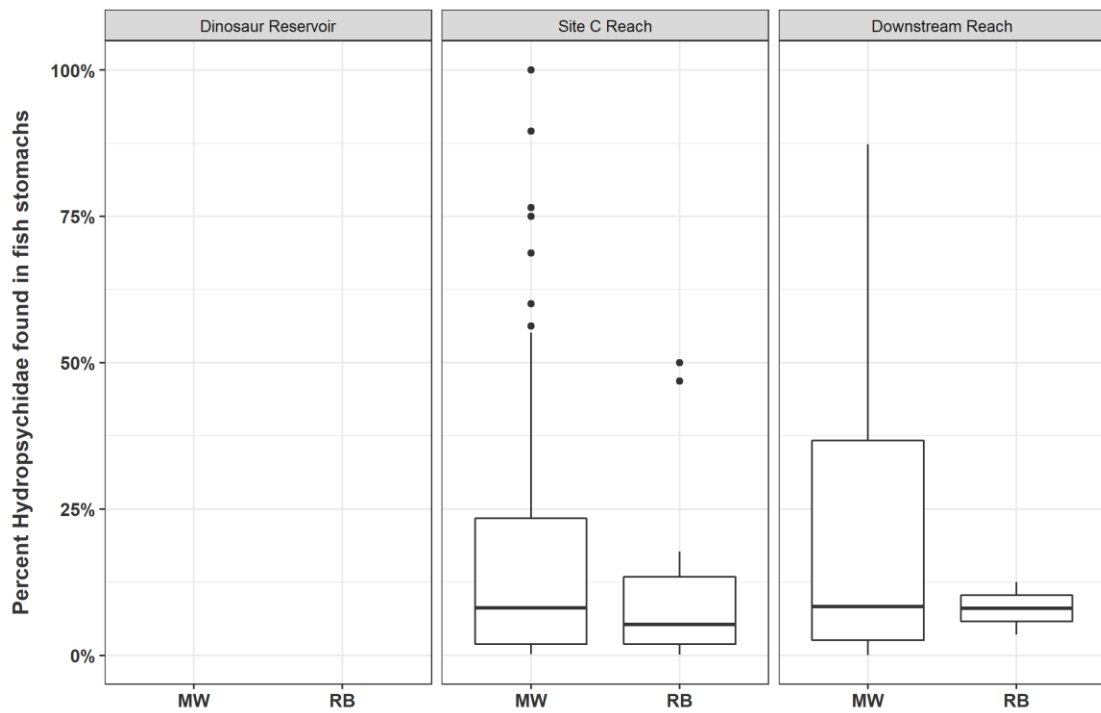


Figure A209 Percentage of Hydropsychidae found in fish stomachs in the Dinosaur Reservoir, Site C Reach, and Downstream Reach



Appendix HH Invertebrate Taxonomic Methods



Methods and QC Report 2018

Project ID: BC Hydro Site C Fall

Client: Ecoscape Environmental



Cordillera
Consulting

Prepared by:

Cordillera Consulting Inc.

Summerland, BC

© 2019

Unit 1, 13216 Henry Ave B1202
Summerland, BC, V0H 1Z0
www.cordilleraconsulting.ca

P:250.494.7553
F: 250.494.7562

Table of Contents

Sample Reception	2
Sample Sorting	4
Sorting Quality Control - Sorting Efficiency	6
Taxonomic Effort	7
Taxonomy Staff	7
Isotope Analysis Procedure	7
References	8
Taxonomic Keys	8

Sample Reception

On October 12 and 23, 2018, Cordillera Consulting received 64 benthic samples and 11 zooplankton samples from Ecoscape Environmental. When samples arrived to Cordillera Consulting, exterior packaging was initially inspected for damage or wet spots that would have indicated damage to the interior containers.

Next, samples were logged into a proprietary software database (INSTAR1) where the clients assigned sample name was recorded along with a Cordillera Consulting (CC) number for cross-reference. Each sample was checked to ensure that all sites and replicates recorded on field sheets or packing lists were delivered intact and with adequate preservative. Any missing, mislabelled or extra samples were reported to the client immediately to confirm the total numbers and correct names on the sample jars. The client representative was notified of the arrival of the shipment and provided a sample inventory once intake was completed.

See table below for sample inventory:

Table 1: Summary of sample information including Cordillera Consulting (CC) number

Site	Sample	CC#	Date	Size	# of Jars
D1	D1-1	CC192130	9/20/2018	250µM	1
D1	D1-1-E	CC192131	9/20/2018	250µM	1
D1	D1-2	CC192132	9/20/2018	250µM	1
D1	D1-2-E	CC192133	9/20/2018	250µM	1
D1	D1-3	CC192134	9/20/2018	250µM	1
D1	D1-3-E	CC192135	9/20/2018	250µM	1
D1	D1-4	CC192136	9/20/2018	250µM	1
D1	D1-4-E	CC192137	9/20/2018	250µM	1
D1	D1-5	CC192138	9/20/2018	250µM	1
D1	D1-5-E	CC192139	9/20/2018	250µM	1
HD	HD-1-E	CC192140	9/20/2018	250µM	1
HD	HD-2-E	CC192141	9/20/2018	250µM	1
HD	HD-3-E	CC192142	9/20/2018	250µM	1
HD	HD-4-E	CC192143	9/20/2018	250µM	1
PD	PD1-1	CC192144	9/20/2018	250µM	1

PD	PD1-2	CC192145	9/20/2018	250µM	1
PD	PD1-3	CC192146	9/20/2018	250µM	1
PD	PD1-4	CC192147	9/20/2018	250µM	1
PD	PD2-1	CC192148	9/20/2018	250µM	1
PD	PD4-1	CC192149	9/20/2018	250µM	1
PD	PD4-2	CC192150	9/20/2018	250µM	1
PD	PD4-3	CC192151	9/20/2018	250µM	1
PD	PD5-1	CC192152	9/20/2018	250µM	1
PR	PR1-1	CC192153	9/20/2018	250µM	1
PR	PR1-1-E	CC192154	9/20/2018	250µM	1
PR	PR1-2	CC192155	9/20/2018	250µM	1
PR	PR1-2-E	CC192156	9/20/2018	250µM	1
PR	PR1-3	CC192157	9/20/2018	250µM	1
PR	PR1-3-E	CC192158	9/20/2018	250µM	1
PR	PR1-4-E	CC192159	9/20/2018	250µM	1
PR	PR2-1	CC192160	9/20/2018	250µM	1
PR	PR2-1-E	CC192161	9/20/2018	250µM	1
PR	PR2-2	CC192162	9/20/2018	250µM	1
PR	PR2-2-E	CC192163	9/20/2018	250µM	1
PR	PR2-3	CC192164	9/20/2018	250µM	1
PR	PR2-3-E	CC192165	9/20/2018	250µM	1
PR	PR2-4	CC192166	9/20/2018	250µM	1
PR	PR2-4-E	CC192167	9/20/2018	250µM	1
PR	PR3-1	CC192168	9/20/2018	250µM	1
PR	PR3-1-E	CC192169	9/20/2018	250µM	1
PR	PR3-2	CC192170	9/20/2018	250µM	1
PR	PR3-2-E	CC192171	9/20/2018	250µM	1
PR	PR3-3	CC192172	9/20/2018	250µM	1
PR	PR3-3-E	CC192173	9/20/2018	250µM	1
PR	PR3-4	CC192174	9/20/2018	250µM	1
PR	PR3-4-E	CC192175	9/20/2018	250µM	1
Zooplankton	D1-ZOO LITTORAL	CC192176	9/20/2018	250µM	1
Zooplankton	D1-ZOO PELAGIC	CC192177	9/20/2018	250µM	1
Zooplankton	HD-ZOO	CC192178	9/20/2018	250µM	1
Zooplankton	MD-ZOO	CC192179	9/20/2018	250µM	1
Zooplankton	PR1-ZOO	CC192180	9/20/2018	250µM	1
Zooplankton	PR2-ZOO	CC192181	9/20/2018	250µM	1
Zooplankton	PR3-ZOO	CC192182	9/20/2018	250µM	1
Zooplankton	W1-ZOO	CC192183	9/20/2018	250µM	1
MD	MD-1-E	CC192433	10/10/2018	250µM	1
MD	MD-2-E	CC192434	10/10/2018	250µM	1
MD	MD-3-E	CC192435	10/10/2018	250µM	1
MD	MD-1	CC192436	10/9/2018	250µM	1
MD	MD-2	CC192437	10/9/2018	250µM	1
MD	MD-3	CC192438	10/9/2018	250µM	2
PD	PD2-2	CC192439	10/9/2018	250µM	1
PD	PD2-3	CC192440	10/9/2018	250µM	1
PD	PD2-4	CC192441	10/9/2018	250µM	1
PD	PD3-1	CC192442	10/10/2018	250µM	1
PD	PD3-2	CC192443	10/10/2018	250µM	1
PD	PD3-3	CC192444	10/10/2018	250µM	1

PD	PD3-4	CC192445	10/10/2018	250µM	1
PD	PD4-4	CC192446	10/10/2018	250µM	1
PD	PD5-2	CC192447	10/11/2018	250µM	1
PD	PD5-3	CC192448	10/11/2018	250µM	1
PD	PD5-4	CC192449	10/11/2018	250µM	1
PR	PR1-4	CC192450	10/7/2018	250µM	1
Zooplankton	W1-ZOOPK	CC192451	10/8/2018	250µM	1
Zooplankton	D1-Littoral	CC192452	10/8/2018	250µM	1
Zooplankton	D1-Pelagic	CC192453	10/8/2018	250µM	1

Sample Sorting

- Using a gridded Petri dish, fine forceps and a low power stereo-microscope (Olympus, Nikon, Leica) the sorting technicians removed the invertebrates and sorted them into family/orders.
- The sorting technician kept a running tally of total numbers excluding organisms from Porifera, Nemata, Platyhelminthes, Ostracoda, Copepoda, Cladocera and terrestrial drop-ins such as aphids. These organisms were marked for their presence (given a value of 1) only and left in the sample. They were not included towards the 300-organism subsample count.
- Where specimens are broken or damaged, only heads were counted.
- Subsampling was conducted with the use of a Marchant Box or Plankton divider.
- When using the Marchant box, cells were extracted at the same time in the order indicated by a random number table. If the 300th organism was found part way into sorting a cell then the balance of that cell was sorted. If the organism count had not reached 300 by the 50th cell then the entire sample was sorted.
- The total number of cells sorted and the number of organisms removed were recorded manually on a bench sheet and then recorded into INSTAR1
- Organisms were stored in vials containing 80% ethanol and an interior label indicating the site names, date of sampling, site code numbers and portion subsampled. This information was also recorded on the laboratory bench sheet and on INSTAR1.
- The sorted portion of the debris was preserved and labeled separately from the unsorted portion and was tested for sorting efficiency (Sorting Quality Control – Sorting Efficiency). The unsorted portion was also labeled and preserved in separate jars.

Percent sub-sampled and total countable invertebrates pulled from the samples were summarized in the table below.

Table 2: Percent sub-sample and invertebrate count for each sample

Site	Sample	Date	CC#	212 micron fraction	# Invertebrates	250 micron fraction	# Invertebrates	1000 micron fraction	# Invertebrates
				% Sampled		% Sampled		% Sampled	
D1	D1-1	20-Sep-18	CC192130			100%	17	100%	1
D1	D1-1-E	20-Sep-18	CC192131			18.75%	300	100%	324
D1	D1-2	20-Sep-18	CC192132			100%	34	100%	21
D1	D1-2-E	20-Sep-18	CC192133			12.5%	211	100%	241
D1	D1-3	20-Sep-18	CC192134			100%	9	100%	35
D1	D1-3-E	20-Sep-18	CC192135			58%	225	100%	37

D1	D1-4	20-Sep-18	CC192136			100%	59	100%	136
D1	D1-4-E	20-Sep-18	CC192137			8%	229	100%	330
D1	D1-5	20-Sep-18	CC192138			100%	45	100%	109
D1	D1-5-E	20-Sep-18	CC192139			12.5%	275	100%	348
HD	HD-1-E	20-Sep-18	CC192140			75%	205	100%	19
HD	HD-2-E	20-Sep-18	CC192141			100%	40	100%	14
HD	HD-3-E	20-Sep-18	CC192142			100%	36	100%	4
HD	HD-4-E	20-Sep-18	CC192143			100%	5	100%	3
PD	PD1-1	20-Sep-18	CC192144			7%	242	100%	642
PD	PD1-2	20-Sep-18	CC192145			25%	379	100%	510
PD	PD1-3	20-Sep-18	CC192146			8%	233	100%	1675
PD	PD1-4	20-Sep-18	CC192147			6%	211	50%	1341
PD	PD2-1	20-Sep-18	CC192148			62%	227	100%	102
PD	PD4-1	20-Sep-18	CC192149			87.5%	208	100%	27
PD	PD4-2	20-Sep-18	CC192150			75%	234	100%	117
PD	PD4-3	20-Sep-18	CC192151			20%	200	100%	199
PD	PD5-1	20-Sep-18	CC192152			21%	296	50%	97
PR	PR1-1	20-Sep-18	CC192153			9%	249	100%	597
PR	PR1-1-E	20-Sep-18	CC192154			19%	213	100%	154
PR	PR1-2	20-Sep-18	CC192155			25%	248	100%	861
PR	PR1-2-E	20-Sep-18	CC192156			44%	213	100%	149
PR	PR1-3	20-Sep-18	CC192157			18%	235	100%	416
PR	PR1-3-E	20-Sep-18	CC192158			100%	206	100%	68
PR	PR1-4-E	20-Sep-18	CC192159			18%	205	100%	594
PR	PR2-1	20-Sep-18	CC192160			12.5%	214	100%	396
PR	PR2-1-E	20-Sep-18	CC192161			34%	259	100%	83
PR	PR2-2	20-Sep-18	CC192162			100%	265	100%	156
PR	PR2-2-E	20-Sep-18	CC192163			55%	233	100%	33
PR	PR2-3	20-Sep-18	CC192164			100%	274	100%	313
PR	PR2-3-E	20-Sep-18	CC192165			25%	224	100%	182
PR	PR2-4	20-Sep-18	CC192166			15%	221	100%	404
PR	PR2-4-E	20-Sep-18	CC192167			27%	220	100%	98
PR	PR3-1	20-Sep-18	CC192168			12.5%	240	50%	451
PR	PR3-1-E	20-Sep-18	CC192169			35%	244	100%	38
PR	PR3-2	20-Sep-18	CC192170			26%	225	100%	180
PR	PR3-2-E	20-Sep-18	CC192171			100%	11	100%	5
PR	PR3-3	20-Sep-18	CC192172			100%	140	100%	29
PR	PR3-3-E	20-Sep-18	CC192173			50%	225	100%	48
PR	PR3-4	20-Sep-18	CC192174			36%	198	100%	316
PR	PR3-4-E	20-Sep-18	CC192175			45%	218	100%	34
Zooplankton	D1-ZOO LITTORAL	20-Sep-18	CC192176	50%	0				
Zooplankton	D1-ZOO PELAGIC	20-Sep-18	CC192177	6.25%	0				
Zooplankton	HD-ZOO	20-Sep-18	CC192178	100%	24				
Zooplankton	MD-ZOO	20-Sep-18	CC192179	100%	45				
Zooplankton	PR1-ZOO	20-Sep-18	CC192180	25%	14				
Zooplankton	PR2-ZOO	20-Sep-18	CC192181	100%	143				
Zooplankton	PR3-ZOO	20-Sep-18	CC192182	100%	20				
Zooplankton	W1-ZOO	20-Sep-18	CC192183	1.5625%	1				
MD	MD-1-E	10-Oct-18	CC192433			100%	35	100%	7
MD	MD-2-E	10-Oct-18	CC192434			100%	66	100%	16

MD	MD-3-E	10-Oct-18	CC192435			100%	3	100%	0
MD	MD-1	09-Oct-18	CC192436			100%	31	100%	36
MD	MD-2	09-Oct-18	CC192437			100%	119	100%	43
MD	MD-3	09-Oct-18	CC192438			100%	262	100%	90
PD	PD2-2	09-Oct-18	CC192439			100%	264	100%	83
PD	PD2-3	09-Oct-18	CC192440			100%	127	100%	140
PD	PD2-4	09-Oct-18	CC192441			100%	220	100%	125
PD	PD3-1	10-Oct-18	CC192442			100%	188	100%	37
PD	PD3-2	10-Oct-18	CC192443			25%	209	100%	224
PD	PD3-3	10-Oct-18	CC192444			43.75%	245	100%	192
PD	PD3-4	10-Oct-18	CC192445			50%	270	100%	215
PD	PD4-4	10-Oct-18	CC192446			100%	66	100%	86
PD	PD5-2	11-Oct-18	CC192447			100%	152	100%	66
PD	PD5-3	11-Oct-18	CC192448			50%	217	100%	199
PD	PD5-4	11-Oct-18	CC192449			100%	180	100%	179
PR	PR1-4	07-Oct-18	CC192450			25%	237	100%	449
Zooplankton	W1-ZOOPK	08-Oct-18	CC192451	1.5625%	0				
Zooplankton	D1-Littoral	08-Oct-18	CC192452	1.5625%	0				
Zooplankton	D1-Pelagic	08-Oct-18	CC192453	7.8125%	1				

Sorting Quality Control - Sorting Efficiency

As a part of Cordillera's laboratory policy, all projects undergo sorting efficiency checks.

- As sorting progresses, 10% of samples were randomly chosen by senior members of the sorting team for resorting.
- All sorters working on a project had at least 1 sample resorted by another sorter.
- An efficiency of 90 % was expected (95% for CABIN samples).
- If 90/95% efficiency was not met, samples from that sorter were resorted.
- To calculate sorting efficiency the following formula was used:

$$\frac{\#OrganismsMissed}{TotalOrganismsFound} * 100 = \% OM$$

Table 3: Summary of sorting efficiency

CC #	Number of Organisms Recovered (initial sort)	Number of Organisms in Re-sort	Percent Recovery
CC192134	44	0	100%
CC192134	44	0	100%
CC192150	351	0	100%
CC192150	351	4	99%
CC192154	587	0	100%
CC192154	587	15	97%
CC192172	169	0	100%
CC192172	169	1	99%
CC192448	416	3	98%
CC192448	416	7	99%
Average Recovery			99%

Taxonomic Effort

The next procedure was the identification to genus-species level where possible of all the organisms in the sample.

- Identifications were made at the genus/species level for all insect organisms found including Chironomidae (Based on CABIN protocol).
- Non-insect organisms (except those not included in CABIN count) were identified to genus/species where possible and to a minimum of family level with intact and mature specimens.
- The Standard Taxonomic Effort lists compiled by the CABIN manual¹, SAFIT², and PNAMP³ were used as a guide line for what level of identification to achieve where the condition and maturity of the organism enabled.
- Organisms from the same families/order were kept in separate vials with 80% ethanol and an interior label of printed laser paper.
- Chironomidae was identified to genus/species level where possible and was aided by slide mounts. CMC-10 was used to clear and mount the slide.
- Oligochaetes was identified to family/genus level with the aid of slide mounts. CMC-10 was used to clear and mount the slide.
- Other Annelida (leeches, polychaetes) were identified to the family/genus/species level with undamaged, mature specimens.
- Mollusca was identified to family and genus/species where possible
- Decapoda, Amphipoda and Isopoda were identified at family/genus/species level where possible.
- Bryozoans and Nemata remained at the phylum level
- Hydrachnidae and Cnidaria were identified at the family/genus level where possible.
- When requested, reference collections were made containing at least one individual from each taxa listed. Organisms represented will have been identified to the lowest practical level.
- Reference collection specimens were stored in 55 mm glass vials with screw-cap lids with polyseal inserts (museum quality). They were labeled with taxa name, site code, date identified and taxonomist name. The same information was applied to labels on the slide mounts.

Taxonomy Staff

The taxonomists for this project were certified by the Society of Freshwater Science (SFS) Taxonomic Certification Program at level 2 which is the required certification for CABIN projects:

Scott Finlayson: Group 1 General Arthropods (East/West); Group 2 EPT (East/West); Group 3 Chironomidae (East/West); Group 4 Oligochaeta

Adam Bliss: Group 1 General Arthropods (East/West); Group 2 EPT (East/West); Group 3 Chironomidae

Rita Avery: Group 1 General Arthropods (East/West); Group 2 EPT (East/West)

Isotope Analysis Procedure

Samples are originally sorted by the sorting team to the Order level, or Family if they are competent. Once the sample has been processed by the sorting team the taxonomist will identify

the organisms in the sample. Each sample is processed one vial at a time. Each Order level vial is then separated to the Family level by the taxonomists. After processing the sample, digital biomass is performed to determine dry weight. Once the entire project is complete the biomass data is analyzed to find samples with enough weight to be useable for isotope analysis, these samples are then separated and kept out and ready to ship when the entire project is complete.

References

¹ McDermott, H., Paull, T., Strachan, S. (May 2014). Laboratory Methods: Processing, Taxonomy, and Quality Control of Benthic Macroinvertebrate Samples, Environment Canada. ISBN: 978-1-100-25417-3

² Southwest Association of Freshwater Invertebrate Taxonomists. (2015). www.safit.org

³ Pacific Northwest Aquatic Monitoring Partnership (Accessed 2015). www.pnamp.org

Taxonomic Keys

Below is a reference list of taxonomic keys utilized by taxonomists at Cordillera Consulting. Cordillera taxonomists routinely seek out new literature to ensure the most accurate identification keys are being utilized. This is not reflective of the exhaustive list of resources that we use for identification. A more complete list of taxonomic resources can be found at Southwest Association of Freshwater Invertebrate Taxonomists. (2015). http://www.safit.org/Docs/SAFIT_Taxonomic_Literature_Database_1_March_2011.enl

Brook, Arthur R. and Leonard A. Kelton. 1967. Aquatic and semiaquatic Heteroptera of Alberta, Saskatchewan and Manitoba (Hemiptera) *Memoirs of the Entomological Society of Canada*. No. 51.

Brown HP & White DS (1978) Notes on Separation and Identification of North American Riffle Beetles (Coleoptera: Dryopidea: Elmidae). *Entomological News* 89 (1&2): 1-13

Clifford, Hugh F. 1991. *Aquatic Invertebrates of Alberta*. University of Alberta Press Edmonton, Alberta.

Epler, John. 2001 *The Larval Chironomids of North and South Carolina*. <http://home.earthlink.net/~johnepler/>

Epler, John. *Identification Manual for the Water Beetles of Florida*. <http://home.earthlink.net/~johnepler/>

Epler, John. *Identification Manual for the Aquatic and Semi-aquatic Heteroptera of Florida*. <http://home.earthlink.net/~johnepler/>

Trond Andersen, Peter S. Cranston & John H. Epler (Eds) (2013) *Chironomidae of the Holarctic Region: Keys and Diagnoses*. Part 1. Larvae. *Insect Systematics and Evolution Supplements* 66: 1-571.

Jacobus, Luke and Pat Randolph. 2005. *Northwest Ephemeroptera Nymphs*. Manual from Northwest Biological Assessment Working Group. Moscow Idaho 2005. Not Published.

Jacobus LM, McCafferty WP (2004) Revisionary Contributions to the Genus *Drunella* (Ephemeroptera : Ephemerellidae). *Journal of the New York Entomological Society* 112: 127-147

Jacobus LM, McCafferty WP (2003) Revisionary Contributions to North American *Ephemerella* and *Serratella* (Ephemeroptera : Ephemerellidae). *Journal of the New York Entomological Society* 111 (4): 174-193.

Kathman, R.D., R.O. Brinkhurst. 1999. *Guide to the Freshwater Oligochaetes of North America*. Aquatic Resources Center, College Grove, Tennessee.

Larson, D.J., Y. Alarie, R.E. Roughly. 2005. *Predaceous Diving Beetles (Coleoptera: Dytiscidae) of the Nearctic Region*. NRC-CNRC Research Press. Ottawa.

Merritt, R.W., K.W. Cummins, M. B. Berg. (eds.). 2007. An introduction to the aquatic insects of North America, 4th. Kendall/Hunt, Dubuque, IA

Morihara DK, McCafferty WP (1979) The Baetis Larvae of North American (Ephemeroptera: Baetidae). Transactions of the American Entomological Society 105: 139-221.

Needham, James, M. May, M. Westfall Jr. 2000. Dragonflies of North America. Scientific Publishers. Gainesville FL.

Prescott David, R.C. and Medea M. Curteanu. 2004. Survey of Aquatic Gastropods of Alberta. Species at Risk Report No. 104. ISSN: 1496-7146 (Online Edition)

Needham, K. 1996. An Identification Guide to the Nymphal Mayflies of British Columbia. Publication #046 Resource Inventory Committee, Government of British Columbia.

Oliver, Donald R. and Mary E. Roussel. 1983. The Insects and Arachnids of Canada Part 11. The Genera of larval midges of Canada. Biosystematics Research Institute. Ottawa, Ontario. Research Branch, Agriculture Canada. Publication 1746.

Proctor, H. The 'Top 18' Water Mite Families in Alberta. Zoology 351. University of Alberta, Edmonton, Alberta.

Rogers, D.C. and M. Hill, 2008. Key to the Freshwater Malacostraca (Crustacea) of the mid-Atlantic Region. EPA-230-R-08-017. US Environmental Protection Agency, Office of Environmental Information, Washington, DC.

Stewart, Kenneth W. and Bill Stark. 2002. The Nymphs of North American Stonefly Genera (Plecoptera). The Caddis Press. Columbus Ohio.

Stewart, Kenneth W. and Mark W. Oswood. 2006 The Stoneflies (Plecoptera) of Alaska and Western Canada. The Caddis Press.

Stonedahl, Gary and John D. Lattin. 1986. The Corixidae of Oregon and Washington (Hemiptera: Heteroptera). Technical Bulletin 150. Oregon State University, Corvallis Oregon.

Thorpe, J. H. and A. P. Covich [Eds.] 1991. Ecology and classification of North American freshwater invertebrates. Academic Press, San Diego.

Tinerella, Paul P. and Ralph W. Gunderson. 2005. The Waterboatmen (Insecta: Heteroptera: Corixidae) of Minnesota. Publication No. 23 Dept. Of Entomology, North Dakota State University, Fargo, North Dakota, USA.

Weiderholm, Torgny (Ed.) 1983. The larvae of Chironomidae (Diptera) of the Holarctic region. Entomologica Scandinavica. Supplement No. 19.

Westfall, Minter J. Jr. and May, Michael L. 1996. Damselflies of North America. Scientific Publishers, Gainesville, FL.

Wiggins, Glenn B. 1998. Larvae of the North American Caddisfly Genera (Tricoptera) 2nd ed. University of Toronto Press. Toronto Ontario.

Methods and QC Report 2018
Project ID: BC Hydro Site C Summer

Client: Ecoscape Environmental

Cordillera
Consulting

Prepared by:
Cordillera Consulting Inc.
Summerland, BC
© 2018

Unit 1, 13216 Henry Ave B1202
Summerland, BC, V0H 1Z0
www.cordilleraconsulting.ca

P:250.494.7553
F: 250.494.7562

Table of Contents

Sample Reception	2
Sample Sorting.....	4
Sorting Quality Control - Sorting Efficiency.....	6
Taxonomic Effort	7
Taxonomy Staff.....	8
Isotope Analysis Procedure	8
References.....	8
Taxonomic Keys.....	8

Sample Reception

On August 13, 2018, Cordillera Consulting received 56 benthic samples and 17 zooplankton samples from Ecoscape Environmental. When samples arrived to Cordillera Consulting, exterior packaging was initially inspected for damage or wet spots that would have indicated damage to the interior containers.

Next, samples were logged into a proprietary software database (INSTAR1) where the clients assigned sample name was recorded along with a Cordillera Consulting (CC) number for cross-reference. Each sample was checked to ensure that all sites and replicates recorded on field sheets or packing lists were delivered intact and with adequate preservative. Any missing, mislabelled or extra samples were reported to the client immediately to confirm the total numbers and correct names on the sample jars. The client representative was notified of the arrival of the shipment and provided a sample inventory once intake was completed.

See table below for sample inventory:

Table 1: Summary of sample information including Cordillera Consulting (CC) number

Site	Sample	CC#	Date	Size	# of Jars
D1	D1-1	CC190139	8/4/2018	250µM	1
D1	D1-1-E	CC190140	8/4/2018	250µM	1
D1	D1-2	CC190141	8/4/2018	250µM	1
D1	D1-2-E	CC190142	8/4/2018	250µM	1
D1	D1-3	CC190143	8/4/2018	250µM	1
D1	D1-3-E	CC190144	8/4/2018	250µM	1
D1	D1-4	CC190145	8/4/2018	250µM	1
D1	D1-4-E	CC190146	8/4/2018	250µM	1
D1	D1-5	CC190147	8/4/2018	250µM	1
D1	D1-5-E	CC190148	8/4/2018	250µM	1
HD	HD-1-E	CC190149	8/4/2018	250µM	1
HD	HD-2-E	CC190150	8/4/2018	250µM	1
HD	HD-3-E	CC190151	8/4/2018	250µM	1
HD	HD-4-E	CC190152	8/4/2018	250µM	1
MD	MD-1-E	CC190153	8/4/2018	250µM	1

MD	MD-2-E	CC190154	8/4/2018	250µM	1
MD	MD-3-E	CC190155	8/4/2018	250µM	1
MD	MD-4-E	CC190156	8/4/2018	250µM	1
PD	PD1-1	CC190157	8/4/2018	250µM	1
PD	PD1-2	CC190158	8/4/2018	250µM	1
PD	PD1-3	CC190159	8/4/2018	250µM	1
PD	PD1-4	CC190160	8/4/2018	250µM	1
PD	PD2-1	CC190161	8/4/2018	250µM	1
PD	PD4-1	CC190162	8/4/2018	250µM	1
PD	PD4-2	CC190163	8/4/2018	250µM	1
PD	PD4-3	CC190164	8/4/2018	250µM	1
PD	PD5-1	CC190165	8/4/2018	250µM	1
PR	PR1-1	CC190166	8/4/2018	250µM	1
PR	PR1-1-E	CC190167	8/4/2018	250µM	1
PR	PR1-2	CC190168	8/4/2018	250µM	1
PR	PR1-2-E	CC190169	8/4/2018	250µM	1
PR	PR1-3	CC190170	8/4/2018	250µM	1
PR	PR1-3-E	CC190171	8/4/2018	250µM	1
PR	PR1-4-E	CC190172	8/4/2018	250µM	1
PR	PR2-1	CC190173	8/4/2018	250µM	1
PR	PR2-1-E	CC190174	8/4/2018	250µM	1
PR	PR2-2	CC190175	8/4/2018	250µM	1
PR	PR2-2-E	CC190176	8/4/2018	250µM	1
PR	PR2-3	CC190177	8/4/2018	250µM	1
PR	PR2-3-E	CC190178	8/4/2018	250µM	1
PR	PR2-4	CC190179	8/4/2018	250µM	1
PR	PR2-4-E	CC190180	8/4/2018	250µM	1
PR	PR3-1	CC190181	8/4/2018	250µM	1
PR	PR3-1-E	CC190182	8/4/2018	250µM	1
PR	PR3-2	CC190183	8/4/2018	250µM	1
PR	PR3-2-E	CC190184	8/4/2018	250µM	1
PR	PR3-3	CC190185	8/4/2018	250µM	1
PR	PR3-3-E	CC190186	8/4/2018	250µM	1
PR	PR3-4	CC190187	8/4/2018	250µM	1
PR	PR3-4-E	CC190188	8/4/2018	250µM	1
Zooplankton	D1 Littoral/May	CC190189	5/11/2018	250µM	1
Zooplankton	D1 Pelagic/May	CC190190	5/11/2018	250µM	1
Zooplankton	D1 Littoral/June	CC190191	6/8/2018	250µM	1
Zooplankton	D1 Pelagic/June	CC190192	6/8/2018	250µM	1
Zooplankton	D1 Littoral/July	CC190193	7/31/2018	250µM	1
Zooplankton	D1 Pelagic/July	CC190194	7/31/2018	250µM	1
Zooplankton	HD-Zoo	CC190195	8/1/2018	250µM	1
Zooplankton	PR1-Zoo	CC190196	8/1/2018	250µM	1
Zooplankton	PR2-Zoo	CC190197	8/1/2018	250µM	1
Zooplankton	PR3-Zoo	CC190198	7/28/2018	250µM	1
Zooplankton	W1-Zoo/May	CC190199	5/11/2018	250µM	1
Zooplankton	W1-Zoo/June	CC190200	6/9/2018	250µM	1
Zooplankton	W1-Zoo/July	CC190201	6/28/2018	250µM	1
PD	PD2-2	CC190530	8/28/2018	250µM	1
PD	PD3-1	CC190531	8/28/2018	250µM	2
PD	PD3-3	CC190532	8/28/2018	250µM	1

PD	PD3-4	CC190533	8/28/2018	250µM	1
PD	PD5-2	CC190534	8/28/2018	250µM	1
PR	PR1-4	CC190535	8/28/2018	250µM	1
Zooplankton	MD-ZOO	CC190536	8/28/2018	250µM	1
Zooplankton	W1-ZOOPK	CC190537	8/25/2018	250µM	1
Zooplankton	D1-LITTORAL ZOOPK	CC190538	8/25/2018	250µM	1
Zooplankton	D1-PELAGIC ZOOPK	CC190539	8/25/2018	250µM	1

Sample Sorting

- Using a gridded Petri dish, fine forceps and a low power stereo-microscope (Olympus, Nikon, Leica) the sorting technicians removed the invertebrates and sorted them into family/orders.
- The sorting technician kept a running tally of total numbers excluding organisms from Porifera, Nemata, Platyhelminthes, Ostracoda, Copepoda, Cladocera and terrestrial drop-ins such as aphids. These organisms were marked for their presence (given a value of 1) only and left in the sample. They were not included towards the 300-organism subsample count.
- Where specimens are broken or damaged, only heads were counted.
- Subsampling was conducted with the use of a Marchant Box or Plankton divider.
- When using the Marchant box, cells were extracted at the same time in the order indicated by a random number table. If the 300th organism was found part way into sorting a cell then the balance of that cell was sorted. If the organism count had not reached 300 by the 50th cell then the entire sample was sorted.
- The total number of cells sorted and the number of organisms removed were recorded manually on a bench sheet and then recorded into INSTAR1
- Organisms were stored in vials containing 80% ethanol and an interior label indicating the site names, date of sampling, site code numbers and portion subsampled. This information was also recorded on the laboratory bench sheet and on INSTAR1.
- The sorted portion of the debris was preserved and labeled separately from the unsorted portion and was tested for sorting efficiency (Sorting Quality Control – Sorting Efficiency). The unsorted portion was also labeled and preserved in separate jars.

Note: Sorting technicians noticed a large amount of Hydra in some samples. To avoid sample bias, only the first 100 hydra were removed from the sample and the total number was estimated and recorded based on the % subsampled. The remainder of the 300 count was made up by other organisms.

Percent sub-sampled and total countable invertebrates pulled from the samples were summarized in the table below.

Table 2: Percent sub-sample and invertebrate count for each sample

Site	Sample	Date	CC#	212 micron fraction		250 micron fraction		1000 micron fraction	
				% Sampled	# Invertebrates	% Sampled	# Invertebrates	% Sampled	# Invertebrates
D1	D1-1	04-Aug-18	CC190139			100%	13	100%	0
D1	D1-1-E	04-Aug-18	CC190140			25%	202	100%	164

D1	D1-2	04-Aug-18	CC190141			100%	50	100%	20
D1	D1-2-E	04-Aug-18	CC190142			35%	212	100%	92
D1	D1-3	04-Aug-18	CC190143			100%	132	100%	72
D1	D1-3-E	04-Aug-18	CC190144			100%	31	100%	31
D1	D1-4	04-Aug-18	CC190145			50%	298	100%	173
D1	D1-4-E	04-Aug-18	CC190146			100%	206	100%	29
D1	D1-5	04-Aug-18	CC190147			100%	146	100%	25
D1	D1-5-E	04-Aug-18	CC190148			50%	210	100%	340
HD	HD-1-E	04-Aug-18	CC190149			100%	55	100%	29
HD	HD-2-E	04-Aug-18	CC190150			100%	137	100%	22
HD	HD-3-E	04-Aug-18	CC190151			100%	71	100%	1
HD	HD-4-E	04-Aug-18	CC190152			100%	71	100%	27
MD	MD-1-E	04-Aug-18	CC190153			100%	46	100%	1
MD	MD-2-E	04-Aug-18	CC190154			100%	4	100%	4
MD	MD-3-E	04-Aug-18	CC190155			100%	20	100%	4
MD	MD-4-E	04-Aug-18	CC190156			100%	14	100%	3
PD	PD1-1	04-Aug-18	CC190157			31.25%	256	100%	129
PD	PD1-2	04-Aug-18	CC190158			20%	226	100%	177
PD	PD1-3	04-Aug-18	CC190159			31.25%	225	100%	56
PD	PD1-4	04-Aug-18	CC190160			10%	218	50%	20
PD	PD2-1	04-Aug-18	CC190161			25%	289	100%	108
PD	PD4-1	04-Aug-18	CC190162			37.5%	198	50%	49
PD	PD4-2	04-Aug-18	CC190163			75%	265	100%	158
PD	PD4-3	04-Aug-18	CC190164			100%	192	100%	19
PD	PD5-1	04-Aug-18	CC190165			25%	226	100%	222
PR	PR1-1	04-Aug-18	CC190166			5%	294	25%	46
PR	PR1-1-E	04-Aug-18	CC190167			12.5%	230	100%	95
PR	PR1-2	04-Aug-18	CC190168			5%	343	25%	408
PR	PR1-2-E	04-Aug-18	CC190169			50%	216	100%	106
PR	PR1-3	04-Aug-18	CC190170			15%	483	50%	118
PR	PR1-3-E	04-Aug-18	CC190171			7%	202	100%	116
PR	PR1-4-E	04-Aug-18	CC190172			100%	112	100%	6
PR	PR2-1	04-Aug-18	CC190173			100%	279	100%	21
PR	PR2-1-E	04-Aug-18	CC190174			25%	239	100%	134
PR	PR2-2	04-Aug-18	CC190175			100%	137	100%	79

PR	PR2-2-E	04-Aug-18	CC190176			100%	204	100%	368
PR	PR2-3	04-Aug-18	CC190177			100%	316	100%	61
PR	PR2-3-E	04-Aug-18	CC190178			21%	223	100%	167
PR	PR2-4	04-Aug-18	CC190179			21%	334	25%	255
PR	PR2-4-E	04-Aug-18	CC190180			25%	280	100%	72
PR	PR3-1	04-Aug-18	CC190181			28%	302	25%	120
PR	PR3-1-E	04-Aug-18	CC190182			100%	221	100%	135
PR	PR3-2	04-Aug-18	CC190183			100%	78	25%	22
PR	PR3-2-E	04-Aug-18	CC190184			100%	148	100%	86
PR	PR3-3	04-Aug-18	CC190185			55%	207	50%	142
PR	PR3-3-E	04-Aug-18	CC190186			100%	244	100%	77
PR	PR3-4	04-Aug-18	CC190187			50%	311	50%	157
PR	PR3-4-E	04-Aug-18	CC190188			100%	222	100%	113
Zooplankton	D1 Littoral/May	11-May-18	CC190189	25%	1				
Zooplankton	D1 Pelagic/May	11-May-18	CC190190	12.5%	3				
Zooplankton	D1 Littoral/June	08-Jun-18	CC190191	3.125%	0				
Zooplankton	D1 Pelagic/June	08-Jun-18	CC190192	3.125%	0				
Zooplankton	D1 Littoral/July	31-Jul-18	CC190193	1.5625%	0				
Zooplankton	D1 Pelagic/July	31-Jul-18	CC190194	1.5625%	0				
Zooplankton	HD-Zoo	01-Aug-18	CC190195	100%	73				
Zooplankton	PR1-Zoo	01-Aug-18	CC190196	12.5%	15				
Zooplankton	PR2-Zoo	01-Aug-18	CC190197	100%	387				
Zooplankton	PR3-Zoo	28-Jul-18	CC190198	100%	138				
Zooplankton	W1-Zoo/May	11-May-18	CC190199	6.25%	0				
Zooplankton	W1-Zoo/June	09-Jun-18	CC190200	1.5625%	0				
Zooplankton	W1-Zoo/July	28-Jun-18	CC190201	1.5625%	0				

Sorting Quality Control - Sorting Efficiency

As a part of Cordillera's laboratory policy, all projects undergo sorting efficiency checks.

- As sorting progresses, 10% of samples were randomly chosen by senior members of the sorting team for resorting.
- All sorters working on a project had at least 1 sample resorting by another sorter.
- An efficiency of 90 % was expected (95% for CABIN samples).
- If 90/95% efficiency was not met, samples from that sorter were resorting.
- To calculate sorting efficiency the following formula was used:

$$\frac{\#OrganismsMissed}{TotalOrganismsFound} * 100 = \% OM$$

Table 3: Summary of sorting efficiency

CC #	Number of Organisms Recovered (initial sort)	Number of Organisms in Re-sort	Percent Recovery
CC190139	13	0	100%
CC190139	13	0	100%
CC190152	98	0	100%
CC190152	98	0	100%
CC190156	17	0	100%
CC190156	17	0	100%
CC190167	325	1	99%
CC190167	325	3	99%
CC190173	300	6	98%
CC190173	300	1	99%
CC190182	356	16	96%
CC190182	356	6	98%
Average Recovery			99%

Taxonomic Effort

The next procedure was the identification to genus-species level where possible of all the organisms in the sample.

- Identifications were made at the genus/species level for all insect organisms found including Chironomidae (Based on CABIN protocol).
- Non-insect organisms (except those not included in CABIN count) were identified to genus/species where possible and to a minimum of family level with intact and mature specimens.
- The Standard Taxonomic Effort lists compiled by the CABIN manual¹, SAFIT², and PNAMP³ were used as a guide line for what level of identification to achieve where the condition and maturity of the organism enabled.
- Organisms from the same families/order were kept in separate vials with 80% ethanol and an interior label of printed laser paper.
- Chironomidae was identified to genus/species level where possible and was aided by slide mounts. CMC-10 was used to clear and mount the slide.
- Oligochaetes was identified to family/genus level with the aid of slide mounts. CMC-10 was used to clear and mount the slide.
- Other Annelida (leeches, polychaetes) were identified to the family/genus/species level with undamaged, mature specimens.
- Mollusca was identified to family and genus/species where possible
- Decapoda, Amphipoda and Isopoda were identified at family/genus/species level where possible.
- Bryozoans and Nemata remained at the phylum level
- Hydrachnidae and Cnidaria were identified at the family/genus level where possible.
- When requested, reference collections were made containing at least one individual from each taxa listed. Organisms represented will have been identified to the lowest practical level.

- Reference collection specimens were stored in 55 mm glass vials with screw-cap lids with polyseal inserts (museum quality). They were labeled with taxa name, site code, date identified and taxonomist name. The same information was applied to labels on the slide mounts.

Taxonomy Staff

The taxonomists for this project were certified by the Society of Freshwater Science (SFS) Taxonomic Certification Program at level 2 which is the required certification for CABIN projects:

Scott Finlayson: Group 1 General Arthropods (East/West); Group 2 EPT (East/West); Group 3 Chironomidae (East/West); Group 4 Oligochaeta

Adam Bliss: Group 1 General Arthropods (East/West); Group 2 EPT (East/West); Group 3 Chironomidae

Rita Avery: Group 1 General Arthropods (East/West); Group 2 EPT (East/West)

Isotope Analysis Procedure

Samples are originally sorted by the sorting team to the Order level, or Family if they are competent. Once the sample has been processed by the sorting team the taxonomist will identify the organisms in the sample. Each sample is processed one vial at a time. Each Order level vial is then separated to the Family level by the taxonomists. After processing the sample, digital biomass is performed to determine dry weight. Once the entire project is complete the biomass data is analyzed to find samples with enough weight to be useable for isotope analysis, these samples are then separated and kept out and ready to ship when the entire project is complete.

References

¹ McDermott, H., Paull, T., Strachan, S. (May 2014). Laboratory Methods: Processing, Taxonomy, and Quality Control of Benthic Macroinvertebrate Samples, Environment Canada. ISBN: 978-1-100-25417-3

² Southwest Association of Freshwater Invertebrate Taxonomists. (2015). www.safit.org

³ Pacific Northwest Aquatic Monitoring Partnership (Accessed 2015). www.pnamp.org

Taxonomic Keys

Below is a reference list of taxonomic keys utilized by taxonomists at Cordillera Consulting. Cordillera taxonomists routinely seek out new literature to ensure the most accurate identification keys are being utilized. This is not reflective of the exhaustive list of resources that we use for identification. A more complete list of taxonomic resources can be found at Southwest Association of Freshwater Invertebrate Taxonomists. (2015). http://www.safit.org/Docs/SAFIT_Taxonomic_Literature_Database_1_March_2011.enl

Brook, Arthur R. and Leonard A. Kelton. 1967. Aquatic and semiaquatic Heteroptera of Alberta, Saskatchewan and Manitoba (Hemiptera) *Memoirs of the Entomological Society of Canada*. No. 51.

Brown HP & White DS (1978) Notes on Separation and Identification of North American Riffle Beetles (Coleoptera: Dryopidea: Elmidae). *Entomological News* 89 (1&2): 1-13

Clifford, Hugh F. 1991. *Aquatic Invertebrates of Alberta*. University of Alberta Press Edmonton, Alberta.

- Epler, John. 2001 The Larval Chironomids of North and South Carolina. <http://home.earthlink.net/~johnnepler/>
- Epler, John. Identification Manual for the Water Beetles of Florida. <http://home.earthlink.net/~johnnepler/>
- Epler, John. Identification Manual for the Aquatic and Semi-aquatic Heteroptera of Florida. <http://home.earthlink.net/~johnnepler/>
- Trond Andersen, Peter S. Cranston & John H. Epler (Eds) (2013) Chironomidae of the Holarctic Region: Keys and Diagnoses. Part 1. Larvae. *Insect Systematics and Evolution Supplements* 66: 1-571.
- Jacobus, Luke and Pat Randolph. 2005. Northwest Ephemeroptera Nymphs. Manual from Northwest Biological Assessment Working Group. Moscow Idaho 2005. Not Published.
- Jacobus LM, McCafferty WP (2004) Revisionary Contributions to the Genus *Drunella* (Ephemeroptera : Ephemerellidae). *Journal of the New York Entomological Society* 112: 127-147
- Jacobus LM, McCafferty WP (2003) Revisionary Contributions to North American *Ephemerella* and *Serratella* (Ephemeroptera : Ephemerellidae). *Journal of the New York Entomological Society* 111 (4): 174-193.
- Kathman,R.D., R.O. Brinkhurst. 1999. Guide to the Freshwater Oligochaetes of North America. Aquatic Resources Center, College Grove, Tennessee.
- Larson, D.J., Y. Alarie, R.E. Roughly.2005. Predaceous Diving Beetles (Coleoptera: Dytiscidae) of the Neararctic Region. NRC-CNRC Research Press. Ottawa.
- Merritt, R.W., K.W. Cummins, M. B. Berg. (eds.). 2007. An introduction to the aquatic insects of North America, 4th. Kendall/Hunt, Dubuque, IA
- Morihara DK, McCafferty WP (1979) The *Baetis* Larvae of North American (Ephemeroptera: Baetidae). *Transactions of the American Entomological Society* 105: 139-221.
- Needham, James, M. May, M. Westfall Jr. 2000. Dragonflies of North America. Scientific Publishers. Gainesville FL.
- Prescott David, R.C.and Medea M. Curteanu.2004. Survey of Aquatic Gastropods of Alberta. Species at Risk Report No. 104. ISSN: 1496-7146 (Online Edition)
- Needham, K. 1996. An Identification Guide to the Nymphal Mayflies of British Columbia. Publication #046 Resource Inventory Committee, Government of British Columbia.
- Oliver, Donald R. and Mary E. Roussel. 1983. The Insects and Arachnids of Canada Part 11. The Genera of larval midges of Canada. Biosystematics Research Institute. Ottawa, Ontario. Research Branch, Agriculture Canada. Publication 1746.
- Proctor, H. The 'Top 18' Water Mite Families in Alberta. *Zoology* 351. University of Alberta, Edmonton, Alberta.
- Rogers, D.C. and M. Hill, 2008. Key to the Freshwater Malacostraca (Crustacea) of the mid-Atlantic Region. EPA-230-R-08-017. US Environmental Protection Agency, Office of Environmental Information, Washington, DC.
- Stewart, Kenneth W. and Bill Stark. 2002. The Nymphs of North American Stonefly Genera (Plecoptera). The Caddis Press. Columbus Ohio.
- Stewart, Kenneth W. and Mark W. Oswood. 2006 The Stoneflies (Plecoptera) of Alaska and Western Canada. The Caddis Press.
- Stonedahl, Gary and John D. Lattin. 1986. The Corixidae of Oregon and Washington (Hemiptera: Heteroptera). Technical Bulletin 150. Oregon State University, Corvallis Oregon.
- Thorpe, J. H. and A. P. Covich [Eds.] 1991. Ecology and classification of North American freshwater invertebrates. Academic Press, San Diego.

Tinerella, Paul P. and Ralph W. Gunderson. 2005. The Waterboatmen (Insecta: Heteroptera: Corixidae) of Minisota. Publication No. 23 Dept. Of Entomology, North Dakota State University, Fargo, North Dakota, USA.

Weiderholm, Torgny (Ed.) 1983. The larvae of Chironomidae (Diptera) of the Holartic region. Entomologica Scandinavica. Supplement No. 19.

Westfall, Minter J. Jr. and May, Michael L. 1996. Damselflies of North America. Scientific Publishers, Gainesville, FL.

Wiggins, Glenn B. 1998. Larvae of the North American Caddisfly Genera (Trichoptera) 2nd ed. University of Toronto Press. Toronto Ontario.